# Health Risk and Exposure Assessment for Ozone

## Second External Review Draft

## Chapter 4 Appendices

## DISCLAIMER

This draft document has been prepared by staff from the Risk and Benefits Group, Health and Environmental Impacts Division, Office of Air Quality Planning and Standards, U.S. Environmental Protection Agency. Any findings and conclusions are those of the authors and do not necessarily reflect the views of the Agency. This draft document is being circulated to facilitate discussion with the Clean Air Scientific Advisory Committee to inform the EPA's consideration of the ozone National Ambient Air Quality Standards.

This information is distributed for the purposes of pre-dissemination peer review under applicable information quality guidelines. It has not been formally disseminated by EPA. It does not represent and should not be construed to represent any Agency determination or policy.

Questions related to this preliminary draft document should be addressed to Dr. Bryan Hubbell, U.S. Environmental Protection Agency, Office of Air Quality Planning and Standards, C539-07, Research Triangle Park, North Carolina 27711 (email: hubbell.bryan@epa.gov).

EPA-452/P-14-004b
February 2014

# *Health Risk and Exposure Assessment for Ozone*

## *Second External Review Draft*

## *Chapter 4 Appendices*

U.S. Environmental Protection Agency
Office of Air and Radiation
Office of Air Quality Planning and Standards
Health and Environmental Impacts Division
Risk and Benefits Group
Research Triangle Park, North Carolina 27711

*This page left intentionally blank*

# Appendix 4-A
# Ambient Air Quality Monitoring Data

## Table of Contents


1. Ambient $O_3$ Monitoring and Air Quality Data ..... 4
   1.1 Overview of Ambient $O_3$ Monitoring ..... 4
   1.2 Ambient $O_3$ Concentration Data ..... 6
   1.3 Data Handling ..... 8
2. Air Quality Inputs for the Exposure and Clinical Risk Assessments ..... 12
   2.1 Urban Case Study Areas ..... 12
   2.2 Air Quality Inputs to the Air Pollutants Exposure (APEX) Model ..... 13
   2.3 Evaluation of Air Quality Spatial Field Techniques ..... 30
3. Air Quality Inputs for the Epidemiology-Based Risk Assessment ..... 34
   3.1 Urban Case Study Areas ..... 34
   3.2 Air Quality Inputs to the Benefits Mapping and Analysis Program (BenMAP) 36
4. References ..... 39

# FIGURES


FIGURE 1: MAP OF U.S. AMBIENT $O_3$ MONITORING SITES IN OPERATION DURING THE 2006-2010 PERIOD ..... 6

FIGURE 2: MAP OF MONITORED 8-HOUR $O_3$ DESIGN VALUES FOR THE 2006-2008 PERIOD ..... 11

FIGURE 3: MAP OF MONITORED 8-HOUR $O_3$ DESIGN VALUES FOR THE 2008-2010 PERIOD ..... 12

FIGURE 4 NUMERICAL EXAMPLE OF THE VORONOI NEIGHBOR AVERAGING (VNA) TECHNIQUE ..... 14

FIGURE 5 MAPS OF DESIGN VALUES AND MAY – SEPTEMBER AVERAGE MDA8 VALUES BASED ON VNA SPATIAL FIELDS FOR ATLANTA. 16

FIGURE 6 MAPS OF DESIGN VALUES AND MAY – SEPTEMBER AVERAGE MDA8 VALUES BASED ON VNA SPATIAL FIELDS FOR BALTIMORE. 17

FIGURE 7 MAPS OF DESIGN VALUES AND MAY – SEPTEMBER AVERAGE MDA8 VALUES BASED ON VNA SPATIAL FIELDS FOR BOSTON. 18

FIGURE 8 MAPS OF DESIGN VALUES AND MAY – SEPTEMBER AVERAGE MDA8 VALUES BASED ON VNA SPATIAL FIELDS FOR CHICAGO. 19

FIGURE 9 MAPS OF DESIGN VALUES AND MAY – SEPTEMBER AVERAGE MDA8 VALUES BASED ON VNA SPATIAL FIELDS FOR CLEVELAND. 20

FIGURE 10 MAPS OF DESIGN VALUES AND MAY – SEPTEMBER AVERAGE MDA8 VALUES BASED ON VNA SPATIAL FIELDS FOR DALLAS. 21

FIGURE 11 MAPS OF DESIGN VALUES AND MAY – SEPTEMBER AVERAGE MDA8 VALUES BASED ON VNA SPATIAL FIELDS FOR DENVER. 22

FIGURE 12 MAPS OF DESIGN VALUES AND MAY – SEPTEMBER AVERAGE MDA8 VALUES BASED ON VNA SPATIAL FIELDS FOR DETROIT. 23

FIGURE 13 MAPS OF DESIGN VALUES AND MAY – SEPTEMBER AVERAGE MDA8 VALUES BASED ON VNA SPATIAL FIELDS FOR HOUSTON. 24

FIGURE 14 MAPS OF DESIGN VALUES AND MAY – SEPTEMBER AVERAGE MDA8 VALUES BASED ON VNA SPATIAL FIELDS FOR LOS ANGELES. 25

FIGURE 15 MAPS OF DESIGN VALUES AND MAY – SEPTEMBER AVERAGE MDA8 VALUES BASED ON VNA SPATIAL FIELDS FOR NEW YORK. 26

FIGURE 16 MAPS OF DESIGN VALUES AND MAY – SEPTEMBER AVERAGE MDA8 VALUES BASED ON VNA SPATIAL FIELDS FOR PHILADELPHIA. 27

FIGURE 17 MAPS OF DESIGN VALUES AND MAY – SEPTEMBER AVERAGE MDA8 VALUES BASED ON VNA SPATIAL FIELDS FOR SACRAMENTO. 28

FIGURE 18 MAPS OF DESIGN VALUES AND MAY – SEPTEMBER AVERAGE MDA8 VALUES BASED ON VNA SPATIAL FIELDS FOR ST. LOUIS. 29

FIGURE 19 MAPS OF DESIGN VALUES AND MAY – SEPTEMBER AVERAGE MDA8 VALUES BASED ON VNA SPATIAL FIELDS FOR WASHINGTON, D.C. 30

FIGURE 20 MAPS OF MONITORED VALUES (LEFT), NEAREST NEIGHBOR SPATIAL FIELDS (CENTER), AND VNA SPATIAL FIELDS (RIGHT) FOR SELECTED HOURS IN ATLANTA (TOP), AND PHILADELPHIA (BOTTOM) ..... 31

FIGURE 21: DENSITY SCATTER PLOTS AND PERFORMANCE STATISTICS FOR THE CROSS-VALIDATION ANALYSIS OF NEAREST NEIGHBOR (NN; LEFT) AND VORONOI NEIGHBOR AVERAGING (VNA; RIGHT) SPATIAL FIELD TECHNIQUES APPLIED TO MONITORED HOURLY $O_3$ CONCENTRATIONS IN ATLANTA, 2005. ..... 32

FIGURE 22: DENSITY SCATTER PLOTS AND PERFORMANCE STATISTICS FOR THE CROSS-VALIDATION ANALYSIS OF NEAREST NEIGHBOR (NN; LEFT) AND VORONOI NEIGHBOR AVERAGING (VNA; RIGHT) SPATIAL FIELD TECHNIQUES APPLIED TO MONITORED HOURLY $O_3$ CONCENTRATIONS IN DETROIT, 2005.....33
FIGURE 23: DENSITY SCATTER PLOTS AND PERFORMANCE STATISTICS FOR THE CROSS-VALIDATION ANALYSIS OF NEAREST NEIGHBOR (NN; LEFT) AND VORONOI NEIGHBOR AVERAGING (VNA; RIGHT) SPATIAL FIELD TECHNIQUES APPLIED TO MONITORED HOURLY $O_3$ CONCENTRATIONS IN PHILADELPHIA, 2005. .....33

## TABLES

TABLE 1: INFORMATION ON THE 15 URBAN CASE STUDY AREAS IN THE EXPOSURE AND CLINICAL RISK ASSESSMENTS ....13
TABLE 2 INFORMATION ON THE 12 URBAN CASE STUDY AREAS IN THE EPIDEMIOLOGY BASED RISK ASSESSMENT .....35
TABLE 3 SUMMARY OF THE AIR QUALITY INPUTS TO BENMAP .....38

# 1. AMBIENT $O_3$ MONITORING AND AIR QUALITY DATA

This section provides a brief overview of ambient $O_3$ monitoring in the U.S. (Section 1.1), the ambient $O_3$ concentration data extracted for use in the risk and exposure assessments (Section 1.2), and the data handling procedures used for determining compliance with the existing and potential alternative standards as well as some other relevant air quality metrics (Section 1.3).

## 1.1 OVERVIEW OF AMBIENT $O_3$ MONITORING

The Clean Air Act establishes air quality monitoring requirements to provide information on ambient concentrations for six criteria pollutants, including $O_3$, and makes provisions for the collection of other ambient air quality measurements, such as $O_3$ precursors. The federal regulations for ambient air quality monitoring, including establishment and periodic assessment of local monitoring networks, approved monitoring methods, operating schedules, and protocols for data reporting, quality assurance, and certification, are in Part 58 of the Code of Federal Regulations.

There were over 1,300 ambient $O_3$ monitoring sites actively operating in the U.S. in 2010. These monitoring sites are operated by over 100 federal, state, local, and tribal agencies, and can be grouped into one of the following networks:

1) State and Local Air Monitoring Stations (SLAMS): Monitoring sites operated by state, local, and tribal governments for the purposes of determining compliance with the National Ambient Air Quality Standards (NAAQS), and providing ambient air quality information to help state and local public health agencies evaluate and implement air quality control programs. There were over 1,100 SLAMS $O_3$ monitoring sites operating in 2010, making up over 80% of the U.S. ambient $O_3$ monitoring network. There are two important subcategories of SLAMS monitors:
   a. National Multi-pollutant Monitoring Network (NCore): Approximately 80 monitoring sites (60 urban and 20 rural) operated by state and local agencies. These sites monitor six criteria pollutants (CO, $NO_2$, $O_3$, $SO_2$, $PM_{10}$, and $PM_{2.5}$) and other important parameters for the purposes of assessing multi-pollutant impacts on public health, and supporting air quality forecasting.
   b. Photochemical Assessment Monitoring Stations (PAMS): Approximately 80 monitoring sites operated by state and local agencies with EPA funding. These sites monitor $O_3$ and its precursors, including NO, $NO_2$, total NOx, total reactive nitrogen (NOy), and over 60 volatile organic compounds (VOCs) for the purposes of understanding $O_3$ chemistry and transport, aiding photochemical modeling, and evaluating $O_3$ precursor emissions control strategies in areas designated nonattainment for the $O_3$ NAAQS. Some PAMS monitoring sites are co-located with NCore monitoring sites.

2) Clean Air Status and Trends Network (CASTNET): Approximately 80 $O_3$ monitoring sites operated year-round by EPA and the National Park Service (NPS) for the purpose of determining $O_3$ levels in national parks and other rural areas.
3) Special Purpose Monitoring Stations (SPMS): These monitoring sites are used to support various air quality monitoring objectives, such as specific public health and welfare impacts studies, model evaluation, or monitoring network assessments. These monitoring sites are often operated on a temporary basis (up to 24 months), and are generally not used to determine compliance with the NAAQS. Some of these monitoring sites may be operated by local industry or other private interest groups.

SLAMS monitoring sites are required to monitor for $O_3$ only during the required $O_3$ monitoring season, which is defined for each state in Table D-3 of 40 CFR Part 58. Many states also operate their $O_3$ monitors outside of the required $O_3$ monitoring season. States that are required to operate some or all of their $O_3$ monitors on a year-round basis include Arizona, California, Hawaii, Louisiana, New Mexico, and Texas. EPA regional offices may approve waivers effectively shortening the length of the required $O_3$ monitoring season for some individual monitoring sites (e.g. rural monitoring sites which may be inaccessible during the winter months). CASTNET and NCore monitoring sites are typically operated on a year-round basis.

The Federal Reference Method (FRM) for $O_3$ measurement is the Chemiluminescence Method (CLM). The first ultraviolet (UV) absorption photometric analyzers were approved as Federal Equivalent Methods (FEMs) in 1977 and gained rapid acceptance for NAAQS compliance purposes due to ease of operation, relatively low cost, and reliability. All SLAMS and CASTNET $O_3$ monitoring sites in the U.S. have been operating UV analyzers since 2005.

Figure 1 shows the locations of the ambient $O_3$ monitoring sites used in the risk and exposure assessments. Gray dots represent SLAMS monitoring sites, green dots represent CASTNET sites, blue dots represent NCore and/or PAMS monitoring sites, and black dots represent SPMS and other monitoring sites for which data were available.

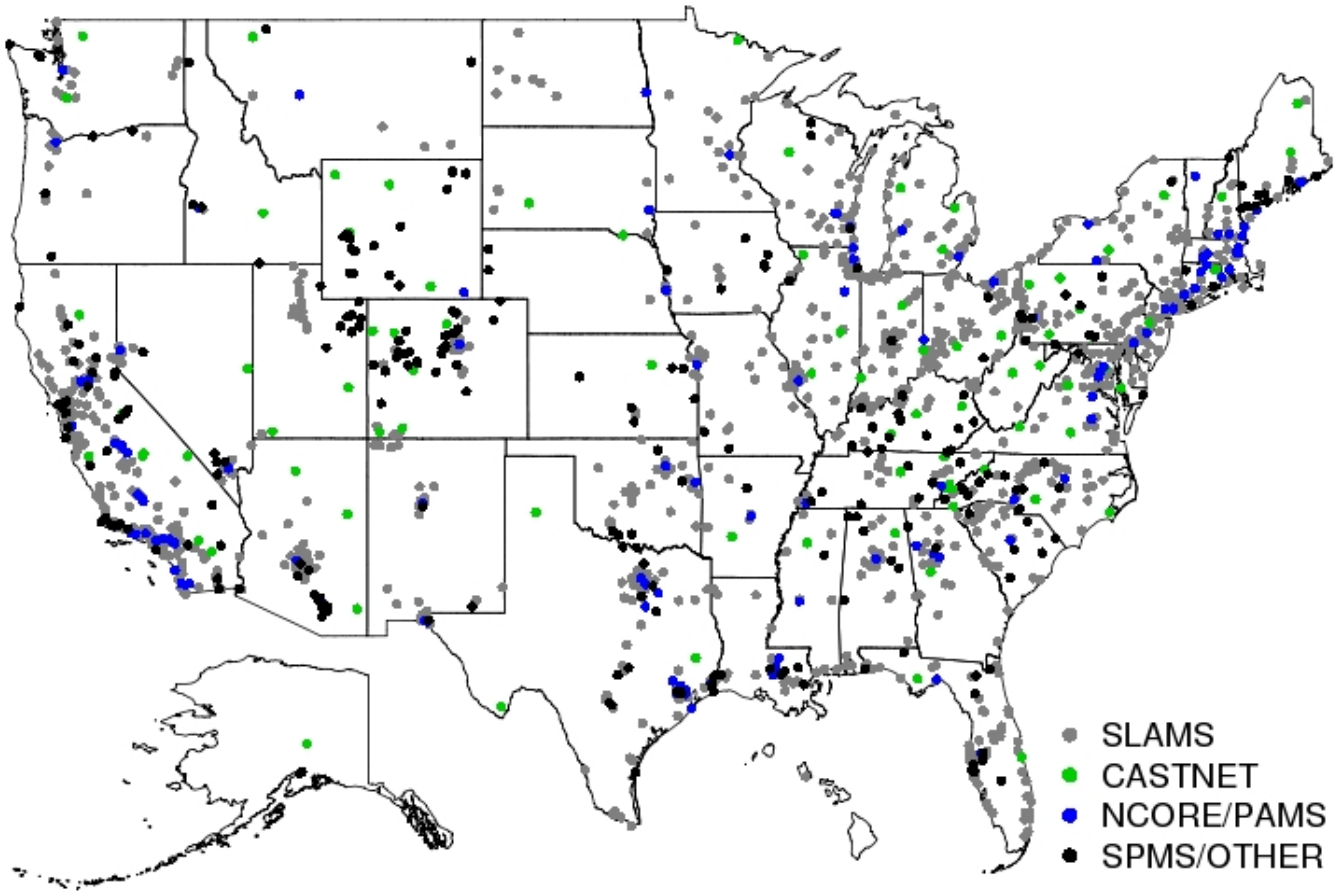


**Figure 1: Map of U.S. ambient $O_3$ monitoring sites in operation during the 2006-2010 period**

## 1.2 AMBIENT $O_3$ CONCENTRATION DATA

EPA's Air Quality System (AQS) database is a national repository for many types of air quality and related monitoring data. AQS contains monitoring data for the six criteria pollutants dating back to the 1970's, as well as more recent additions such as $PM_{2.5}$ speciation, air toxics, and meteorology data. As of 2010, over 100 federal, state, local, and tribal agencies submitted hourly $O_3$ concentration data collected from over 1,300 ambient monitoring sites to AQS.

Air quality monitoring data from 1,468 ambient $O_3$ monitoring sites in the U.S. were extracted for use in the risk and exposure assessments. The initial dataset consisted of hourly $O_3$ concentrations in ppb collected from these monitors between 1/1/2006 and 12/31/2010. Data for nearly 1,400 of these monitors were extracted from the AQS database in October 2012, and the remaining data were extracted from the CASTNET database at the same time. CASTNET monitors operated by the National Park Service were included in the data extracted from AQS, but the CASTNET monitors operated by EPA did not begin reporting data to AQS until 2011. Data collected from these EPA operated CASTNET monitors prior to 2011 did not meet EPA's quality assurance requirements, but the data were subject to

quality assurance criteria, and it is generally agreed that data collected from CASTNET monitors prior to 2011 is of comparable quality to the regulatory data stored in AQS.

There were a number of subtle, yet noteworthy differences between the air quality data used in the 1st draft REA and the air quality data used in this draft.

1. In the 1st draft REA, multiple AQS data extractions were used for the air quality inputs to various parts of the risk and exposure assessments. In this draft, all air quality inputs were derived from the data extraction described above.
2. In the 1st draft REA, data collected from EPA operated CASTNET sites and other non-regulatory monitoring sites were not included in the air quality inputs to the risk and exposure assessments. In this draft, these monitors were included, but were not used to make determinations of meeting the existing standard or the potential alternative standards.
3. In the 1st draft REA, data collected with $O_3$ analyzers not using federal reference or equivalent methods were not included in the air quality inputs to the risk and exposure assessments. In this draft, these monitors were included, but were not used to make determinations of meeting the existing standard or the potential alternative standards.
4. In the 1st draft REA, reported hourly $O_3$ concentrations lower than the minimum detection limit (MDL, 5 ppb for most $O_3$ analyzers) were replaced with a value of ½ MDL. This is called the "standard sample value" for criteria pollutant data extracted from AQS. In this draft, the actual reported sample values were used, effectively allowing concentrations down to 0 ppb.
5. In the 1st draft REA, hourly $O_3$ concentrations flagged by the monitoring agencies and concurred by EPA as having been affected by exceptional events were removed from the air quality inputs to the risk and exposure assessments. In this draft, these data were included, but were not used to make determinations of meeting the existing standard or the potential alternative standards, which is consistent with EPA's exceptional events policy.
6. In this draft, missing data gaps of 1 or 2 hours in length were filled in using linear interpolation. These short gaps often occur at regular intervals in the ambient data due to an EPA requirement for monitoring agencies to perform routine quality control checks on their $O_3$ monitors. Quality control checks are typically performed between midnight and 6:00 AM when $O_3$ concentrations are low. Missing data gaps of 3 hours or more in length were not replaced, and interpolated values were not used to make determinations of meeting the existing standard or the potential alternative standards.
7. In this draft, hourly $O_3$ concentrations from 7 monitoring sites where multiple $O_3$ analyzers were operated simultaneously in the same physical location were combined to create a single hourly site record using the highest reported hourly concentration in each hour.
8. In some instances, EPA regional offices may approve the data combinations for pairs of nearby $O_3$ monitoring sites affected by short distance site relocations for the purpose of making NAAQS

determinations. In this draft, hourly $O_3$ concentrations from 12 such pairs of monitoring sites were combined to create a single hourly site record for each pair.

## 1.3 **DATA HANDLING**

To determine whether or not the NAAQS have been met at an ambient air quality monitoring site, a statistic commonly referred to as a "design value" must be calculated based on 3 consecutive years of data collected from that site. The form of the existing $O_3$ NAAQS design value statistic is the 3-year average of the annual 4$^{th}$ highest daily maximum 8-hour $O_3$ concentration in ppb, with all decimal digits truncated. The existing $O_3$ NAAQS are met at an ambient monitoring site when the design value is less than or equal to 75 ppb. The data handling protocols for calculating design values for the existing $O_3$ NAAQS are in 40 CFR Part 50, Appendix P. In counties or other geographic areas with multiple monitors, the area-wide design value is defined as the design value at the highest individual monitoring site, and the area is said to have met the NAAQS if all monitors in the area are meeting the NAAQS. The initial hourly $O_3$ concentration dataset was split into two design value periods, 2006-2008 and 2008-2010, and subsequent analyses were conducted independently for these two periods.

The following daily summary statistics were calculated from the hourly $O_3$ concentrations:

1. Daily Maximum 8-hour Average (MDA8) Concentration: There are 24 consecutive 8-hour periods in each day (midnight – 8:00 AM, 1:00 AM – 9:00 AM, ..., 11:00 PM – 7:00 AM). Rolling 8-hour averages were calculated for each period with 6, 7, or 8 hours of data available, using 6, 7, or 8 as the divisor, respectively, and 8-hour periods with fewer than 6 hours of data available were not used. The 8-hour average values were stored in the 1$^{st}$, or start, hour of the 8-hour period. The MDA8 value is the highest of the 8-hour average values for each day, and the MDA8 values for two consecutive days may have some hours in common. MDA8 values were considered to be valid if there were sufficient data available to calculate at least 18 of 24 possible 8-hour averages, or, if used for design value calculations, if the MDA8 value is greater than the level of the standard. This is the daily metric used in design values and the Smith et al, 2009 short-term mortality study.
2. Daily 10:00 AM – 6:00 PM Mean Concentration: This is the rolling 8-hour average value as defined above for the 8-hour period starting at 10:00 AM. This is the daily metric used in the Zanobetti & Schwartz, 2008 short-term mortality study.
3. Daily Maximum 1-hour Concentration: This is the highest hourly $O_3$ concentration reported during a given day. Daily Maximum 1-hour values were considered to be valid if there were at least 18 hourly $O_3$ concentrations reported in a given day. This is the daily metric used in the Jerrett et al, 2009 long-term mortality study.
4. Daily 24-hour Average Concentration: This is the simple arithmetic average of the hourly $O_3$ concentrations reported during a given day. Daily 24-hour average values were considered to be

valid if there were at least 18 hourly $O_3$ concentrations reported in a given day. This is the daily metric used in the Bell et al, 2004 short-term mortality study.

The daily summary statistics described above were then used to calculate the following annual summary statistics:

1. Annual 4$^{th}$ Highest MDA8 Concentration: This is the 4$^{th}$ highest valid MDA8 value measured at a given monitoring site in a given year. The 4$^{th}$ highest MDA8 values were considered to be valid if there were valid MDA8 values available for at least 75% of the days in the required $O_3$ monitoring season, or, if used for design value calculations, if the 4$^{th}$ highest MDA8 value was greater than the level of the standard. Data collected outside of the required $O_3$ monitoring season were used in determining the 4$^{th}$ highest MDA8 value, but were not used in determining validity.
2. May – September Average MDA8: This is the average of all available valid MDA8 values at a given monitoring site during the May – September period (153 days). The May – September average MDA8 values were considered to be valid if valid MDA8 values were available for at least 114 days (75%) in May – September of a given year. Three-year averages of these values were calculated for the 2006-2008 period and used to create the May – September average MDA8 national fused air quality surface described in Appendix 4c. This surface was then used in the national-scale risk assessment based on Smith et al, 2009 described in Chapter 8.
3. June – August Average Daily 10:00 AM – 6:00 PM Mean: This is the average of all available daily 10:00 AM – 6:00 PM mean values at a given monitoring site during the June – August period (92 days). The June – August average daily mean values were considered to be valid if daily 10:00 AM – 6:00 PM mean values were available for at least 70 days (75%) in June – August of a given year. Three-year averages of these values were calculated for the 2006-2008 period and used to create the June – August average daily 10:00 AM – 6:00 PM mean national fused air quality surface described in Appendix 4c. This surface was then used in the national-scale risk assessment based on Zanobetti & Schwartz, 2008 described in Chapter 8.
4. April – September Average Daily Maximum 1-hour Concentration: This is the average of all available valid daily maximum 1-hour values at a given monitoring site during the April – September period. The April – September average daily maximum 1-hour values were considered to be valid if valid daily maximum 1-hour values were available for at least 137 days (75%) in April – September of a given year. Three-year averages of these values were calculated for the 2006-2008 period and used to create the April - September average daily maximum 1-hour national fused air quality surface described in Appendix 4c. This surface was then used in the national-scale risk assessment based on Jerrett et al, 2009 described in Chapter 8.

The design value statistic for the existing $O_3$ standard is the 3-year average of the annual 4$^{th}$ highest MDA8 values described above. Design values greater than the level of the existing standard (76

ppb or higher) are automatically valid. Design values less than or equal to the level of the existing standard must be based on 3 valid 4$^{th}$ highest MDA8 values, with the additional requirement that the 3-year average of the annual data completeness statistics (percent of valid MDA8 values within the required $O_3$ monitoring season) must be at least 90%. These same criteria were chosen to determine design values for the potential alternative standards. The implications of this choice are that in some cases, a monitoring site may have different design values based on the level of the standard. This may occur for one of two reasons:

1. A monitoring site with insufficient data to determine a design value at higher standard level may have sufficient data to show a violation at a lower standard level. For example, if a monitoring site has a 3-year average annual 4$^{th}$ highest MDA8 value of 72 ppb, but does not meet the data completeness criteria described above, then the site has a design value of 72 ppb for the potential alternative standards of 70 ppb, 65 ppb, and 60 ppb, but does not have a design value for the existing standard of 75 ppb.
2. EPA's current practice is to use only "valid" MDA8 values when determining the annual 4$^{th}$ highest MDA8 value. A valid MDA8 value is either based on at least 18 of 24 possible 8-hour average values, or it is greater than the level of the standard. This can cause the design value to change based on the level of the standard, due to whether certain days are considered valid or not. For example, suppose the five highest MDA8 values at a particular monitoring site for a given year are 78 ppb, 76 ppb, 75 ppb, 74 ppb, and 70 ppb, but the 4$^{th}$ highest value is based on only 12 valid 8-hour averages. Then for the existing standard, the 4$^{th}$ highest MDA8 value is 70 ppb, but for the 70 ppb alternative standard, the 4$^{th}$ highest MDA8 value is 74 ppb.

Figure 2 and Figure 3 show the design values for the existing $O_3$ NAAQS for all regulatory monitoring sites in the U.S. for the 2006-2008 and 2008-2010 periods, respectively. In general, $O_3$ design values were lower in 2008-2010 than in 2006-2008, especially in the Eastern U.S. There were 518 $O_3$ monitors in the U.S. with design values above the existing standard in 2006-2008, compared to only 179 in 2008-2010.

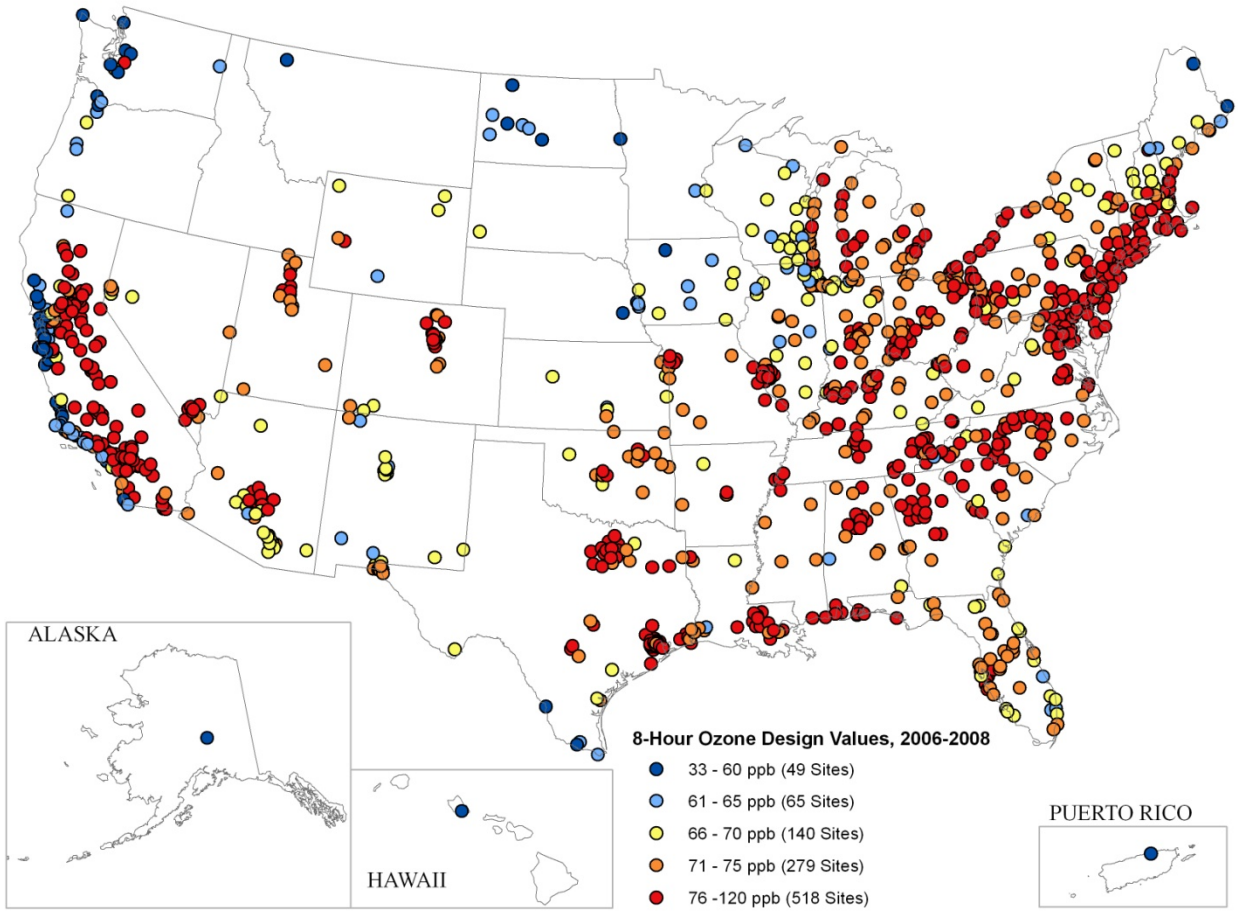


**Figure 2: Map of monitored 8-hour $O_3$ design values for the 2006-2008 period**

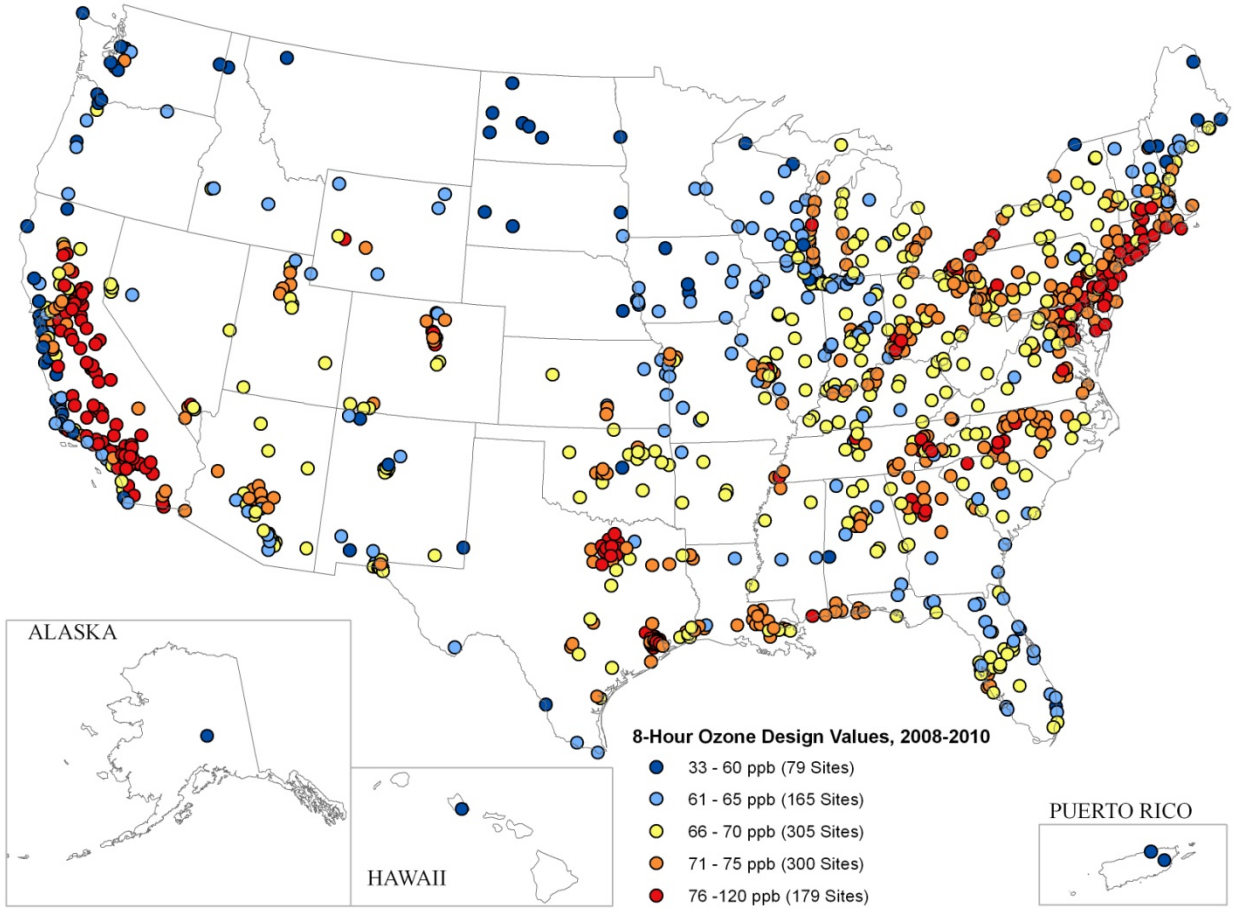


**Figure 3: Map of monitored 8-hour $O_3$ design values for the 2008-2010 period**

# 2. AIR QUALITY INPUTS FOR THE EXPOSURE AND CLINICAL RISK ASSESSMENTS

This section describes the 15 urban case study areas used in the exposure and clinical risk assessments described in Chapters 5 and 6 (Section 2.1), the hourly $O_3$ concentration spatial fields used as inputs to the Air Pollutants Exposure Model (APEX; Section 2.2), and some methods evaluations supporting the change from nearest neighbor to the Voronoi Neighbor Averaging (VNA) technique for generating the spatial fields (Section 2.3).

## 2.1 URBAN CASE STUDY AREAS

The 15 urban case study areas in the exposure (Chapter 5) and clinical risk (Chapter 6) assessments covered a large spatial extent, with boundaries generally similar to those covered by the respective Combined Statistical Areas (CSA) defined by the U.S. Census Bureau. Table 1 gives some basic information about the 15 urban case study areas in the exposure and clinical risk assessments,

including the number of counties, number of ambient $O_3$ monitoring sites, the required $O_3$ monitoring season, and the 2006-2008 and 2008-2010 design values. All 15 urban case study areas had 8-hour $O_3$ design values above the existing standard in 2006-2008, while 13 areas had 8-hour $O_3$ design values above the existing standard in 2008-2010. Chicago (74 ppb) and Detroit (75 ppb) had design values meeting the existing standard during the 2008-2010 period. The design values in the 15 urban areas decreased by an average of 6 ppb between 2006-2008 and 2008-2010, ranging from no change in Sacramento to a decrease of 15 ppb in Atlanta.

| Area Name | # of Counties | # of $O_3$ Monitors | Population (2010) | Required $O_3$ Monitoring Season | 2006-2008 DV (ppb) | 2008-2010 DV (ppb) |
|---|---|---|---|---|---|---|
| Atlanta | 33 | 13 | 5,618,431 | March - October | 95 | 80 |
| Baltimore | 7 | 7 | 2,710,489 | April - October | 91 | 89 |
| Boston | 10 | 14 | 5,723,468 | April - September | 83 | 77 |
| Chicago | 16 | 26 | 9,686,021 | April - October | 78 | 74 |
| Cleveland | 8 | 13 | 2,881,937 | April - October | 82 | 77 |
| Dallas | 11 | 20 | 6,366,542 | January - December | 89 | 86 |
| Denver | 13 | 26 | 3,390,504 | March - September | 86 | 77 |
| Detroit | 9 | 12 | 5,218,852 | April - September | 81 | 75 |
| Houston | 10 | 22 | 5,946,800 | January - December | 91 | 85 |
| Los Angeles | 5 | 54 | 17,877,006 | January - December | 119 | 112 |
| New York | 27 | 31 | 21,056,173 | April - October | 90 | 84 |
| Philadelphia | 15 | 19 | 7,070,622 | April - October | 92 | 83 |
| Sacramento | 7 | 26 | 2,755,972 | January - December | 102 | 102 |
| St. Louis | 17 | 17 | 2,837,592 | April - October | 85 | 77 |
| Washington | 26 | 22 | 5,838,518 | April - October | 87 | 81 |

**Table 1: Information on the 15 Urban Case Study Areas in the Exposure and Clinical Risk Assessments**

## 2.2 AIR QUALITY INPUTS TO THE AIR POLLUTANTS EXPOSURE (APEX) MODEL

The Air Pollutants Exposure Model (APEX) described in Chapter 5 requires spatial fields of air quality concentrations with no missing values as inputs. In the 1st draft REA, the spatial fields were generated using hourly $O_3$ concentrations from the nearest available monitoring site for each census tract in four of the 15 urban case study areas (Atlanta, Denver, Los Angeles, and New York). In this draft, the spatial fields were generated with hourly $O_3$ concentrations interpolated using the Voronoi Neighbor Averaging (VNA; Gold, 1997; Chen et al, 2004) technique described below for each census tract in the 15 urban case study areas. The following paragraphs provide a numerical example of VNA used to estimate an $O_3$ concentration value for census tract "E" in figure 4 below.

The first step in the VNA technique is to identify the set of nearest monitors for each census tract. The left-hand panel of Figure 4 presents a numerical example with nine census tracts (squares) and seven monitoring sites (stars), with the focus on identifying the set of nearest neighboring sites to

census tract "E" in the center of the panel. The Delaunay triangulation algorithm identifies the set of nearest neighboring monitors by drawing a set of polygons called the "Voronoi diagram" around the census tract "E" centroid and each of the monitoring sites. Voronoi diagrams have the special property that each edge of each of the polygons are the same distance from the two closest points, as shown in the right-hand panel of Figure 4.

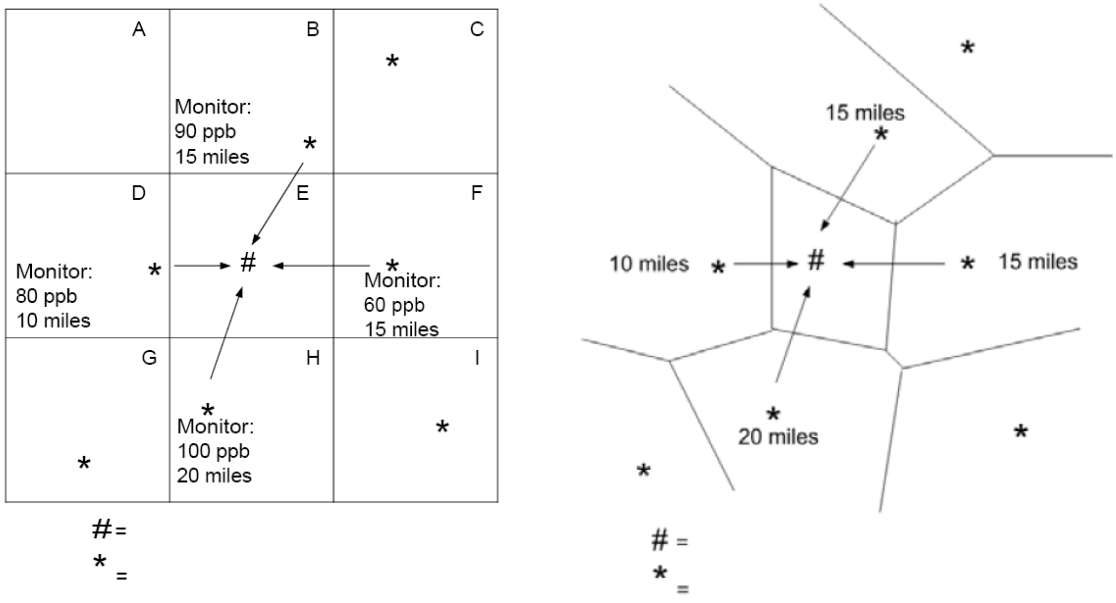


**Figure 4 Numerical example of the Voronoi Neighbor Averaging (VNA) technique**

The VNA technique then chooses the monitoring sites whose polygons share a boundary with the census tract "E" centroid. These monitors are the "Voronoi neighbors", which are used to estimate the concentration value for census tract "E". The VNA estimate of the concentration value in census tract "E" is the inverse distance squared weighted average of the four monitored concentrations. The further the monitor is from the center of census tract "E", the smaller the weight. For example, the weight for the monitor in census tract "D" 10 miles from the census tract "E" centroid is calculated as follows:

$$\frac{1/10^2}{1/10^2+1/15^2+1/15^2+1/20^2} = 0.4675 \quad \textbf{(Equation 1)}$$

The weights for the other monitors are calculated in a similar fashion. The final VNA estimate for census tract "E" is calculated as follows:

$$VNA(E) = 0.4675 * 80 + 0.2078 * 90 + 0.2078 * 60 + 0.1169 * 100 = 80.3\ ppb \quad \textbf{(Equation 2)}$$

The observed hourly $O_3$ concentrations in the 15 urban case study areas were used to calculate VNA estimates for approximately 24,935 census tracts * 43,824 hours ≈ 1.1 billion values. The actual number of values was lower than this, because values were not calcuated for hours outside the required

monitoring season. However, the same VNA procedure was also used to create hourly spatial surfaces based on air quality adjusted to meet the existing standard of 75 ppb, and air quality adjusted to meet the potential alternative standards of 70 ppb, 65 ppb, 60 ppb, and 55 ppb, which effectively increased the total number of VNA estimates by roughly a factor of 5. The computations were executed using the R statistical computing program (R, 2012), with the Delaunay triangulation algorithm implemented in the "deldir" package (Turner, 2012).

Figure 5 through Figure 19 show maps of the 2006-2008 and 2008-2010 design values and May–September "seasonal" average MDA8 values in the 15 urban case study areas based on the VNA spatial fields. The top panels in each figure show the design values, while the bottom panels show the seasonal average values. The left-hand panels in each figure show the 2006-2008 values, while the right-hand panels show the 2008-2010 values. The colored circles in each panel represent census tract centroids, and the colored squares represent monitoring sites. In each panel, counties colored pink indicate the study area boundaries used in the Zanobetti & Schwartz (2008) and/or Smith et al (2009b) epidemiology studies[1], where applicable. Counties colored gray indicate additional counties within the CBSA boundaries, and counties colored peach indicate any additional counties included in the exposure and lung function risk assessments. Note that the maps show some monitors outside of the study area boundaries. This is because the VNA surfaces were generated using data from monitors within a 50 km radius of the study area boundaries, in addition to the monitors inside the study areas.

[1] The Zanobetti and Schwartz (2008) and Smith et al (2009) study area boundaries were identical for 6 of the 12 urban case study areas, and had at least one county in common for all 12 urban case study areas. The counties colored pink in figures 5 through 19 refer to counties included in either of those two studies.

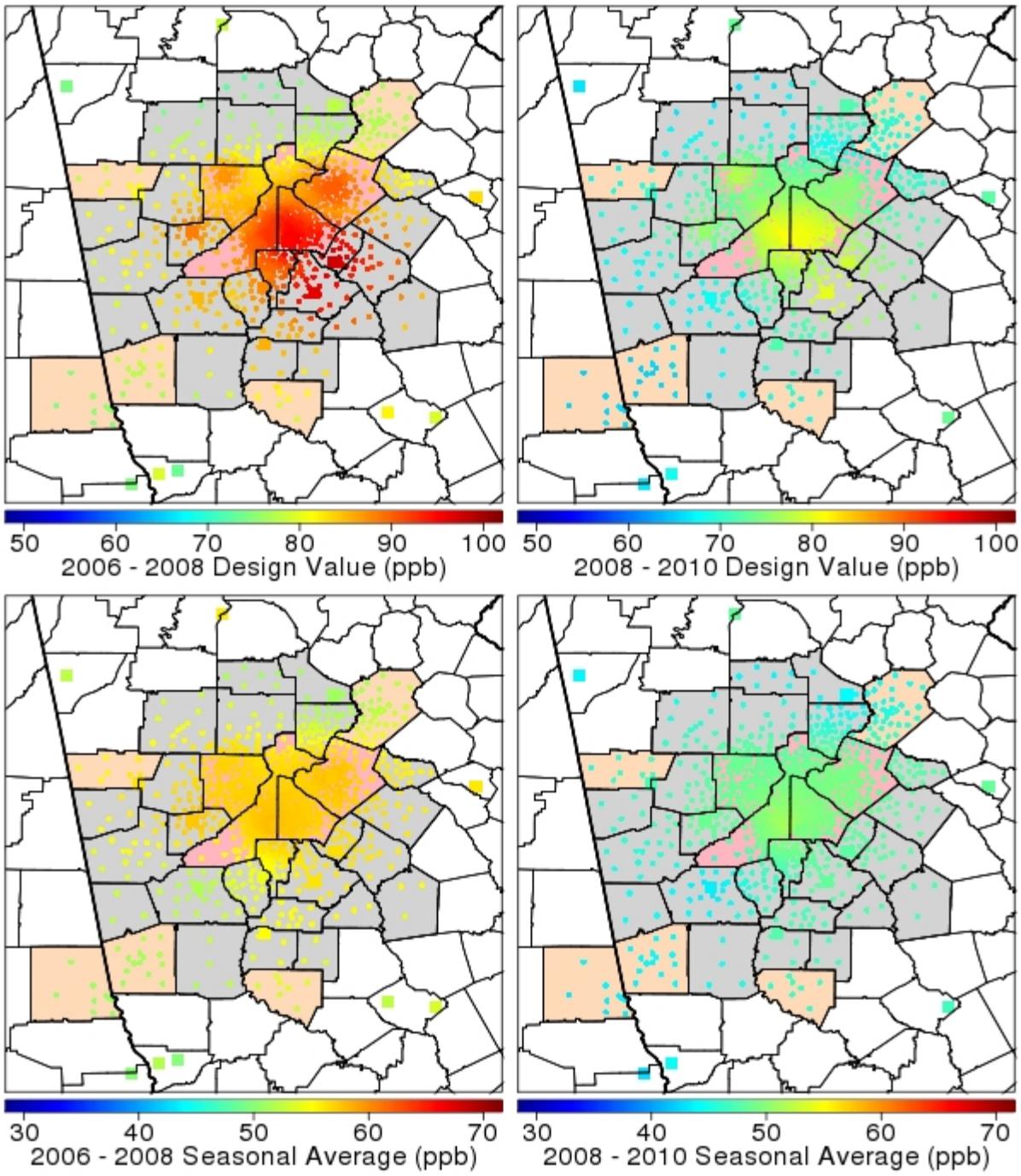


**Figure 5** **Maps of design values and May – September average MDA8 values based on VNA spatial fields for Atlanta.**

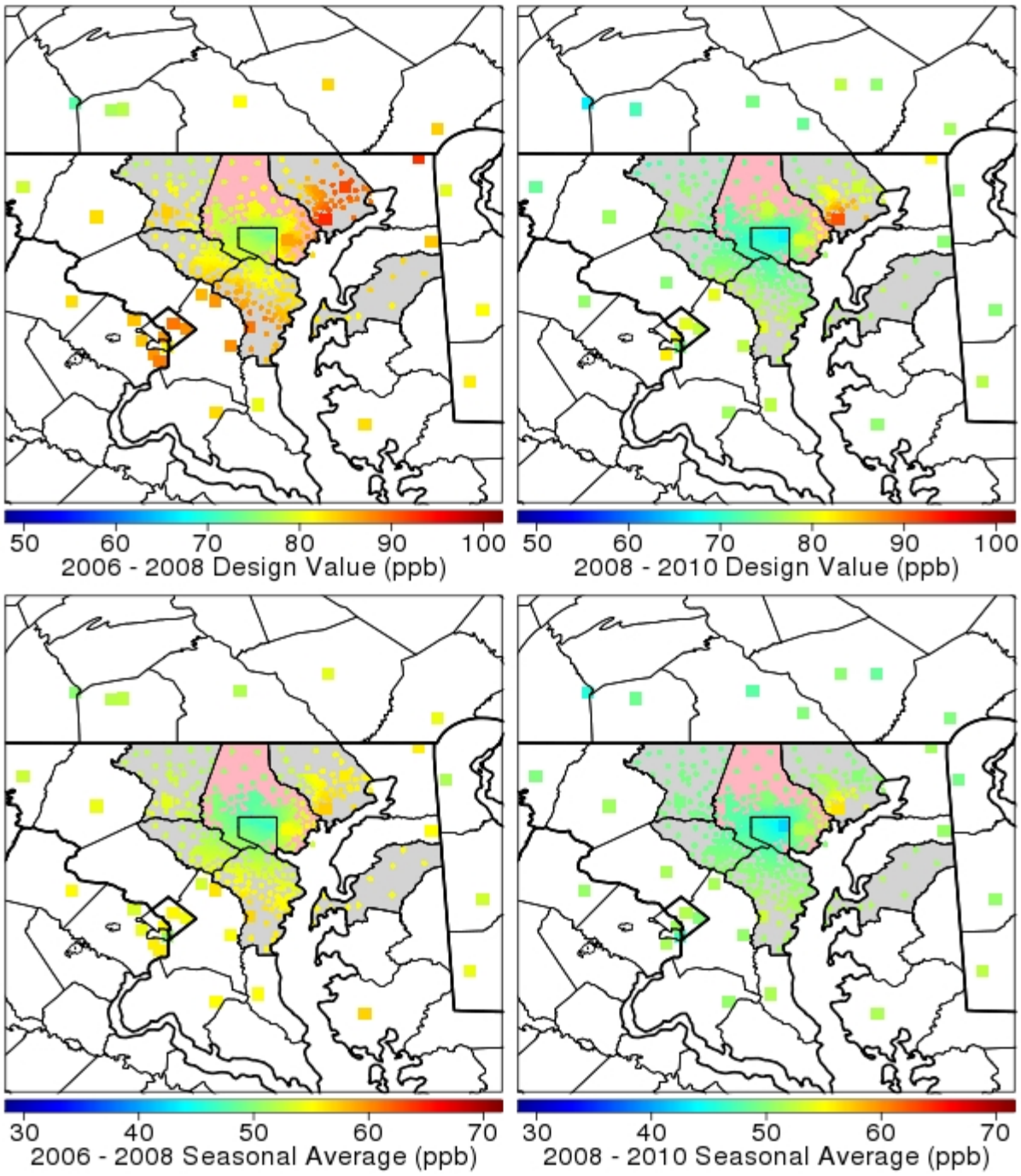


**Figure 6** **Maps of design values and May – September average MDA8 values based on VNA spatial fields for Baltimore.**

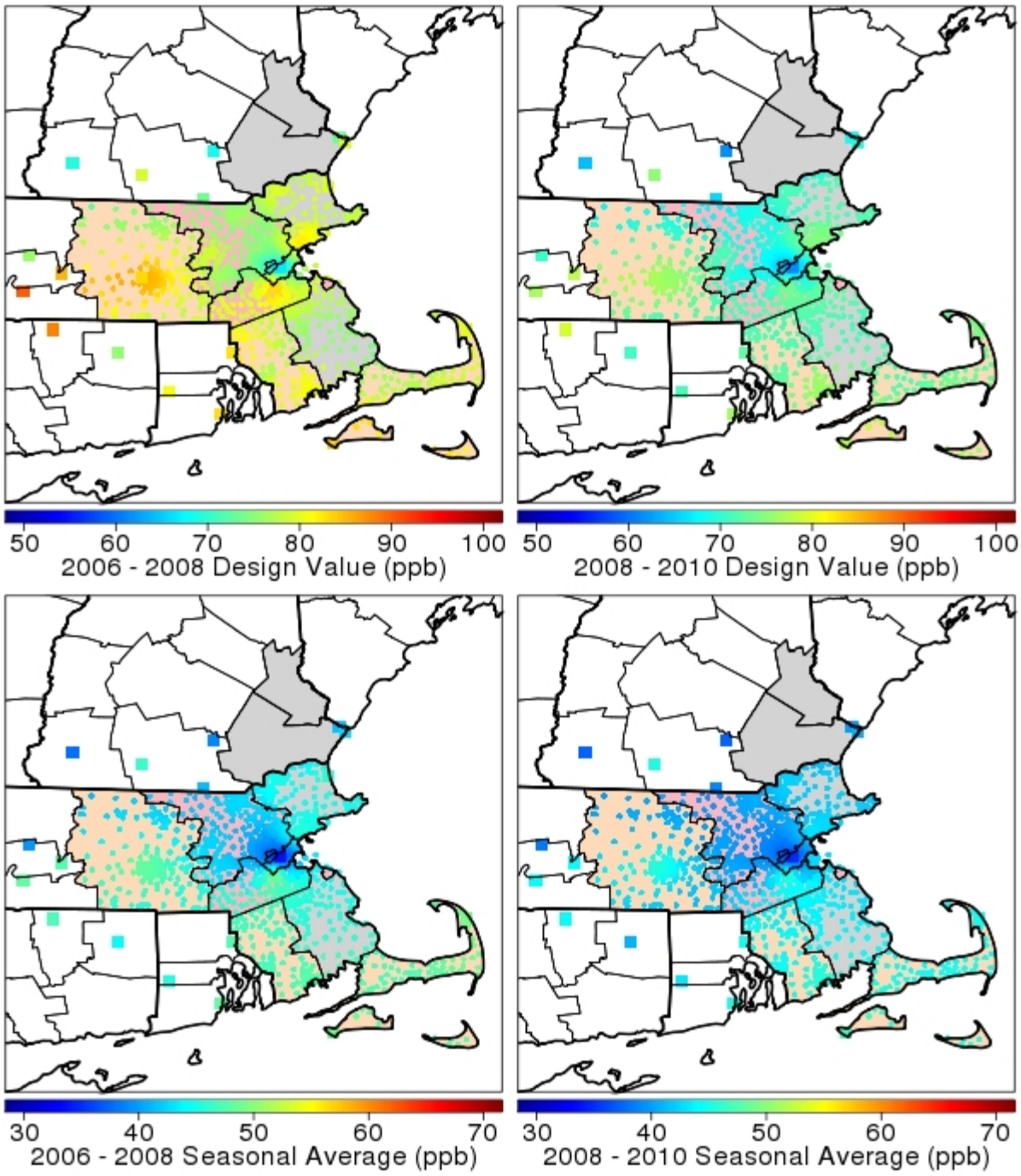


**Figure 7** **Maps of design values and May – September average MDA8 values based on VNA spatial fields for Boston.**

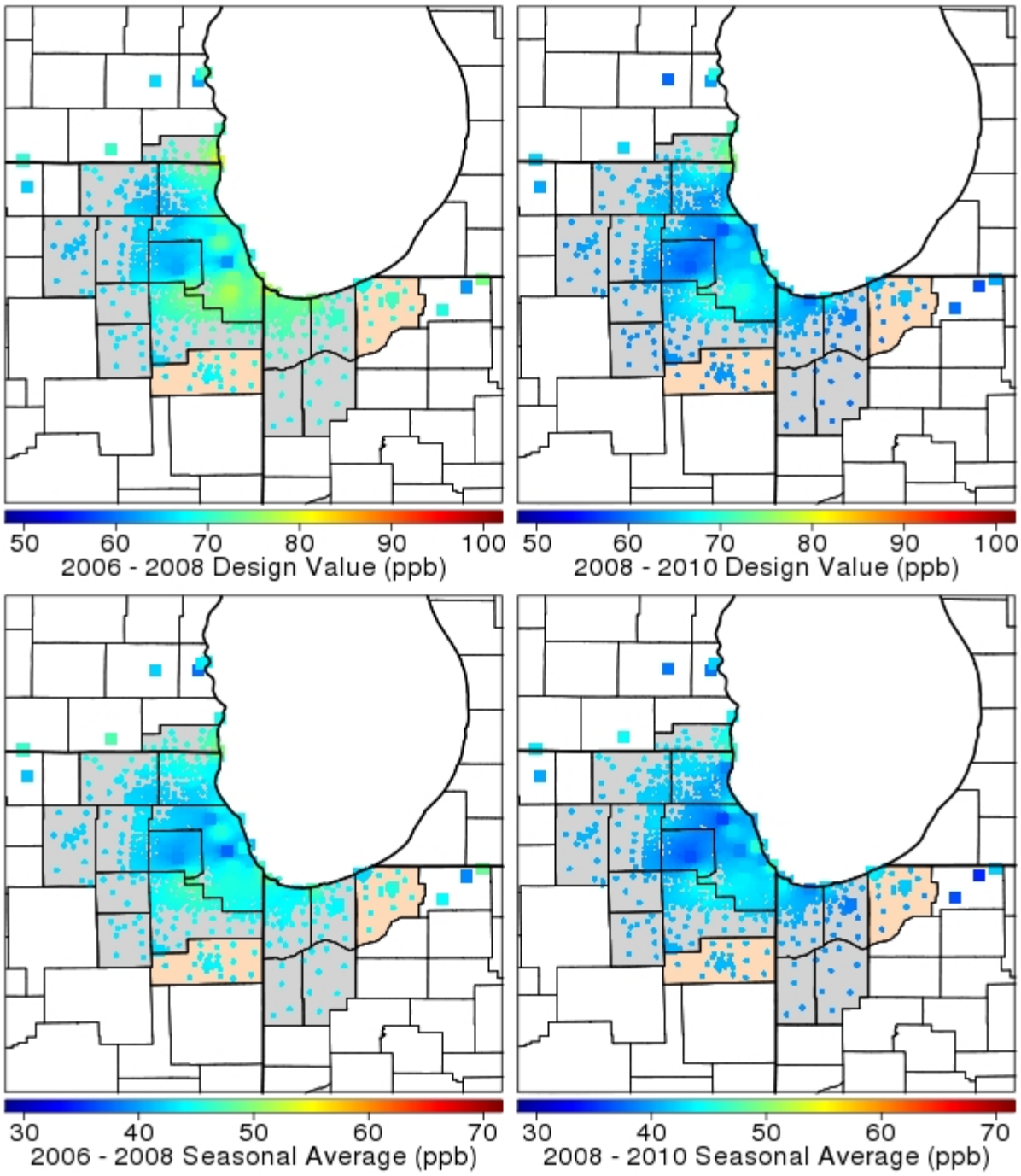


**Figure 8** **Maps of design values and May – September average MDA8 values based on VNA spatial fields for Chicago.**

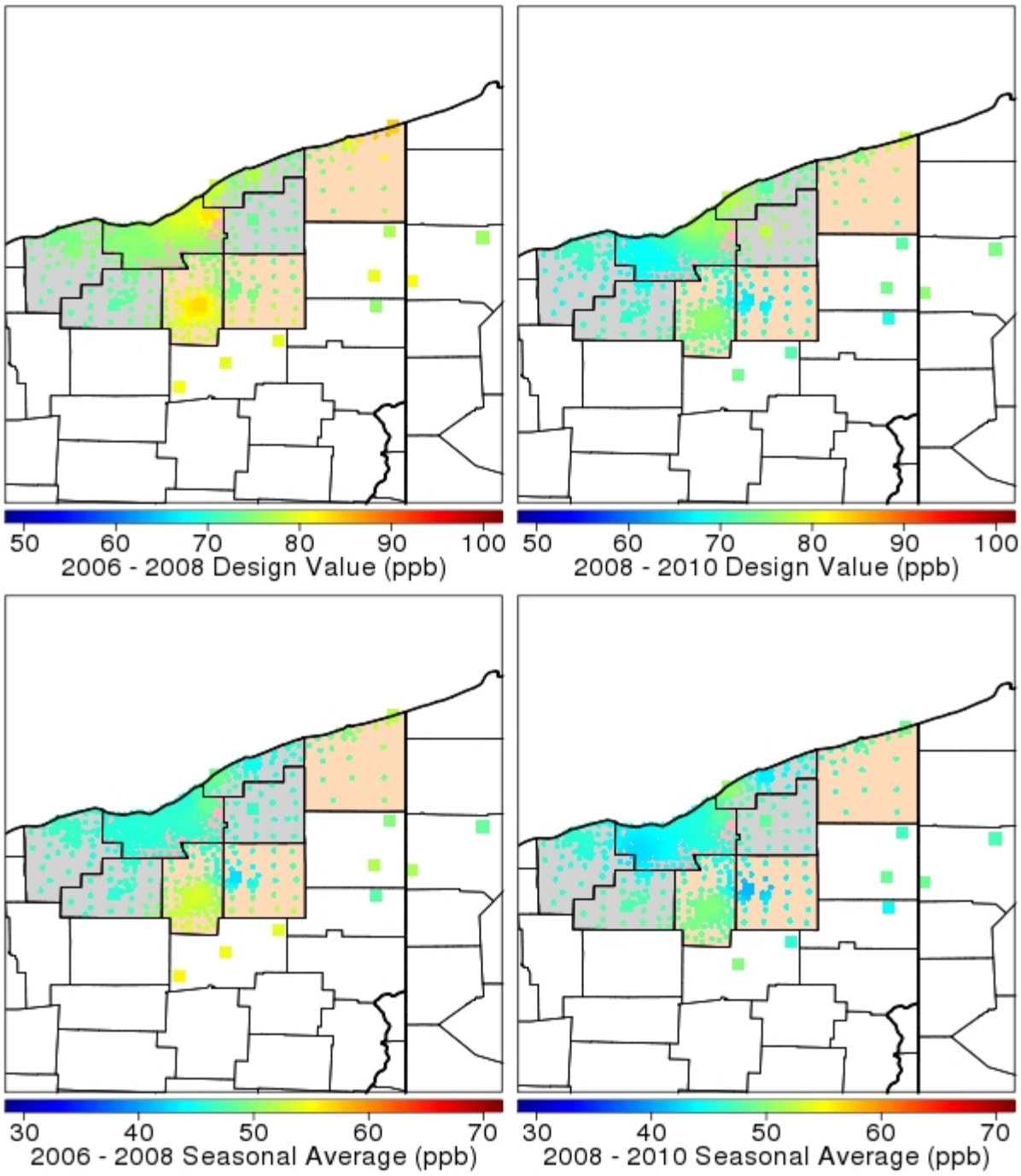


**Figure 9** **Maps of design values and May – September average MDA8 values based on VNA spatial fields for Cleveland.**

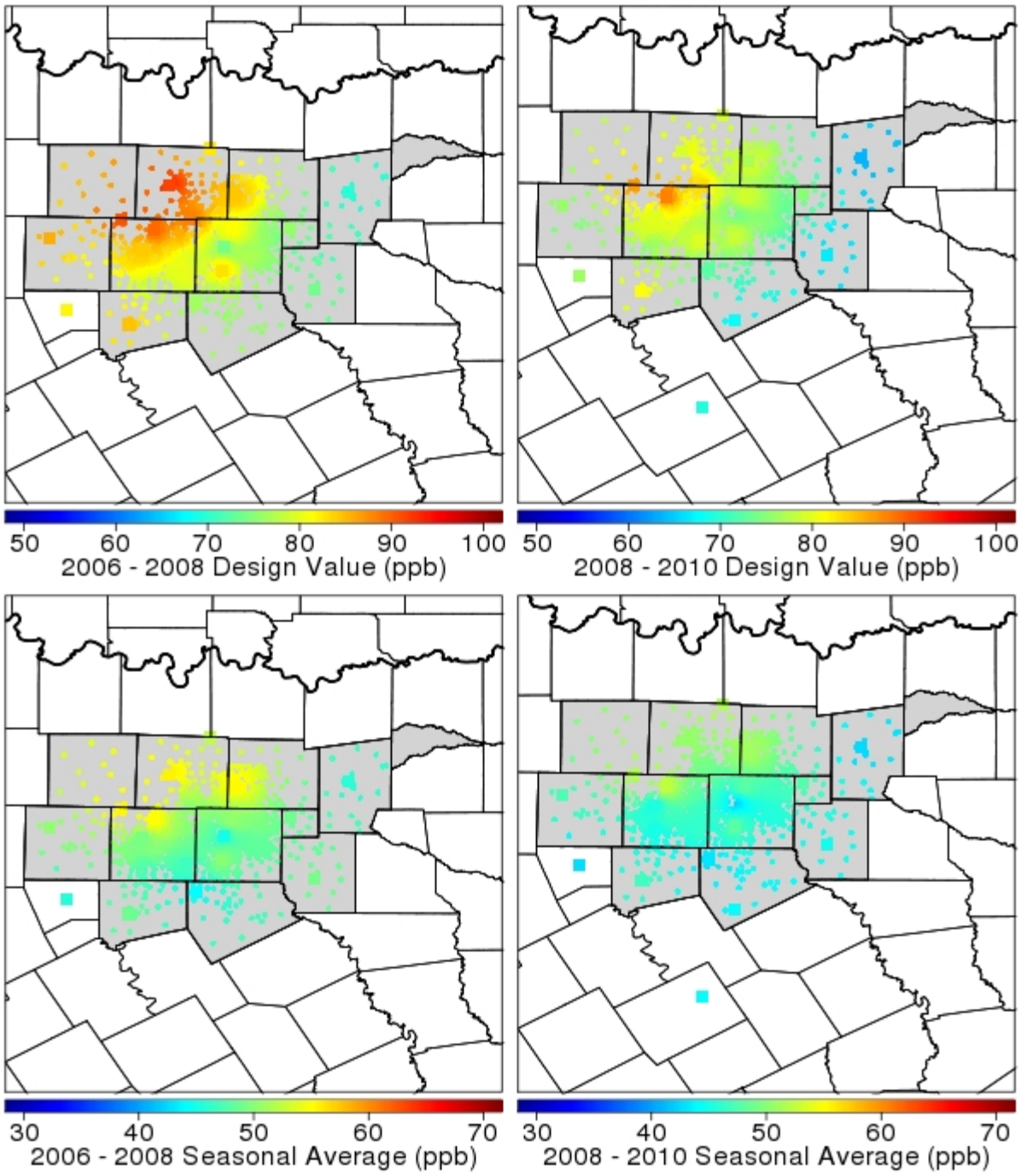


**Figure 10** **Maps of design values and May – September average MDA8 values based on VNA spatial fields for Dallas.**

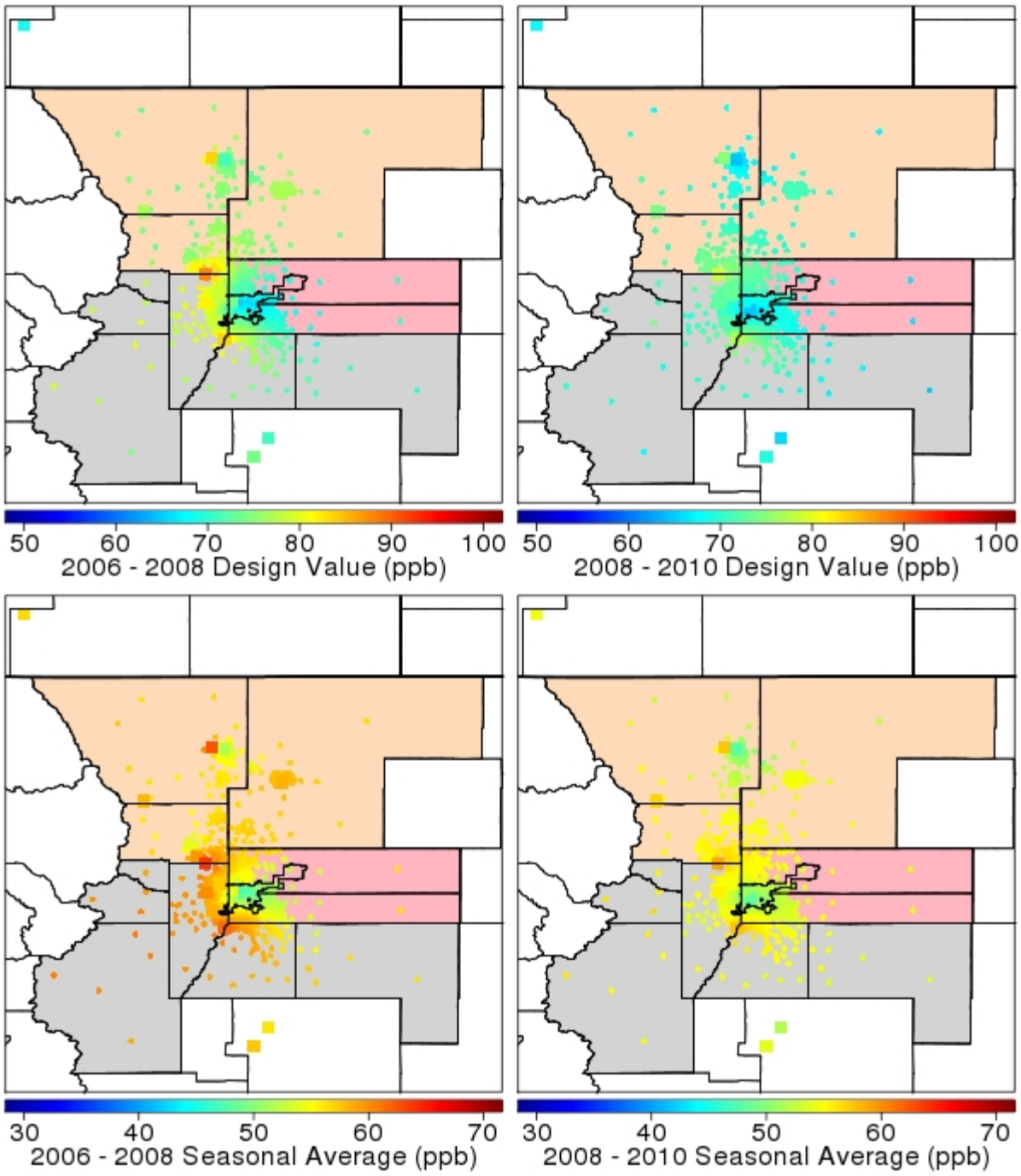


**Figure 11** **Maps of design values and May – September average MDA8 values based on VNA spatial fields for Denver.**

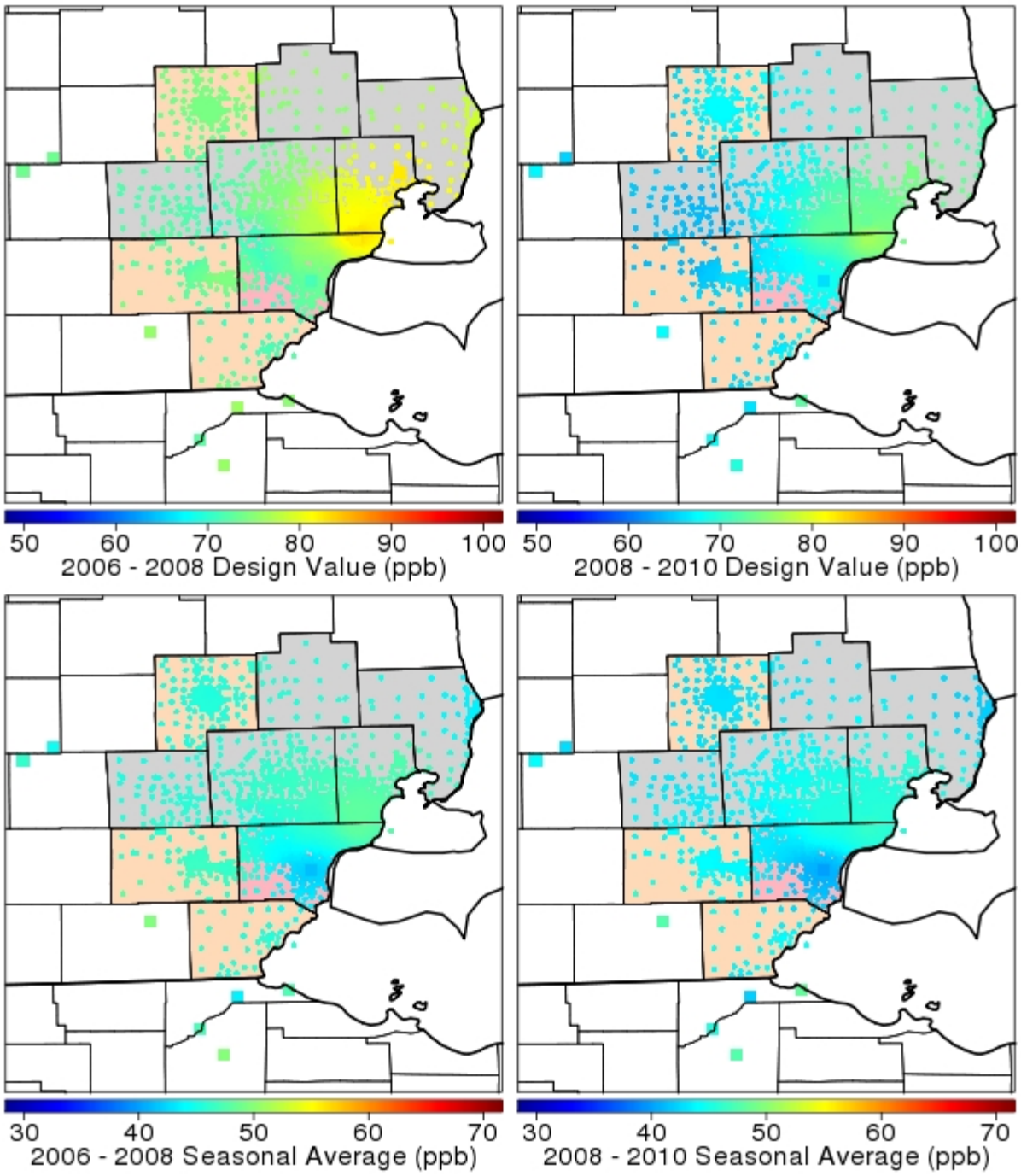


**Figure 12 Maps of design values and May – September average MDA8 values based on VNA spatial fields for Detroit.**

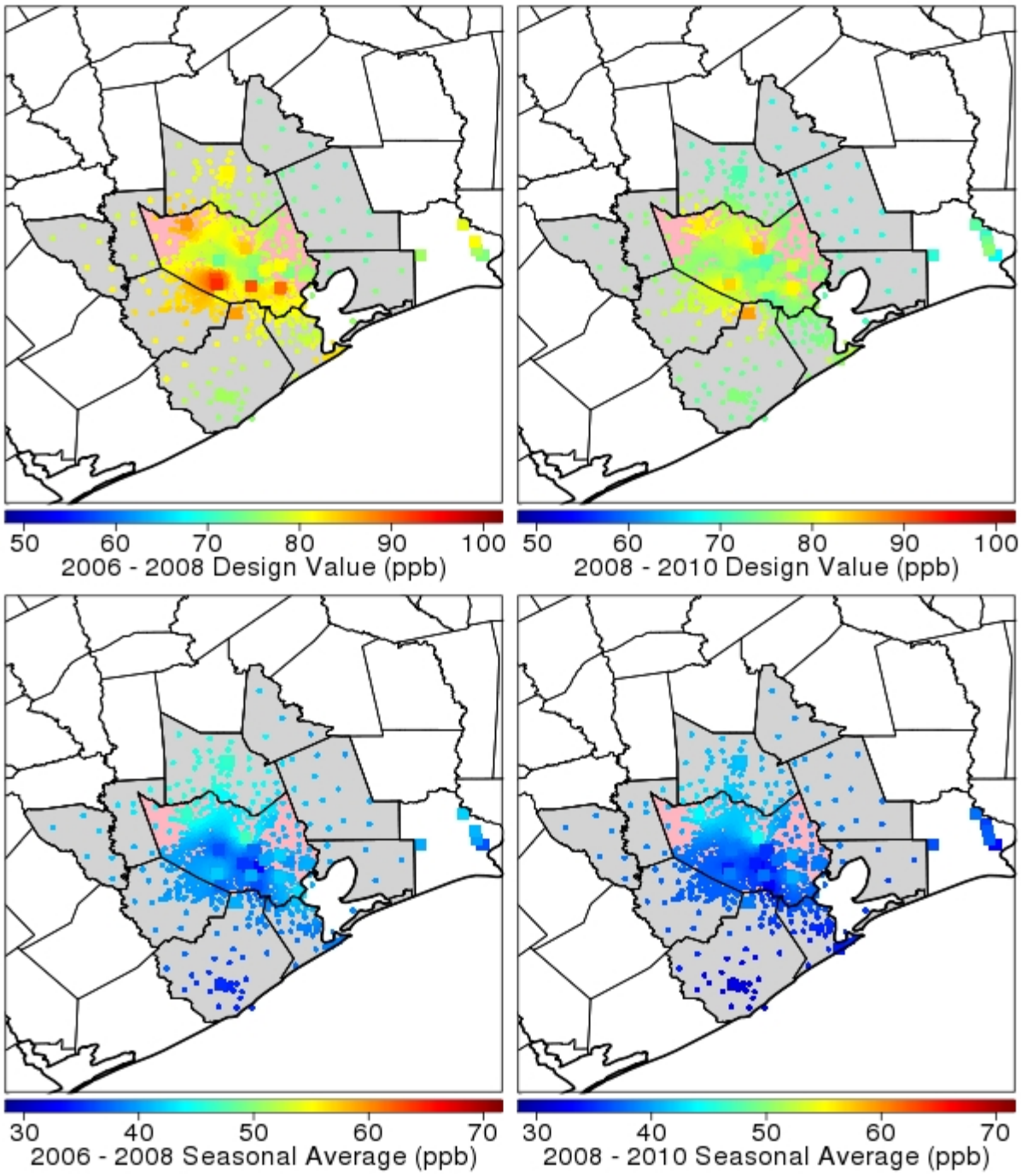


**Figure 13 Maps of design values and May – September average MDA8 values based on VNA spatial fields for Houston.**

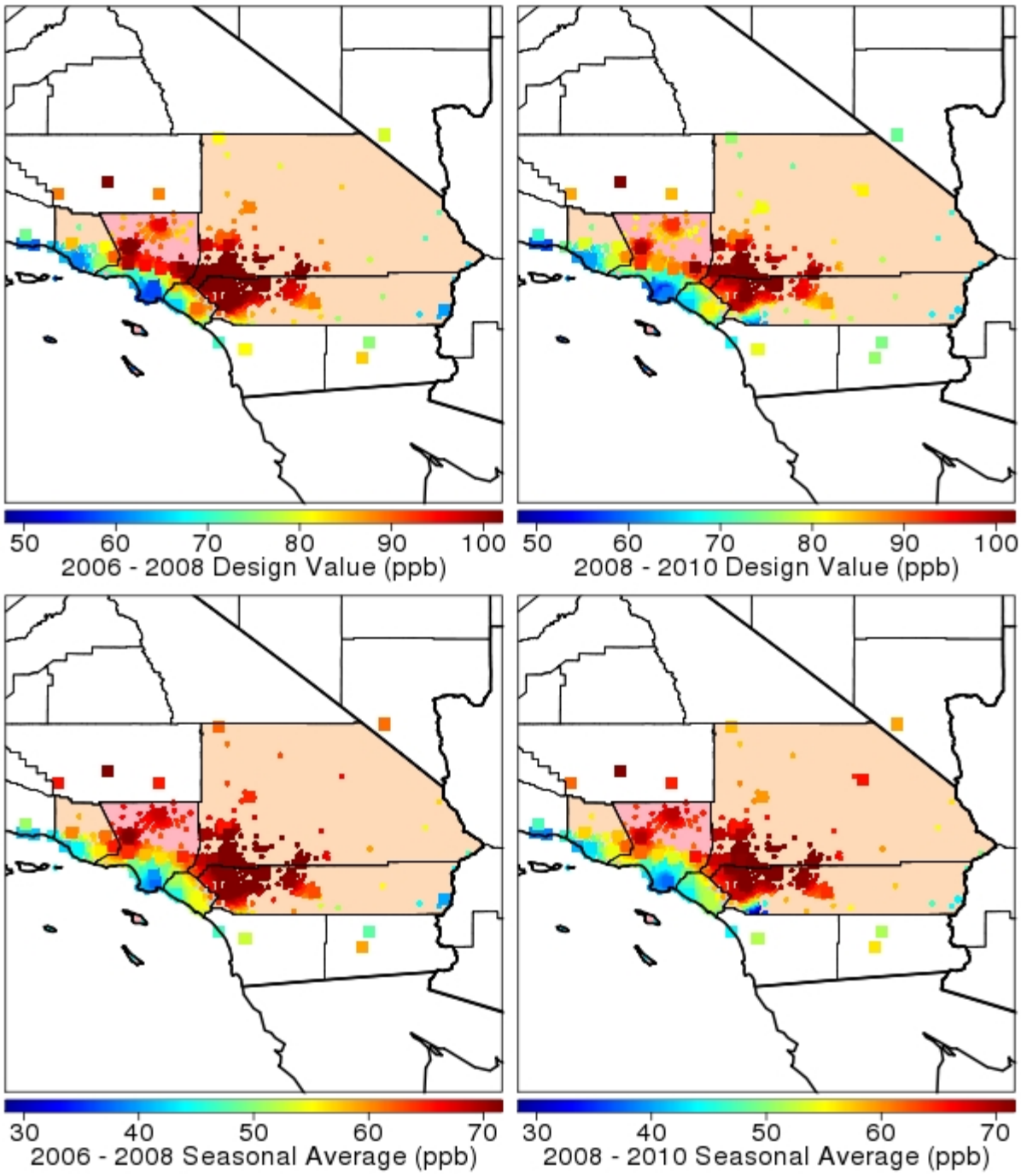


**Figure 14** **Maps of design values and May – September average MDA8 values based on VNA spatial fields for Los Angeles.**

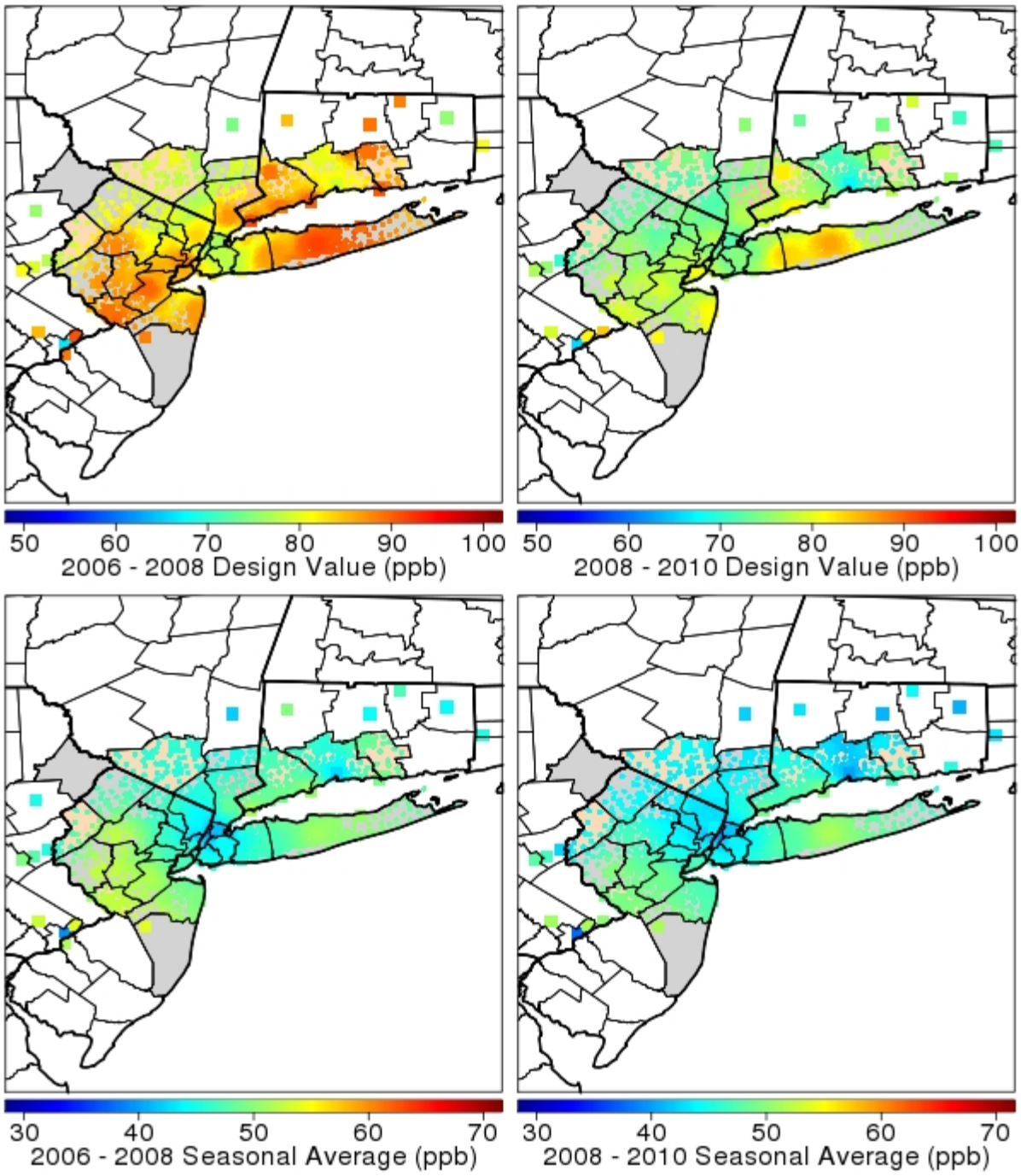


**Figure 15 Maps of design values and May – September average MDA8 values based on VNA spatial fields for New York.**

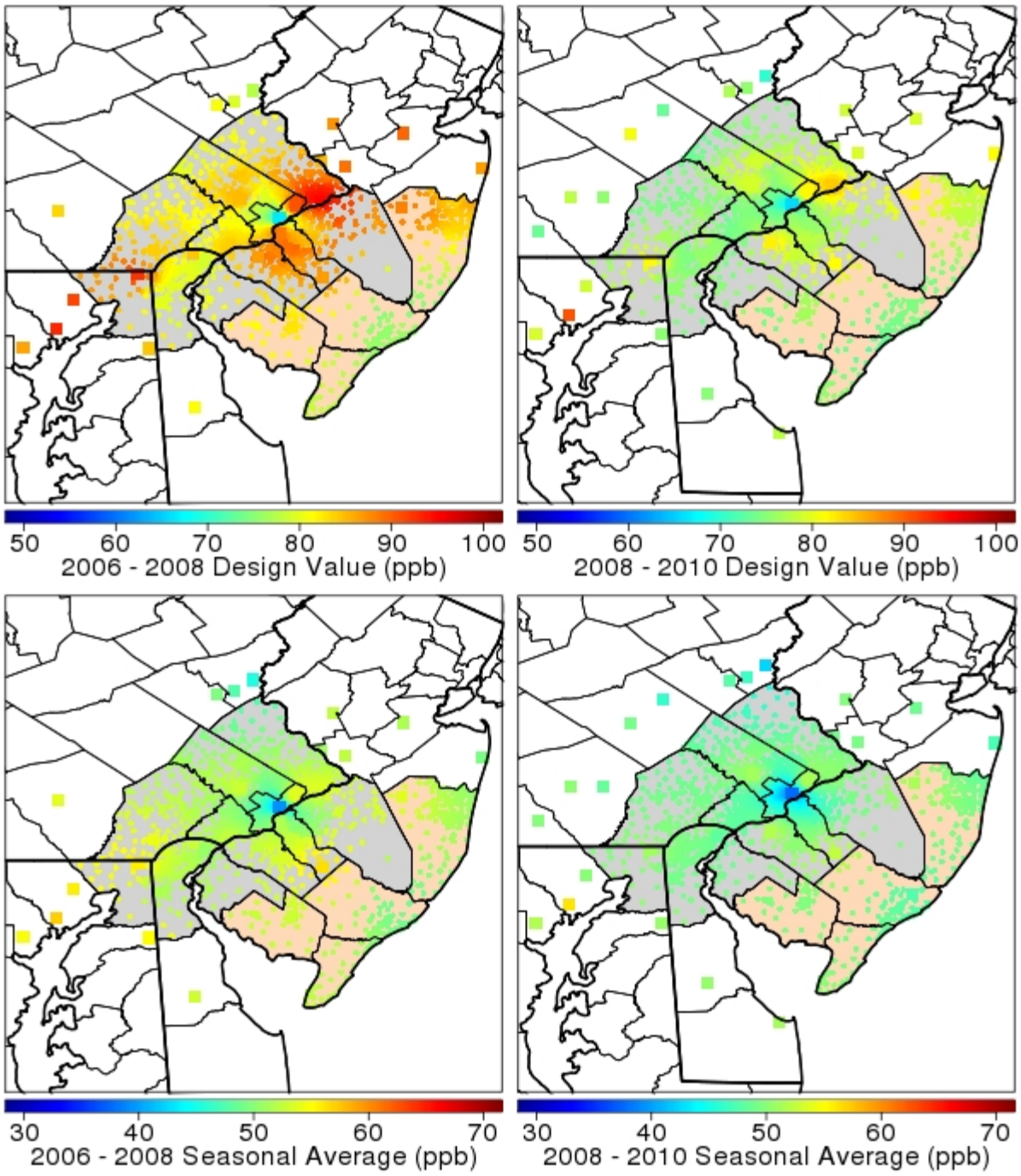


**Figure 16** **Maps of design values and May – September average MDA8 values based on VNA spatial fields for Philadelphia.**

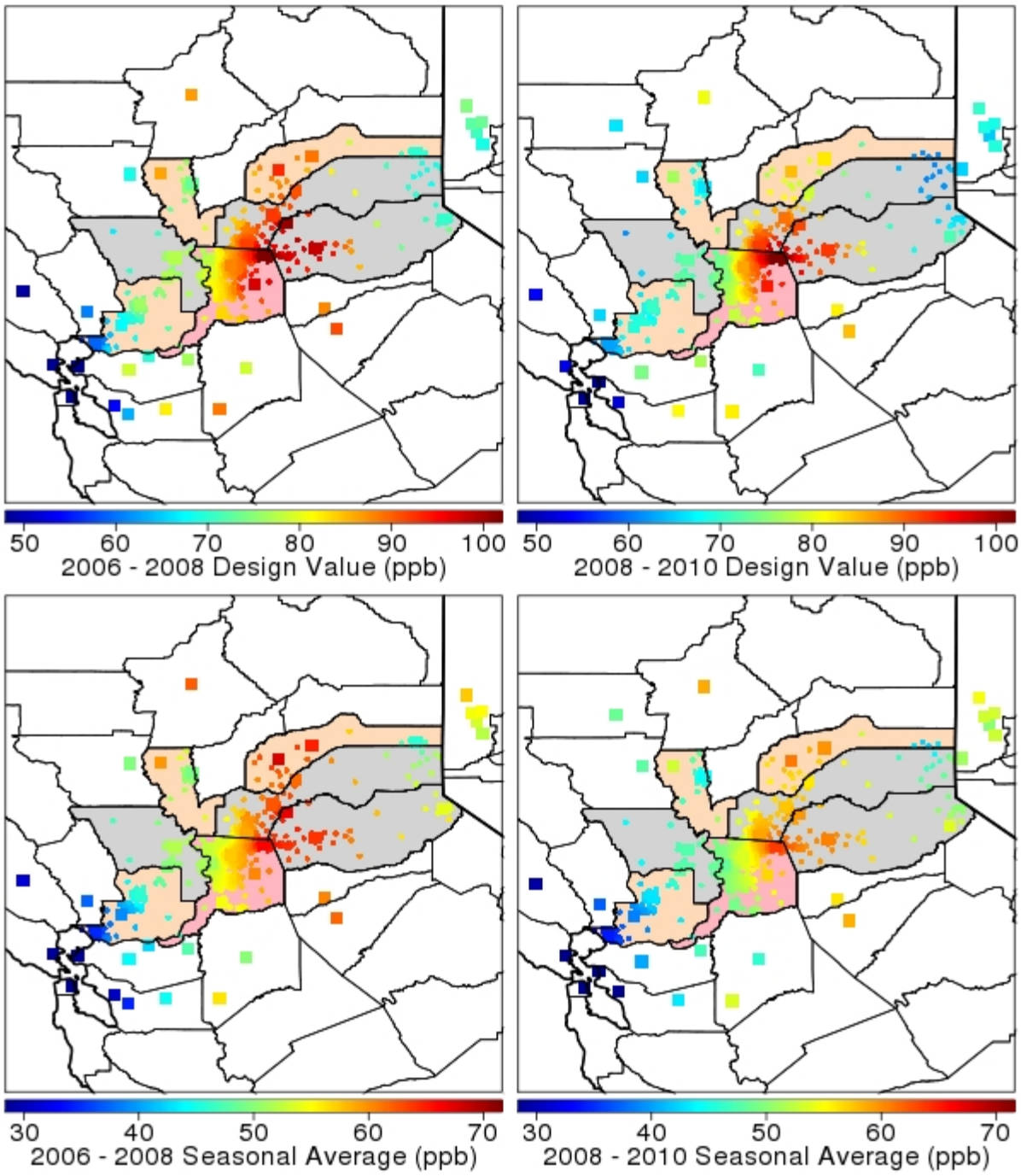


**Figure 17** **Maps of design values and May – September average MDA8 values based on VNA spatial fields for Sacramento.**

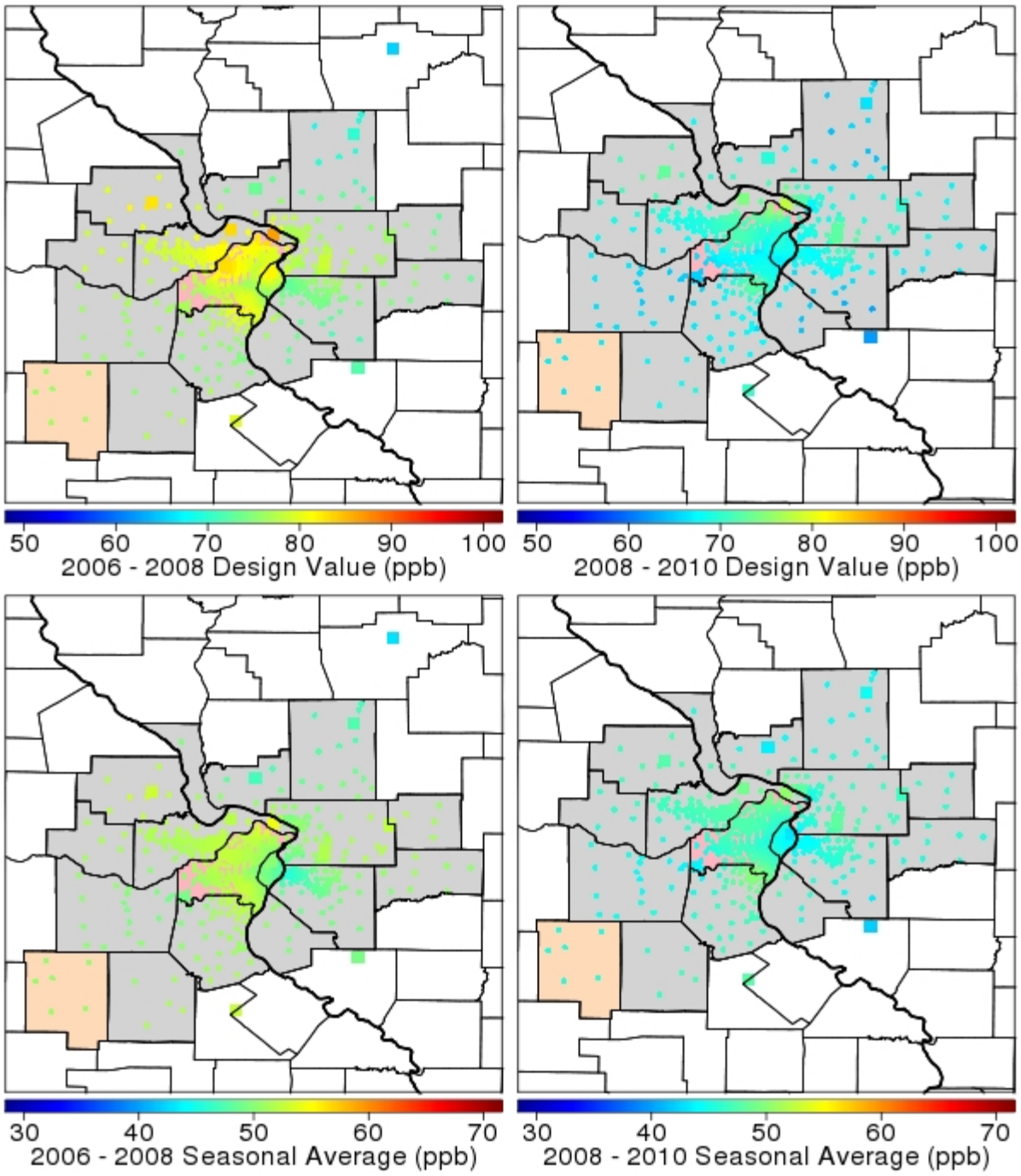


**Figure 18 Maps of design values and May – September average MDA8 values based on VNA spatial fields for St. Louis.**

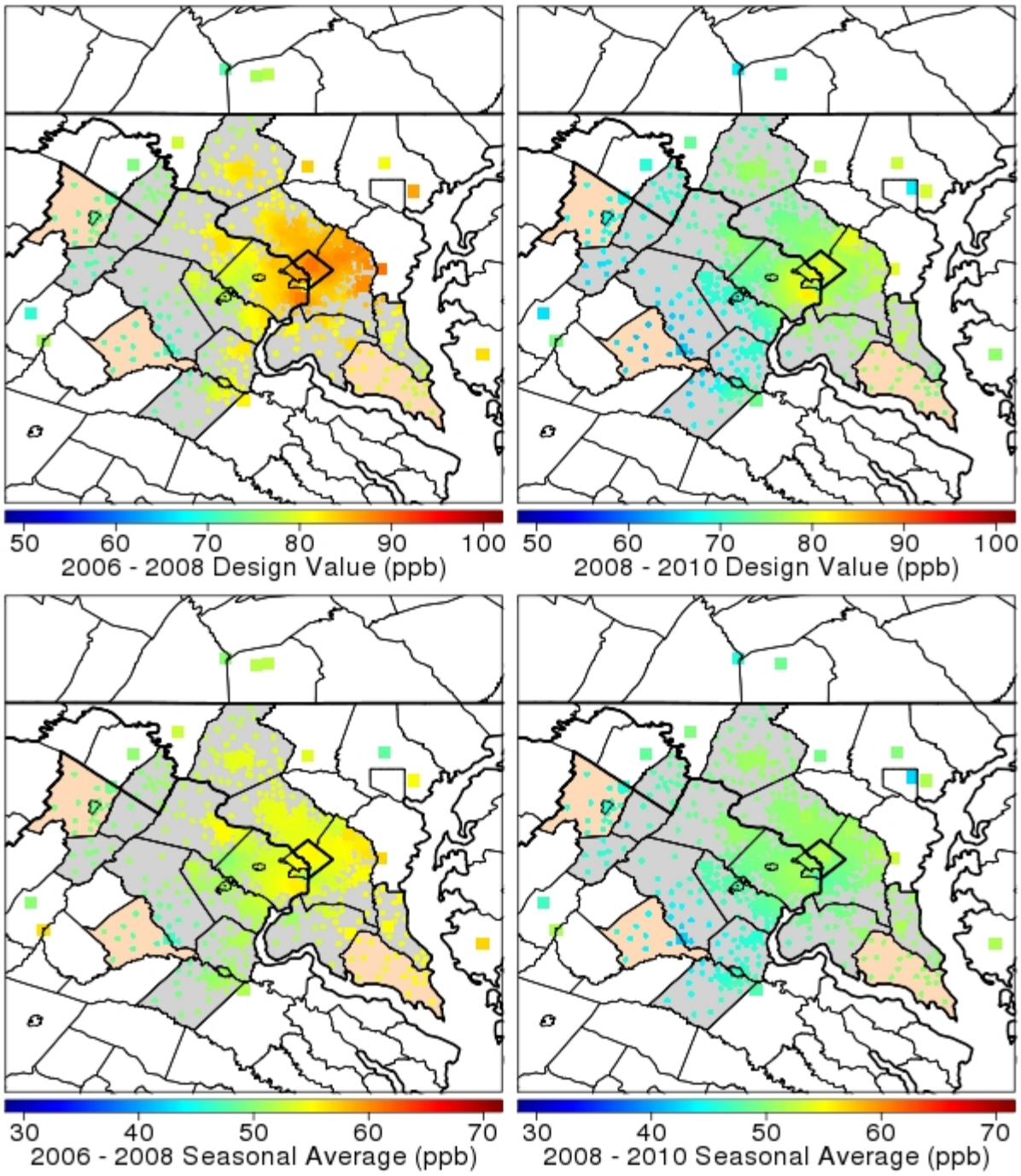


**Figure 19 Maps of design values and May – September average MDA8 values based on VNA spatial fields for Washington, D.C.**

## 2.3 EVALUATION OF AIR QUALITY SPATIAL FIELD TECHNIQUES

As mentioned previously, in the 1st draft REA the air quality spatial fields used as inputs to APEX were based on hourly $O_3$ concentrations from the nearest monitoring site, while in this draft the spatial fields were based on the VNA technique described in the previous section. This section presents

an evaluation comparing the relative accuracy of the nearest neighbor (NN) and VNA techniques for generating spatial fields of hourly $O_3$ concentrations.

The evaluations were conducted over 4km gridded domains in Atlanta, Detroit, and Philadelphia using monitored hourly $O_3$ concentrations from 2005. Due to potential discrepancies in the availability of data, only data collected within the required $O_3$ monitoring seasons for each area (March – October for Atlanta; April – September for Detroit; April – October for Philadelphia) were considered. Figure 20 below shows maps of the monitored values (AQS, left), NN values (center), and VNA values (right) in Atlanta (top) and Philadelphia (bottom) for a single selected hour in each area. These maps show an extreme example of the differences in the NN and VNA spatial fields. The NN fields (center column) have very sharp breaks between air quality monitors, while the VNA fields (right column) tend to produce much smoother surfaces. The NN fields also have a tendency to spread concentrations out over a large area if the monitoring network is sparse. For example, the highest concentration at the monitor in southern Atlanta is spread out over a large area in the NN fields, but this effect is somewhat mitigated in the VNA fields.

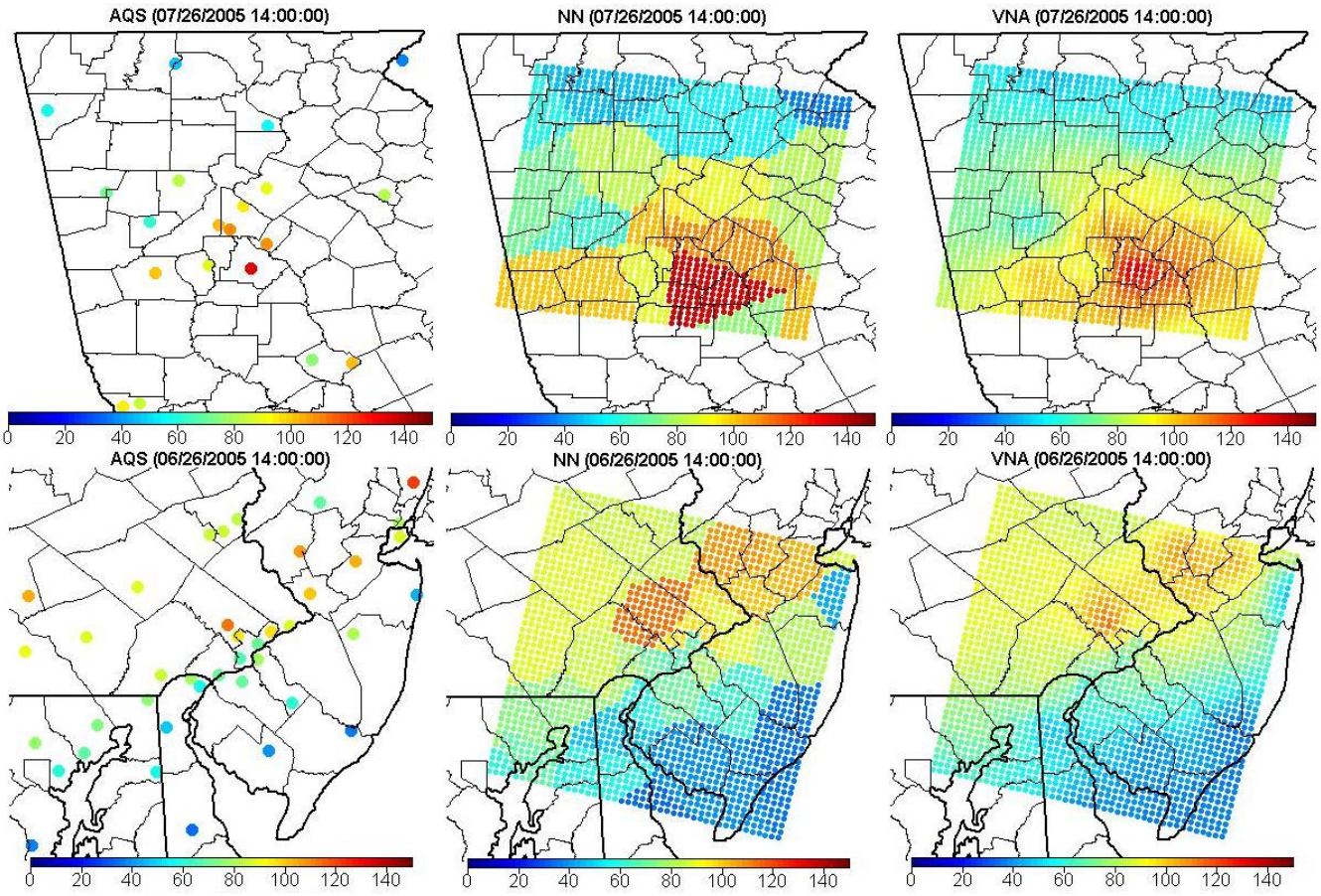


**Figure 20 Maps of monitored values (left), nearest neighbor spatial fields (center), and VNA spatial fields (right) for selected hours in Atlanta (top), and Philadelphia (bottom)**

A cross-validation analysis was performed to evaluate the relative accuracy of the estimates from these two methods. For each hour in the required $O_3$ season, the concentrations from each monitor in the 4 km gridded domain were withheld (one at a time) from the input dataset, and the concentrations from the remaining monitors were used to estimate the concentration at the monitoring site that was withheld using NN and VNA. Additional monitoring sites within a 50 km radius of the 4 km gridded domain were used in the estimates, but were not included in the set of monitors that were withheld from the analysis. The estimated values were then compared to the respective monitored concentrations that were withheld, and the relative accuracy of NN and VNA were assessed using three summary statistics: the coefficient of variation ($R^2$), the mean bias, and the root mean squared error (RMSE).

Figure 21 (Atlanta), Figure 22 (Detroit), and Figure 23 (Philadelphia) show density scatter plots and performance statistics for the NN and VNA spatial fields based on the cross-validation analysis described above for the three urban areas. Each figure shows the monitored hourly $O_3$ concentrations in ppb (AQS; x-axis) from the monitors which were withheld from the analysis, versus the respective values estimated using the NN (left panel) and VNA (right panel) techniques. In each panel, the plot region was split into 2 ppb x 2 ppb squares, with the colors indicating the number of points falling into each square. The diagonal line in each panel is a one-to-one reference line, and performance statistics for each method are included in the upper left-hand corner. High $R^2$ values, low mean bias values, and low RMSE values are indicative of good performance.

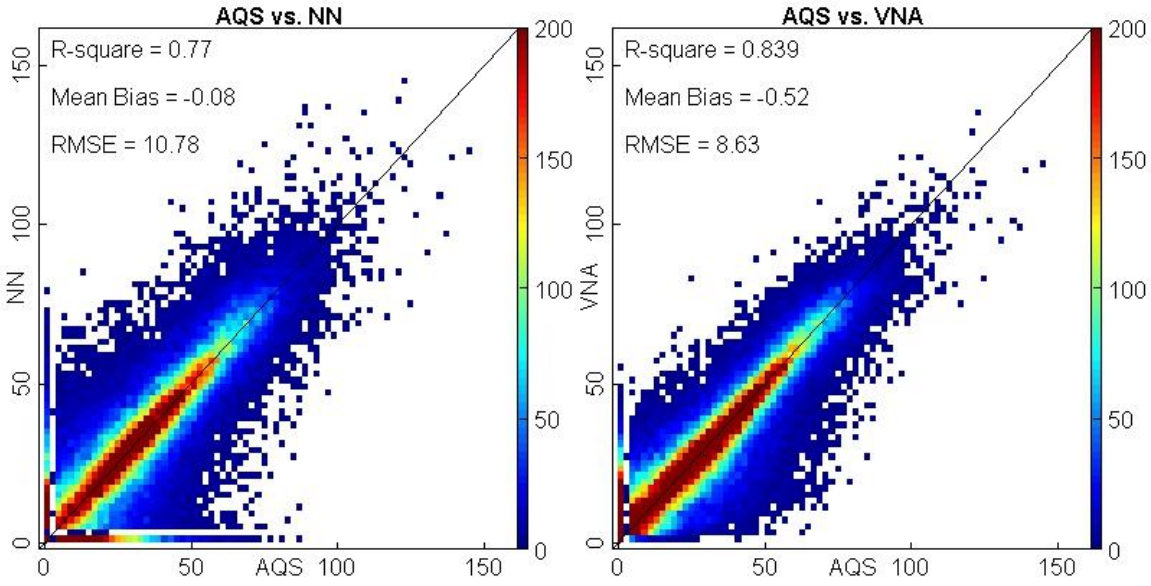


**Figure 21: Density scatter plots and performance statistics for the cross-validation analysis of nearest neighbor (NN; left) and Voronoi Neighbor Averaging (VNA; right) spatial field techniques applied to monitored hourly $O_3$ concentrations in Atlanta, 2005.**

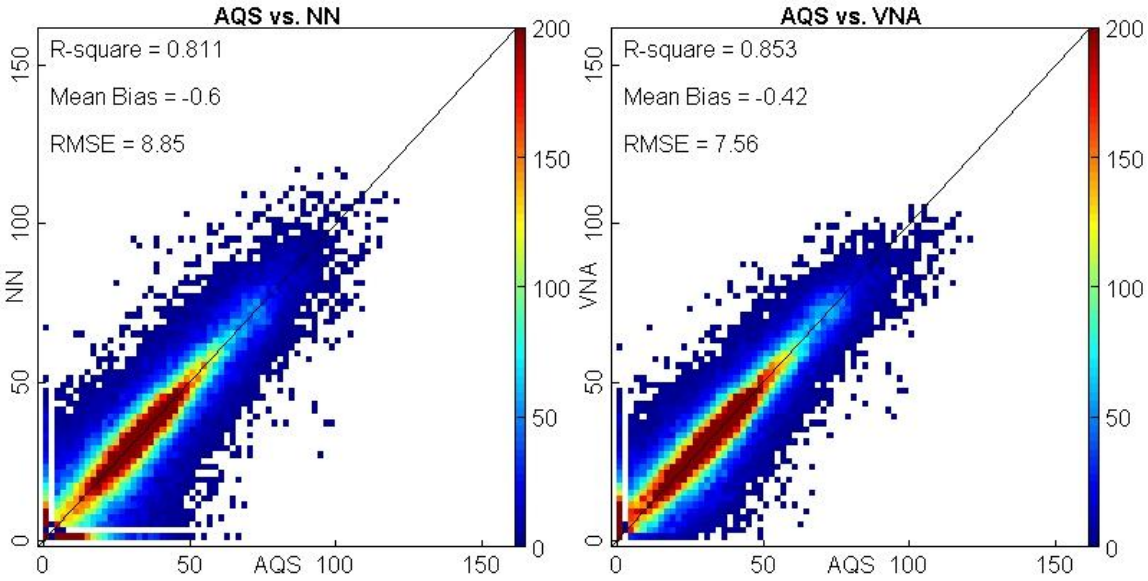


**Figure 22: Density scatter plots and performance statistics for the cross-validation analysis of nearest neighbor (NN; left) and Voronoi Neighbor Averaging (VNA; right) spatial field techniques applied to monitored hourly $O_3$ concentrations in Detroit, 2005.**

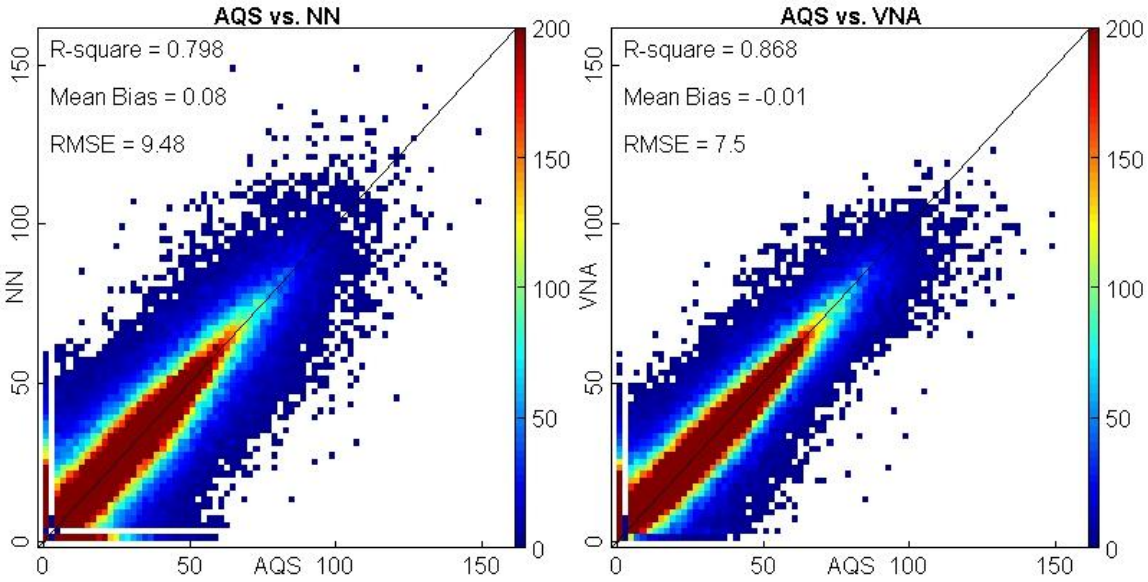


**Figure 23: Density scatter plots and performance statistics for the cross-validation analysis of nearest neighbor (NN; left) and Voronoi Neighbor Averaging (VNA; right) spatial field techniques applied to monitored hourly $O_3$ concentrations in Philadelphia, 2005.**

Both techniques had relatively low mean bias statistics in all three urban areas (< 1 ppb in all cases). However, the VNA estimates had higher $R^2$ statistics and lower RMSE statistics than the NN estimates in all three urban areas, both of which indicate that the VNA technique consistently produces more accurate estimates than NN. This is also reflected by the fact that there is generally less scatter in

the density plots based on the VNA estimates than those based on the NN estimates. From a physical perspective, the VNA technique is also more appealing since it does not produce sharp breakpoints in the estimated values between adjacent monitors when the reported concentrations are different.

# 3. AIR QUALITY INPUTS FOR THE EPIDEMIOLOGY-BASED RISK ASSESSMENT

This section describes the 12 urban case study areas for the epidemiology-based risk assessment described in Chapter 7 (Section 3.1), and the spatially averaged "composite monitor" values used as inputs to the Benefits Mapping and Analysis Program (BenMAP; Section 3.2).

## 3.1 URBAN CASE STUDY AREAS

Three distinct sets of boundaries were considered for the 12 urban case study areas in the epidemiology-based risk assessment:

1. Core Based Statistical Areas[2] ("CBSA" boundaries)
2. Area boundaries defined in the Zanobetti & Schwartz, 2008 study ("Z & S" boundaries)
3. Area boundaries defined in Smith et al, 2009 study ("Smith" boundaries)

In the 1st draft REA, the short-term mortality risk estimates were based on the concentration response functions estimated in the Zanobetti & Schwartz, 2008 study using the Z & S boundaries. In this draft, the primary set of short-term and long-term mortality risk estimates described in Chapter 7 are based on the concentration response functions estimated in the Smith et al, 2009 study using the CBSA boundaries. The other two sets of boundaries are used in sensitivity analyses. The first sensitivity analysis uses the Z&S boundaries to assess the impact of changing from the quadratic rollback method used to adjust air quality in the 1st draft REA to the HDDM adjustment method described in Chapter 4 and Appendix 4d of this draft. The second sensitivity analysis uses the Smith boundaries to assess the impact of pairing air quality information based on the CBSA boundaries with the concentration-response functions which were derived from air quality information based on the Smith boundaries.

Table 2 gives some basic information about the 12 urban case study areas in the epidemiology-based risk assessment for each set of boundaries. In general, the Z & S and Smith areas were generally smaller and more focused on the urban population centers than the CBSAs. The Z & S and Smith areas were identical in 6 of the 12 urban case study areas, and had at least one county in common for all 12 study areas. The CBSAs were typically smaller than the respective study areas described in Section 2.1 for the exposure and clinical risk assessments, with the exceptions of Baltimore, Dallas, and Houston,

[2] Core Based Statistical Areas (CBSAs) are used by the Office of Management and Budget (OMB) to group U.S. counties into urbanized areas. These groupings are updated by OMB every 5 years. The CBSAs used in the epidemiology based risk assessment are based on the OMB deliniations from 2008. For more information see: http://www.whitehouse.gov/sites/default/files/omb/assets/bulletins/b10-02.pdf

where the areas were identical. The final two columns of Table 2 show the annual 4th highest MDA8 values in ppb based on monitors within the three sets of boundaries for 2007 and 2009, the two years upon which the risk estimates in Chapter 7 are focused.

| Area Name | Boundary Definition | # of Counties | # of $O_3$ Monitors | Population (2010) | 2007 4th high (ppb) | 2009 4th high (ppb) |
|---|---|---|---|---|---|---|
| Atlanta | CBSA | 28 | 13 | 5,268,860 | 102 | 77 |
| | Z & S | 4 | 5 | 3,105,873 | 98 | 77 |
| | Smith | 2 | 3 | 1,612,474 | 98 | 77 |
| Baltimore | CBSA | 7 | 7 | 2,710,489 | 92 | 83 |
| | Z & S | 2 | 3 | 1,425,990 | 83 | 71 |
| | Smith | 1 | 1 | 620,961 | 73 | 66 |
| Boston | CBSA | 7 | 11 | 4,552,402 | 89 | 75 |
| | Z & S | 3 | 5 | 2,895,958 | 88 | 75 |
| | Smith | 1 | 2 | 722,023 | 72 | 75 |
| Cleveland | CBSA | 5 | 10 | 2,077,240 | 83 | 72 |
| | Z & S | 1 | 4 | 1,280,122 | 83 | 71 |
| | Smith | 1 | 4 | 1,280,122 | 83 | 71 |
| Denver | CBSA | 10 | 16 | 2,543,482 | 97 | 79 |
| | Z & S | 1 | 3 | 600,158 | 76 | 63 |
| | Smith | 3 | 6 | 1,613,764 | 76 | 72 |
| Detroit | CBSA | 6 | 8 | 4,296,250 | 93 | 73 |
| | Z & S | 1 | 4 | 1,820,584 | 92 | 73 |
| | Smith | 1 | 4 | 1,820,584 | 92 | 73 |
| Houston | CBSA | 10 | 22 | 5,946,800 | 90 | 91 |
| | Z & S | 1 | 17 | 4,092,459 | 90 | 86 |
| | Smith | 1 | 17 | 4,092,459 | 90 | 86 |
| Los Angeles | CBSA | 2 | 21 | 12,828,837 | 105 | 108 |
| | Z & S | 1 | 17 | 9,818,605 | 105 | 108 |
| | Smith | 1 | 17 | 9,818,605 | 105 | 108 |
| New York | CBSA | 23 | 22 | 18,897,109 | 94 | 81 |
| | Z & S | 5 | 6 | 8,175,133 | 83 | 78 |
| | Smith | 6 | 7 | 9,124,246 | 94 | 78 |
| Philadelphia | CBSA | 11 | 15 | 5,965,343 | 102 | 74 |
| | Z & S | 1 | 4 | 1,526,006 | 95 | 72 |
| | Smith | 1 | 4 | 1,526,006 | 95 | 72 |
| Sacramento | CBSA | 4 | 17 | 2,149,127 | 93 | 96 |
| | Z & S | 1 | 8 | 1,418,788 | 90 | 96 |
| | Smith | 1 | 8 | 1,418,788 | 90 | 96 |
| St. Louis | CBSA | 16 | 17 | 2,812,896 | 94 | 74 |
| | Z & S | 2 | 5 | 1,318,248 | 94 | 70 |
| | Smith | 1 | 2 | 319,294 | 91 | 65 |

**Table 2 Information on the 12 Urban Case Study Areas in the Epidemiology Based Risk Assessment**

Since $O_3$ is not emitted directly but formed indirectly through photochemical reactions, precursor emissions may continue to react and form $O_3$ downwind of emissions sources, and thus the highest $O_3$ concentrations are often measured downwind of the highest concentration of precursor emissions in the urban population center. This phenomenon is reflected in Table 2, where the highest monitored value in the CBSA occurs outside of the Smith boundaries in 9 of 12 areas in 2007, and in 7 of 12 areas in 2009. In addition, there were some instances where the highest monitored $O_3$ concentrations occurred outside of the CBSAs, but within the respective study areas used in the exposure and clinical risk assessments, which were designed to always include the monitor associated with the highest area-wide design value. For example, in Los Angeles, the CBSA includes Los Angeles County, CA and Orange County, CA, but the highest $O_3$ concentrations are typically measured further downwind in Riverside County, CA and San Bernardino County, CA.

## 3.2 AIR QUALITY INPUTS TO THE BENEFITS MAPPING AND ANALYSIS PROGRAM (BENMAP)

The air quality monitoring data used as inputs to the Benefits Mapping and Analysis Program (BenMAP) were daily time-series of spatially averaged "composite monitor" values for the 12 urban case study areas based on monitored air quality data. These composite monitor values were calculated by taking hour-by-hour spatial averages of the hourly $O_3$ concentrations for all monitors within a given study area, then calculating the four daily metrics described in Section 1.3:

1. Daily Maximum 8-hour Average (MDA8) Concentration
2. Daily 10:00 AM – 6:00 PM Mean Concentration
3. Daily Maximum 1-hour Concentration
4. Daily 24-hour Average Concentration

These four daily metrics were calculated based on each of the three sets of urban case study area boundaries listed in the previous section, for a total of 12 daily metric/area boundary combinations. Although these 12 values were provided based on available monitoring data for each day in the 2006-2010 period, only a subset of these data were used for the air quality inputs to BenMAP. Since the BenMAP software is designed to run for only one year at a time, we chose to focus on air quality data from 2007 and 2009. In most cases, the 2007 data was meant to represent a year with high $O_3$ levels, while 2009 was meant to represent a year with low $O_3$ levels. In some areas, the data were also subset to a particular "$O_3$ season", either to match the period used in the respective epidemiology study, or to avoid the potential disparity in data availability which could arise if the air quality data included months outside of the required $O_3$ monitoring season. Appendix 4d contains "box and whisker" plots showing the distribution of composite monitor values in each area for current air quality, air quality adjusted to meet the existing $O_3$ standard, and air quality adjusted to meet the potential alternative standards of 70

ppb, 65 ppb, and 60 ppb. These plots are stratified to show the effects of varying spatial extents (CBSAs vs. Z & S areas), $O_3$ season lengths (June – August vs. April – October), and years (2007 vs. 2009).

Table 3 gives a list of the air quality inputs to the various BenMAP outputs discussed in Chapter 7, including the health endpoints modeled, the epidemiology studies from which the concentration-response functions were derived, which urban case study areas were modeled, which air quality metrics were used, which $O_3$ season was modeled, and which set of boundaries were used in calculating the composite monitor values. Rows shaded pink represent air quality inputs used in primary risk estimates, while rows shaded blue represent air quality inputs for risk estimates included as sensitivity analyses.

| Health Endpoint | Epidemiology Study | Urban Case Study Area(s) | Air Quality Metric | $O_3$ Season | Study Area Boundaries |
|---|---|---|---|---|---|
| Emergency Room Visits, Respiratory | Darrow et al, 2011 | Atlanta, GA | MDA8 | March - October | CBSA |
| Asthma Exacerbation, Wheeze | Gent et al, 2003 | Boston, MA | 1-Hour Max | April - September | CBSA |
| Asthma Exacerbation, Wheeze | Gent et al, 2004 | Boston, MA | MDA8 | April - September | CBSA |
| Emergency Room Visits, Asthma | Ito et al, 2007 | New York, NY | MDA8 | April - September | CBSA |
| Mortality, Long-Term (Total and Respiratory) | Jerrett et al, 2009 | all 12 areas | Seasonal Average[3] | April - September | CBSA |
| Hospital Admissions, All Respiratory | Katsouyanni et al, 2009 | Detroit, MI | 1-Hour Max | June - August | CBSA |
| Hospital Admissions, All Respiratory | Lin et al, 2000 | Los Angeles, CA | 24-Hour Average | June - August | CBSA |
| Hospital Admissions, Chronic Lung Disease | Lin et al, 2008 | New York, NY | 1-Hour Max | April - October | CBSA |
| Hospital Admissions, Chronic Lung Disease | Medina-Ramon et al, 2006 | all 12 areas | MDA8 | May - September | CBSA |
| Hospital Admissions, Asthma | Silverman and Ito, 2010 | New York, NY | MDA8 | April - August | CBSA |
| Mortality, Non-Accidental | Smith et al, 2009 | all 12 areas | MDA8 | Required $O_3$ season | CBSA |
| Mortality, Non-Accidental | Smith et al, 2009 | all 12 areas | MDA8 | April - October | CBSA |
| Mortality, Non-Accidental | Smith et al, 2009 | all 12 areas | MDA8 | June - August | CBSA |
| Mortality, Non-Accidental | Smith et al, 2009 | all 12 areas | MDA8 | Required $O_3$ season | Smith |
| Emergency Room Visits, Respiratory | Strickland et al, 2010 | Atlanta, GA | MDA8 | May - October | CBSA |
| Emergency Room Visits, Respiratory | Tolbert et al, 2007 | Atlanta, GA | MDA8 | March - October | CBSA |
| Mortality, All Cause | Zanobetti and Schwartz, 2008 | all 12 areas | 10AM-6PM Mean | June - August | CBSA |
| Mortality, All Cause | Zanobetti and Schwartz, 2008 | all 12 areas | 10AM-6PM Mean | June - August | Z & S |

**Table 3 Summary of the air quality inputs to BenMAP**

[3] For the Jerrett et al, 2009 long-term mortality study, the air quality inputs were based on an annual metric instead of a daily metric. The annual metric was the April – September average of the daily maximum 1-hour concentrations.

# 4. REFERENCES


Abt Associates, Inc. (2010). Environmental Benefits and Mapping Program (Version 4.0). Bethesda, MD. Prepared for U.S. Environmental Protection Agency, Office of Air Quality Planning and Standards, Research Triangle Park, NC. Available on the Internet at: http://www.epa.gov/air/benmap.

Bell, M.L., McDermott, A., Zeger S.L., Samet, J.M., Dominici, F. (2004). Ozone and Short-Term Mortality in 95 U.S. Urban Communities, 1987-2000. Journal of the Air and Waste Management Association, 292:2372-2378.

Chen, J., Zhao, R., Li, Z. (2004). Voronoi-based k-order Neighbor Relations for Spatial Analysis. Journal of Photogrammetry and Remote Sensing, 59(1-2), 60-72.

Gold, C. (1997). Voronoi methods in GIS. In: Algorithmic Foundation of Geographic Information Systems (va Kereveld M., Nievergelt, J., Roos, T., Widmayer, P., eds). Lecture Notes in Computer Sicnece, Vol 1340. Berlin: Springer-Verlag, 21-35.

Jerrett, M., Burnett, R.T., Pope III C.A., Ito, K., Thurston, G., Krewski, D., Shi, Y., Calle, E., Thun, M. (2009). Long-Term $O_3$ Exposure and Mortality. New England Journal of Medicine, 360:1085-1095.

R Core Team (2012). R: A language and environment for statistical computing. R Foundation for Statistical Computing, Vienna, Austria. http://www.R-project.org/.

Smith, R.L.; Xu, B., Switzer, P. (2009). Reassessing the Relationship between Ozone and Short-Term Mortality in 95 U.S. Urban Communities. Inhalation Toxicology, 21: 37-61.

Turner, R. (2012). deldir: Delaunay Triangulation and Dirichlet (Voronoi) Tessellation. R package version 0.0-19. http://CRAN.R-project.org/package=deldir

U.S. Environmental Protection Agency. (2012a). Integrated Science Assessment for Ozone and Related Photochemical Oxidants: Final Report. U.S. Environmental Protection Agency, Research Triangle Park, NC. EPA/600/R-10/076C. Available on the Internet at: http://www.epa.gov/ttn/naaqs/standards/ozone/s_o3_2008_isa.html

U.S. Environmental Protection Agency. (2012b). Health Risk and Exposure Assessment for Ozone, First External Review Draft. U.S. Environmental Protection Agency, Research Triangle Park, NC. EPA/600/R-10/076C. Available on the Internet at: http://www.epa.gov/ttn/naaqs/standards/ozone/s_o3_2008_rea.html

U.S. Environmental Protection Agency. (2012c). Total Risk Integrated Methodology (TRIM) - Air Pollutants Exposure Model (APEX) Documentation (TRIM-Expo / APEX, Version 4.4). Available on the Internet at: http://www.epa.gov/ttn/fera/human_apex.html

Wells, B., Wesson, K., Jenkins, S. (2012). Analysis of Recent U.S. Ozone Air Quality Data to Support the $O_3$ NAAQS Review and Quadratic Rollback Simulations to Support the First Draft of the Risk and Exposure Assessment. Available on the Internet at: http://www.epa.gov/ttn/naaqs/standards/ozone/s_o3_td.html

Zanobetti, A., and J. Schwartz (2008). Mortality Displacement in the Association of Ozone with Mortality: An Analysis of 48 Cities in the United States. American Journal of Respiratory and Critical Care Medicine, 177:184-189.

# Appendix 4-B
# Modeling Technical Support Document for the 2013 Ozone Risk and Exposure Assessment

## Table of Contents


Model set-up and simulation ..... 1

Model domain 1

Model time period ..... 3

Model inputs: meteorology ..... 3

Model inputs: emissions ..... 5

Model inputs: Boundary conditions ..... 7

Model inputs: Initial conditions ..... 7

Evaluation of modeled ozone concentrations ..... 7

Operational Evaluation in the Northeast U.S. ..... 9

Operational Evaluation in the Southeast U.S. ..... 27

Operational Evaluation in the Midwest ..... 34

Operational Evaluation in the Central U.S. ..... 46

Operational Evaluation in the Western U.S. ..... 59

References 72


## Table of Figures


FIGURE 1: MAP OF THE CMAQ MODELING DOMAIN. ..... 2

FIGURE 2: MAP OF NORMALIZED MEAN BIAS FOR MDA8 OZONE CONCENTRATIONS IN THE NORTHEASTERN US FOR WINTER MONTHS IN 2007. ..... 11

FIGURE 3: MAP OF NORMALIZED MEAN BIAS FOR MDA8 OZONE CONCENTRATIONS IN THE NORTHEASTERN US FOR SPRING MONTHS IN 2007. ..... 12

FIGURE 4: MAP OF NORMALIZED MEAN BIAS FOR MDA8 OZONE CONCENTRATIONS IN THE NORTHEASTERN US FOR SUMMER MONTHS IN 2007. ..... 13

FIGURE 5: MAP OF NORMALIZED MEAN BIAS FOR MDA8 OZONE CONCENTRATIONS IN THE NORTHEASTERN US FOR FALL MONTHS IN 2007. ..... 14

FIGURE 6: TIME SERIES OF MODEL PERFORMANCE FOR 8-HR DAILY MAXIMUM OZONE CONCENTRATIONS AT BOSTON MONITORING SITES FOR APRIL-OCTOBER 2007. OBSERVED VALUES SHOWN IN BLACK AND MODELED VALUES SHOWN IN RED..... 15
FIGURE 7: TIME SERIES OF MODEL PERFORMANCE FOR HOURLY OZONE CONCENTRATIONS AT BOSTON MONITORING SITES FOR JANUARY 2007. OBSERVED VALUES SHOWN IN BLACK AND MODELED VALUES SHOWN IN RED. ..... 15
FIGURE 8: TIME SERIES OF MODEL PERFORMANCE FOR HOURLY OZONE CONCENTRATIONS AT BOSTON MONITORING SITES FOR APRIL 2007. OBSERVED VALUES SHOWN IN BLACK AND MODELED VALUES SHOWN IN RED. ..... 16
FIGURE 9: TIME SERIES OF MODEL PERFORMANCE FOR HOURLY OZONE CONCENTRATIONS AT BOSTON MONITORING SITES FOR JULY 2007. OBSERVED VALUES SHOWN IN BLACK AND MODELED VALUES SHOWN IN RED. ..... 16
FIGURE 10: TIME SERIES OF MODEL PERFORMANCE FOR HOURLY OZONE CONCENTRATIONS AT BOSTON MONITORING SITES FOR OCTOBER 2007. OBSERVED VALUES SHOWN IN BLACK AND MODELED VALUES SHOWN IN RED. ..... 17
FIGURE 11: TIME SERIES OF MODEL PERFORMANCE FOR 8-HR DAILY MAXIMUM OZONE CONCENTRATIONS AT NEW YORK MONITORING SITES FOR APRIL-OCTOBER 2007. OBSERVED VALUES SHOWN IN BLACK AND MODELED VALUES SHOWN IN RED. ..... 18
FIGURE 12: TIME SERIES OF MODEL PERFORMANCE FOR HOURLY OZONE CONCENTRATIONS AT NEW YORK MONITORING SITES FOR JANUARY 2007. OBSERVED VALUES SHOWN IN BLACK AND MODELED VALUES SHOWN IN RED. ..... 18
FIGURE 13: TIME SERIES OF MODEL PERFORMANCE FOR HOURLY OZONE CONCENTRATIONS AT NEW YORK MONITORING SITES FOR APRIL 2007. OBSERVED VALUES SHOWN IN BLACK AND MODELED VALUES SHOWN IN RED. ..... 19
FIGURE 14: TIME SERIES OF MODEL PERFORMANCE FOR HOURLY OZONE CONCENTRATIONS AT NEW YORK MONITORING SITES FOR JULY 2007. OBSERVED VALUES SHOWN IN BLACK AND MODELED VALUES SHOWN IN RED. ..... 19
FIGURE 15: TIME SERIES OF MODEL PERFORMANCE FOR HOURLY OZONE CONCENTRATIONS AT NEW YORK MONITORING SITES FOR OCTOBER 2007. OBSERVED VALUES SHOWN IN BLACK AND MODELED VALUES SHOWN IN RED..... 19
FIGURE 16: TIME SERIES OF MODEL PERFORMANCE FOR 8-HR DAILY MAXIMUM OZONE CONCENTRATIONS AT PHILADELPHIA MONITORING SITES FOR APRIL-OCTOBER 2007. OBSERVED VALUES SHOWN IN BLACK AND MODELED VALUES SHOWN IN RED. ..... 20
FIGURE 17: TIME SERIES OF MODEL PERFORMANCE FOR HOURLY OZONE CONCENTRATIONS AT PHILADELPHIA MONITORING SITES FOR JANUARY 2007. OBSERVED VALUES SHOWN IN BLACK AND MODELED VALUES SHOWN IN RED. ..... 21
FIGURE 18: TIME SERIES OF MODEL PERFORMANCE FOR HOURLY OZONE CONCENTRATIONS AT PHILADELPHIA MONITORING SITES FOR APRIL 2007. OBSERVED VALUES SHOWN IN BLACK AND MODELED VALUES SHOWN IN RED..... 21
FIGURE 19: TIME SERIES OF MODEL PERFORMANCE FOR HOURLY OZONE CONCENTRATIONS AT PHILADELPHIA MONITORING SITES FOR JULY 2007. OBSERVED VALUES SHOWN IN BLACK AND MODELED VALUES SHOWN IN RED. ..... 21
FIGURE 20: TIME SERIES OF MODEL PERFORMANCE FOR HOURLY OZONE CONCENTRATIONS AT PHILADELPHIA MONITORING SITES FOR OCTOBER 2007. OBSERVED VALUES SHOWN IN BLACK AND MODELED VALUES SHOWN IN RED..... 22
FIGURE 21: TIME SERIES OF MODEL PERFORMANCE FOR 8-HR DAILY MAXIMUM OZONE CONCENTRATIONS AT BALTIMORE MONITORING SITES FOR APRIL-OCTOBER 2007. OBSERVED VALUES SHOWN IN BLACK AND MODELED VALUES SHOWN IN RED. ..... 23
FIGURE 22: TIME SERIES OF MODEL PERFORMANCE FOR HOURLY OZONE CONCENTRATIONS AT BALTIMORE MONITORING SITES FOR JANUARY 2007. OBSERVED VALUES SHOWN IN BLACK AND MODELED VALUES SHOWN IN RED. ..... 23
FIGURE 23: TIME SERIES OF MODEL PERFORMANCE FOR HOURLY OZONE CONCENTRATIONS AT BALTIMORE MONITORING SITES FOR APRIL 2007. OBSERVED VALUES SHOWN IN BLACK AND MODELED VALUES SHOWN IN RED. ..... 24
FIGURE 24: TIME SERIES OF MODEL PERFORMANCE FOR HOURLY OZONE CONCENTRATIONS AT BALTIMORE MONITORING SITES FOR JULY 2007. OBSERVED VALUES SHOWN IN BLACK AND MODELED VALUES SHOWN IN RED. ..... 24
FIGURE 25: TIME SERIES OF MODEL PERFORMANCE FOR HOURLY OZONE CONCENTRATIONS AT BALTIMORE MONITORING SITES FOR OCTOBER 2007. OBSERVED VALUES SHOWN IN BLACK AND MODELED VALUES SHOWN IN RED..... 25

FIGURE 26: TIME SERIES OF MODEL PERFORMANCE FOR 8-HR DAILY MAXIMUM OZONE CONCENTRATIONS AT WASHINGTON D.C. MONITORING SITES FOR APRIL-OCTOBER 2007. OBSERVED VALUES SHOWN IN BLACK AND MODELED VALUES SHOWN IN RED. . 25
FIGURE 27: TIME SERIES OF MODEL PERFORMANCE FOR HOURLY OZONE CONCENTRATIONS AT WASHINGTON D.C. MONITORING SITES FOR JANUARY 2007. OBSERVED VALUES SHOWN IN BLACK AND MODELED VALUES SHOWN IN RED. ..... 26
FIGURE 28: TIME SERIES OF MODEL PERFORMANCE FOR HOURLY OZONE CONCENTRATIONS AT WASHINGTON D.C. MONITORING SITES FOR APRIL 2007. OBSERVED VALUES SHOWN IN BLACK AND MODELED VALUES SHOWN IN RED. ..... 26
FIGURE 29: TIME SERIES OF MODEL PERFORMANCE FOR HOURLY OZONE CONCENTRATIONS AT WASHINGTON D.C. MONITORING SITES FOR JULY 2007. OBSERVED VALUES SHOWN IN BLACK AND MODELED VALUES SHOWN IN RED. ..... 27
FIGURE 30: TIME SERIES OF MODEL PERFORMANCE FOR HOURLY OZONE CONCENTRATIONS AT WASHINGTON D.C. MONITORING SITES FOR OCTOBER 2007. OBSERVED VALUES SHOWN IN BLACK AND MODELED VALUES SHOWN IN RED. ..... 27
FIGURE 31: MAP OF NORMALIZED MEAN BIAS FOR MDA8 OZONE CONCENTRATIONS IN THE SOUTHEASTERN US FOR WINTER MONTHS IN 2007. ..... 29
FIGURE 32: MAP OF NORMALIZED MEAN BIAS FOR MDA8 OZONE CONCENTRATIONS IN THE SOUTHEASTERN US FOR SPRING MONTHS IN 2007. ..... 30
FIGURE 33: MAP OF NORMALIZED MEAN BIAS FOR MDA8 OZONE CONCENTRATIONS IN THE SOUTHEASTERN US FOR SUMMER MONTHS IN 2007. ..... 31
FIGURE 34: MAP OF NORMALIZED MEAN BIAS FOR MDA8 OZONE CONCENTRATIONS IN THE SOUTHEASTERN US FOR FALL MONTHS IN 2007. ..... 32
FIGURE 35: TIME SERIES OF MODEL PERFORMANCE FOR 8-HR DAILY MAXIMUM OZONE CONCENTRATIONS AT ATLANTA MONITORING SITES FOR APRIL-OCTOBER 2007. OBSERVED VALUES SHOWN IN BLACK AND MODELED VALUES SHOWN IN RED. ..... 33
FIGURE 36: TIME SERIES OF MODEL PERFORMANCE FOR HOURLY OZONE CONCENTRATIONS AT ATLANTA MONITORING SITES FOR APRIL 2007. OBSERVED VALUES SHOWN IN BLACK AND MODELED VALUES SHOWN IN RED. ..... 33
FIGURE 37: TIME SERIES OF MODEL PERFORMANCE FOR HOURLY OZONE CONCENTRATIONS AT ATLANTA MONITORING SITES FOR JULY 2007. OBSERVED VALUES SHOWN IN BLACK AND MODELED VALUES SHOWN IN RED. ..... 34
FIGURE 38: TIME SERIES OF MODEL PERFORMANCE FOR HOURLY OZONE CONCENTRATIONS AT ATLANTA MONITORING SITES FOR OCTOBER 2007. OBSERVED VALUES SHOWN IN BLACK AND MODELED VALUES SHOWN IN RED. ..... 34
FIGURE 39: MAP OF NORMALIZED MEAN BIAS FOR MDA8 OZONE CONCENTRATIONS IN THE MIDWEST FOR WINTER MONTHS IN 2007. ..... 36
FIGURE 40: MAP OF NORMALIZED MEAN BIAS FOR MDA8 OZONE CONCENTRATIONS IN THE MIDWEST FOR SPRING MONTHS IN 2007. 37
FIGURE 41: MAP OF NORMALIZED MEAN BIAS FOR MDA8 OZONE CONCENTRATIONS IN THE MIDWEST FOR SUMMER MONTHS IN 2007. ..... 38
FIGURE 42: MAP OF NORMALIZED MEAN BIAS FOR MDA8 OZONE CONCENTRATIONS IN THE MIDWEST FOR FALL MONTHS IN 2007. ... 39
FIGURE 43: TIME SERIES OF MODEL PERFORMANCE FOR 8-HR DAILY MAXIMUM OZONE CONCENTRATIONS AT CHICAGO MONITORING SITES FOR APRIL-OCTOBER 2007. OBSERVED VALUES SHOWN IN BLACK AND MODELED VALUES SHOWN IN RED. ..... 40
FIGURE 44: TIME SERIES OF MODEL PERFORMANCE FOR HOURLY OZONE CONCENTRATIONS AT CHICAGO MONITORING SITES FOR JANUARY 2007. OBSERVED VALUES SHOWN IN BLACK AND MODELED VALUES SHOWN IN RED. ..... 40
FIGURE 45: TIME SERIES OF MODEL PERFORMANCE FOR HOURLY OZONE CONCENTRATIONS AT CHICAGO MONITORING SITES FOR APRIL 2007. OBSERVED VALUES SHOWN IN BLACK AND MODELED VALUES SHOWN IN RED. ..... 41
FIGURE 46: TIME SERIES OF MODEL PERFORMANCE FOR HOURLY OZONE CONCENTRATIONS AT CHICAGO MONITORING SITES FOR JULY 2007. OBSERVED VALUES SHOWN IN BLACK AND MODELED VALUES SHOWN IN RED. ..... 41

FIGURE 47: TIME SERIES OF MODEL PERFORMANCE FOR HOURLY OZONE CONCENTRATIONS AT CHICAGO MONITORING SITES FOR OCTOBER 2007. OBSERVED VALUES SHOWN IN BLACK AND MODELED VALUES SHOWN IN RED..... 42
FIGURE 48: TIME SERIES OF MODEL PERFORMANCE FOR 8-HR DAILY MAXIMUM OZONE CONCENTRATIONS AT CLEVELAND MONITORING SITES FOR APRIL-OCTOBER 2007. OBSERVED VALUES SHOWN IN BLACK AND MODELED VALUES SHOWN IN RED. ..... 42
FIGURE 49: TIME SERIES OF MODEL PERFORMANCE FOR HOURLY OZONE CONCENTRATIONS AT CLEVELAND MONITORING SITES FOR APRIL 2007. OBSERVED VALUES SHOWN IN BLACK AND MODELED VALUES SHOWN IN RED. ..... 43
FIGURE 50: TIME SERIES OF MODEL PERFORMANCE FOR HOURLY OZONE CONCENTRATIONS AT CLEVELAND MONITORING SITES FOR JULY 2007. OBSERVED VALUES SHOWN IN BLACK AND MODELED VALUES SHOWN IN RED. ..... 43
FIGURE 51: TIME SERIES OF MODEL PERFORMANCE FOR HOURLY OZONE CONCENTRATIONS AT CLEVELAND MONITORING SITES FOR OCTOBER 2007. OBSERVED VALUES SHOWN IN BLACK AND MODELED VALUES SHOWN IN RED..... 44
FIGURE 52: TIME SERIES OF MODEL PERFORMANCE FOR 8-HR DAILY MAXIMUM OZONE CONCENTRATIONS AT DETROIT MONITORING SITES FOR APRIL-OCTOBER 2007. OBSERVED VALUES SHOWN IN BLACK AND MODELED VALUES SHOWN IN RED..... 45
FIGURE 53: TIME SERIES OF MODEL PERFORMANCE FOR HOURLY OZONE CONCENTRATIONS AT DETROIT MONITORING SITES FOR APRIL 2007. OBSERVED VALUES SHOWN IN BLACK AND MODELED VALUES SHOWN IN RED. ..... 45
FIGURE 54: TIME SERIES OF MODEL PERFORMANCE FOR HOURLY OZONE CONCENTRATIONS AT DETROIT MONITORING SITES FOR JULY 2007. OBSERVED VALUES SHOWN IN BLACK AND MODELED VALUES SHOWN IN RED. ..... 46
FIGURE 55: MAP OF NORMALIZED MEAN BIAS FOR MDA8 OZONE CONCENTRATIONS IN THE CENTRAL US FOR WINTER MONTHS IN 2007. ..... 48
FIGURE 56: MAP OF NORMALIZED MEAN BIAS FOR MDA8 OZONE CONCENTRATIONS IN THE CENTRAL US FOR SPRING MONTHS IN 2007. ..... 49
FIGURE 57: MAP OF NORMALIZED MEAN BIAS FOR MDA8 OZONE CONCENTRATIONS IN THE CENTRAL US FOR SUMMER MONTHS IN 2007. ..... 50
FIGURE 58: MAP OF NORMALIZED MEAN BIAS FOR MDA8 OZONE CONCENTRATIONS IN THE CENTRAL US FOR FALL MONTHS IN 2007. 51
FIGURE 59: TIME SERIES OF MODEL PERFORMANCE FOR 8-HR DAILY MAXIMUM OZONE CONCENTRATIONS AT SAINT LOUIS MONITORING SITES FOR APRIL-OCTOBER 2007. OBSERVED VALUES SHOWN IN BLACK AND MODELED VALUES SHOWN IN RED. ..... 52
FIGURE 60: TIME SERIES OF MODEL PERFORMANCE FOR HOURLY OZONE CONCENTRATIONS AT SAINT LOUIS MONITORING SITES FOR JANUARY 2007. OBSERVED VALUES SHOWN IN BLACK AND MODELED VALUES SHOWN IN RED. ..... 52
FIGURE 61: TIME SERIES OF MODEL PERFORMANCE FOR HOURLY OZONE CONCENTRATIONS AT SAINT LOUIS MONITORING SITES FOR APRIL 2007. OBSERVED VALUES SHOWN IN BLACK AND MODELED VALUES SHOWN IN RED. ..... 53
FIGURE 62: TIME SERIES OF MODEL PERFORMANCE FOR HOURLY OZONE CONCENTRATIONS AT SAINT LOUIS MONITORING SITES FOR JULY 2007. OBSERVED VALUES SHOWN IN BLACK AND MODELED VALUES SHOWN IN RED. ..... 53
FIGURE 63: TIME SERIES OF MODEL PERFORMANCE FOR HOURLY OZONE CONCENTRATIONS AT SAINT LOUIS MONITORING SITES FOR OCTOBER 2007. OBSERVED VALUES SHOWN IN BLACK AND MODELED VALUES SHOWN IN RED..... 54
FIGURE 64: TIME SERIES OF MODEL PERFORMANCE FOR 8-HR DAILY MAXIMUM OZONE CONCENTRATIONS AT DALLAS MONITORING SITES FOR APRIL-OCTOBER 2007. OBSERVED VALUES SHOWN IN BLACK AND MODELED VALUES SHOWN IN RED..... 55
FIGURE 65: TIME SERIES OF MODEL PERFORMANCE FOR HOURLY OZONE CONCENTRATIONS AT DALLAS MONITORING SITES FOR JANUARY 2007. OBSERVED VALUES SHOWN IN BLACK AND MODELED VALUES SHOWN IN RED. ..... 55
FIGURE 66: TIME SERIES OF MODEL PERFORMANCE FOR HOURLY OZONE CONCENTRATIONS AT DALLAS MONITORING SITES FOR APRIL 2007. OBSERVED VALUES SHOWN IN BLACK AND MODELED VALUES SHOWN IN RED. ..... 56
FIGURE 67: TIME SERIES OF MODEL PERFORMANCE FOR HOURLY OZONE CONCENTRATIONS AT DALLAS MONITORING SITES FOR JULY 2007. OBSERVED VALUES SHOWN IN BLACK AND MODELED VALUES SHOWN IN RED. ..... 56

FIGURE 68: TIME SERIES OF MODEL PERFORMANCE FOR HOURLY OZONE CONCENTRATIONS AT DALLAS MONITORING SITES FOR OCTOBER 2007. OBSERVED VALUES SHOWN IN BLACK AND MODELED VALUES SHOWN IN RED. ..... 57
FIGURE 69: TIME SERIES OF MODEL PERFORMANCE FOR 8-HR DAILY MAXIMUM OZONE CONCENTRATIONS AT HOUSTON MONITORING SITES FOR APRIL-OCTOBER 2007. OBSERVED VALUES SHOWN IN BLACK AND MODELED VALUES SHOWN IN RED. ..... 57
FIGURE 70: TIME SERIES OF MODEL PERFORMANCE FOR HOURLY OZONE CONCENTRATIONS AT HOUSTON MONITORING SITES FOR JANUARY 2007. OBSERVED VALUES SHOWN IN BLACK AND MODELED VALUES SHOWN IN RED. ..... 58
FIGURE 71: TIME SERIES OF MODEL PERFORMANCE FOR HOURLY OZONE CONCENTRATIONS AT HOUSTON MONITORING SITES FOR APRIL 2007. OBSERVED VALUES SHOWN IN BLACK AND MODELED VALUES SHOWN IN RED. ..... 58
FIGURE 72: TIME SERIES OF MODEL PERFORMANCE FOR HOURLY OZONE CONCENTRATIONS AT HOUSTON MONITORING SITES FOR JULY 2007. OBSERVED VALUES SHOWN IN BLACK AND MODELED VALUES SHOWN IN RED. ..... 59
FIGURE 73: TIME SERIES OF MODEL PERFORMANCE FOR HOURLY OZONE CONCENTRATIONS AT HOUSTON MONITORING SITES FOR OCTOBER 2007. OBSERVED VALUES SHOWN IN BLACK AND MODELED VALUES SHOWN IN RED..... 59
FIGURE 74: MAP OF NORMALIZED MEAN BIAS FOR MDA8 OZONE CONCENTRATIONS IN THE WESTERN US FOR WINTER MONTHS IN 2007. ..... 61
FIGURE 75: MAP OF NORMALIZED MEAN BIAS FOR MDA8 OZONE CONCENTRATIONS IN THE WESTERN US FOR SPRING MONTHS IN 2007. ..... 62
FIGURE 76: MAP OF NORMALIZED MEAN BIAS FOR MDA8 OZONE CONCENTRATIONS IN THE WESTERN US FOR SUMMER MONTHS IN 2007. ..... 63
FIGURE 77: MAP OF NORMALIZED MEAN BIAS FOR MDA8 OZONE CONCENTRATIONS IN THE WESTERN US FOR FALL MONTHS IN 2007. ..... 64
FIGURE 78: TIME SERIES OF MODEL PERFORMANCE FOR 8-HR DAILY MAXIMUM OZONE CONCENTRATIONS AT DENVER MONITORING SITES FOR APRIL-OCTOBER 2007. OBSERVED VALUES SHOWN IN BLACK AND MODELED VALUES SHOWN IN RED..... 65
FIGURE 79: TIME SERIES OF MODEL PERFORMANCE FOR HOURLY OZONE CONCENTRATIONS AT DENVER MONITORING SITES FOR APRIL 2007. OBSERVED VALUES SHOWN IN BLACK AND MODELED VALUES SHOWN IN RED. ..... 65
FIGURE 80: TIME SERIES OF MODEL PERFORMANCE FOR HOURLY OZONE CONCENTRATIONS AT DENVER MONITORING SITES FOR JULY 2007. OBSERVED VALUES SHOWN IN BLACK AND MODELED VALUES SHOWN IN RED. ..... 66
FIGURE 81: TIME SERIES OF MODEL PERFORMANCE FOR HOURLY OZONE CONCENTRATIONS AT DENVER MONITORING SITES FOR OCTOBER 2007. OBSERVED VALUES SHOWN IN BLACK AND MODELED VALUES SHOWN IN RED. ..... 66
FIGURE 87: TIME SERIES OF MODEL PERFORMANCE FOR 8-HR DAILY MAXIMUM OZONE CONCENTRATIONS AT SACRAMENTO MONITORING SITES FOR APRIL-OCTOBER 2007. OBSERVED VALUES SHOWN IN BLACK AND MODELED VALUES SHOWN IN RED. ..... 67
FIGURE 88: TIME SERIES OF MODEL PERFORMANCE FOR HOURLY OZONE CONCENTRATIONS AT SACRAMENTO MONITORING SITES FOR JANUARY 2007. OBSERVED VALUES SHOWN IN BLACK AND MODELED VALUES SHOWN IN RED. ..... 67
FIGURE 89: TIME SERIES OF MODEL PERFORMANCE FOR HOURLY OZONE CONCENTRATIONS AT SACRAMENTO MONITORING SITES FOR APRIL 2007. OBSERVED VALUES SHOWN IN BLACK AND MODELED VALUES SHOWN IN RED..... 68
FIGURE 90: TIME SERIES OF MODEL PERFORMANCE FOR HOURLY OZONE CONCENTRATIONS AT SACRAMENTO MONITORING SITES FOR JULY 2007. OBSERVED VALUES SHOWN IN BLACK AND MODELED VALUES SHOWN IN RED. ..... 68
FIGURE 91: TIME SERIES OF MODEL PERFORMANCE FOR HOURLY OZONE CONCENTRATIONS AT SACRAMENTO MONITORING SITES FOR OCTOBER 2007. OBSERVED VALUES SHOWN IN BLACK AND MODELED VALUES SHOWN IN RED..... 69
FIGURE 92: TIME SERIES OF MODEL PERFORMANCE FOR 8-HR DAILY MAXIMUM OZONE CONCENTRATIONS AT LOS ANGELES MONITORING SITES FOR APRIL-OCTOBER 2007. OBSERVED VALUES SHOWN IN BLACK AND MODELED VALUES SHOWN IN RED. ..... 70

FIGURE 93: TIME SERIES OF MODEL PERFORMANCE FOR HOURLY OZONE CONCENTRATIONS AT LOS ANGELES MONITORING SITES FOR JANUARY 2007. OBSERVED VALUES SHOWN IN BLACK AND MODELED VALUES SHOWN IN RED. ..... 70
FIGURE 94: TIME SERIES OF MODEL PERFORMANCE FOR HOURLY OZONE CONCENTRATIONS AT LOS ANGELES MONITORING SITES FOR APRIL 2007. OBSERVED VALUES SHOWN IN BLACK AND MODELED VALUES SHOWN IN RED. ..... 71
FIGURE 95: TIME SERIES OF MODEL PERFORMANCE FOR HOURLY OZONE CONCENTRATIONS AT LOS ANGELES MONITORING SITES FOR JULY 2007. OBSERVED VALUES SHOWN IN BLACK AND MODELED VALUES SHOWN IN RED. ..... 71
FIGURE 96: TIME SERIES OF MODEL PERFORMANCE FOR HOURLY OZONE CONCENTRATIONS AT LOS ANGELES MONITORING SITES FOR OCTOBER 2007. OBSERVED VALUES SHOWN IN BLACK AND MODELED VALUES SHOWN IN RED ..... 71
FIGURE 97: MAP OF MEAN OBSERVED MDA8 OZONE CONCENTRATIONS AT LOS ANGELES MONITORING SITES FOR SUMMER MONTHS (JUNE, JULY, AUG) 2007. ..... 72
FIGURE 98: MAP OF NORMALIZED MEAN BIAS FOR MDA8 OZONE CONCENTRATIONS AT LOS ANGELES MONITORING SITES FOR SUMMER MONTHS (JUNE, JULY, AUG) 2007. ..... 72

# Table of Tables

TABLE 1: GEOGRAPHIC ELEMENTS OF DOMAIN USED IN THE CMAQ/HDDM MODELING ..... 2
TABLE 2: VERTICAL LAYER STRUCTURE FOR 2007 WRF AND CMAQ SIMULATIONS ..... 4
TABLE 3: SUMMARY OF EMISSIONS TOTALS BY SECTOR FOR THE 12KM EASTERN US DOMAIN ..... 6
TABLE 4: SUMMARY OF CMAQ MODEL PERFORMANCE AT AQS MONITORING SITES IN THE NORTHEASTERN US ..... 10
TABLE 5: SUMMARY OF CMAQ MODEL PERFORMANCE AT AQS MONITORING SITES IN THE BOSTON AREA ..... 14
TABLE 6: SUMMARY OF CMAQ MODEL PERFORMANCE AT AQS MONITORING SITES IN THE NEW YORK AREA ..... 17
TABLE 7: SUMMARY OF CMAQ MODEL PERFORMANCE AT AQS MONITORING SITES IN THE PHILADELPHIA AREA ..... 19
TABLE 8: SUMMARY OF CMAQ MODEL PERFORMANCE AT AQS MONITORING SITES IN THE BALTIMORE AREA ..... 22
TABLE 9: SUMMARY OF CMAQ MODEL PERFORMANCE AT AQS MONITORING SITES IN THE WASHINGTON D.C. AREA ..... 25
TABLE 10: SUMMARY OF CMAQ MODEL PERFORMANCE AT AQS MONITORING SITES IN THE SOUTHEASTERN US ..... 28
TABLE 11: SUMMARY OF CMAQ MODEL PERFORMANCE AT AQS MONITORING SITES IN THE ATLANTA AREA ..... 32
TABLE 12: SUMMARY OF CMAQ MODEL PERFORMANCE AT AQS MONITORING SITES IN THE MIDWEST ..... 35
TABLE 13: SUMMARY OF CMAQ MODEL PERFORMANCE AT AQS MONITORING SITES IN THE CHICAGO AREA ..... 39
TABLE 14: SUMMARY OF CMAQ MODEL PERFORMANCE AT AQS MONITORING SITES IN THE CLEVELAND AREA ..... 42
TABLE 15: SUMMARY OF CMAQ MODEL PERFORMANCE AT AQS MONITORING SITES IN THE DETROIT AREA ..... 44
TABLE 16: SUMMARY OF CMAQ MODEL PERFORMANCE AT AQS MONITORING SITES IN THE CENTRAL US ..... 47
TABLE 17: SUMMARY OF CMAQ MODEL PERFORMANCE AT AQS MONITORING SITES IN THE SAINT LOUIS AREA ..... 51
TABLE 18: SUMMARY OF CMAQ MODEL PERFORMANCE AT AQS MONITORING SITES IN THE DALLAS AREA ..... 54
TABLE 19: SUMMARY OF CMAQ MODEL PERFORMANCE AT AQS MONITORING SITES IN THE HOUSTON AREA ..... 57
TABLE 20: SUMMARY OF CMAQ MODEL PERFORMANCE AT AQS MONITORING SITES IN THE WESTERN US ..... 60
TABLE 21: SUMMARY OF CMAQ MODEL PERFORMANCE AT AQS MONITORING SITES IN THE DENVER AREA ..... 64
TABLE 23: SUMMARY OF CMAQ MODEL PERFORMANCE AT AQS MONITORING SITES IN THE SACRAMENTO AREA ..... 66
TABLE 24: SUMMARY OF CMAQ MODEL PERFORMANCE AT AQS MONITORING SITES IN THE LOS ANGELES AREA ..... 69

# MODEL SET-UP AND SIMULATION

The air quality modeling underlying the HDDM adjustment methodology described in chapter 4 and appendix 4d was performed using CMAQv4.7.1 with HDDM for ozone (www.cmaq-model.org). A modified version of CMAQ-HDDM-3D was used that tracked species concentrations through all modeled processes, but tracked ozone sensitivities through the chemistry, transport, and dry deposition subroutines only and did not account for the effects of aerosol and cloud processing due to the uncertainties in these model processes with respect to ozone sensitivity as well as to conserve computational costs. CMAQ was run using the carbon bond 2005 (CB05) gas-phase chemical mechanism (Gery et al 1989; Yarwood et al, 2005) and the AERO5 aerosol module which includes ISORROPIA for gas-particle partitioning of inorganic species (Nenes et al 1998) and secondary organic aerosol treatment as described in Carlton et al (2010).

## MODEL DOMAIN

For this analysis, all CMAQ/HDDM runs were performed for a domain that covers the 48 contiguous states included portions of southern Canada and Northern Mexico with a 12 x 12 km resolution (Figure 1). The CMAQ simulations were performed with 24 vertical layers with a top at about 17,600 meters, or 50 millibars (mb). Tables 1 and 2 provides some basic geographic information regarding the CMAQ domain and vertical layer structure, respectively. Results from the lowest layer of the model were used for analyses to support the ozone NAAQS REA.

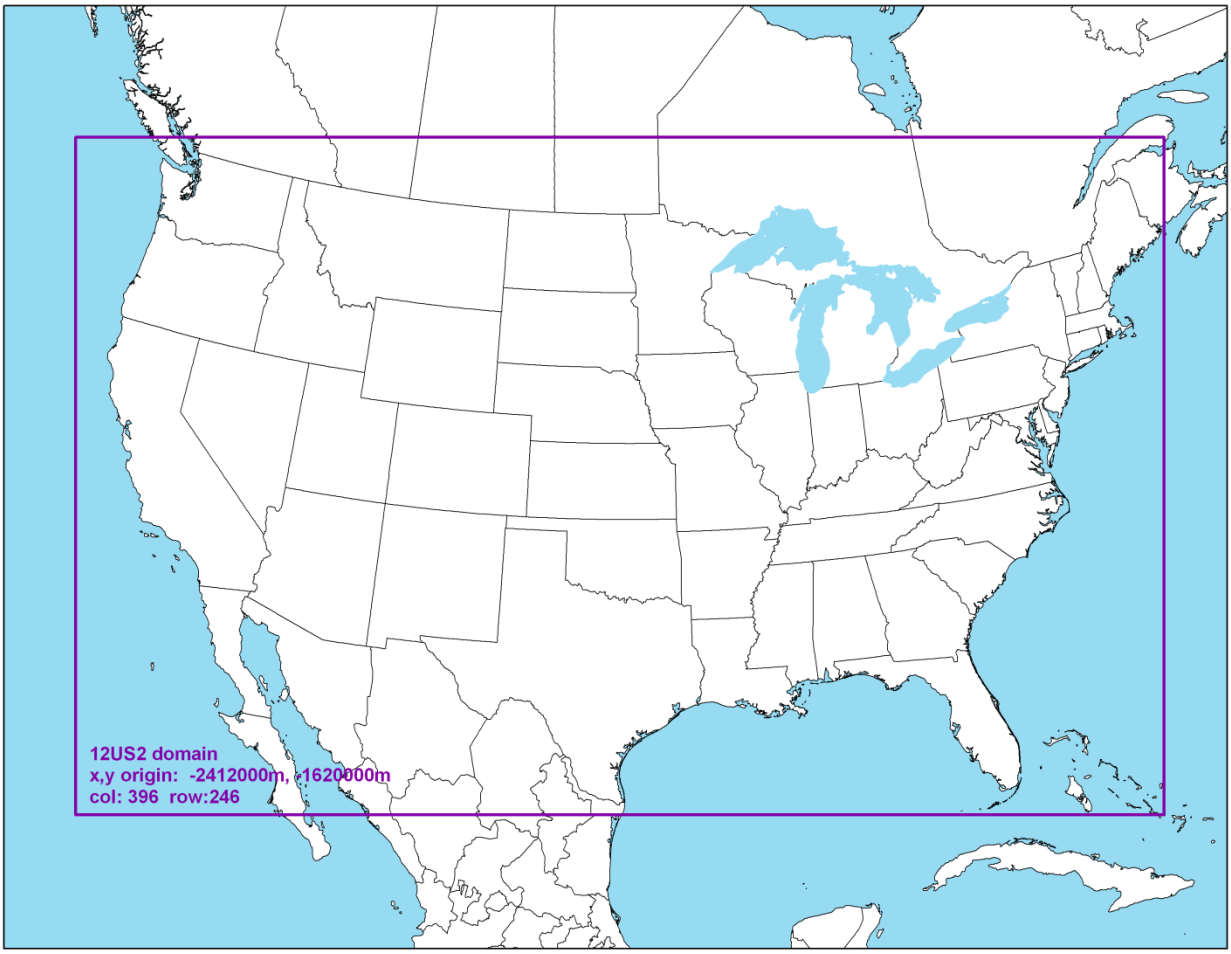


**Figure 1: Map of the CMAQ modeling domain.**

**Table 1: Geographic elements of domain used in the CMAQ/HDDM modeling**

| | **CMAQ Modeling Configuration: National Grid** |
|---|---|
| **Map Projection** | Lambert Conformal Projection |
| **Grid Resolution** | 12 km |
| **True Latitudes** | 33 deg N and 45 deg N |
| **Dimensions** | 396 x 246 x 24 |
| **Vertical extent** | 24 Layers: Surface to 50 millibar level (see Table 2) |

## MODEL TIME PERIOD

The CMAQ/HDDM modeling was performed for January and April-October of 2007. The simulations included 10 day "ramp-up" periods from December 22-31, 2006 and from March 22-31 2007 to minimize the effects of initial conditions. The ramp-up days were not considered in the analysis for the HDDM results.

## MODEL INPUTS: METEOROLOGY

CMAQ model simulations require inputs of meteorological fields, emissions, and initial and boundary conditions. The gridded meteorological data for the entire year of 2007 at the 12 km continental United States scale domain was derived from version 3.1 of the Weather Research and Forecasting Model (WRF), Advanced Research WRF (ARW) core (Skamarock et al., 2008). The WRF Model is a next-generation mesoscale numerical weather prediction system developed for both operational forecasting and atmospheric research applications (http://wrf-model.org). The 2007 WRF simulation included the physics options of the Pleim-Xiu land surface model (LSM), Asymmetric Convective Model version 2 planetary boundary layer (PBL) scheme, Morrison double moment microphysics, Kain-Fritsch cumulus parameterization scheme and the RRTMG long-wave radiation (LWR) scheme (Gilliam and Pleim, 2010).

The WRF meteorological outputs were processed to create model-ready inputs for CMAQ using the Meteorology-Chemistry Interface Processor (MCIP) package (Otte et al., 2010), version 3.6, to derive the specific inputs to CMAQ: horizontal wind components (i.e., speed and direction), temperature, moisture, vertical diffusion rates, and rainfall rates for each grid cell in each vertical layer. The WRF simulation used the same CMAQ map projection, a lambert conformal projection centered at (-97, 40) with true latitudes at 33 and 45 degrees north. The 12 km WRF domain consisted of 459 by 299 grid cells. The WRF simulation utilized 34 vertical layers with a surface layer of approximately 38 meters. Table 2 shows the vertical layer structure used in WRF and the layer collapsing approach to generate the CMAQ meteorological inputs. CMAQ resolved the vertical atmosphere with 24 layers, preserving greater resolution in the PBL.

**Table 2: Vertical layer structure for 2007 WRF and CMAQ simulations**

| Layer Top Height (m) | Pressure (mb) | | WRF | Depth (m) | | CMAQ | Depth (m) |
|---|---|---|---|---|---|---|---|
| 17,145 | 50 | | 34 | 2,655 | | 24 | 4,552 |
| 14,490 | 95 | | 33 | 1,896 | | | |
| 12,593 | 140 | | 32 | 1,499 | | 23 | 2,749 |
| 11,094 | 185 | | 31 | 1,250 | | | |
| 9,844 | 230 | | 30 | 1,078 | | 22 | 2,029 |
| 8,766 | 275 | | 29 | 951 | | | |
| 7,815 | 320 | | 28 | 853 | | 21 | 1,627 |
| 6,962 | 365 | | 27 | 775 | | | |
| 6,188 | 410 | | 26 | 711 | | 20 | 1,368 |
| 5,477 | 455 | | 25 | 657 | | | |
| 4,820 | 500 | | 24 | 612 | | 19 | 1,185 |
| 4,208 | 545 | | 23 | 573 | | | |
| 3,635 | 590 | | 22 | 539 | | 18 | 539 |
| 3,095 | 635 | | 21 | 509 | | 17 | 509 |
| 2,586 | 680 | | 20 | 388 | | 16 | 388 |
| 2,198 | 716 | | 19 | 281 | | 15 | 281 |
| 1,917 | 743 | | 18 | 273 | | 14 | 273 |
| 1,644 | 770 | | 17 | 178 | | 13 | 178 |
| 1,466 | 788 | | 16 | 174 | | 12 | 174 |
| 1,292 | 806 | | 15 | 171 | | 11 | 171 |
| 1,121 | 824 | | 14 | 168 | | 10 | 168 |
| 952 | 842 | | 13 | 165 | | 9 | 165 |
| 787 | 860 | | 12 | 82 | | 8 | 163 |
| 705 | 869 | | 11 | 81 | | | |
| 624 | 878 | | 10 | 80 | | 7 | 160 |
| 544 | 887 | | 9 | 80 | | | |
| 465 | 896 | | 8 | 79 | | 6 | 157 |
| 386 | 905 | | 7 | 78 | | | |
| 307 | 914 | | 6 | 78 | | 5 | 78 |
| 230 | 923 | | 5 | 77 | | 4 | 77 |
| 153 | 932 | | 4 | 38 | | 3 | 76 |
| 114 | 937 | | 3 | 38 | | | |
| 76 | 941 | | 2 | 38 | | 2 | 38 |
| 38 | 946 | | 1 | 38 | | 1 | 38 |

In terms of the 2007 WRF meteorological model performance evaluation, an approach which included a combination of qualitative and quantitative analyses was used to assess the

adequacy of the WRF simulated fields (U.S. EPA, 2011). The qualitative aspects involved comparisons of the model-estimated synoptic patterns against observed patterns from historical weather chart archives. Additionally, the evaluations compared spatial patterns of monthly average rainfall and monthly maximum planetary boundary layer (PBL) heights. The statistical portion of the evaluation examined the model bias and error for temperature, water vapor mixing ratio, solar radiation, and wind fields. These statistical values were calculated on a monthly basis.

**MODEL INPUTS: EMISSIONS**

The emissions data used are based on the 2007 Version 5 emissions modeling platform developed for the Particulate Matter (PM) NAAQS rule (US EPA 2012a, US EPA 2012b). Some small updates to the 2007v5 platform are enumerated below. First we give a general summary of the emissions processing performed for the PM NAAQS 2007 modeling emissions inputs (more details are available in US EPA 2012a, 2012b, and in the PM NAAQS section of http://www.epa.gov/ttn/chief/emch/index.html). The 2008 National Emissions Inventory, Version 2 (http://www.epa.gov/ttn/chief/net/2008inventory.html) was the starting point for these emissions, with updates to specific source categories made where necessary to better represent the year 2007. Emissions were processed to photochemical model inputs with the SMOKE modeling system version 3.1 (Houyoux et al., 2000). For this analysis, emissions from wildfires and prescribed burns are estimated based on a multi-year average of data from 2003 through 2010. Electric generating utilities (EGUs) emissions for 2007 are temporalized based on average temporal profiles from 3 years of data. In addition, US emissions are included from other point sources, area sources, agricultural sources (ammonia only), anthropogenic fugitive dust sources, nonroad mobile sources, onroad mobile sources, and biogenic sources. Onroad mobile sources were created using EPA's MOVES 2010b model (www.epa.gov/otaq/models/moves), except that California emissions were adjusted to match the county total emissions obtained directly from the California Air Resources Board. Biogenic emissions were estimated using the Biogenic Emissions Inventory System version 3.14 (BEISv3.14) (Pierce et al, 1998). Other North American emissions are based on a 2006 Canadian inventory and 2008 Mexican inventory. Emissions totals within the 12 km Eastern domain are summarized in Table 3 for CO, NH3, NOx, PM10, PM2.5, SO2, and VOC.
There are a few differences between the emissions data used for this analysis and the data documented in the PM NAAQS 2007v5 platform technical support document (TSD). First, the years used to compute the average fires were 2003-2010, versus 2003-2009 for the PM NAAQS. Second, point source emissions for South Dakota were updated with more recent data.

Finally, a correction was made the spatial surrogates used for oil and gas emissions in the Western Regional Air Partnership states and updated spatial surrogates for gas stations and dry cleaners were used.

**Table 3: Summary of emissions totals by sector for the 12km Eastern US domain**

| Sector Name | Sector description | Emissions (1000 tons/year) | | | | | | |
|---|---|---|---|---|---|---|---|---|
| | | CO | $NH_3$ | $NO_X$ | $PM_{10}$ | $PM_{2.5}$ | $SO_2$ | VOC |
| afdust | Anthropogenic fugitive dust | | | | 5,854 | 825 | | |
| ag | Agricultural sources | | 3,595 | | | | | |
| c1c2rail | Locomotive and marine mobile sources (except C3 marine) | 219 | 0.6 | 1,338 | 44 | 41 | 49 | 60 |
| avefire | Average year fire emissions | 15,598 | 256 | 216 | 1,589 | 1,347 | 118 | 2,797 |
| nonpt | Area sources | 4,335 | 155 | 1,229 | 768 | 676 | 402 | 6,671 |
| nonroad | Off road equipment | 17,834 | 1.9 | 1,878 | 188 | 178 | 101 | 2,781 |
| onroad | Onroad mobile vehicles | 36,757 | 145 | 7,561 | 363 | 277 | 40 | 3,186 |
| othar | Canada and Mexico area sources | 4,225 | 671 | 918 | 1,510 | 451 | 154 | 1,815 |
| othon | Canada and Mexico onroad mobile sources | 5,173 | 25 | 631 | 23 | 18 | 11 | 405 |
| othpt | Canada and Mexico point sources | 1,331 | 21 | 1,280 | 241 | 159 | 2,504 | 626 |
| ptipm | Point sources: electric generation units | 704 | 25 | 3,357 | 437 | 330 | 9,136 | 43 |
| ptnonipm | Point sources other than electric generating units | 2,934 | 68 | 2,077 | 583 | 409 | 1,589 | 1,074 |
| c3marine US | C3 marine vessels within 4 miles of the US coast | 13 | | 138 | 12 | 11 | 105 | 5.1 |
| c3marine non US | C3 marine vessels more than 4 miles off the US coast | 86 | | 1,047 | 87 | 80 | 646 | 38 |
| beis | Biogenic emissions | 8,211 | | 1,931 | | | | 48,616 |
| total US anthro | Total US anthropogenic emissions used in HDDM (NOx and VOC only) | | | 17,578 | | | | 13,819 |
| total | Domain-wide total | 97,420 | 4,964 | 23,602 | 11,699 | 4,802 | 14,854 | 68,117 |

### MODEL INPUTS: BOUNDARY AND INITIAL CONDITIONS

The lateral boundary concentrations for the 12km US2 domain are provided by a three-dimensional global atmospheric chemistry model, the GEOS-CHEM (Yantosca, 2004) model (standard version 8-03-02 with version 8-02-03 chemistry). The global GEOS-CHEM model simulates atmospheric chemical and physical processes driven by assimilated meteorological observations from the NASA's Goddard Earth Observing System (GEOS-5). This model was run for 2007 with a grid resolution of 2.0 degree x 2.5 degree (latitude-longitude) and 46 vertical layers up to 0.01 hPa. The predictions were processed using the GEOS-2-CMAQ tool (Akhtar et al., 2012, Henderson et al, 2013) and used to provide one-way dynamic boundary conditions at one-hour intervals. The ozone from these GEOS-Chem runs was evaluated by comparing to satellite vertical profiles and ground-based measurements and found acceptable model performance (Akhtar et al, 2012; Henderson et al 2013).

Initial conditions were extracted from a slightly older model simulation using GEOS-CHEM (Yantosca, 2004) version 8-02-03. The model simulation from which the initial conditions were extracted was also run with a grid resolution of 2.0 of 2.0 degree x 2.5 degree (latitude-longitude) and 47 vertical layers. A GEOS-Chem evaluation was conducted for the purpose of validating the 2007 GEOS-Chem simulation outputs for their use as inputs to the CMAQ modeling system. This evaluation included reproducing GEOS-Chem evaluation plots reported in the literature for previous versions of the model (Lam, 2010)

## EVALUATION OF MODELED OZONE CONCENTRATIONS

CMAQ is a peer-reviewed, community air quality model that simulates the formation and fate of photochemical oxidants, aerosol concentrations, acid deposition, and air toxics, over multiple scales for given input sets of meteorological conditions and emissions. In order to assure that CMAQ is an appropriate tool to estimate the AQ changes expected to result from a given set of emissions reductions, the model is typically evaluated for each new application. This evaluation consists of assessments of the model itself and an assessment of this particular application of the model.

An independent panel consisting of academic and government experts assessed the science within the CMAQ model version 4.7.1 in September 2011 (http://www.epa.gov/AMD/Reviews/2011_CMAQ_Review_FinalReport.pdf). Among the conclusions of this peer-review report was the finding that the CMAQ science and evaluation

efforts was of “very high quality” and have provided a “foundation for the more reliable use of the CMAQ modeling system”.

As CMAQ model version 4.7.1 was being developed, a series of incremental diagnostic tests were performed to assess how model performance varied across a variety of model improvements. This analysis is summarized in Foley et al. (2010) as well as Godowitch et al., (2011). While time and resource intensive, this systematic incremental testing shows “the effect of each scientific improvement on the simulated fields.” This evaluation allowed for a clear comparison with previous model versions and provided assurance that CMAQ v4.7.1 yielded equivalent or improved performance relative to previous CMAQ versions.

Numerous dynamic evaluations of CMAQ’s ability to simulate the change in air quality resulting from emissions reductions have been conducted and summarized in the peer-reviewed literature. For instance, Napelenok et al (2011) concluded that the CMAQ model “is able to reproduce the observed change in daily maximum 8-hour ozone levels” at the majority of locations when emissions uncertainty is considered. Other dynamic evaluations (Zhou et al., 2013, Godowitch et al., 2010, Gilliland et al., 2008, Godowitch et al., 2007) have suggested that CMAQ may be a conservative estimate of the air quality improvements resulting from emissions reductions.

This TSD summarizes the ability of the model to reproduce 2007 conditions simulated using specific emissions, meteorological, initial conditions and boundary conditions inputs described above. This operational evaluation shows that the CMAQ model predictions for 2007 are equivalent or better than typical regional modeling simulations as summarized in Simon et al. (2012).

In the following sections we present general model performance statistics and plots for five regions of the U.S. We compare model predictions of maximum daily 8-hr average (MDA8) ozone concentrations to measurements reported in EPA’s Air Quality System (AQS) which is a repository of air pollution measurements made by EPA, state, local, and tribal agencies. For the 2007 model performance evaluation, we ran CMAQ for 2007 using the same emissions as those used for the 2007 HDDM runs, except that we included actual wild fires instead of average fires and we used CEM data to for hourly EGU emissions (US EPA, 2012b) instead of the multi-year average temporal method used for the HDDM runs.

The model statistics presented here include mean bias, mean error, normalized mean bias, and normalized mean error as calculated in Simon et al. (2012). Our analysis focuses on regional model evaluation statistics from five US regions as well as evaluations of the 15 urban areas included in the Risk and Exposure Assessment. The five regions are defined as follows: Northeast (Connecticut, Delaware, District of Columbia, Maine, Maryland, Massachusetts,

New Hampshire, New Jersey, New York, Pennsylvania, Rhode Island, Vermont), Southeast (Alabama, Florida, Georgia, Kentucky, Mississippi, North Carolina, South Carolina, Tennessee, Virginia, West Virginia), Midwest (Illinois, Indiana, Michigan, Ohio, Wisconsin), Central (Arkansas, Iowa, Kansas, Louisiana, Minnesota, Missouri, Nebraska, Oklahoma, Texas), and West (Arizona, California, Colorado, Idaho, Nevada, New Mexico, Oregon, Utah, Wyoming). Statistics for model performance in these regions and urban areas are shown by season in Table 4-Table 23 for observed days with MDA8 ozone values >= 60 ppb, observed days with MDA8 ozone < 60 ppb, and for all observed days. Plots are provided to show regional maps of Normalized Mean Bias by season and time series of modeled and measured ozone concentrations in each urban area. Time series are provided for MDA8 ozone from April-October 2007 and for hourly ozone from one month from each season in 2007 (January, April, July, October) where monitoring data is available. Note that time series show average concentrations across all monitors within each urban area and the number of monitors included in this average sometimes changes by season since different monitors within each area take measurements over different periods of the year.

**OPERATIONAL EVALUATION IN THE NORTHEAST U.S.**

Table 4 shows that in the Northeaster US, model mean bias was generally less than 6 ppb and normalized mean bias was less than 15% in most cases. High ozone days and summertime days were more likely to be under-estimated by the model while low ozone days and wintertime days were more likely to be over-estimated by the model. Performance was best in the spring and fall and had the largest errors in the winter. Five of the 15 urban areas evaluated were in the Northeast: Boston, New York, Philadelphia, Baltimore, and Washington D.C.

Model performance at Boston area monitoring sites (Table 5) was similar to that at other Northeastern US sites. The time series plots show that the model has skill at reproducing measured day-to-day variability in MDA8 ozone concentrations (Figure 6). Hourly daytime and nighttime ozone concentrations are also well modeled in all seasons with exception of a few 2-3 day periods in July in which the model over-estimates daytime and nighttime ozone with some over-estimates of daytime peaks in October (Figure 7-Figure 10)[1].

Bulk performance statistics for MDA8 model estimates in New York (Table 6) also look equivalent to both the Boston statistics and those of the Northeast as a whole. Again, the 7-month time series of MDA8 ozone at NY area sites shows that the model captures synoptic variations in ozone concentrations (Figure 11). Hourly New York area ozone in January is

[1] Note that the Y-axis scale for the various time series are not consistent

generally well captured by the model, although CMAQ does somewhat under-estimate the daytime peaks (Figure 12). The April time series (Figure 13) shows that the model captures the range of measured daytime and nighttime ozone values but has a 3-day period of over-estimates in early April and a week-long period of under-estimates later in the month. July and October ozone is well captured by the model on both low and high ozone days and at night (Figure 14 and Figure 15).

Bulk model performance statistics for Philadelphia (Table 7) are equivalent to those for the Northeast as a whole. The time series plots show that variations of MDA8 are well captured in Philadelphia (Figure 16) and that the model does a reasonable job of estimating day to night ozone changes in all seasons but has some under-estimates of daytime ozone in January (Figure 17) and some over-estimates of daytime and nighttime ozone in October (Figure 20).

Baltimore MDA8 ozone performance (Table 8) is generally similar to ozone performance in the rest of the Northeast except for summertime values which are somewhat more overestimated in Baltimore (8 ppb MB in Baltimore versus 4 ppb MB in the Northeast). Still, these bias and error statistics are well within the range of state-of-the-science model performance described by Simon et al (2012).As shown by the time series in Figure 21, most model overestimates in this area occur from late July to late August. Outside of that time period, the MDA8 variations from April-October are well captured by the model. The hourly time series plots for Baltimore generally show reasonable agreement between the observed and modeled values although the period of over-estimated daytime ozone concentrations in July is apparent in Figure 24.

Bulk statistics for Washington D.C. sites (Table 9) are similar to statistics for the rest of the Northeast region. The period of overestimated MDA8 values in late July through August which was seen in nearby Baltimore is less pronounced in Washington D.C. (Figure 26). Hourly time series generally show reasonable performance with some overestimates of nighttime ozone in October (Figure 30).

**Table 4: Summary of CMAQ model performance at AQS monitoring sites in the Northeastern US**

| | | No. of obs | MB (ppb) | NMB (%) | ME (ppb) | NME (%) |
|---|---|---|---|---|---|---|
| Winter | Days < 60 | 5085 | -4.65 | -17.0 | 5.83 | 21.2 |
| | Days ≥ 60 | 0 | NA | NA | NA | NA |
| | All Days | 5085 | -4.65 | -17.0 | 5.83 | 21.2 |
| Spring | Days < 60 | 10420 | -0.69 | -1.4 | 5.63 | 13.2 |
| | Days ≥ 60 | 1856 | -6.34 | -9.1 | 8.25 | 11.8 |
| | All Days | 12276 | -1.47 | -3.1 | 6.03 | 12.9 |

| | | | | | | |
|---|---|---|---|---|---|---|
| Summer | Days < 60 | 11859 | 5.58 | 13.4 | 7.99 | 19.2 |
| | Days ≥ 60 | 4114 | -0.51 | -0.7 | 7.78 | 10.9 |
| | All Days | 15973 | 4.01 | 8.2 | 7.93 | 16.1 |
| Fall | Days < 60 | 10036 | 2.86 | 8.1 | 6.23 | 17.7 |
| | Days ≥ 60 | 1030 | -4.21 | -6.1 | 8.06 | 11.7 |
| | All Days | 11066 | 2.21 | 5.8 | 6.40 | 16.7 |

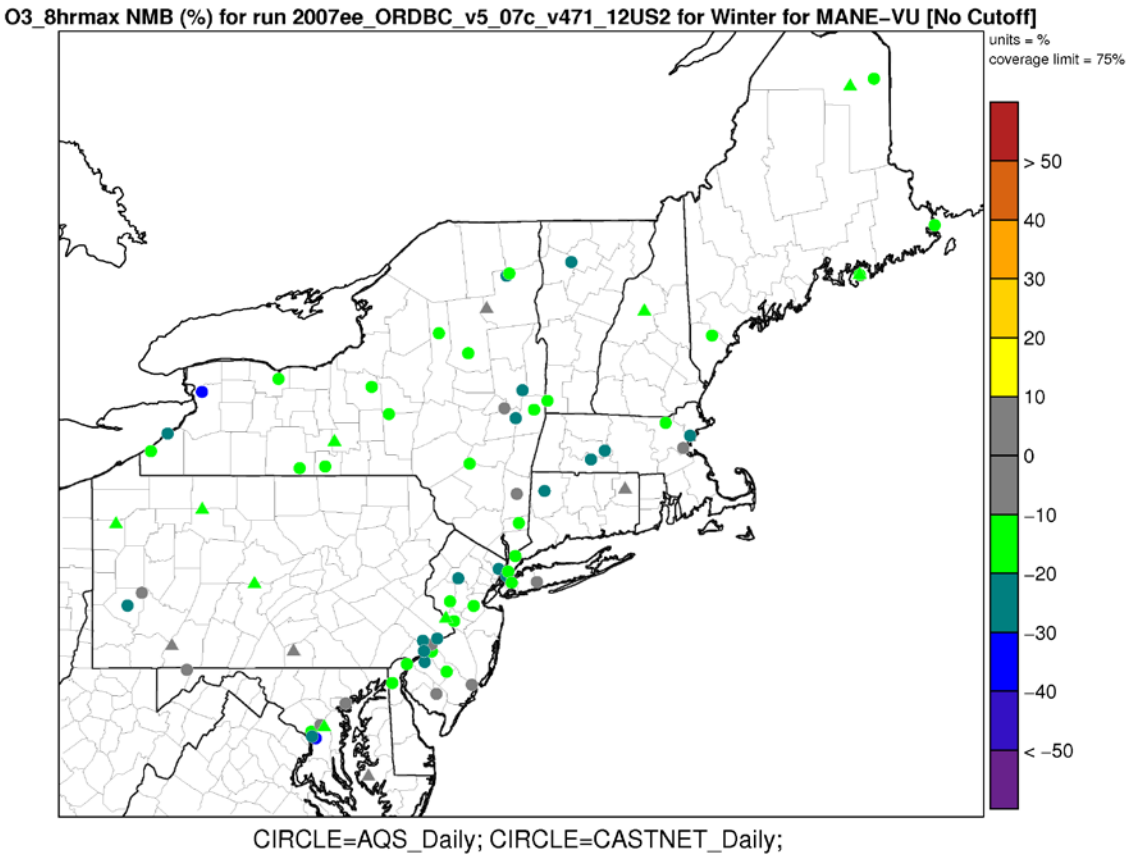


**Figure 2: Map of normalized mean bias for MDA8 ozone concentrations in the Northeastern US for winter months in 2007.**

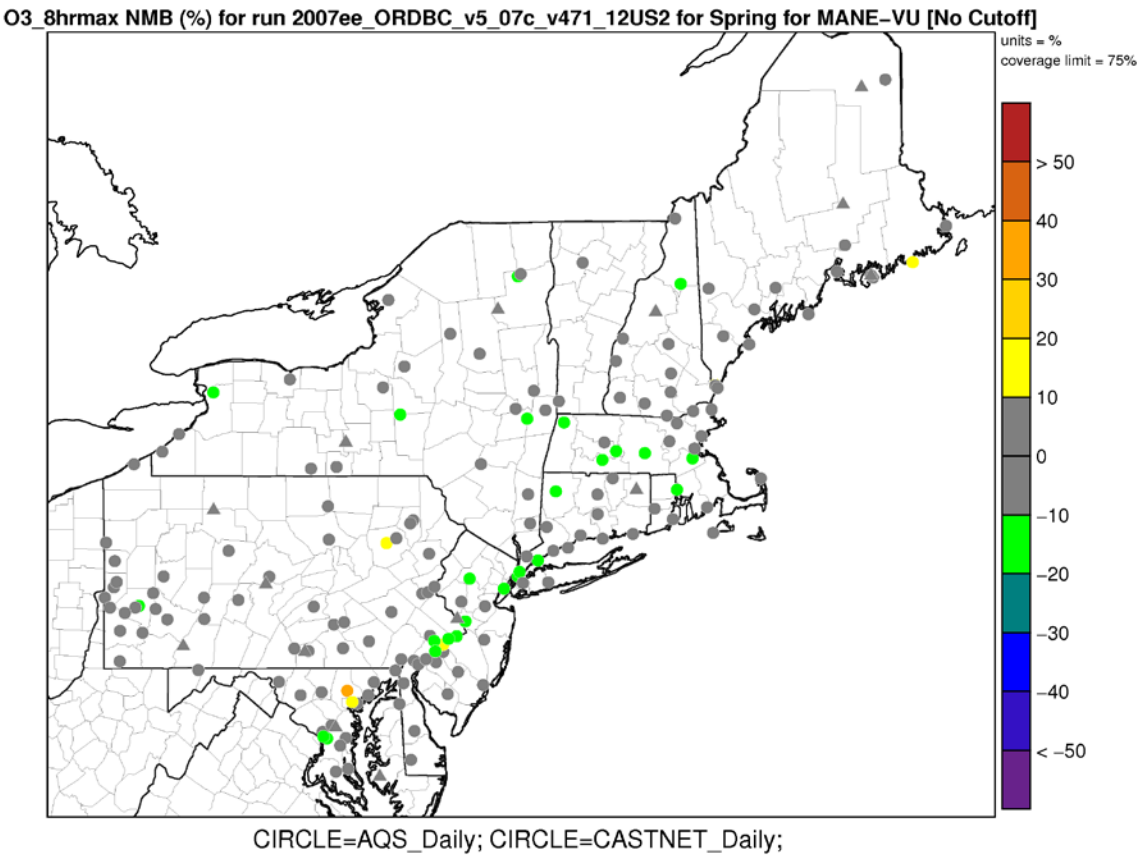


**Figure 3: Map of normalized mean bias for MDA8 ozone concentrations in the Northeastern US for spring months in 2007.**

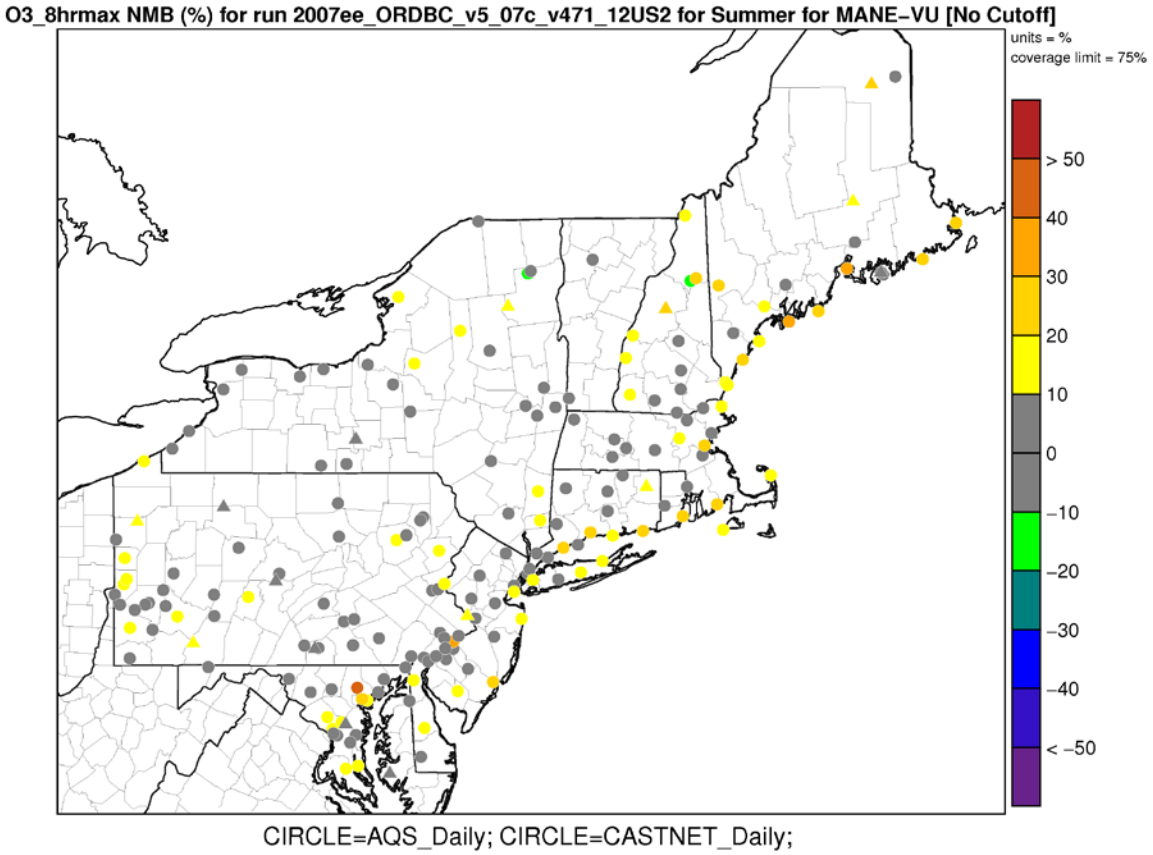


**Figure 4: Map of normalized mean bias for MDA8 ozone concentrations in the Northeastern US for summer months in 2007.**

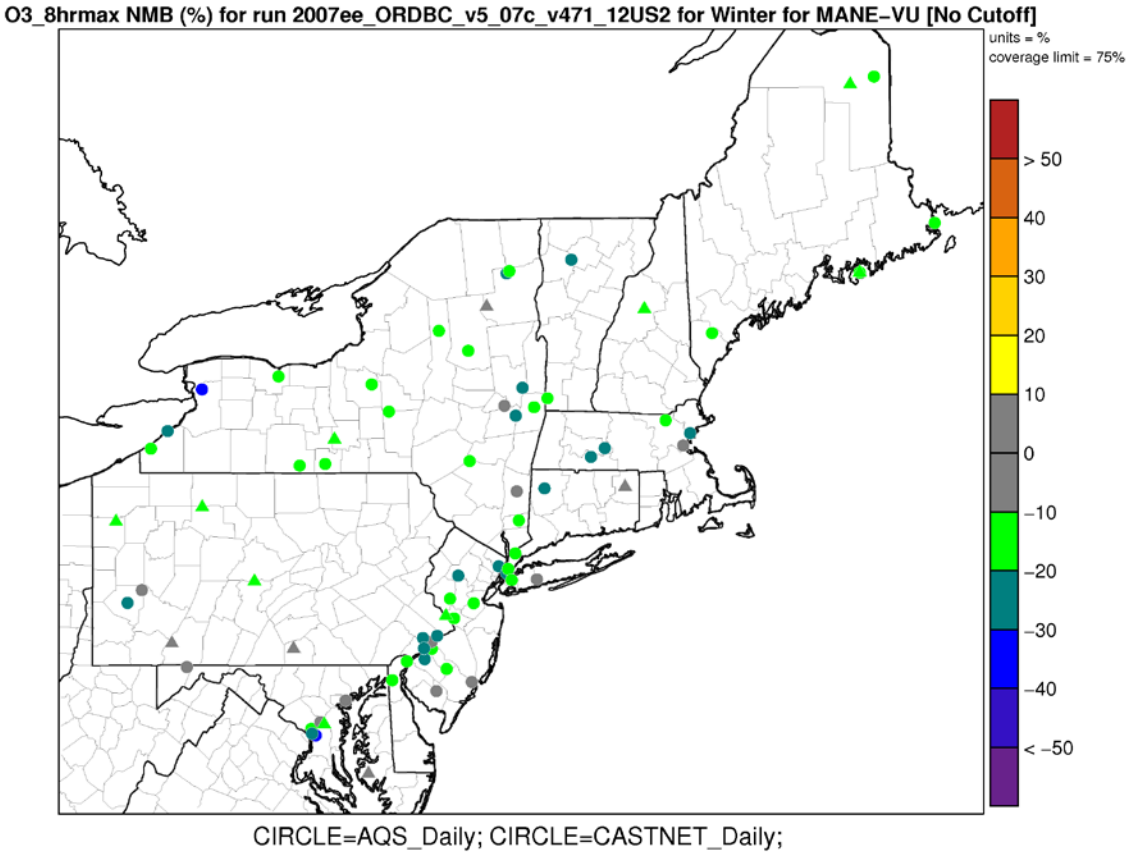


**Figure 5: Map of normalized mean bias for MDA8 ozone concentrations in the Northeastern US for fall months in 2007.**

**Table 5: Summary of CMAQ model performance at AQS monitoring sites in the Boston area**

| | | No. of obs | MB (ppb) | NMB (%) | ME (ppb) | NME (%) |
|---|---|---|---|---|---|---|
| Winter | Days < 60 | 265 | -3.91 | -15.1 | 5.40 | 20.9 |
| | Days ≥ 60 | 0 | NA | NA | NA | NA |
| | All Days | 265 | -3.91 | -15.1 | 5.40 | 20.9 |
| Spring | Days < 60 | 680 | -1.32 | -3.1 | 5.73 | 13.5 |
| | Days ≥ 60 | 87 | -4.95 | -7.0 | 8.46 | 11.9 |
| | All Days | 767 | -1.73 | -3.8 | 6.04 | 13.2 |
| Summer | Days < 60 | 784 | 6.71 | 16.5 | 8.47 | 20.8 |
| | Days ≥ 60 | 210 | -2.88 | -4.0 | 8.76 | 12.1 |
| | All Days | 994 | 4.69 | 9.9 | 8.53 | 18.0 |

| | | | | | | |
|---|---|---|---|---|---|---|
| Fall | Days < 60 | 433 | 3.69 | 11.3 | 6.22 | 19.0 |
| | Days ≥ 60 | 62 | -6.48 | -9.1 | 9.92 | 13.9 |
| | All Days | 495 | 2.42 | 6.4 | 6.68 | 17.8 |

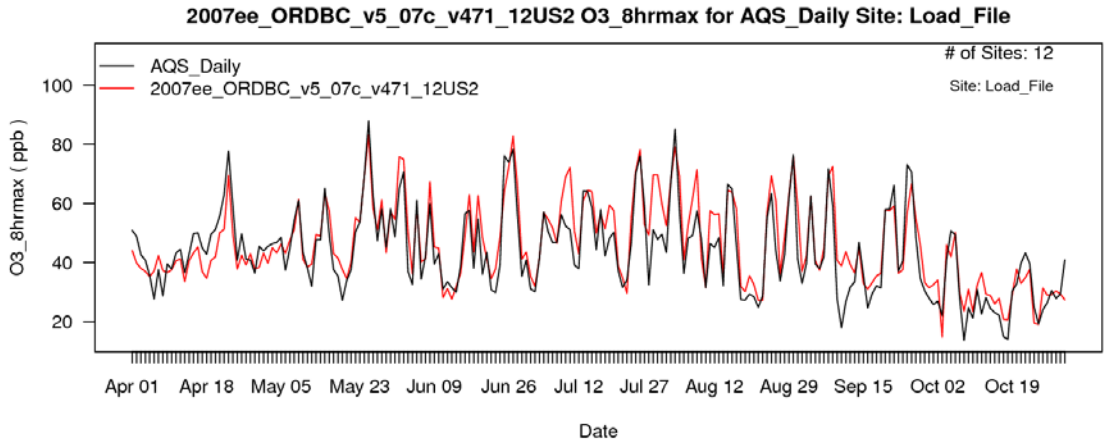


**Figure 6: Time series of 8-hr daily maximum ozone concentrations at Boston monitoring sites for April-October 2007. Observed values shown in black and modeled values shown in red.**

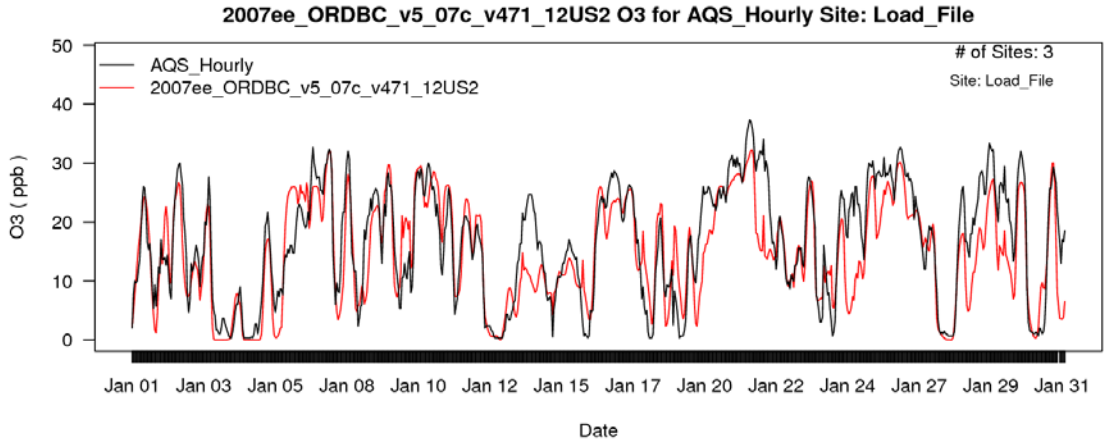


**Figure 7: Time series of hourly ozone concentrations at Boston monitoring sites for January 2007. Observed values shown in black and modeled values shown in red.**

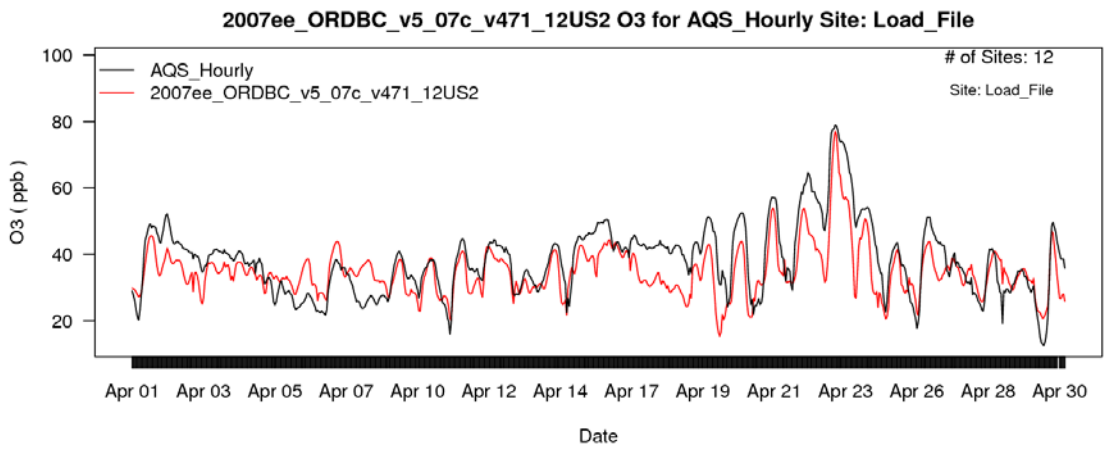


**Figure 8: Time series of hourly ozone concentrations at Boston monitoring sites for April 2007. Observed values shown in black and modeled values shown in red.**

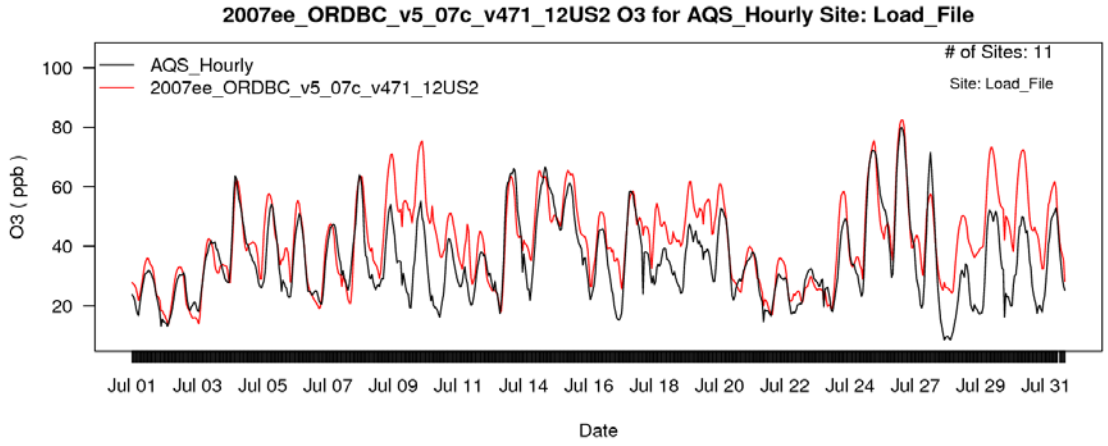


**Figure 9: Time series of hourly ozone concentrations at Boston monitoring sites for July 2007. Observed values shown in black and modeled values shown in red.**

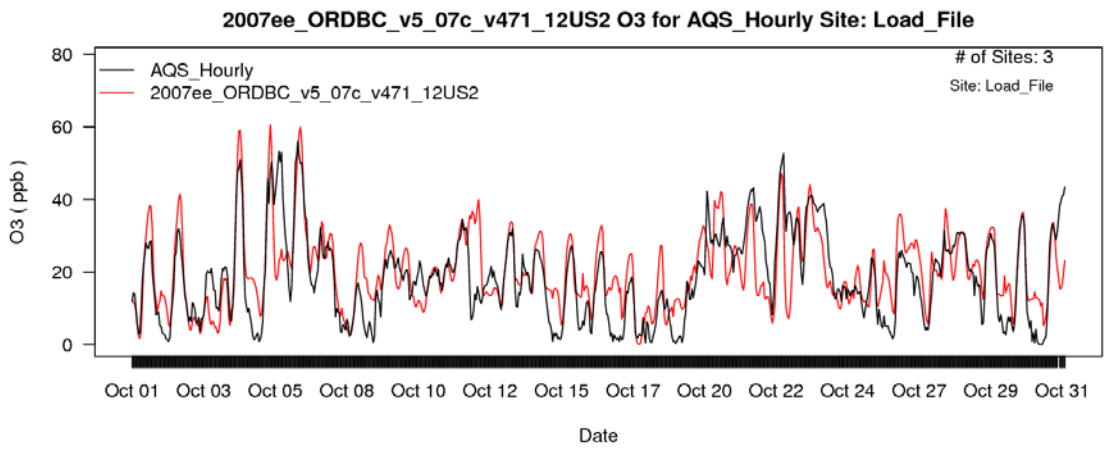


**Figure 10: Time series of hourly ozone concentrations at Boston monitoring sites for October 2007. Observed values shown in black and modeled values shown in red.**

**Table 6: Summary of CMAQ model performance at AQS monitoring sites in the New York area**

| | | No. of obs | MB (ppb) | NMB (%) | ME (ppb) | NME (%) |
|---|---|---|---|---|---|---|
| Winter | Days < 60 | 916 | -4.14 | -17.8 | 5.34 | 22.9 |
| | Days ≥ 60 | 0 | NA | NA | NA | NA |
| | All Days | 916 | -4.14 | -17.8 | 5.34 | 22.9 |
| Spring | Days < 60 | 1547 | -1.20 | -3.0 | 6.04 | 15.0 |
| | Days ≥ 60 | 200 | -6.05 | -8.5 | 9.45 | 13.2 |
| | All Days | 1747 | -1.75 | -4.0 | 6.43 | 14.7 |
| Summer | Days < 60 | 1469 | 5.16 | 12.3 | 8.53 | 20.4 |
| | Days ≥ 60 | 635 | 1.48 | 2.0 | 9.25 | 12.7 |
| | All Days | 2104 | 4.05 | 7.9 | 8.75 | 17.1 |
| Fall | Days < 60 | 1443 | 2.01 | 6.2 | 6.40 | 19.7 |
| | Days ≥ 60 | 108 | -5.60 | -8.1 | 8.90 | 12.8 |
| | All Days | 1551 | 1.48 | 4.2 | 6.58 | 18.7 |

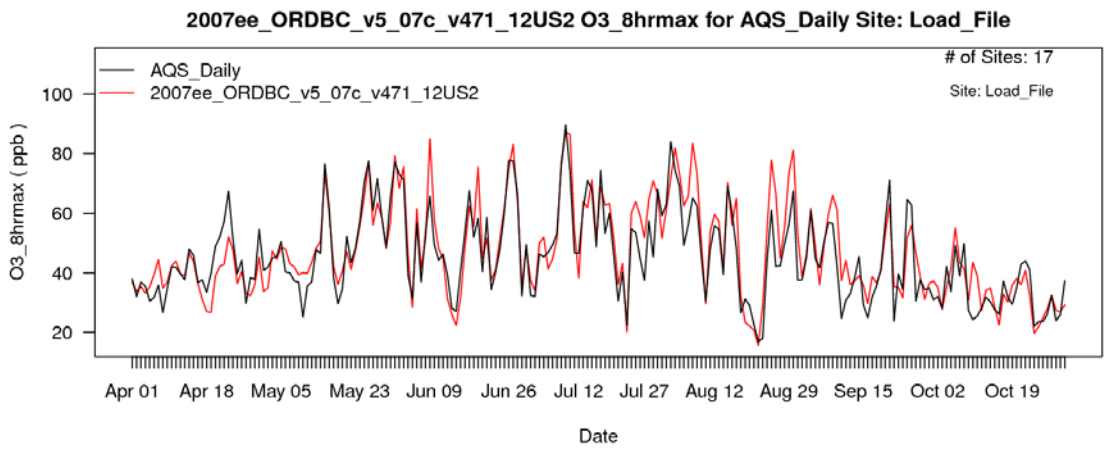


**Figure 11: Time series of 8-hr daily maximum ozone concentrations at New York monitoring sites for April-October 2007. Observed values shown in black and modeled values shown in red.**

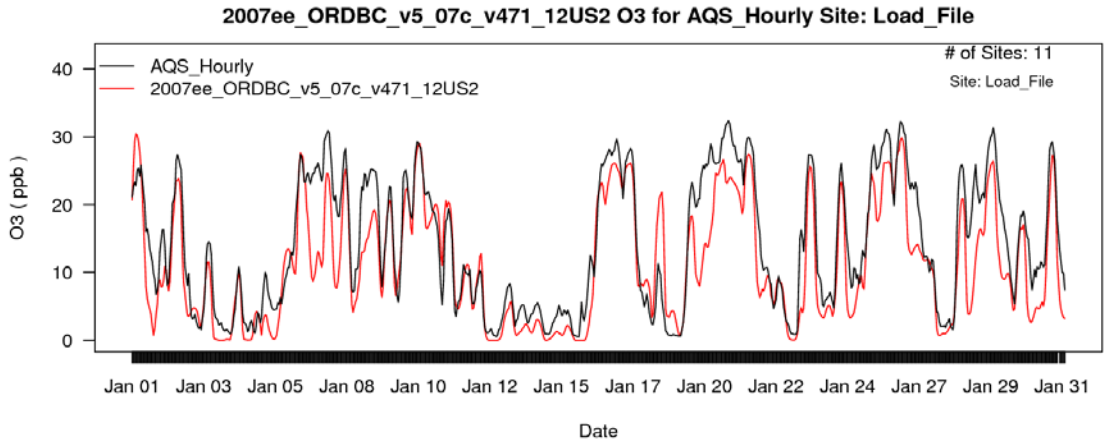


**Figure 12: Time series of hourly ozone concentrations at New York monitoring sites for January 2007. Observed values shown in black and modeled values shown in red.**

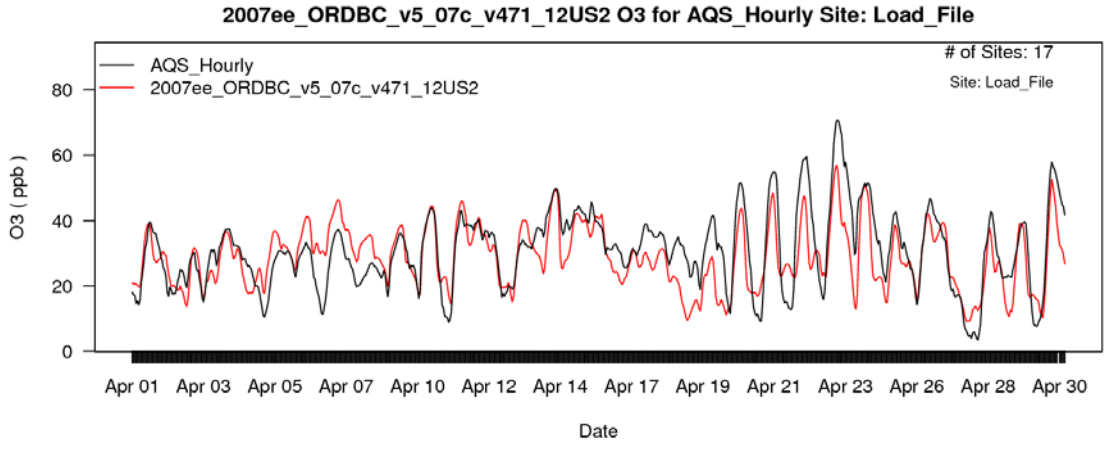

**Figure 13: Time series of hourly ozone concentrations at New York monitoring sites for April 2007. Observed values shown in black and modeled values shown in red.**

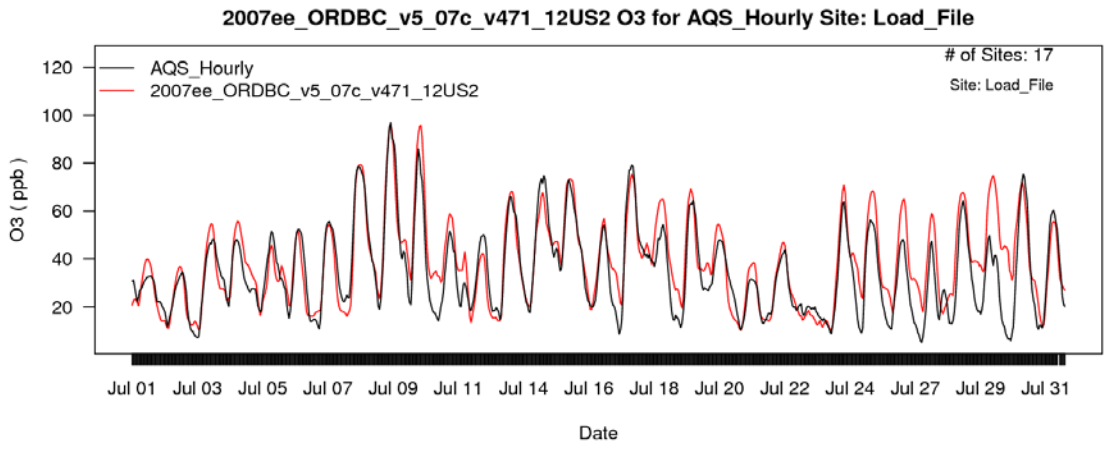


**Figure 14: Time series of hourly ozone concentrations at New York monitoring sites for July 2007. Observed values shown in black and modeled values shown in red.**

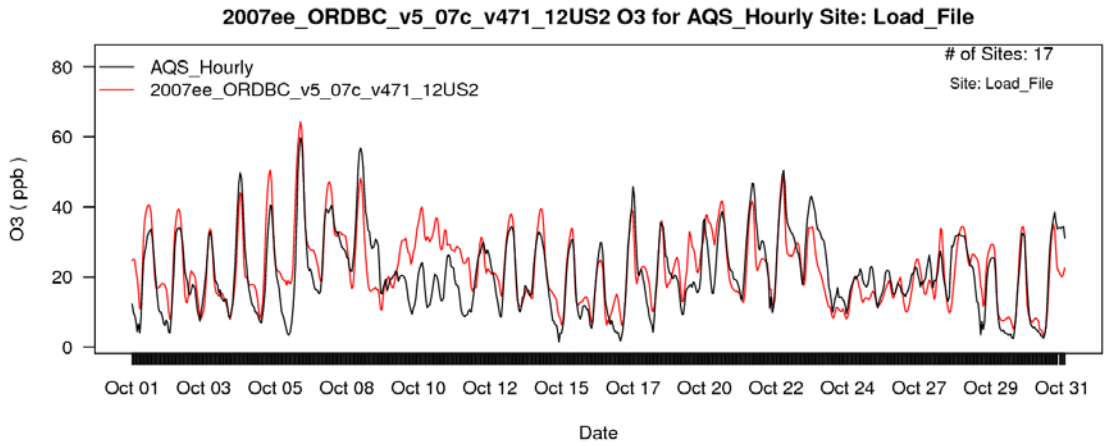


**Figure 15: Time series of hourly ozone concentrations at New York monitoring sites for October 2007. Observed values shown in black and modeled values shown in red.**

**Table 7: Summary of CMAQ model performance at AQS monitoring sites in the Philadelphia area**

| | | No. of obs | MB (ppb) | NMB (%) | ME (ppb) | NME (%) |
|---|---|---|---|---|---|---|
| Winter | Days < 60 | 684 | -3.48 | -14.4 | 5.15 | 21.3 |
| | Days ≥ 60 | 0 | NA | NA | NA | NA |
| | All Days | 684 | -3.48 | -14.4 | 5.15 | 21.3 |

| | | | | | | |
|---|---|---|---|---|---|---|
| Spring | Days < 60 | 942 | -0.80 | -1.9 | 5.93 | 14.1 |
| | Days ≥ 60 | 204 | -7.01 | -9.9 | 8.6 | 12.1 |
| | All Days | 1146 | -1.91 | -4.0 | 6.40 | 13.5 |
| Summer | Days < 60 | 778 | 6.25 | 9.44 | 14.1 | 21.3 |
| | Days ≥ 60 | 507 | 1.23 | 1.7 | 7.80 | 10.8 |
| | All Days | 1285 | 4.27 | 7.7 | 8.79 | 15.9 |
| Fall | Days < 60 | 1005 | 2.69 | 7.8 | 6.01 | 17.4 |
| | Days ≥ 60 | 103 | -4.51 | -6.7 | 7.68 | 11.4 |
| | All Days | 1108 | 2.02 | 5.4 | 6.16 | 16.4 |

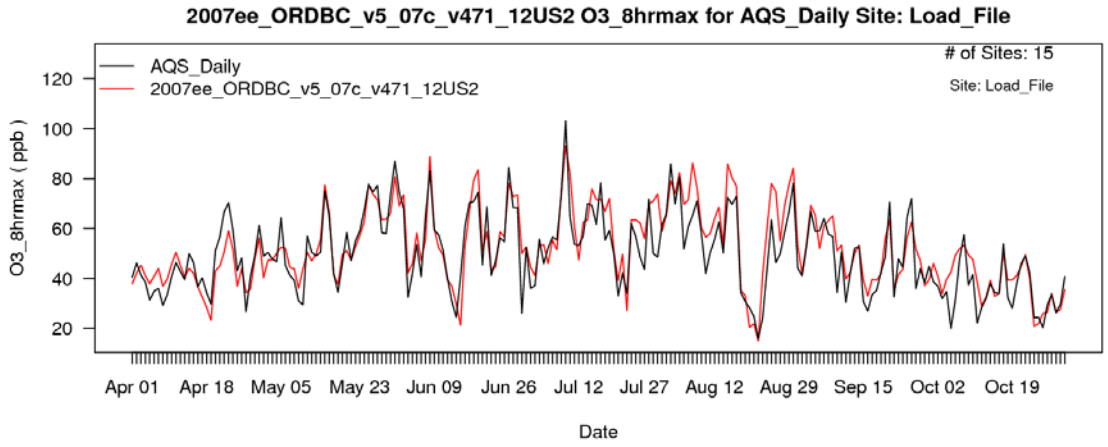


**Figure 16: Time series of 8-hr daily maximum ozone concentrations at Philadelphia monitoring sites for April-October 2007. Observed values shown in black and modeled values shown in red.**

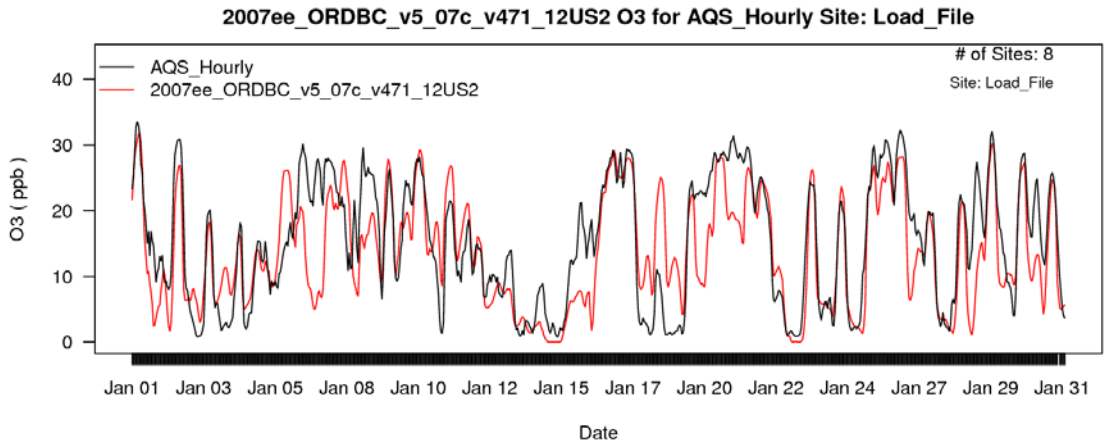

**Figure 17: Time series of hourly ozone concentrations at Philadelphia monitoring sites for January 2007. Observed values shown in black and modeled values shown in red.**

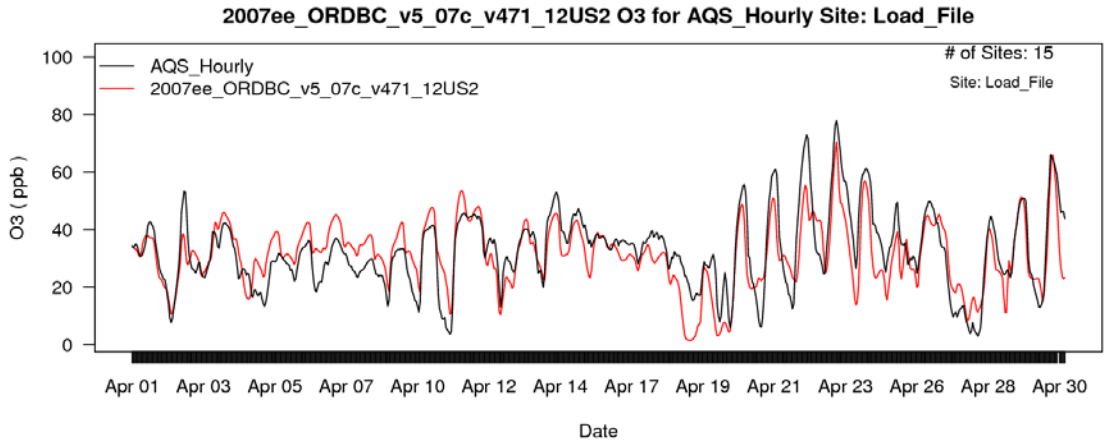


**Figure 18: Time series of hourly ozone concentrations at Philadelphia monitoring sites for April 2007. Observed values shown in black and modeled values shown in red.**

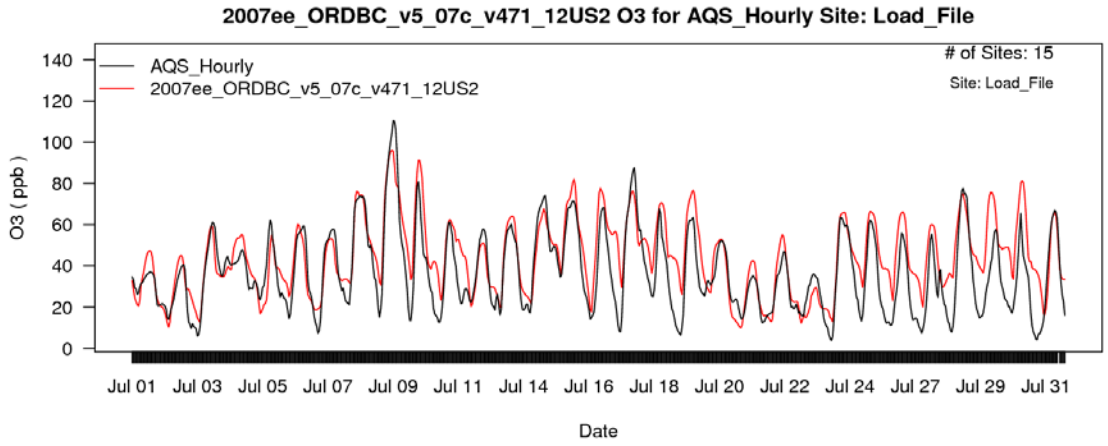


**Figure 19: Time series of hourly ozone concentrations at Philadelphia monitoring sites for July 2007. Observed values shown in black and modeled values shown in red.**

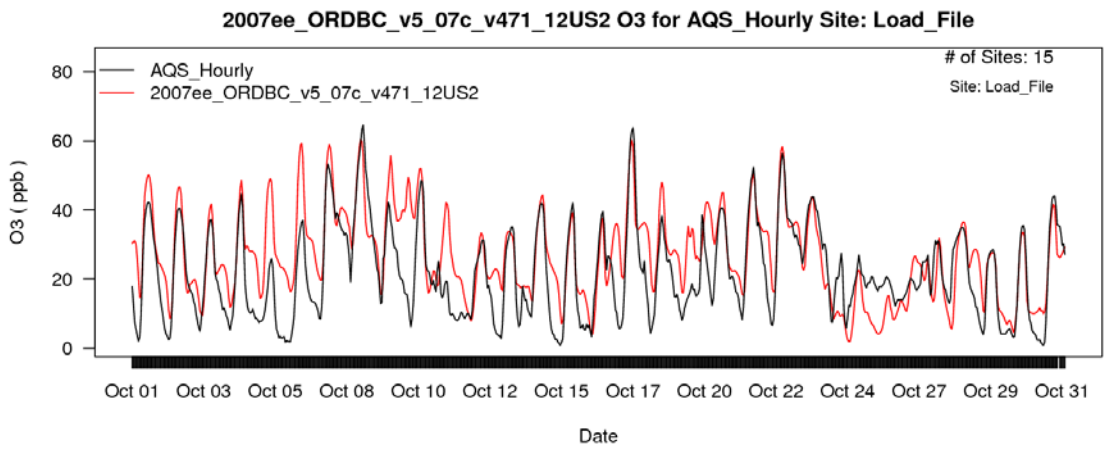


**Figure 20: Time series of hourly ozone concentrations at Philadelphia monitoring sites for October 2007. Observed values shown in black and modeled values shown in red.**

**Table 8: Summary of CMAQ model performance at AQS monitoring sites in the Baltimore area**

| | | No. of obs | MB (ppb) | NMB (%) | ME (ppb) | NME (%) |
|---|---|---|---|---|---|---|
| Winter | Days < 60 | 78 | -1.50 | -7.0 | 4.63 | 21.5 |
| | Days ≥ 60 | 0 | NA | NA | NA | NA |
| | All Days | 78 | -1.50 | -7.0 | 4.63 | 21.5 |
| Spring | Days < 60 | 358 | 4.62 | 11.1 | 6.81 | 16.3 |
| | Days ≥ 60 | 92 | -0.86 | -1.2 | 5.92 | 8.5 |
| | All Days | 450 | 3.50 | 7.4 | 6.62 | 14.0 |
| Summer | Days < 60 | 382 | 10.40 | 23.2 | 11.60 | 25.8 |
| | Days ≥ 60 | 255 | 4.18 | 5.7 | 8.95 | 12.3 |
| | All Days | 637 | 7.90 | 14.1 | 10.50 | 18.8 |
| Fall | Days < 60 | 389 | 6.63 | 17.9 | 8.35 | 22.5 |
| | Days ≥ 60 | 51 | -1.07 | -1.5 | 7.67 | 11.0 |
| | All Days | 440 | 5.74 | 14.1 | 8.27 | 20.2 |

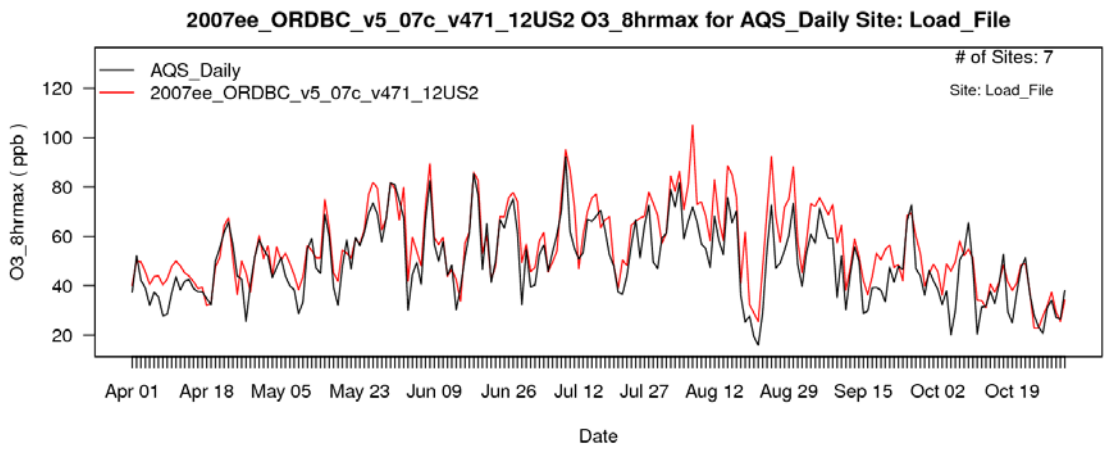


**Figure 21: Time series of 8-hr daily maximum ozone concentrations at Baltimore monitoring sites for April-October 2007. Observed values shown in black and modeled values shown in red.**

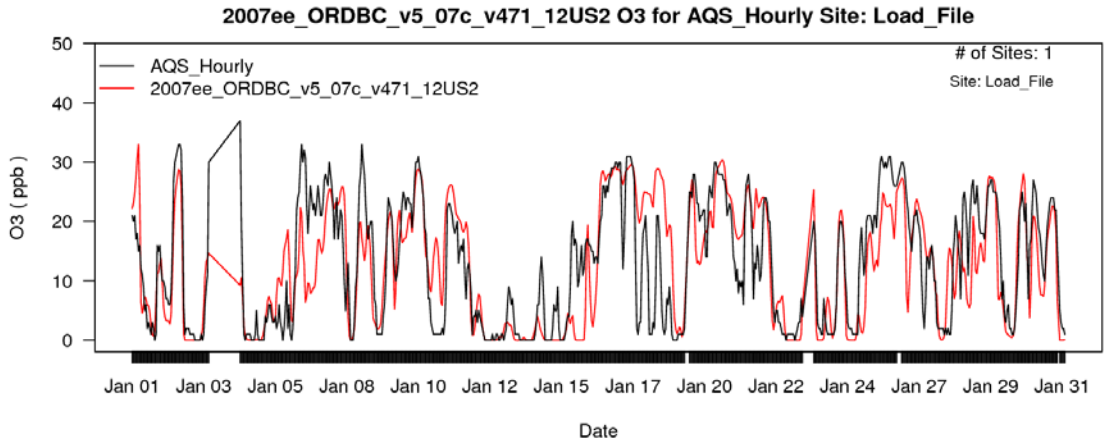


**Figure 22: Time series of hourly ozone concentrations at Baltimore monitoring sites for January 2007. Observed values shown in black and modeled values shown in red.**

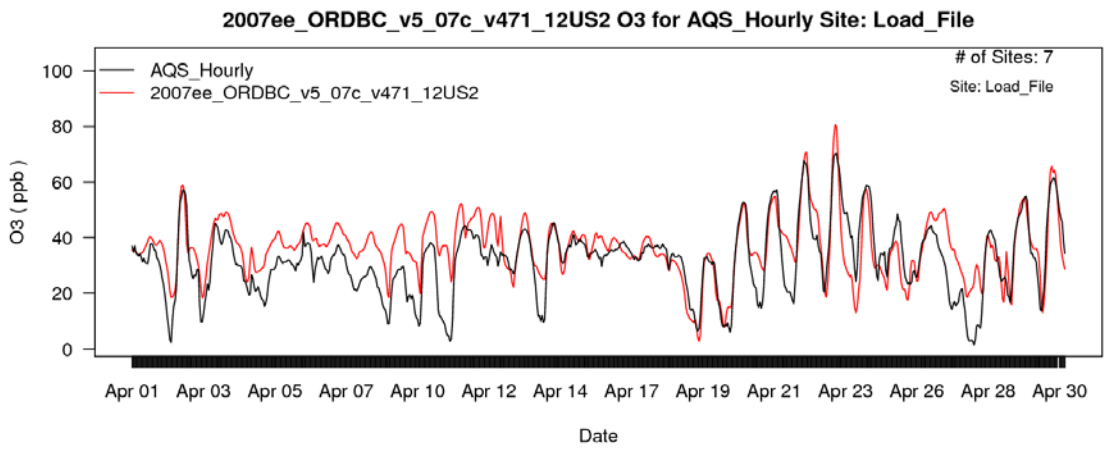


**Figure 23: Time series of hourly ozone concentrations at Baltimore monitoring sites for April 2007. Observed values shown in black and modeled values shown in red.**

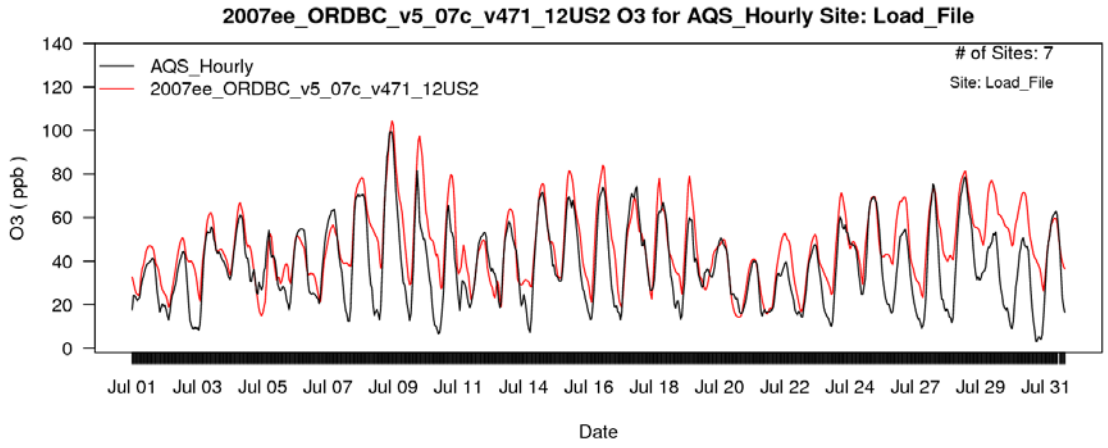


**Figure 24: Time series of hourly ozone concentrations at Baltimore monitoring sites for July 2007. Observed values shown in black and modeled values shown in red.**

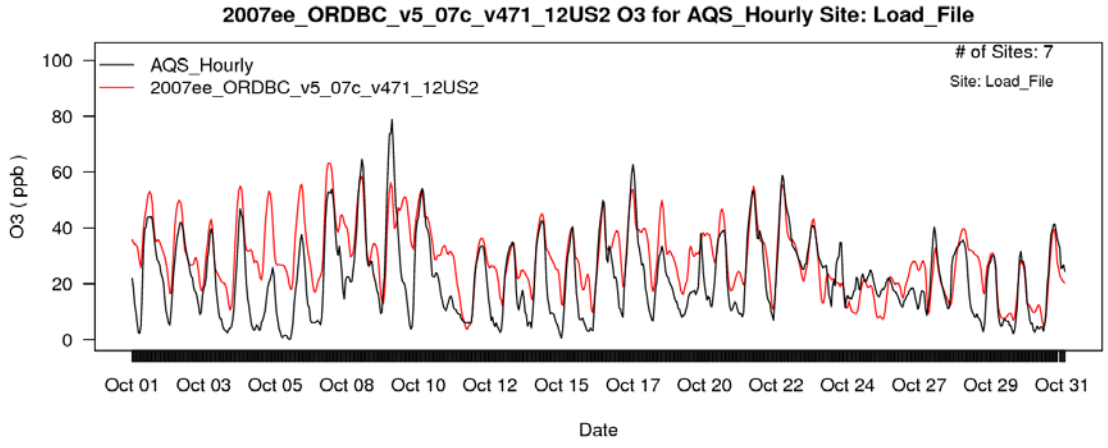

**Figure 25: Time series of hourly ozone concentrations at Baltimore monitoring sites for October 2007. Observed values shown in black and modeled values shown in red.**

**Table 9: Summary of CMAQ model performance at AQS monitoring sites in the Washington D.C. area**

| | | No. of obs | MB (ppb) | NMB (%) | ME (ppb) | NME (%) |
|---|---|---|---|---|---|---|
| Winter | Days < 60 | 565 | -4.97 | -20.5 | 6.12 | 25.2 |
| | Days ≥ 60 | 0 | NA | NA | NA | NA |
| | All Days | 565 | -4.97 | -20.5 | 6.12 | 25.2 |
| Spring | Days < 60 | 1120 | -0.95 | -2.2 | 6.11 | 14.2 |
| | Days ≥ 60 | 334 | -4.98 | -7.3 | 7.00 | 10.2 |
| | All Days | 1454 | -1.88 | -3.8 | 6.31 | 12.9 |
| Summer | Days < 60 | 1066 | 6.55 | 13.9 | 8.24 | 17.5 |
| | Days ≥ 60 | 819 | 2.36 | 3.3 | 7.13 | 10.2 |
| | All Days | 1885 | 4.73 | 8.3 | 7.76 | 13.6 |
| Fall | Days < 60 | 1188 | 2.07 | 5.4 | 7.22 | 19.0 |
| | Days ≥ 60 | 106 | -2.03 | -3.0 | 8.37 | 12.4 |
| | All Days | 1394 | 1.46 | 3.5 | 7.39 | 17.4 |

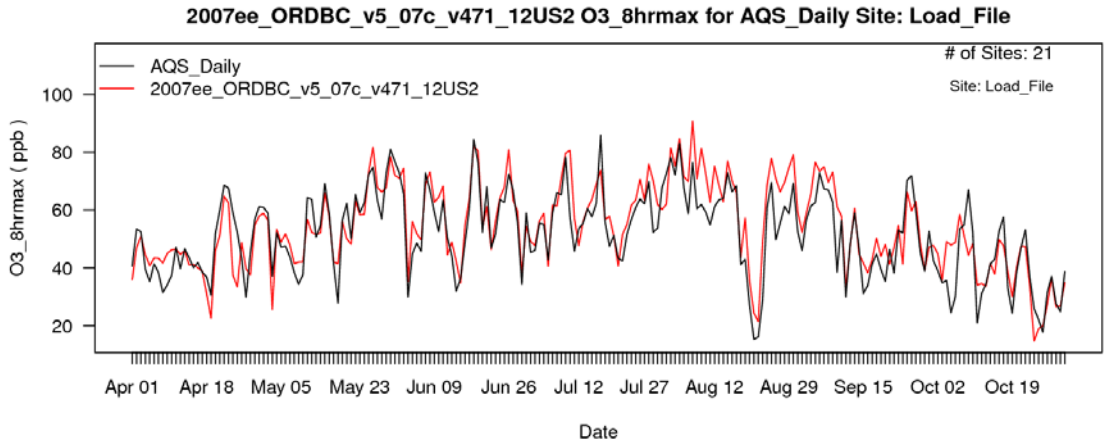


**Figure 26: Time series of 8-hr daily maximum ozone concentrations at Washington D.C. monitoring sites for April-October 2007. Observed values shown in black and modeled values shown in red.**

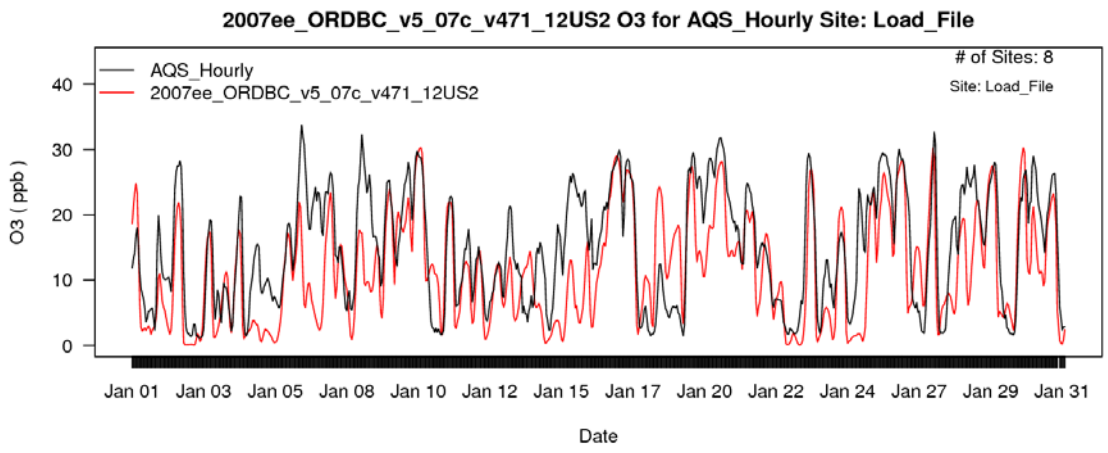


**Figure 27: Time series of hourly ozone concentrations at Washington D.C. monitoring sites for January 2007. Observed values shown in black and modeled values shown in red.**

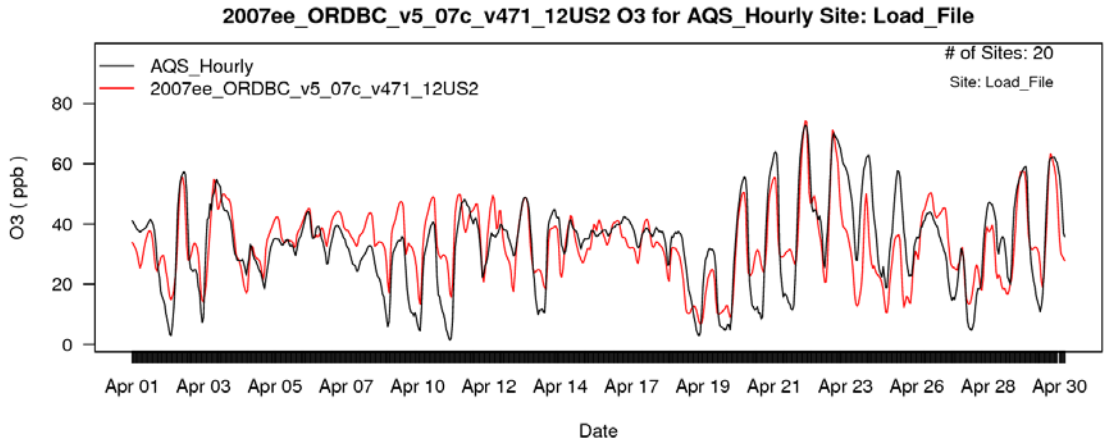


**Figure 28: Time series of hourly ozone concentrations at Washington D.C. monitoring sites for April 2007. Observed values shown in black and modeled values shown in red.**

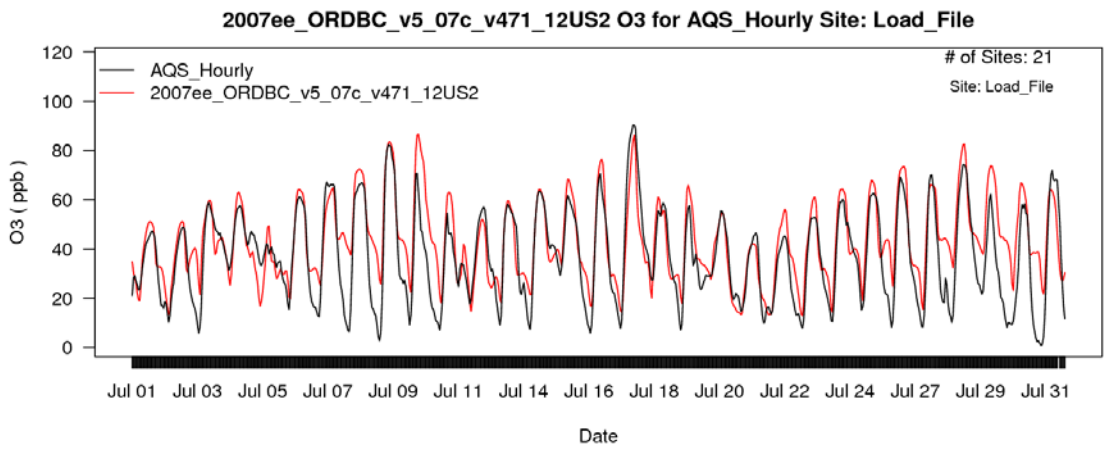


**Figure 29: Time series of hourly ozone concentrations at Washington D.C. monitoring sites for July 2007. Observed values shown in black and modeled values shown in red.**

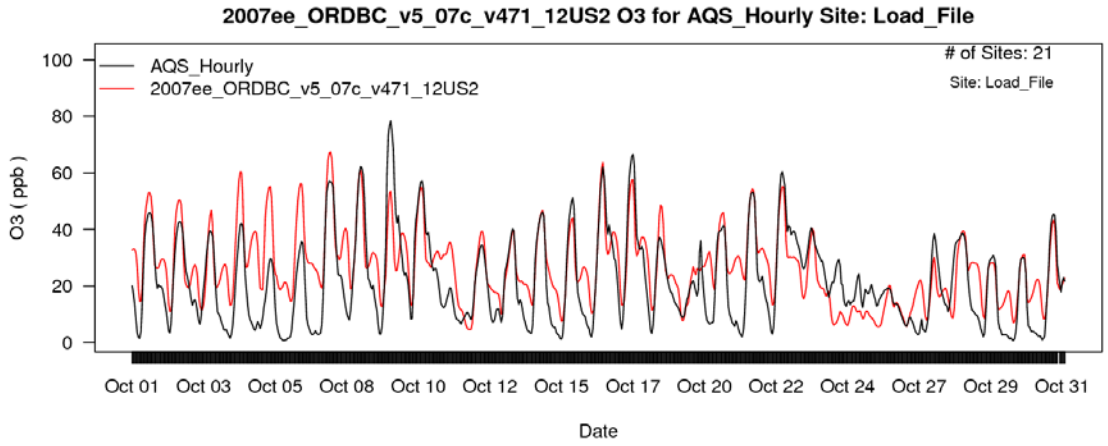


**Figure 30: Time series of hourly ozone concentrations at Washington D.C. monitoring sites for October 2007. Observed values shown in black and modeled values shown in red.**

## OPERATIONAL EVALUATION IN THE SOUTHEAST U.S.

Model performance in the Southeastern US was in the range of reported performance for state of the science models (Simon et al., 2012). Mean bias for MDA8 ozone was less than 5 ppb at most sites in the winter and spring and less than 10 ppb at most sites in the summer and fall seasons. Normalized mean bias was generally less than 10% at most sites in the winter and spring and less than 25% at most sites in the summer and fall. Also, there were very few days above 60 ppb in the winter season (4 days at two sites and 0,1, or 2 days at all other sites), but

the model generally had trouble capturing ozone on those days and had mean biases in the range of -5 to -15 ppb on those days. The higher biases in the summer and fall are most pronounced along the Gulf coast and at sites in Florida. Atlanta was the only one of the 15 urban areas from the REA which was located in the Southeast region.

There were no ozone measurements in the Atlanta area during the winter season. Mean bias and normalized mean bias at Atlanta sites for the spring, summer, and fall months were typical of performance throughout the Southeast region. The April to June MDA8 ozone time series (Figure 35) shows that the model does a good job of capturing the variability between high and low ozone days. The hourly time series plots for April (Figure 36), July (Figure 37), and October (Figure 38) show reasonable model performance during daytime hours but some persistent overestimates of nighttime ozone, especially in April and July.

**Table 10: Summary of CMAQ model performance at AQS monitoring sites in the Southeastern US**

| | | No. of obs | MB (ppb) | NMB (%) | ME (ppb) | NME (%) |
|---|---|---|---|---|---|---|
| Winter | Days < 60 | 6378 | 0.13 | 0.4 | 5.32 | 15.7 |
| | Days ≥ 60 | 53 | -10.40 | -16.1 | 11.10 | 17.2 |
| | All Days | 6431 | 0.04 | 0.1 | 5.37 | 15.7 |
| Spring | Days < 60 | 13326 | 1.10 | 2.3 | 5.22 | 10.8 |
| | Days ≥ 60 | 5190 | -4.94 | -7.4 | 6.45 | 9.6 |
| | All Days | 18516 | -0.60 | -1.1 | 5.57 | 10.4 |
| Summer | Days < 60 | 14129 | 10.3 | 23.2 | 11.2 | 25.3 |
| | Days ≥ 60 | 6336 | 0.3 | 0.5 | 6.7 | 9.6 |
| | All Days | 20465 | 7.20 | 13.8 | 9.82 | 18.8 |
| Fall | Days < 60 | 14105 | 5.43 | 13.9 | 7.67 | 19.7 |
| | Days ≥ 60 | 1743 | -1.44 | -2.1 | 6.40 | 9.5 |
| | All Days | 15848 | 4.67 | 11.1 | 7.53 | 17.9 |

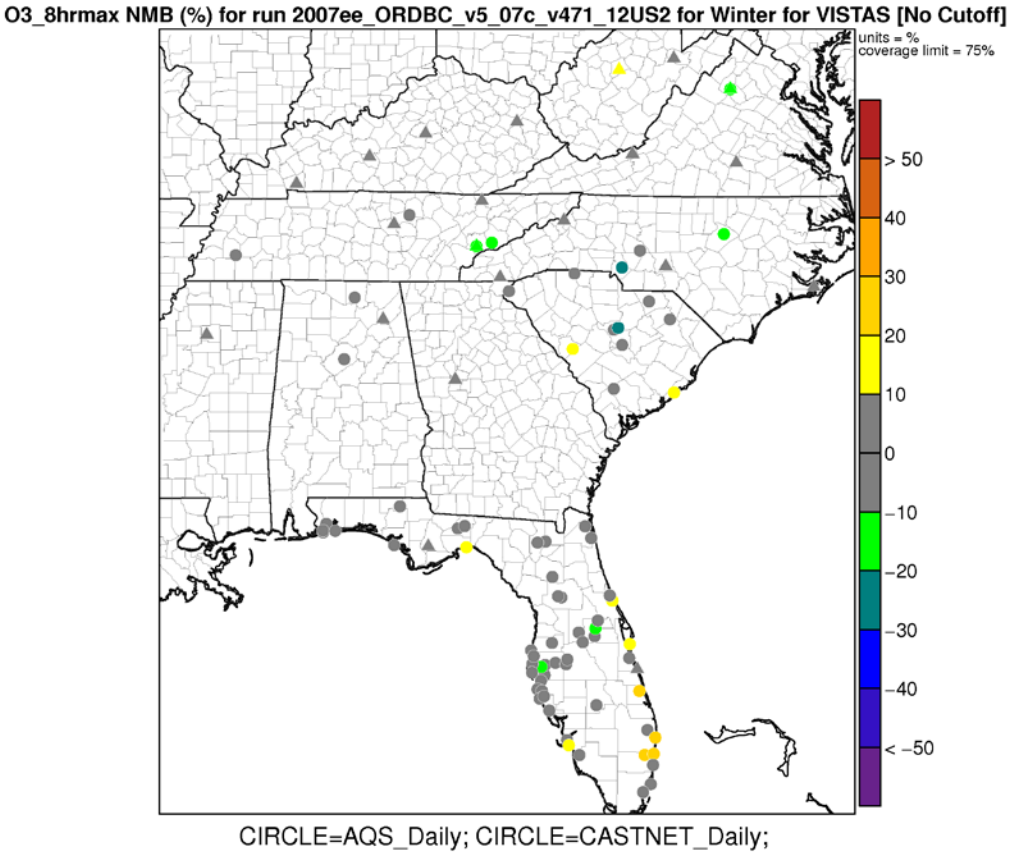


**Figure 31: Map of normalized mean bias for MDA8 ozone concentrations in the Southeastern US for winter months in 2007.**

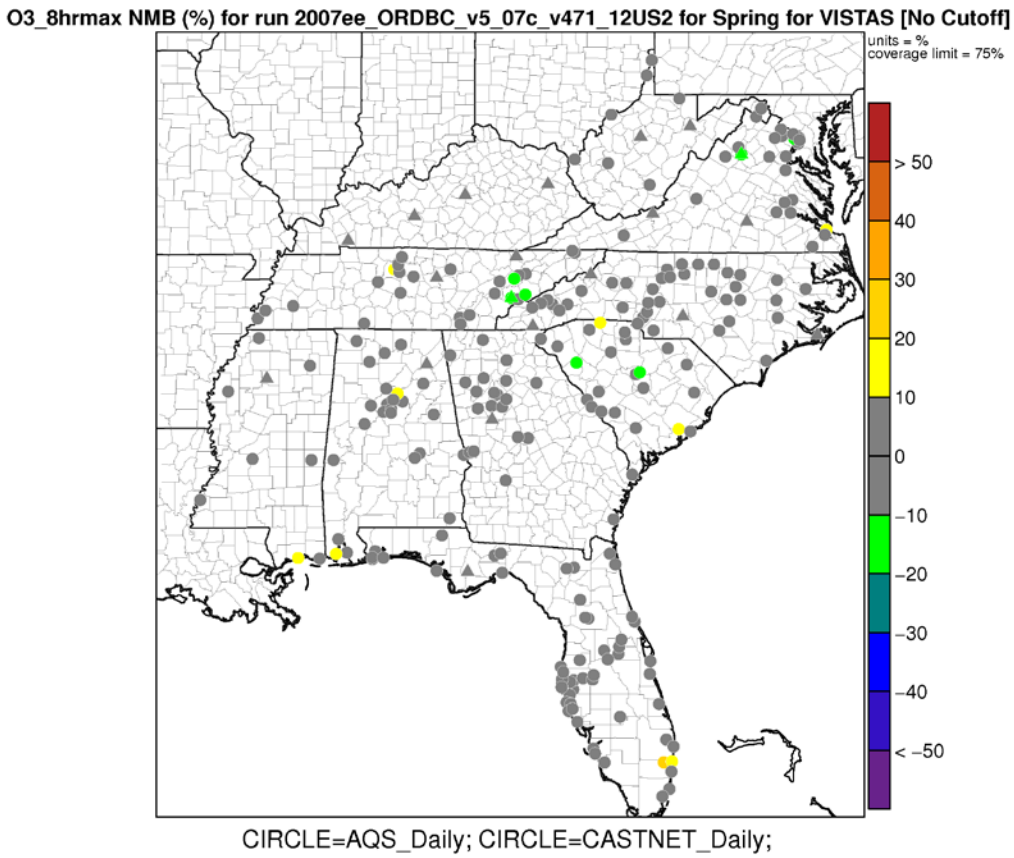


**Figure 32: Map of normalized mean bias for MDA8 ozone concentrations in the Southeastern US for spring months in 2007.**

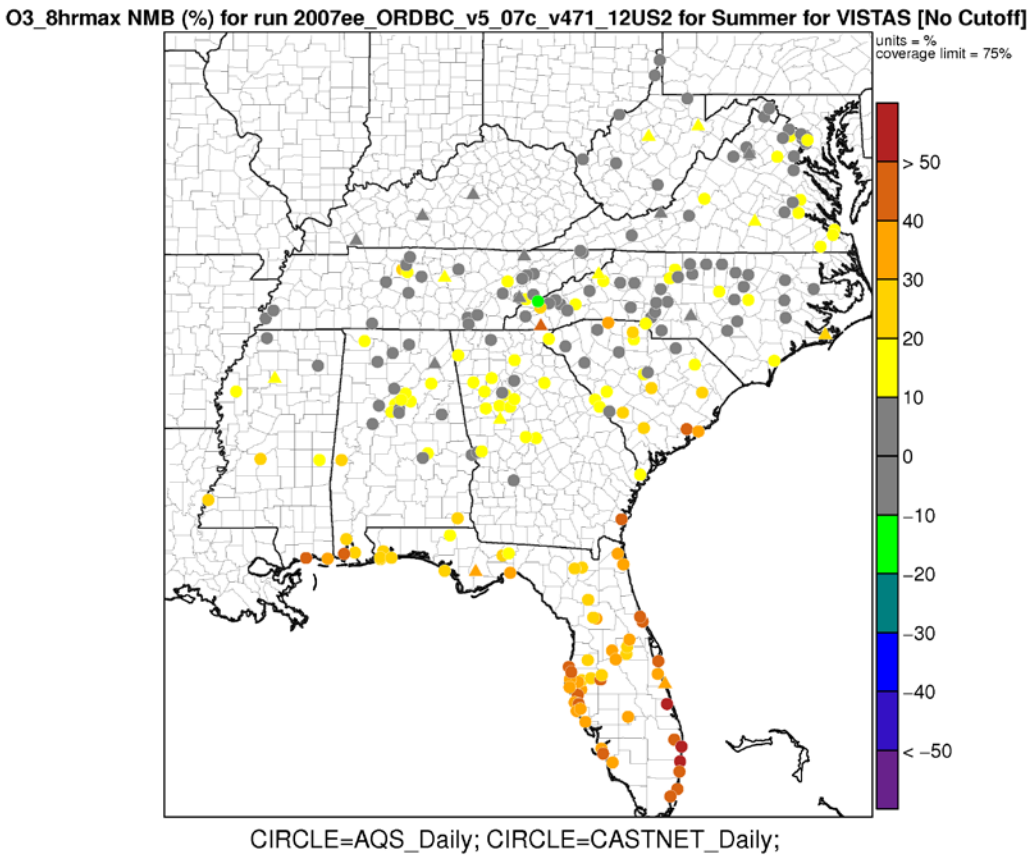


**Figure 33: Map of normalized mean bias for MDA8 ozone concentrations in the Southeastern US for summer months in 2007.**

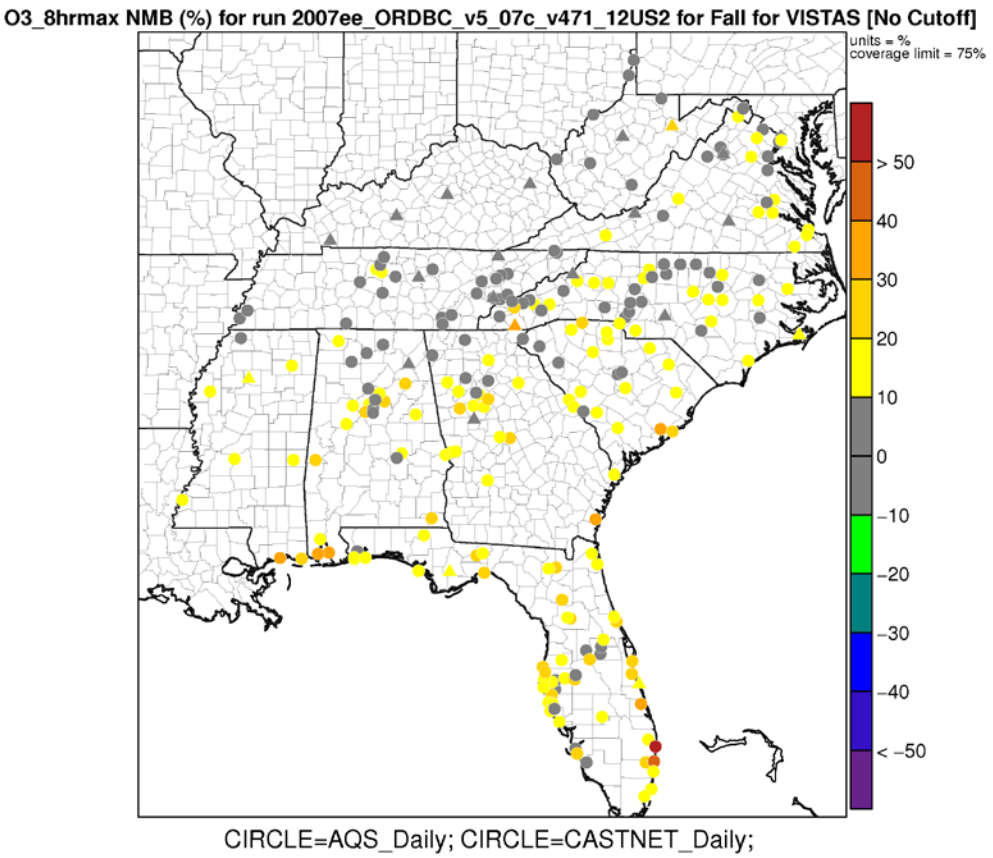


**Figure 34: Map of normalized mean bias for MDA8 ozone concentrations in the Southeastern US for fall months in 2007.**

**Table 11: Summary of CMAQ model performance at AQS monitoring sites in the Atlanta area**

| | | No. of obs | MB (ppb) | NMB (%) | ME (ppb) | NME (%) |
|---|---|---|---|---|---|---|
| Winter | Days < 60 | 0 | NA | NA | NA | NA |
| | Days ≥ 60 | 0 | NA | NA | NA | NA |
| | All Days | 0 | NA | NA | NA | NA |
| Spring | Days < 60 | 703 | 0.52 | 1.1 | 5.99 | 12.5 |
| | Days ≥ 60 | 295 | -3.08 | -4.6 | 6.03 | 9.0 |
| | All Days | 998 | -0.54 | -1.0 | 6.00 | 11.2 |
| Summer | Days < 60 | 510 | 10.00 | 21.7 | 11.50 | 24.8 |
| | Days ≥ 60 | 467 | 3.77 | 5.2 | 8.46 | 11.5 |
| | All Days | 977 | 7.04 | 11.9 | 10.00 | 17.0 |

| | | | | | | |
|---|---|---|---|---|---|---|
| Fall | Days < 60 | 575 | 5.45 | 13.7 | 7.72 | 19.4 |
| | Days ≥ 60 | 87 | 4.01 | 5.9 | 6.27 | 9.2 |
| | All Days | 662 | 5.26 | 12.1 | 7.53 | 17.3 |

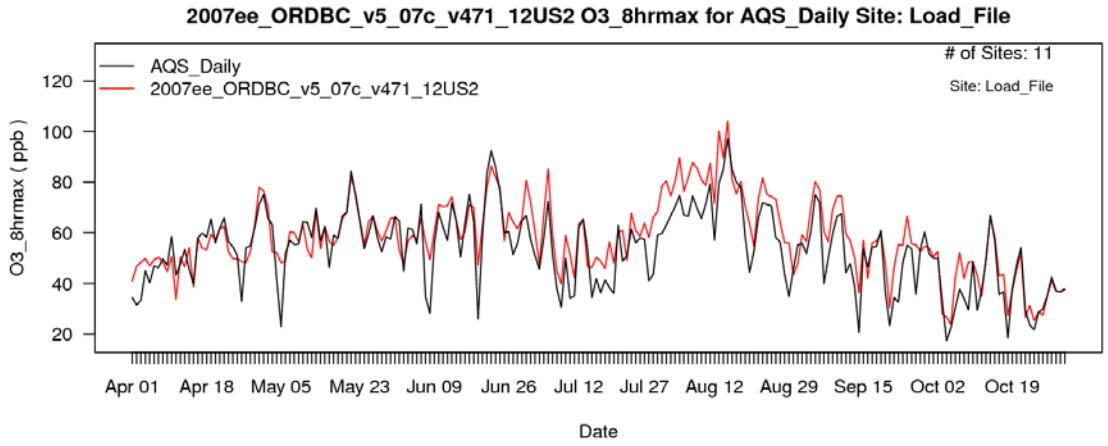


**Figure 35: Time series of 8-hr daily maximum ozone concentrations at Atlanta monitoring sites for April-October 2007. Observed values shown in black and modeled values shown in red.**

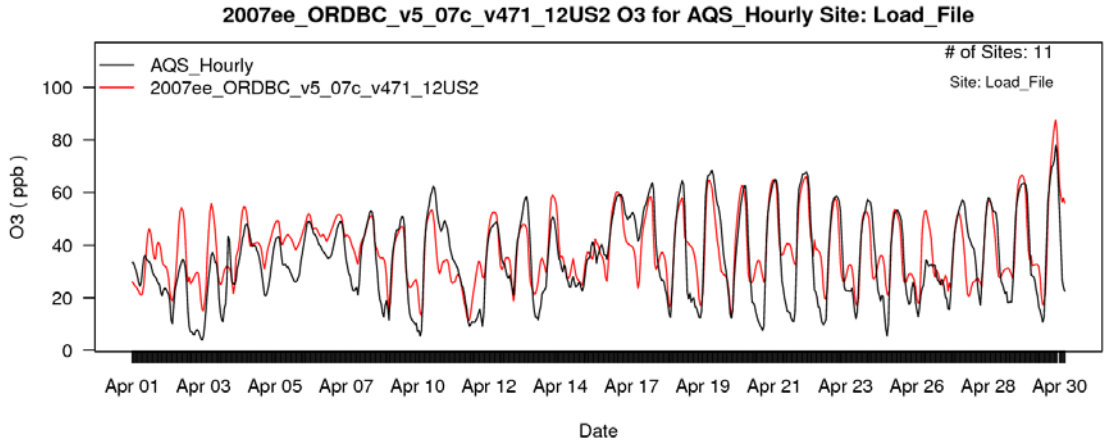


**Figure 36: Time series of hourly ozone concentrations at Atlanta monitoring sites for April 2007. Observed values shown in black and modeled values shown in red.**

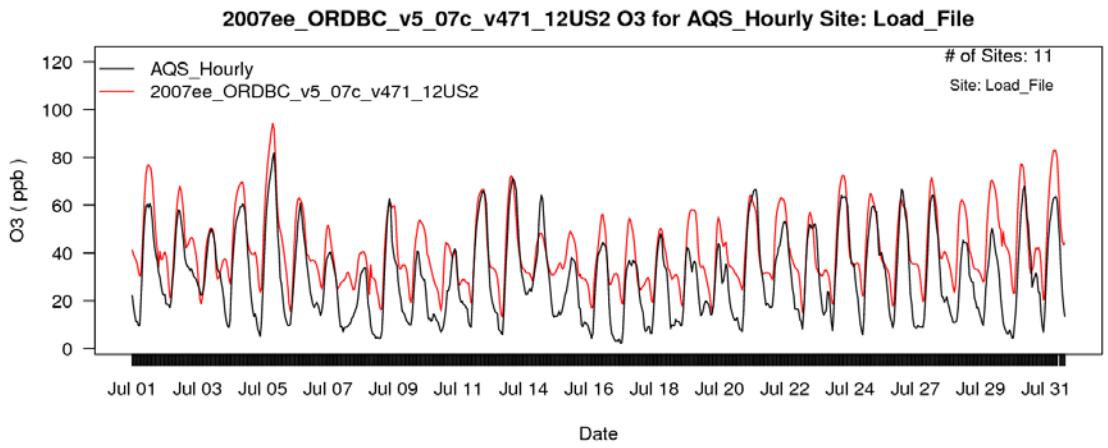


**Figure 37: Time series of hourly ozone concentrations at Atlanta monitoring sites for July 2007. Observed values shown in black and modeled values shown in red.**

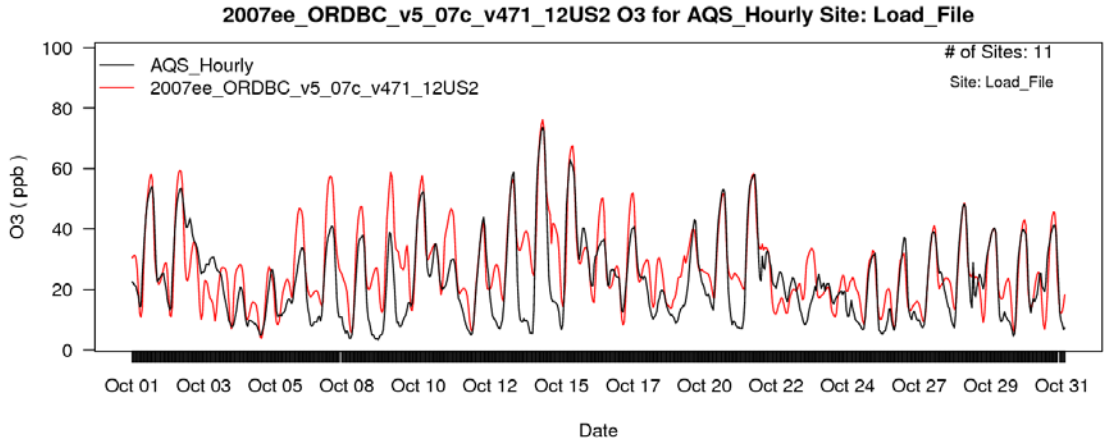


**Figure 38: Time series of hourly ozone concentrations at Atlanta monitoring sites for October 2007. Observed values shown in black and modeled values shown in red.**

## OPERATIONAL EVALUATION IN THE MIDWEST

The model performed well compared to observed ozone concentrations in the Midwest. Mean bias for MDA8 ozone was around 5 ppb or less at most sites in the winter, spring, and fall and less than 7 ppb at most sites in the summer. Normalized mean bias for MDA8 ozone was less than 15% at most sites except in the winter when it was somewhat higher (less than 20% at most sites) due to lower observed ozone concentrations. The model was more likely to be biased high on low ozone days and biased low on higher ozone days. No distinct spatial trends are apparent from the maps of normalized mean bias (Figure 39-Figure 42). Three urban areas

in the Midwest were examined more closely for this evaluation: Chicago, Cleveland, and Detroit.

Chicago performance statistics for MDA8 ozone were similar to those of the rest of the region. The time series of MDA8 ozone from Apr-Oct 2007 (Figure 43) as well as the hourly time series for January, April, July, and October (Figure 44-Figure 47) all show that the model does a good job of capturing synoptic variations in ozone observed in Chicago and reasonably captures both day and nighttime measured concentrations.

No measurements were made during the winter season in Cleveland. MB for MDA8 ozone on high days (≥ 60 ppb) was similar to MB in the rest of the region, but MB on low ozone days was somewhat higher than was typically seen in the Midwest (4 ppb vs. 1 ppb in the spring, 11 ppb vs. 6 ppb in the summer, and 4 ppb vs. 3 ppb in the fall). The time series plots for Cleveland sites show good correlation with observed ozone, although a period of moderate model over-estimates in daytime ozone is depicted in July (Figure 48 and Figure 50). Nighttime ozone concentrations are often overestimated by the model except in the time series shown for April, July, and October the latter portion of October, 2007.

Detroit area sites did not report any ozone measurements during the winter of 2007. Detroit performance statistics for MDA8 ozone were similar to those from the rest of the Midwest; however under-estimates on high ozone days were more pronounced in Detroit than in the rest of the region. The time series shows that the model accurately estimates both day and nighttime hourly ozone in Detroit in April and July and generally captures the variations in MDA8 ozone across the April-October time period.

**Table 12: Summary of CMAQ model performance at AQS monitoring sites in the Midwest**

| | | No. of obs | MB (ppb) | NMB (%) | ME (ppb) | NME (%) |
|---|---|---|---|---|---|---|
| Winter | Days < 60 | 2824 | -3.76 | -15.1 | 5.36 | 21.5 |
| | Days ≥ 60 | 0 | NA | NA | NA | NA |
| | All Days | 2824 | -3.76 | -15.1 | 5.36 | 21.5 |
| Spring | Days < 60 | 9447 | 1.11 | 2.6 | 5.55 | 12.8 |
| | Days ≥ 60 | 2403 | -6.19 | -8.9 | 7.38 | 10.6 |
| | All Days | 11850 | -0.37 | -0.8 | 5.92 | 12.2 |
| Summer | Days < 60 | 12478 | 6.31 | 14.2 | 8.39 | 18.8 |
| | Days ≥ 60 | 4114 | -1.19 | -1.7 | 7.56 | 10.8 |
| | All Days | 16592 | 4.45 | 8.8 | 8.18 | 16.1 |
| Fall | Days < 60 | 8207 | 2.94 | 8.2 | 6.22 | 17.3 |

| | | | | | | |
|---|---|---|---|---|---|---|
| | Days ≥ 60 | 1382 | -4.48 | -6.5 | 7.72 | 11.1 |
| | All Days | 9589 | 1.87 | 4.6 | 6.44 | 15.8 |

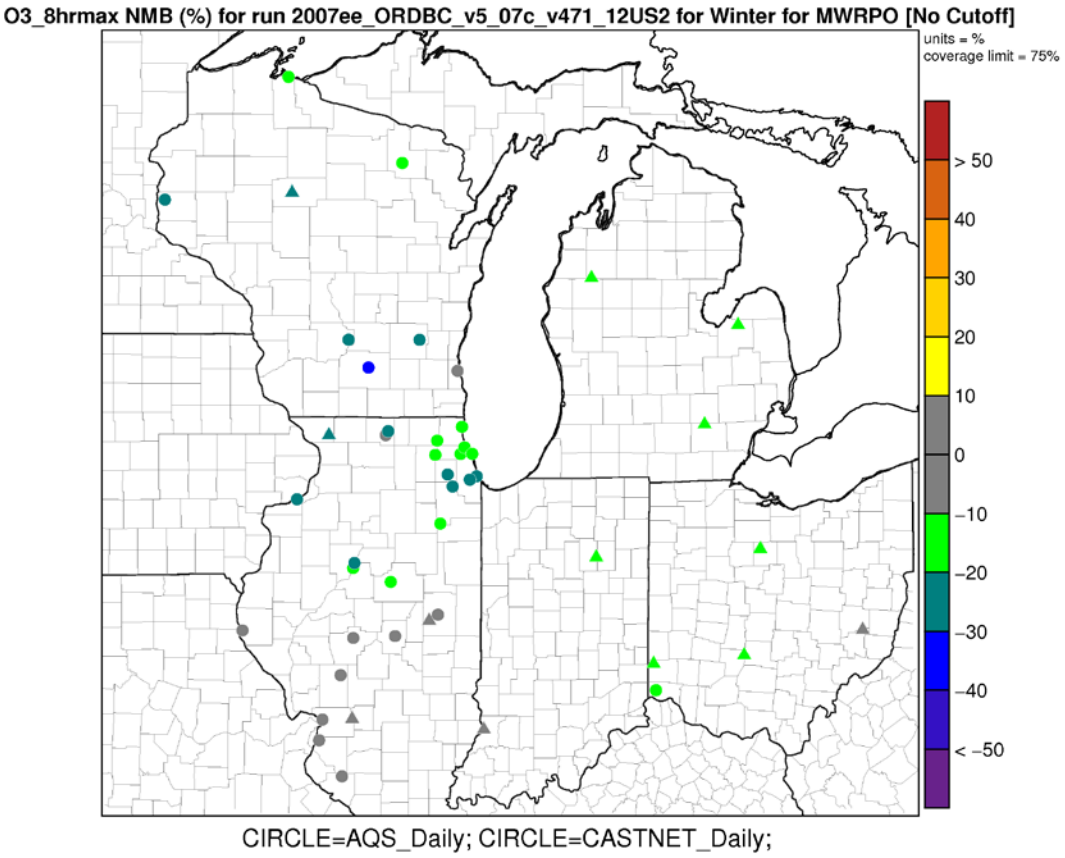


**Figure 39: Map of normalized mean bias for MDA8 ozone concentrations in the Midwest for winter months in 2007.**

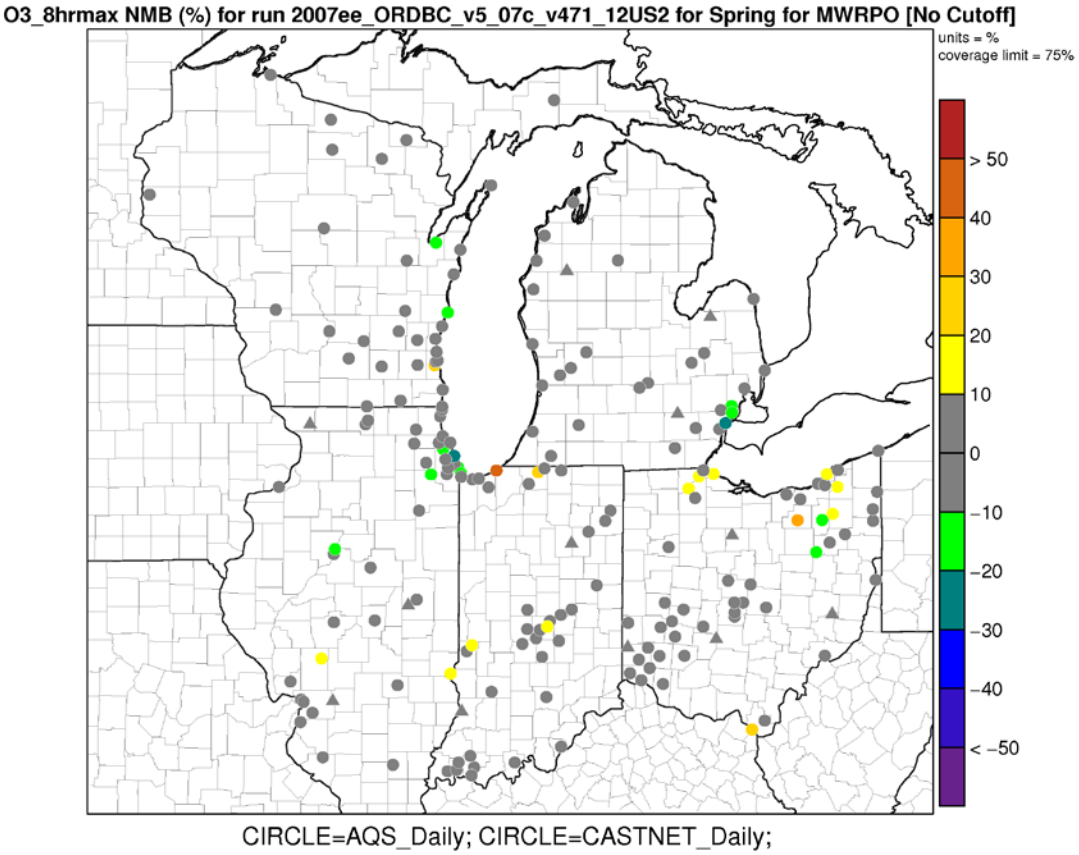


**Figure 40: Map of normalized mean bias for MDA8 ozone concentrations in the Midwest for spring months in 2007.**

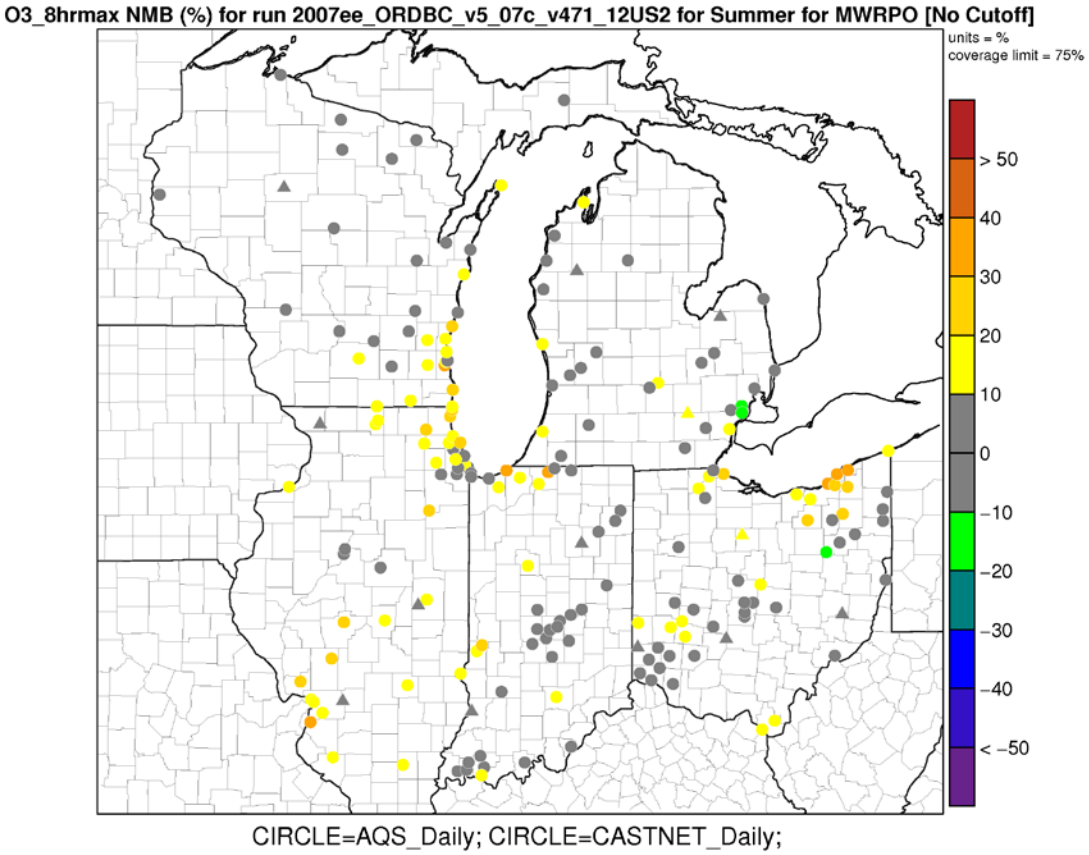


**Figure 41: Map of normalized mean bias for MDA8 ozone concentrations in the Midwest for summer months in 2007.**

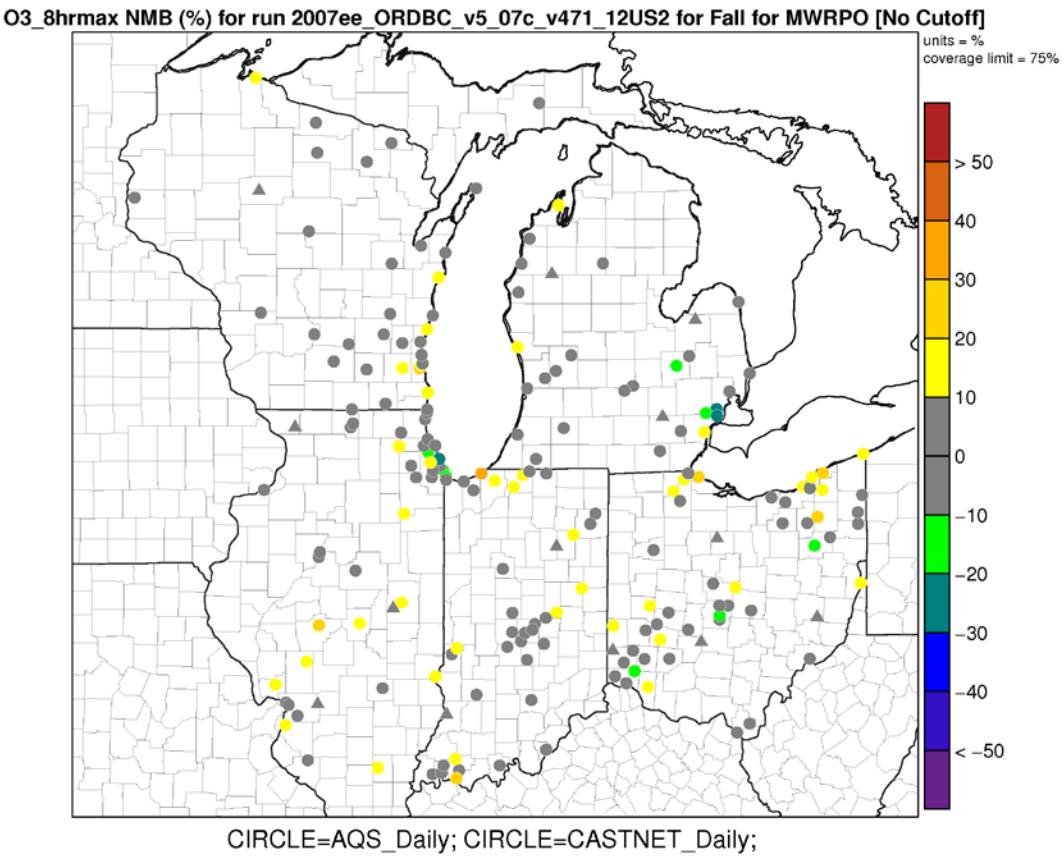


**Figure 42: Map of normalized mean bias for MDA8 ozone concentrations in the Midwest for fall months in 2007.**

**Table 13: Summary of CMAQ model performance at AQS monitoring sites in the Chicago area**

| | | No. of obs | MB (ppb) | NMB (%) | ME (ppb) | NME (%) |
|---|---|---|---|---|---|---|
| Winter | Days < 60 | 963 | -3.93 | -17.5 | 5.13 | 22.9 |
| | Days ≥ 60 | 0 | NA | NA | NA | NA |
| | All Days | 963 | -3.93 | -17.5 | 5.13 | 22.9 |
| Spring | Days < 60 | 1510 | 0.70 | 1.7 | 6.02 | 15.1 |
| | Days ≥ 60 | 218 | -5.55 | -8.1 | 6.62 | 9.7 |
| | All Days | 1728 | -0.09 | -0.2 | 6.1 | 14.0 |
| Summer | Days < 60 | 1700 | 8.10 | 18.8 | 10.0 | 23.2 |
| | Days ≥ 60 | 448 | 1.70 | 2.5 | 8.65 | 12.5 |
| | All Days | 2148 | 6.76 | 13.9 | 9.74 | 20.0 |

| | | | | | | |
|---|---|---|---|---|---|---|
| Fall | Days < 60 | 1375 | 1.93 | 6.1 | 5.62 | 17.8 |
| | Days ≥ 60 | 136 | -4.61 | -6.7 | 9.05 | 13.2 |
| | All Days | 1511 | 1.34 | 3.8 | 5.93 | 17.0 |

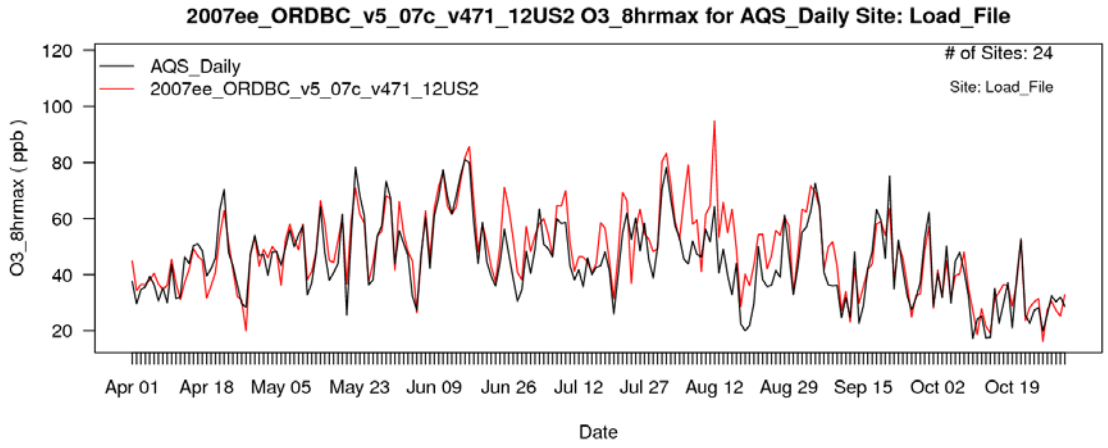


**Figure 43: Time series of 8-hr daily maximum ozone concentrations at Chicago monitoring sites for April-October 2007. Observed values shown in black and modeled values shown in red.**

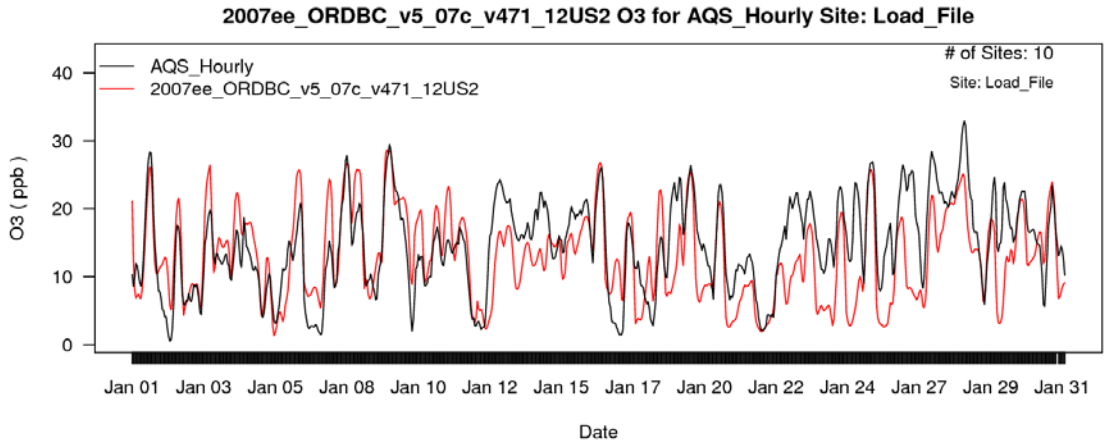


**Figure 44: Time series of hourly ozone concentrations at Chicago monitoring sites for January 2007. Observed values shown in black and modeled values shown in red.**

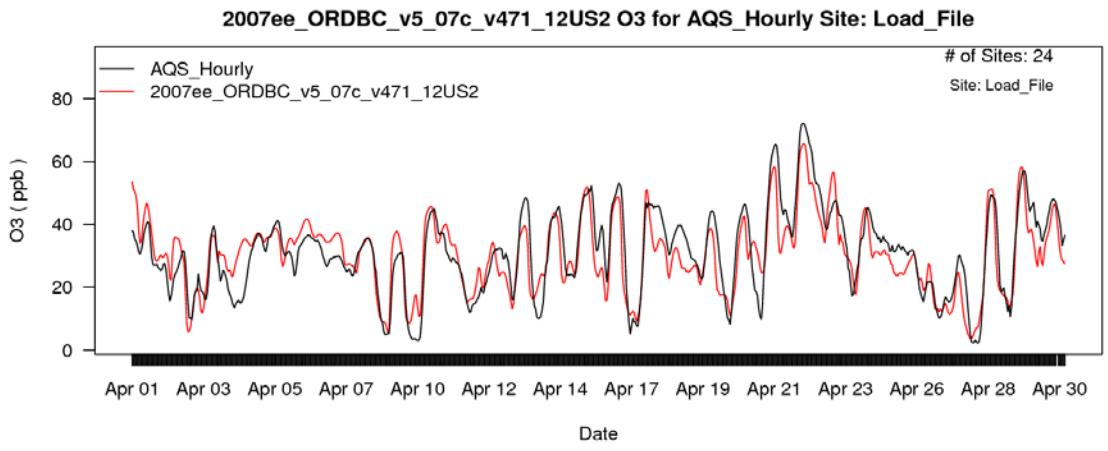


**Figure 45: Time series of hourly ozone concentrations at Chicago monitoring sites for April 2007. Observed values shown in black and modeled values shown in red.**

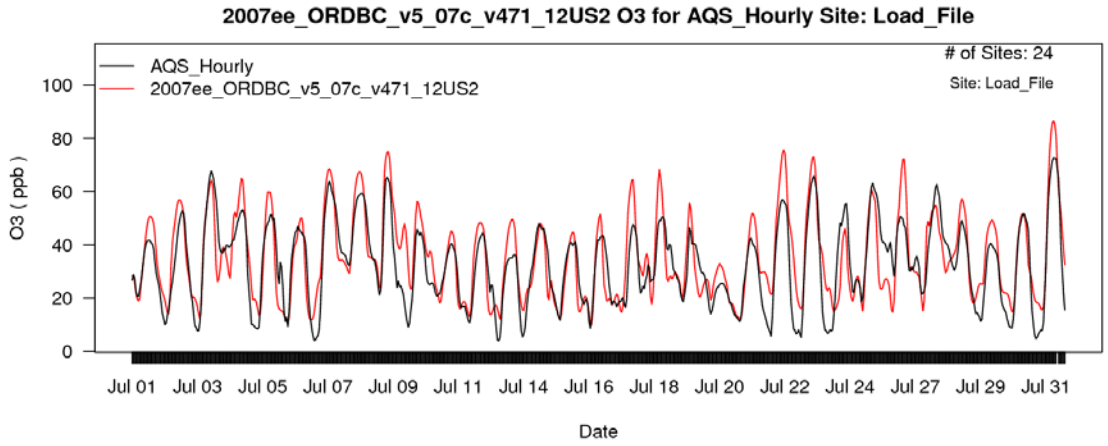


**Figure 46: Time series of hourly ozone concentrations at Chicago monitoring sites for July 2007. Observed values shown in black and modeled values shown in red.**

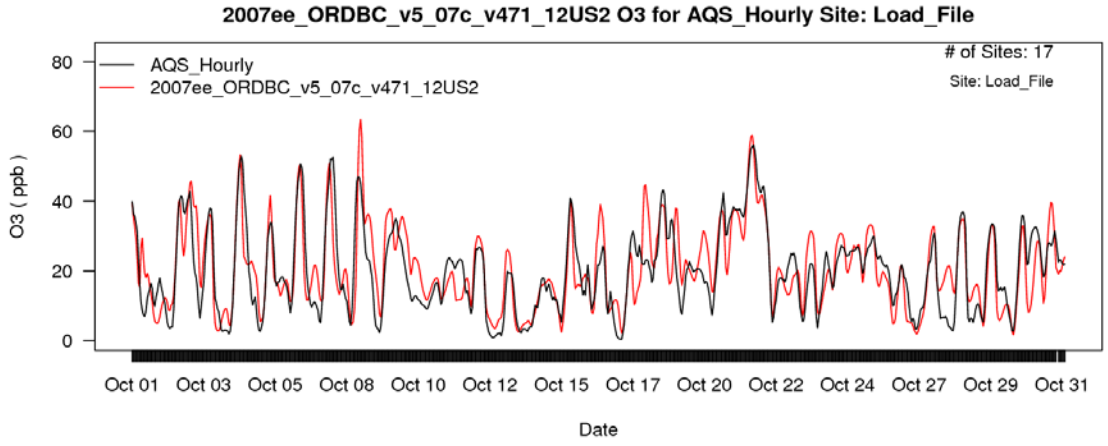

**Figure 47: Time series of hourly ozone concentrations at Chicago monitoring sites for October 2007. Observed values shown in black and modeled values shown in red.**

**Table 14: Summary of CMAQ model performance at AQS monitoring sites in the Cleveland area**

| | | No. of obs | MB (ppb) | NMB (%) | ME (ppb) | NME (%) |
|---|---|---|---|---|---|---|
| Winter | Days < 60 | 0 | NA | NA | NA | NA |
| | Days ≥ 60 | 0 | NA | NA | NA | NA |
| | All Days | 0 | NA | NA | NA | NA |
| Spring | Days < 60 | 491 | 4.35 | 10.5 | 7.03 | 17.0 |
| | Days ≥ 60 | 113 | -4.80 | -6.7 | 8.46 | 11.7 |
| | All Days | 604 | 2.64 | 5.6 | 7.30 | 15.5 |
| Summer | Days < 60 | 714 | 11.00 | 25.8 | 12.90 | 30.3 |
| | Days ≥ 60 | 187 | 2.25 | 3.2 | 9.48 | 13.6 |
| | All Days | 901 | 9.16 | 19.0 | 12.20 | 25.3 |
| Fall | Days < 60 | 543 | 4.41 | 11.6 | 7.38 | 19.4 |
| | Days ≥ 60 | 60 | -4.48 | -6.5 | 8.97 | 13.1 |
| | All Days | 603 | 3.52 | 8.6 | 7.54 | 18.4 |

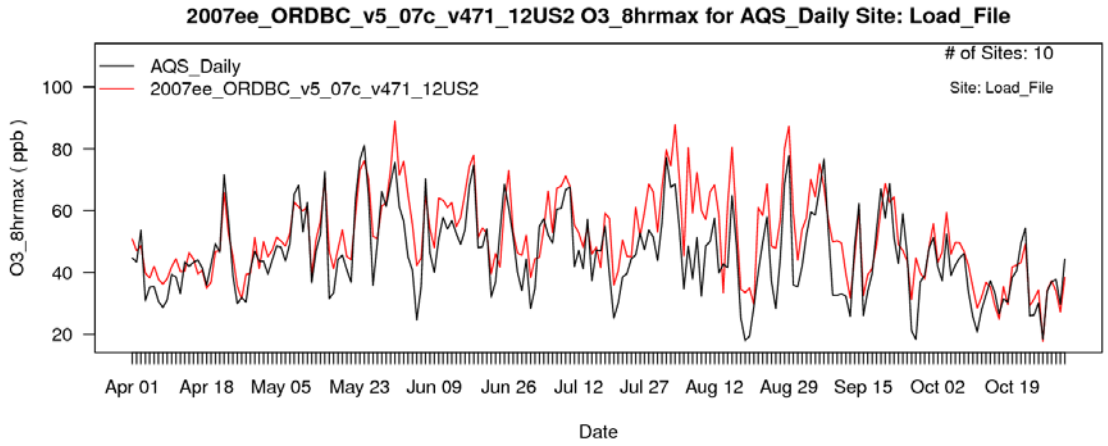


**Figure 48: Time series of 8-hr daily maximum ozone concentrations at Cleveland monitoring sites for April-October 2007. Observed values shown in black and modeled values shown in red.**

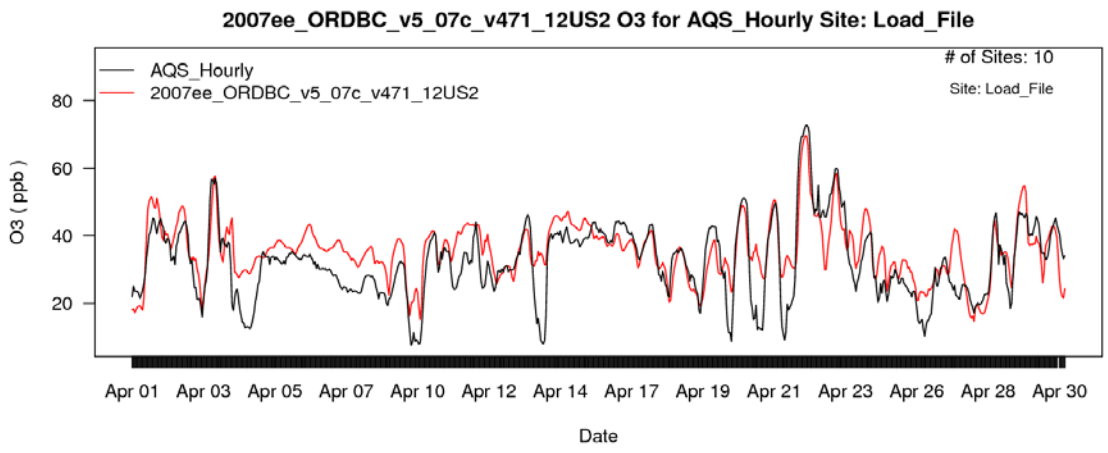


**Figure 49: Time series of hourly ozone concentrations at Cleveland monitoring sites for April 2007. Observed values shown in black and modeled values shown in red.**

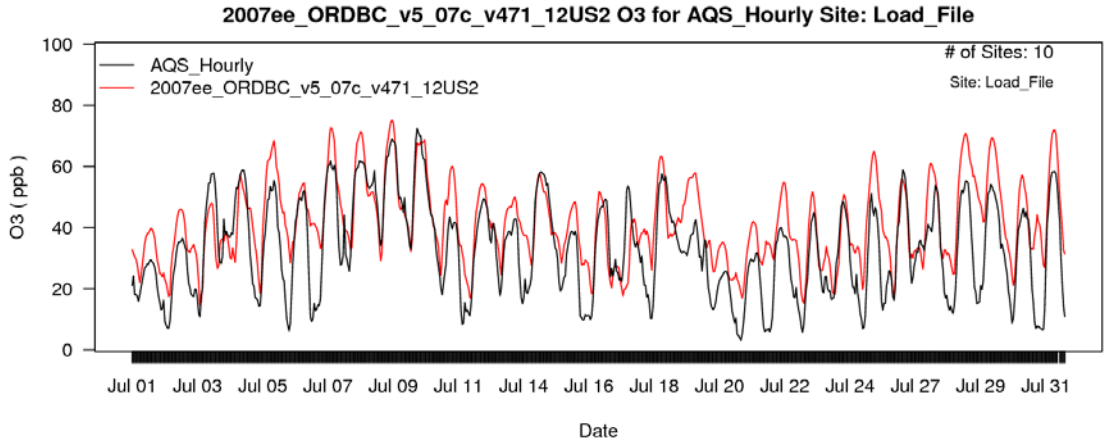


**Figure 50: Time series of hourly ozone concentrations at Cleveland monitoring sites for July 2007. Observed values shown in black and modeled values shown in red.**

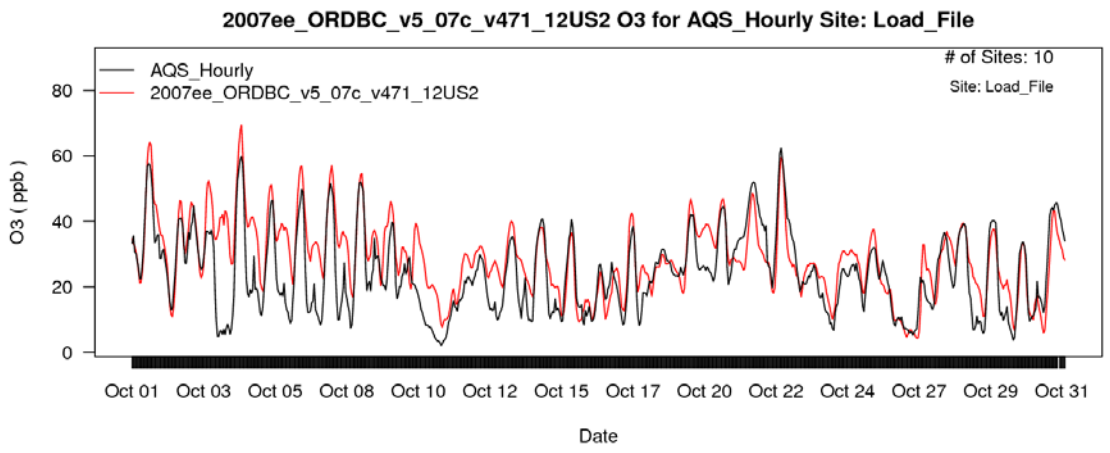


**Figure 51: Time series of hourly ozone concentrations at Cleveland monitoring sites for October 2007. Observed values shown in black and modeled values shown in red.**

**Table 15: Summary of CMAQ model performance at AQS monitoring sites in the Detroit area**

| | | No. of obs | MB (ppb) | NMB (%) | ME (ppb) | NME (%) |
|---|---|---|---|---|---|---|
| Winter | Days < 60 | 0 | NA | NA | NA | NA |
| | Days ≥ 60 | 0 | NA | NA | NA | NA |
| | All Days | 0 | NA | NA | NA | NA |
| Spring | Days < 60 | 443 | -1.04 | -2.5 | 4.93 | 11.7 |
| | Days ≥ 60 | 90 | -8.61 | -11.7 | 9.15 | 12.4 |
| | All Days | 533 | -2.32 | -4.9 | 5.64 | 11.9 |
| Summer | Days < 60 | 614 | 1.65 | 3.9 | 7.19 | 16.7 |
| | Days ≥ 60 | 191 | -7.16 | -9.9 | 10.9 | 15.1 |
| | All Days | 805 | -0.44 | -0.8 | 8.07 | 16.2 |
| Fall | Days < 60 | 220 | -1.01 | -2.6 | 6.65 | 17.1 |
| | Days ≥ 60 | 46 | -14.70 | -21.2 | 15.6 | 22.6 |
| | All Days | 166 | -3.38 | -7.7 | 8.2 | 18.6 |

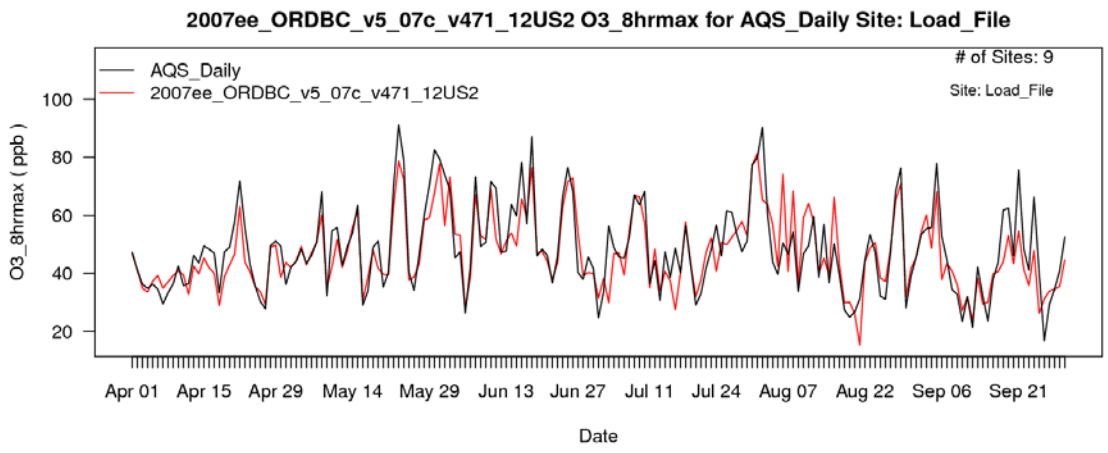


**Figure 52: Time series of 8-hr daily maximum ozone concentrations at Detroit monitoring sites for April-October 2007. Observed values shown in black and modeled values shown in red.**

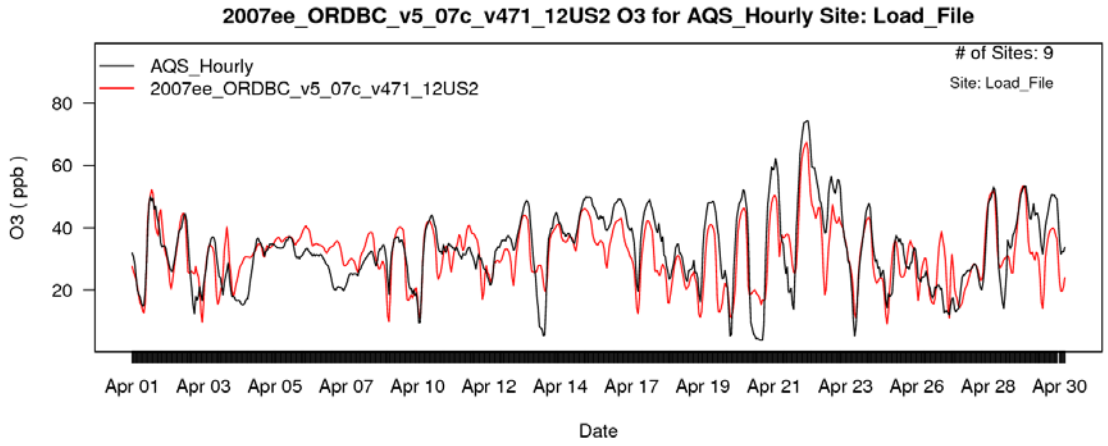


**Figure 53: Time series of hourly ozone concentrations at Detroit monitoring sites for April 2007. Observed values shown in black and modeled values shown in red.**

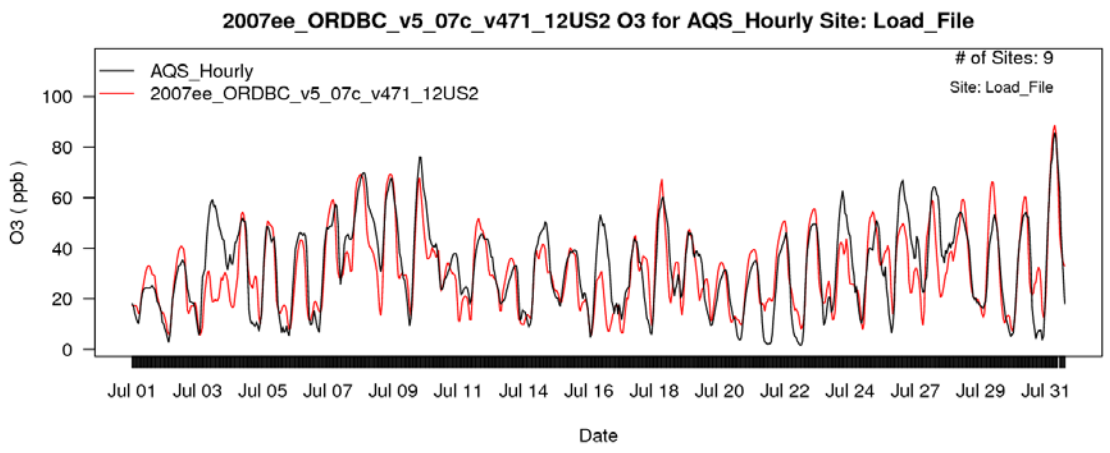


**Figure 54: Time series of hourly ozone concentrations at Detroit monitoring sites for July 2007. Observed values shown in black and modeled values shown in red.**

## OPERATIONAL EVALUATION IN THE CENTRAL U.S.

Mean bias for MDA8 ozone concentrations were in the range of 4 ppb or less at Central US monitoring sites during the winter and spring and less than 13 ppb and 6 ppb in the summer and fall respectively. Normalized mean bias was less than 15% at most sites in winter, spring, and fall and less than 35% at most sites in the summer. Summertime model overestimates were primarily located along the Gulf coast of Texas and Louisiana, mostly occurring on days with MDA8 ozone concentrations less than 60 ppb. This is similar to summertime overestimates reported for the Southern US which also were more pronounced along the Gulf Coast. Houston, Dallas, and Saint Louis were the three cities from the 15 REA areas which were located in the Central US region.

Saint Louis mean bias for MDA8 was moderately better than mean bias in the rest of the region for winter and spring periods and substantially better than the mean bias in the rest of the Central region in the summer and fall. The time series plots show that the model does a good job of replicating the observed variations in ozone (both MDA8 and hourly). Nighttime ozone is generally well simulated with the exception of a few several day periods in July when nighttime concentrations were overestimated by the model.

Dallas performance statistics for MDA8 ozone were very similar to those presented for the Central region as a whole with the exception of comparisons made for the fall season which showed that Dallas performed substantially better than average for the region. The time series plot of MDA8 ozone modeled and measured values (Figure 64) demonstrate consistent high bias on very low ozone days in May through early September but not in April or October.

Hourly ozone is fairly well replicated in January (Figure 65), April (Figure 66), and October (Figure 68) but is overestimated during July both on low ozone days and at night (Figure 67).

As mentioned above, the largest summertime overestimates in MDA8 ozone in the Central US occur along the Texas Gulf coast. This is demonstrated by the Houston model performance statistics. Houston model performance is relatively good and is equivalent to that in the rest of the Central US during the winter, spring, and fall seasons and on high days during the summer. However summertime MDA8 ozone is overestimated by 15 ppb and 48% on summer days with observed levels less than 60 ppb in the Houston area. This summertime overestimate of low ozone days is demonstrated in the time series plots in Figure 69 and Figure 72.

**Table 16: Summary of CMAQ model performance at AQS monitoring sites in the central US**

| | | No. of obs | MB (ppb) | NMB (%) | ME (ppb) | NME (%) |
|---|---|---|---|---|---|---|
| Winter | Days < 60 | 11190 | -0.42 | -1.4 | 5.61 | 18.7 |
| | Days ≥ 60 | 33 | -13.9 | -21.5 | 14.5 | 22.4 |
| | All Days | 11223 | -0.46 | -1.5 | 5.64 | 18.7 |
| Spring | Days < 60 | 13077 | 2.88 | 6.7 | 6.35 | 14.7 |
| | Days ≥ 60 | 2137 | -6.68 | -10.0 | 8.26 | 12.4 |
| | All Days | 15214 | 1.54 | 3.3 | 6.62 | 14.2 |
| Summer | Days < 60 | 14142 | 11.4 | 29.7 | 12.6 | 32.8 |
| | Days ≥ 60 | 2477 | 0.60 | 0.9 | 7.77 | 11.1 |
| | All Days | 16619 | 9.82 | 22.8 | 11.9 | 27.5 |
| Fall | Days < 60 | 13209 | 4.39 | 11.8 | 7.54 | 20.3 |
| | Days ≥ 60 | 1359 | -3.33 | -4.9 | 7.04 | 10.4 |
| | All Days | 14568 | 3.67 | 9.2 | 7.49 | 18.7 |

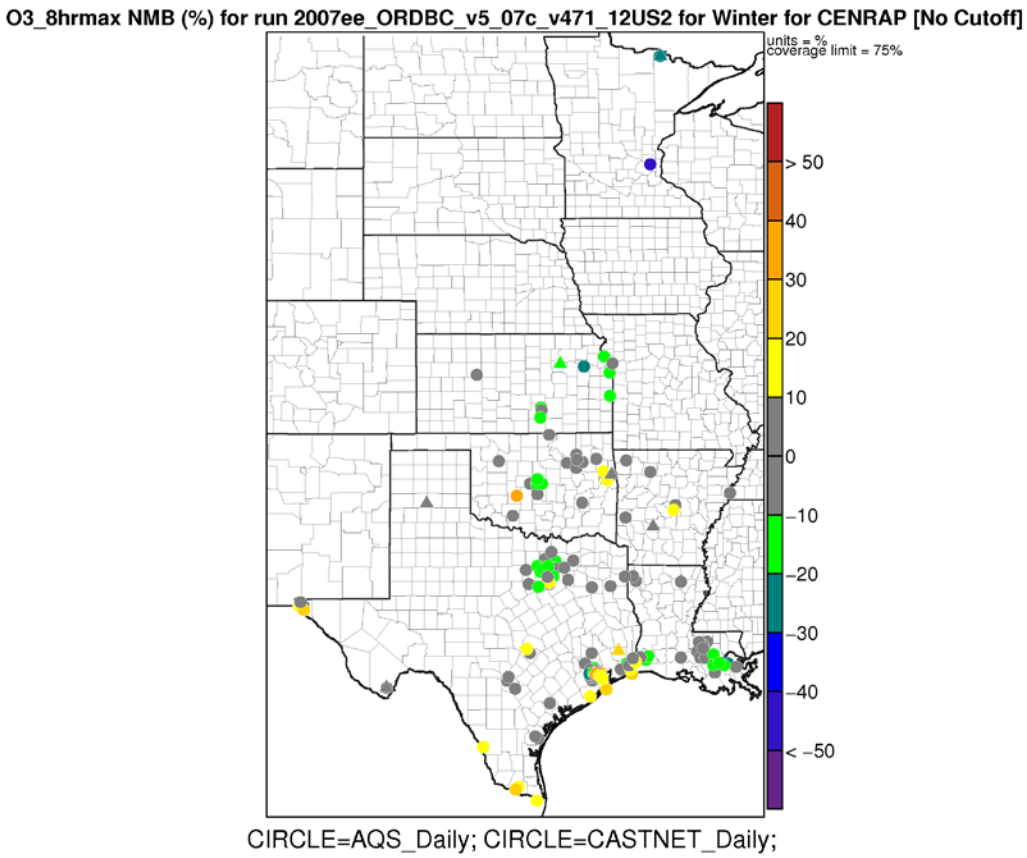


**Figure 55: Map of normalized mean bias for MDA8 ozone concentrations in the Central US for winter months in 2007.**

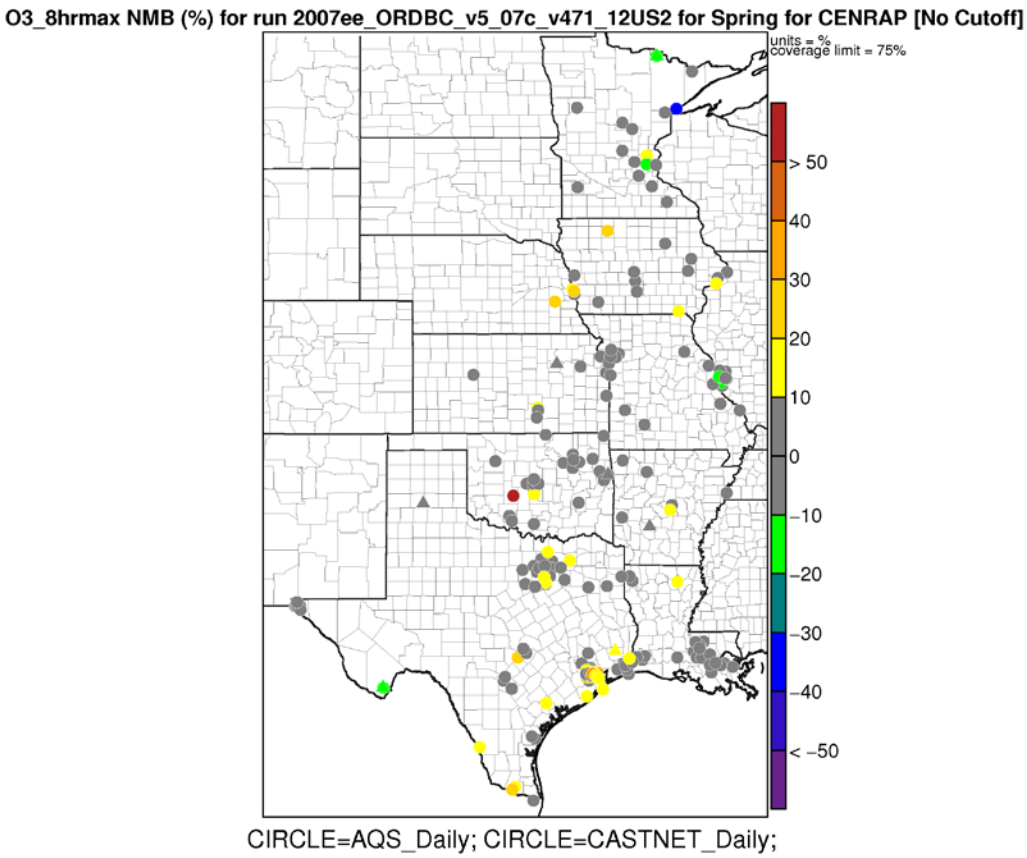


**Figure 56: Map of normalized mean bias for MDA8 ozone concentrations in the Central US for spring months in 2007.**

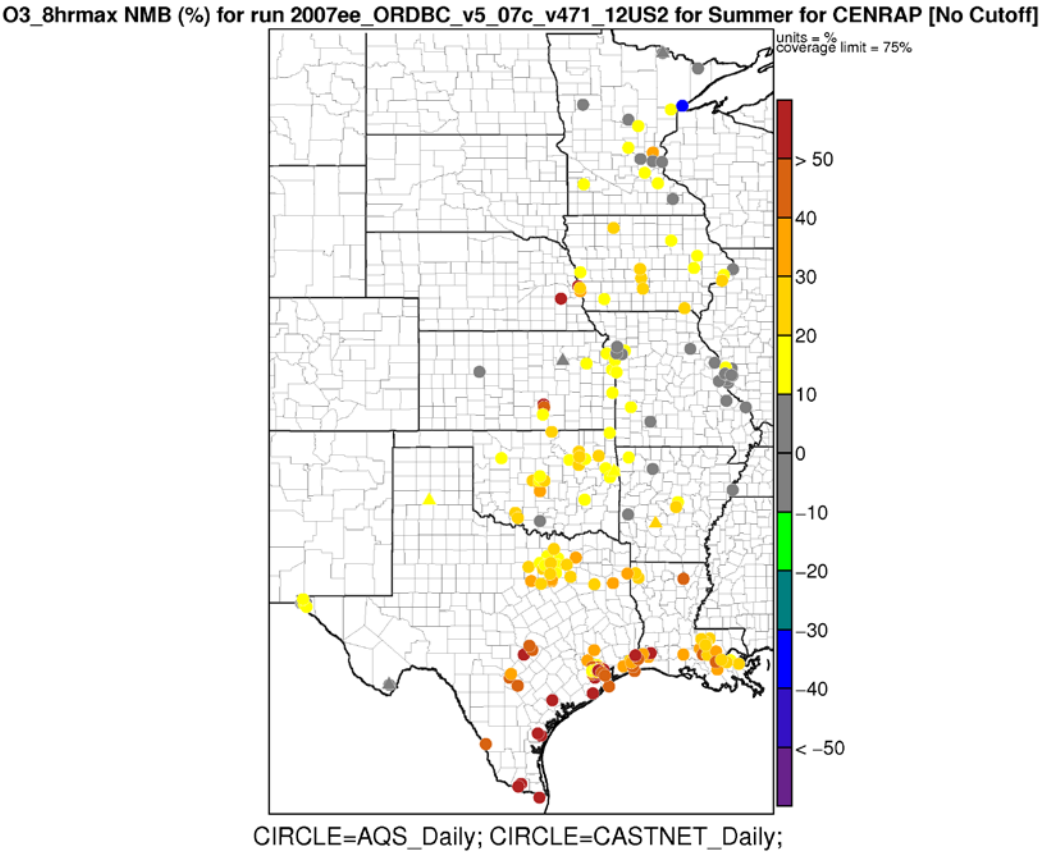


**Figure 57: Map of normalized mean bias for MDA8 ozone concentrations in the Central US for summer months in 2007.**

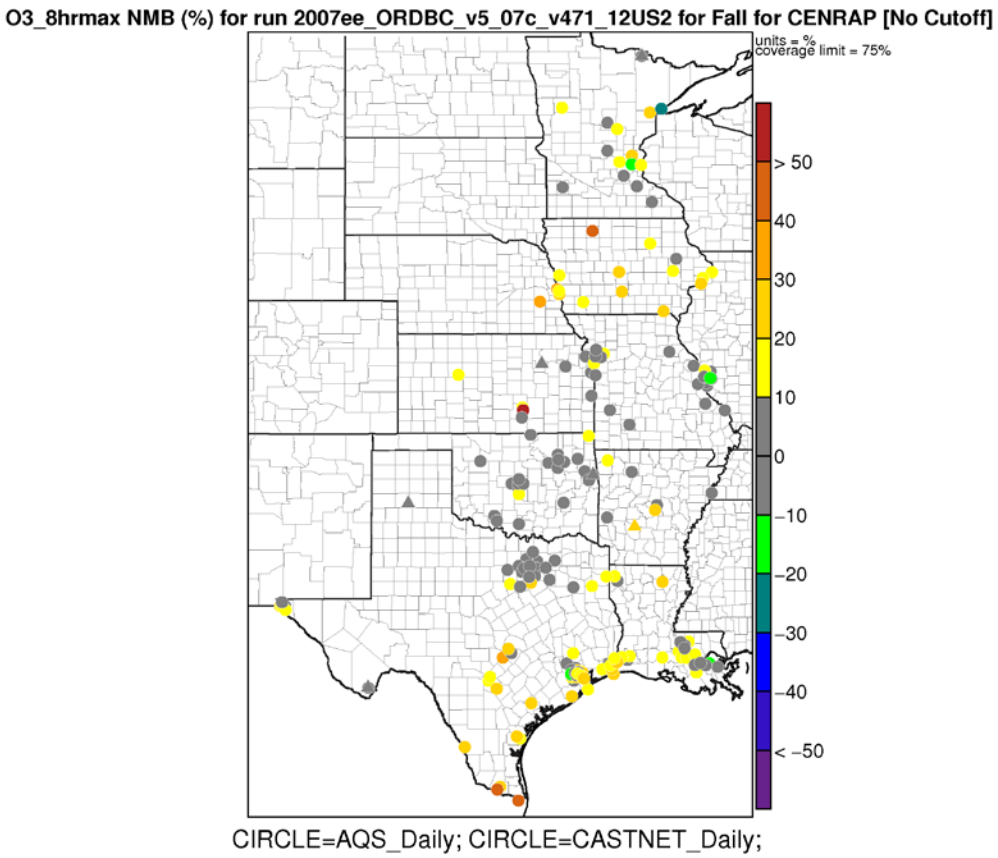


**Figure 58: Map of normalized mean bias for MDA8 ozone concentrations in the Central US for fall months in 2007.**

**Table 17: Summary of CMAQ model performance at AQS monitoring sites in the Saint Louis area**

| | | No. of obs | MB (ppb) | NMB (%) | ME (ppb) | NME (%) |
|---|---|---|---|---|---|---|
| Winter | Days < 60 | 266 | -0.16 | -0.7 | 4.10 | 18.1 |
| | Days ≥ 60 | 0 | NA | NA | NA | NA |
| | All Days | 266 | -0.16 | -0.7 | 4.10 | 18.1 |
| Spring | Days < 60 | 812 | 1.09 | 2.5 | 5.31 | 11.9 |
| | Days ≥ 60 | 139 | -6.93 | -10.6 | 7.85 | 12.0 |
| | All Days | 951 | -0.08 | -0.2 | 5.68 | 11.9 |
| Summer | Days < 60 | 834 | 8.71 | 18.9 | 9.83 | 21.4 |
| | Days ≥ 60 | 447 | 0.66 | 0.9 | 9.34 | 12.7 |
| | All Days | 1281 | 5.90 | 10.6 | 9.66 | 17.4 |

| | | | | | | |
|---|---|---|---|---|---|---|
| Fall | Days < 60 | 829 | 2.38 | 6.6 | 6.34 | 17.6 |
| | Days ≥ 60 | 113 | -6.19 | -8.8 | 8.46 | 12.1 |
| | All Days | 942 | 1.35 | 3.4 | 6.60 | 16.4 |

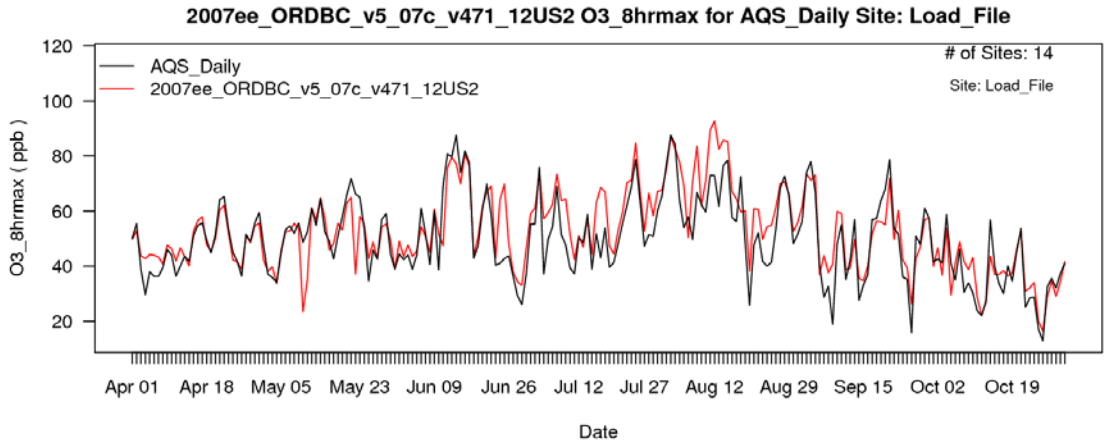


**Figure 59: Time series of 8-hr daily maximum ozone concentrations at Saint Louis monitoring sites for April-October 2007. Observed values shown in black and modeled values shown in red.**

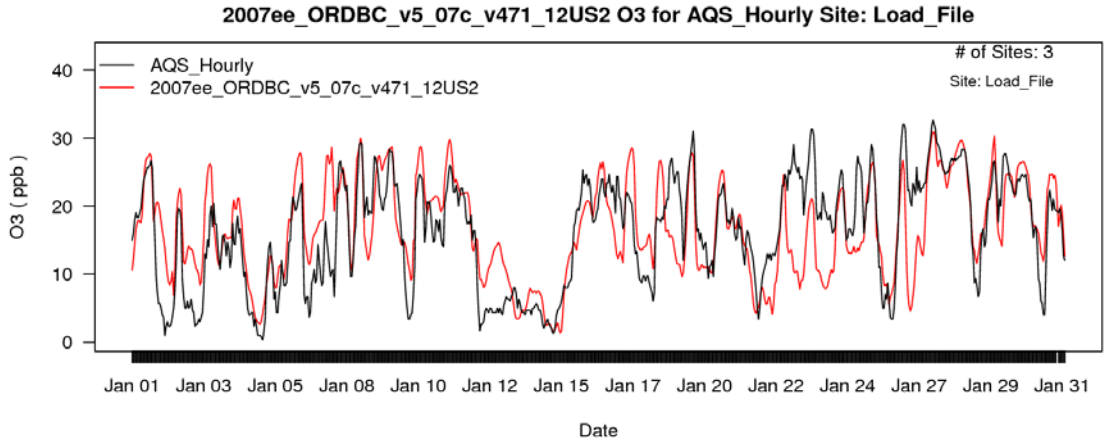


**Figure 60: Time series of hourly ozone concentrations at Saint Louis monitoring sites for January 2007. Observed values shown in black and modeled values shown in red.**

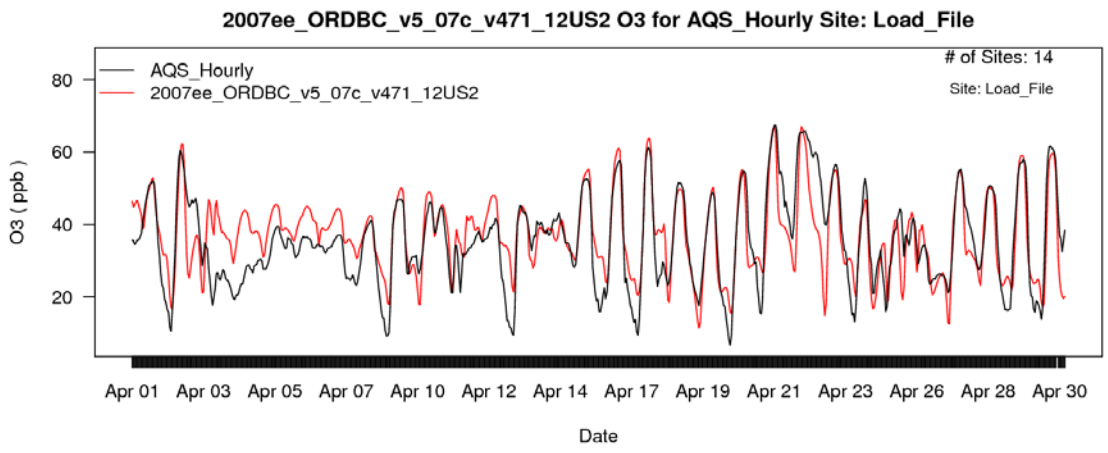


**Figure 61: Time series of hourly ozone concentrations at Saint Louis monitoring sites for April 2007. Observed values shown in black and modeled values shown in red.**

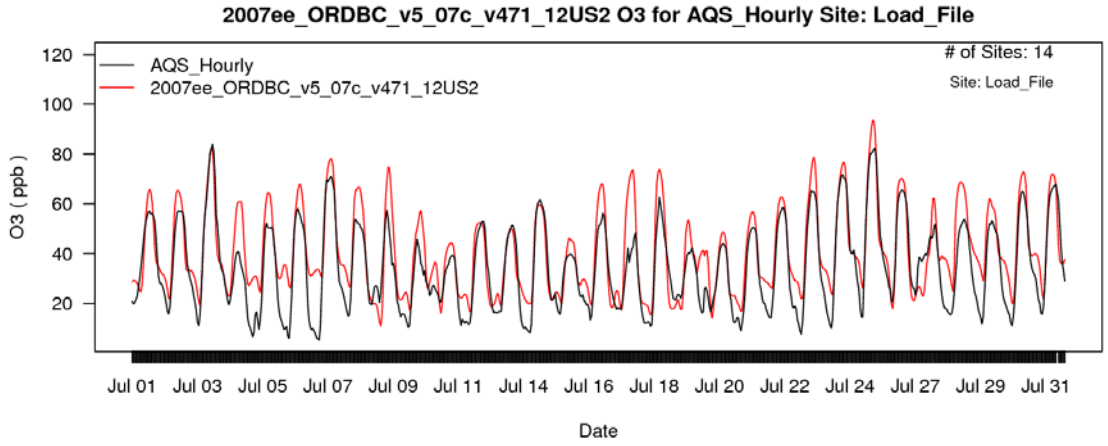


**Figure 62: Time series of hourly ozone concentrations at Saint Louis monitoring sites for July 2007. Observed values shown in black and modeled values shown in red.**

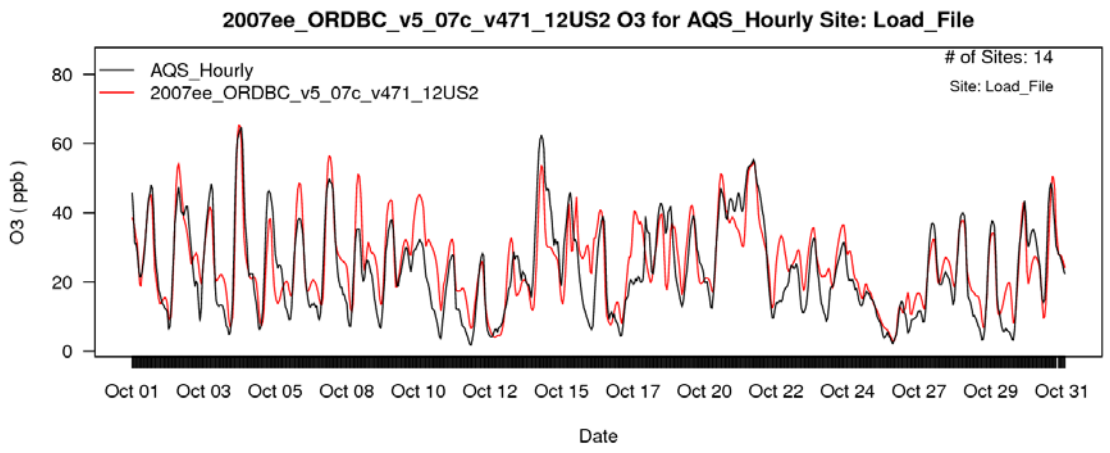


**Figure 63: Time series of hourly ozone concentrations at Saint Louis monitoring sites for October 2007. Observed values shown in black and modeled values shown in red.**

**Table 18: Summary of CMAQ model performance at AQS monitoring sites in the Dallas area**

| | | No. of obs | MB (ppb) | NMB (%) | ME (ppb) | NME (%) |
|---|---|---|---|---|---|---|
| Winter | Days < 60 | 1483 | -2.12 | -7.4 | 5.30 | 18.6 |
| | Days ≥ 60 | 0 | NA | NA | NA | NA |
| | All Days | 1483 | -2.12 | -7.4 | 5.30 | 18.6 |
| Spring | Days < 60 | 1360 | 2.92 | 7.0 | 6.77 | 16.2 |
| | Days ≥ 60 | 168 | -8.10 | -12.3 | 9.38 | 14.2 |
| | All Days | 1528 | 1.71 | 3.8 | 7.05 | 15.8 |
| Summer | Days < 60 | 1289 | 11.10 | 28.3 | 12.30 | 31.5 |
| | Days ≥ 60 | 260 | 3.35 | 4.7 | 8.59 | 12.0 |
| | All Days | 1549 | 9.77 | 21.9 | 11.70 | 26.3 |
| Fall | Days < 60 | 1306 | 1.67 | 4.3 | 6.89 | 17.8 |
| | Days ≥ 60 | 223 | -2.77 | -4.1 | 6.69 | 9.8 |
| | All Days | 1529 | 1.02 | 2.4 | 6.86 | 15.9 |

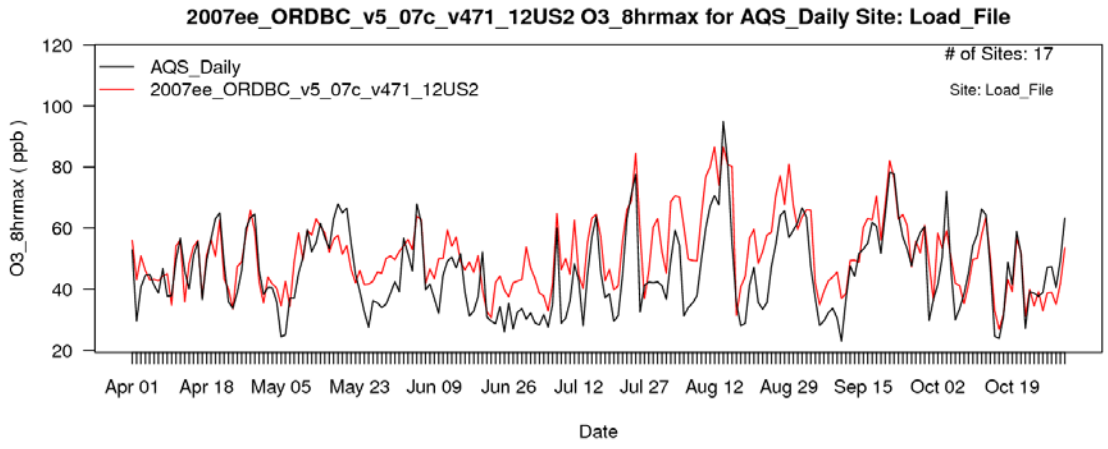


**Figure 64: Time series of 8-hr daily maximum ozone concentrations at Dallas monitoring sites for April-October 2007. Observed values shown in black and modeled values shown in red.**

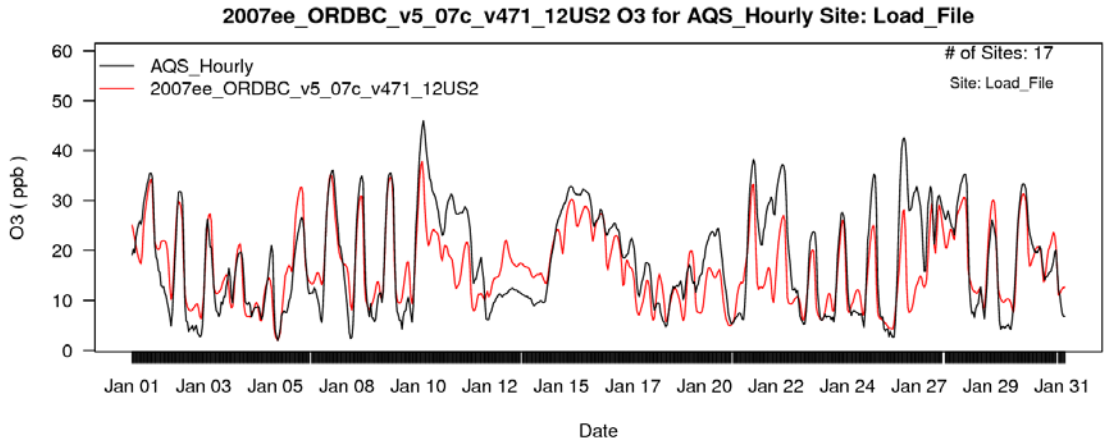


**Figure 65: Time series of hourly ozone concentrations at Dallas monitoring sites for January 2007. Observed values shown in black and modeled values shown in red.**

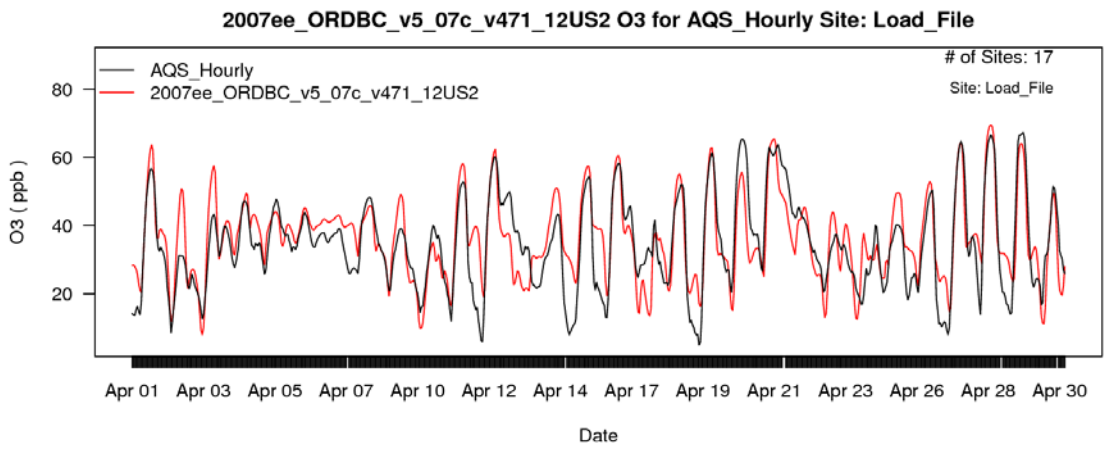


**Figure 66: Time series of hourly ozone concentrations at Dallas monitoring sites for April 2007. Observed values shown in black and modeled values shown in red.**

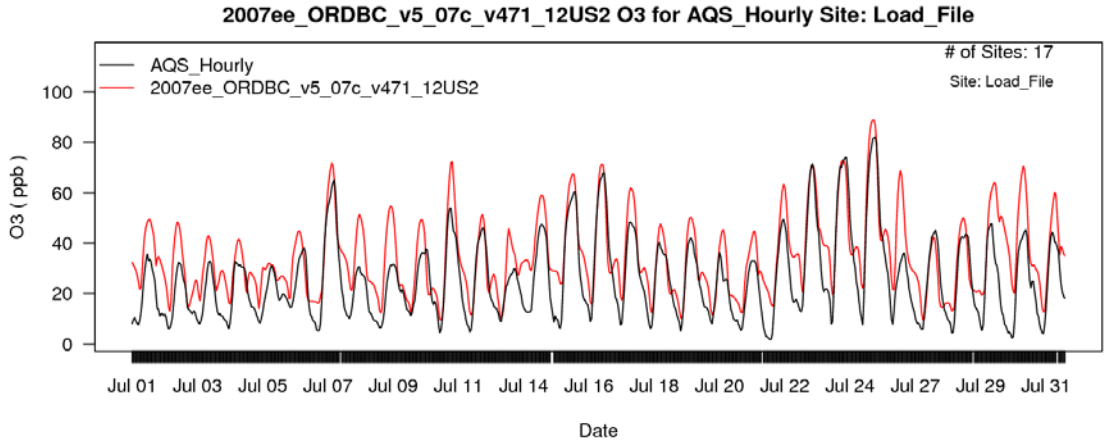


**Figure 67: Time series of hourly ozone concentrations at Dallas monitoring sites for July 2007. Observed values shown in black and modeled values shown in red.**

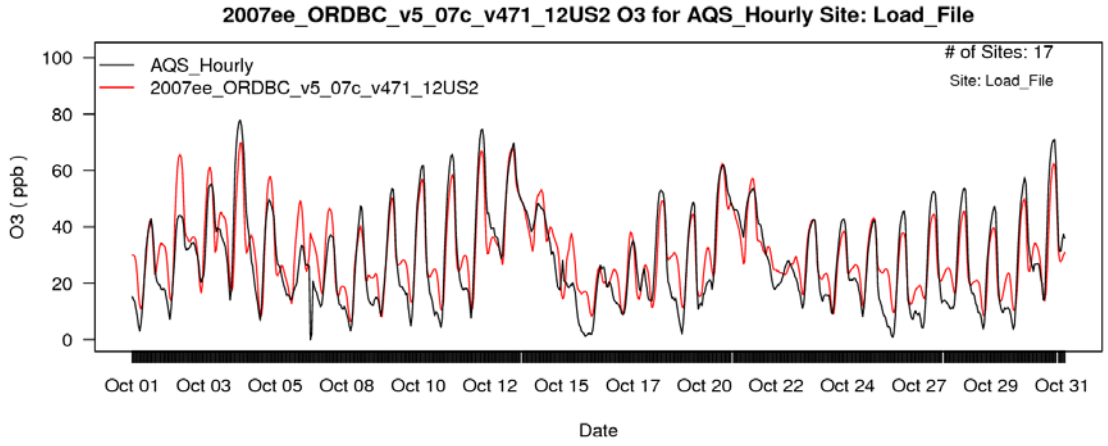

**Figure 68: Time series of hourly ozone concentrations at Dallas monitoring sites for October 2007. Observed values shown in black and modeled values shown in red.**

**Table 19: Summary of CMAQ model performance at AQS monitoring sites in the Houston area**

| | | No. of obs | MB (ppb) | NMB (%) | ME (ppb) | NME (%) |
|---|---|---|---|---|---|---|
| Winter | Days < 60 | 1772 | 0.48 | 1.8 | 5.97 | 22.2 |
| | Days ≥ 60 | 0 | NA | NA | NA | NA |
| | All Days | 1772 | 0.48 | 1.8 | 5.97 | 22.2 |
| Spring | Days < 60 | 1569 | 5.82 | 14.5 | 9.05 | 22.5 |
| | Days ≥ 60 | 276 | -5.23 | -7.7 | 10.40 | 15.2 |
| | All Days | 1845 | 4.17 | 9.4 | 9.25 | 20.8 |
| Summer | Days < 60 | 1706 | 15.00 | 48.4 | 16.8 | 54.2 |
| | Days ≥ 60 | 165 | 1.71 | 2.5 | 11.00 | 15.8 |
| | All Days | 1871 | 13.80 | 40.2 | 16.30 | 47.3 |
| Fall | Days < 60 | 1608 | 5.41 | 14.9 | 8.73 | 24.1 |
| | Days ≥ 60 | 259 | -3.38 | -4.8 | 9.05 | 12.8 |
| | All Days | 1867 | 4.19 | 10.2 | 8.78 | 21.4 |

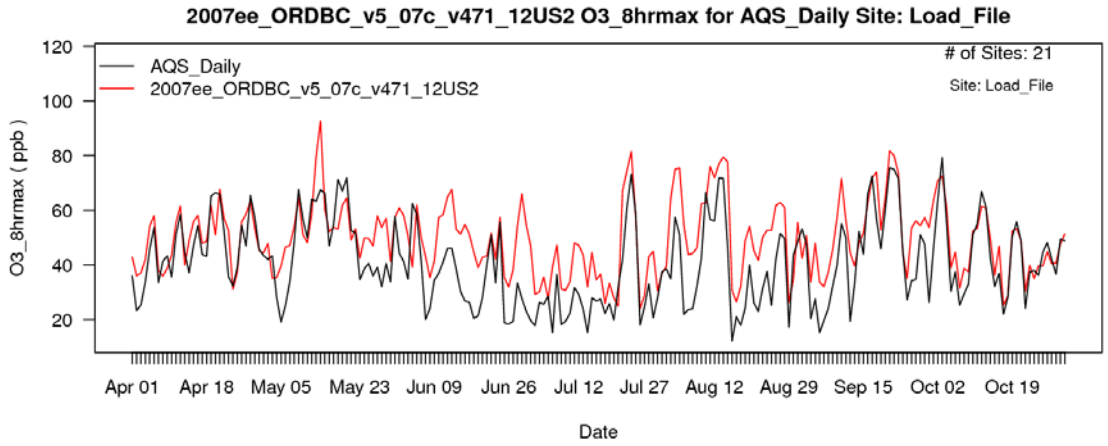


**Figure 69: Time series of 8-hr daily maximum ozone concentrations at Houston monitoring sites for April-October 2007. Observed values shown in black and modeled values shown in red.**

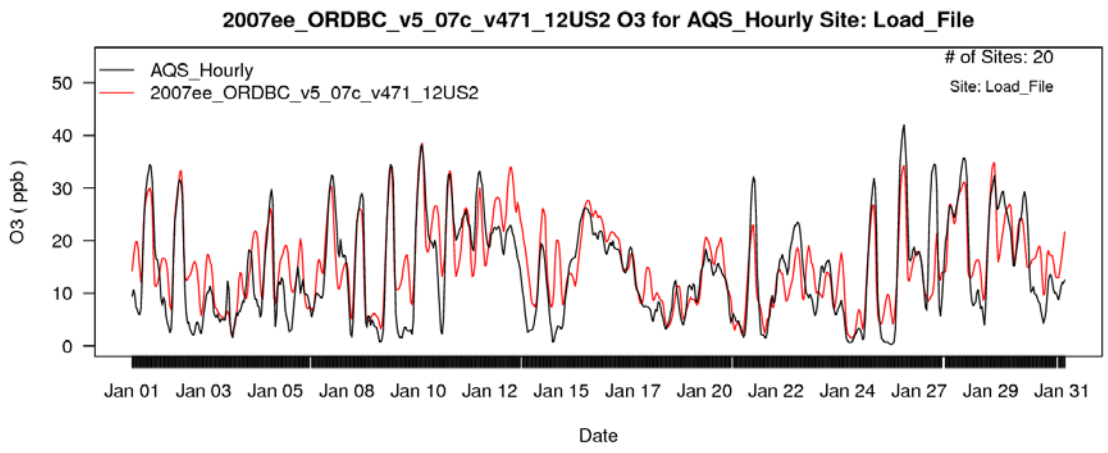


**Figure 70: Time series of hourly ozone concentrations at Houston monitoring sites for January 2007. Observed values shown in black and modeled values shown in red.**

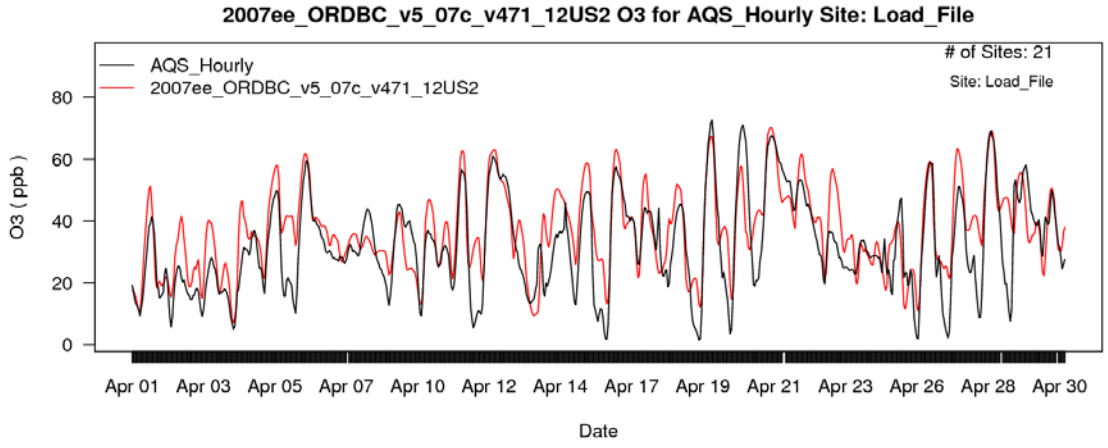


**Figure 71: Time series of hourly ozone concentrations at Houston monitoring sites for April 2007. Observed values shown in black and modeled values shown in red.**

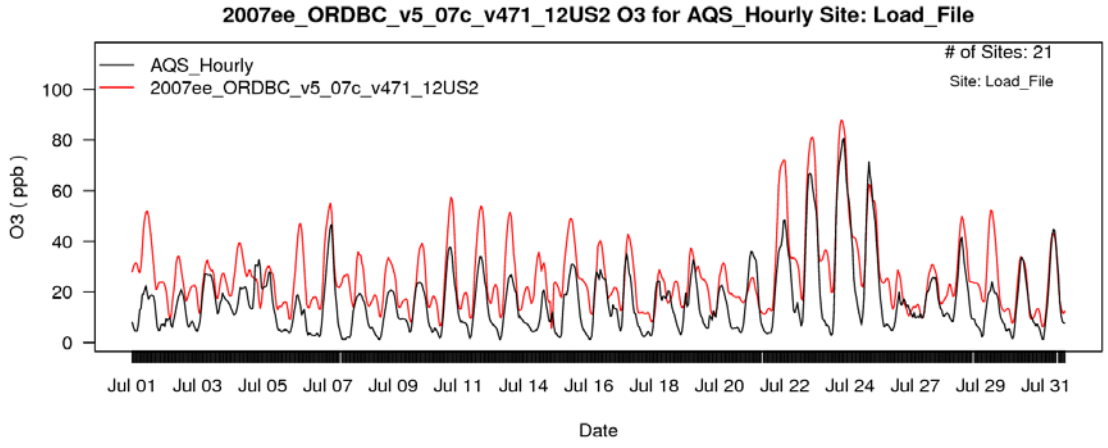

**Figure 72: Time series of hourly ozone concentrations at Houston monitoring sites for July 2007. Observed values shown in black and modeled values shown in red.**

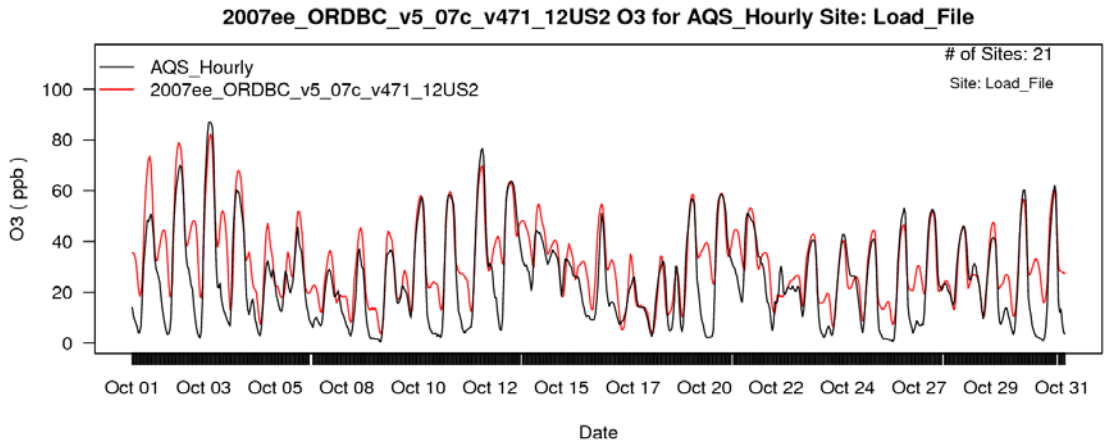


**Figure 73: Time series of hourly ozone concentrations at Houston monitoring sites for October 2007. Observed values shown in black and modeled values shown in red.**

## OPERATIONAL EVALUATION IN THE WESTERN U.S.

Again model statistics for MDA8 ozone in the Western US are in the range of what has been reported for state of the science model performance in the literature (Simon et al, 2012). Mean bias at most sites was less than 6 ppb in the winter, spring, and fall and less than 10 ppb in the summer. Normalized mean bias at most monitoring locations was less than 10% in the winter and spring, less than 20% in the summer and less than 15% in the fall. Only 3 sites in the West recorded ozone concentrations equal to or above 60 ppb in winter (a Riverside California site reported 13 days and the other two sites in Sacramento, CA and Sublette county WY reported only 2 and 3 days above 60 ppb). These high wintertime observations were substantially underestimated by the model with an average MB of -34.5 ppb but likely for different reasons. The high days in Riverside California are probably due to traditionally understood ozone formation that occurs on warm sunny days. The high ozone concentrations in Wyoming are an example of wintertime ozone formation that occurs during cold pool meteorology events which have substantial snow cover and extreme temperature inversions and are still an active area of research. Some spatial trends in normalized mean bias are apparent in the winter (Figure 74) and in the summer (Figure 76). Wintertime ozone is more likely to be overestimated on the West Coast and more likely to be underestimated in the Intermountain West. Summertime model overestimates are greatest along the Southern Coast of California in locations that generally have low observed ozone concentrations. Three urban areas from the

REA are located in the Western US and are evaluated in this section: Denver, Sacramento, and Los Angeles.

Denver area model performance was generally comparable to model performance in the rest of the Western US although summertime overestimates of MDA8 were somewhat greater in Denver. These summertime overestimates can be seen on many days in Figure 78 and Figure 80. Figure 79 shows that the model generally captures measured hourly ozone concentrations in the Denver area on mid to high ozone days but often overestimates very low ozone days in the spring. Fall hourly ozone estimates from the model are reasonably well captured in Figure 81.

Sacramento area model performance for MDA8 ozone values was reasonably good in all seasons except for the 2 days with high observed ozone in the winter. The model underestimated those high wintertime concentrations by 32 ppb. Other than those days, model bias was generally less than 10% in the Sacramento area. The time series figures of MDA8 and hourly ozone concentrations show that the model does well at capturing the day to day and day to night ozone variations in all seasons.

Los Angeles generally had reasonable model performance with low normalized mean bias number (0-8%) with two exceptions. The thirteen high wintertime ozone days measured in central Riverside County were not captured by the model which had a mean bias for those days at that site of -36 ppb and -45%. Also, the model tended to overestimate ozone on summertime days with observed concentrations below 60 ppb (15 ppb mean bias). These low ozone summer ozone concentrations generally occurred along the coast (Figure 92). A map of summertime normalized mean bias (Figure 93) clearly shows that the low ozone sites are the locations with the largest model bias. Monitors away from the coast generally had fairly low bias (0-20%) with the exception of two sites in western Riverside County. The summer ozone overestimates shown in the MDA8 time series (Figure 87) are therefore due to performance at those coastal sites. The hourly time series for January (Figure 88), April (Figure 89), and October (Figure 90) generally show good hourly ozone performance during the day but model overestimates at night.

**Table 20: Summary of CMAQ model performance at AQS monitoring sites in the western US**

| | | No. of obs | MB (ppb) | NMB (%) | ME (ppb) | NME (%) |
|---|---|---|---|---|---|---|
| Winter | Days < 60 | 23890 | 1.31 | 4.1 | 5.79 | 17.9 |
| | Days ≥ 60 | 18 | -34.5 | -45.8 | 34.5 | 45.8 |
| | All Days | 23908 | 1.29 | 4.0 | 5.81 | 17.9 |

| | | | | | | |
|---|---|---|---|---|---|---|
| Spring | Days < 60 | 22670 | 0.61 | 1.3 | 5.61 | 12.1 |
| | Days ≥ 60 | 5101 | -4.84 | -7.2 | 7.30 | 10.9 |
| | All Days | 27771 | -0.40 | -0.8 | 5.92 | 11.8 |
| Summer | Days < 60 | 21098 | 7.50 | 17.0 | 9.96 | 22.6 |
| | Days ≥ 60 | 9708 | 1.29 | 2.8 | 8.94 | 12.8 |
| | All Days | 30806 | 5.74 | 11.0 | 9.64 | 18.5 |
| Fall | Days < 60 | 26055 | 3.40 | 8.9 | 7.08 | 18.4 |
| | Days ≥ 60 | 1691 | -3.32 | -4.9 | 9.81 | 14.4 |
| | All Days | 27746 | 2.99 | 7.4 | 7.25 | 18.0 |

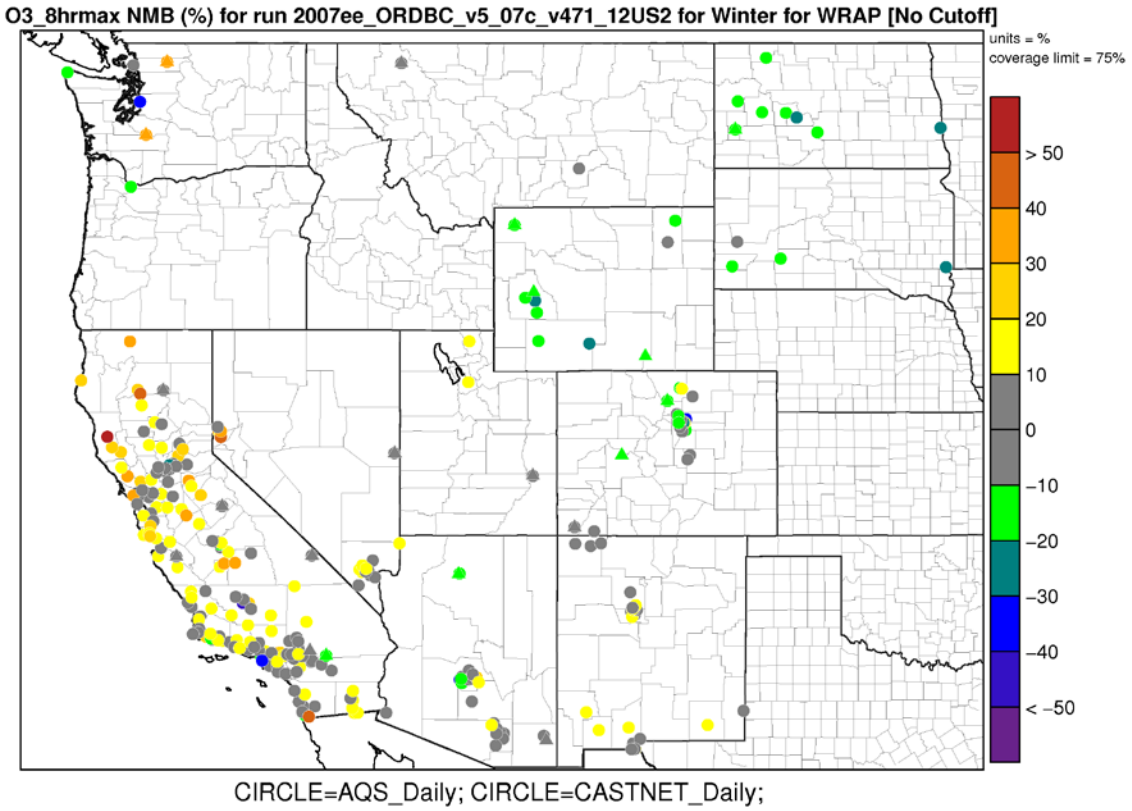


**Figure 74: Map of normalized mean bias for MDA8 ozone concentrations in the Western US for winter months in 2007.**

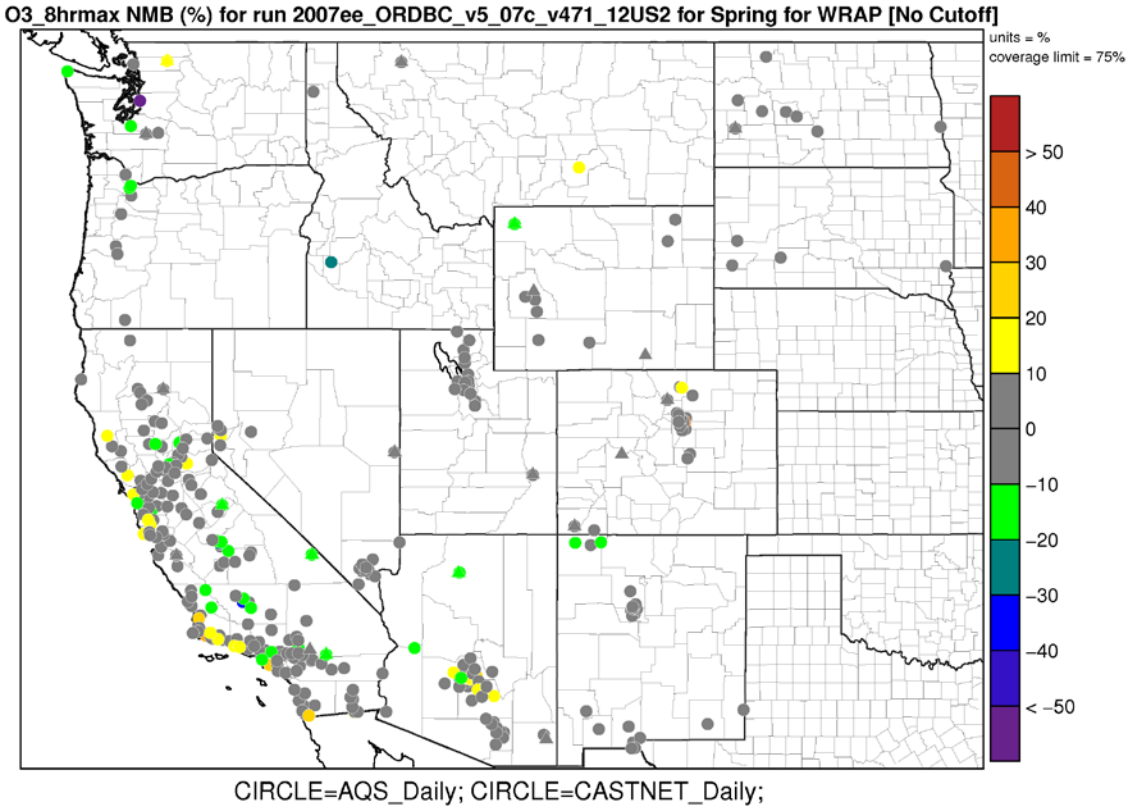


**Figure 75: Map of normalized mean bias for MDA8 ozone concentrations in the Western US for spring months in 2007.**

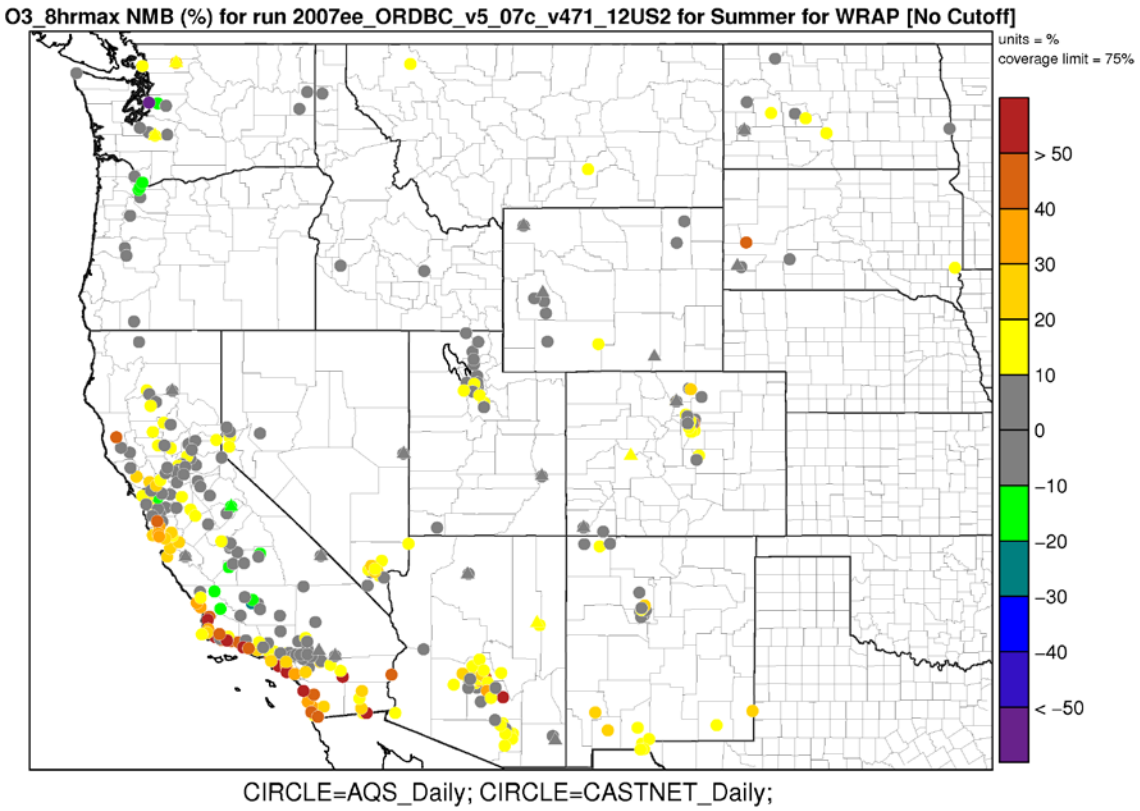


**Figure 76: Map of normalized mean bias for MDA8 ozone concentrations in the Western US for summer months in 2007.**

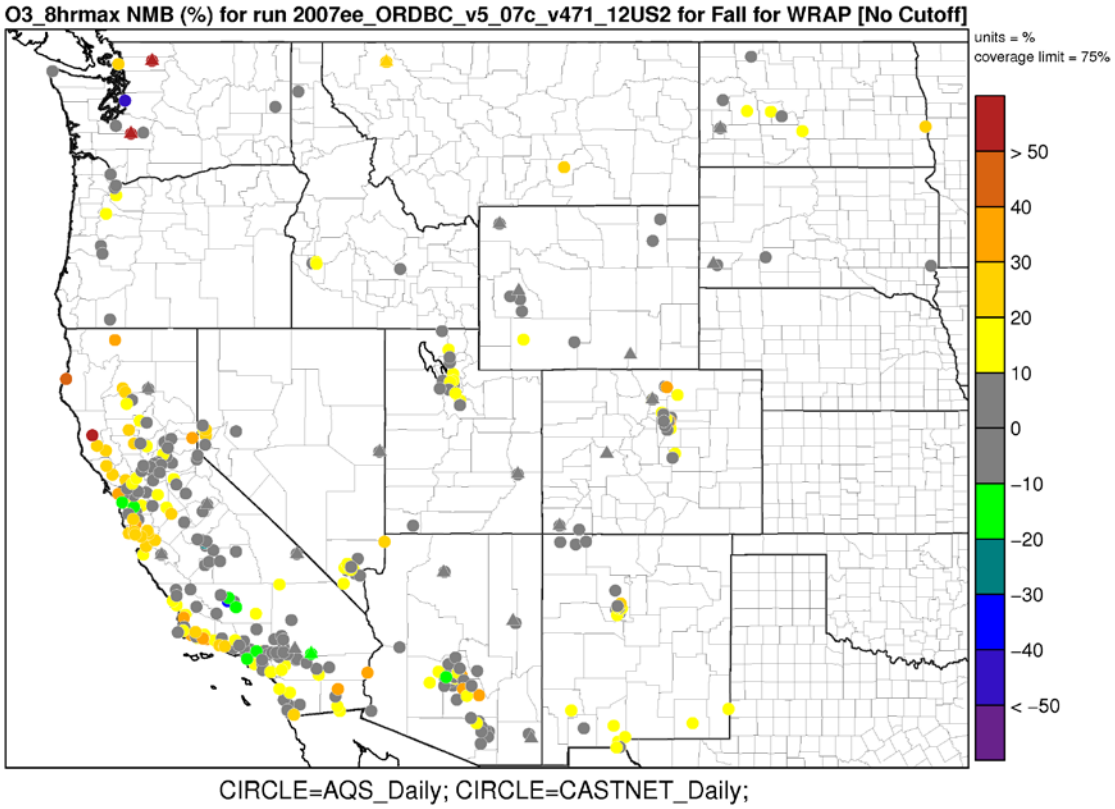


**Figure 77: Map of normalized mean bias for MDA8 ozone concentrations in the Western US for fall months in 2007.**

**Table 21: Summary of CMAQ model performance at AQS monitoring sites in the Denver area**

| | | No. of obs | MB (ppb) | NMB (%) | ME (ppb) | NMB (%) |
|---|---|---|---|---|---|---|
| Winter | Days < 60 | 1006 | -3.84 | -11.5 | 7.23 | 21.6 |
| | Days ≥ 60 | 0 | NA | NA | NA | NA |
| | All Days | 1006 | -3.84 | -11.5 | 7.23 | 21.6 |
| Spring | Days < 60 | 893 | 3.36 | 7.3 | 6.24 | 13.7 |
| | Days ≥ 60 | 182 | -2.42 | -3.7 | 6.06 | 9.4 |
| | All Days | 1075 | 2.38 | 4.9 | 6.21 | 12.7 |
| Summer | Days < 60 | 427 | 10.2 | 19.4 | 11.5 | 21.9 |
| | Days ≥ 60 | 653 | 4.94 | 7.2 | 8.18 | 11.9 |
| | All Days | 1080 | 7.02 | 11.3 | 9.49 | 15.2 |

| | | | | | | |
|---|---|---|---|---|---|---|
| Fall | Days < 60 | 993 | 3.19 | 8.4 | 6.47 | 17.0 |
| | Days ≥ 60 | 53 | -1.59 | -2.5 | 6.38 | 9.8 |
| | All Days | 1046 | 2.95 | 7.5 | 6.46 | 16.4 |

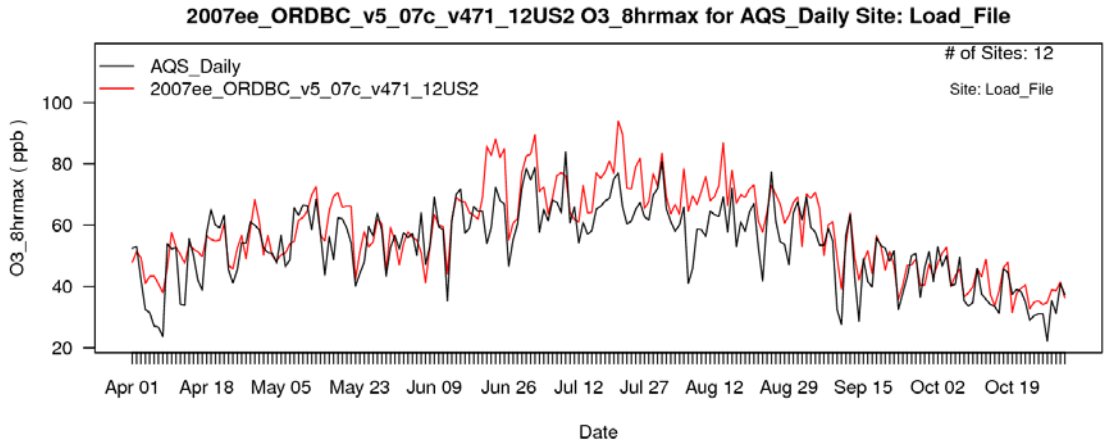


**Figure 78: Time series of 8-hr daily maximum ozone concentrations at Denver monitoring sites for April-October 2007. Observed values shown in black and modeled values shown in red.**

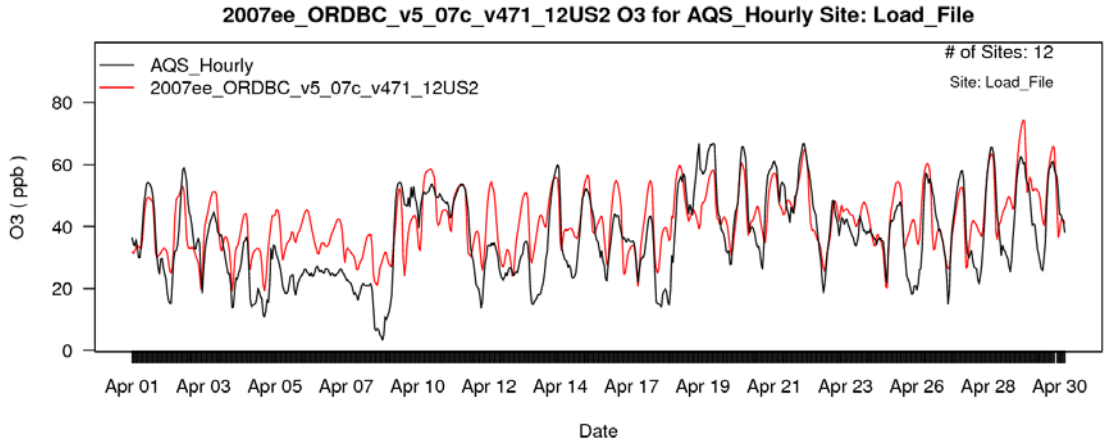


**Figure 79: Time series of hourly ozone concentrations at Denver monitoring sites for April 2007. Observed values shown in black and modeled values shown in red.**

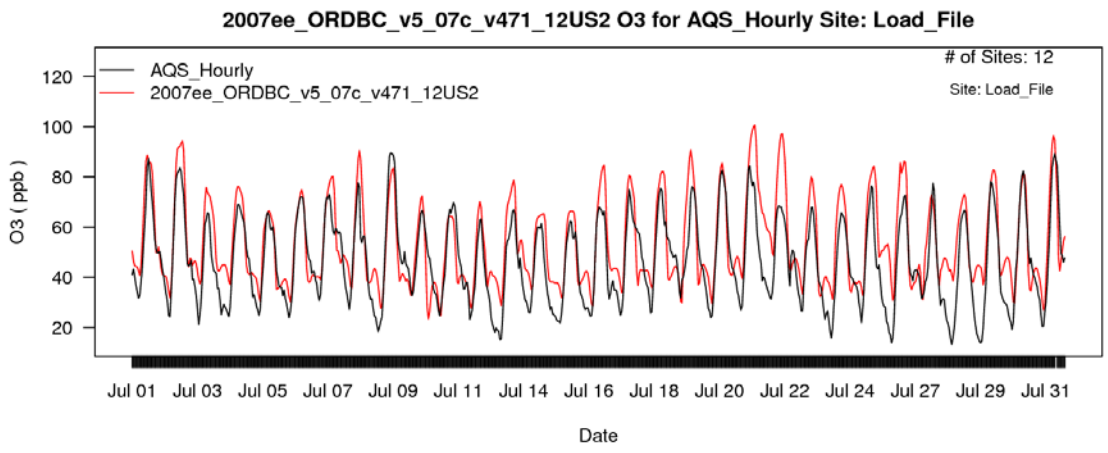


**Figure 80: Time series of hourly ozone concentrations at Denver monitoring sites for July 2007. Observed values shown in black and modeled values shown in red.**

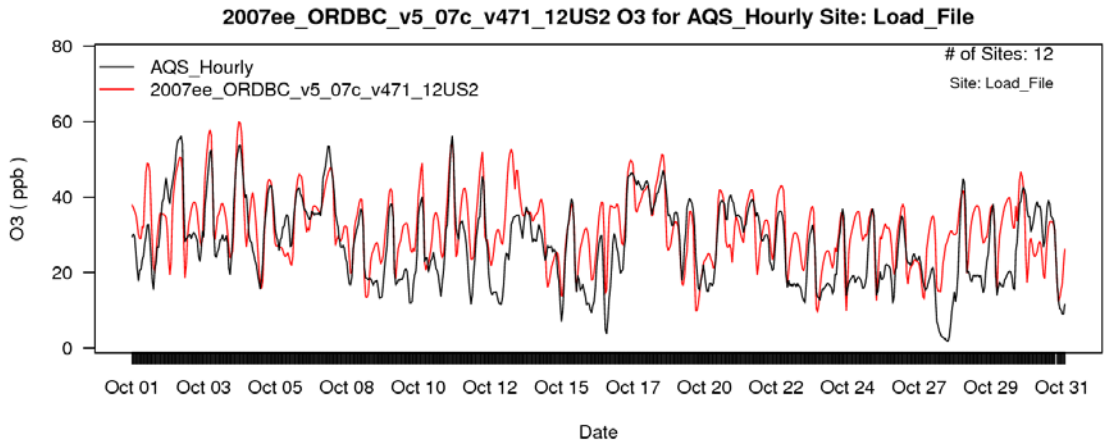


**Figure 81: Time series of hourly ozone concentrations at Denver monitoring sites for October 2007. Observed values shown in black and modeled values shown in red.**

**Table 22: Summary of CMAQ model performance at AQS monitoring sites in the Sacramento area**

| | | No. of obs | MB (ppb) | NMB (%) | ME (ppb) | NME (%) |
|---|---|---|---|---|---|---|
| Winter | Days < 60 | 1374 | 1.04 | 3.5 | 5.41 | 18.4 |
| | Days ≥ 60 | 2 | -31.80 | -49.8 | 31.80 | 49.8 |
| | All Days | 1376 | 0.99 | 3.4 | 5.45 | 18.5 |
| Spring | Days < 60 | 1516 | -0.89 | -2.0 | 5.28 | 11.8 |
| | Days ≥ 60 | 239 | -4.83 | -7.1 | 6.37 | 9.3 |
| | All Days | 1755 | -1.42 | -3.0 | 5.43 | 11.3 |

| | | | | | | |
|---|---|---|---|---|---|---|
| Summer | Days < 60 | 1443 | 4.10 | 9.1 | 6.58 | 14.6 |
| | Days ≥ 60 | 619 | -1.39 | -2.0 | 7.81 | 11.2 |
| | All Days | 2062 | 2.45 | 4.7 | 6.95 | 13.2 |
| Fall | Days < 60 | 1809 | 1.80 | 4.8 | 6.30 | 16.7 |
| | Days ≥ 60 | 150 | -7.82 | -11.1 | 10.10 | 14.3 |
| | All Days | 1959 | 1.06 | 2.6 | 6.59 | 16.4 |

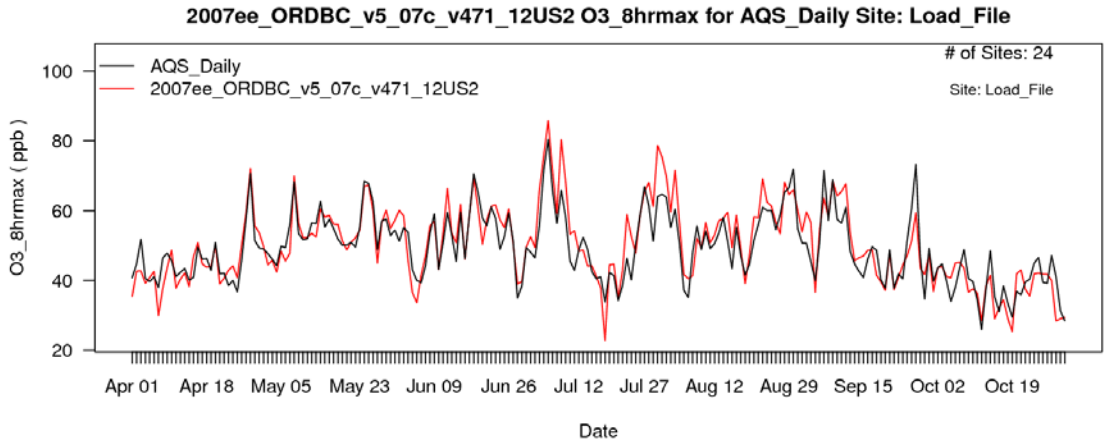


**Figure 82: Time series of 8-hr daily maximum ozone concentrations at Sacramento monitoring sites for April-October 2007. Observed values shown in black and modeled values shown in red.**

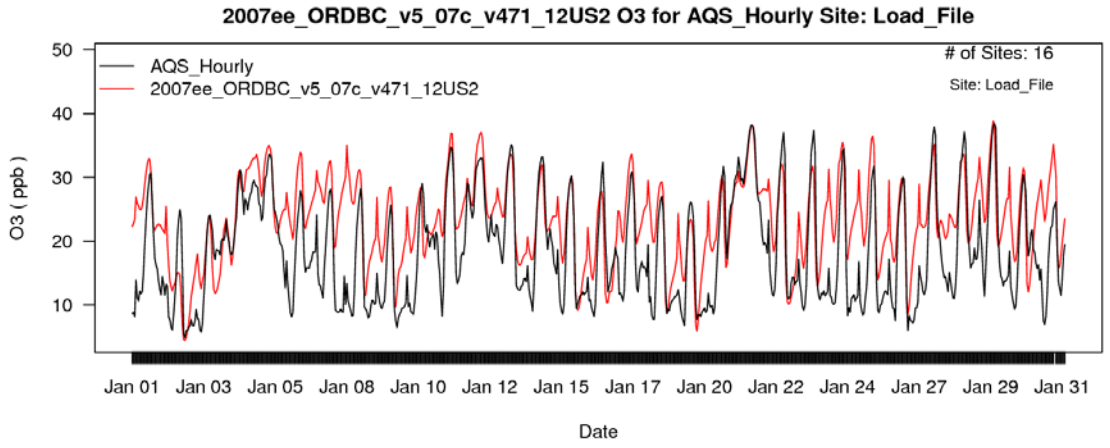


**Figure 83: Time series of hourly ozone concentrations at Sacramento monitoring sites for January 2007. Observed values shown in black and modeled values shown in red.**

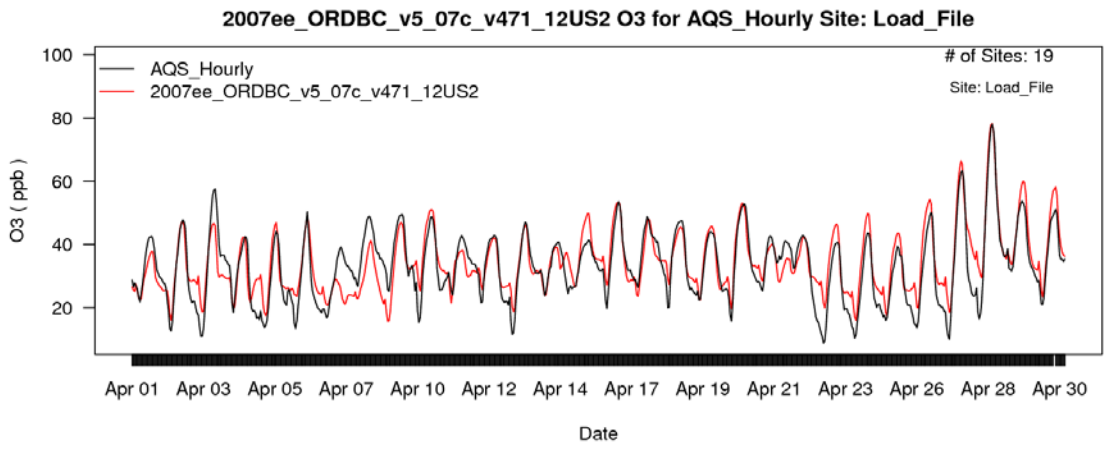


**Figure 84: Time series of hourly ozone concentrations at Sacramento monitoring sites for April 2007. Observed values shown in black and modeled values shown in red.**

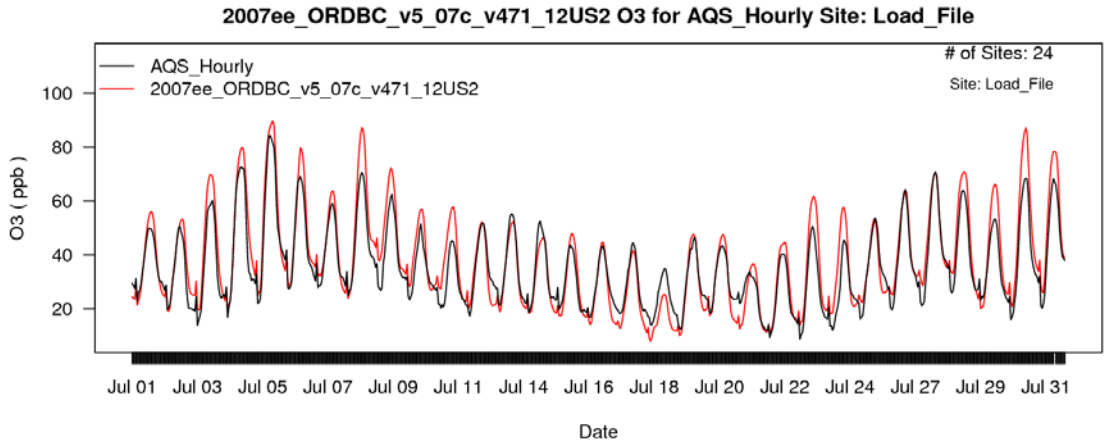


**Figure 85: Time series of hourly ozone concentrations at Sacramento monitoring sites for July 2007. Observed values shown in black and modeled values shown in red.**

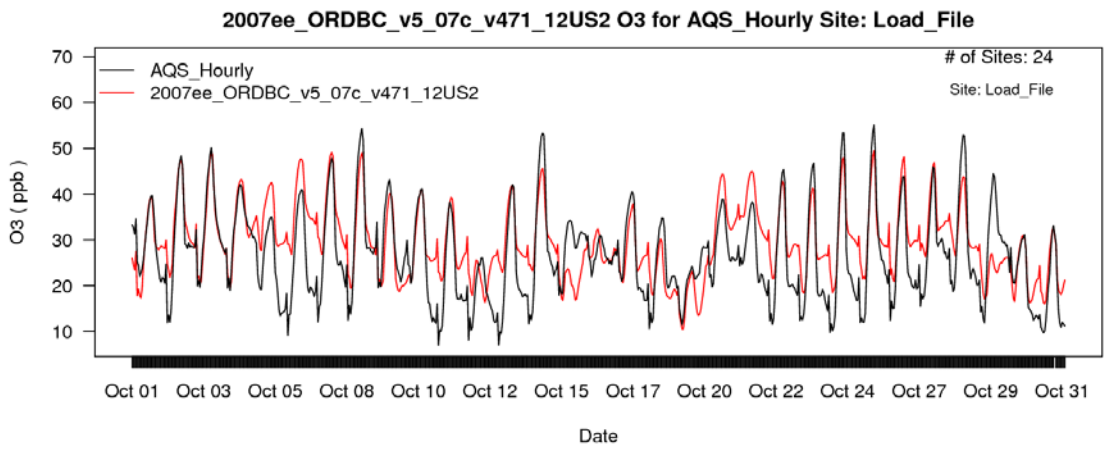


**Figure 86: Time series of hourly ozone concentrations at Sacramento monitoring sites for October 2007. Observed values shown in black and modeled values shown in red.**

**Table 23: Summary of CMAQ model performance at AQS monitoring sites in the Los Angeles area**

| | | No. of obs | MB (ppb) | NMB (%) | ME (ppb) | NME (%) |
|---|---|---|---|---|---|---|
| Winter | Days < 60 | 3710 | 1.40 | 4.4 | 5.39 | 16.9 |
| | Days ≥ 60 | 13 | -35.60 | -44.9 | 35.6 | 44.9 |
| | All Days | 3723 | 1.27 | 4.0 | 5.49 | 17.2 |
| Spring | Days < 60 | 2911 | 1.55 | 3.3 | 6.12 | 13.0 |
| | Days ≥ 60 | 968 | -3.76 | -5.4 | 7.20 | 10.4 |
| | All Days | 3879 | 0.22 | 0.4 | 6.39 | 12.2 |
| Summer | Days < 60 | 1972 | 15.0 | 32.7 | 16.2 | 35.3 |
| | Days ≥ 60 | 1896 | 3.35 | 4.4 | 10.4 | 13.7 |
| | All Days | 3868 | 9.27 | 15.4 | 13.3 | 22.1 |
| Fall | Days < 60 | 3461 | 2.95 | 7.7 | 8.30 | 21.5 |
| | Days ≥ 60 | 335 | -2.66 | -3.8 | 10.60 | 15.1 |
| | All Days | 3796 | 2.46 | 5.9 | 8.51 | 20.5 |

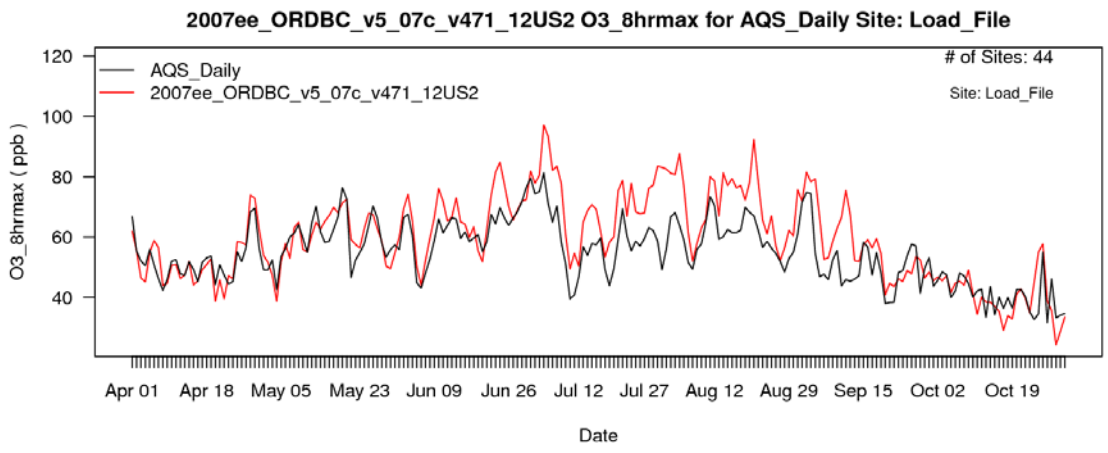


**Figure 87: Time series of 8-hr daily maximum ozone concentrations at Los Angeles monitoring sites for April-October 2007. Observed values shown in black and modeled values shown in red.**

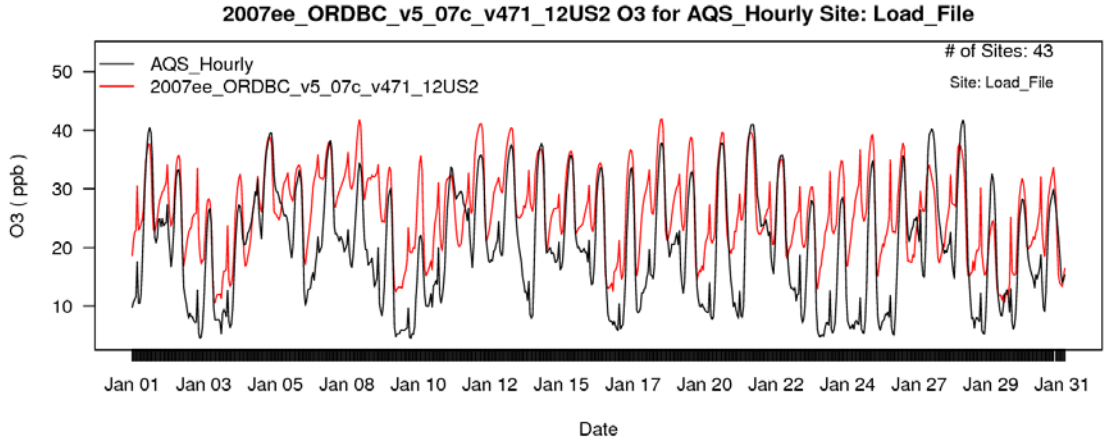


**Figure 88: Time series of hourly ozone concentrations at Los Angeles monitoring sites for January 2007. Observed values shown in black and modeled values shown in red.**

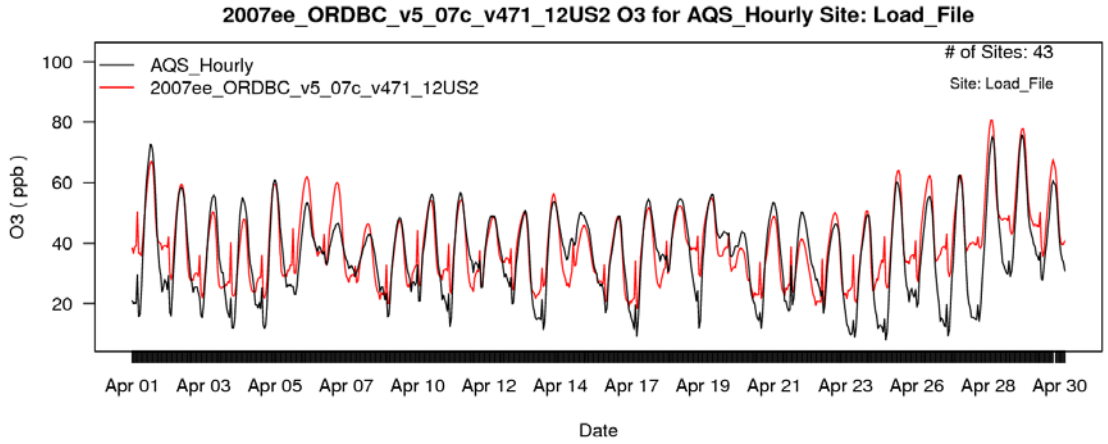

**Figure 89: Time series of hourly ozone concentrations at Los Angeles monitoring sites for April 2007. Observed values shown in black and modeled values shown in red.**

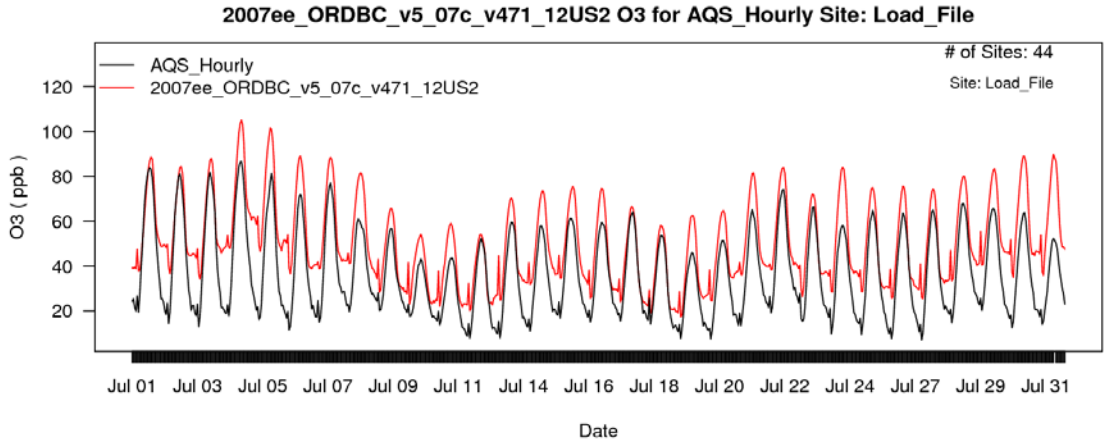


**Figure 90: Time series of hourly ozone concentrations at Los Angeles monitoring sites for July 2007. Observed values shown in black and modeled values shown in red.**

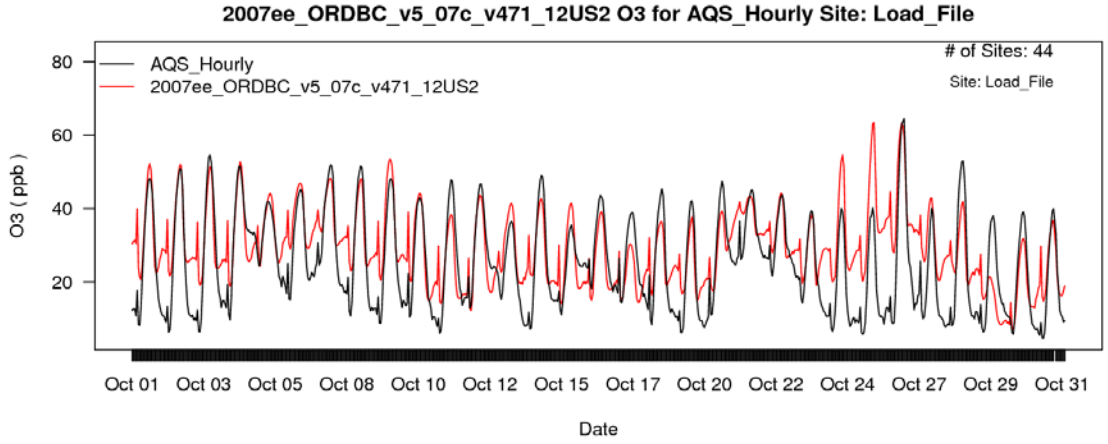


**Figure 91: Time series of hourly ozone concentrations at Los Angeles monitoring sites for October 2007. Observed values shown in black and modeled values shown in red.**

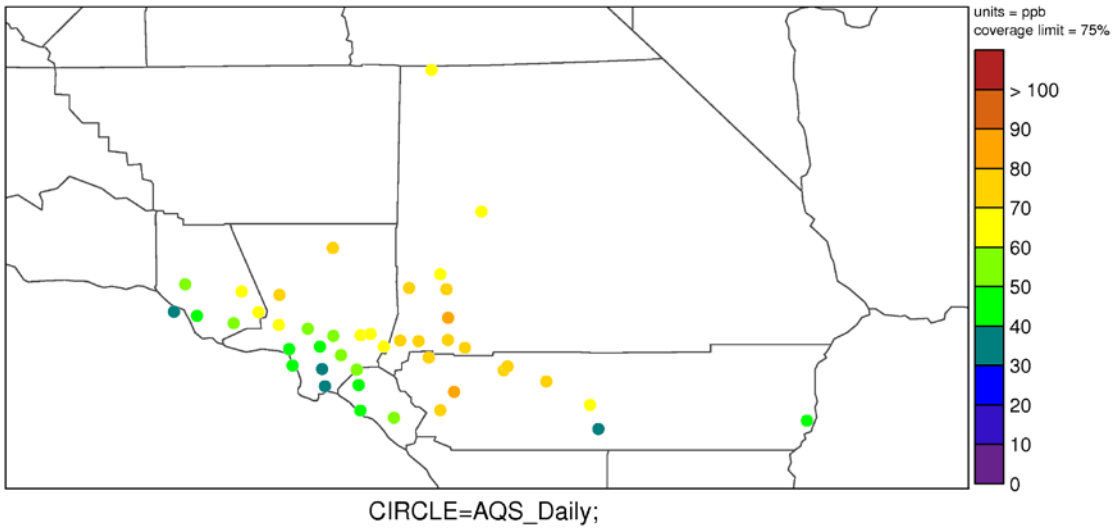


**Figure 92: Map of mean observed MDA8 ozone concentrations at Los Angeles monitoring sites for summer months (June, July, Aug) 2007.**

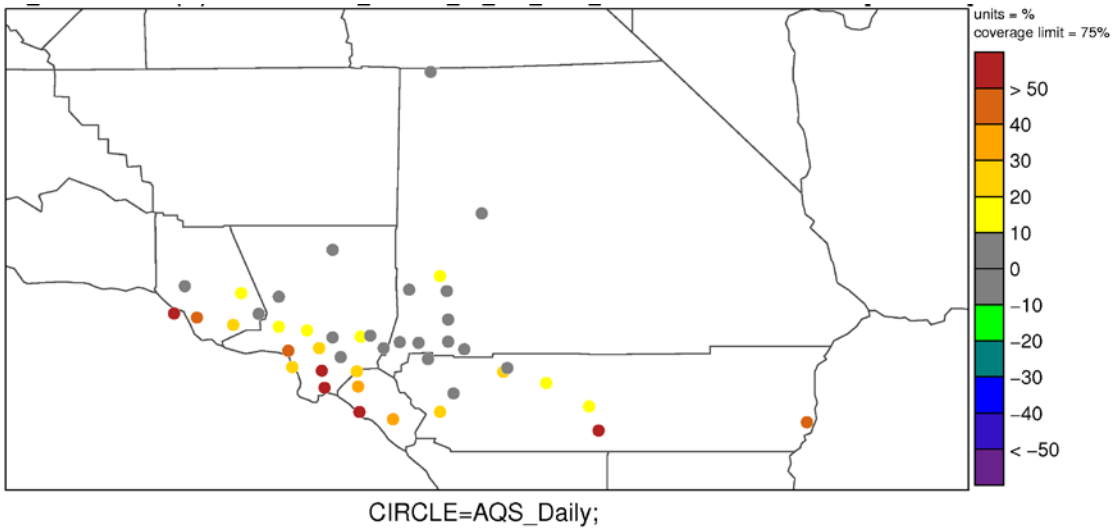


**Figure 93: Map of normalized mean bias for MDA8 ozone concentrations at Los Angeles monitoring sites for summer months (June, July, Aug) 2007.**

## REFERENCES

Akhtar, F., Henderson, B., Appel, W., Napelenok, S., Hutzell, B., Pye, H., Foley, K. (2012). Multiyear Boundary Conditions for CMAQ 5.0 from GEOS-Chem with Secondary Organic Aerosol Extensions, 11th annual Community Modeling and Analysis System conference, Chapel Hill, NC, October 2012.

Carlton, A.G., Bhave, P.V., Napelenok, S.L., Edney, E.D., Sarwar, G., Pinder, R.W., Pouliot, G.A., Houyoux, M. (2010). Model Representation of Secondary Organic Aerosol in CMAQv4.7. *Environmental Science & Technology*, 44: 8553-8560.

Foley, K.M., Roselle, S.J., Appel, K.W., Bhave, P.V., Pleim, J.E., Otte, T.L., Mathur, R., Sarwar, G., Young, J.O., Gilliam, R.C., Nolte, C.G., Kelly, J.T., Gilliland, A.B., Bash, J.O. (2010). Incremental testing of the Community Multiscale Air Quality (CMAQ) modeling system version 4.7, *Geoscientific Model Development*, 3: 205-226.

Gery, M.W., Whitten, G.Z., Killus, J.P., Dodge, M.C. (1989). A photochemical kinetics mechanism for urban and regional scale computer modeling. *Journal of Geophysical Research-Atmospheres*, 94: 12925-12956.

Gilliam, R.C., Pleim, J.E. (2010). Performance Assessment of New Land Surface and Planetary Boundary Layer Physics in the WRF-ARW. *Journal of Applied Meteorology and Climatology*, 49: 760-774.

Gilliland, A.B., Hogrefe, C., Pinder, R.W., Godowitch, J.M., Foley, K.L., Rao, S.T. (2008). Dynamic evaluation of regional air quality models: assessing changes in O3 stemming from changes in emission and meteorology. *Atmospheric Environment*, 42: 5110-5123.

Godowitch, J.M, Gilliam, R.C., Rao, S.T. (2011). Diagnostic evaluation of ozone production and horizontal transport in a regional photochemical air quality modeling system. *Atmospheric Environment*, 45: 3977-3987.

Godowitch, J.M., Pouliot, G.A., Rao, S.T. (2010). Assessing multi-year changes in modeled and observed urban NOx concentrations from a dynamic model evaluation perspective. *Atmospheric Environment*, 44: 2894-2901.

Godowitch, J.M., Hogrefe, C., Rao, S.T. (2008). Diagnostic analysis of a regional air quality model: changes in modeled processes affecting ozone and chemical-transport indicators form NOx point source emissions reductions. *Journal of Geophysical Research-Atmospheres*, 113(D19): D19303, DOI: 10.1029/2007JD009537.

Grell, G. A., Dudhia, A. J., and Stauffer, D. R. (1994). A description of the Fifth-Generation Penn State/NCAR Mesoscale Model (MM5). NCAR Technical Note NCAR/TN-398+STR. Available at http://www.mmm.ucar.edu/mm5/doc1.html.

Henderson, B.H., Akhtar, F., Pye, H.O.T., Napelenok, S.L., Hutzell, W.T. (2013) A database and tool for boundary conditions for regional air quality modeling: description and evaluation, Geoscientific Model Development Discussions, 6, 4665-4704.

Henze, D.K., J.H. Seinfeld, N.L. Ng, J.H. Kroll, T-M. Fu, D.J. Jacob, C.L. Heald (2008). Global modeling of secondary organic aerosol formation from aromatic hydrocarbons: High-vs.low-yield pathways. *Atmos. Chem. Phys*., 8: 2405-2420.

Lam, Y.F., Fu, J.S., Jacob, D.J., Jang, C., Dolwick, P., 2010 2006-2008 GEOS-Chem for CMAQ Initial and Boundary Conditions. 9th Annual CMAS Conference, October 11-13, 2010, Chapel Hill, NC.

Nenes, A., Pandis, S.N., Pilinis, C. (1998). ISORROPIA: A new thermodynamic equilibrium model for multiphase multicomponent inorganic aerosols. *Aquatic Geochemistry*, 4: 123-152.

Napelenok, S.L., Foley, K.M, Kang. D.W., Mathur, R., Pierce, T., Rao, S.T. (2011). Dynamic evaluation of regional air quality model's response to emission reduction in the presence of uncertain emission inventories. *Atmospheric Environment*, 45: 4091-4098.

Otte T.L., Pleim, J.E. (2010). The Meteorology-Chemistry Interface Processor (MCIP) for the CMAQ modeling system: updates through v3.4.1. *Geoscientific Model Development*, 3: 243-256.

Simon, H., Baker, K.R., Phillips, S. (2012). Compilation and interpretation of photochemical model performance statistics published between 2006 and 2012. *Atmospheric Environment*, 61: 124-139.

Skamarock, W.C., Klemp, J.B., Dudhia, J., Gill, D.O., Barker, D.M., Dudia, M.G., Huang, X., Wang, W., Powers, J.G. (2008). A Description of the Advanced Research WRF Version 3.

U.S. Environmental Protection Agency (2011). Meteorological Model Performance for Annual 2007 Simulations, Office of Air Quality Planning and Standards, Research Triangle Park, NC., 27711, EPA-454/R-11-007.

U.S. Environmental Protection Agency (2012a), Air Quality Modeling Technical Support Document for the Regulatory Impact Analysis for the Revisions of the National Ambient Air Quality Standard for Particulate Matter. Office of Air Quality Planning and Standards, Research Triangle Park, NC, December 2012. Available at: http://www.epa.gov/ttn/naaqs/standards/pm/data/201212aqm.pdf

U.S. Environmental Protection Agency (2012b). Technical Support Document: Preparation of Emissions Inventories of the Version 5, 2007-based Platform. Office of Air Quality Planning and Standards, Research Triangle Park, NC. December 2012.

Yantosca, B. (2004). GEOS-CHEMv7-01-02 User's Guide, Atmospheric Chemistry Modeling Group, Harvard University, Cambridge, MA, October 15, 2004.

Yarwood, G., Rao, S., Yocke, M., Whitten, G.Z. (2005). Updates to the Carbon Bond chemical mechanism: CB05. Final Report to the US EPA, RT-0400675, December 8, 2005: http://www.camx.com/publ/pdfs/CB05_Final_Report_120805.pdf.

Zhou, W., Cohan, D.S., Napelenok, S.L. (2013). Reconciling NOx emissions reductions and ozone trends in the U.S., 2002-2006, *Atmospheric Environment*, 70: 236-244.

# Appendix 4-C
# Air Quality Spatial Fields for the National Mortality Risk Burden Assessment

## Table of Contents


1. Overview ..... 3
2. Air Quality Spatial Field Techniques ..... 4
   - 2.1 Voronoi Neighbor Averaging (VNA) ..... 4
   - 2.2 Community Multi-scale Air Quality (CMAQ) Model ..... 5
   - 2.3 Enhanced Voronoi Neighbor Averaging (eVNA) ..... 6
   - 2.4 Downscaler (DS) ..... 7
3. Evaluation of Air Quality Spatial Field Techniques ..... 9
   - 3.1 Data ..... 9
   - 3.2 Methods ..... 9
   - 3.3 Results ..... 11
4. Air Quality Inputs to the National Mortality Risk Burden Assessment ..... 14
5. References ..... 18

## FIGURES

FIGURE 1 NUMERICAL EXAMPLE OF THE VORONOI NEIGHBOR AVERAGING (VNA) TECHNIQUE APPLIED TO A MODEL GRID DOMAIN..5
FIGURE 2 NUMERICAL EXAMPLE OF THE ENHANCED VORONOI NEIGHBOR AVERAGING (EVNA) TECHNIQUE APPLIED TO A MODEL GRID DOMAIN.....7
FIGURE 3 EXAMPLE OF THE "4-FOLD" CROSS-VALIDATION SCHEME USED IN THE EVALUATION OF THE AIR QUALITY SPATIAL FIELD TECHNIQUES FOR THE SOUTHERN LAKE MICHIGAN AREA .....11
FIGURE 4 CROSS-VALIDATION RESULTS FOR THE 2007 ANNUAL 4TH HIGHEST DAILY MAXIMUM $O_3$ CONCENTRATIONS.....12
FIGURE 5 CROSS-VALIDATION RESULTS FOR THE 2007 MAY-SEPTEMBER MEAN OF THE DAILY MAXIMUM 8-HOUR $O_3$ CONCENTRATIONS .....13
FIGURE 6 MAY-SEPTEMBER AVERAGE DAILY MAXIMUM 8-HOUR $O_3$ CONCENTRATIONS IN PPB, BASED ON A DOWNSCALER FUSION OF 2006-2008 AVERAGE MONITORED VALUES WITH A 2007 CMAQ MODEL SIMULATION .....15
FIGURE 7 JUNE-AUGUST AVERAGE DAILY 10AM-6PM MEAN $O_3$ CONCENTRATIONS IN PPB, BASED ON A DOWNSCALER FUSION OF 2006-2008 AVERAGE MONITORED VALUES WITH A 2007 CMAQ MODEL SIMULATION .....16
FIGURE 8 APRIL-SEPTEMBER AVERAGE DAILY MAXIMUM 1-HOUR $O_3$ CONCENTRATIONS IN PPB, BASED ON A DOWNSCALER FUSION OF 2006-2008 AVERAGE MONITORED VALUES WITH A 2007 CMAQ MODEL SIMULATION.....17

## TABLES

TABLE 1 SUMMARY OF THE CROSS-VALIDATION PERFORMANCE METRICS FOR THE FOUR AIR QUALITY SPATIAL FIELD TECHNIQUES ..14

# 1. **OVERVIEW**

The need for greater spatial and temporal coverage of air quality concentration estimates has grown in recent years as epidemiology and exposure studies that link air quality to health effects have become more robust and as regulatory needs have increased. These health studies have historically relied upon direct measurements of air quality concentrations, but prohibitive logistics and costs limit the spatial coverage and temporal resolution of available ambient monitoring networks. Numerical methods of interpolation, which predict unknown values from data observed at known locations, have historically been used by researchers to extend the spatial coverage of these monitoring networks with a high degree of confidence to inform exposure studies. However, simple kriging approaches such as Voronoi Neighbor Averaging (VNA) do not take advantage of the greater availability of model predictions of air quality concentrations that can enhance the predictive capabilities of numerical methods. Such "data fusion" methods employ both ambient air quality monitoring data and air quality modeling simulation data as inputs, and therefore take advantage of the measurement data's accuracy at specific locations and the air quality model's spatial coverage to generate more robust spatial predictions. For regulatory purposes, the enhanced Voronoi Neighbor Averaging (eVNA) has been the preferred method used by EPA to make spatial predictions of ozone as part of conducting health benefit assessments (EPA, 2010). Given the interest and value of these methods, research and development efforts have focused on improving their predictive capabilities. This includes the Office of Research and Development's development of the Downscaler (DS) model that can potentially provide predictions that are improved over those of eVNA (Berrocal et al, 2011).

This appendix describes the methods, evaluation, and results of four different techniques for predicting air quality concentrations. These four techniques are:

1) VNA (interpolating the monitoring data),
2) CMAQ (using the absolute modeled air quality concentrations),
3) eVNA, and
4) Downscaler.

EPA used the method with the best performance based on the evaluation to generate national air quality spatial fields of seasonally averaged $O_3$ concentrations as inputs to the national mortality risk burden assessment in Chapter 8 of the 2nd draft $O_3$ Health Risk and Exposure Assessment.

Air quality spatial fields are also used in two other applications for the risk and exposure assessments. In Appendix 4a to the 2nd Draft $O_3$ Health Risk and Exposure Assessment, we describe the methodology used to create urban-scale spatial fields of hourly $O_3$ concentrations for use in the exposure modeling. In Appendix 4a to the 2nd Draft Welfare Risk and Exposure

Assessment, we evaluate these same four spatial field techniques for use in creating national-scale air quality spatial fields for the W126 exposure metric.

# 2. AIR QUALITY SPATIAL FIELD TECHNIQUES

This section briefly describes the methodology of each of the four techniques considered for generating air quality spatial fields as inputs to the national risk mortality burden analyses described in Chapter 8.

## 2.1 VORONOI NEIGHBOR AVERAGING (VNA)

The Voronoi Neighbor Averaging (VNA; Gold, 1997; Chen et al, 2004) interpolation technique uses inverse distance squared weighted averages of the ambient concentrations from a set of nearest neighboring monitors to estimate the concentration at a specified location (in this case CMAQ grid cell centers). VNA identifies the nearest neighboring monitors for the center of each grid cell using a Delaunay triangulation algorithm, then takes the inverse distance squared weighted average of the hourly $O_3$ concentrations from each neighboring monitor to estimate an hourly $O_3$ concentration value for the center of the grid cell. The following paragraphs provide a numerical example of the VNA technique applied to a model grid domain.

The first step in VNA is to identify the set of nearest monitors for each grid cell in the domain. The left-hand panel of **Error! Reference source not found.** below presents a numerical example with nine model grid cells and seven monitoring sites, with the focus on identifying the set of nearest neighboring sites to the center of grid cell "E", the center cell. The Delaunay triangulation algorithm identifies the set of nearest neighboring monitors by drawing a set of polygons called the "Voronoi diagram" around the center of grid cell "E" and each of the monitoring sites. Voronoi diagrams have the special property that the each edge of the polygons are the same distance from the two closest points, as shown in the right-hand panel below.

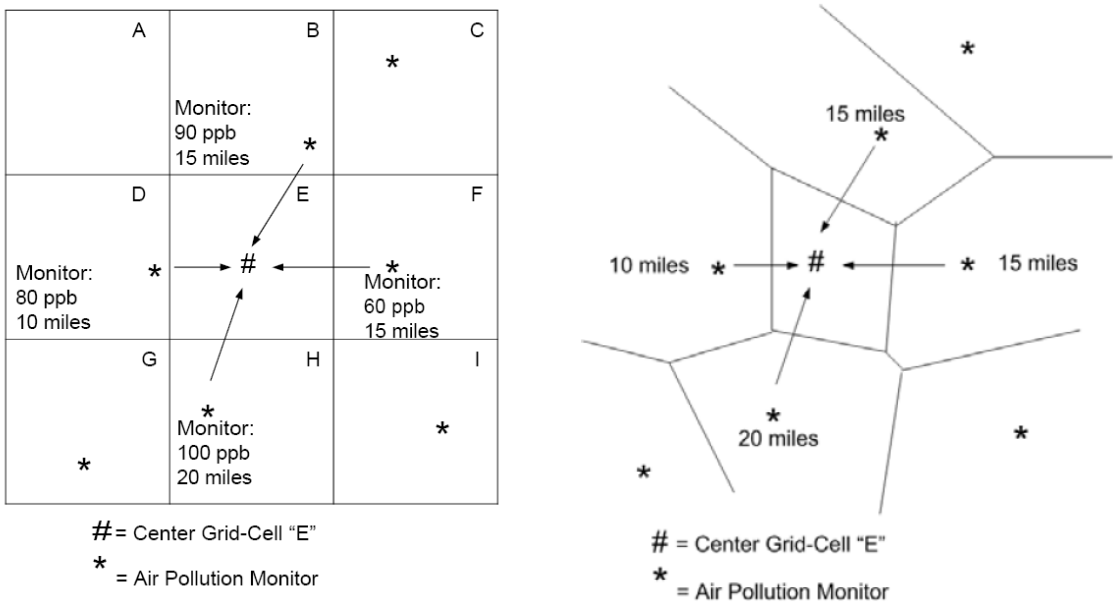


**Figure 1 Numerical example of the Voronoi Neighbor Averaging (VNA) technique applied to a model grid domain**

VNA then chooses the monitoring sites that share a boundary with the center of grid cell "E". These are the nearest neighboring sites, which are used to estimate the concentration value for grid cell "E". The VNA estimate of the concentration value in grid cell "E" is the inverse distance squared weighted average of the four monitored concentrations. The further the monitor is from grid cell "E", the smaller the weight.

For example, the weight for the monitor in grid cell "D" 10 miles from the center of grid cell "E" is calculated as follows:

$$\frac{1/10^2}{1/10^2+1/15^2+1/15^2+1/20^2} = 0.4675 \qquad \textbf{(Equation 1)}$$

The weights for the other monitors are calculated in a similar fashion. The final VNA estimate for grid cell "E" is calculated as follows:

$$VNA(E) = 0.4675 * 80 + 0.2078 * 90 + 0.2078 * 60 + 0.1169 * 100 = 80.3\ ppb$$

**(Equation 2)**

## 2.2 COMMUNITY MULTI-SCALE AIR QUALITY (CMAQ) MODEL

For more than a decade, the EPA's Community Multi-scale Air Quality (CMAQ; Foley et al, 2010) model has been a valuable computational tool used by EPA and states to inform air quality management programs. The CMAQ system simultaneously models multiple air pollutants, including ozone, particulate matter, and a variety of air toxics to help regulators

determine the best air quality management scenarios for their communities, states, and countries. CMAQ is also used by states to assess implementation actions needed to attain National Ambient Air Quality Standards.

The CMAQ system includes emissions, meteorology, and photochemical modeling components. Research continues in all of these areas to reduce biases and uncertainties in model simulations. CMAQ is a multi-scale system that has been applied over continental, national, regional, and urban modeling domains with progressively finer resolution in a series of nested grids. The CMAQ modeling community includes researchers, regulators, and forecasters in academia, government, and the private sector with thousands of users worldwide.

Modeled air quality concentrations from CMAQ simulations have a twofold purpose in the generation and analysis of air quality spatial fields. First, the modeled concentrations are "fused" with the ambient measurement data using the eVNA and DS techniques. Second, the original modeled concentrations are evaluated against the resulting concentration estimates from the other spatial field techniques, to ensure that those techniques successfully reduce biases in the modeled air quality fields.

## 2.3 ENHANCED VORONOI NEIGHBOR AVERAGING (EVNA)

Enhanced Voronoi Neighbor Averaging (eVNA; Timin et al, 2010) is a direct extension of VNA used to combine monitored and modeled air quality concentration data. Continuing from the previous numerical example for VNA, suppose the model grid cells containing monitors are associated with modeled concentrations as shown in Figure 2 below. The modeled concentrations are used to weight the VNA estimates relative to the modeled concentration gradient:

$$eVNA(E) = \sum_{i=1}^{n_i} Weight_i * Monitor_i * \frac{Model_E}{Model_i} \quad \textbf{(Equation 3)}$$

where $Monitor_i$ represents the monitored concentration for a nearest neighboring monitor,
$Weight_i$ represents the inverse distance squared weight for $Monitor_i$,
$Model_E$ represents the modeled concentration for grid cell "E", and
$Model_i$ represents the modeled concentration in the grid cell containing $Monitor_i$.

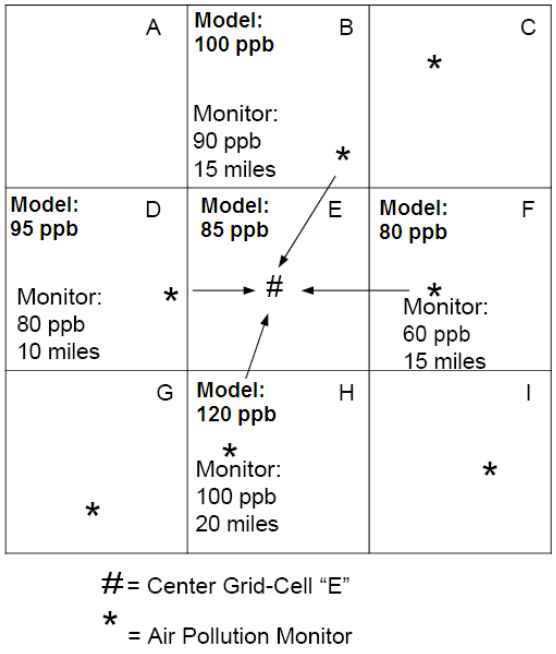


**Figure 2 Numerical example of the Enhanced Voronoi Neighbor Averaging (eVNA) technique applied to a model grid domain**

Based on the values shown in Figure 2, the eVNA estimate for grid cell "E" is calculated as follows:

$$eVNA(E) = \left(0.4675 * 80 * \frac{85}{95}\right) + \left(0.2078 * 90 * \frac{85}{100}\right) + \left(0.2078 * 60 * \frac{85}{80}\right) + \left(0.1169 * 100 * \frac{85}{120}\right) = 70.9\ ppb$$

**(Equation 4)**

In this example, eVNA adjusts the modeled concentration in grid cell "E" downward to reflect the tendency for the model to over-predict the monitored concentrations. In general, the eVNA method attempts to use the monitored concentrations to adjust for model biases, while preserving local gradients in the modeled concentration fields. The computations for VNA and eVNA were executed using the R statistical computing program (R, 2012), with the Delaunay triangulation algorithm implemented in the "deldir" package (Turner, 2012).

## 2.4 DOWNSCALER (DS)

The Downscaler (DS) model is EPA's most recently developed "data fusion" method for spatially predicting air pollution concentrations. DS essentially operates by calibrating CMAQ data to the observational data, and then uses the resulting relationship to predict "observed" concentrations at new spatial points in the domain. Although similar in principle to a linear regression, spatial modeling aspects have been incorporated for improving the model fit, and a

Bayesian[1] approaching to fitting is used to generate an uncertainty value associated with each concentration prediction. The uncertainties that DS produces are a major distinguishing feature from earlier fusion methods previously used by EPA such as the "Hierarchical Bayesian" (HB) model (McMillan et al, 2009). The term "downscaler" refers to the fact that DS takes grid-averaged predictions from an air quality model such as CMAQ for input and produces point-based estimates, thus "scaling down" the area of data representation. Although this allows air pollution concentration estimates to be made at point locations where no observations exist, caution is needed when interpreting any within-grid cell spatial gradients generated by DS since they may not exist in the input datasets. The theory, development, and initial evaluation of DS can be found in the earlier papers of Berrocal, Gelfand, and Holland (2009, 2010, and 2011).

DS develops a relationship between observed and modeled concentrations, and then uses that relationship to spatially predict what measurements would be at new locations in the spatial domain based on the input data. This process is separately applied for each time step (daily in this work) of data, and for each of the pollutants under study (ozone and PM2.5). In its most general form, the model can be expressed in an equation similar to that of linear regression:

$$Y(s,t) = \sim\beta_0(s,t) + \beta_1(t) * \sim x(s,t) + \varepsilon(s,t) \qquad \text{(Equation 1)}$$

where $Y(s,t)$ is the observed concentration at point $s$ and time $t$,

$\sim x(s,t)$ is the CMAQ concentration at point s and time t, (This value is a weighted average of both the grid cell containing the monitor and neighboring grid cells.)

$\sim\beta_0(s,t)$ is the intercept, composed of global and local components,

$\beta_1(t)$ is the global slope, (Local components of the slope are contained in the $\sim x(s,t)$ term),

$\varepsilon(s,t)$ is the model residual error.

DS has additional properties that differentiate it from linear regression:

1) Rather than just finding a single optimal solution to Equation 1, DS uses a Bayesian approach so that uncertainties can be generated along with each concentration prediction. This involves drawing random samples of model parameters from built-in "prior" distributions and assessing their fit on the data on the order of thousands of times. After each iteration, properties of the prior distributions are adjusted to try to improve the fit of the next iteration. The resulting collection of $\sim\beta_0$ and $\beta_1$ values at each space-time point are the "posterior" distributions, and the means and standard distributions of these are used to predict concentrations and associated uncertainties at new spatial points.

2) The model is "heirarchical" in structure, meaning that the top level parameters in Equation 1 (ie $\sim\beta_0(s,t)$, $\beta_1(t)$, $\sim x(s,t)$) are actually defined in terms of further parameters and sub-parameters in the DS code. For example, the overall slope and intercept is defined to be the sum

[1] Bayesian statistical modeling refers to methods that are based on Bayes' theorem, and model the world in terms of probabilities based on previously acquired knowledge.

of a global (one value for the entire spatial domain) and local (values specific to each spatial point) component. This gives more flexibility in fitting a model to the data to optimize the fit (i.e. minimize $\varepsilon(s,t)$).

EPA has recently used DS in other applications, such as providing spatial predictions of national daily 8-hour ozone and fine particulate matter ($PM_{2.5}$) concentrations at a census tract resolution to the Centers for Disease Control (CDC) for the Public Health Air Surveillance Evaluation (PHASE) project as part of their Environmental Public Health Tracking (EPHT) program.

# 3. EVALUATION OF AIR QUALITY SPATIAL FIELD TECHNIQUES

This section describes the data, methods, and results of an evaluation that was performed in order to assess the relative accuracy of the predictions generated by the four air quality spatial field techniques described in the previous section.

## 3.1 DATA

The evaluation was designed to assess the relative ability of each spatial field technique to reproduce monitored concentrations for two annual air quality metrics: 1) the 4$^{th}$ highest daily maximum 8-hour $O_3$ concentration (henceforth referred to as the "4$^{th}$ max"), and 2) the May – September mean of the daily maximum 8-hour $O_3$ concentrations (henceforth referred to as the "seasonal mean"). For the ambient monitoring data, these two metrics were calculated for all monitors in the contiguous U.S. with complete data for 2007 based on the initial dataset and the data completeness criteria described in Appendix 4a. For the air quality modeling data, the two metrics were calculated from hourly $O_3$ concentrations based on a CMAQ simulation with a 12 km gridded domain covering the contiguous U.S., and 2007 emissions and meteorology inputs (EPA, 2012b).

## 3.2 METHODS

Cross-validation is a method commonly used to evaluate the ability of statistical models to make accurate predictions. In a cross-validation analysis, the data are split into two subsets, the "calibration" subset, and the "validation" subset. The calibration subset is used to "fit" the model, usually by estimating parameters which establish a relationship between the variable of interest and one or more dependent variables. The resulting model fit is then applied to the dependent variable(s) in the validation subset, and the predictive ability of the model is assessed by how accurately it is able to reproduce the variable of interest in the validation subset.

The evaluation used a systematic "4-fold" cross-validation scheme based on the CMAQ modeling domain (e.g., 12 km x 12 km grid covering the continental U.S.). The CMAQ modeling domain was divided into four groups, or "folds", so that each 2x2 block of 12 km grid cells had one member in each fold. Figure 3 shows an example of the resulting four folds with $O_3$ monitor locations for the area surrounding southern Lake Michigan. Four cross-validations were performed using VNA, eVNA, and DS, for both the $4^{th}$ max and seasonal mean metrics. The calibration subset in the first cross-validation consisted of the monitors in folds 2, 3, and 4 as shown in Figure 3 (blue dots), while the validation subset consisted of the monitors in fold 1 (red dots). The remaining cross-validations were performed in a similar manner, with three of the four folds used as the calibration subset and the final fold used as the validation subset. Thus, this method resulted in four cross-validation partitions, each with approximately 75% of the monitoring data used in the calibration subset, and the remaining 25% used in the validation subset. Each monitor was included in the validation subset exactly once, resulting in a validation dataset of observed $4^{th}$ max and seasonal mean values paired with VNA, eVNA, and DS predictions of those values at monitor locations. The CMAQ predictions were simply the modeled $4^{th}$ max and seasonal mean values for the 12 km grid cells containing $O_3$ monitors.

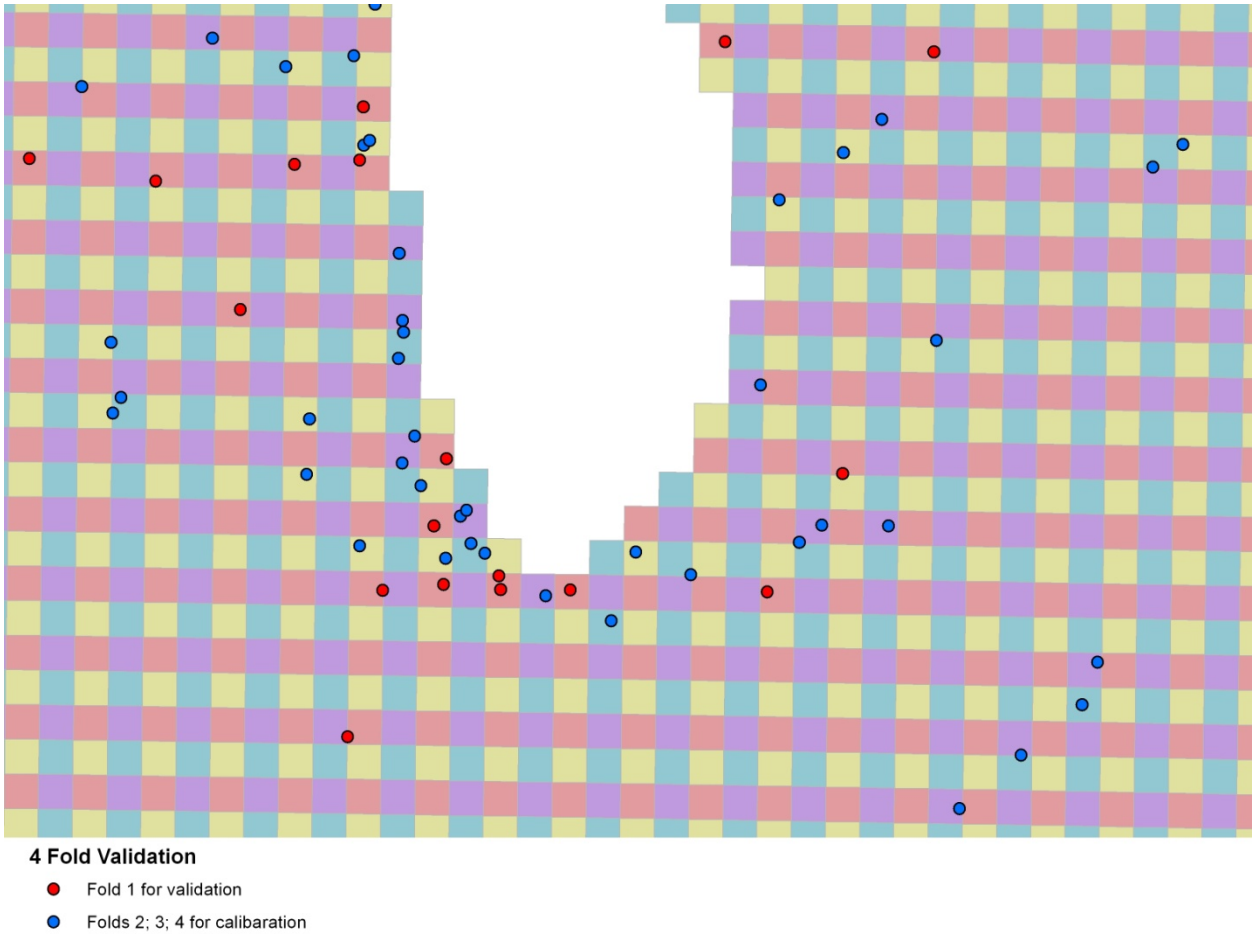


**Figure 3 Example of the "4-fold" cross-validation scheme used in the evaluation of the air quality spatial field techniques for the southern Lake Michigan area**

## 3.3 RESULTS

The cross-validation predictions based on the four air quality spatial field techniques were compared with the observed 4$^{th}$ max and seasonal mean values based on the ambient data. The comparison focused on three performance metrics: 1) the root mean squared error (RMSE), 2) the coefficient of variation ($R^2$), and 3) the mean bias (MB). The results of these comparisons are shown in Figure 4 (4$^{th}$ max) and Figure 5 (seasonal mean), and Table 1 contains a summary of the three performance metrics for each technique.

The cross-validation results clearly showed that VNA, eVNA, and DS more accurately predict monitored 4$^{th}$ max and seasonal mean concentrations than the CMAQ model. The scatter plots and the mean bias statistics indicated that both eVNA and DS were effective at reducing the amount of bias present in the modeled concentrations. The differences between VNA, eVNA, and DS were much smaller, but the performance statistics consistently indicated that overall DS was able to most accurately reproduce the observed values. DS had the highest $R^2$ values, and

the lowest RMSE and MB values of the four techniques for both air quality metrics. In contrast to eVNA, DS seemed to be an improvement over VNA, which did not make use of the modeled concentration data. Based on these results, DS was deemed the most appropriate technique for generating spatial fields of seasonal mean $O_3$ concentrations for the national risk mortality burden analyses.

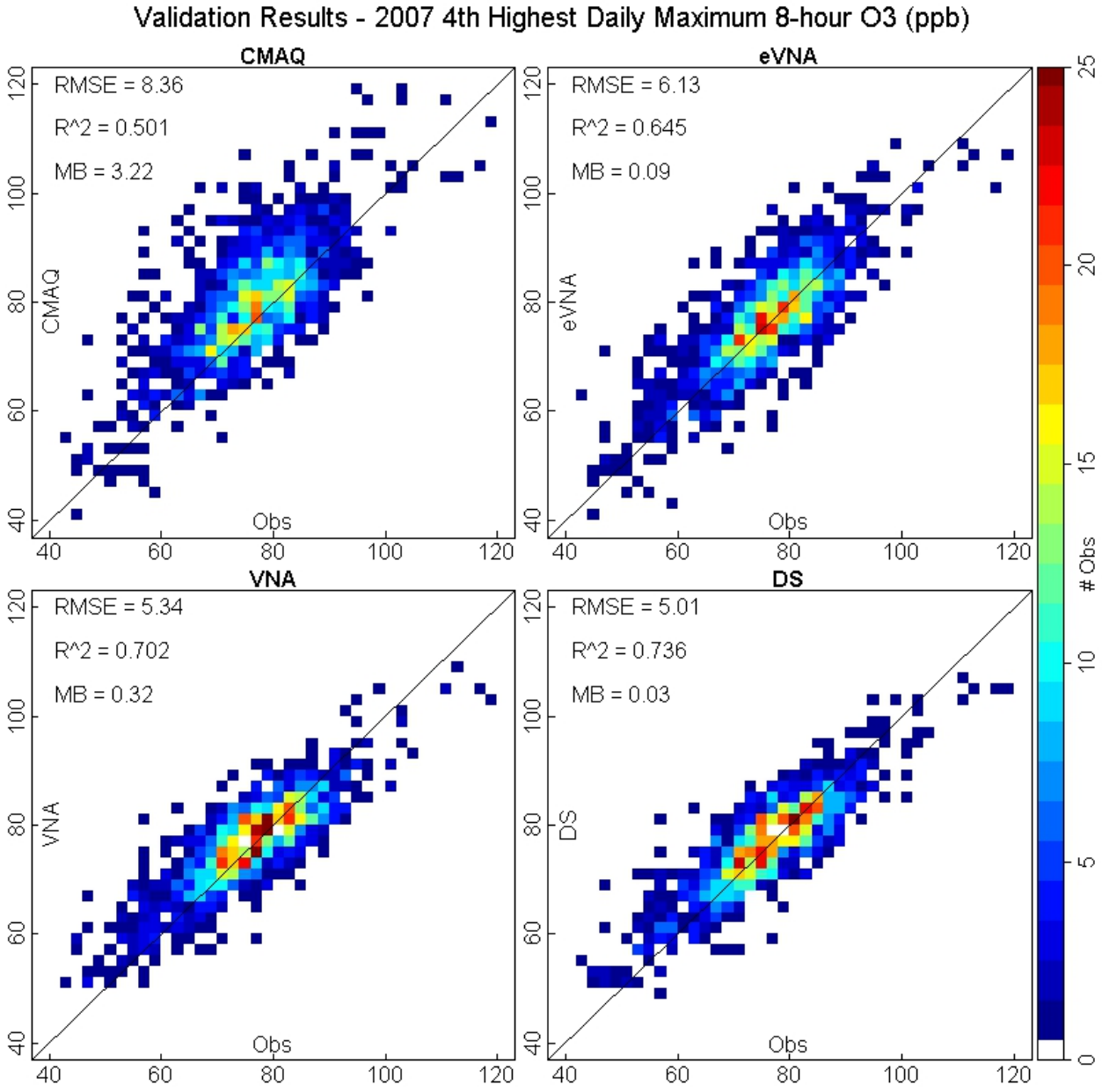


**Figure 4 Cross-validation results for the 2007 annual 4th highest daily maximum $O_3$ concentrations**

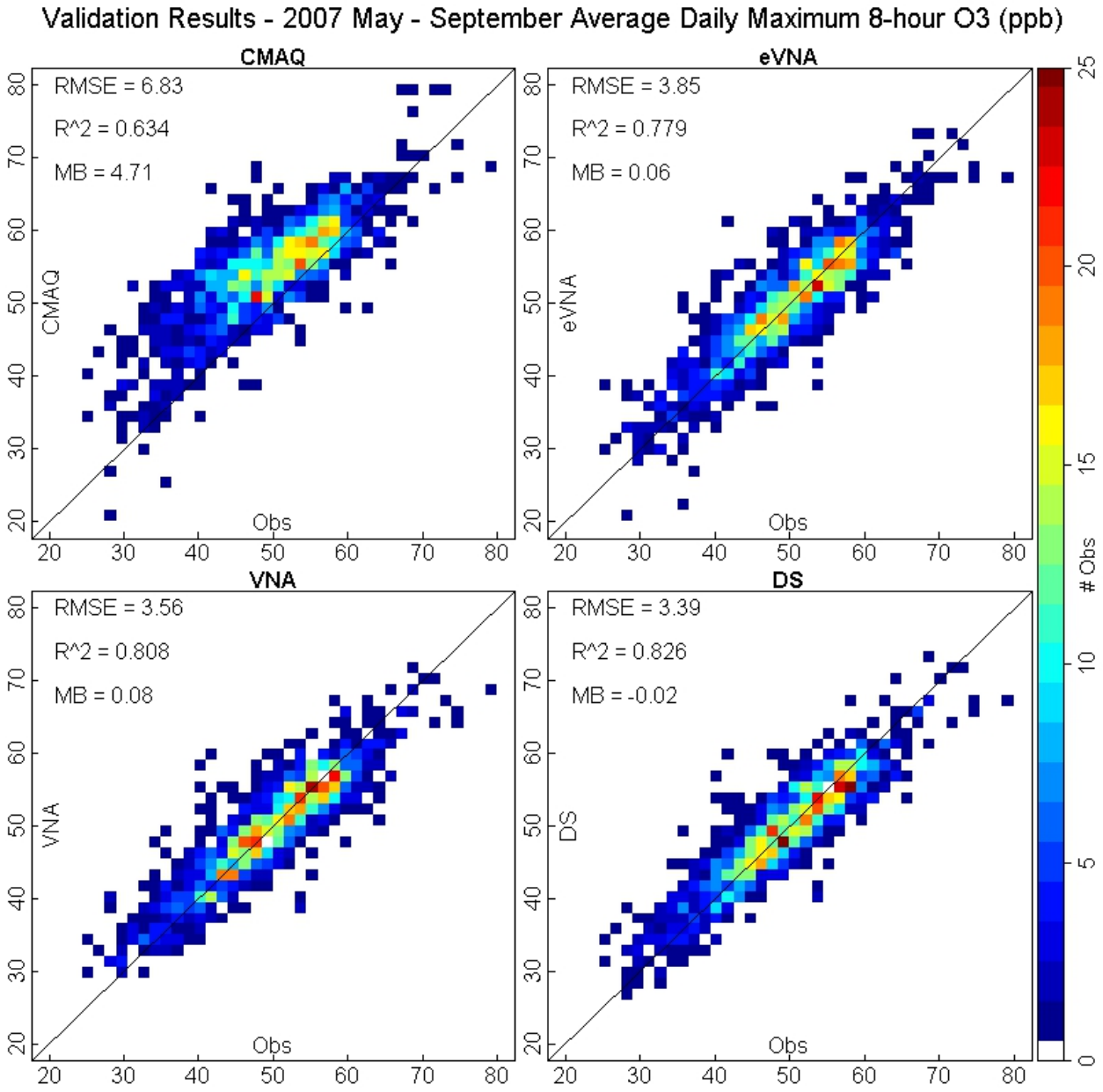


**Figure 5** **Cross-validation results for the 2007 May-September mean of the daily maximum 8-hour $O_3$ concentrations**

| Performance Metric | $O_3$ Metric | VNA | CMAQ | eVNA | DS |
|---|---|---|---|---|---|
| RMSE | $4^{th}$ max | 5.34 | 8.36 | 6.13 | 5.01 |
| RMSE | seasonal mean | 3.56 | 6.83 | 3.85 | 3.39 |
| $R^2$ | $4^{th}$ max | 0.702 | 0.501 | 0.645 | 0.736 |
| $R^2$ | seasonal mean | 0.808 | 0.634 | 0.779 | 0.826 |
| MB | $4^{th}$ max | 0.32 | 3.22 | 0.09 | 0.03 |
| MB | seasonal mean | 0.08 | 4.71 | 0.06 | -0.02 |

**Table 1 Summary of the cross-validation performance metrics for the four air quality spatial field techniques**

# 4. AIR QUALITY INPUTS TO THE NATIONAL MORTALITY RISK BURDEN ASSESSMENT

Three air quality spatial fields were created using DS as inputs to the national mortality risk burden analyses. These fields were based on three seasonal mean $O_3$ metrics:

1) May-September average daily maximum 8-hour $O_3$ concentration (consistent with the metric used by Smith et al. 2009);
2) June-August average daily 10am-6pm mean $O_3$ concentration (consistent with the metric used by Zanobetti and Schwartz 2008); and
3) April-September average daily maximum 1-hour $O_3$ concentration (consistent with the metric used by Jerrett et al 2009).

For the ambient monitoring data, the 2006-2008 average of these annual metrics were calculated for all monitors in the contiguous U.S. with complete data for 2006-2008 based on the initial dataset and the data completeness criteria described in Appendix 4a. For the air quality modeling data, these metrics were calculated from hourly $O_3$ concentrations based on a CMAQ simulation with a 12 km gridded domain covering the contiguous U.S., and 2007 emissions and meteorology inputs. This simulation differed from the one used for the evaluations in that the wildfire and power plant emissions inputs were based on multi-year averages instead of year-specific estimates. Appendix 4b contains a complete description of this CMAQ simulation and provides relevant model evaluation results.

Figure 6, Figure 7, and Figure 8 show maps of the DS air quality spatial fields for the May-September average daily maximum 8-hour $O_3$ concentrations, the June-August average daily 10am-6pm mean $O_3$ concentrations, and the April-September average daily maximum 1-hour $O_3$ concentrations, respectively. The overall spatial pattern seen in these three fields is very similar, with the highest concentration values for each metric occurring in Southern California.

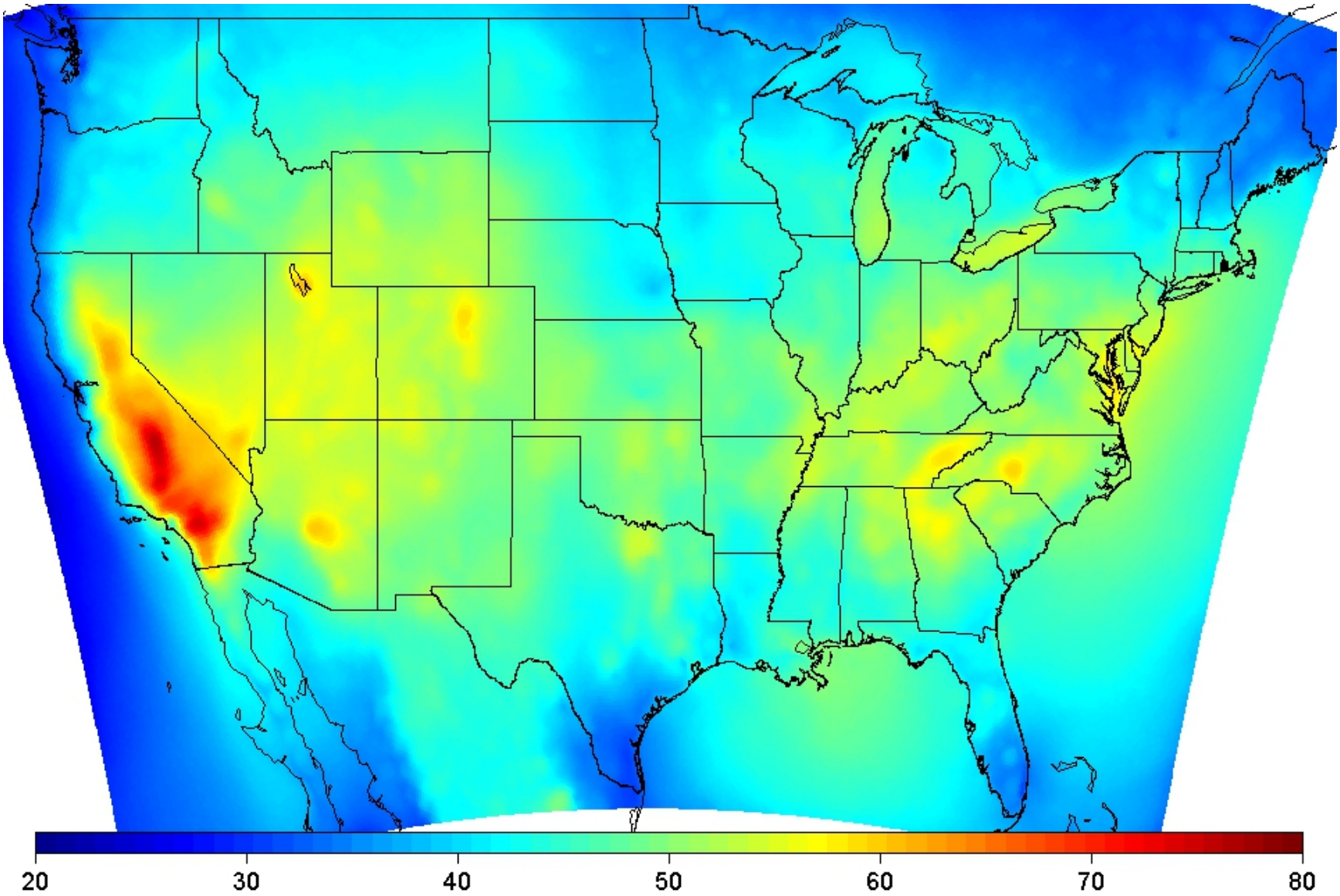


**Figure 6** **May-September average daily maximum 8-hour $O_3$ concentrations in ppb, based on a Downscaler fusion of 2006-2008 average monitored values with a 2007 CMAQ model simulation**

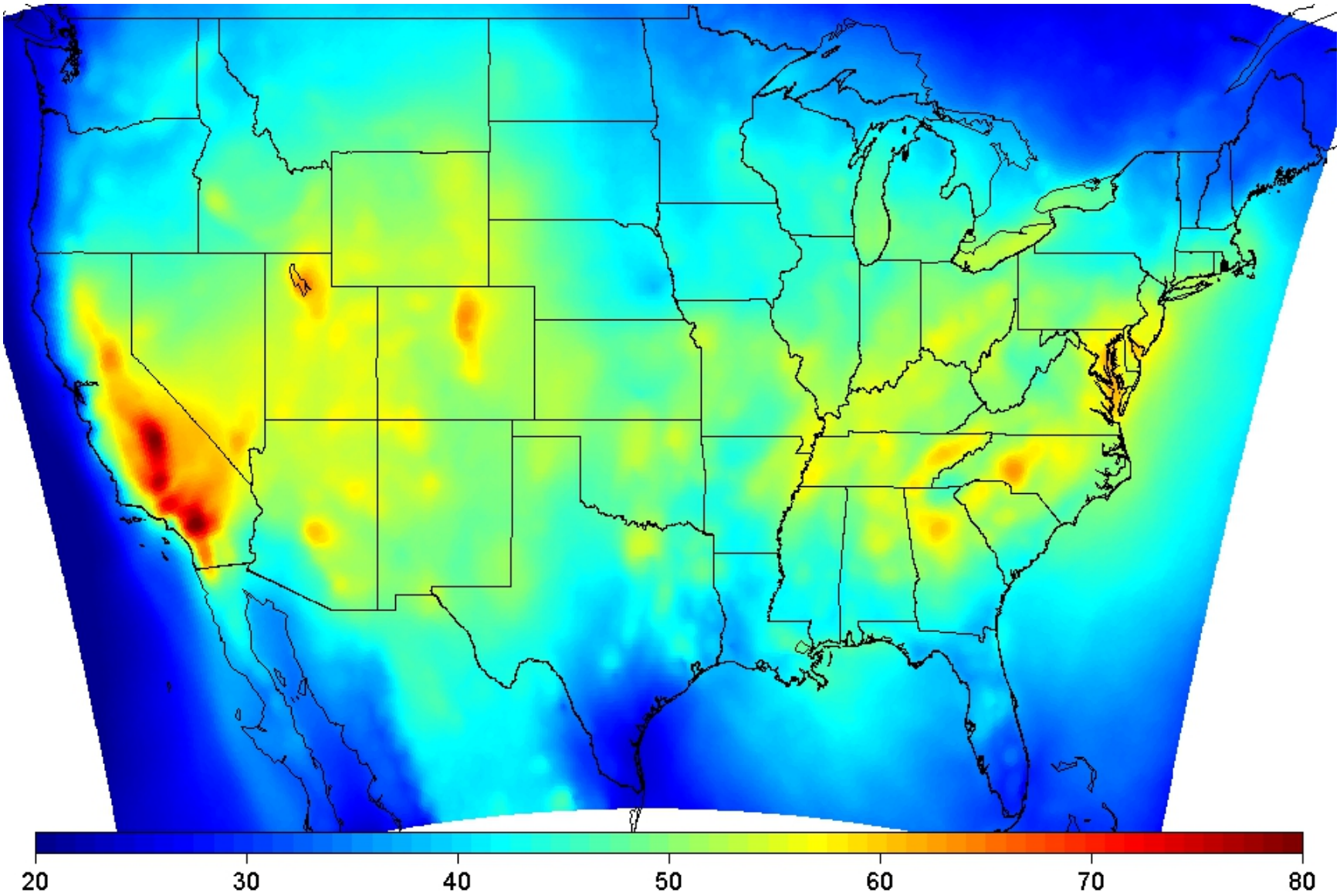


**Figure 7** **June-August average daily 10am-6pm mean $O_3$ concentrations in ppb, based on a Downscaler fusion of 2006-2008 average monitored values with a 2007 CMAQ model simulation**

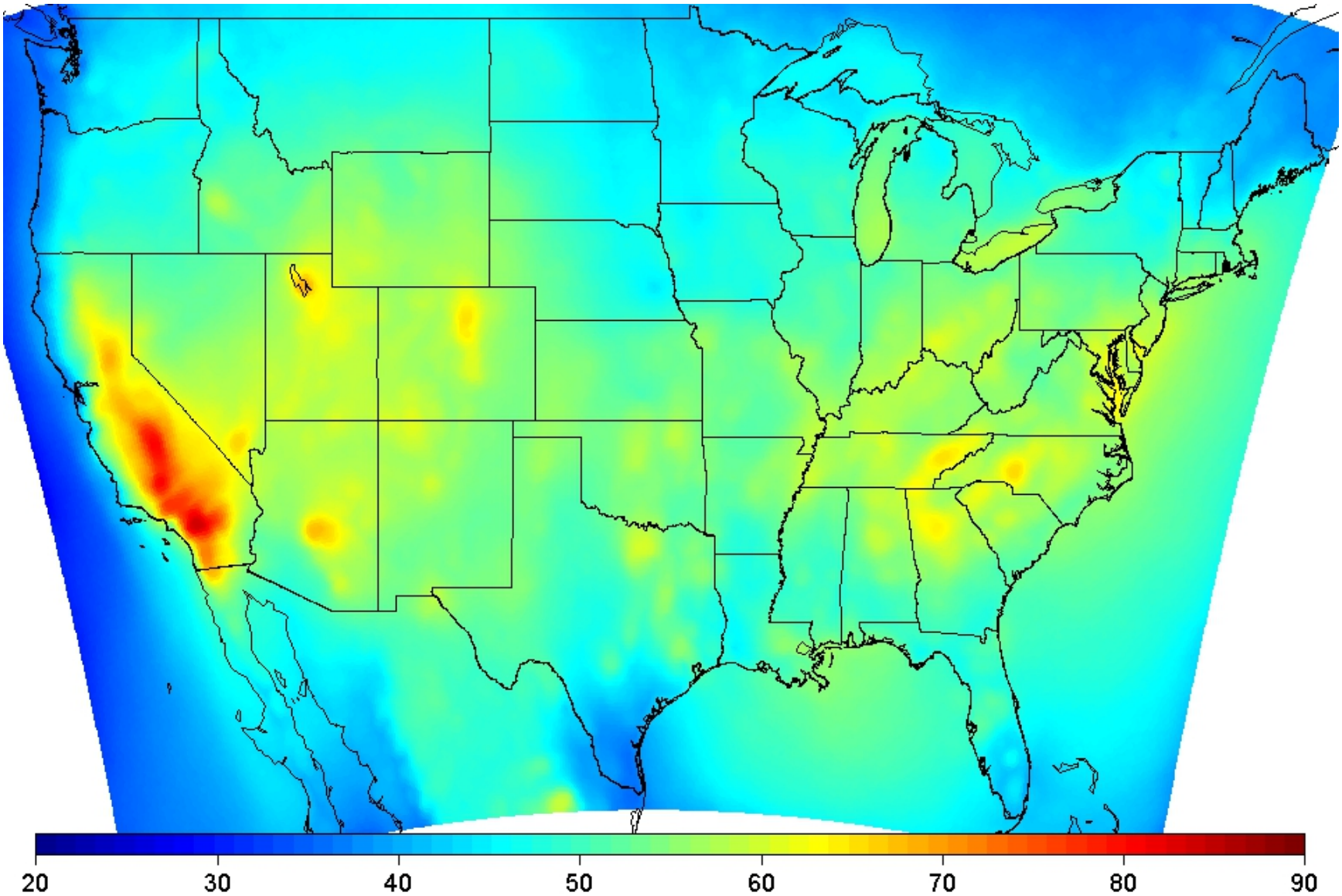


**Figure 8** **April-September average daily maximum 1-hour $O_3$ concentrations in ppb, based on a Downscaler fusion of 2006-2008 average monitored values with a 2007 CMAQ model simulation**

## 5. **REFERENCES**


Abt Associates, Inc. (2010). Environmental Benefits and Mapping Program (Version 4.0). Bethesda, MD. Prepared for U.S. Environmental Protection Agency Office of Air Quality Planning and Standards. Research Triangle Park, NC. Available on the Internet at <http://www.epa.gov/air/benmap>.

Berrocal, V.J., Gelfand, A.E., Holland, D.M. (2009). A Spatio-Temporal Downscaler for Output from Numerical Models. Journal of Agricultural, Biological, and Environmental Statistics, 15(2), 176–197.

Berrocal, V.J., Gelfand, A.E., Holland, D.M. (2010). A Bivariate Space-Time Downscaler Under Space and Time Misalignment. Annals of Applied Statistics, 4(4), 1942-1975.

Berrocal, V.J., Gelfand, A.E., Holland, D.M. (2011). Space-Time Data Fusion Under Error in Computer Model Output: An Application to Modeling Air Quality. Biometrics, 68(3), 837-848.

Chen, J., Zhao, R., Li, Z. (2004). Voronoi-based k-order neighbor relations for spatial analysis. ISPRS J Photogrammetry Remote Sensing, 59(1-2), 60-72.

Foley, K.M., Roselle, S.J., Appel, K.W., Pleim, J.E., Otte, T.L., Mathur, R., Sarwar, G., Young, J.O., Gilliam, R.C., Nolte, C.G., Kelly, J.T., Gilliland, A.B., Bash, J.O. (2010). Incremental testing of the Community Multiscale Air Quality (CMAQ) modeling system version 4.7. Geoscientific Model Development, 3, 205-226.

Gold, C. (1997). Voronoi methods in GIS. In: Algorithmic Foundation of Geographic Information Systems (va Kereveld M., Nievergelt, J., Roos, T., Widmayer, P., eds). Lecture Notes in Computer Sicnece, Vol 1340. Berlin: Springer-Verlag, 21-35.

Hall, E., Eyth, A., Phillips, S. (2012). Hierarchical Bayesian Model (HBM)-Derived Estimates of Air Quality for 2007: Annual Report. EPA/600/R-12/538. Available on the Internet at: http://www.epa.gov/heasd/sources/projects/CDC/AnnualReports/2007_HBM.pdf

Jerrett, M., R.T. Burnett, C.A. Pope III, K. Ito, G. Thurston, D. Krewski, Y. Shi, E. Calle, M. Thun. (2009). Long-term O3 exposure and mortality. N. Eng. J. Med., 360:1085-1095.

McMillan, N.J., Holland, D.M., Morara, M., Feng, J. (2009). Combining Numerical Model Output and Particulate Data using Bayesian Space-Time Modeling. Environmetrics, Vol. 21, 48-65.

R Core Team (2012). R: A language and environment for statistical computing. R Foundation for Statistical Computing, Vienna, Austria. http://www.R-project.org/.

Smith, RL; Xu, B; Switzer, P. (2009). Reassessing the relationship between ozone and short-term mortality in U.S. urban communities. Inhal Toxicol 21: 37-61.

Timin B, Wesson K, Thurman J. (2010). Application of Model and Ambient Data Fusion Techniques to Predict Current and Future Year $PM_{2.5}$ Concentrations in Unmonitored Areas. Pp. 175-179 in Steyn DG, Rao St (eds). Air Pollution Modeling and Its Application XX. Netherlands: Springer.

Turner, R. (2012). deldir: Delaunay Triangulation and Dirichlet (Voronoi) Tessellation. R package version 0.0-19. http://CRAN.R-project.org/package=deldir

U.S. Environmental Protection Agency. (2012a). Health Risk and Exposure Assessment for Ozone, First External Review Draft. Available on the Internet at: http://www.epa.gov/ttn/naaqs/standards/ozone/s_o3_2008_rea.html

U.S. Environmental Protection Agency. (2012b). Air Quality Modeling Technical Support Document for the Regulatory Impact Analysis for the Revisions to the National Ambient Air Quality Standards for Particulate Matter. Available on the Internet at: http://www.epa.gov/ttn/naaqs/standards/pm/data/201212aqm.pdf

Wells, B., Wesson, K., Jenkins, S. (2012). Analysis of Recent U.S. Ozone Air Quality Data to Support the O3 NAAQS Review and Quadratic Rollback Simulations to Support the First Draft of the Risk and Exposure Assessment. Available on the Internet at: http://www.epa.gov/ttn/naaqs/standards/ozone/s_o3_td.html

Zanobetti, A., and J. Schwartz (2008). Mortality Displacement in the Association of Ozone with Mortality: An Analysis of 48 Cities in the United States. American Journal of Respiratory and Critical Care Medicine, 177, 184-189.

# Appendix 4-D
# Model-based Air Quality Adjustment Using the Higher-order Decoupled Direct Method (HDDM)

## Table of Contents


1. Motivation for a New Technique to Simulate Ozone Concentrations Under Alternative Standards ..... 1

2. Higher-order Decoupled Direct Method (HDDM) ..... 2

2.1 Capabilities ..... 2

2.2 Limitations ..... 4

3. Applying HDDM/CMAQ to Adjust Ozone to Just Meet Current and Alternative Standards: Methodology ..... 5

3.1 Conceptual Framework ..... 5

3.2 Application to Measured $O_3$ Concentrations in 15 Urban Areas ..... 6

3.2.1 Multi-step Application of HDDM Sensitivities ..... 7

3.2.2 Relationships between HDDM Sensitivities and Modeled $O_3$ Concentrations 16

3.2.3 Application of Sensitivity Regressions to Ambient Data ..... 24

3.2.4 Alternate Methodologies ..... 25

4. Applying HDDM/CMAQ to Adjust Ozone to Just Meet Current and Alternative Standards: Results ..... 26

4.1 Emission Reductions Applied to Meet Alternative Standards ..... 26

4.2 Design Values ..... 27

4.3 Distribution of Hourly $O_3$ Concentrations ..... 39

4.4 Standard Errors for Predicted Hourly $O_3$ Concentrations ..... 56

4.5 Air Quality Inputs for the Epidemiology-Based Risk Assessment ..... 59

4.6 Air Quality Inputs for the Exposure and Clinical Risk Assessment ..... 66

4.7 Comparing Air Quality Adjustments Based on NOx Reductions Only to Air Quality Adjustments Based on NOx and VOC Reductions ..... 131

5. References ..... 144

# Table of Figures


FIGURE 1: FLOW DIAGRAM DEMONSTRATING DDM MODEL-BASED $O_3$ ADJUSTMENT APPROACH ..... 6

FIGURE 2: CONCEPTUAL PICTURE OF 3-STEP APPLICATION OF HDDM SENSITIVITIES ..... 9

FIGURE 3: COMPARISON OF BRUTE FORCE AND 3-STEP HDDM $O_3$ ESTIMATES FOR 50% NOX CUT CONDITIONS: ATLANTA, BALTIMORE, BOSTON, CHICAGO, CLEVELAND, DALLAS, DENVER, AND DETROIT. ..... 13

FIGURE 4: COMPARISON OF BRUTE FORCE AND 3-STEP HDDM $O_3$ ESTIMATES FOR 50% NOX CUT CONDITIONS: HOUSTON, LOS ANGELES, NEW YORK, PHILADELPHIA, SACRAMENTO, ST. LOUIS, AND WASHINGTON D.C. ..... 14

FIGURE 5: COMPARISON OF BRUTE FORCE AND 3-STEP HDDM $O_3$ ESTIMATES FOR 90% NOX CUT CONDITIONS: ATLANTA, BALTIMORE, BOSTON, CHICAGO, CLEVELAND, DALLAS, DENVER, AND DETROIT. ..... 15

FIGURE 6: COMPARISON OF BRUTE FORCE AND 3-STEP HDDM $O_3$ ESTIMATES FOR 90% NOX CUT CONDITIONS: HOUSTON, LOS ANGELES, NEW YORK, PHILADELPHIA, SACRAMENTO, ST. LOUIS, AND WASHINGTON D.C. ..... 16

FIGURE 7: RELATIONSHIP BETWEEN $S_{NOx}$ AND HOURLY $O_3$ AT A $NO_x$-LIMITED SITE DOWNWIND OF ATLANTA (SUMMER). RELATIONSHIPS ARE SHOWN FOR ONE NIGHTTIME HOUR, ONE MORNING RUSH-HOUR HOUR, ONE DAYTIME HOUR, AND ONE EVENING RUSH-HOUR HOUR. THE SOLID BLUE LINE SHOW THE LINEAR REGRESSION FOR THESE POINTS AND THE DOTTED BLUE LINE SHOWS THE FLOOR VALUE USED FOR $S_{NOx}$ BASED ON THE $5^{TH}$ PERCENTILE MODELED VALUE. ..... 19

FIGURE 8: RELATIONSHIP BETWEEN $S_{NOx}$ AND HOURLY $O_3$ AT A $NO_x$-SATURATED SITE IN QUEENS COUNTY, NY (AUTUMN). RELATIONSHIPS ARE SHOWN FOR ONE NIGHTTIME HOUR, ONE MORNING RUSH-HOUR HOUR, ONE DAYTIME HOUR, AND ONE EVENING RUSH-HOUR HOUR. THE SOLID BLUE LINE SHOW THE LINEAR REGRESSION FOR THESE POINTS AND THE DOTTED BLUE LINE SHOWS THE FLOOR VALUE USED FOR $S_{NOx}$ BASED ON THE $5^{TH}$ PERCENTILE MODELED VALUE. ..... 20

FIGURE 9: RELATIONSHIP BETWEEN $S_{NOx}$ AND HOURLY $O_3$ AT A $NO_x$-SATURATED SITE IN SUFFOLK COUNTY, NY ON LONG ISLAND (SPRING). RELATIONSHIPS ARE SHOWN FOR ONE NIGHTTIME HOUR, ONE MORNING RUSH-HOUR HOUR, ONE DAYTIME HOUR, AND ONE EVENING RUSH-HOUR HOUR. THE SOLID BLUE LINE SHOW THE LINEAR REGRESSION FOR THESE POINTS AND THE DOTTED BLUE LINE SHOWS THE FLOOR VALUE USED FOR $S_{NOx}$ BASED ON THE $5^{TH}$ PERCENTILE MODELED VALUE. ..... 21

FIGURE 10: RELATIONSHIP BETWEEN $S^2_{NOx}$ AND $S_{NOx}$ AT A $NO_x$-LIMITED SITE DOWNWIND OF ATLANTA (SUMMER). RELATIONSHIPS ARE SHOWN FOR ONE NIGHTTIME HOUR, ONE MORNING RUSH-HOUR HOUR, ONE DAYTIME HOUR, AND ONE EVENING RUSH-HOUR HOUR. THE SOLID BLUE LINE SHOWS THE LINEAR REGRESSION FOR THESE POINTS. ..... 22

FIGURE 11: RELATIONSHIP BETWEEN $S^2_{NOx}$ AND $S_{NOx}$ AT A $NO_x$-SATURATED SITE IN QUEENS COUNTY, NY (AUTUMN). RELATIONSHIPS ARE SHOWN FOR ONE NIGHTTIME HOUR, ONE MORNING RUSH-HOUR HOUR, ONE DAYTIME HOUR, AND ONE EVENING RUSH-HOUR HOUR. THE SOLID BLUE LINE SHOWS THE LINEAR REGRESSION FOR THESE POINTS. ..... 23

FIGURE 12: RELATIONSHIP BETWEEN $S^2_{NOx}$ AND $S_{NOx}$ AT A $NO_x$-SATURATED SITE IN SUFFOLK COUNTY, NY ON LONG ISLAND (SPRING). RELATIONSHIPS ARE SHOWN FOR ONE NIGHTTIME HOUR, ONE MORNING RUSH-HOUR HOUR, ONE DAYTIME HOUR, AND ONE EVENING RUSH-HOUR HOUR. THE SOLID BLUE LINE SHOWS THE LINEAR REGRESSION FOR THESE POINTS. ..... 24

FIGURE 13: HOURLY $O_3$ DISTRIBUTIONS AT ATLANTA AREA REGULATORY MONITORING SITES FOR OBSERVED AIR QUALITY, AND AIR QUALITY ADJUSTED TO MEET THE EXISTING (75 PPB) AND ALTERNATIVE (65 PPB) STANDARDS FOR 2006-2008 (LEFT) AND 2008-2010 (RIGHT). ..... 41

FIGURE 14: HOURLY $O_3$ DISTRIBUTIONS AT BALTIMORE AREA REGULATORY MONITORING SITES FOR OBSERVED AIR QUALITY, AND AIR QUALITY ADJUSTED TO MEET THE EXISTING (75 PPB) AND ALTERNATIVE (65 PPB) STANDARDS FOR 2006-2008 (LEFT) AND 2008-2010 (RIGHT). ..... 42

FIGURE 15: HOURLY $O_3$ DISTRIBUTIONS AT BOSTON AREA REGULATORY MONITORING SITES FOR OBSERVED AIR QUALITY, AND AIR QUALITY ADJUSTED TO MEET THE EXISTING (75 PPB) AND ALTERNATIVE (65 PPB) STANDARDS FOR 2006-2008 (LEFT) AND 2008-2010 (RIGHT). ..... 42
FIGURE 16: HOURLY $O_3$ DISTRIBUTIONS AT CHICAGO AREA REGULATORY MONITORING SITES FOR OBSERVED AIR QUALITY, AND AIR QUALITY ADJUSTED TO MEET THE EXISTING (75 PPB) AND ALTERNATIVE (65 PPB) STANDARDS FOR 2006-2008 (LEFT) AND 2008-2010 (RIGHT). ..... 43
FIGURE 17: HOURLY $O_3$ DISTRIBUTIONS AT CLEVELAND AREA REGULATORY MONITORING SITES FOR OBSERVED AIR QUALITY, AND AIR QUALITY ADJUSTED TO MEET THE EXISTING (75 PPB) AND ALTERNATIVE (65 PPB) STANDARDS FOR 2006-2008 (LEFT) AND 2008-2010 (RIGHT). ..... 43
FIGURE 18: HOURLY $O_3$ DISTRIBUTIONS AT DALLAS AREA REGULATORY MONITORING SITES FOR OBSERVED AIR QUALITY, AND AIR QUALITY ADJUSTED TO MEET THE EXISTING (75 PPB) AND ALTERNATIVE (65 PPB) STANDARDS FOR 2006-2008 (LEFT) AND 2008-2010 (RIGHT). ..... 44
FIGURE 19: HOURLY $O_3$ DISTRIBUTIONS AT DENVER AREA REGULATORY MONITORING SITES FOR OBSERVED AIR QUALITY, AND AIR QUALITY ADJUSTED TO MEET THE EXISTING (75 PPB) AND ALTERNATIVE (65 PPB) STANDARDS FOR 2006-2008 (LEFT) AND 2008-2010 (RIGHT). ..... 44
FIGURE 20: HOURLY $O_3$ DISTRIBUTIONS AT DETROIT AREA REGULATORY MONITORING SITES FOR OBSERVED AIR QUALITY, AND AIR QUALITY ADJUSTED TO MEET THE EXISTING (75 PPB) AND ALTERNATIVE (65 PPB) STANDARDS FOR 2006-2008 (LEFT) AND 2008-2010 (RIGHT). ..... 45
FIGURE 21: HOURLY $O_3$ DISTRIBUTIONS AT HOUSTON AREA REGULATORY MONITORING SITES FOR OBSERVED AIR QUALITY, AND AIR QUALITY ADJUSTED TO MEET THE EXISTING (75 PPB) AND ALTERNATIVE (65 PPB) STANDARDS FOR 2006-2008 (LEFT) AND 2008-2010 (RIGHT). ..... 45
FIGURE 22: HOURLY $O_3$ DISTRIBUTIONS AT LOS ANGELES AREA REGULATORY MONITORING SITES FOR OBSERVED AIR QUALITY, AND AIR QUALITY ADJUSTED TO MEET THE EXISTING (75 PPB) AND ALTERNATIVE (65 PPB) STANDARDS FOR 2006-2008 (LEFT) AND 2008-2010 (RIGHT). ..... 46
FIGURE 23: HOURLY $O_3$ DISTRIBUTIONS AT NEW YORK AREA REGULATORY MONITORING SITES FOR OBSERVED AIR QUALITY, AND AIR QUALITY ADJUSTED TO MEET THE EXISTING (75 PPB) AND ALTERNATIVE (65 PPB) STANDARDS FOR 2006-2008 (LEFT) AND 2008-2010 (RIGHT). ..... 46
FIGURE 24: HOURLY $O_3$ DISTRIBUTIONS AT PHILADELPHIA AREA REGULATORY MONITORING SITES FOR OBSERVED AIR QUALITY, AND AIR QUALITY ADJUSTED TO MEET THE EXISTING (75 PPB) AND ALTERNATIVE (65 PPB) STANDARDS FOR 2006-2008 (LEFT) AND 2008-2010 (RIGHT). ..... 47
FIGURE 25: HOURLY $O_3$ DISTRIBUTIONS AT SACRAMENTO AREA REGULATORY MONITORING SITES FOR OBSERVED AIR QUALITY, AND AIR QUALITY ADJUSTED TO MEET THE EXISTING (75 PPB) AND ALTERNATIVE (65 PPB) STANDARDS FOR 2006-2008 (LEFT) AND 2008-2010 (RIGHT). ..... 47
FIGURE 26: HOURLY $O_3$ DISTRIBUTIONS AT ST. LOUIS AREA REGULATORY MONITORING SITES FOR OBSERVED AIR QUALITY, AND AIR QUALITY ADJUSTED TO MEET THE EXISTING (75 PPB) AND ALTERNATIVE (65 PPB) STANDARDS FOR 2006-2008 (LEFT) AND 2008-2010 (RIGHT). ..... 48
FIGURE 27: HOURLY $O_3$ DISTRIBUTIONS AT WASHINGTON, D.C. AREA REGULATORY MONITORING SITES FOR OBSERVED AIR QUALITY, AND AIR QUALITY ADJUSTED TO MEET THE EXISTING (75 PPB) AND ALTERNATIVE (65 PPB) STANDARDS FOR 2006-2008 (LEFT) AND 2008-2010 (RIGHT). ..... 48

FIGURE 28: MONTHLY $O_3$ DISTRIBUTIONS AT ATLANTA AREA REGULATORY MONITORING SITES FOR OBSERVED AIR QUALITY, AND AIR QUALITY ADJUSTED TO MEET THE EXISTING (75 PPB) AND ALTERNATIVE (65 PPB) STANDARDS FOR 2006-2008 (LEFT) AND 2008-2010 (RIGHT). ..... 49
FIGURE 29: MONTHLY $O_3$ DISTRIBUTIONS AT BALTIMORE AREA REGULATORY MONITORING SITES FOR OBSERVED AIR QUALITY, AND AIR QUALITY ADJUSTED TO MEET THE EXISTING (75 PPB) AND ALTERNATIVE (65 PPB) STANDARDS FOR 2006-2008 (LEFT) AND 2008-2010 (RIGHT). ..... 49
FIGURE 30: MONTHLY $O_3$ DISTRIBUTIONS AT BOSTON AREA REGULATORY MONITORING SITES FOR OBSERVED AIR QUALITY, AND AIR QUALITY ADJUSTED TO MEET THE EXISTING (75 PPB) AND ALTERNATIVE (65 PPB) STANDARDS FOR 2006-2008 (LEFT) AND 2008-2010 (RIGHT). ..... 50
FIGURE 31: MONTHLY $O_3$ DISTRIBUTIONS AT CHICAGO AREA REGULATORY MONITORING SITES FOR OBSERVED AIR QUALITY, AND AIR QUALITY ADJUSTED TO MEET THE EXISTING (75 PPB) AND ALTERNATIVE (65 PPB) STANDARDS FOR 2006-2008 (LEFT) AND 2008-2010 (RIGHT). ..... 50
FIGURE 32: MONTHLY $O_3$ DISTRIBUTIONS AT CLEVELAND AREA REGULATORY MONITORING SITES FOR OBSERVED AIR QUALITY, AND AIR QUALITY ADJUSTED TO MEET THE EXISTING (75 PPB) AND ALTERNATIVE (65 PPB) STANDARDS FOR 2006-2008 (LEFT) AND 2008-2010 (RIGHT). ..... 51
FIGURE 33: MONTHLY $O_3$ DISTRIBUTIONS AT DALLAS AREA REGULATORY MONITORING SITES FOR OBSERVED AIR QUALITY, AND AIR QUALITY ADJUSTED TO MEET THE EXISTING (75 PPB) AND ALTERNATIVE (65 PPB) STANDARDS FOR 2006-2008 (LEFT) AND 2008-2010 (RIGHT). ..... 51
FIGURE 34: MONTHLY $O_3$ DISTRIBUTIONS AT DENVER AREA REGULATORY MONITORING SITES FOR OBSERVED AIR QUALITY, AND AIR QUALITY ADJUSTED TO MEET THE EXISTING (75 PPB) AND ALTERNATIVE (65 PPB) STANDARDS FOR 2006-2008 (LEFT) AND 2008-2010 (RIGHT). ..... 52
FIGURE 35: MONTHLY $O_3$ DISTRIBUTIONS AT DETROIT AREA REGULATORY MONITORING SITES FOR OBSERVED AIR QUALITY, AND AIR QUALITY ADJUSTED TO MEET THE EXISTING (75 PPB) AND ALTERNATIVE (65 PPB) STANDARDS FOR 2006-2008 (LEFT) AND 2008-2010 (RIGHT). ..... 52
FIGURE 36: MONTHLY $O_3$ DISTRIBUTIONS AT HOUSTON AREA REGULATORY MONITORING SITES FOR OBSERVED AIR QUALITY, AND AIR QUALITY ADJUSTED TO MEET THE EXISTING (75 PPB) AND ALTERNATIVE (65 PPB) STANDARDS FOR 2006-2008 (LEFT) AND 2008-2010 (RIGHT). ..... 53
FIGURE 37: MONTHLY $O_3$ DISTRIBUTIONS AT LOS ANGELES AREA REGULATORY MONITORING SITES FOR OBSERVED AIR QUALITY, AND AIR QUALITY ADJUSTED TO MEET THE EXISTING (75 PPB) AND ALTERNATIVE (65 PPB) STANDARDS FOR 2006-2008 (LEFT) AND 2008-2010 (RIGHT). ..... 53
FIGURE 38: MONTHLY $O_3$ DISTRIBUTIONS AT NEW YORK AREA REGULATORY MONITORING SITES FOR OBSERVED AIR QUALITY, AND AIR QUALITY ADJUSTED TO MEET THE EXISTING (75 PPB) AND ALTERNATIVE (65 PPB) STANDARDS FOR 2006-2008 (LEFT) AND 2008-2010 (RIGHT). ..... 54
FIGURE 39: MONTHLY $O_3$ DISTRIBUTIONS AT PHILADELPHIA AREA REGULATORY MONITORING SITES FOR OBSERVED AIR QUALITY, AND AIR QUALITY ADJUSTED TO MEET THE EXISTING (75 PPB) AND ALTERNATIVE (65 PPB) STANDARDS FOR 2006-2008 (LEFT) AND 2008-2010 (RIGHT). ..... 54
FIGURE 40: MONTHLY $O_3$ DISTRIBUTIONS AT SACRAMENTO AREA REGULATORY MONITORING SITES FOR OBSERVED AIR QUALITY, AND AIR QUALITY ADJUSTED TO MEET THE EXISTING (75 PPB) AND ALTERNATIVE (65 PPB) STANDARDS FOR 2006-2008 (LEFT) AND 2008-2010 (RIGHT). ..... 55

FIGURE 41: MONTHLY $O_3$ DISTRIBUTIONS AT ST. LOUIS AREA REGULATORY MONITORING SITES FOR OBSERVED AIR QUALITY, AND AIR QUALITY ADJUSTED TO MEET THE EXISTING (75 PPB) AND ALTERNATIVE (65 PPB) STANDARDS FOR 2006-2008 (LEFT) AND 2008-2010 (RIGHT). ..... 55
FIGURE 42: MONTHLY $O_3$ DISTRIBUTIONS AT WASHINGTON, D.C. AREA REGULATORY MONITORING SITES FOR OBSERVED AIR QUALITY, AND AIR QUALITY ADJUSTED TO MEET THE EXISTING (75 PPB) AND ALTERNATIVE (65 PPB) STANDARDS FOR 2006-2008 (LEFT) AND 2008-2010 (RIGHT). ..... 56
FIGURE 43: COMPOSITE MONITOR DAILY MAXIMUM 8-HOUR $O_3$ VALUES FOR ATLANTA BASED ON OBSERVED AND ADJUSTED AIR QUALITY. ..... 61
FIGURE 44: COMPOSITE MONITOR DAILY MAXIMUM 8-HOUR $O_3$ VALUES FOR BALTIMORE BASED ON OBSERVED AND ADJUSTED AIR QUALITY. ..... 61
FIGURE 45: COMPOSITE MONITOR DAILY MAXIMUM 8-HOUR $O_3$ VALUES FOR BOSTON BASED ON OBSERVED AND ADJUSTED AIR QUALITY. ..... 62
FIGURE 46: COMPOSITE MONITOR DAILY MAXIMUM 8-HOUR $O_3$ VALUES FOR CLEVELAND BASED ON OBSERVED AND ADJUSTED AIR QUALITY. ..... 62
FIGURE 47: COMPOSITE MONITOR DAILY MAXIMUM 8-HOUR $O_3$ VALUES FOR DENVER BASED ON OBSERVED AND ADJUSTED AIR QUALITY. ..... 63
FIGURE 48: COMPOSITE MONITOR DAILY MAXIMUM 8-HOUR $O_3$ VALUES FOR DETROIT BASED ON OBSERVED AND ADJUSTED AIR QUALITY. ..... 63
FIGURE 49: COMPOSITE MONITOR DAILY MAXIMUM 8-HOUR $O_3$ VALUES FOR HOUSTON BASED ON OBSERVED AND ADJUSTED AIR QUALITY. ..... 64
FIGURE 50: COMPOSITE MONITOR DAILY MAXIMUM 8-HOUR $O_3$ VALUES FOR LOS ANGELES BASED ON OBSERVED AND ADJUSTED AIR QUALITY. ..... 64
FIGURE 51: COMPOSITE MONITOR DAILY MAXIMUM 8-HOUR $O_3$ VALUES FOR NEW YORK BASED ON OBSERVED AND ADJUSTED AIR QUALITY. ..... 65
FIGURE 52: COMPOSITE MONITOR DAILY MAXIMUM 8-HOUR $O_3$ VALUES FOR PHILADELPHIA BASED ON OBSERVED AND ADJUSTED AIR QUALITY. ..... 65
FIGURE 53: COMPOSITE MONITOR DAILY MAXIMUM 8-HOUR $O_3$ VALUES FOR SACRAMENTO BASED ON OBSERVED AND ADJUSTED AIR QUALITY. ..... 66
FIGURE 54: COMPOSITE MONITOR DAILY MAXIMUM 8-HOUR $O_3$ VALUES FOR ST. LOUIS BASED ON OBSERVED AND ADJUSTED AIR QUALITY. ..... 66
FIGURE 55: CHANGE IN VNA ESTIMATES OF THE DAILY MAXIMUM 8-HOUR AVERAGE (MDA8) $O_3$ CONCENTRATIONS BASED ON HDDM ADJUSTMENTS IN ATLANTA. ..... 71
FIGURE 56: CHANGE IN VNA ESTIMATES OF THE DAILY MAXIMUM 8-HOUR AVERAGE (MDA8) $O_3$ CONCENTRATIONS BASED ON HDDM ADJUSTMENTS IN BALTIMORE. ..... 72
FIGURE 57: CHANGE IN VNA ESTIMATES OF THE DAILY MAXIMUM 8-HOUR AVERAGE (MDA8) $O_3$ CONCENTRATIONS BASED ON HDDM ADJUSTMENTS IN BOSTON. ..... 73
FIGURE 58: CHANGE IN VNA ESTIMATES OF THE DAILY MAXIMUM 8-HOUR AVERAGE (MDA8) $O_3$ CONCENTRATIONS BASED ON HDDM ADJUSTMENTS IN CHICAGO. ..... 74
FIGURE 59: CHANGE IN VNA ESTIMATES OF THE DAILY MAXIMUM 8-HOUR AVERAGE (MDA8) $O_3$ CONCENTRATIONS BASED ON HDDM ADJUSTMENTS IN CLEVELAND. ..... 75

FIGURE 60: CHANGE IN VNA ESTIMATES OF THE DAILY MAXIMUM 8-HOUR AVERAGE (MDA8) $O_3$ CONCENTRATIONS BASED ON HDDM ADJUSTMENTS IN DALLAS. ..... 76
FIGURE 61: CHANGE IN VNA ESTIMATES OF THE DAILY MAXIMUM 8-HOUR AVERAGE (MDA8) $O_3$ CONCENTRATIONS BASED ON HDDM ADJUSTMENTS IN DENVER. ..... 77
FIGURE 62: CHANGE IN VNA ESTIMATES OF THE DAILY MAXIMUM 8-HOUR AVERAGE (MDA8) $O_3$ CONCENTRATIONS BASED ON HDDM ADJUSTMENTS IN DETROIT. ..... 78
FIGURE 63: CHANGE IN VNA ESTIMATES OF THE DAILY MAXIMUM 8-HOUR AVERAGE (MDA8) $O_3$ CONCENTRATIONS BASED ON HDDM ADJUSTMENTS IN HOUSTON. ..... 79
FIGURE 64: CHANGE IN VNA ESTIMATES OF THE DAILY MAXIMUM 8-HOUR AVERAGE (MDA8) $O_3$ CONCENTRATIONS BASED ON HDDM ADJUSTMENTS IN LOS ANGELES. ..... 80
FIGURE 65: CHANGE IN VNA ESTIMATES OF THE DAILY MAXIMUM 8-HOUR AVERAGE (MDA8) $O_3$ CONCENTRATIONS BASED ON HDDM ADJUSTMENTS IN NEW YORK. ..... 81
FIGURE 66: CHANGE IN VNA ESTIMATES OF THE DAILY MAXIMUM 8-HOUR AVERAGE (MDA8) $O_3$ CONCENTRATIONS BASED ON HDDM ADJUSTMENTS IN PHILADELPHIA. ..... 82
FIGURE 67: CHANGE IN VNA ESTIMATES OF THE DAILY MAXIMUM 8-HOUR AVERAGE (MDA8) $O_3$ CONCENTRATIONS BASED ON HDDM ADJUSTMENTS IN SACRAMENTO. ..... 83
FIGURE 68: CHANGE IN VNA ESTIMATES OF THE DAILY MAXIMUM 8-HOUR AVERAGE (MDA8) $O_3$ CONCENTRATIONS BASED ON HDDM ADJUSTMENTS IN ST. LOUIS. ..... 84
FIGURE 69: CHANGE IN VNA ESTIMATES OF THE DAILY MAXIMUM 8-HOUR AVERAGE (MDA8) O3 CONCENTRATIONS BASED ON HDDM ADJUSTMENTS IN WASHINGTON, D.C. ..... 85
FIGURE 70: CHANGES IN ANNUAL 4$^{TH}$ HIGHEST MDA8 AND MAY-SEPTEMBER AVERAGE MDA8 VALUES BASED ON HDDM ADJUSTMENTS FOR ATLANTA, 2006-2008. THE POINTS ARE COLORED ACCORDING TO THE CHANGE IN PPB, AND VALUES FALLING OUTSIDE THE RANGE IN THE COLOR BAR WERE SET TO THE NEAREST VALUE WITHIN THE COLOR BAR. ..... 86
FIGURE 71: CHANGES IN ANNUAL 4$^{TH}$ HIGHEST MDA8 AND MAY-SEPTEMBER AVERAGE MDA8 VALUES BASED ON HDDM ADJUSTMENTS FOR ATLANTA, 2008-2010. THE POINTS ARE COLORED ACCORDING TO THE CHANGE IN PPB, AND VALUES FALLING OUTSIDE THE RANGE IN THE COLOR BAR WERE SET TO THE NEAREST VALUE WITHIN THE COLOR BAR. ..... 87
FIGURE 72: CHANGES IN ANNUAL 4$^{TH}$ HIGHEST MDA8 AND MAY-SEPTEMBER AVERAGE MDA8 VALUES BASED ON HDDM ADJUSTMENTS FOR BALTIMORE, 2006-2008. THE POINTS ARE COLORED ACCORDING TO THE CHANGE IN PPB, AND VALUES FALLING OUTSIDE THE RANGE IN THE COLOR BAR WERE SET TO THE NEAREST VALUE WITHIN THE COLOR BAR. ..... 88
FIGURE 73: CHANGES IN ANNUAL 4$^{TH}$ HIGHEST MDA8 AND MAY-SEPTEMBER AVERAGE MDA8 VALUES BASED ON HDDM ADJUSTMENTS FOR BALTIMORE, 2008-2010. THE POINTS ARE COLORED ACCORDING TO THE CHANGE IN PPB, AND VALUES FALLING OUTSIDE THE RANGE IN THE COLOR BAR WERE SET TO THE NEAREST VALUE WITHIN THE COLOR BAR. ..... 89
FIGURE 74: CHANGES IN ANNUAL 4$^{TH}$ HIGHEST MDA8 AND MAY-SEPTEMBER AVERAGE MDA8 VALUES BASED ON HDDM ADJUSTMENTS FOR BOSTON, 2006-2008. THE POINTS ARE COLORED ACCORDING TO THE CHANGE IN PPB, AND VALUES FALLING OUTSIDE THE RANGE IN THE COLOR BAR WERE SET TO THE NEAREST VALUE WITHIN THE COLOR BAR. ..... 90
FIGURE 75: CHANGES IN ANNUAL 4$^{TH}$ HIGHEST MDA8 AND MAY-SEPTEMBER AVERAGE MDA8 VALUES BASED ON HDDM ADJUSTMENTS FOR BOSTON, 2008-2010. THE POINTS ARE COLORED ACCORDING TO THE CHANGE IN PPB, AND VALUES FALLING OUTSIDE THE RANGE IN THE COLOR BAR WERE SET TO THE NEAREST VALUE WITHIN THE COLOR BAR. ..... 91
FIGURE 76: CHANGES IN ANNUAL 4$^{TH}$ HIGHEST MDA8 AND MAY-SEPTEMBER AVERAGE MDA8 VALUES BASED ON HDDM ADJUSTMENTS FOR CHICAGO, 2006-2008. THE POINTS ARE COLORED ACCORDING TO THE CHANGE IN PPB, AND VALUES FALLING OUTSIDE THE RANGE IN THE COLOR BAR WERE SET TO THE NEAREST VALUE WITHIN THE COLOR BAR. ..... 92

FIGURE 77: CHANGES IN ANNUAL 4TH HIGHEST MDA8 AND MAY-SEPTEMBER AVERAGE MDA8 VALUES BASED ON HDDM ADJUSTMENTS FOR CHICAGO, 2008-2010. THE POINTS ARE COLORED ACCORDING TO THE CHANGE IN PPB, AND VALUES FALLING OUTSIDE THE RANGE IN THE COLOR BAR WERE SET TO THE NEAREST VALUE WITHIN THE COLOR BAR. ..... 93
FIGURE 78: CHANGES IN ANNUAL 4TH HIGHEST MDA8 AND MAY-SEPTEMBER AVERAGE MDA8 VALUES BASED ON HDDM ADJUSTMENTS FOR CLEVELAND, 2006-2008. THE POINTS ARE COLORED ACCORDING TO THE CHANGE IN PPB, AND VALUES FALLING OUTSIDE THE RANGE IN THE COLOR BAR WERE SET TO THE NEAREST VALUE WITHIN THE COLOR BAR. ..... 94
FIGURE 79: CHANGES IN ANNUAL 4TH HIGHEST MDA8 AND MAY-SEPTEMBER AVERAGE MDA8 VALUES BASED ON HDDM ADJUSTMENTS FOR CLEVELAND, 2008-2010. THE POINTS ARE COLORED ACCORDING TO THE CHANGE IN PPB, AND VALUES FALLING OUTSIDE THE RANGE IN THE COLOR BAR WERE SET TO THE NEAREST VALUE WITHIN THE COLOR BAR. ..... 95
FIGURE 80: CHANGES IN ANNUAL 4TH HIGHEST MDA8 AND MAY-SEPTEMBER AVERAGE MDA8 VALUES BASED ON HDDM ADJUSTMENTS FOR DALLAS, 2006-2008. THE POINTS ARE COLORED ACCORDING TO THE CHANGE IN PPB, AND VALUES FALLING OUTSIDE THE RANGE IN THE COLOR BAR WERE SET TO THE NEAREST VALUE WITHIN THE COLOR BAR. ..... 96
FIGURE 81: CHANGES IN ANNUAL 4TH HIGHEST MDA8 AND MAY-SEPTEMBER AVERAGE MDA8 VALUES BASED ON HDDM ADJUSTMENTS FOR DALLAS, 2008-2010. THE POINTS ARE COLORED ACCORDING TO THE CHANGE IN PPB, AND VALUES FALLING OUTSIDE THE RANGE IN THE COLOR BAR WERE SET TO THE NEAREST VALUE WITHIN THE COLOR BAR. ..... 97
FIGURE 82: CHANGES IN ANNUAL 4TH HIGHEST MDA8 AND MAY-SEPTEMBER AVERAGE MDA8 VALUES BASED ON HDDM ADJUSTMENTS FOR DENVER, 2006-2008. THE POINTS ARE COLORED ACCORDING TO THE CHANGE IN PPB, AND VALUES FALLING OUTSIDE THE RANGE IN THE COLOR BAR WERE SET TO THE NEAREST VALUE WITHIN THE COLOR BAR. ..... 98
FIGURE 83: CHANGES IN ANNUAL 4TH HIGHEST MDA8 AND MAY-SEPTEMBER AVERAGE MDA8 VALUES BASED ON HDDM ADJUSTMENTS FOR DENVER, 2008-2010. THE POINTS ARE COLORED ACCORDING TO THE CHANGE IN PPB, AND VALUES FALLING OUTSIDE THE RANGE IN THE COLOR BAR WERE SET TO THE NEAREST VALUE WITHIN THE COLOR BAR. ..... 99
FIGURE 84: CHANGES IN ANNUAL 4TH HIGHEST MDA8 AND MAY-SEPTEMBER AVERAGE MDA8 VALUES BASED ON HDDM ADJUSTMENTS FOR DETROIT, 2006-2008. THE POINTS ARE COLORED ACCORDING TO THE CHANGE IN PPB, AND VALUES FALLING OUTSIDE THE RANGE IN THE COLOR BAR WERE SET TO THE NEAREST VALUE WITHIN THE COLOR BAR. ..... 100
FIGURE 85: CHANGES IN ANNUAL 4TH HIGHEST MDA8 AND MAY-SEPTEMBER AVERAGE MDA8 VALUES BASED ON HDDM ADJUSTMENTS FOR DETROIT, 2008-2010. THE POINTS ARE COLORED ACCORDING TO THE CHANGE IN PPB, AND VALUES FALLING OUTSIDE THE RANGE IN THE COLOR BAR WERE SET TO THE NEAREST VALUE WITHIN THE COLOR BAR. ..... 101
FIGURE 86: CHANGES IN ANNUAL 4TH HIGHEST MDA8 AND MAY-SEPTEMBER AVERAGE MDA8 VALUES BASED ON HDDM ADJUSTMENTS FOR HOUSTON, 2006-2008. THE POINTS ARE COLORED ACCORDING TO THE CHANGE IN PPB, AND VALUES FALLING OUTSIDE THE RANGE IN THE COLOR BAR WERE SET TO THE NEAREST VALUE WITHIN THE COLOR BAR. ..... 102
FIGURE 87: CHANGES IN ANNUAL 4TH HIGHEST MDA8 AND MAY-SEPTEMBER AVERAGE MDA8 VALUES BASED ON HDDM ADJUSTMENTS FOR HOUSTON, 2008-2010. THE POINTS ARE COLORED ACCORDING TO THE CHANGE IN PPB, AND VALUES FALLING OUTSIDE THE RANGE IN THE COLOR BAR WERE SET TO THE NEAREST VALUE WITHIN THE COLOR BAR. ..... 103
FIGURE 88: CHANGES IN ANNUAL 4TH HIGHEST MDA8 AND MAY-SEPTEMBER AVERAGE MDA8 VALUES BASED ON HDDM ADJUSTMENTS FOR LOS ANGELES, 2006-2008. THE POINTS ARE COLORED ACCORDING TO THE CHANGE IN PPB, AND VALUES FALLING OUTSIDE THE RANGE IN THE COLOR BAR WERE SET TO THE NEAREST VALUE WITHIN THE COLOR BAR. ..... 104
FIGURE 89: CHANGES IN ANNUAL 4TH HIGHEST MDA8 AND MAY-SEPTEMBER AVERAGE MDA8 VALUES BASED ON HDDM ADJUSTMENTS FOR LOS ANGELES, 2008-2010. THE POINTS ARE COLORED ACCORDING TO THE CHANGE IN PPB, AND VALUES FALLING OUTSIDE THE RANGE IN THE COLOR BAR WERE SET TO THE NEAREST VALUE WITHIN THE COLOR BAR. ..... 105

FIGURE 90: CHANGES IN ANNUAL 4TH HIGHEST MDA8 AND MAY-SEPTEMBER AVERAGE MDA8 VALUES BASED ON HDDM ADJUSTMENTS FOR NEW YORK, 2006-2008. THE POINTS ARE COLORED ACCORDING TO THE CHANGE IN PPB, AND VALUES FALLING OUTSIDE THE RANGE IN THE COLOR BAR WERE SET TO THE NEAREST VALUE WITHIN THE COLOR BAR. ..... 106
FIGURE 91: CHANGES IN ANNUAL 4TH HIGHEST MDA8 AND MAY-SEPTEMBER AVERAGE MDA8 VALUES BASED ON HDDM ADJUSTMENTS FOR NEW YORK, 2008-2010. THE POINTS ARE COLORED ACCORDING TO THE CHANGE IN PPB, AND VALUES FALLING OUTSIDE THE RANGE IN THE COLOR BAR WERE SET TO THE NEAREST VALUE WITHIN THE COLOR BAR. ..... 107
FIGURE 92: CHANGES IN ANNUAL 4TH HIGHEST MDA8 AND MAY-SEPTEMBER AVERAGE MDA8 VALUES BASED ON HDDM ADJUSTMENTS FOR PHILADELPHIA, 2006-2008. THE POINTS ARE COLORED ACCORDING TO THE CHANGE IN PPB, AND VALUES FALLING OUTSIDE THE RANGE IN THE COLOR BAR WERE SET TO THE NEAREST VALUE WITHIN THE COLOR BAR. ..... 108
FIGURE 93: CHANGES IN ANNUAL 4TH HIGHEST MDA8 AND MAY-SEPTEMBER AVERAGE MDA8 VALUES BASED ON HDDM ADJUSTMENTS FOR PHILADELPHIA, 2008-2010. THE POINTS ARE COLORED ACCORDING TO THE CHANGE IN PPB, AND VALUES FALLING OUTSIDE THE RANGE IN THE COLOR BAR WERE SET TO THE NEAREST VALUE WITHIN THE COLOR BAR. ..... 109
FIGURE 94: CHANGES IN ANNUAL 4TH HIGHEST MDA8 AND MAY-SEPTEMBER AVERAGE MDA8 VALUES BASED ON HDDM ADJUSTMENTS FOR SACRAMENTO, 2006-2008. THE POINTS ARE COLORED ACCORDING TO THE CHANGE IN PPB, AND VALUES FALLING OUTSIDE THE RANGE IN THE COLOR BAR WERE SET TO THE NEAREST VALUE WITHIN THE COLOR BAR. ..... 110
FIGURE 95: CHANGES IN ANNUAL 4TH HIGHEST MDA8 AND MAY-SEPTEMBER AVERAGE MDA8 VALUES BASED ON HDDM ADJUSTMENTS FOR SACRAMENTO, 2008-2010. THE POINTS ARE COLORED ACCORDING TO THE CHANGE IN PPB, AND VALUES FALLING OUTSIDE THE RANGE IN THE COLOR BAR WERE SET TO THE NEAREST VALUE WITHIN THE COLOR BAR. ..... 111
FIGURE 96: CHANGES IN ANNUAL 4TH HIGHEST MDA8 AND MAY-SEPTEMBER AVERAGE MDA8 VALUES BASED ON HDDM ADJUSTMENTS FOR ST. LOUIS, 2006-2008. THE POINTS ARE COLORED ACCORDING TO THE CHANGE IN PPB, AND VALUES FALLING OUTSIDE THE RANGE IN THE COLOR BAR WERE SET TO THE NEAREST VALUE WITHIN THE COLOR BAR. ..... 112
FIGURE 97: CHANGES IN ANNUAL 4TH HIGHEST MDA8 AND MAY-SEPTEMBER AVERAGE MDA8 VALUES BASED ON HDDM ADJUSTMENTS FOR ST. LOUIS, 2008-2010. THE POINTS ARE COLORED ACCORDING TO THE CHANGE IN PPB, AND VALUES FALLING OUTSIDE THE RANGE IN THE COLOR BAR WERE SET TO THE NEAREST VALUE WITHIN THE COLOR BAR. ..... 113
FIGURE 98: CHANGES IN ANNUAL 4TH HIGHEST MDA8 AND MAY-SEPTEMBER AVERAGE MDA8 VALUES BASED ON HDDM ADJUSTMENTS FOR WASHINGTON, D.C., 2006-2008. THE POINTS ARE COLORED ACCORDING TO THE CHANGE IN PPB, AND VALUES FALLING OUTSIDE THE RANGE IN THE COLOR BAR WERE SET TO THE NEAREST VALUE WITHIN THE COLOR BAR. ..... 114
FIGURE 99: CHANGES IN ANNUAL 4TH HIGHEST MDA8 AND MAY-SEPTEMBER AVERAGE MDA8 VALUES BASED ON HDDM ADJUSTMENTS FOR WASHINGTON D.C., 2008-2010. THE POINTS ARE COLORED ACCORDING TO THE CHANGE IN PPB, AND VALUES FALLING OUTSIDE THE RANGE IN THE COLOR BAR WERE SET TO THE NEAREST VALUE WITHIN THE COLOR BAR. ..... 115
FIGURE 100: CHANGES IN VNA ESTIMATES OF ANNUAL 4TH HIGHEST MDA8 AND MAY – SEPTEMBER AVERAGE MDA8 BASED ON HDDM ADJUSTMENTS FOR ATLANTA VERSUS POPULATION AND POPULATION DENSITY. ..... 116
FIGURE 101: CHANGES IN VNA ESTIMATES OF ANNUAL 4TH HIGHEST MDA8 AND MAY – SEPTEMBER AVERAGE MDA8 BASED ON HDDM ADJUSTMENTS FOR BALTIMORE VERSUS POPULATION AND POPULATION DENSITY. ..... 117
FIGURE 102: CHANGES IN VNA ESTIMATES OF ANNUAL 4TH HIGHEST MDA8 AND MAY – SEPTEMBER AVERAGE MDA8 BASED ON HDDM ADJUSTMENTS FOR BOSTON VERSUS POPULATION AND POPULATION DENSITY. ..... 118
FIGURE 103: CHANGES IN VNA ESTIMATES OF ANNUAL 4TH HIGHEST MDA8 AND MAY – SEPTEMBER AVERAGE MDA8 BASED ON HDDM ADJUSTMENTS FOR CHICAGO VERSUS POPULATION AND POPULATION DENSITY. ..... 119
FIGURE 104: CHANGES IN VNA ESTIMATES OF ANNUAL 4TH HIGHEST MDA8 AND MAY – SEPTEMBER AVERAGE MDA8 BASED ON HDDM ADJUSTMENTS FOR CLEVELAND VERSUS POPULATION AND POPULATION DENSITY. ..... 120

FIGURE 105: CHANGES IN VNA ESTIMATES OF ANNUAL 4TH HIGHEST MDA8 AND MAY – SEPTEMBER AVERAGE MDA8 BASED ON HDDM ADJUSTMENTS FOR DALLAS VERSUS POPULATION AND POPULATION DENSITY. ..... 121
FIGURE 106: CHANGES IN VNA ESTIMATES OF ANNUAL 4TH HIGHEST MDA8 AND MAY – SEPTEMBER AVERAGE MDA8 BASED ON HDDM ADJUSTMENTS FOR DENVER VERSUS POPULATION AND POPULATION DENSITY. ..... 122
FIGURE 107: CHANGES IN VNA ESTIMATES OF ANNUAL 4TH HIGHEST MDA8 AND MAY – SEPTEMBER AVERAGE MDA8 BASED ON HDDM ADJUSTMENTS FOR DETROIT VERSUS POPULATION AND POPULATION DENSITY. ..... 123
FIGURE 108: CHANGES IN VNA ESTIMATES OF ANNUAL 4TH HIGHEST MDA8 AND MAY – SEPTEMBER AVERAGE MDA8 BASED ON HDDM ADJUSTMENTS FOR HOUSTON VERSUS POPULATION AND POPULATION DENSITY. ..... 124
FIGURE 109: CHANGES IN VNA ESTIMATES OF ANNUAL 4TH HIGHEST MDA8 AND MAY – SEPTEMBER AVERAGE MDA8 BASED ON HDDM ADJUSTMENTS FOR LOS ANGELES VERSUS POPULATION AND POPULATION DENSITY. ..... 125
FIGURE 110: CHANGES IN VNA ESTIMATES OF ANNUAL 4TH HIGHEST MDA8 AND MAY – SEPTEMBER AVERAGE MDA8 BASED ON HDDM ADJUSTMENTS FOR NEW YORK VERSUS POPULATION AND POPULATION DENSITY. ..... 126
FIGURE 111: CHANGES IN VNA ESTIMATES OF ANNUAL 4TH HIGHEST MDA8 AND MAY – SEPTEMBER AVERAGE MDA8 BASED ON HDDM ADJUSTMENTS FOR PHILADELPHIA VERSUS POPULATION AND POPULATION DENSITY. ..... 127
FIGURE 112: CHANGES IN VNA ESTIMATES OF ANNUAL 4TH HIGHEST MDA8 AND MAY – SEPTEMBER AVERAGE MDA8 BASED ON HDDM ADJUSTMENTS FOR SACRAMENTO VERSUS POPULATION AND POPULATION DENSITY. ..... 128
FIGURE 113: CHANGES IN VNA ESTIMATES OF ANNUAL 4TH HIGHEST MDA8 AND MAY – SEPTEMBER AVERAGE MDA8 BASED ON HDDM ADJUSTMENTS FOR ST. LOUIS VERSUS POPULATION AND POPULATION DENSITY. ..... 129
FIGURE 114: CHANGES IN VNA ESTIMATES OF ANNUAL 4TH HIGHEST MDA8 AND MAY – SEPTEMBER AVERAGE MDA8 BASED ON HDDM ADJUSTMENTS FOR WASHINGTON, D.C. VERSUS POPULATION AND POPULATION DENSITY. ..... 130
FIGURE 115: COMPOSITE MONITOR DAILY MAXIMUM 8-HOUR $O_3$ VALUES FOR DENVER BASED ON OBSERVED AND ADJUSTED AIR QUALITY FOR THE NOX ONLY AND NOX/VOC SCENARIOS. ..... 133
FIGURE 116: COMPOSITE MONITOR DAILY MAXIMUM 8-HOUR $O_3$ VALUES FOR DETROIT BASED ON OBSERVED AND ADJUSTED AIR QUALITY FOR THE NOX ONLY AND NOX/VOC SCENARIOS. ..... 134
FIGURE 117: COMPOSITE MONITOR DAILY MAXIMUM 8-HOUR $O_3$ VALUES FOR HOUSTON BASED ON OBSERVED AND ADJUSTED AIR QUALITY FOR THE NOX ONLY AND NOX/VOC SCENARIOS. ..... 134
FIGURE 118: COMPOSITE MONITOR DAILY MAXIMUM 8-HOUR $O_3$ VALUES FOR LOS ANGELES BASED ON OBSERVED AND ADJUSTED AIR QUALITY FOR THE NOX ONLY AND NOX/VOC SCENARIOS. ..... 135
FIGURE 119: COMPOSITE MONITOR DAILY MAXIMUM 8-HOUR $O_3$ VALUES FOR NEW YORK BASED ON OBSERVED AND ADJUSTED AIR QUALITY FOR THE NOX ONLY AND NOX/VOC SCENARIOS. ..... 135
FIGURE 120: COMPOSITE MONITOR DAILY MAXIMUM 8-HOUR $O_3$ VALUES FOR PHILADELPHIA BASED ON OBSERVED AND ADJUSTED AIR QUALITY FOR THE NOX ONLY AND NOX/VOC SCENARIOS. ..... 136
FIGURE 121: COMPOSITE MONITOR DAILY MAXIMUM 8-HOUR $O_3$ VALUES FOR SACRAMENTO BASED ON OBSERVED AND ADJUSTED AIR QUALITY FOR THE NOX ONLY AND NOX/VOC SCENARIOS. ..... 136
FIGURE 122: APRIL-OCTOBER SEASONAL AVERAGE OF DAILY MAXIMUM 8-HOUR $O_3$ VALUES AT DENVER AREA MONITOR LOCATIONS FOR OBSERVED 2006-2008 CONDITIONS (LEFT PANEL), 75 PPB ADJUSTMENT SCENARIOS (MIDDLE PANELS), AND 65 PPB ADJUSTMENT SCENARIOS (RIGHT PANELS). NOX ONLY ADJUSTMENTS ARE SHOWN IN TOP PANELS, NOX/VOC ADJUSTMENTS ARE SHOWN IN BOTTOM PANELS. ..... 138
FIGURE 123: APRIL-OCTOBER SEASONAL AVERAGE OF DAILY MAXIMUM 8-HOUR $O_3$ VALUES AT DETROIT AREA MONITOR LOCATIONS FOR OBSERVED 2006-2008 CONDITIONS (LEFT PANEL), 75 PPB ADJUSTMENT SCENARIOS (MIDDLE PANELS), AND 65 PPB ADJUSTMENT

scenarios (right panels). NOx only adjustments are shown in top panels, NOx/VOC adjustments are shown in bottom panels. ..... 139
Figure 124: April-October seasonal average of daily maximum 8-hour $O_3$ values at Houston area monitor locations for observed 2006-2008 conditions (left panel), 75 ppb adjustment scenarios (middle panels), and 65 ppb adjustment scenarios (right panels). NOx only adjustments are shown in top panels, NOx/VOC adjustments are shown in bottom panels. ..... 140
Figure 125: April-October seasonal average of daily maximum 8-hour $O_3$ values at Los Angeles area monitor locations for observed 2006-2008 conditions (left panel), 75 ppb adjustment scenarios (middle panels), and 65 ppb adjustment scenarios (right panels). NOx only adjustments are shown in top panels, NOx/VOC adjustments are shown in bottom panels. ..... 141
Figure 126: April-October seasonal average of daily maximum 8-hour $O_3$ values at New York area monitor locations for observed 2006-2008 conditions (left panel), 75 ppb adjustment scenarios (middle panels), and 65 ppb adjustment scenarios (right panels). NOx only adjustments are shown in top panels, NOx/VOC adjustments are shown in bottom panels. ..... 142
Figure 127: April-October seasonal average of daily maximum 8-hour $O_3$ values at Philadelphia area monitor locations for observed 2006-2008 conditions (left panel), 75 ppb adjustment scenarios (middle panels), and 65 ppb adjustment scenarios (right panels). NOx only adjustments are shown in top panels, NOx/VOC adjustments are shown in bottom panels. ..... 143
Figure 128: April-October seasonal average of daily maximum 8-hour $O_3$ values at Sacramento area monitor locations for observed 2006-2008 conditions (left panel), 75 ppb adjustment scenarios (middle panels), and 65 ppb adjustment scenarios (right panels). NOx only adjustments are shown in top panels, NOx/VOC adjustments are shown in bottom panels. ..... 144

# Table of Tables


TABLE 1: X AND Y CUTPOINTS USED IN EQUATIONS (4) AND (8). NOTE: THE NOX/VOC SENSITIVITY CASE WAS ONLY PERFORMED IN TWO CITIES. ..... 12

TABLE 2: PERCENT EMISSIONS REDUCTIONS USED FOR EACH URBAN AREA TO OBTAIN EACH STANDARD. ..... 26

TABLE 3: DESIGN VALUES FOR THE ATLANTA AREA REGULATORY MONITORS FROM OBSERVED DATA AND FOR ADJUSTMENTS TO MEET THE EXISTING AND POTENTIAL ALTERNATIVE STANDARDS IN 2006-2008 AND 2008-2010. ..... 29

TABLE 4: DESIGN VALUES FOR THE BALTIMORE AREA REGULATORY MONITORS FROM OBSERVED DATA AND FOR ADJUSTMENTS TO MEET THE EXISTING AND POTENTIAL ALTERNATIVE STANDARDS IN 2006-2008 AND 2008-2010. ..... 29

TABLE 5: DESIGN VALUES FOR THE BOSTON AREA REGULATORY MONITORS FROM OBSERVED DATA AND FOR ADJUSTMENTS TO MEET THE EXISTING AND POTENTIAL ALTERNATIVE STANDARDS IN 2006-2008 AND 2008-2010. ..... 30

TABLE 6: DESIGN VALUES FOR THE CHICAGO AREA REGULATORY MONITORS FROM OBSERVED DATA AND FOR ADJUSTMENTS TO MEET THE EXISTING AND POTENTIAL ALTERNATIVE STANDARDS USING NOX AND VOC EMISSIONS REDUCTIONS IN 2006-2008 AND 2008-2010. ..... 30

TABLE 7: DESIGN VALUES FOR THE CLEVELAND AREA REGULATORY MONITORS FROM OBSERVED DATA AND FOR ADJUSTMENTS TO MEET THE EXISTING AND POTENTIAL ALTERNATIVE STANDARDS IN 2006-2008 AND 2008-2010. ..... 31

TABLE 8: DESIGN VALUES FOR THE DALLAS AREA REGULATORY MONITORS FROM OBSERVED DATA AND FOR ADJUSTMENTS TO MEET THE EXISTING AND POTENTIAL ALTERNATIVE STANDARDS IN 2006-2008 AND 2008-2010. ..... 31

TABLE 9: DESIGN VALUES FOR THE DENVER AREA REGULATORY MONITORS FROM OBSERVED DATA AND FOR ADJUSTMENTS TO MEET THE EXISTING AND POTENTIAL ALTERNATIVE STANDARDS USING NOX AND VOC EMISSIONS REDUCTIONS IN 2006-2008 AND 2008-2010. ..... 32

TABLE 10: DESIGN VALUES FOR THE DETROIT AREA REGULATORY MONITORS FROM OBSERVED DATA AND FOR ADJUSTMENTS TO MEET THE EXISTING AND POTENTIAL ALTERNATIVE STANDARDS IN 2006-2008 AND 2008-2010. ..... 33

TABLE 11: DESIGN VALUES FOR THE HOUSTON AREA REGULATORY MONITORS FROM OBSERVED DATA AND FOR ADJUSTMENTS TO MEET THE EXISTING AND POTENTIAL ALTERNATIVE STANDARDS IN 2006-2008 AND 2008-2010. ..... 33

TABLE 12: DESIGN VALUES FOR THE LOS ANGELES AREA REGULATORY MONITORS FROM OBSERVED DATA AND FOR ADJUSTMENTS TO MEET THE EXISTING AND POTENTIAL ALTERNATIVE STANDARDS USING THE LOWER BOUND OF THE $95^{TH}$ PERCENT CONFIDENCE INTERVAL OF ESTIMATED HOURLY $O_3$ IN 2006-2008 AND 2008-2010. ..... 34

TABLE 13: DESIGN VALUES FOR THE NEW YORK AREA REGULATORY MONITORS FROM OBSERVED DATA AND FOR ADJUSTMENTS TO MEET THE EXISTING AND POTENTIAL ALTERNATIVE STANDARDS USING THE LOWER BOUND OF THE $95^{TH}$ PERCENT CONFIDENCE INTERVAL OF ESTIMATED HOURLY $O_3$ IN 2006-2008 AND 2008-2010. ..... 35

TABLE 14: DESIGN VALUES FOR THE PHILADELPHIA AREA REGULATORY MONITORS FROM OBSERVED DATA AND FOR ADJUSTMENTS TO MEET THE EXISTING AND POTENTIAL ALTERNATIVE STANDARDS IN 2006-2008 AND 2008-2010. ..... 36

TABLE 15: DESIGN VALUES FOR THE SACRAMENTO AREA REGULATORY MONITORS FROM OBSERVED DATA AND FOR ADJUSTMENTS TO MEET THE EXISTING AND POTENTIAL ALTERNATIVE STANDARDS IN 2006-2008 AND 2008-2010. ..... 37

TABLE 16: DESIGN VALUES FOR THE SAINT LOUIS AREA REGULATORY MONITORS FROM OBSERVED DATA AND FOR ADJUSTMENTS TO MEET THE EXISTING AND POTENTIAL ALTERNATIVE STANDARDS IN 2006-2008 AND 2008-2010. ..... 38

TABLE 17: DESIGN VALUES FOR THE WASHINGTON D.C. AREA REGULATORY MONITORS FROM OBSERVED DATA AND FOR ADJUSTMENTS TO MEET THE EXISTING AND POTENTIAL ALTERNATIVE STANDARDS IN 2006-2008 AND 2008-2010 ..... 38

TABLE 18: MEAN STANDARD ERROR (PPB) IN ADJUSTED HOURLY $O_3$ CONCENTRATION IN EACH URBAN AREA FOR EACH STANDARD. ..... 56

TABLE 19: 95TH PERCENTILE STANDARD ERROR (PPB) IN ADJUSTED HOURLY $O_3$ CONCENTRATION IN EACH URBAN AREA FOR EACH STANDARD. ..... 57
TABLE 20: COMPARISON OF NOX-ONLY AND NOX/VOC EMISSION REDUCTIONS APPLIED IN SENSITIVITY ANALYSES FOR SEVEN URBAN AREAS. ..... 132

# 1. MOTIVATION FOR A NEW TECHNIQUE TO SIMULATE OZONE CONCENTRATIONS UNDER ALTERNATIVE STANDARDS

As part of the reviews of the National Ambient Air Quality Standards (NAAQS) for $O_3$, EPA estimates health risks after $O_3$ has been adjusted to just meet the existing standard and potential alternative standards. The first draft documents for this review rely upon the quadratic rollback method used in previous reviews to adjust or "roll back" hourly $O_3$ concentrations in urban areas. Although the quadratic rollback method simulates historical patterns of air quality changes more closely than some alternative methods (e.g. simply shaving peak concentrations off at the NAAQS level), its implementation requires some assumptions that may not always hold true. Specifically, the quadratic rollback method assumes that all monitors in an urban area will have the same response to emissions changes not allowing for temporally varying response depending on time of day. In addition, it assumes that ozone concentrations never increase in response to emissions reductions. However, during NOx-saturated (i.e. VOC limited) conditions, NOx reductions can result in ozone increases (Seinfeld and Pandis, 1998). Finally, since the quadratic rollback method is purely a mathematical technique and does not account for physical and chemical atmospheric processes or the sources of emissions precursors that lead to $O_3$ formation, a backstop or "floor" must be used to ensure that predicted $O_3$ is not reduced below "background" concentrations[1].

EPA has received comments during past $O_3$ NAAQS reviews and during the January 9-10, 2012 and Sep 11-13, 2013 Clean Air Scientific Advisory Committee (CASAC) meetings for this $O_3$ NAAQS review which encourage the use of alternate methods to quadratic rollback. In addition, the National Research Council of the National Academies (NRC, 2008) recommended that EPA explore how emissions reductions might effect temporal and spatial variations in $O_3$ concentrations, and that EPA include information on how $NO_x$ versus VOC control strategies might affect risk and exposure to $O_3$.

Photochemical modeling can simulate the $O_3$ response to emission reductions while avoiding the limitations presented by the quadratic rollback method. While there are uncertainties inherent in any modeling exercise due to uncertainties in inputs and model parameters, photochemical modeling provides a more representative characterization of the

[1] Background $O_3$ has been characterized in previous reviews of the $O_3$ NAAQS as "policy relevant background" or PRB, defined as $O_3$ concentrations that would exist in the absence of North American anthropogenic emissions. In the current review, we have refined the concept of background $O_3$ to recognize that there are several possible definitions of background $O_3$, reflecting both the geographic source of emissions, e.g. U.S., North American, Global non-U.S., and whether emissions are anthropogenic or natural in origin. In the cases described in this document, "background" refers to $O_3$ that would exist in absence of U.S. anthropogenic emissions.

spatial and temporal responses of $O_3$ to emissions reductions. In this document we present a model-based $O_3$ adjustment methodology that allows for adjustments to $O_3$ concentrations. This new approach is firmly rooted in the latest atmospheric modeling science and was peer reviewed in Simon et al (2012). This analysis uses EPA's Community Multi-scale Air Quality (CMAQ) photochemical model (www.cmaq-model.org) instrumented with the Higher order Direct Decoupled Method (HDDM) - a tool that generates modeled sensitivities of $O_3$ to emissions changes - to estimate the distribution of $O_3$ concentrations associated with achievement of the existing $O_3$ standard and alternative standards for multiple urban areas. The HDDM sensitivities are applied to ambient measurements of $O_3$ to estimate how $O_3$ concentrations would respond to changes in U.S. anthropogenic emissions. We use this methodology to estimate $O_3$ concentrations meeting the existing and potential alternative standards in the 2nd drafts of the risk and exposure assessments and the 2nd draft policy assessment. The photochemical modeling incorporates emissions from non-anthropogenic sources and anthropogenic emissions from sources in the U.S and in portions of Canada and Mexico. Pollution from sources in other locations within and outside of North America is included as transport into the boundary of the modeling domain. Because the application of the model-based approach focuses on reductions in U.S. anthropogenic emissions while holding constant those emissions that influence U.S. background, all changes in $O_3$ will be relative to U.S. background. This does not mean that background $O_3$ concentrations will be constant between recent ambient $O_3$ conditions and after just meeting the existing or alternative standard levels, because of nonlinearities in the formation of ozone.

# 2. HIGHER-ORDER DECOUPLED DIRECT METHOD (HDDM)

## 2.1 CAPABILITIES

Chemical transport models, such as CMAQ, simulate the effects of physical and chemical processes in the atmosphere to predict 3-D gridded pollutant concentrations (Foley et al, 2010, Appel et al, 2008, Appel et al, 2007, Byun and Schere, 2006). These models account for the impacts of emissions, transport, chemistry, and deposition on spatially and temporally varying pollutant concentrations. Required model inputs include time-varying emissions and meteorology fields, time varying concentrations of pollutants at the boundaries of the model domain (i.e. boundary conditions), and a characterization of the 3-D field of chemical concentrations to initialize the model (i.e. initial conditions).

Beyond modeling the concentrations of ambient $O_3$, chemical transport models can be used to estimate the response of ambient $O_3$ concentrations to changes in emissions. One

technique to simulate the response of $O_3$ to emissions changes, the brute force method, requires the modeler to explicitly model this response by directly altering the emissions inputs in the model simulation. This technique provides an estimate of the $O_3$ concentration at the altered emission level, but often does not provide accurate information regarding the response of $O_3$ to other levels of emissions since the chemistry for $O_3$ formation is nonlinear. Therefore, when using only brute force techniques a new model simulation would need to be performed for every emissions scenario under consideration.

Other analytical techniques have been developed to estimate the $O_3$ response to emissions perturbations without performing multiple simulations. One such method is termed the Decoupled Direct Method (DDM) (Dunker 1984). DDM, solves for sensitivity coefficients which are defined as the partial derivative of the atmospheric diffusion equations that underly the model calculations, Equations (2) and (3).

$$\boldsymbol{s_{ij}(t)} = \frac{\partial C_i(t)}{\partial p_j} \qquad \text{Equation (2)}$$

$$\boldsymbol{S_{ij}(t)} = \widetilde{P}_j \frac{\partial C_i(t)}{\partial p_j} = \widetilde{P}_j \frac{\partial C_i(t)}{\partial (\epsilon_j \widetilde{P}_j)} = \frac{\partial C_i(t)}{\partial \epsilon_j} \qquad \text{Equation (3)}$$

Here, $s_{ij}(t)$, the sensitivity, gives the change in model concentration, $C_i$, (for instance $O_3$ concentration) with an incremental change in any input parameter, $p_j$ (in this case emissions). Equation (3) allows us to normalize the sensitivity coefficient, $S_{ij}(t)$, so that it shows response in relative terms for the input rather than in absolute units. Therefore, $\tilde{P}_j$ (x,t) is the normalized input and $\varepsilon_j$ is a scaling variable (Yang et al, 1997). In general terms, the sensitivity coefficient tells us how a model output ($O_3$ concentration) will change if a model input (emissions of $NO_x$ or VOC) is perturbed. This first order sensitivity coefficient, $S_{ij}(t)$ is quite suitable for small perturbations, but gives a linear response which is unlikely to represent the results of large perturbations in very nonlinear chemical environments. Second (and third) order derivatives can be calculated to give higher order sensitivity coefficients (Hakami et al, 2003). Higher order sensitivity coefficients give the curvature and inflection points for the response curve and can capture the nonlinearities in the response of $O_3$ to emissions changes. Using Higher order DDM (HDDM) allows for the sensitivities to be more appropriately applied over larger emissions perturbations. Hakami et al. (2003) report that for an application in California, HDDM gave reasonable approximations of $O_3$ changes compared to brute force results for perturbations of emissions up to 50% using the first three terms of the Taylor series expansion, Equation (4).

$$\boldsymbol{C}(+\Delta\boldsymbol{\epsilon}) = \boldsymbol{C}(\mathbf{0}) + \Delta\boldsymbol{\epsilon}\boldsymbol{S}(\mathbf{0}) + \frac{\Delta\boldsymbol{\epsilon}^2}{\mathbf{2}}\boldsymbol{S}^2(\mathbf{0}) + \ \ldots + \frac{\Delta\boldsymbol{\epsilon}^n}{\boldsymbol{n}!}\boldsymbol{S}^n(\mathbf{0}) + \boldsymbol{R}_{n+1} \qquad \text{Equation (4)}$$

Here $\Delta\epsilon$ represents the relative change in emissions (for instance $\Delta\epsilon$ = -0.2 would be equivalent to reducing emissions by 20%), $S^n(0)$ is the n-th order sensitivity coefficient, C(0) is the concentration under baseline conditions (no perturbation in emissions) and $R_{n+1}$ is a remainder term.

A variant of DDM called DDM-3D has been implemented into several chemical transport models, including CMAQ, for both $O_3$ and particulate matter (PM) predictions (Dunker, 1984; Yang et al, 1997; Hakami et al, 2003; Cohan et al, 2005; Napelenok et al, 2006; Koo et al., 2010; Zhang et al, 2012). These implementations allow the modeler to define the parameters for which first and higher order sensitivities will be calculated. For instance, the sensitivity can be calculated for emissions from a specific source type, for emissions in a specific geographic region, and for emissions of a single $O_3$ precursor or for multiple $O_3$ precursors. In addition, sensitivities can be calculated to boundary conditions, initial conditions, and various other model inputs. Sensitivities to different sets of parameters can be calculated in a single model simulation but computation time increases as the number of sensitivities increases. Outputs from an HDDM simulation consist of time varying 3-D fields of first and second order sensitivities.

For the purposes of the $O_3$ NAAQS analysis, HDDM provides an improved approach compared to existing quadratic rollback techniques for several reasons. First, it captures non-linearity of $O_3$ response to emissions changes, representing both increases and decreases in $O_3$ concentrations resulting from emissions reductions. Second, HDDM characterizes different $O_3$ response at different locations (downtown urban versus downwind suburban) and at different times of day allowing us to incorporate temporal and spatial variations in response into the $O_3$ adjustment methodology. Finally, HDDM eliminates the need to use "background" $O_3$ as a floor for rollback since predicted sensitivities are based on model formulations that explicitly account for background sources.

## 2.2 LIMITATIONS

In addition to the many potential benefits of using HDDM to understand and characterize $O_3$ response to emissions changes, there are several limitations. First, HDDM encompasses all of the uncertainties of the base photochemical model formulation and inputs. So uncertainties in how the physical and chemical processes are treated in the model and in the model inputs propagate to the HDDM results. Also, HDDM can capture response to larger emissions perturbations than DDM but it is still most accurate for small perturbations. The larger the relative change in emissions, the less likely that the HDDM sensitivities will properly

capture the change in $O_3$ that would be predicted by a brute force model simulation. Several studies have reported reasonable performance of HDDM for $O_3$ up to 50% emissions perturbations (Hakami et al, 2003; Cohan et al., 2005; Hakami et al, 2004), but the magnitude of perturbation over which HDDM will give accurate estimates will depend on the specific modeling episode, size of the model domain, emissions and meteorological inputs, and the size of the emissions source to which the sensitivity is being calculated. In this work, we applied sensitivities derived from model simulations done under varying NOx levels (see Section 3.2.1) and found that using this technique we were able to replicate brute force estimates using HDDM sensitivities for up to 90% NOx reductions with a mean bias of less than 3 ppb and a mean error of less than 4 ppb.

# 3. APPLYING HDDM/CMAQ TO ADJUST OZONE TO JUST MEET CURRENT AND ALTERNATIVE STANDARDS: METHODOLOGY

## 3.1 CONCEPTUAL FRAMEWORK

This section outlines the methodology from Simon et al (2012) in which we apply CMAQ/HDDM to estimate hourly $O_3$ concentrations that might result from meeting the existing and potential alternative standards. As part of the methodology, photochemical modeling results are not used in an absolute sense, but instead are applied to modulate ambient measurements, thus tying estimated $O_3$ distributions to measured values. The basic steps are outlined below and in Figure 1 Details are given in section 3. The inputs, set-up, and evaluation of the modeling system are described in Appendix 4-B.

- **Step 1:** Run CMAQ simulation with HDDM to determine hourly $O_3$ sensitivities to $NO_x$ emissions and VOC emissions for the grid cells containing monitoring sites in an urban area.
- **Step 2:** For each monitoring site, season, and hour of the day use linear regression to relate first order sensitivities of $NO_x$ and VOC ($S_{NOx}$ and $S_{VOC}$) to modeled $O_3$ and second order sensitivities to NOx and VOC ($S^2_{NOx}$ and $S^2_{VOC}$) to the first order sensitivities.
- **Step 3:** For each measured hourly $O_3$ value, calculate the first and second order sensitivities based on monitoring site-, season-, and hour-specific functions calculated in Step 2.
- **Step 4:** Adjust measured hourly 2006-2010 $O_3$ concentrations for incrementally increasing levels of emissions reductions using assigned sensitivities and then

recalculate 2006-2008 and 2008-2010 design values until all monitors in an urban area are in attainment of existing and potential alternative levels of the standard.

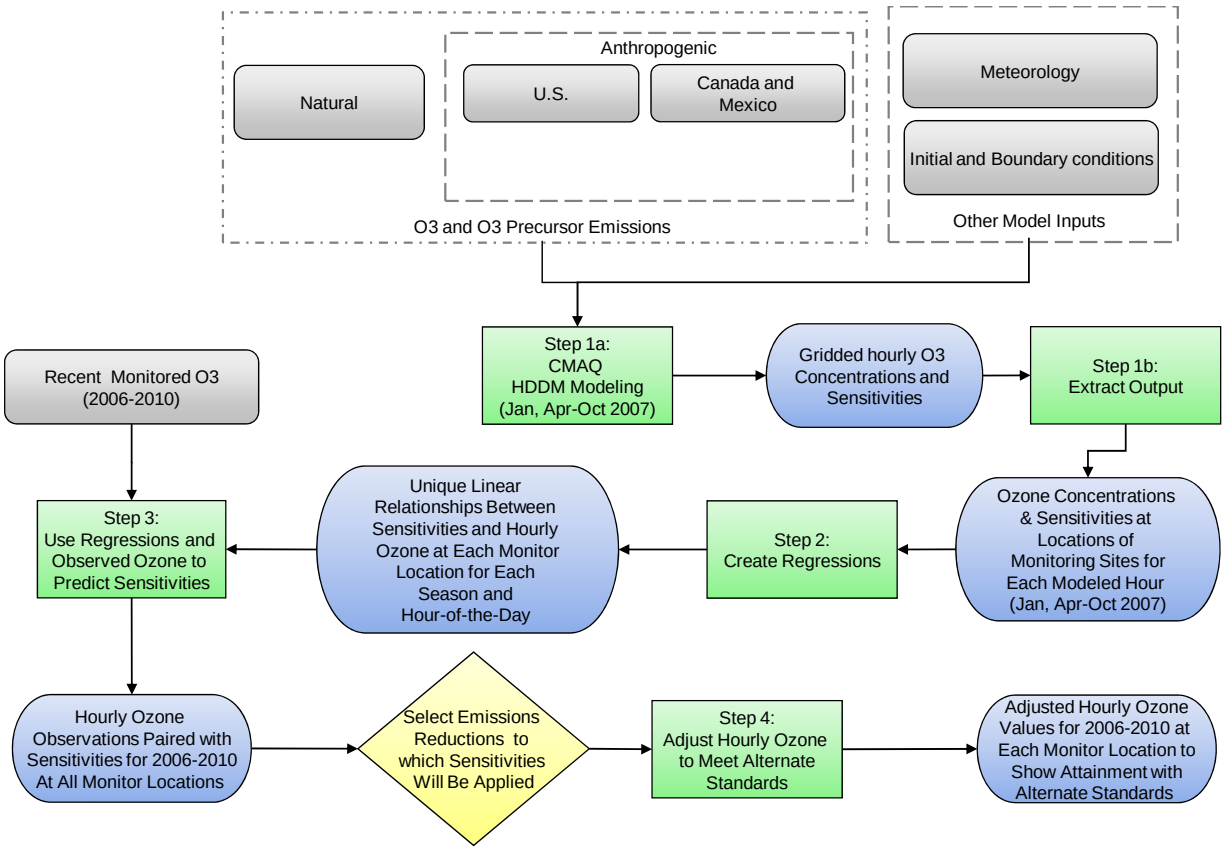


**Figure 1: Flow diagram demonstrating DDM model-based $O_3$ adjustment approach**

## 3.2 APPLICATION TO MEASURED $O_3$ CONCENTRATIONS IN 15 URBAN AREAS

In this analysis, we apply the model-based adjustment approach described above for attainment of the existing standard and three potential alternative standards. The analysis covers the 15 urban areas listed in Chapter 4 using photochemical modeling for January, and April-October of 2007 and ambient data for the years 2006-2010. When running CMAQ with HDDM, additional information is required to designate model inputs for calculating sensitivities. In this analysis, HDDM was set up to calculate the sensitivity of $O_3$

concentrations to U.S. anthropogenic $NO_x$ and VOC emissions[2]. US anthropogenic emissions were defined as all emissions in the following sectors: commercial marine and rail, onroad mobile, offroad mobile, Electric Generating Unit (power plant) point sources, non-EGU point, and non-point area. These sectors accounted for 17.6 million of the total domain-wide 23.6 million tons per year of $NO_x$ emissions and 13.8 million of the total domain-wide 68.1 million tons per year of VOC emissions. Sensitivities were not determined for biogenic, fire, Canadian, or Mexican emissions. In addition, sensitivities were not calculated for any emissions originating from outside the domain (i.e. entering through the use of boundary concentrations).

### 3.2.1 Multi-step Application of HDDM Sensitivities

As discussed in Section 2.2 of this appendix, HDDM has been reported to reasonably replicate brute force emissions reductions up to a 50% change in emissions. For this analysis, it was desirable to have confidence that the HDDM sensitivities could replicate the entire range of emissions reductions. Evaluations of the HDDM estimates compared to brute force emissions reduction model runs confirm that the HDDM estimates of $O_3$ response to $NO_x$ reductions are fairly comparable for a 50% change. However, HDDM and brute force estimates begin to diverge in comparisons under larger emissions changes (90%). Consequently four additional CMAQ/HDDM runs were performed under different levels of NOx and VOC emissions reductions in order to characterize ozone sensitivities to NOx reductions over a larger range of emissions perterbations. One CMAQ/HDDM simulation was performed with US anthropogenic $NO_x$ cut by 50%. A second additional simulation was performed with a 90% $NO_x$ reduction. Another set of CMAQ/HDDM simulations were performed for simultaneous $NO_x$ and VOC cuts (50% $NO_x$ and 50% VOC; 90% $NO_x$ and 90% VOC). Emissions of other species were not modified from the base case in these four simulations. These additional HDDM simulations give ozone sensitivities to $NO_x$ and VOC under conditions with lower $NO_x$ (or $NO_x$ and VOC) emissions in the US. These sensitivities are used in a multistep adjustment approach.

Figure 2 gives a conceptual picture of the multistep adjustment procedure using first-order sensitivities. Sensitivities from the base run are used to adjust $O_3$ concentrations for NOx emissions reductions up to X%. Additional emission reductions beyond X% use sensitivities from the 50% NOx cut run until reductions exceed (X+Y)%. Finally, sensitivities from the 90% NOx cut run are applied for any emission reductions beyond (X+Y)%. In order to more closely approximate the non-linear $O_3$ response to any level of emissions reductions, $2^{nd}$ order terms are added to the multistep approximation method in Equations (4)-(7). P represents the percentage

[2] Sensitivities only tracked U.S. emissions in the contiguous 48 states.

$NO_x$ cut for which the $\Delta O_3$ values are being calculated, $S$ and $S^2$ are the first and second order $O_3$ sensitivities to US $NO_x$ emissions, and X and Y are described above. Alternately, Equation (8) can be used with Equations (5)-(7) if simultaneous $NO_x$ and $VOC_c$ cuts are being simulated. Note that the 50% and 90% cut sensitivities used in Equation (8) come from model runs which cut both VOC and NOx by these percentages in contrast to the NOx cut only sensitivities that are used in Equation 4. Consequently, Equation (8) works only for equal percentage cuts in both $NO_x$ and VOC emissions. In equations (4)-(7), we cap $\Delta O_3$, so that $O_3$ never drops below zero due to emissions changes.

$$\Delta O_3 = -a \times S_{NOx_{base}} + \frac{a^2}{2} \times S^2_{NOx_{base}} - b \times S_{NOx_{50}\%cut} + \frac{b^2}{2} \times S^2_{NOx_{50}\%cut} \\ -c \times S_{NOx_{90}\%cut} + \frac{c^2}{2} \times S^2_{NOx_{90}\%cut} \qquad \text{Equation (4)}$$

$$a = \begin{cases} \frac{P}{100} & for\ P \le X \\ \frac{X}{100} & for\ P > X \end{cases} \qquad \text{Equation (5)}$$

$$b = \begin{cases} 0 & for\ P \le X \\ \frac{2\times(P-X)}{100} & for\ X < P \le (X+Y) \\ \frac{2\times Y}{100} & for\ P > (X+Y) \end{cases} \qquad \text{Equation (6)}$$

$$c = \begin{matrix} 0 & for\ P \le (X+Y) \\ \frac{10\times(P-(X+Y))}{100} & for\ 100 \ge P > (X+Y) \end{matrix} \qquad \text{Equation (7)}$$

$$\Delta O_3 = -a \times S_{NOx_{base}} + \frac{a^2}{2} \times S^2_{NOx_{base}} - a \times S_{VOC_{base}} + \frac{a^2}{2} \times S^2_{VOC_{base}} + a^2 \times S^2_{NOx,VOC_{base}} \\ -b \times S_{NOx_{50}\%cut} + \frac{b^2}{2} \times S^2_{NOx_{50}\%cut} - b \times S_{VOC_{50}\%cut} + \frac{b^2}{2} \times S^2_{VOC_{50}\%cut} + b^2 \times S^2_{NOx,VOC_{50}\%cut} \\ -c \times S_{NOx_{50}\%cut} + \frac{c^2}{2} \times S^2_{NOx_{50}\%cut} - c \times S_{VOC_{50}\%cut} + \frac{c^2}{2} \times S^2_{VOC_{50}\%cut} + c^2 \times S^2_{NOx,VOC_{50}\%cut} \qquad \text{Equation (8)}$$

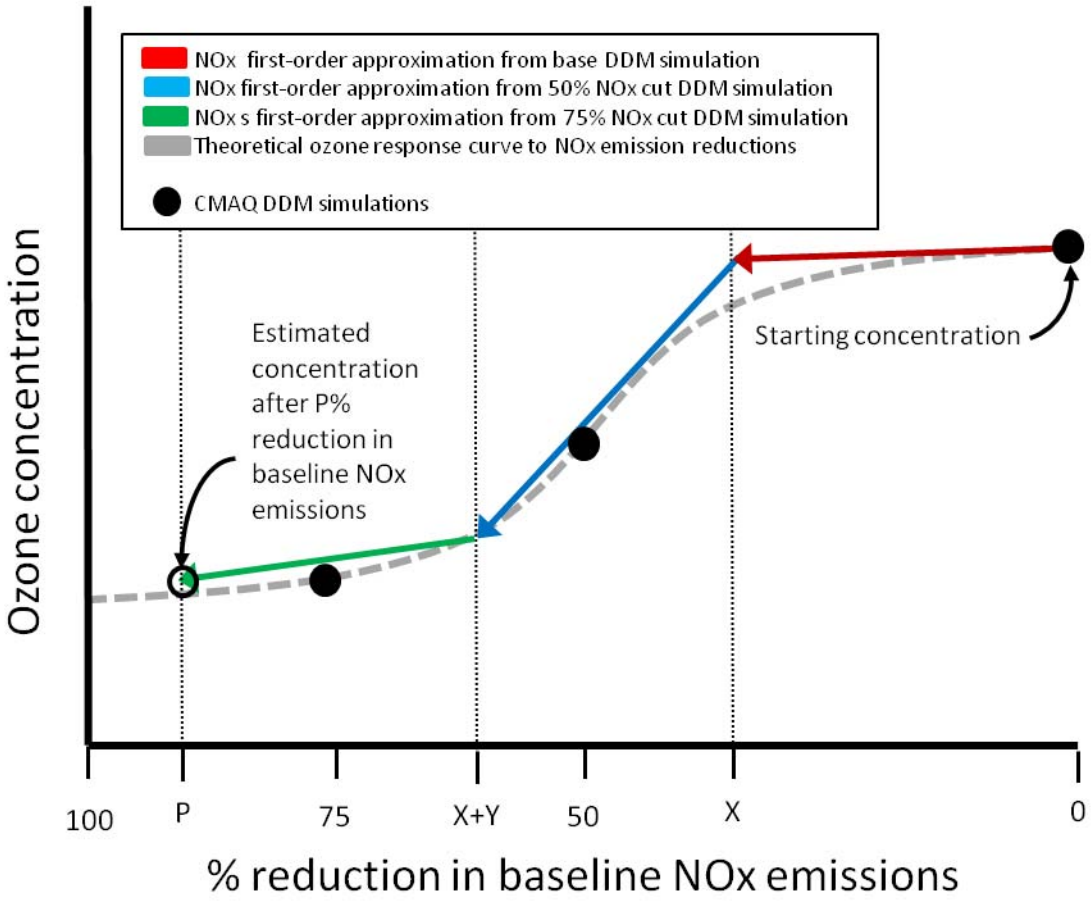


**Figure 2: Conceptual picture of 3-step application of HDDM sensitivities**

The ideal value for equation transition points, X and Y, are determined by minimizing the least square mean error between the adjusted concentrations using the multistep approach and modeled concentrations from brute force NOx cut runs. We first determined the value of X which gave the lowest error compared to brute forces estimates at 50% NOx cuts. Then holding X constant, we determined the value of Y which gave the lowest error compared to brute force estimates at 90% NOx cuts. This process was performed independently for each of the 15 urban areas in this analysis.

Error in HDDM estimates of hourly $O_3$ is defined here as the difference between HDDM estimates and brute force $O_3$. Based on equations (4)-(7), this can be calculated from Equations (9) and (10) for 50% NOx cuts:

$$\varepsilon = \Delta Ozone_{HDDM,50} - \Delta Ozone_{BF,50}$$ Equation (9)

$$\varepsilon = \frac{-X}{100} \times S_{NOx_base} + \frac{X^2}{2 \times 100^2} \times S^2_{NOx_base} - \frac{2(50 - X)}{100} \times S_{NOx_{50}\%cut} + \frac{\left(2 \times (50 - X)\right)^2}{2 \times 100^2} \times S^2_{NOx_{50}\%cut} - \Delta Ozone_{BF,50}$$ Equation (10)

Equation (10) can be rearranged to appear in the form: $AX^2 + BX + C$:

$$\varepsilon = \left(\frac{S^2_{NOx_{base}}}{2 \times 100^2} + \frac{4 \times S^2_{NOx_{50}\%cut}}{2 \times 100^2}\right) X^2 + \left(\frac{-S_{NOx_{base}}}{100} + \frac{2 \times S_{NOx_{50}\%cut}}{100} - \frac{400 \times S^2_{NOx_{50}\%cut}}{2 \times 100^2}\right) X + \left(-S_{NOx_{50}\%cut} + \frac{S^2_{NOx_{50}\%cut}}{2} - \Delta Ozone_{BF,50}\right)$$ Equation (11)

$$A = \left(\frac{S^2_{NOx_base}}{2 \times 100^2} + \frac{4 \times S^2_{NOx_{50}\%cut}}{2 \times 100^2}\right)$$ Equation (12)

$$B = \left(\frac{-S_{NOx_base}}{100} + \frac{2 \times S_{NOx_{50}\%cut}}{100} - \frac{400 \times S^2_{NOx_{50}\%cut}}{2 \times 100^2}\right)$$ Equation (13)

$$C = \left(-S_{NOx_{50}\%cut} + \frac{S^2_{NOx_{50}\%cut}}{2} - \Delta Ozone_{BF,50}\right)$$ Equation (14)

Next, the error is squared, summed over all points (error can be calculated for each hourly $O_3$ value at each monitoring location), and the derivative is set to 0 to determine X which gives the least squares error (Equations (15), (16), and (17)).

$$\varepsilon^2 = A^2X^4 + 2ABX^3 + (2AC + B^2)X^2 + 2BCX + C^2$$ Equation (15)

$$\sum \varepsilon^2 = (\sum A^2)X^4 + (\sum 2AB)X^3 + (\sum 2AC + B^2)X^2 + (\sum 2BC)X + \sum C^2$$ Equation (16)

$$(\sum \varepsilon^2)' = (4\sum A^2)X^3 + (3\sum 2AB)X^2 + (2\sum 2AC + B^2)X + (\sum 2BC) = 0$$ Equation (17)

The value of X that gives the least squares error will occur at one of the 3 roots of the trinomial in Equation (17) or at 0 or 50. All real roots, 0, and 50 were input into equation (16) and X was set to the value which resulted in the lowest error in each city. An analogous procedure was followed to determine Y using the 90% NOx cut brute force simulation and Equations (18) through (24).

$$\varepsilon = \frac{-X}{100} \times S_{NOx_{base}} + \frac{X^2}{2 \times 100^2} \times S^2_{NOx_{base}} - \frac{2Y}{100} \times S_{NOx_{50}\%cut} + \frac{2^2Y^2}{2 \times 100^2} \times S^2_{NOx_{50}\%cut} - \frac{10\big(90-(X+Y)\big)}{100} \times S_{NOx_{90}\%cut} + \frac{\left(10^2(90-(X+Y))\right)^2}{2\times100^2} \times S^2_{NOx_{90}\%cut} - \Delta Ozone_{BF,90}$$

Equation (18)

$$\varepsilon^2 = A^2Y^4 + 2ABY^3 + (2AC + B^2)Y^2 + 2BCY + C^2$$ Equation (19)

$$A = \left(\frac{4\times S^2_{NOx_{50}\%cut}}{2\times100^2} + \frac{100\times S^2_{NO90\%cut}}{2\times100^2}\right)$$ Equation (20)

$$B = \left(\frac{-2\times S_{NOx_{50}\%cut}}{100} + \frac{10\times S_{NO90\%cut}}{100} - \frac{200\times(90-X)S^2_{NOx_{90}\%cut}}{2\times100^2}\right)$$ Equation (21)

$$C = \left(\frac{-X}{100}S_{NOx_base} + \frac{X^2}{2\times100^2}S^2_{NOx_base} - \frac{10\times(90-X)}{100}S_{NOx_{90}\%cut} + \frac{100\times(90-X)^2}{2\times100^2}S^2_{NOx_{90}\%cut} - \Delta Ozone_{BF,90}\right)$$

Equation (22)

$$\sum\varepsilon^2 = (\sum A^2)Y^4 + (\sum 2AB)Y^3 + (\sum 2AC + B^2)Y^2 + (\sum 2BC)Y + \sum C^2$$ Equation (23)

$$(\sum\varepsilon^2)' = (4\sum A^2)Y^3 + (3\sum 2AB)Y^2 + (2\sum 2AC + B^2)Y + (\sum 2BC) = 0$$ Equation (24)

This methodology can also be adjusted to calculate least squares error cutpoints for the combined $NO_x$ and VOC emissions reduction case. X and Y cutpoints which have the least square error in each urban area are shown in

Table 1. This 3-step adjustment methodology was shown to be a robust method for minimizing error in the HDDM applications for larger percentage changes in emissions by Simon et al (2012). Figure 3 through Figure 6 are density scatter plots that compare hourly ozone estimates from brute force with hourly ozone estimates from the 3-step HDDM adjustments at all monitor locations in each of the 15 urban areas evaluated in this study. The colors in these plots depict the percentage of points falling at any one location. Mean error for the 50% and 90% 3-step HDDM adjustment NOx cut cases compared to brute force results are less than 1 ppb and 4 ppb respectively in all 15 case study areas.

**Table 1: X and Y cutpoints used in Equations (4) and (8). Note: the NOx/VOC sensitivity case was only performed in two cities.**

| Urban Area | NOx cuts only | | NOx and VOC combined cuts | |
|---|---|---|---|---|
| | X | Y | X | Y |
| Atlanta | 40 | 46 | | |
| Baltimore | 40 | 46 | | |
| Boston | 39 | 45 | | |
| Chicago | 38 | 45 | 40 | 46 |
| Cleveland | 42 | 45 | | |
| Dallas | 37 | 46 | | |
| Denver | 39 | 45 | 43 | 45 |
| Detroit | 38 | 45 | | |
| Houston | 37 | 44 | | |
| Los Angeles | 38 | 46 | | |
| New York | 37 | 45 | | |
| Philadelphia | 40 | 45 | | |
| Sacramento | 38 | 45 | | |
| Saint Louis | 39 | 45 | | |
| Washington D.C. | 40 | 46 | | |

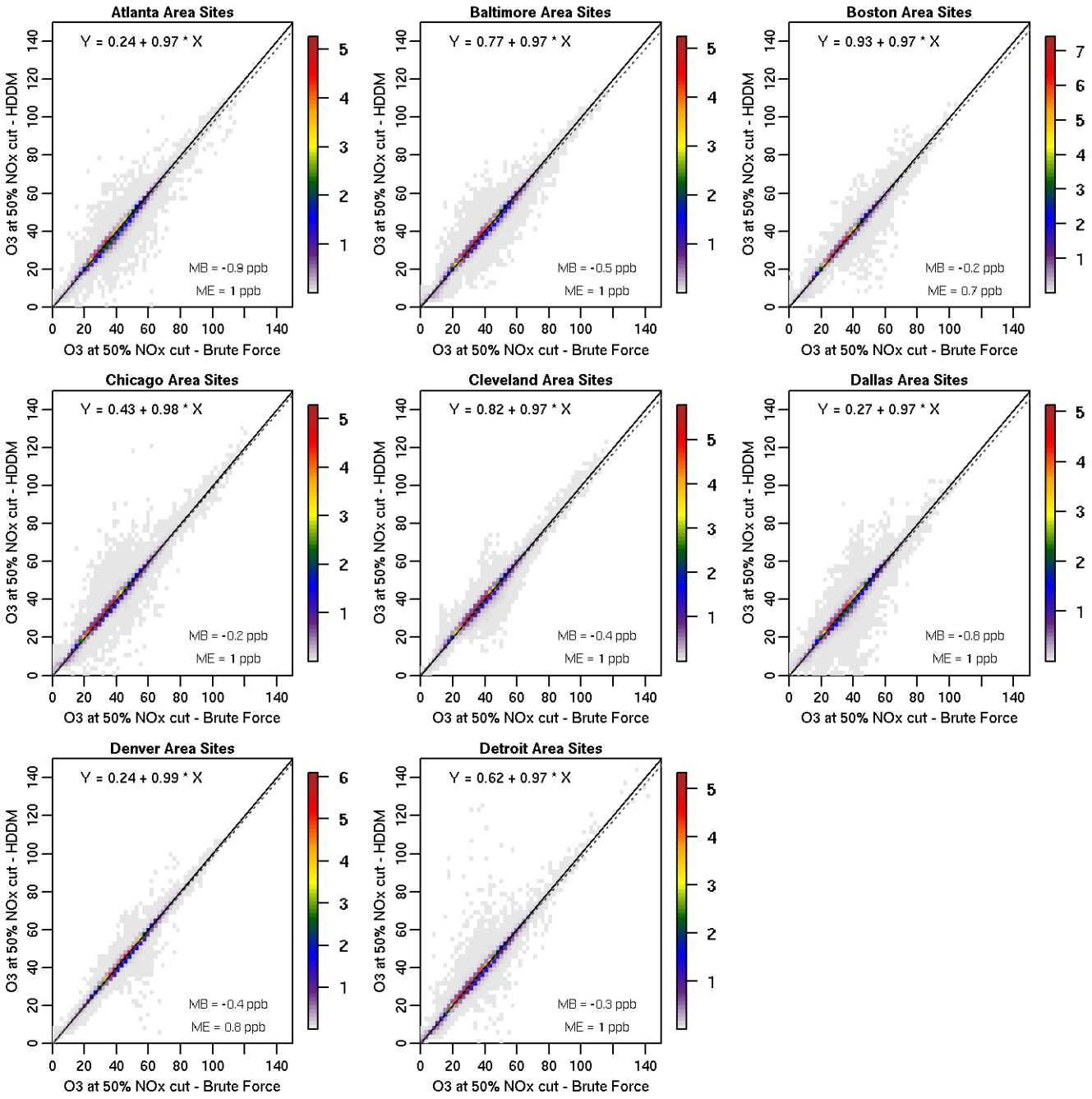


**Figure 3: Comparison of brute force and 3-step HDDM $O_3$ estimates for 50% NOx cut conditions: Atlanta, Baltimore, Boston, Chicago, Cleveland, Dallas, Denver, and Detroit.**

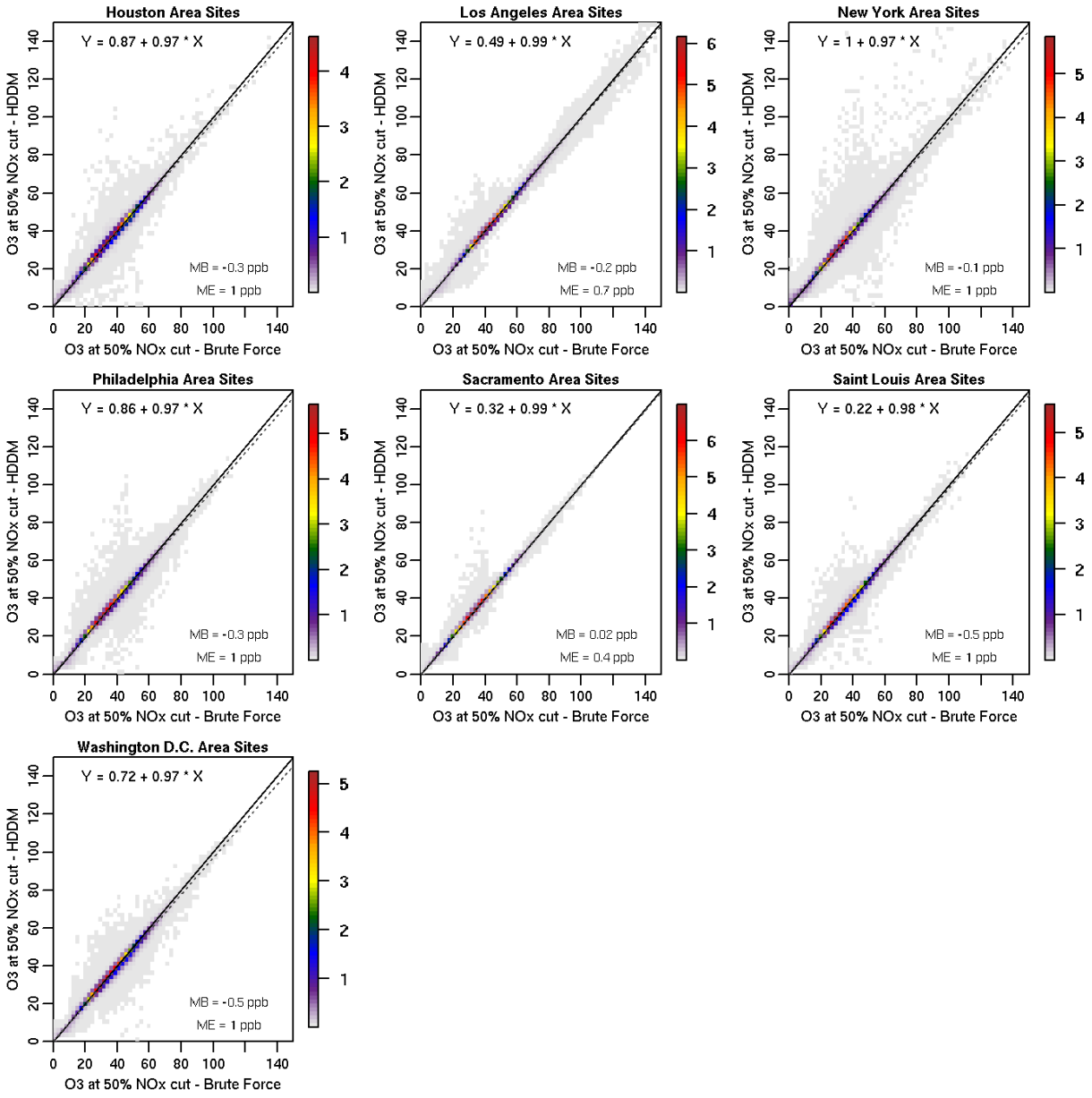


**Figure 4: Comparison of brute force and 3-step HDDM $O_3$ estimates for 50% NOx cut conditions: Houston, Los Angeles, New York, Philadelphia, Sacramento, St. Louis, and Washington D.C.**

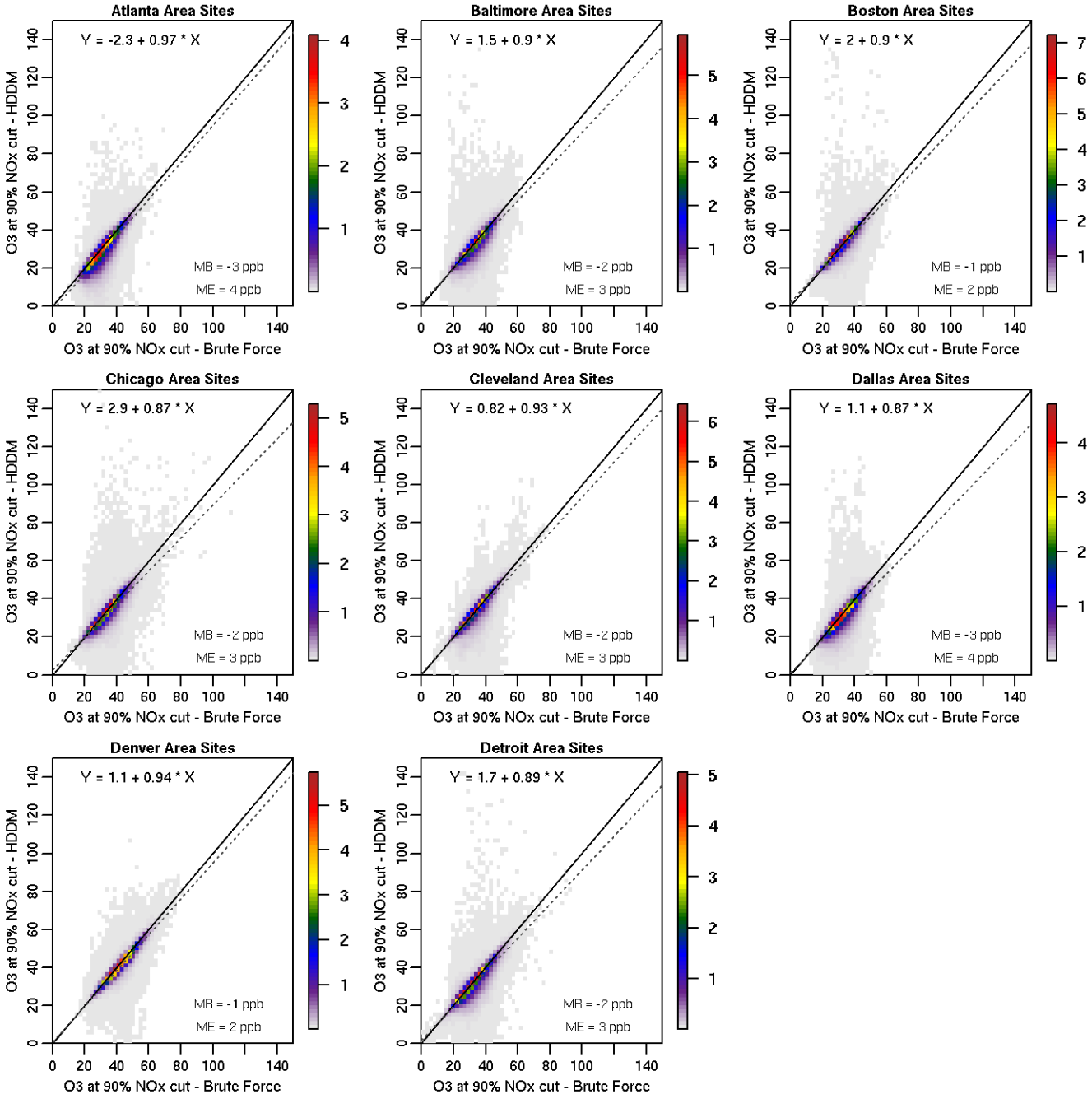


**Figure 5: Comparison of brute force and 3-step HDDM $O_3$ estimates for 90% NOx cut conditions: Atlanta, Baltimore, Boston, Chicago, Cleveland, Dallas, Denver, and Detroit.**

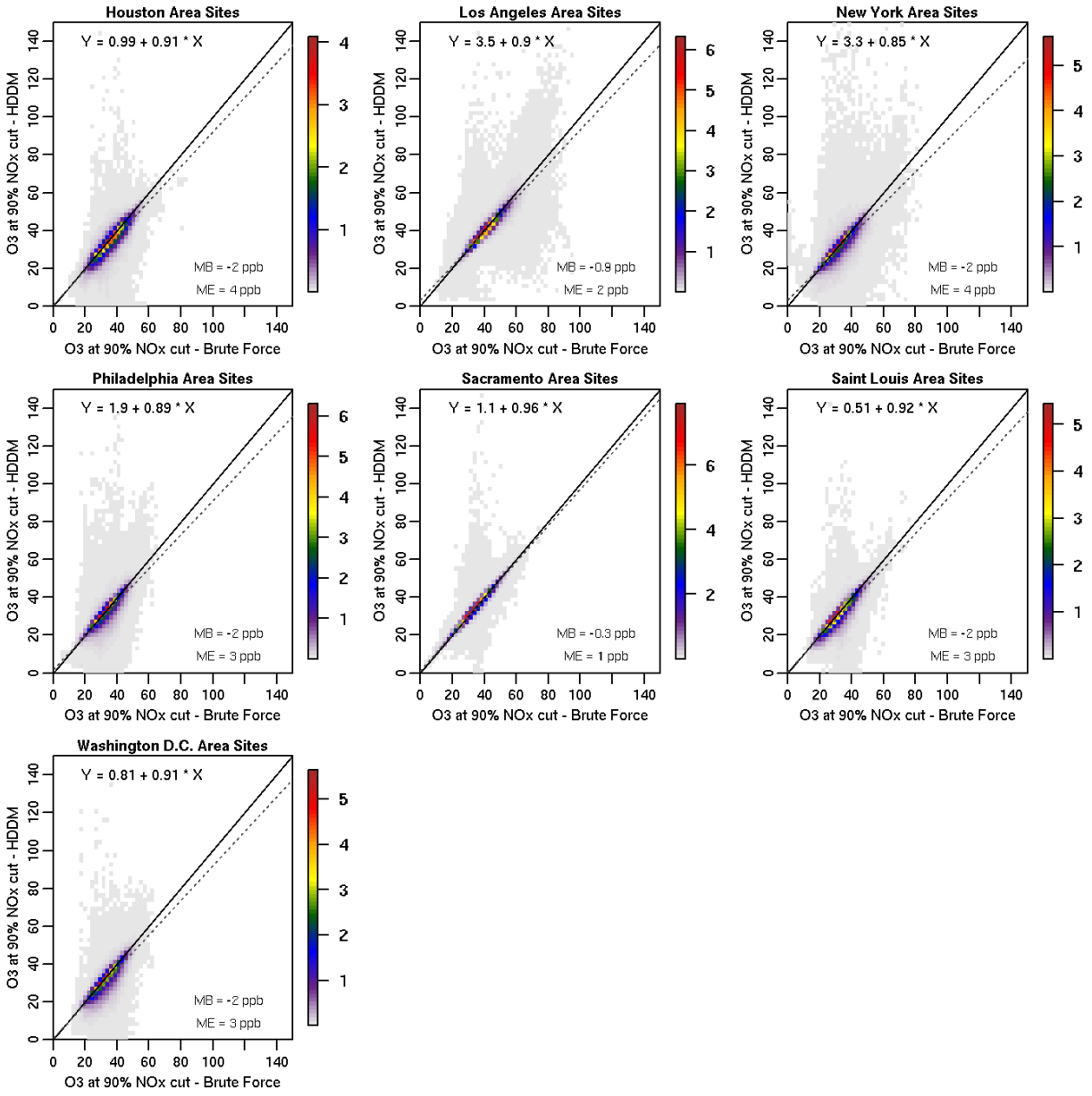


**Figure 6: Comparison of brute force and 3-step HDDM $O_3$ estimates for 90% NOx cut conditions: Houston, Los Angeles, New York, Philadelphia, Sacramento, St. Louis, and Washington D.C.**

### 3.2.2 Relationships between HDDM Sensitivities and Modeled $O_3$ Concentrations

First and second order hourly $O_3$ sensitivities to VOC and $NO_x$ were extracted from the HDDM simulation for model grid cells that contained the $O_3$ monitors in the 15 urban areas. Extracted data included modeled sensitivities at monitor locations for all modeled hours in 2007. These sensitivities cannot be applied directly to observed values for two reasons: 1) high modeled $O_3$ days/hours do not always occur concurrently with high observed $O_3$ days/hours and

2) the modeling time period includes 8 months in 2007 but the time period we are analyzing in this REA includes five full years of ambient data, 2006-2010. As to the first point, photochemical models are generally used in a relative sense for purposes of projecting design values to assess attainment with the NAAQS standard. In this manner, model predictions are "anchored" to measured ambient values. In general, the average response on high modeled days is used for this purpose. This allows for more confidence in calculated results when "less than ideal model performance [occurs] on individual days" (US EPA, 2007). Similarly, for this analysis we believe it is appropriate to account for the fact the model does not always perfectly agree with measurements and that sensitivities from a low $O_3$ modeled day would not be appropriate to apply to a high $O_3$ measured day (and vice-versa) even if they occur on the same calendar day. For the second point, due to current resource and time constraints we were only able to model 8 months in 2007. However, the $O_3$ exposure analysis evaluates the effects of $O_3$ decreases for two 3-year periods in 2006-2008 and 2008-2010 most of which is outside the modeled time period. For both of these reasons, a method was developed to generalize the modeled site-, season-, and hour-specific sensitivities so that they could be applied to ambient data during 2006-2010[3].

Simon et al. (2012) describe how first order sensitivities are generally well correlated with hourly modeled $O_3$ concentrations and second order sensitivities are well correlated to first order sensitivities. Based on their analysis, we create a separate linear regression for $S_{NOx}$ and $S_{VOC}$ as functions of hourly $O_3$ (i.e. $S_{NOx} = m \times O_3 + b$) for every site, season[4], and hour-of-the day examined in this analysis. For instance, for summer 8-am hours at Detroit Site 260990009, $S_{NOx}$ and $O_3$ values from all 8 am hours in June-August 2007 are used to fit this relationship. Since only 8 months were modeled (Jan, April-October) regressions for summer season relationships include more data points (92) than those for winter (31), spring (61), and fall (61). Similarly, $S^2_{NOx}$ and $S^2_{VOC}$ were calculated as a function of $S_{NOx}$ and $S_{VOC}$ respectively and $S^2_{NOx,VOC}$ was calculated as a linear combination of both $S_{NOx}$ and $S_{VOC}$. Figure 7, Figure 8, and Figure 9 show examples of these regressions for first order NOx sensitivities for a NOx-limited site (summertime, downwind of Atlanta), a NOx-saturated site (autumn, Queens NY), and a transitional site which switches between chemical regimes (spring, Long Island NY). Example relationships are shown for four different times of day with different $O_3$ response behavior:

[3] The 8 months modeled covered a variety of conditions such that we can use the results from this modeled time period in conjunction with the ambient data from the longer 5-year period for estimating response and applying adjustments

[4] Here seasons are defined as follows:
For ambient data, Winter = December, January, February; Spring = March, April, May; Summer = June, July, August; Fall = September, October, November.
For modeled data, Winter = January; Spring = April, May; Summer = June, July, August; Fall = September, October

nighttime (1:00 LST), mid-afternoon (15:00 LST), morning rush-hour (8:00 LST), and evening rush-hour (18:00 LST). The Atlanta area NOx-limited site (Figure 7) generally showed positive sensitivities which would lead to decreasing ozone with decreasing emissions. However some limited $O_3$ increases with NOx reductions from NOx (negative sensitivities) occurred at this site during nighttime and rush-hour times. The Queens site had negative sensitivities at these four hours on almost all days indicating strongly NOx saturated conditions. The slopes from the regressions at the Queens site were negative indicating larger ozone increases are high concentrations. Finally, the Long Island site had both positive and negative sensitivities but the slope was positive resulting in ozone increases for low basecase concentrations but ozone decreases at higher basecase concentrations. Correlations were strongest at the NOx limited site and during rush-hour and nighttime periods for the other sites. Figure 10, Figure 11, and Figure 12 show these regressions from the same sites and time-periods for second order sensitivities.

Comparisons between brute force and HDDM $O_3$ estimates shown in Figure 5 and Figure 6, demonstrate that for the vast majority of data points, HDDM replicates brute force with minimal errors. However, these figures show a small number of instances in which HDDM predicts very high hourly $O_3$ (> 100 ppb) while the brute force emissions simulations show much lower $O_3$ (< 40 ppb). In such cases, base modeled $O_3$ is low due to NOx titration and increases occur with reductions of $NO_x$. The HDDM sensitivities for these few points appear to be too high to be applied over large emissions changes because of strongly nonlinear chemistry. While the brute force simulations predict modest increases in $O_3$ at these hours, the HDDM method predicts very large increase in $O_3$ at these hours. To avoid outlier sensitivities from biasing this analysis, we set a floor value for negative $S_{NOx}$ values (ozone increases) in each regression so that $S_{NOx}$ never drops below the $5^{th}$ percentile modeled $S_{NOx}$ (for each site, hour, season grouping) when negative $S_{NOx}$ values are simulated (see dotted blue lines in Figure 7, Figure 8, and Figure 9). In addition, $S_{NOx}$ is prevented from dropping below 0 when all modeled $S_{NOx}$ values were positive (i.e. no modeled increases in ozone). These floor values have the most influence when regressions with highly NOx-saturated conditions, such as those shown for Queens NY, are applied to ambient $O_3$ values that are higher than the modeled range. For instance in Figure 9, if there were any measured autumn 18:00 $O_3$ concentrations above 30 ppb at that site in 2006-2010, the floor would prevent the extrapolation of $O_3$ increases from the modeled time period to conditions that do not apply. This floor is necessary for $O_3$ increases which, if extrapolated, could unrealistically increase $O_3$ without a bound. In contrast, the $O_3$ decreases can never exceed the total measured $O_3$ so positive NOx sensitivities have a built-in upper bound.

For the 50% and 90% emissions cut CMAQ/HDDM simulation, regressions were performed for first order $NO_x$ and VOC sensitivities with modeled $O_3$ from the base HDDM simulation. The regression technique was performed for the first and second order NOx and VOC sensitivities from the base run and the 50% emissions cut and 90% emissions cut simulations. The sensitivities from the emissions cut runs were fitted to hourly $O_3$ concentrations in the base simulation. Simon et al. (2012) found that correlation coefficients using for sensitivities from NOx cut simulations to base case $O_3$ concentrations were similar to those with $O_3$ concentrations from the NOx cut runs.

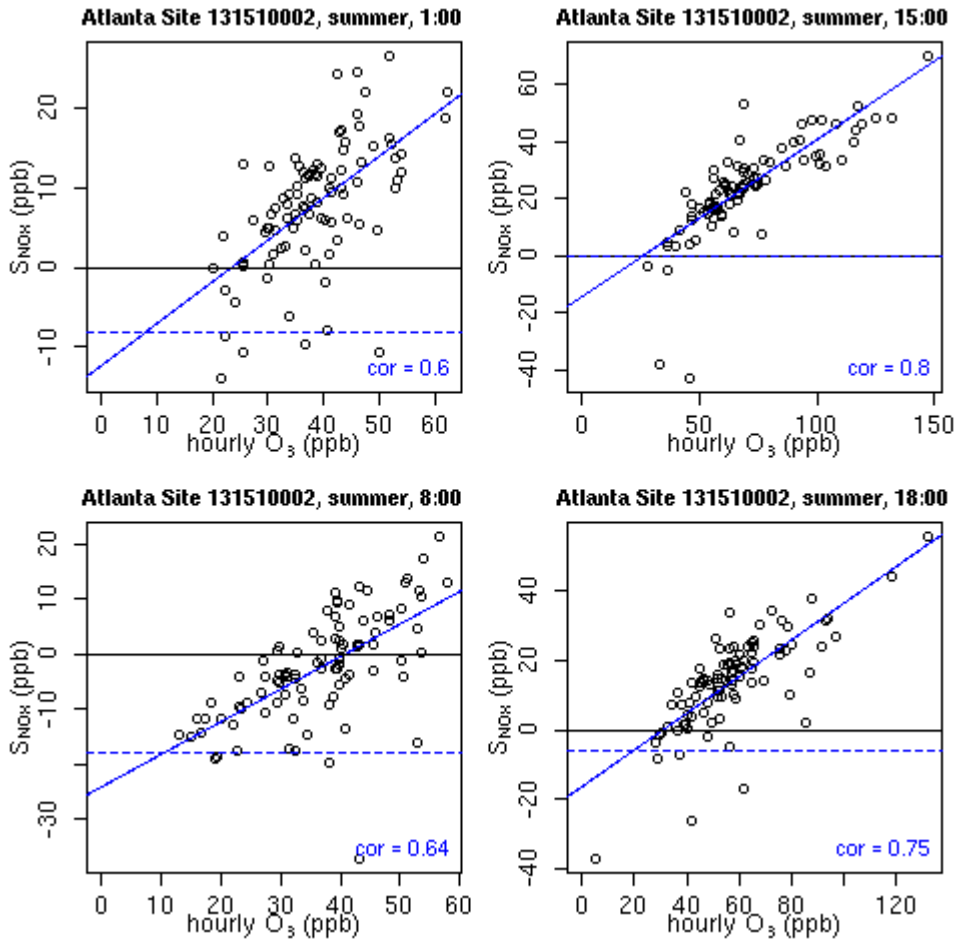


**Figure 7: Relationship between $S_{NOx}$ and hourly $O_3$ at a $NO_x$-limited site downwind of Atlanta (summer). Relationships are shown for one nighttime hour, one morning rush-hour hour, one daytime hour, and one evening rush-hour hour. The solid blue line show the linear regression for these points and the dotted blue line shows the floor value used for $S_{NOx}$ based on the 5th percentile modeled value.**

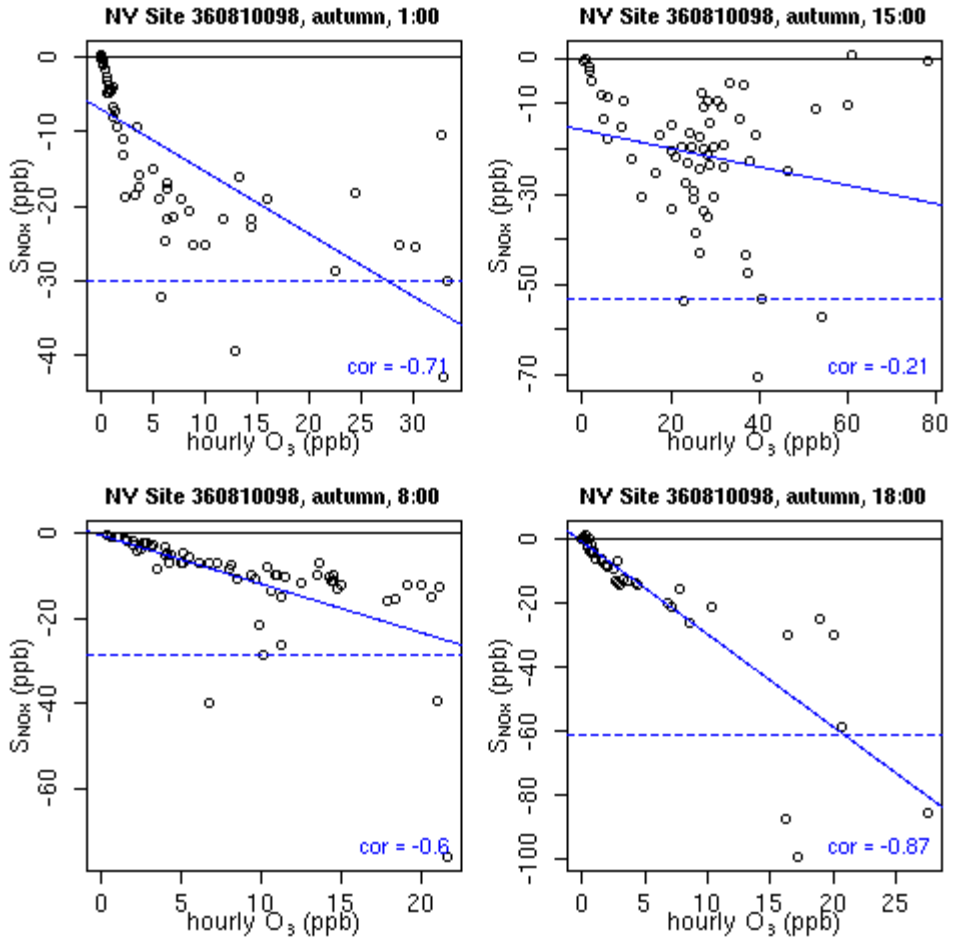


**Figure 8: Relationship between $S_{NOx}$ and hourly $O_3$ at a $NO_x$-saturated site in Queens County, NY (autumn). Relationships are shown for one nighttime hour, one morning rush-hour hour, one daytime hour, and one evening rush-hour hour. The solid blue line show the linear regression for these points and the dotted blue line shows the floor value used for $S_{NOx}$ based on the 5$^{th}$ percentile modeled value.**

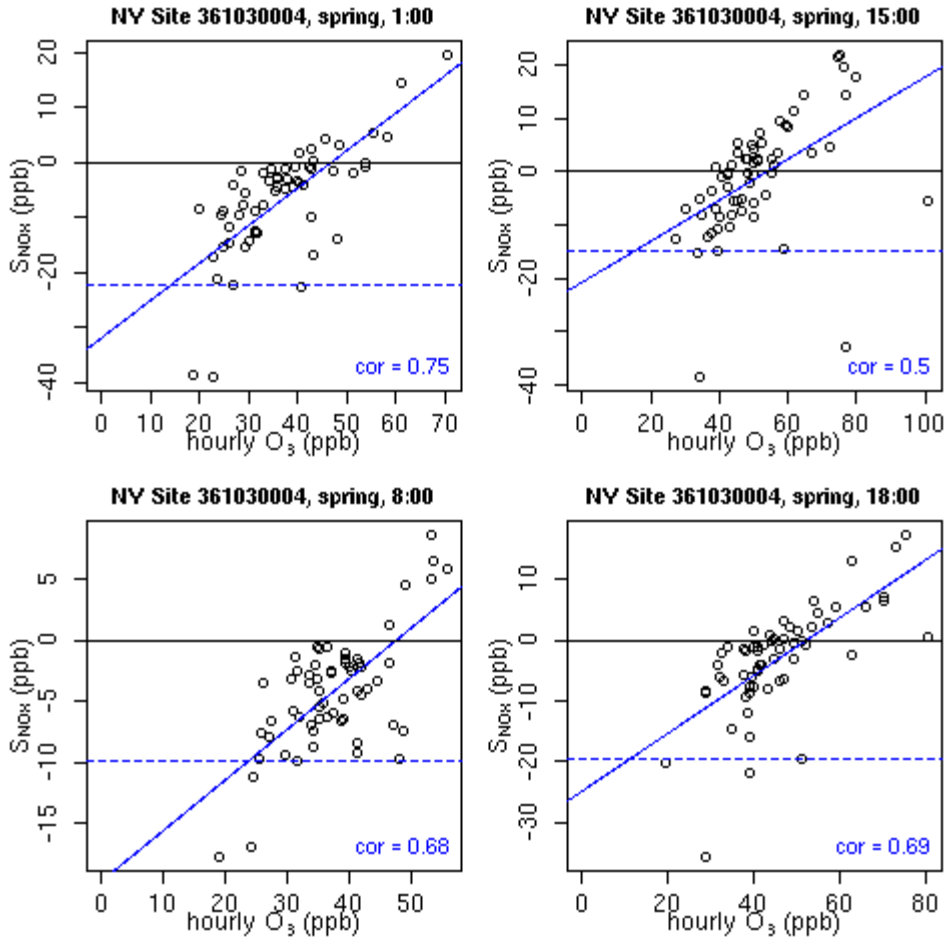


**Figure 9: Relationship between $S_{NOx}$ and hourly $O_3$ at a $NO_x$-saturated site in Suffolk County, NY on Long Island (spring). Relationships are shown for one nighttime hour, one morning rush-hour hour, one daytime hour, and one evening rush-hour hour. The solid blue line show the linear regression for these points and the dotted blue line shows the floor value used for $S_{NOx}$ based on the 5$^{th}$ percentile modeled value.**

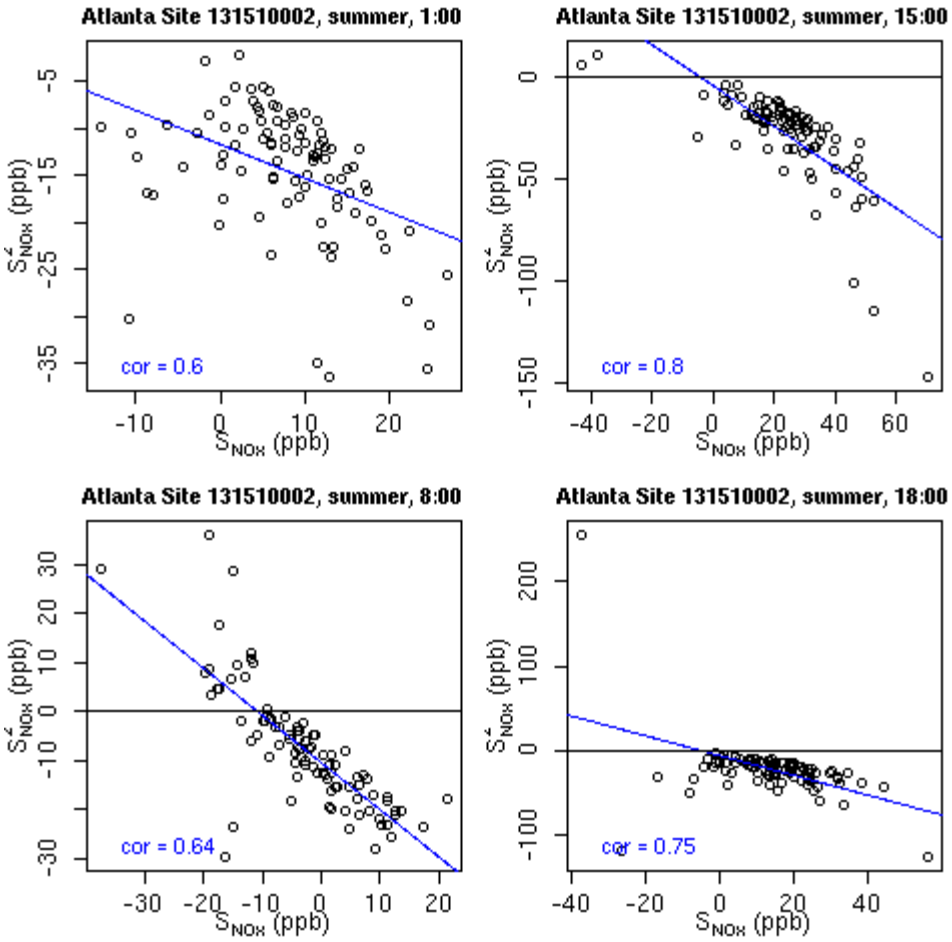


**Figure 10: Relationship between $S^2_{NOx}$ and $S_{NOx}$ at a $NO_x$-limited site downwind of Atlanta (summer). Relationships are shown for one nighttime hour, one morning rush-hour hour, one daytime hour, and one evening rush-hour hour. The solid blue line shows the linear regression for these points.**

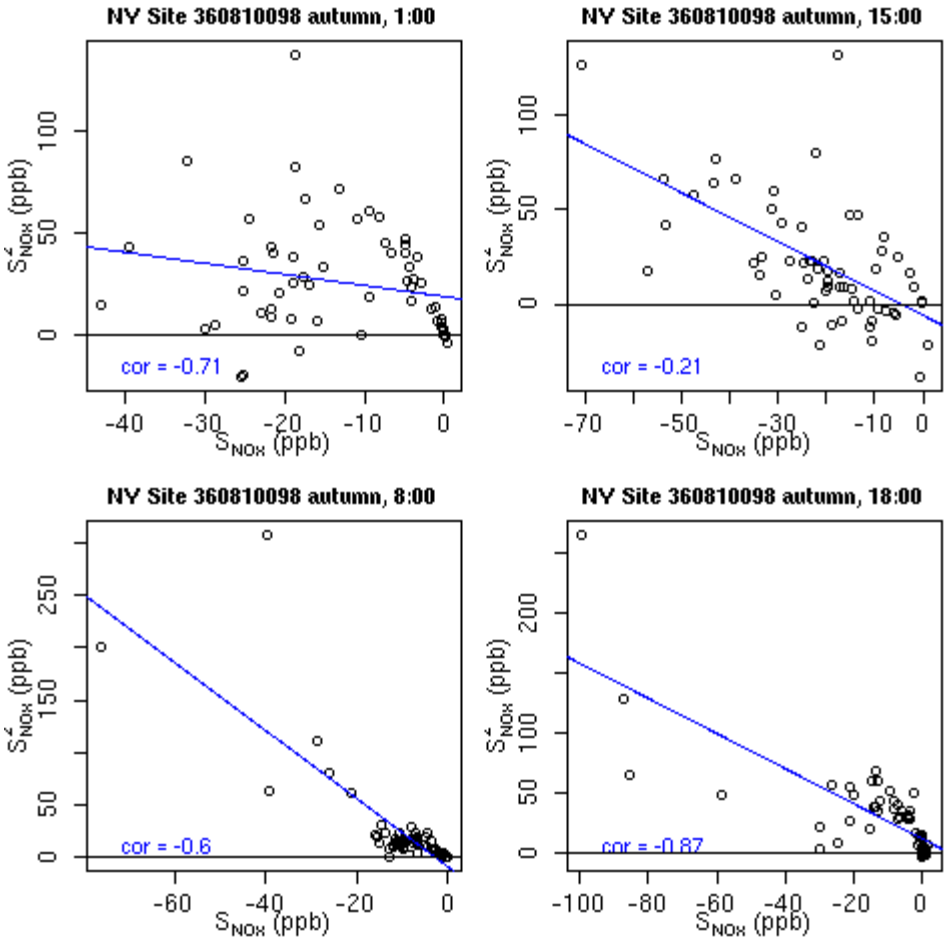


**Figure 11: Relationship between $S^2_{NOx}$ and $S_{NOx}$ at a $NO_x$-saturated site in Queens County, NY (autumn). Relationships are shown for one nighttime hour, one morning rush-hour hour, one daytime hour, and one evening rush-hour hour. The solid blue line shows the linear regression for these points.**

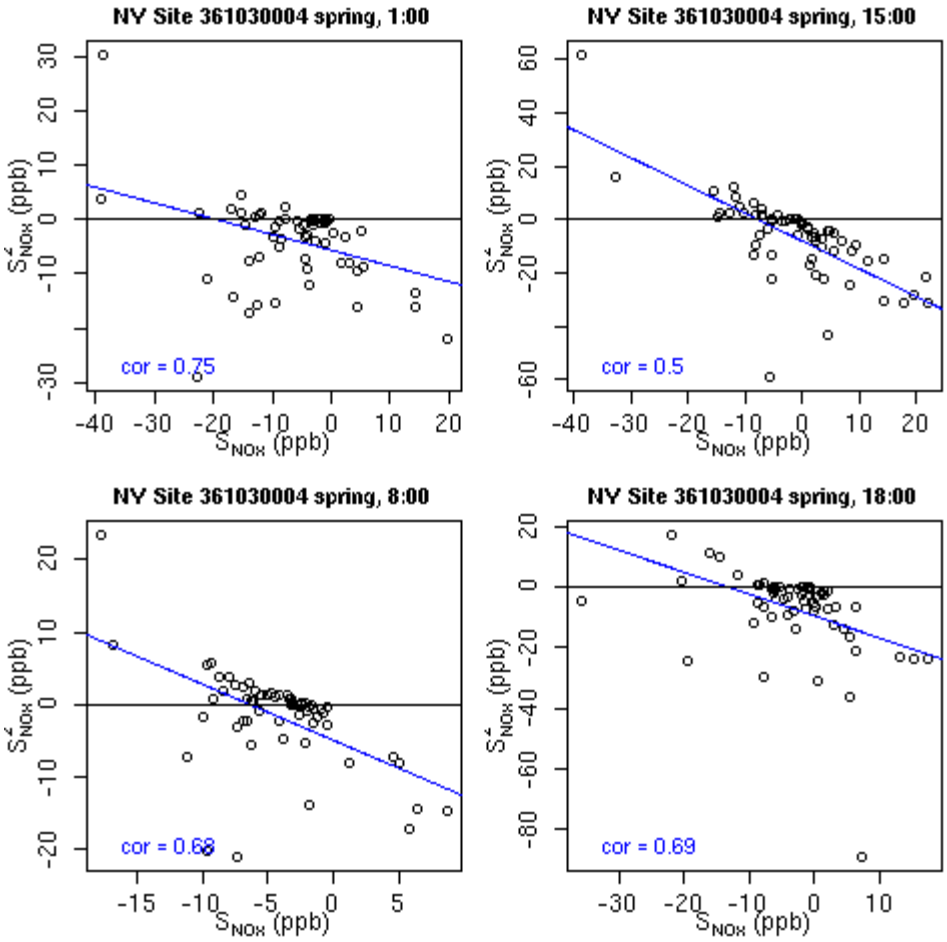


**Figure 12: Relationship between $S^2_{NOx}$ and $S_{NOx}$ at a $NO_x$-saturated site in Suffolk County, NY on Long Island (spring). Relationships are shown for one nighttime hour, one morning rush-hour hour, one daytime hour, and one evening rush-hour hour. The solid blue line shows the linear regression for these points.**

### 3.2.3 Application of Sensitivity Regressions to Ambient Data

To apply the HDDM adjustments to observed data, sensitivities must be determined for each hour from 2006-2010 at each site based on the linear relationship from the modeled data and the observed $O_3$ concentration. The linear regression model also allows us to quantify the standard error of each predicted sensitivity value at each hour and site.

Observed hourly $O_3$ from 2006-2010 at each monitor location was adjusted by applying incrementally increasing NOx reductions (equations (4)-(8)) and recalculating MDA8 values at each step until all monitors in an urban area achieved design values at the standard level being evaluated (75, 70, 65, or 60 ppb). Therefore all monitors within an urban area were treated as responding to the same percentage reduction in $NO_x$ or $NO_x$/VOC emissions. The standard error associated with each predicted sensitivity from the linear model can be propagated through Equations (4) and (8) to quantify the standard error in the final predicted $O_3$ concentration. This

gives a measure of variability in the sensitivities at any given $O_3$ concentration and allows us to quantify how much our predicted $O_3$ could change given that variability.

### 3.2.4 Alternate Methodologies

The methodology used for most of the 15 urban areas is described above. In most cases the $O_3$ response was calculated using Equation (4) which represents a $NO_x$ only control strategy. In addition, sensitivities applied to observed data were based on the predicted sensitivity for that hourly $O_3$ from the site, season, and hour-specific regression. However, two alternate scenarios were used for a few cities as described below.

A combined $NO_x$/VOC control strategy was applied to two cities for which controlling monitors were sensitive to changes in VOC emissions: Chicago and Denver. These were the only case study areas in which the addition of VOC reductions allowed attainment of the targeted standard levels with smaller reductions in NOx emissions than would be required if VOC emissions were held constant. In these cases, Equation (8) was applied in place of Equation (4) and the X,Y cutpoints described in

Table 1 were derived for the $NO_x$/VOC control case based on brute force runs that reduced the two $O_3$ precursors by equal percentages.

In two cities, New York and Los Angeles, results were affected by aberrant behavior at a few monitors which occurred during rush-hour and nighttime hours. At a few highly urbanized monitors during some seasons, the ozone increases during highly titrated rush-hour and nighttime hours appear to be overestimated, leading to predictions that when NOx was reduced ozone would peak during rush-hour periods on the very highest ozone days (compare outlier dots for 65 ppb standard at 9:00-17:00 to outlier dots for 65 ppb standard at 18:00-8:00 in Figure 23). Even at these monitors, the majority of days did not have this problem as shown by the more normal diurnal pattern for the boxes (interquartile range) and whiskers (1.5 × interquartile range) in Figure 23. As mentioned above, for each predicted hourly $O_3$ concentration we calculated a standard error based on the uncertainty in the fitted regressions representing the variability in modeled sensitivities which is not explained by hourly $O_3$ levels alone for each site, season, and hour. So, in addition to the predicted $O_3$, we can create alternate hourly $O_3$ datasets based on the standard error in these values. To address the aberrant behavior on the very highest ozone days in the adjustment scenarios in New York and Los Angeles, we

took the 95th percentile confidence interval for each hourly $O_3$ prediction and used the lower bound value to determine the $NO_x$ reductions required to meet the existing and potential alternative standards and to calculate the hourly $O_3$ that would occur under that reduced emission scenario. During most hours and at most monitors, the 95th percentile range was small (less than +/- 2.7 ppb) so the use of the lower-bound of the 95th percentile range made little difference in predicted ozone concentrations (see Table 18 and Table 19). However, using the lower bound of the 95th percent confidence interval allowed us to dampen the effect of overpredicted ozone increases during rush-hour times. Since the $O_3$ concentrations for each standard level were created using consistent methodology, these $O_3$ datasets can be used to compare between standards in these cities. In addition, at a single standard level (for instance 75 ppb) these $O_3$ values can be compared against those obtained using the base methodology in order to quantify uncertainty due to variability in modeled sensitivities. However, $O_3$ values for one standard obtained using the 95th percentile confidence interval lower bound are not contrasted against $O_3$ concentrations for a potential alternative standard which were obtained using the base methodology since these datasets are not directly comparable.

# 4. APPLYING HDDM/CMAQ TO ADJUST OZONE TO JUST MEET CURRENT AND ALTERNATIVE STANDARDS: RESULTS

## 4.1 EMISSION REDUCTIONS APPLIED TO MEET ALTERNATIVE STANDARDS

Table 2 reports the percentage reduction in domain-wide emissions that were used to reach the existing and potential alternative standard levels in each urban area. Percentages in Chicago and Denver represent reductions in anthropogenic $NO_x$ and VOC. Percentages in all other cities represent reductions only in anthropogenic $NO_x$ emissions. Percentages in New York and in Los Angeles were calculated based on air quality estimates at the lower end of the 95th percentile confidence interval as discussed above in section 3.2.4. Please note that these reductions and broad nationwide emission cuts are not intended to represent recommended control scenarios since they would not be the most efficient method for achieving the standard in many localized areas.

**Table 2: Percent emissions reductions used for each urban area to obtain each standard.**

| Urban Area | Years | Standard Level* | | | |
|---|---|---|---|---|---|
| | | 75 ppb | 70 ppb | 65 ppb | 60 ppb |
| Atlanta | 2006-2008 | 50% | 58% | 64% | 71% |
| | 2008-2010 | 23% | 43% | 54% | 62% |
| Baltimore | 2006-2008 | 46% | 54% | 61% | 69% |
| | 2008-2010 | 44% | 52% | 60% | 67% |

| | | | | | |
|---|---|---|---|---|---|
| Boston | 2006-2008 | 40% | 49% | 61% | 70% |
| | 2008-2010 | 13% | 40% | 53% | 65% |
| Chicago | 2006-2008 | 19% | 52% | 66% | 80% |
| | 2008-2010 | N/A | 27% | 55% | 70% |
| Cleveland | 2006-2008 | 48% | 61% | 73% | 88% |
| | 2008-2010 | 50% | 64% | 77% | 88% |
| Dallas | 2006-2008 | 50% | 57% | 65% | 72% |
| | 2008-2010 | 50% | 58% | 64% | 71% |
| Denver | 2006-2008 | 51% | 65% | 78% | 87% |
| | 2008-2010 | 15% | 46% | 64% | 87% |
| Detroit | 2006-2008 | 59% | 69% | 76% | 84% |
| | 2008-2010 | N/A | 54% | 66% | 78% |
| Houston | 2006-2008 | 62% | 68% | 74% | 82% |
| | 2008-2010 | 42% | 53% | 63% | 75% |
| Los Angeles | 2006-2008 | 87.1% | 89.3% | 91.2% | 93.2% |
| | 2008-2010 | 87% | 89% | 91% | 93% |
| New York | 2006-2008 | 64% | 74% | 92% | N/A |
| | 2008-2010 | 52% | 67% | 89% | N/A |
| Philadelphia | 2006-2008 | 54% | 61% | 68% | 74% |
| | 2008-2010 | 42% | 52% | 61% | 68% |
| Sacramento | 2006-2008 | 63% | 70% | 76% | 84%[5] |
| | 2008-2010 | 64% | 71% | 77% | 84% |
| Saint Louis | 2006-2008 | 45% | 56% | 66% | 75% |
| | 2008-2010 | 10% | 34% | 50% | 63% |
| Washington D.C. | 2006-2008 | 53% | 60% | 67% | 74% |
| | 2008-2010 | 31% | 50% | 60% | 71% |

* N/A values for the 75 ppb standard level mean that a particular urban area did not have any design values above 75 for that 3-year period so no controls were needed. N/A values for the 60 ppb standard level mean that this adjustment methodology was not able to bring design values down to 60 for that particular city and 3-year period.

## 4.2 **DESIGN VALUES**

Table 3 through Table 17 report the design values for sites in each of the urban areas for recent years (2006-2008 and 2008-2010) and for adjusted $O_3$ levels representing just meeting standards of 75, 70, 65, and 60 ppb. In each table, the highest design value for each scenario is

[5] An error was discovered in the Sacramento adjustment to 60 ppb for the 2006-2008 design value period in which 84% NOx cuts were applied instead of 85% NOx cuts. The 84% NOx cuts thus simulate meeting a standard of 61 ppb for Sacramento for those years. Results for the 85% NOx cut case are not expected to be substantially different from the 84% NOx cut case that was analyzed.

displayed in bold text. These tables demonstrate that in some urban areas high $O_3$ values at monitors in different locations have different magnitudes of response to reductions in NOx (and VOC) emissions. Atlanta monitor 132470001, a downwind monitor, had the highest design value for 2006-2008. With the NOx reduction scenarios to meet various standard levels, the two downtown monitors (131210055 and 130890002) switch to being the highest monitors in the area. These downtown locations which have large amounts of spatially concentrated NOx emissions are expected to be more VOC limited and therefore less responsive to NOx emission reductions than surrounding rural and suburban areas. This phenomenon occurs to varying degrees in each of the 15 urban areas included in this analysis. For instance, the difference in response between monitors on high days is very pronounced in Cleveland and in New York. In Cleveland, a downwind monitor located East of the city along Lake Erie was the high monitor for both 2006-2008 and 2008-2010 (39071001). That monitor responded more dramatically to NOx cuts than another monitor (390850003) which was closer to the city. As a result of adjusting air quality to show attainment of a 60 ppb standard at monitor 390850003, the design value at monitor 390071001 was lowered to 45 ppb for the 2006-2008 data and 44 ppb for the 2008-2010 data. Similarly in the New York area, the highest measured $O_3$ values occurred at downwind sites in Connecticut and on Long Island. Two highly urbanized sites (360050110 in the Bronx and 360610135 in Manhattan) have lower observed design values but become the controlling monitors in the adjustment scenarios for 75, 70, and 65 ppb. In contrast, several cities do not show this change in location of the highest monitor after adjustments to show attainment with potential alternative standards. For example, the highest monitor for the 2008-2010 design value period in the Dallas area (484393009, located on the North side of Fort Worth) remained the highest monitor through all adjustment scenarios for that time period. Similarly, the controlling monitor in Sacramento (060670012, a downwind suburban site) remained the highest or second highest site for all adjustment scenarios. However, in the Sacramento case, another downwind monitor (060610006) which did not have as high of an observed design value, responded less to emissions changes and essentially "caught up" to the controlling monitor in the 65 and 60 ppb scenarios.

It is important to note that a model-based adjustment technique is uniquely capable of capturing this type of spatial heterogeneity in response to emissions reductions. The quadratic rollback technique used in the first draft REA forces $O_3$ at all monitoring sites in an urban area to respond identically.

**Table 3: Design values for the Atlanta area regulatory monitors from observed data and for adjustments to meet the existing and potential alternative standards in 2006-2008 and 2008-2010.**

| | 2006-2008 | | | | | 2008-2010 | | | | |
|---|---|---|---|---|---|---|---|---|---|---|
| **Monitor** | obs | 75 ppb | 70 ppb | 65 ppb | 60 ppb | obs | 75 ppb | 70 ppb | 65 ppb | 60 ppb |
| **132470001** | **95** | 72 | 66 | 61 | 55 | 78 | 71 | 64 | 59 | 55 |
| **132230003** | 80 | 62 | 58 | 55 | 51 | 70 | 64 | 59 | 55 | 52 |
| **131510002** | 94 | 72 | 65 | 61 | 55 | 79 | 73 | 66 | 60 | 55 |
| **131350002** | 88 | 71 | 67 | 63 | 58 | 74 | 71 | 66 | 61 | 58 |
| **131210055** | 91 | **75** | **70** | **65** | 59 | **80** | **75** | **70** | **65** | **60** |
| **131130001** | 86 | 67 | 61 | 57 | 53 | N/A | N/A | N/A | N/A | N/A |
| **130970004** | 87 | 68 | 63 | 59 | 54 | 75 | 69 | 64 | 59 | 55 |
| **130890002** | 93 | **75** | **70** | **65** | **60** | 79 | **75** | **70** | 64 | **60** |
| **130850001** | 77 | 59 | 55 | 53 | 49 | 71 | 66 | 60 | 56 | 52 |
| **130770002** | 84 | 65 | 60 | 56 | 52 | 68 | 63 | 58 | 54 | 51 |
| **130670003** | 85 | 68 | 63 | 59 | 53 | 76 | 72 | 66 | 62 | 57 |

The highest DV for each scenario is shown in **bold**. N/A values indicate that there was not enough ambient data to compute a design value for that monitor during a specific 3-year period.

**Table 4: Design values for the Baltimore area regulatory monitors from observed data and for adjustments to meet the existing and potential alternative standards in 2006-2008 and 2008-2010.**

| | 2006-2008 | | | | | 2008-2010 | | | | |
|---|---|---|---|---|---|---|---|---|---|---|
| **Monitor** | obs | 75 ppb | 70 ppb | 65 ppb | 60 ppb | obs | 75 ppb | 70 ppb | 65 ppb | 60 ppb |
| **240030014** | 87 | 72 | 66 | 61 | 56 | 79 | 67 | 63 | 58 | 54 |
| **240051007** | 80 | 68 | 63 | 59 | 53 | 77 | 68 | 64 | 60 | 56 |
| **240053001** | 85 | 74 | 69 | **65** | **60** | 78 | 69 | 65 | 62 | 58 |
| **240130001** | 83 | 68 | 63 | 59 | 53 | 76 | 64 | 60 | 56 | 53 |
| **240251001** | **91** | **75** | **70** | **65** | 59 | **89** | **75** | **70** | **65** | **60** |
| **240259001** | 89 | 75 | 69 | 65 | 59 | 78 | 68 | 64 | 60 | 56 |
| **245100054** | 66 | 61 | 58 | 56 | 52 | 67 | 62 | 59 | 55 | 53 |

The highest DV for each scenario is shown in **bold**.

**Table 5: Design values for the Boston area regulatory monitors from observed data and for adjustments to meet the existing and potential alternative standards in 2006-2008 and 2008-2010.**

| Monitor | 2006-2008 | | | | | 2008-2010 | | | | |
|---|---|---|---|---|---|---|---|---|---|---|
| | obs | 75 ppb | 70 ppb | 65 ppb | 60 ppb | obs | 75 ppb | 70 ppb | 65 ppb | 60 ppb |
| **250010002** | 79 | 70 | 67 | 62 | 58 | 73 | 72 | 68 | 63 | 58 |
| **250051002** | 80 | 70 | 67 | 62 | 57 | 75 | 73 | 67 | 62 | 57 |
| **250070001** | **83** | 74 | **70** | **65** | **60** | **78** | **75** | 69 | **65** | **60** |
| **250092006** | 81 | 73 | 69 | 62 | 57 | 74 | 72 | 68 | 63 | 56 |
| **250094004** | 78 | 72 | 68 | 63 | 58 | N/A | N/A | N/A | N/A | N/A |
| **250095005** | 79 | 72 | 68 | 62 | 56 | 71 | 69 | 66 | 62 | 56 |
| **250170009** | 75 | 68 | 64 | 58 | 52 | 68 | 66 | 62 | 58 | 53 |
| **250171102** | 78 | 70 | 66 | 59 | 53 | 71 | 69 | 64 | 58 | 53 |
| **250213003** | 82 | 73 | 68 | 62 | 56 | 73 | 72 | 68 | 62 | 57 |
| **250250041** | 74 | 72 | 69 | 63 | 58 | 72 | 72 | **70** | **65** | **60** |
| **250250042** | 67 | 66 | 64 | 60 | 56 | 62 | 63 | 63 | 60 | 57 |
| **250270015** | 82 | **75** | **70** | 63 | 58 | 76 | 74 | **70** | **65** | 58 |

The highest DV for each scenario is shown in **bold**. N/A values indicate that there was not enough ambient data to compute a design value for that monitor during a specific 3-year period.

**Table 6: Design values for the Chicago area regulatory monitors from observed data and for adjustments to meet the existing and potential alternative standards using NOx and VOC emissions reductions in 2006-2008 and 2008-2010.**

| Monitor | 2006-2008 | | | | | 2008-2010 | | | | |
|---|---|---|---|---|---|---|---|---|---|---|
| | obs | 75 ppb | 70 ppb | 65 ppb | 60 ppb | obs | 75 ppb | 70 ppb | 65 ppb | 60 ppb |
| **170310001** | 76 | 73 | 65 | 59 | 53 | 69 | 69 | 66 | 60 | 54 |
| **170310032** | 74 | 74 | **70** | **65** | 58 | 68 | 68 | 69 | **65** | **60** |
| **170310064** | 71 | 70 | 66 | 62 | 56 | 64 | 64 | 65 | 61 | 57 |
| **170310076** | 73 | 72 | 67 | 62 | 56 | 67 | 67 | 65 | 60 | 56 |
| **170311003** | 73 | 73 | **70** | **65** | **60** | 66 | 66 | 66 | 63 | **60** |
| **170311601** | 75 | 72 | 66 | 60 | 53 | 70 | 70 | 67 | 60 | 55 |
| **170314002** | 62 | 63 | 61 | 58 | 54 | 65 | 65 | 65 | 62 | 58 |
| **170314007** | 66 | 66 | 62 | 58 | 53 | 59 | 59 | 59 | 57 | 53 |
| **170314201** | 71 | 70 | 66 | 62 | 56 | 69 | 69 | 68 | 63 | 59 |
| **170317002** | 70 | 68 | 63 | 58 | 53 | 63 | 63 | 62 | 58 | 53 |
| **170436001** | 63 | 63 | 59 | 54 | 49 | 60 | 60 | 58 | 54 | 51 |
| **170890005** | 66 | 63 | 57 | 53 | 47 | 66 | 66 | 62 | 56 | 51 |

| | | | | | | | | | | |
|---|---|---|---|---|---|---|---|---|---|---|
| **170971002** | 71 | 69 | 63 | 58 | 54 | 64 | 64 | 61 | 56 | 52 |
| **170971007** | 72 | 71 | 64 | 59 | 54 | 73 | 73 | **70** | 64 | 59 |
| **171110001** | 64 | 61 | 55 | 51 | 47 | 64 | 64 | 61 | 55 | 51 |
| **171971011** | 66 | 63 | 55 | 50 | 46 | 62 | 62 | 59 | 52 | 49 |
| **180890022** | 73 | 70 | 64 | 59 | 53 | 61 | 61 | 59 | 54 | 50 |
| **180890030** | 77 | **75** | **70** | **65** | **60** | 64 | 64 | 63 | 60 | 56 |
| **180892008** | 73 | 71 | 66 | 62 | 56 | 67 | 67 | 65 | 62 | 57 |
| **180910005** | 69 | 66 | 58 | 53 | 47 | 65 | 65 | 61 | 55 | 51 |
| **180910010** | 70 | 67 | 58 | 53 | 47 | 65 | 65 | 61 | 54 | 49 |
| **181270024** | 74 | 72 | 65 | 60 | 56 | 67 | 67 | 64 | 59 | 55 |
| **181270026** | 70 | 67 | 59 | 54 | 50 | 62 | 62 | 58 | 53 | 49 |
| **550590019** | **78** | **75** | 68 | 62 | 56 | **74** | **74** | **70** | 64 | 59 |

The highest DV for each scenario is shown in **bold**.

**Table 7: Design values for the Cleveland area regulatory monitors from observed data and for adjustments to meet the existing and potential alternative standards in 2006-2008 and 2008-2010.**

| | 2006-2008 | | | | | 2008-2010 | | | | |
|---|---|---|---|---|---|---|---|---|---|---|
| **Monitor** | obs | 75 ppb | 70 ppb | 65 ppb | 60 ppb | obs | 75 ppb | 70 ppb | 65 ppb | 60 ppb |
| **390071001** | **84** | 69 | 62 | 55 | 45 | **77** | 64 | 58 | 50 | 44 |
| **390350034** | 78 | 74 | 69 | 64 | 57 | 75 | 72 | 67 | 62 | 57 |
| **390350064** | 74 | 67 | 61 | 56 | 47 | 68 | 62 | 57 | 51 | 45 |
| **390355002** | 81 | 74 | 68 | 61 | 50 | 75 | 68 | 62 | 55 | 48 |
| **390550004** | 73 | 61 | 55 | 49 | 42 | **77** | 63 | 55 | 48 | 42 |
| **390850003** | 78 | **75** | **70** | **65** | **60** | 76 | **75** | **70** | **65** | **60** |
| **390850007** | 76 | 72 | 67 | 62 | 55 | 72 | 70 | 66 | 60 | 56 |
| **390930018** | 74 | 65 | 59 | 53 | 44 | 70 | 62 | 56 | 49 | 43 |
| **391030003** | 72 | 61 | 55 | 49 | 41 | 70 | 58 | 52 | 47 | 41 |
| **391331001** | 73 | 62 | 56 | 50 | 42 | 67 | 57 | 51 | 46 | 41 |
| **391530020** | 82 | 69 | 62 | 54 | 44 | 75 | 64 | 57 | 50 | 44 |

The highest DV for each scenario is shown in **bold.**

**Table 8: Design values for the Dallas area regulatory monitors from observed data and for adjustments to meet the existing and potential alternative standards in 2006-2008 and 2008-2010.**

| | 2006-2008 | | | | | 2008-2010 | | | | |
|---|---|---|---|---|---|---|---|---|---|---|
| **Monitor** | obs | 75 ppb | 70 ppb | 65 ppb | 60 ppb | obs | 75 ppb | 70 ppb | 65 ppb | 60 ppb |
| **480850005** | 83 | 70 | 66 | 61 | 57 | 77 | 66 | 62 | 57 | 54 |
| **481130069** | 74 | 67 | 63 | 59 | 56 | 67 | 63 | 59 | 56 | 54 |
| **481130075** | 80 | 71 | 68 | 63 | 59 | 78 | 71 | 67 | 63 | 58 |
| **481130087** | 82 | 65 | 63 | 59 | 55 | 78 | 65 | 61 | 58 | 54 |

| | | | | | | | | | | |
|---|---|---|---|---|---|---|---|---|---|---|
| **481210034** | **91** | 73 | 68 | 62 | 56 | 80 | 67 | 62 | 57 | 53 |
| **481211032** | 81 | 65 | 62 | 57 | 53 | 78 | 65 | 60 | 55 | 51 |
| **481390016** | 75 | 62 | 59 | 55 | 51 | 72 | 61 | 57 | 54 | 50 |
| **481391044** | N/A | N/A | N/A | N/A | N/A | 68 | 56 | 53 | 50 | 47 |
| **482311006** | 70 | 56 | 54 | 51 | 47 | 64 | 54 | 50 | 47 | 45 |
| **482510003** | 83 | 69 | 66 | 61 | 56 | 80 | 69 | 65 | 59 | 55 |
| **482570005** | 73 | 59 | 57 | 53 | 50 | 67 | 56 | 53 | 50 | 47 |
| **483670081** | 84 | 66 | 62 | 57 | 52 | 75 | 61 | 57 | 54 | 50 |
| **483970001** | 75 | 61 | 57 | 53 | 49 | 74 | 62 | 57 | 53 | 49 |
| **484390075** | 89 | **75** | **70** | 64 | 58 | 85 | 74 | 69 | 63 | 58 |
| **484391002** | 83 | 71 | 68 | 64 | **60** | 79 | 70 | 66 | 62 | 58 |
| **484392003** | 87 | **75** | **70** | **65** | **60** | **86** | **75** | **70** | **65** | **60** |
| **484393009** | 87 | 73 | 68 | 63 | 57 | 82 | 71 | 66 | 61 | 55 |
| **484393011** | 79 | 64 | 61 | 58 | 54 | 79 | 66 | 61 | 58 | 54 |

The highest DV for each scenario is shown in **bold**. N/A values indicate that there was not enough ambient data to compute a design value for that monitor during a specific 3-year period.

**Table 9: Design values for the Denver area regulatory monitors from observed data and for adjustments to meet the existing and potential alternative standards using NOx and VOC emissions reductions in 2006-2008 and 2008-2010.**

| | 2006-2008 | | | | | 2008-2010 | | | | |
|---|---|---|---|---|---|---|---|---|---|---|
| **Monitor** | obs | 75 ppb | 70 ppb | 65 ppb | 60 ppb | obs | 75 ppb | 70 ppb | 65 ppb | 60 ppb |
| **080013001** | 71 | 69 | 66 | **65** | **60** | 70 | 70 | 69 | **65** | **60** |
| **080050002** | 71 | 65 | 61 | 58 | 54 | 67 | 66 | 63 | 59 | 52 |
| **080130011** | 81 | 70 | 65 | 60 | 55 | 73 | 71 | 66 | 61 | 53 |
| **080310014** | 73 | 70 | 67 | 64 | **60** | 68 | 68 | 67 | 64 | **60** |
| **080310025** | N/A | N/A | N/A | N/A | N/A | 65 | 64 | 62 | 59 | 56 |
| **080350004** | 82 | 72 | 67 | 61 | 56 | 76 | 74 | 69 | 64 | 54 |
| **080590002** | 78 | 73 | 69 | 64 | 58 | 73 | 72 | **70** | 65 | 56 |
| **080590005** | 78 | 70 | 65 | 61 | 56 | 72 | 71 | 67 | 61 | 54 |
| **080590006** | **86** | **75** | **70** | 64 | 58 | **77** | **75** | **70** | **65** | 55 |
| **080590011** | 81 | **75** | **70** | **65** | 59 | 72 | 72 | **70** | **65** | 57 |
| **080690011** | 82 | 70 | 65 | 59 | 55 | 74 | 72 | 65 | 60 | 52 |
| **080691004** | 71 | 61 | 57 | 53 | 50 | 65 | 63 | 57 | 53 | 48 |
| **081230009** | 76 | 66 | 62 | 57 | 53 | 71 | 69 | 63 | 59 | 52 |

The highest DV for each scenario is shown in **bold**. N/A values indicate that there was not enough ambient data to compute a design value for that monitor during a specific 3-year period.

**Table 10: Design values for the Detroit area regulatory monitors from observed data and for adjustments to meet the existing and potential alternative standards in 2006-2008 and 2008-2010.**

| Monitor | 2006-2008 | | | | | 2008-2010 | | | | |
|---|---|---|---|---|---|---|---|---|---|---|
| | obs | 75 ppb | 70 ppb | 65 ppb | 60 ppb | obs | 75 ppb | 70 ppb | 65 ppb | 60 ppb |
| **260490021** | 74 | 61 | 56 | 52 | 49 | 68 | 68 | 59 | 54 | 49 |
| **260492001** | 76 | 58 | 54 | 50 | 46 | 68 | 68 | 56 | 51 | 47 |
| **260990009** | 81 | 69 | 64 | 61 | 57 | 74 | 74 | 66 | 61 | 57 |
| **260991003** | 80 | **75** | **70** | **65** | **60** | 73 | 73 | **70** | **65** | **60** |
| **261250001** | 76 | 70 | 65 | 60 | 55 | 72 | 72 | 69 | 64 | 57 |
| **261470005** | 78 | 63 | 58 | 55 | 51 | 71 | 71 | 60 | 56 | 51 |
| **261610008** | 74 | 61 | 56 | 53 | 49 | 66 | 66 | 58 | 54 | 49 |
| **261630001** | 71 | 64 | 59 | 56 | 51 | 66 | 66 | 62 | 58 | 53 |
| **261630019** | **82** | 74 | 69 | 64 | 59 | **75** | **75** | **70** | **65** | 59 |

The highest DV for each scenario is shown in **bold**.

**Table 11: Design values for the Houston area regulatory monitors from observed data and for adjustments to meet the existing and potential alternative standards in 2006-2008 and 2008-2010.**

| Monitor | 2006-2008 | | | | | 2008-2010 | | | | |
|---|---|---|---|---|---|---|---|---|---|---|
| | obs | 75 ppb | 70 ppb | 65 ppb | 60 ppb | obs | 75 ppb | 70 ppb | 65 ppb | 60 ppb |
| **480391004** | 85 | 63 | 59 | 55 | 50 | **85** | 73 | 67 | 61 | 54 |
| **480391016** | 76 | 56 | 53 | 51 | 47 | 74 | 63 | 60 | 55 | 50 |
| **481671034** | N/A | N/A | N/A | N/A | N/A | 75 | 65 | 61 | 57 | 52 |
| **482010024** | 83 | 64 | 60 | 56 | 51 | 83 | **75** | 69 | 63 | 55 |
| **482010026** | 80 | 61 | 57 | 54 | 50 | 78 | 68 | 63 | 58 | 52 |
| **482010029** | 85 | 63 | 58 | 54 | 47 | 81 | 72 | 66 | 59 | 51 |
| **482010046** | 75 | 60 | 57 | 54 | 49 | 72 | 66 | 61 | 56 | 51 |
| **482010047** | 76 | 61 | 58 | 54 | 49 | 76 | 73 | 68 | 62 | 55 |
| **482010051** | 80 | 63 | 59 | 56 | 51 | 77 | 71 | 66 | 61 | 55 |
| **482010055** | **91** | 70 | 65 | 60 | 53 | 82 | 75 | 69 | 64 | 57 |
| **482010062** | 81 | 62 | 58 | 55 | 50 | 72 | 65 | 62 | 57 | 52 |
| **482010066** | 89 | **75** | **70** | **65** | **60** | 75 | **75** | **70** | **65** | 59 |
| **482010070** | 74 | 66 | 64 | 61 | 59 | 73 | 71 | 68 | 64 | **60** |
| **482010075** | 76 | 66 | 64 | 62 | 59 | 74 | 73 | 69 | 65 | **60** |
| **482010416** | 89 | 70 | 65 | 62 | 56 | 77 | 72 | 67 | 62 | 57 |
| **482011015** | 74 | 57 | 55 | 52 | 48 | 73 | 65 | 61 | 57 | 52 |
| **482011034** | 80 | 63 | 60 | 57 | 53 | 76 | 71 | 66 | 62 | 55 |

| | | | | | | | | | | |
|---|---|---|---|---|---|---|---|---|---|---|
| **482011035** | 73 | 59 | 56 | 53 | 49 | 75 | 69 | 64 | 59 | 53 |
| **482011039** | 87 | 63 | 59 | 56 | 51 | 81 | 68 | 65 | 59 | 53 |
| **482011050** | 80 | 61 | 58 | 55 | 51 | 75 | 67 | 62 | 58 | 53 |
| **483390078** | 80 | 56 | 52 | 49 | 45 | 71 | 61 | 56 | 50 | 45 |

The highest DV for each scenario is shown in **bold**. N/A values indicate that there was not enough ambient data to compute a design value for that monitor during a specific 3-year period.

**Table 12: Design values for the Los Angeles area regulatory monitors from observed data and for adjustments to meet the existing and potential alternative standards using the lower bound of the 95$^{th}$ percent confidence interval of estimated hourly $O_3$ in 2006-2008 and 2008-2010.**

| | 2006-2008 | | | | | 2008-2010 | | | | |
|---|---|---|---|---|---|---|---|---|---|---|
| **Monitor** | obs | 75 ppb | 70 ppb | 65 ppb | 60 ppb | obs | 75 ppb | 70 ppb | 65 ppb | 60 ppb |
| **060370002** | 96 | 63 | 60 | 56 | 53 | 89 | 63 | 60 | 56 | 52 |
| **060370016** | 107 | 64 | 60 | 57 | 53 | 103 | 65 | 61 | 57 | 53 |
| **060370113** | 69 | 54 | 52 | 50 | 48 | 72 | 55 | 53 | 50 | 48 |
| **060371002** | 92 | 69 | 64 | 59 | 54 | 84 | 69 | 64 | 59 | 54 |
| **060371103** | 73 | 68 | 64 | 61 | 56 | 70 | 68 | 64 | 60 | 56 |
| **060371201** | 97 | 54 | 52 | 50 | 47 | 91 | 53 | 51 | 49 | 47 |
| **060371301** | 58 | 56 | 54 | 52 | 50 | N/A | N/A | N/A | N/A | N/A |
| **060371602** | 78 | 71 | 67 | 63 | 59 | 69 | 68 | 64 | 61 | 57 |
| **060371701** | 103 | 63 | 59 | 55 | 52 | 90 | 62 | 58 | 55 | 51 |
| **060372005** | 92 | **75** | **70** | **65** | **60** | 87 | **75** | **70** | **65** | **60** |
| **060374002** | 59 | 54 | 52 | 52 | 50 | 61 | 55 | 54 | 53 | 52 |
| **060375005** | 64 | 56 | 54 | 53 | 51 | 61 | 56 | 54 | 52 | 50 |
| **060376012** | 105 | 57 | 54 | 51 | 47 | 97 | 57 | 54 | 50 | 47 |
| **060379033** | 94 | 55 | 52 | 49 | 47 | 91 | 54 | 52 | 50 | 48 |
| **060590007** | 73 | 58 | 56 | 54 | 51 | 68 | 58 | 55 | 53 | 51 |
| **060591003** | 66 | 52 | 51 | 50 | 48 | 66 | 53 | 52 | 51 | 49 |
| **060592022** | 87 | 55 | 52 | 50 | 48 | 81 | 54 | 52 | 50 | 47 |
| **060595001** | 83 | 61 | 57 | 54 | 51 | 74 | 60 | 57 | 54 | 51 |
| **060650004** | N/A | N/A | N/A | N/A | N/A | 97 | 60 | 56 | 53 | 49 |
| **060650008** | 79 | 55 | 53 | 52 | 51 | 81 | 55 | 54 | 53 | 52 |
| **060650012** | 102 | 58 | 55 | 52 | 49 | 102 | 58 | 55 | 52 | 49 |
| **060651010** | N/A | N/A | N/A | N/A | N/A | 78 | 52 | 51 | 49 | 48 |
| **060651016** | 105 | 60 | 57 | 54 | 51 | 102 | 59 | 56 | 53 | 50 |
| **060651999** | N/A | N/A | N/A | N/A | N/A | 77 | 52 | 51 | 49 | 48 |

| | | | | | | | | | | |
|---|---|---|---|---|---|---|---|---|---|---|
| **060652002** | 86 | 55 | 54 | 52 | 51 | 85 | 55 | 53 | 52 | 50 |
| **060655001** | 97 | 56 | 54 | 52 | 50 | 95 | 55 | 54 | 52 | 49 |
| **060656001** | 107 | 57 | 54 | 51 | 47 | 102 | 55 | 52 | 50 | 47 |
| **060658001** | 107 | 63 | 59 | 55 | 51 | 97 | 60 | 56 | 53 | 49 |
| **060658005** | N/A | N/A | N/A | N/A | N/A | 93 | 58 | 55 | 51 | 48 |
| **060659001** | 102 | 55 | 52 | 49 | 46 | 96 | 53 | 51 | 48 | 46 |
| **060659003** | 63 | 48 | 47 | 46 | 45 | 63 | 48 | 47 | 47 | 46 |
| **060710001** | 86 | 57 | 56 | 54 | 53 | 80 | 54 | 52 | 51 | 50 |
| **060710005** | **119** | 70 | 65 | 61 | 55 | **112** | 68 | 64 | 59 | 55 |
| **060710012** | 96 | 60 | 57 | 56 | 54 | 99 | 60 | 57 | 55 | 54 |
| **060710306** | 89 | 60 | 57 | 56 | 54 | 87 | 58 | 56 | 53 | 52 |
| **060711004** | 110 | 67 | 62 | 57 | 52 | 100 | 65 | 61 | 56 | 52 |
| **060711234** | 80 | 56 | 55 | 54 | 53 | 75 | 54 | 53 | 52 | 51 |
| **060712002** | 112 | 68 | 63 | 58 | 53 | 101 | 65 | 61 | 56 | 51 |
| **060714001** | 96 | 60 | 56 | 53 | 50 | 96 | 60 | 57 | 53 | 50 |
| **060714003** | 116 | 68 | 63 | 59 | 54 | 103 | 65 | 61 | 56 | 51 |
| **060719004** | 116 | 67 | 62 | 58 | 53 | 102 | 64 | 60 | 55 | 50 |
| **061110007** | 75 | 47 | 46 | 44 | 43 | 78 | 48 | 46 | 45 | 44 |
| **061110009** | 80 | 47 | 46 | 44 | 43 | 79 | 47 | 46 | 45 | 43 |
| **061111004** | 83 | 49 | 48 | 46 | 45 | 79 | 47 | 46 | 45 | 44 |
| **061112002** | 88 | 49 | 48 | 46 | 44 | 86 | 49 | 48 | 46 | 44 |
| **061112003** | 64 | 48 | 47 | 46 | 46 | 63 | 47 | 46 | 46 | 45 |
| **061113001** | 61 | 47 | 46 | 46 | 45 | 63 | 47 | 46 | 45 | 44 |

The highest DV for each scenario is shown in **bold**. N/A values indicate that there was not enough ambient data to compute a design value for that monitor during a specific 3-year period.

**Table 13: Design values for the New York area regulatory monitors from observed data and for adjustments to meet the existing and potential alternative standards using the lower bound of the 95$^{th}$ percent confidence interval of estimated hourly $O_3$ in 2006-2008 and 2008-2010.**

| | 2006-2008 | | | | 2008-2010 | | | |
|---|---|---|---|---|---|---|---|---|
| **Monitor** | obs | 75 ppb | 70 ppb | 65 ppb | obs | 75 ppb | 70 ppb | 65 ppb |
| **090010017** | 99 | **75** | 67 | 39 | 91 | 74 | 65 | 43 |
| **090011123** | 102 | 60 | 50 | 36 | 91 | 64 | 54 | 37 |
| **090013007** | 102 | 70 | 61 | 40 | 89 | 68 | 60 | 42 |
| **090019003** | 106 | 66 | 58 | 39 | 91 | 70 | 61 | 41 |
| **090070007** | 104 | 62 | 53 | 37 | 86 | 63 | 54 | 40 |
| **090090027** | 90 | 61 | 54 | 37 | 77 | 61 | 53 | 39 |

| | | | | | | | | |
|---|---|---|---|---|---|---|---|---|
| **090093002** | **108** | 64 | 56 | 40 | 88 | 64 | 55 | 41 |
| **340030006** | N/A | N/A | N/A | N/A | 84 | 71 | 63 | 46 |
| **340170006** | 92 | 69 | 64 | 60 | 91 | 71 | 64 | 60 |
| **340190001** | 94 | 54 | 45 | 38 | 88 | 59 | 49 | 39 |
| **340210005** | 101 | 59 | 50 | 36 | 87 | 63 | 53 | 39 |
| **340230011** | 100 | 59 | 50 | 37 | 86 | 64 | 53 | 39 |
| **340250005** | 94 | 58 | 51 | 37 | 87 | 65 | 55 | 39 |
| **340273001** | 94 | 51 | 42 | 38 | 87 | 56 | 46 | 40 |
| **340315001** | 86 | 53 | 45 | 37 | 83 | 60 | 50 | 37 |
| **360050110** | 89 | 74 | **70** | **65** | 76 | 70 | 66 | 60 |
| **360050133** | 87 | 70 | 66 | 54 | 82 | 72 | 65 | 54 |
| **360610135** | N/A | N/A | N/A | N/A | 80 | **75** | **70** | **65** |
| **360715001** | 97 | 49 | 41 | 35 | 88 | 54 | 45 | 36 |
| **360790005** | 91 | 53 | 46 | 35 | 87 | 59 | 50 | 37 |
| **360810124** | 88 | 65 | 58 | 44 | 85 | 70 | 61 | 46 |
| **360850067** | 95 | 61 | 55 | 45 | 90 | 66 | 59 | 47 |
| **361030002** | 98 | 65 | 58 | 40 | 90 | 71 | 61 | 43 |
| **361030004** | 102 | 61 | 53 | 40 | 84 | 61 | 54 | 42 |
| **361030009** | 104 | 65 | 58 | 41 | **92** | 70 | 61 | 44 |
| **361192004** | 104 | 64 | 56 | 37 | 87 | 67 | 57 | 38 |

The highest DV for each scenario is shown in **bold**. N/A values indicate that there was not enough ambient data to compute a design value for that monitor during a specific 3-year period.

**Table 14: Design values for the Philadelphia area regulatory monitors from observed data and for adjustments to meet the existing and potential alternative standards in 2006-2008 and 2008-2010.**

| | 2006-2008 | | | | | 2008-2010 | | | | |
|---|---|---|---|---|---|---|---|---|---|---|
| **Monitor** | obs | 75 ppb | 70 ppb | 65 ppb | 60 ppb | obs | 75 ppb | 70 ppb | 65 ppb | 60 ppb |
| **100031007** | 80 | 60 | 57 | 53 | 50 | 75 | 64 | 59 | 55 | 51 |
| **100031010** | 83 | 65 | 60 | 56 | 51 | 76 | 67 | 62 | 57 | 53 |
| **100031013** | 78 | 64 | 60 | 56 | 53 | 75 | 67 | 63 | 59 | 56 |
| **240150003** | 90 | 68 | 63 | 58 | 52 | 80 | 68 | 63 | 58 | 54 |
| **340010006** | N/A | N/A | N/A | N/A | N/A | 74 | 64 | 60 | 56 | 52 |
| **340070003** | 87 | **75** | **70** | **65** | **60** | N/A | N/A | N/A | N/A | N/A |
| **340071001** | 86 | 65 | 60 | 55 | 52 | 80 | 69 | 63 | 59 | 54 |
| **340110007** | 81 | 61 | 57 | 52 | 49 | 76 | 63 | 59 | 54 | 51 |
| **340150002** | 87 | 70 | 65 | 60 | 55 | 81 | 72 | 67 | 62 | 57 |
| **340290006** | 87 | 67 | 62 | 57 | 53 | 81 | 69 | 64 | 59 | 55 |
| **420170012** | **92** | **75** | **70** | 64 | 58 | **83** | 74 | 69 | 64 | **60** |
| **420290100** | 82 | 63 | 59 | 54 | 50 | 76 | 65 | 60 | 56 | 52 |
| **420450002** | 83 | 68 | 64 | 59 | 55 | 74 | 68 | 64 | 59 | 55 |

| | | | | | | | | | | |
|---|---|---|---|---|---|---|---|---|---|---|
| **420910013** | 84 | 67 | 62 | 57 | 53 | 78 | 71 | 66 | 61 | 56 |
| **421010004** | 67 | 59 | 56 | 53 | 50 | 66 | 62 | 59 | 55 | 52 |
| **421010024** | 89 | 74 | 69 | 63 | 58 | 82 | **75** | **70** | **65** | **60** |

The highest DV for each scenario is shown in **bold**. N/A values indicate that there was not enough ambient data to compute a design value for that monitor during a specific 3-year period.

**Table 15: Design values for the Sacramento area regulatory monitors from observed data and for adjustments to meet the existing and potential alternative standards in 2006-2008 and 2008-2010.**

| | 2006-2008 | | | | | 2008-2010 | | | | |
|---|---|---|---|---|---|---|---|---|---|---|
| **Monitor** | obs | 75 ppb | 70 ppb | 65 ppb | 60 ppb | obs | 75 ppb | 70 ppb | 65 ppb | 60 ppb |
| **060170010** | 96 | 71 | 66 | 63 | 56 | 90 | 67 | 63 | 59 | 54 |
| **060170012** | 76 | 66 | 64 | 63 | 60 | 71 | 61 | 60 | 59 | 57 |
| **060170013** | 70 | 61 | 59 | 58 | 57 | N/A | N/A | N/A | N/A | N/A |
| **060170020** | 98 | 74 | 69 | 64 | 58 | 89 | 68 | 64 | 60 | 55 |
| **060570005** | 91 | 69 | 66 | 62 | 57 | 84 | 63 | 60 | 57 | 53 |
| **060570007** | 87 | 66 | 63 | 60 | 56 | 81 | 63 | 59 | 57 | 54 |
| **060571001** | 70 | 61 | 59 | 58 | 57 | N/A | N/A | N/A | N/A | N/A |
| **060610002** | 90 | 69 | 65 | 61 | 56 | 87 | 66 | 62 | 58 | 54 |
| **060610004** | 89 | 67 | 63 | 60 | 55 | 78 | 59 | 56 | 53 | 49 |
| **060610006** | 90 | 73 | 68 | 64 | 59 | 90 | 73 | 69 | **65** | **60** |
| **060670002** | 78 | 64 | 61 | 58 | 54 | 75 | 62 | 58 | 55 | 52 |
| **060670006** | 87 | 71 | 66 | 62 | 56 | 85 | 69 | 65 | 61 | 56 |
| **060670010** | 79 | 65 | 62 | 59 | 55 | 75 | 62 | 59 | 56 | 53 |
| **060670011** | 82 | 65 | 61 | 58 | 53 | 77 | 61 | 57 | 54 | 51 |
| **060670012** | **99** | **75** | **70** | **65** | 59 | **99** | **75** | **70** | **65** | 59 |
| **060670013** | 78 | 64 | 61 | 59 | 54 | N/A | N/A | N/A | N/A | N/A |
| **060670014** | N/A | N/A | N/A | N/A | N/A | 57 | 51 | 49 | 47 | 45 |
| **060675003** | 95 | 72 | 68 | 64 | 58 | 92 | 70 | 65 | 61 | 55 |
| **060950004** | 60 | 57 | 56 | 55 | 53 | 63 | 59 | 58 | 56 | 54 |
| **060950005** | 68 | 57 | 55 | 52 | 49 | 69 | 58 | 55 | 53 | 50 |
| **060953003** | 75 | 59 | 55 | 53 | 49 | 70 | 56 | 53 | 51 | 49 |
| **061010003** | 72 | 59 | 56 | 53 | 48 | 66 | 54 | 51 | 49 | 46 |
| **061010004** | 85 | 69 | 66 | 64 | **61** | 76 | 62 | 60 | 58 | 56 |
| **061130004** | 76 | 59 | 55 | 52 | 48 | 72 | 56 | 53 | 50 | 47 |
| **061131003** | 76 | 59 | 56 | 53 | 49 | 72 | 56 | 53 | 50 | 47 |

The highest DV for each scenario is shown in **bold**. N/A values indicate that there was not enough ambient data to compute a design value for that monitor during a specific 3-year period.

**Table 16: Design values for the Saint Louis area regulatory monitors from observed data and for adjustments to meet the existing and potential alternative standards in 2006-2008 and 2008-2010.**

| | 2006-2008 | | | | | 2008-2010 | | | | |
|---|---|---|---|---|---|---|---|---|---|---|
| **Monitor** | obs | 75 ppb | 70 ppb | 65 ppb | 60 ppb | obs | 75 ppb | 70 ppb | 65 ppb | 60 ppb |
| **170831001** | 73 | 61 | 57 | 52 | 48 | 69 | 67 | 62 | 57 | 52 |
| **171170002** | 70 | 58 | 54 | 50 | 46 | 66 | 64 | 60 | 55 | 51 |
| **171190008** | 76 | 67 | 62 | 57 | 52 | 71 | 70 | 67 | 61 | 56 |
| **171191009** | 78 | 67 | 62 | 57 | 52 | 72 | 70 | 66 | 61 | 56 |
| **171193007** | 77 | 68 | 63 | 57 | 52 | 68 | 67 | 63 | 59 | 53 |
| **171630010** | 72 | 65 | 60 | 55 | 51 | 68 | 67 | 64 | 59 | 55 |
| **290990019** | N/A | N/A | N/A | N/A | N/A | 72 | 70 | 67 | 62 | 56 |
| **291130003** | 81 | 67 | 62 | 56 | 51 | 72 | 70 | 65 | 60 | 55 |
| **291831002** | N/A | N/A | N/A | N/A | N/A | **77** | **75** | **70** | **65** | 59 |
| **291831004** | N/A | N/A | N/A | N/A | N/A | 74 | 72 | 66 | 61 | 54 |
| **291890004** | 78 | 71 | 66 | 60 | 55 | N/A | N/A | N/A | N/A | N/A |
| **291890005** | 76 | 65 | 60 | 55 | 50 | 65 | 64 | 59 | 55 | 51 |
| **291890014** | **82** | 73 | 68 | 62 | 57 | 71 | 70 | 66 | 62 | 57 |
| **295100085** | N/A | N/A | N/A | N/A | N/A | 68 | 68 | 69 | 65 | **60** |
| **295100086** | 81 | **75** | **70** | **65** | **60** | N/A | N/A | N/A | N/A | N/A |

The highest DV for each scenario is shown in **bold**. N/A values indicate that there was not enough ambient data to compute a design value for that monitor during a specific 3-year period.

**Table 17: Design values for the Washington D.C. area regulatory monitors from observed data and for adjustments to meet the existing and potential alternative standards in 2006-2008 and 2008-2010.**

| | 2006-2008 | | | | | 2008-2010 | | | | |
|---|---|---|---|---|---|---|---|---|---|---|
| **Monitor** | obs | 75 ppb | 70 ppb | 65 ppb | 60 ppb | obs | 75 ppb | 70 ppb | 65 ppb | 60 ppb |
| **110010025** | 80 | 62 | 58 | 53 | 48 | 75 | 68 | 60 | 55 | 49 |
| **110010041** | 86 | 73 | 69 | 64 | 59 | 77 | 74 | 69 | **65** | **60** |
| **110010043** | **87** | **75** | **70** | **65** | **60** | 79 | **75** | **70** | **65** | **60** |
| **240090011** | 79 | 61 | 57 | 54 | 49 | 77 | 69 | 61 | 56 | 49 |
| **240170010** | 82 | 63 | 59 | 55 | 50 | 75 | 68 | 61 | 56 | 50 |
| **240210037** | 82 | 65 | 61 | 56 | 52 | 75 | 69 | 63 | 58 | 52 |
| **240313001** | 84 | 68 | 63 | 59 | 54 | 74 | 68 | 63 | 59 | 53 |
| **240330030** | 83 | 68 | 64 | 60 | 54 | 79 | 74 | 67 | 62 | 55 |
| **240338003** | **87** | 65 | 60 | 56 | 52 | 77 | 70 | 62 | 57 | 51 |
| **510130020** | 85 | 70 | 66 | 62 | 56 | 79 | 74 | 68 | 63 | 57 |
| **510590005** | 79 | 61 | 58 | 54 | 50 | 67 | 62 | 57 | 53 | 50 |
| **510590018** | 86 | 68 | 64 | 60 | 56 | 73 | 68 | 62 | 58 | 52 |
| **510590030** | 85 | 69 | 64 | 60 | 55 | **81** | **75** | 68 | 63 | 55 |

| | | | | | | | | | | |
|---|---|---|---|---|---|---|---|---|---|---|
| **510591005** | 83 | 68 | 64 | 59 | 54 | 68 | 65 | 60 | 57 | 54 |
| **510595001** | 83 | 66 | 61 | 57 | 52 | 66 | 62 | 58 | 54 | 51 |
| **510610002** | 70 | 54 | 51 | 48 | 45 | 65 | 59 | 53 | 50 | 45 |
| **510690010** | 72 | 55 | 52 | 49 | 46 | 68 | 61 | 55 | 51 | 46 |
| **511071005** | 82 | 62 | 58 | 53 | 49 | 75 | 68 | 60 | 56 | 50 |
| **511530009** | 78 | 58 | 54 | 49 | 46 | 70 | 61 | 55 | 51 | 46 |
| **511790001** | 81 | 60 | 56 | 52 | 48 | 70 | 63 | 57 | 53 | 48 |
| **515100009** | 81 | 65 | 61 | 56 | 53 | 74 | 68 | 61 | 56 | 51 |

The highest DV for each scenario is shown in **bold**.

### 4.3 DISTRIBUTION OF HOURLY $O_3$ CONCENTRATIONS

Figure 13 through Figure 27 display diurnal boxplots of hourly $O_3$ concentrations at monitor locations in each urban area for observed air quality, air quality adjusted to meet the existing standard, and an example of air quality adjusted to meet a potential alternative standard (65 ppb), for 2006-2008 and 2008-2010. Note that these plots include data from multiple monitoring sites within each urban area so they generally encompass the overall distribution of $O_3$ at both the urban core sites and the downwind suburban sites. The hourly plots show similar patterns in most cities for which $O_3$ concentrations during daytime hours decrease from observed air quality (black) to air quality adjusted to meet the existing standard (red), and decrease further when adjusted to meet a potential alternative standard of 65 ppb (blue). These daytime decreases are generally seen most on high $O_3$ days represented by outlier dots. In some cities the mid-range $O_3$ days, represented by the $25^{th}$ – $75^{th}$ percentile boxes, remained fairly constant (Boston) and in other cities, mid-range $O_3$ days decreased (Atlanta). Although daytime $O_3$ decreases, concentrations during morning rush-hour generally increase. These increases are associated with VOC-limited and NOx titration conditions near NOx sources during rush-hour periods. Reducing NOx under those conditions results in less $O_3$ titration and thus increases $O_3$ concentrations. Nighttime increases in $O_3$ are often seen to a lesser extent than morning rush-hour increases. These phenomena generally lead to a flattening of the diurnal $O_3$ pattern with smaller differences between daytime and nighttime concentrations as NOx emissions are reduced. Cases that required more substantial $NO_x$ cuts to reach 75 and 65 ppb standards generally have more pronounced patterns of decreases in daytime $O_3$ and increases in nighttime $O_3$ leading to a flatter diurnal $O_3$ pattern (e.g. Los Angeles in Figure 22). Two cities, Houston and New York, do not follow this general pattern. In Houston (Figure 21), mid-range $O_3$ values increase during daytime hours as the highest $O_3$ concentrations decrease. This pattern is consistent with NOx-limited conditions on high $O_3$ days but VOC-limited conditions on mid-range $O_3$ days or potentially NOx-limited conditions at high $O_3$ sites and VOC limited conditions at mid-range $O_3$ sites. Therefore NOx reductions, which are applied applied on all

days, increase $O_3$ on mid-range $O_3$ days. Note that mid-range $O_3$ days in Houston start out quite low (20-30 ppb) and increase modestly. The changes in $O_3$ from observed air quality to the existing standard in New York look similar to the trends shown for other cities, but the diurnal $O_3$ pattern for the 65 ppb potential alternative standard has some unrealistic features which were previously discussed in section 3.2.4 of this appendix. The steep NOx cuts (~90%) applied to meet a 65 ppb standard in New York result in a very flat diurnal pattern for mid-range values (see boxes from Figure 23) but the outliers represented by dots in Figure 23 show an inverse diurnal pattern with lower $O_3$ concentrations during the day and higher values at night. This is a result of the modeled sensitivities showing that nighttime $O_3$ does not respond to NOx emissions changes on high $O_3$ nights while daytime $O_3$ does respond to NOx emission changes during those same days. Thus the daytime values drop substantially while the nighttime values show no change. These results are not seen when the sensitivities are applied for the more modest cuts (50-65%) to reach 75 ppb. The diurnal pattern in New York for the 65 ppb case for the highest days is clearly unrealistic as there is no chemical process expected to result in daytime values lower than values at night, rather it appears to be an artifact of applying this model-based methodology to extremely large emissions reductions in a location where relationships derived under 3 discrete conditions (base, 50% NOx cut, 90% NOx cut) cannot fully characterize sensitivities over the entire range of possible reductions. As discussed previously in section 3.2.4, the use of the lower bound from the 95$^{th}$ percentile confidence interval can mitigate some of this behavior, but in the case of New York some unrealistic outliers still remain. It should be noted, however that this unrealistic diurnal pattern is only seen in the outlier points, and is not seen the box and whiskers which represent 1.5 times the interquartile range (most of the data).

Figure 28 through Figure 42 display the same information as Figure 13 through Figure 27 but for monthly rather than hourly distributions. Note that missing months in these plots indicate that there was no monitor data available for those months and years. Similar to the diurnal plots, the seasonal distributions become flatter when meeting 75 and 65 ppb standard levels especially for the highest ozone days. This is due to more ozone decreases during summer months and more ozone increases in winter months. The ozone increases in the winter are consistent with the understanding that solar insolation rates are lower in the winter reducing total photochemical activity and shifting the net affect of NOx emissions on ozone which can both create ozone through photochemical pathways and destroy ozone through titration. In addition, the decreases on the highest ozone days and increases on the lowest ozone days show a visible compression of the ozone distribution in these plots similar to what was seen in the diurnal plots. The changes for mid-range ozone days also show a pattern of shifting higher mid-range ozone earlier in the year. While in most cities, the highest interquartile ozone

concentrations in the recent conditions occur in the summer months (June-August), in many areas the highest interquartile ozone concentrations shift to spring months (April-May) for the adjustment scenarios of meeting 75 and 65 ppb standard levels. This pattern can be seen most dramatically in Atlanta, Baltimore, Boston, Denver, Los Angeles, New York, Philadelphia, Sacramento, and Washington D.C. This pattern is consistent with higher contribution from non-U.S. anthropogenic sources at lower standard levels than under recent observed conditions. Many of these non-U.S. anthropogenic sources such as stratospheric intrusions and international transport have been shown to peak during spring months as discussed in the Integrated Science Assessment (EPA, 2013).

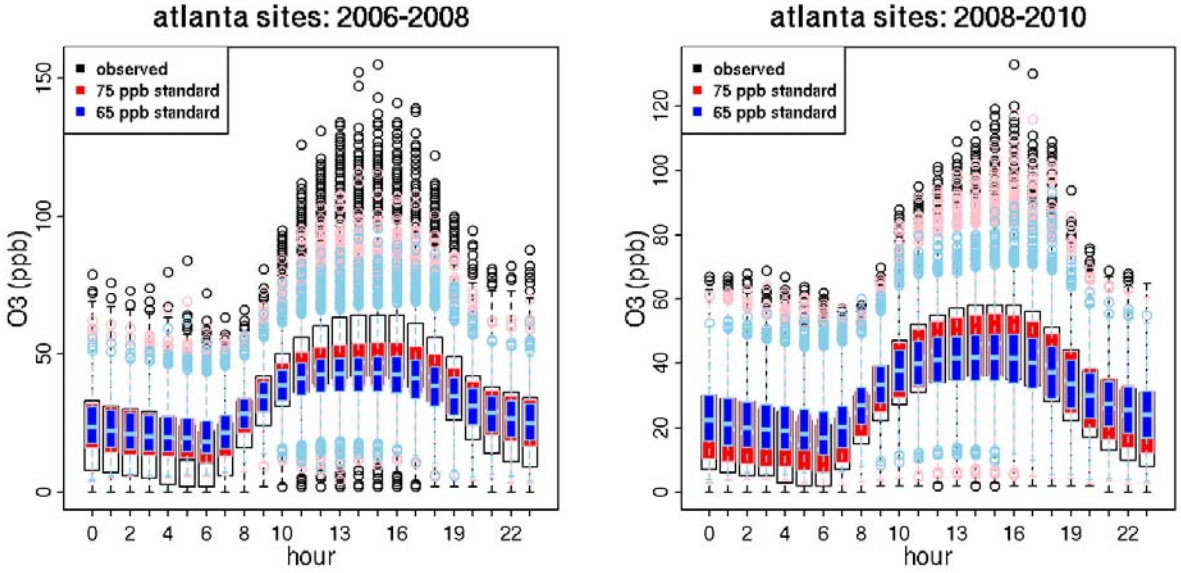


**Figure 13: Hourly $O_3$ distributions at Atlanta area regulatory monitoring sites for observed air quality, and air quality adjusted to meet the existing (75 ppb) and alternative (65 ppb) standards for 2006-2008 (left) and 2008-2010 (right).**

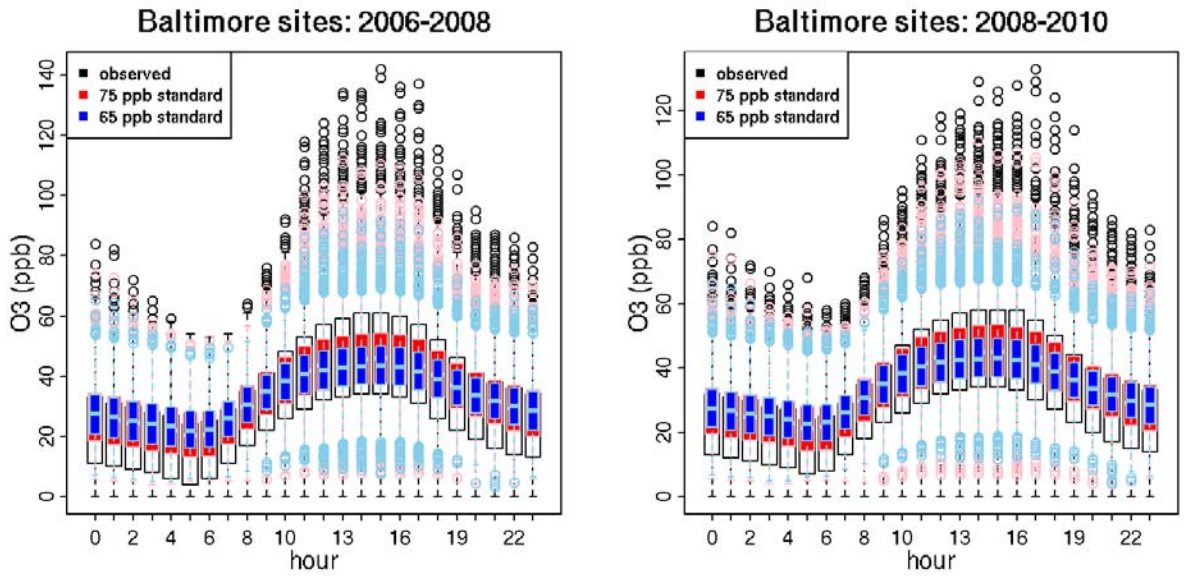


**Figure 14: Hourly $O_3$ distributions at Baltimore area regulatory monitoring sites for observed air quality, and air quality adjusted to meet the existing (75 ppb) and alternative (65 ppb) standards for 2006-2008 (left) and 2008-2010 (right).**

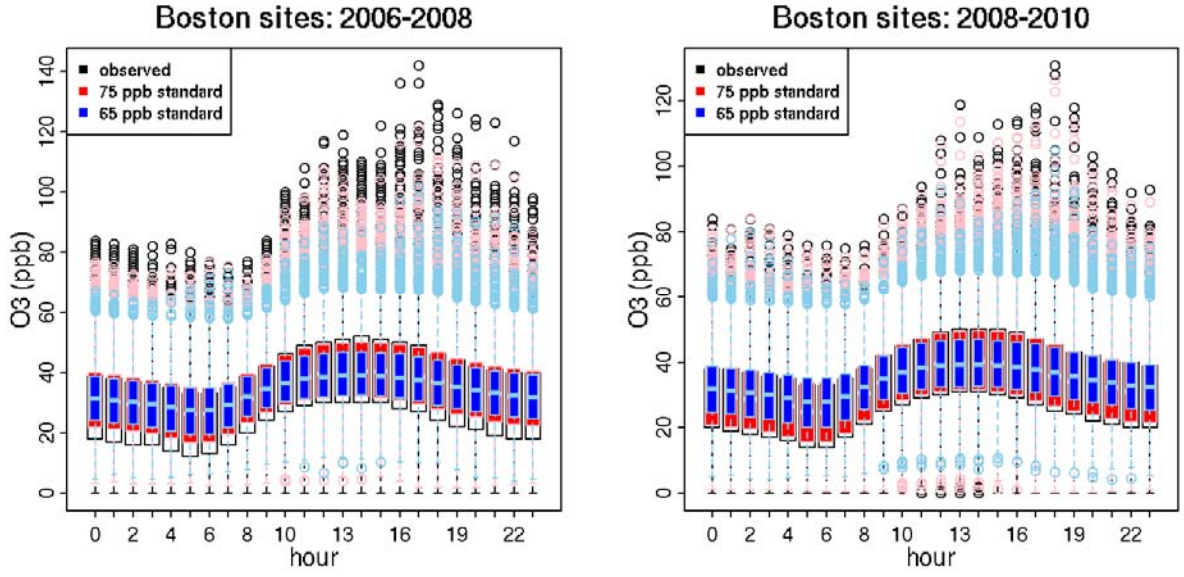


**Figure 15: Hourly $O_3$ distributions at Boston area regulatory monitoring sites for observed air quality, and air quality adjusted to meet the existing (75 ppb) and alternative (65 ppb) standards for 2006-2008 (left) and 2008-2010 (right).**

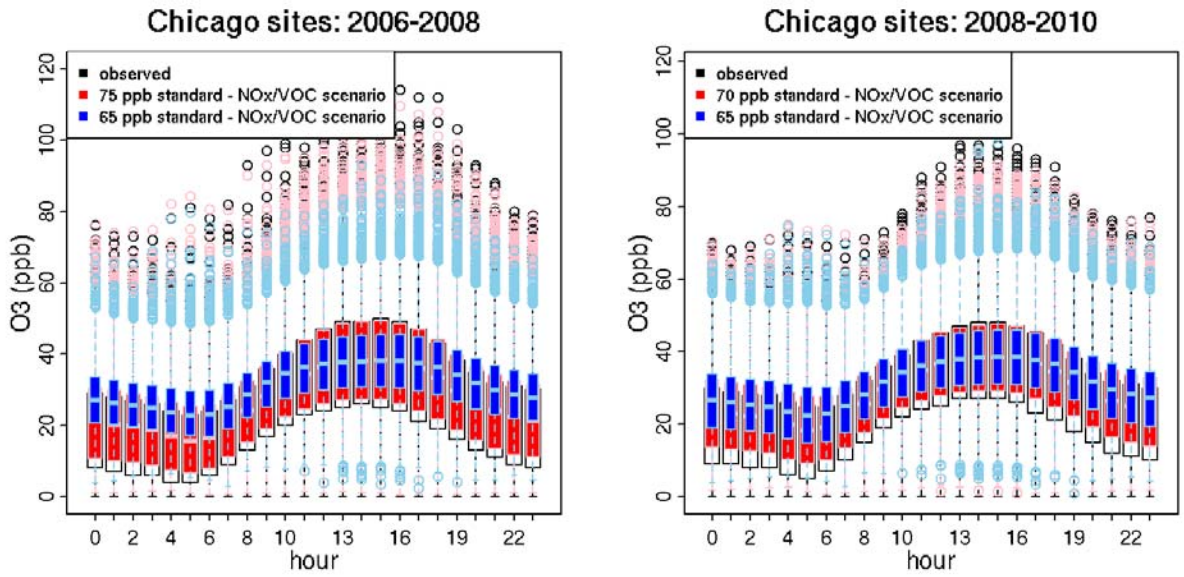


**Figure 16: Hourly $O_3$ distributions at Chicago area regulatory monitoring sites for observed air quality, and air quality adjusted to meet the existing (75 ppb) and alternative (65 ppb) standards for 2006-2008 (left) and 2008-2010 (right).**

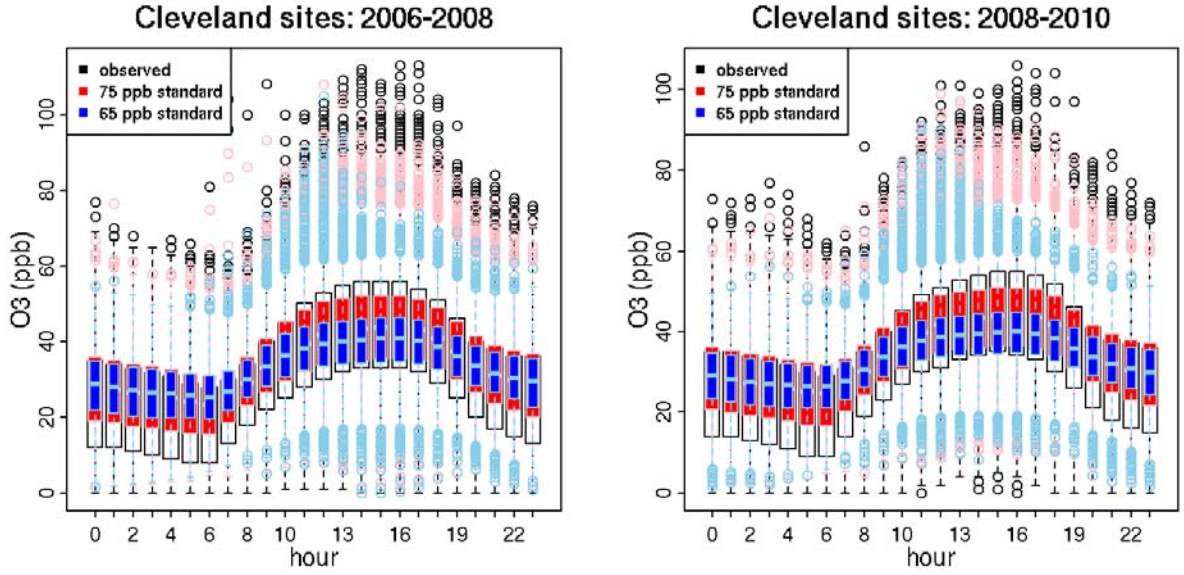


**Figure 17: Hourly $O_3$ distributions at Cleveland area regulatory monitoring sites for observed air quality, and air quality adjusted to meet the existing (75 ppb) and alternative (65 ppb) standards for 2006-2008 (left) and 2008-2010 (right).**

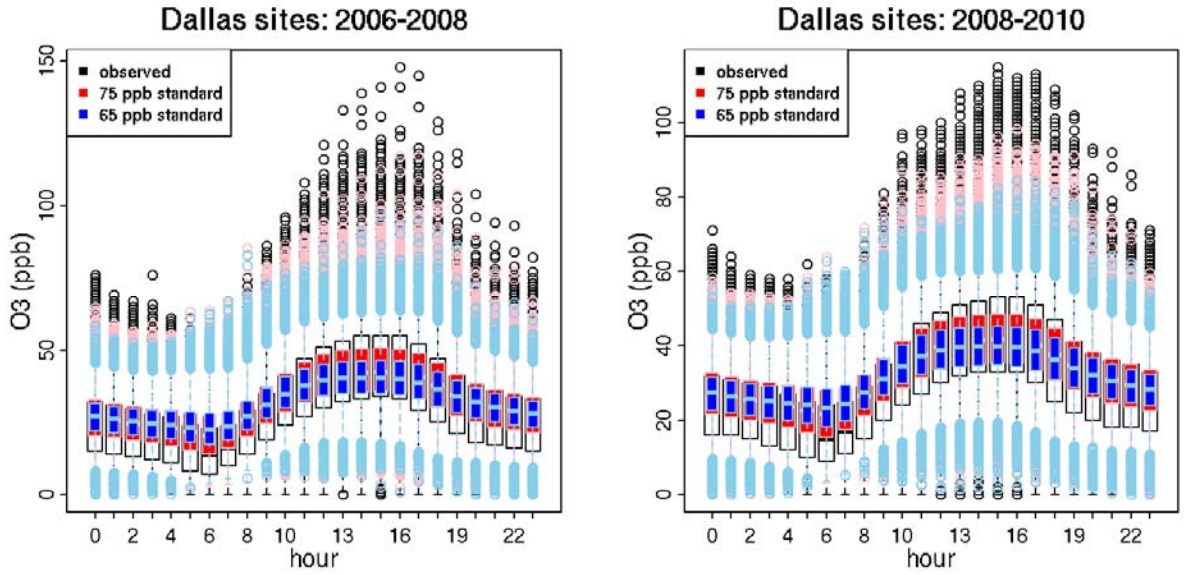


**Figure 18: Hourly $O_3$ distributions at Dallas area regulatory monitoring sites for observed air quality, and air quality adjusted to meet the existing (75 ppb) and alternative (65 ppb) standards for 2006-2008 (left) and 2008-2010 (right).**

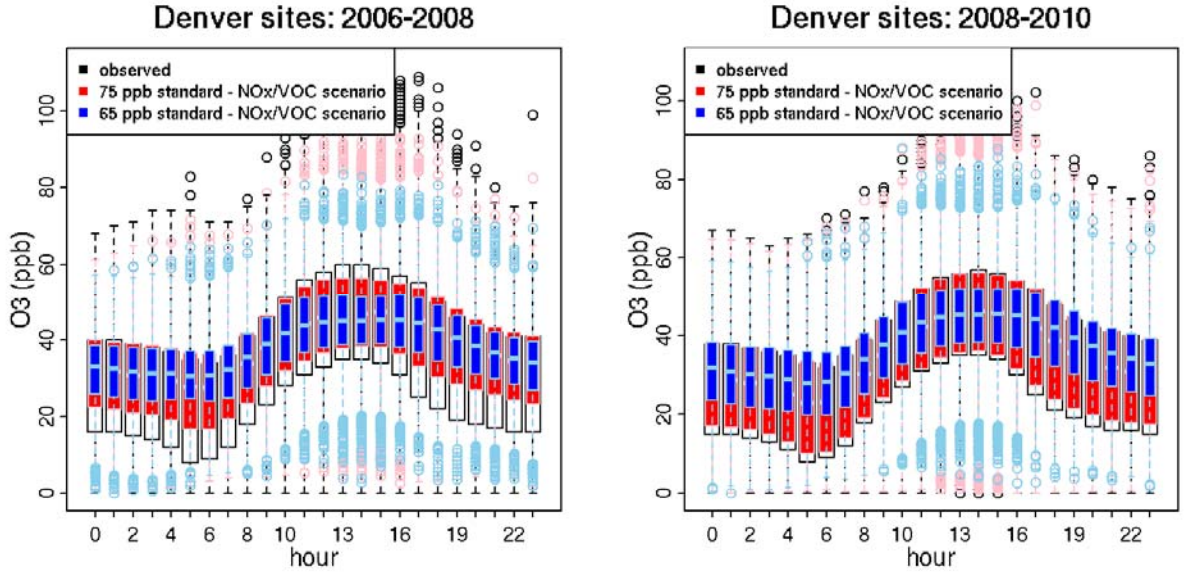


**Figure 19: Hourly $O_3$ distributions at Denver area regulatory monitoring sites for observed air quality, and air quality adjusted to meet the existing (75 ppb) and alternative (65 ppb) standards for 2006-2008 (left) and 2008-2010 (right).**

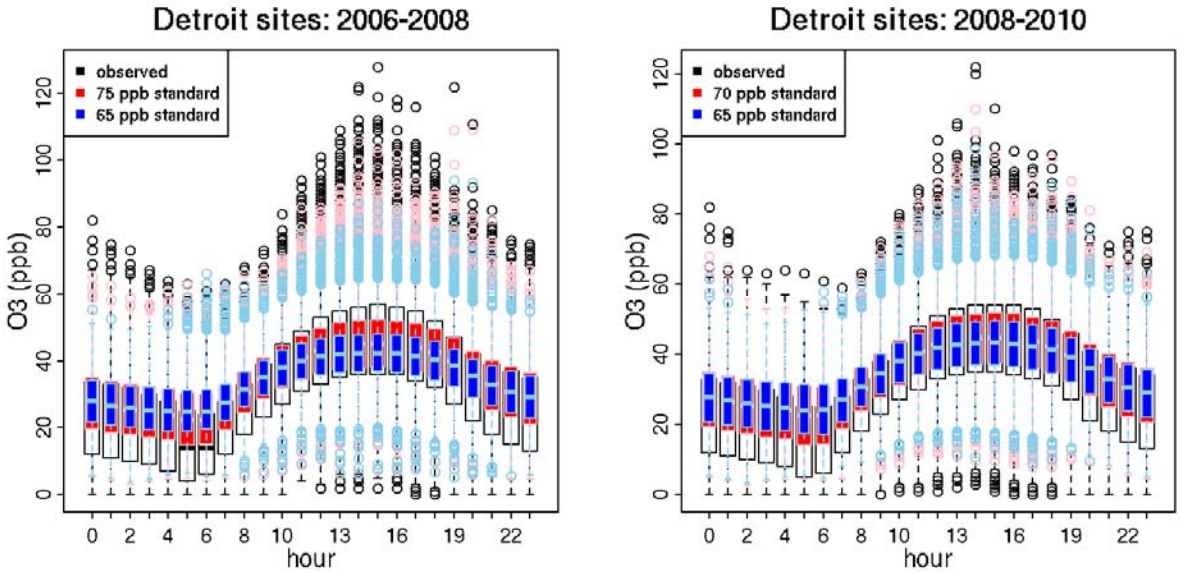


**Figure 20: Hourly $O_3$ distributions at Detroit area regulatory monitoring sites for observed air quality, and air quality adjusted to meet the existing (75 ppb) and alternative (65 ppb) standards for 2006-2008 (left) and 2008-2010 (right).**

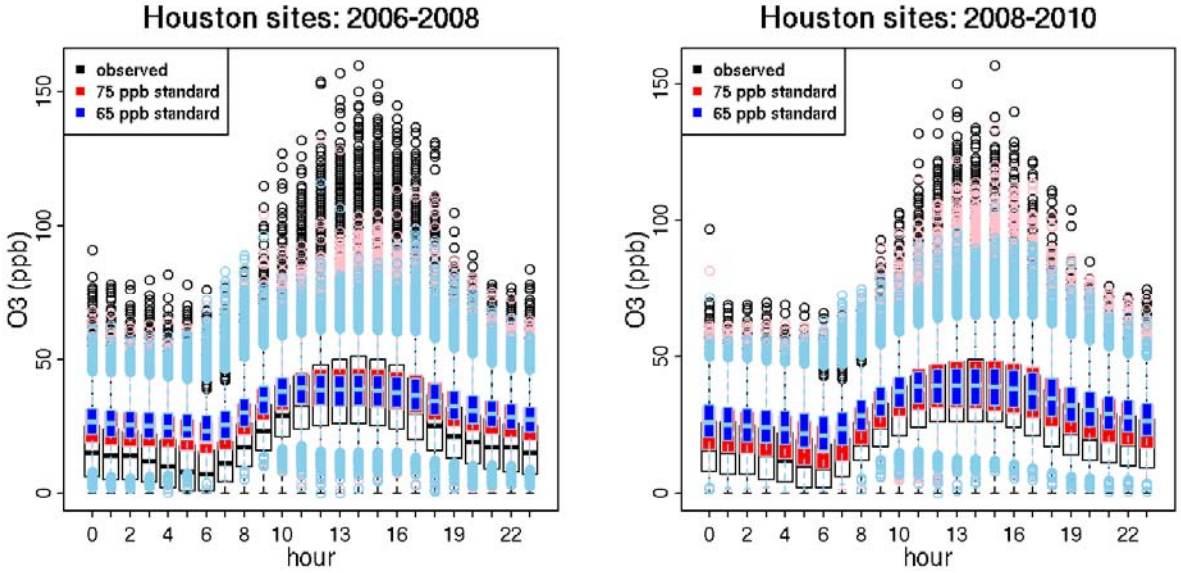


**Figure 21: Hourly $O_3$ distributions at Houston area regulatory monitoring sites for observed air quality, and air quality adjusted to meet the existing (75 ppb) and alternative (65 ppb) standards for 2006-2008 (left) and 2008-2010 (right).**

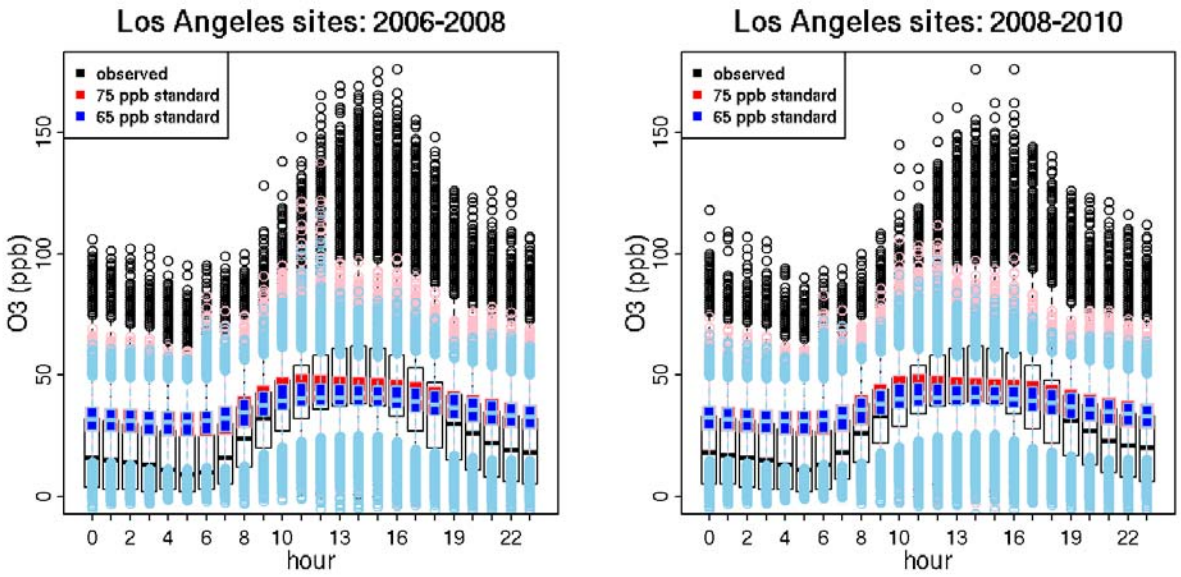


**Figure 22: Hourly $O_3$ distributions at Los Angeles area regulatory monitoring sites for observed air quality, and air quality adjusted to meet the existing (75 ppb) and alternative (65 ppb) standards for 2006-2008 (left) and 2008-2010 (right).**

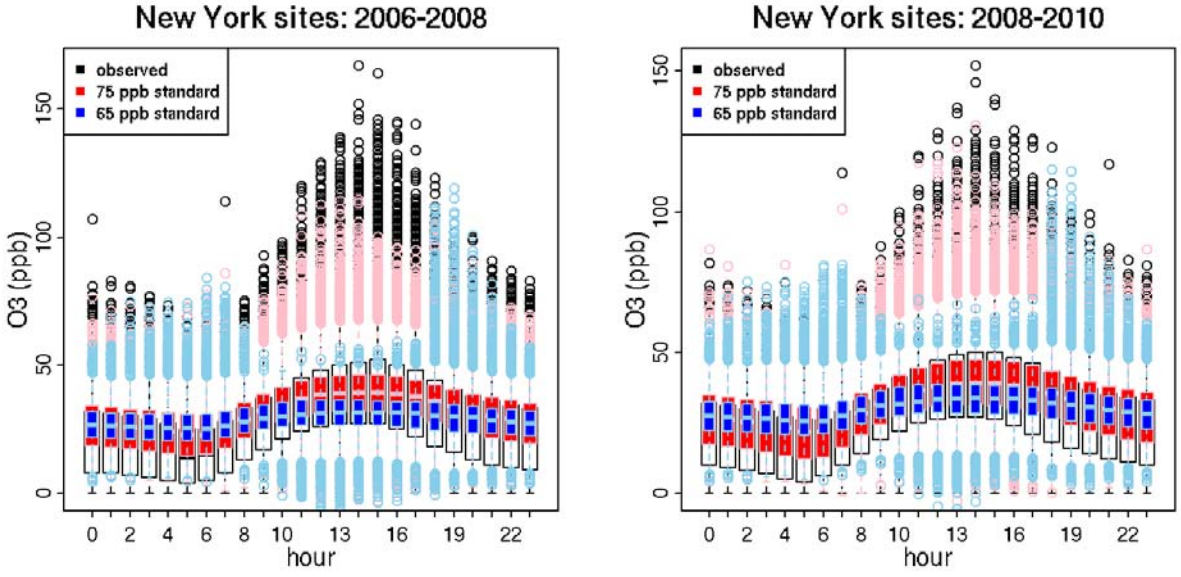


**Figure 23: Hourly $O_3$ distributions at New York area regulatory monitoring sites for observed air quality, and air quality adjusted to meet the existing (75 ppb) and alternative (65 ppb) standards for 2006-2008 (left) and 2008-2010 (right).**

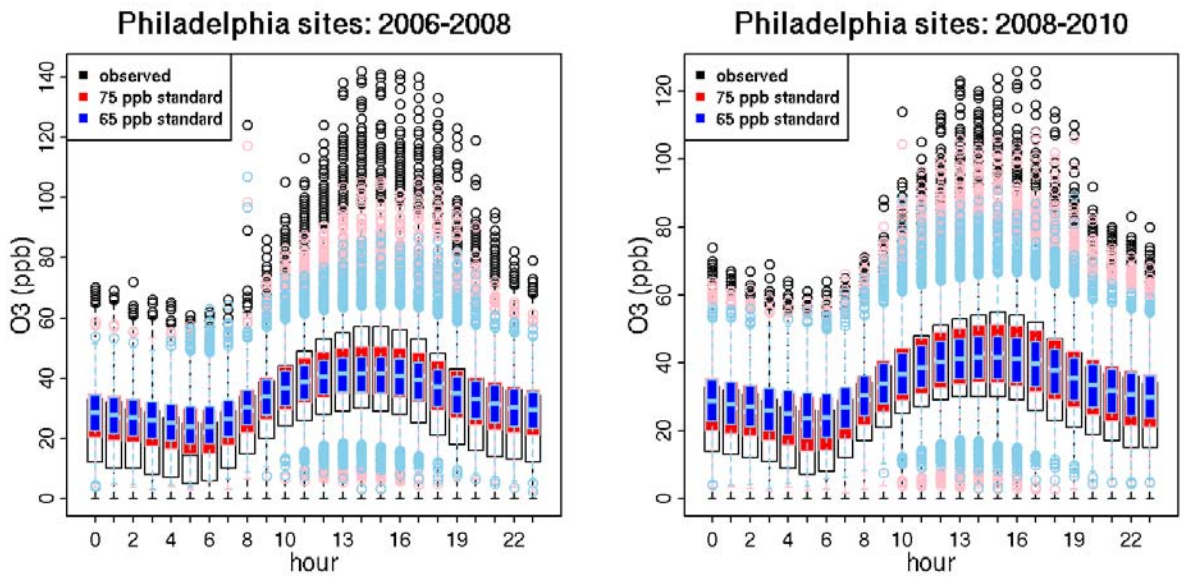


**Figure 24: Hourly $O_3$ distributions at Philadelphia area regulatory monitoring sites for observed air quality, and air quality adjusted to meet the existing (75 ppb) and alternative (65 ppb) standards for 2006-2008 (left) and 2008-2010 (right).**

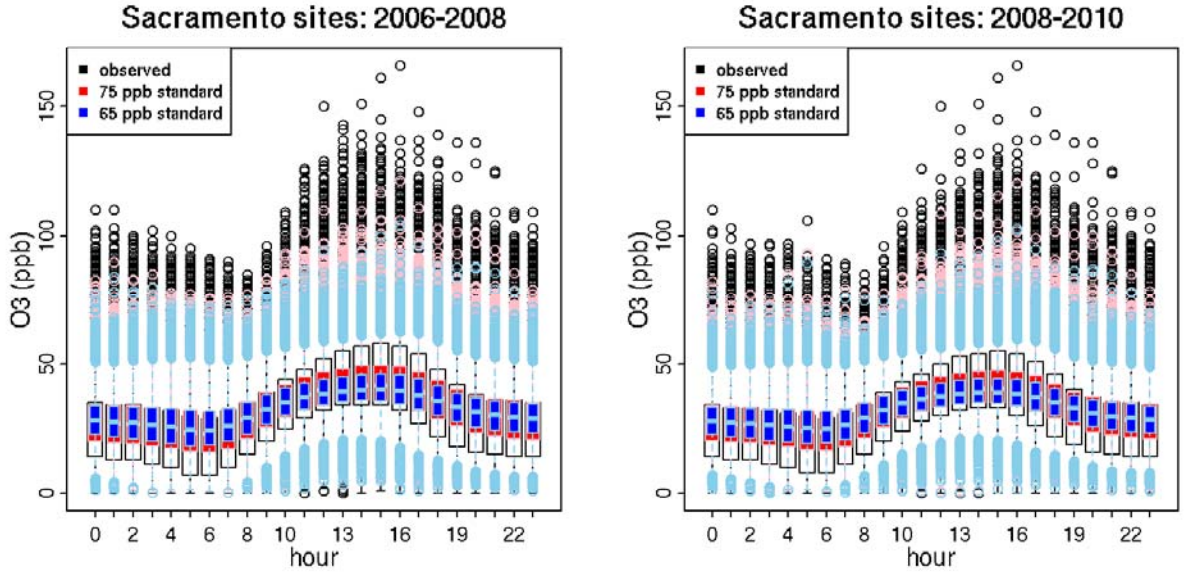


**Figure 25: Hourly $O_3$ distributions at Sacramento area regulatory monitoring sites for observed air quality, and air quality adjusted to meet the existing (75 ppb) and alternative (65 ppb) standards for 2006-2008 (left) and 2008-2010 (right).**

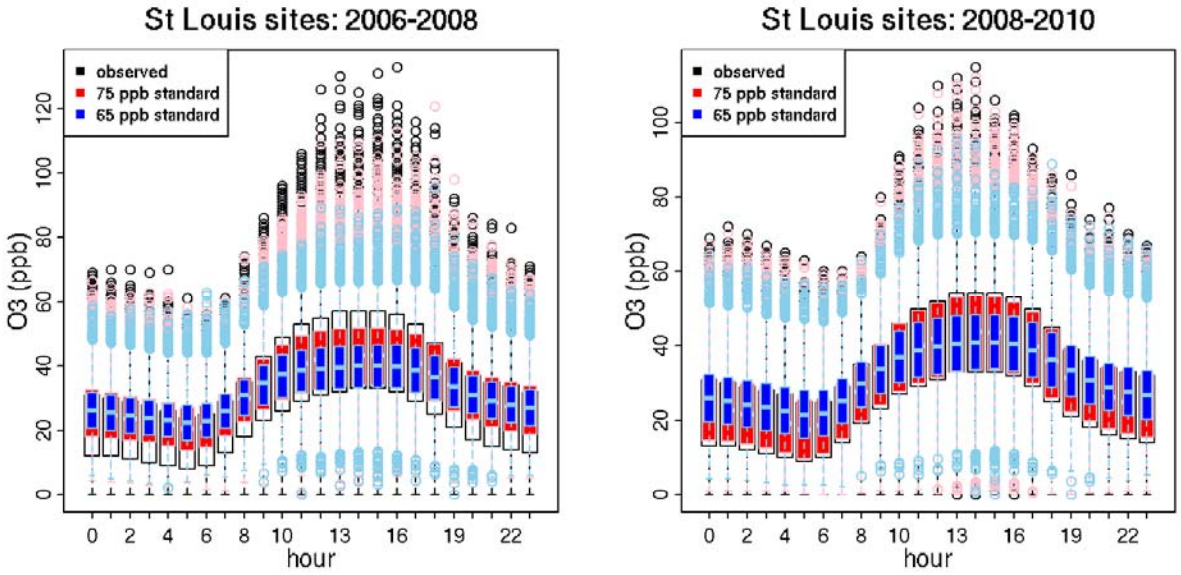


**Figure 26: Hourly $O_3$ distributions at St. Louis area regulatory monitoring sites for observed air quality, and air quality adjusted to meet the existing (75 ppb) and alternative (65 ppb) standards for 2006-2008 (left) and 2008-2010 (right).**

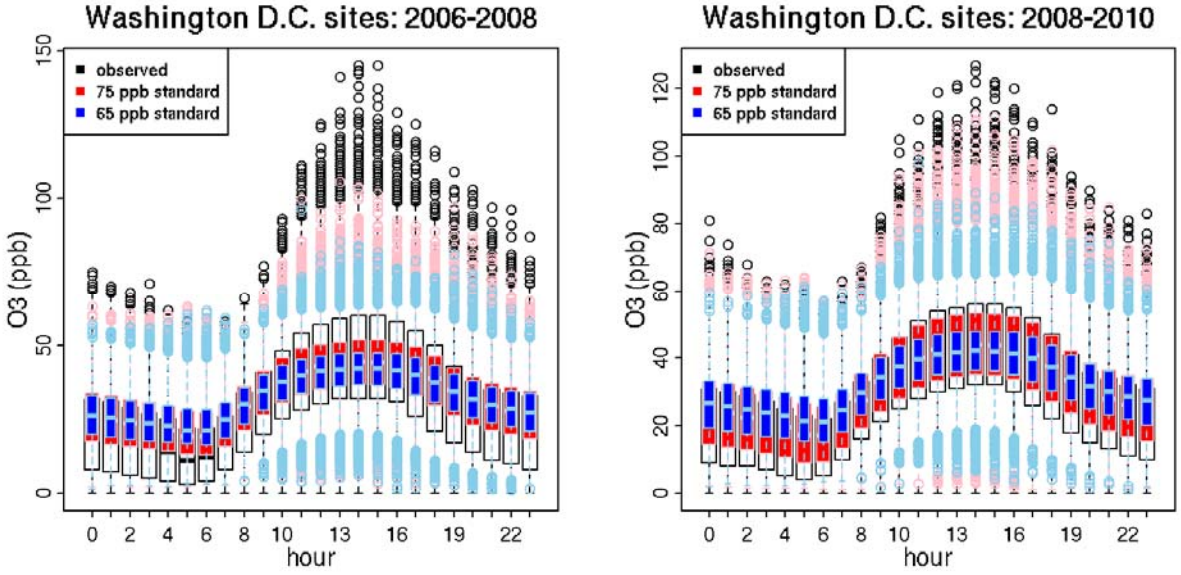


**Figure 27: Hourly $O_3$ distributions at Washington, D.C. area regulatory monitoring sites for observed air quality, and air quality adjusted to meet the existing (75 ppb) and alternative (65 ppb) standards for 2006-2008 (left) and 2008-2010 (right).**

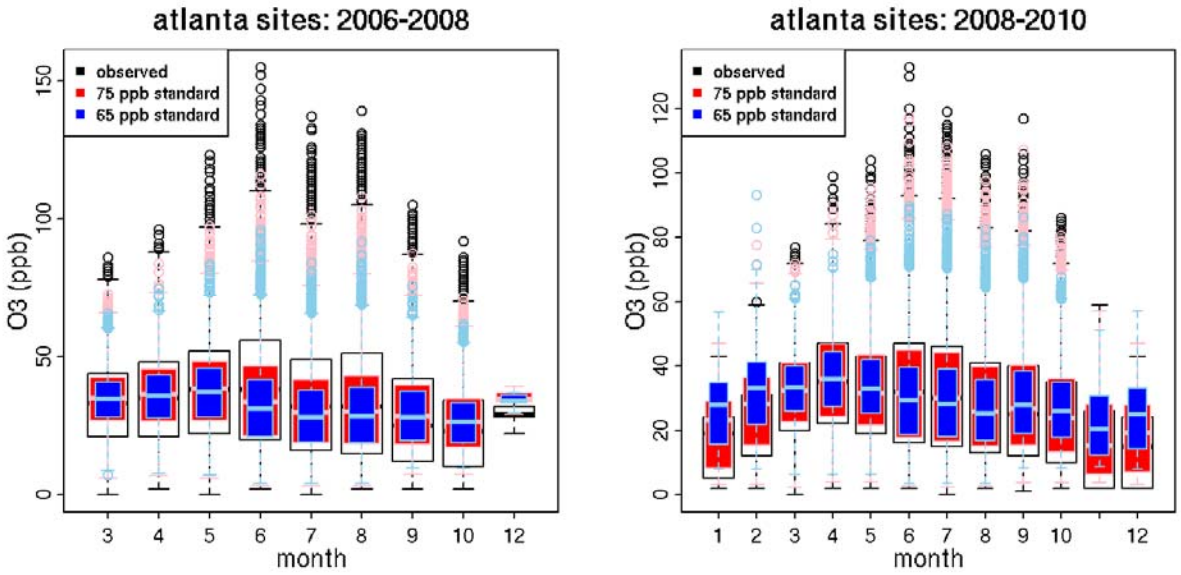


**Figure 28: Monthly $O_3$ distributions at Atlanta area regulatory monitoring sites for observed air quality, and air quality adjusted to meet the existing (75 ppb) and alternative (65 ppb) standards for 2006-2008 (left) and 2008-2010 (right).**

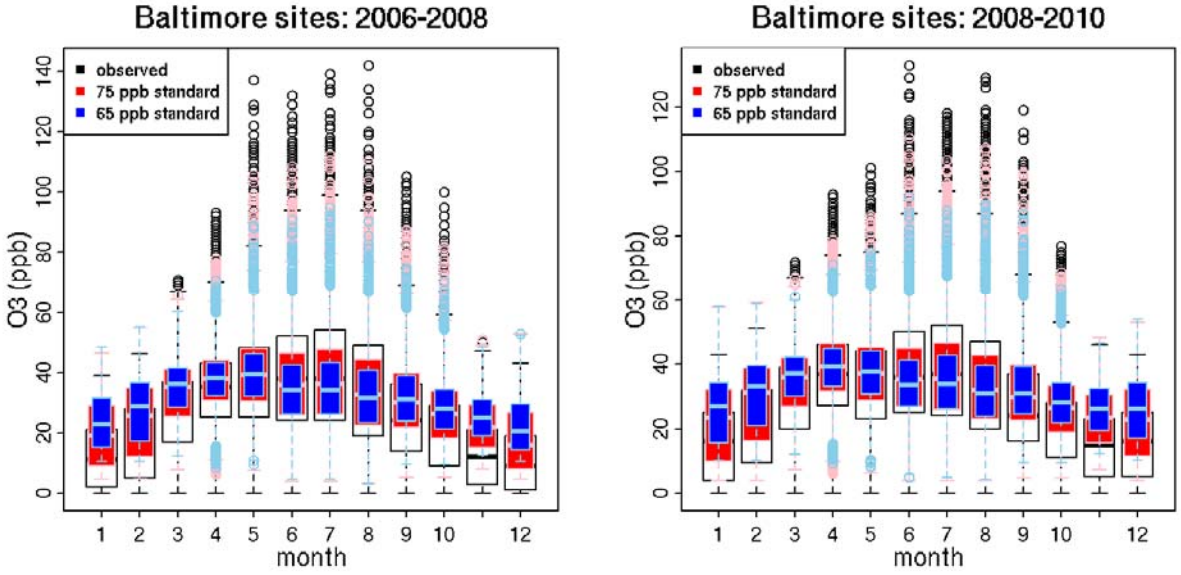


**Figure 29: Monthly $O_3$ distributions at Baltimore area regulatory monitoring sites for observed air quality, and air quality adjusted to meet the existing (75 ppb) and alternative (65 ppb) standards for 2006-2008 (left) and 2008-2010 (right).**

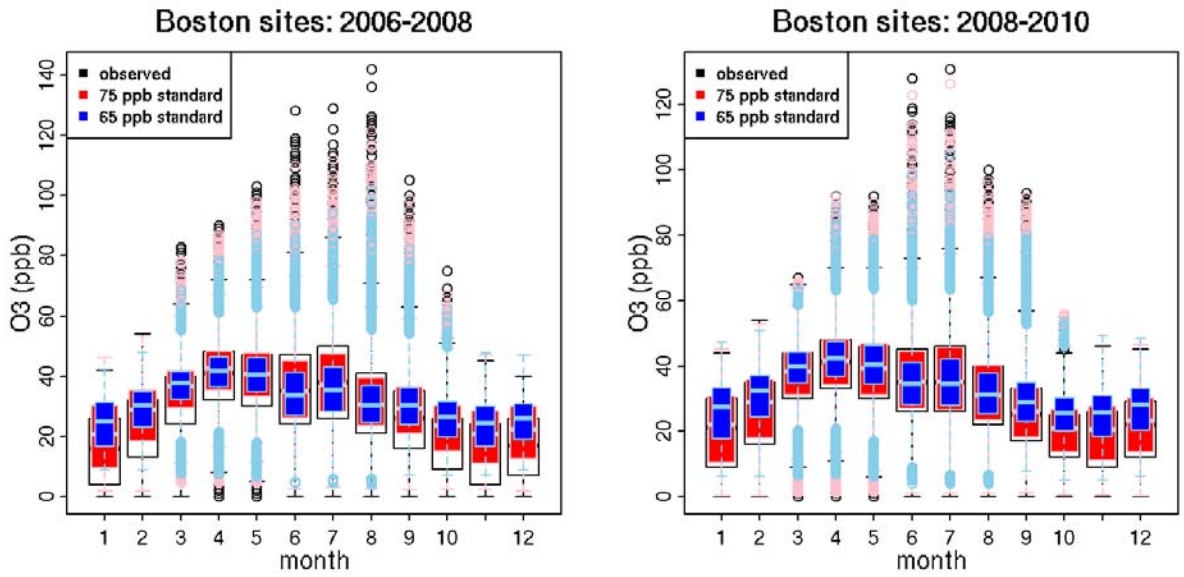


**Figure 30: Monthly $O_3$ distributions at Boston area regulatory monitoring sites for observed air quality, and air quality adjusted to meet the existing (75 ppb) and alternative (65 ppb) standards for 2006-2008 (left) and 2008-2010 (right).**

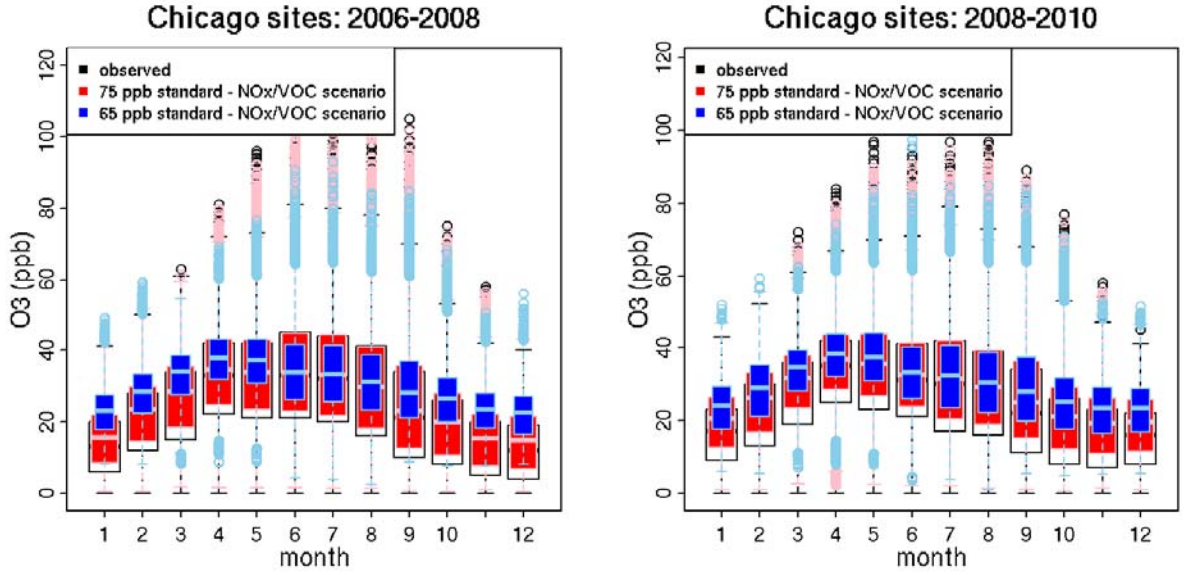


**Figure 31: Monthly $O_3$ distributions at Chicago area regulatory monitoring sites for observed air quality, and air quality adjusted to meet the existing (75 ppb) and alternative (65 ppb) standards for 2006-2008 (left) and 2008-2010 (right).**

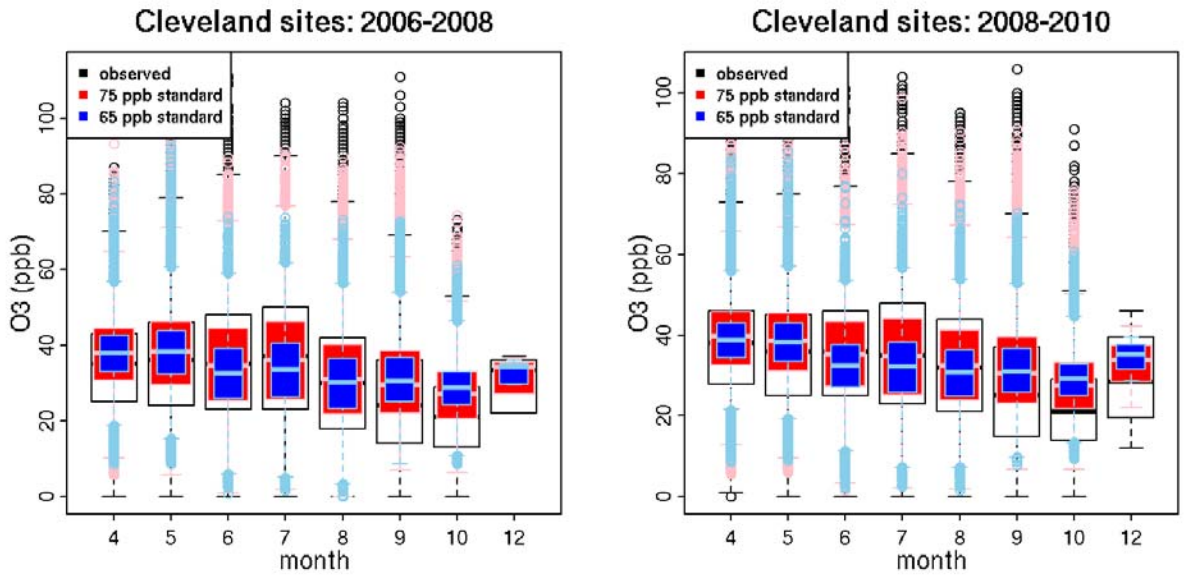


**Figure 32: Monthly $O_3$ distributions at Cleveland area regulatory monitoring sites for observed air quality, and air quality adjusted to meet the existing (75 ppb) and alternative (65 ppb) standards for 2006-2008 (left) and 2008-2010 (right).**

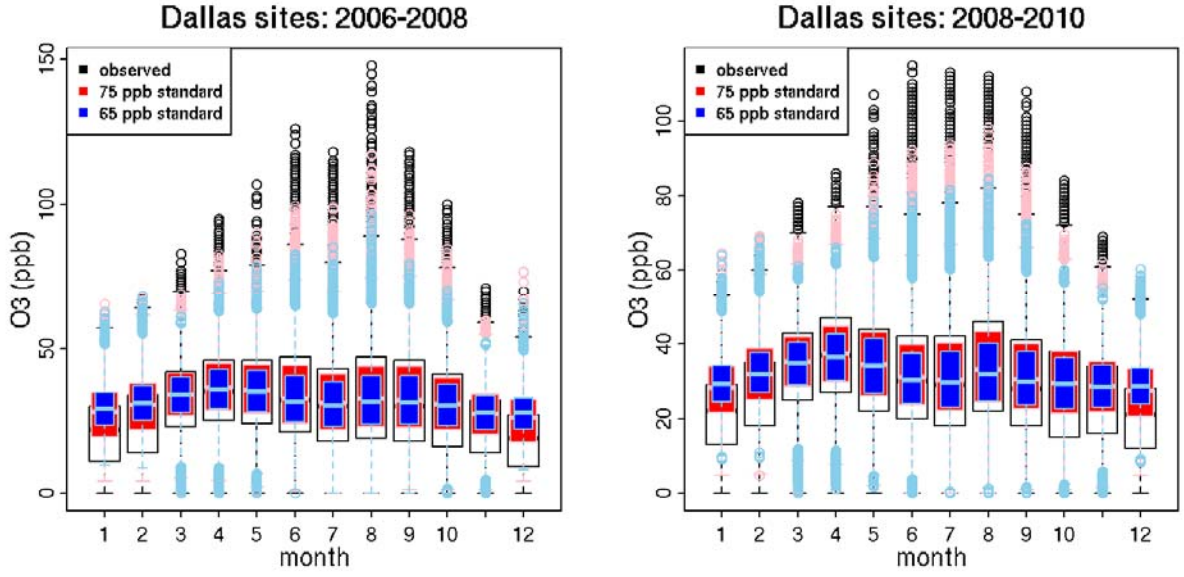


**Figure 33: Monthly $O_3$ distributions at Dallas area regulatory monitoring sites for observed air quality, and air quality adjusted to meet the existing (75 ppb) and alternative (65 ppb) standards for 2006-2008 (left) and 2008-2010 (right).**

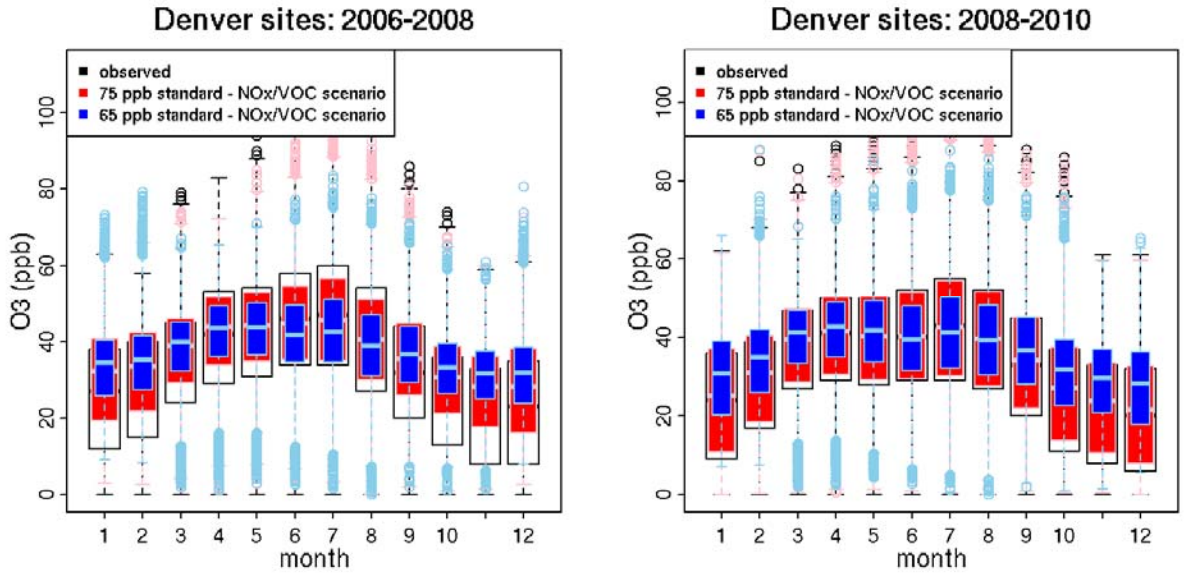


**Figure 34: Monthly $O_3$ distributions at Denver area regulatory monitoring sites for observed air quality, and air quality adjusted to meet the existing (75 ppb) and alternative (65 ppb) standards for 2006-2008 (left) and 2008-2010 (right).**

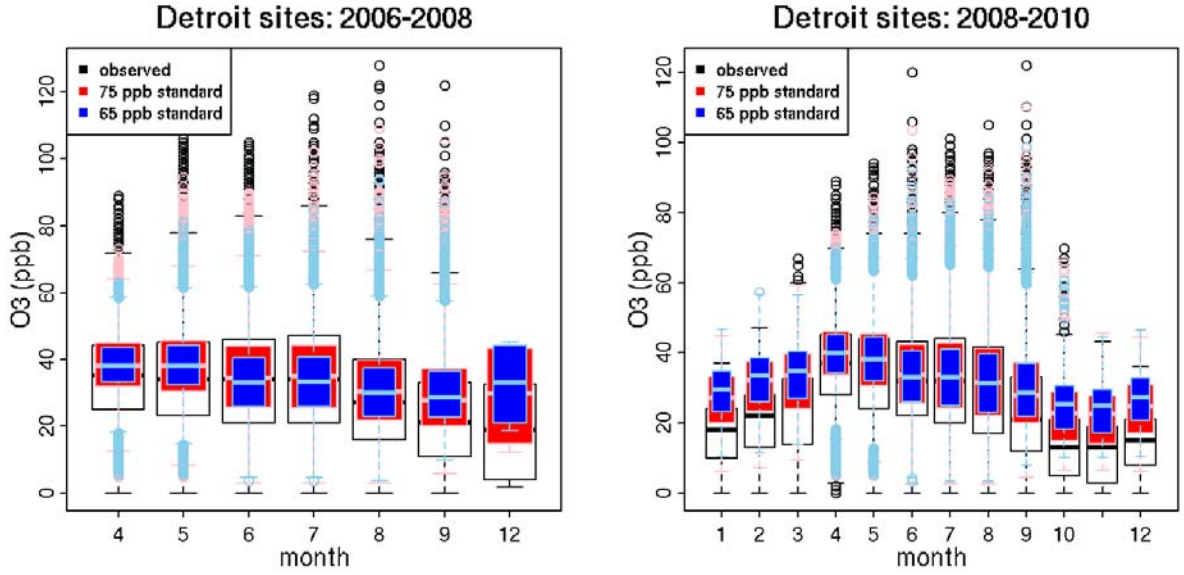


**Figure 35: Monthly $O_3$ distributions at Detroit area regulatory monitoring sites for observed air quality, and air quality adjusted to meet the existing (75 ppb) and alternative (65 ppb) standards for 2006-2008 (left) and 2008-2010 (right).**

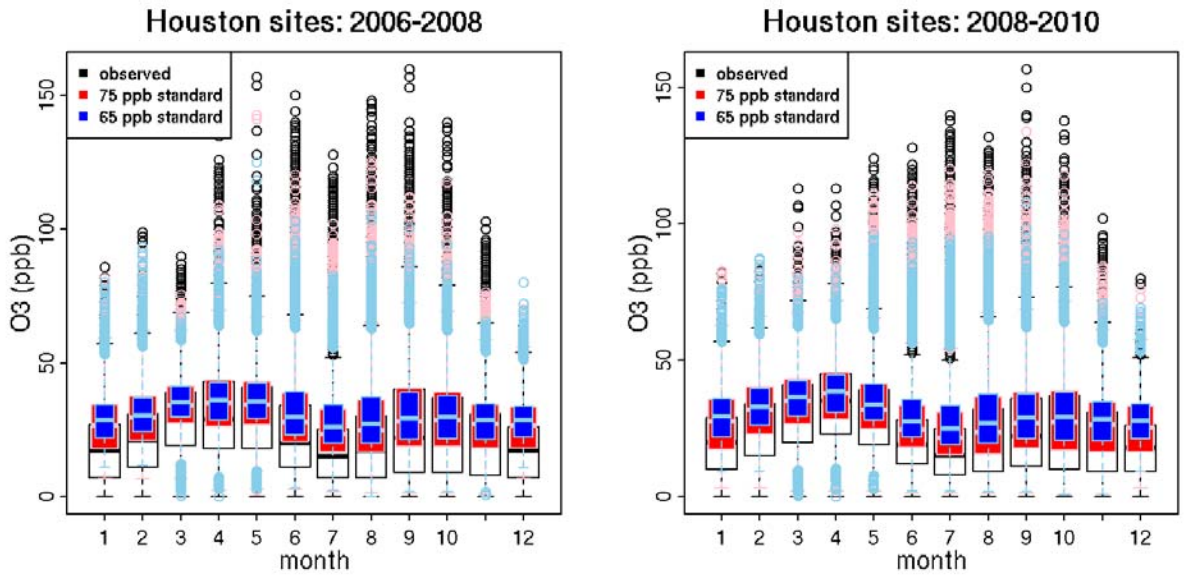


**Figure 36: Monthly $O_3$ distributions at Houston area regulatory monitoring sites for observed air quality, and air quality adjusted to meet the existing (75 ppb) and alternative (65 ppb) standards for 2006-2008 (left) and 2008-2010 (right).**

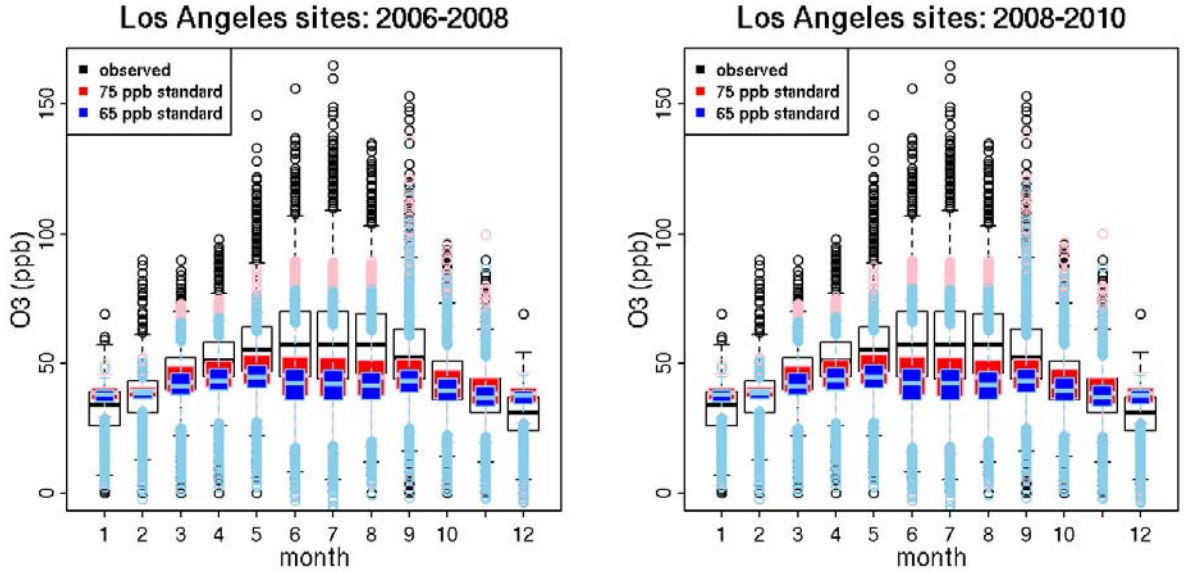


**Figure 37: Monthly $O_3$ distributions at Los Angeles area regulatory monitoring sites for observed air quality, and air quality adjusted to meet the existing (75 ppb) and alternative (65 ppb) standards for 2006-2008 (left) and 2008-2010 (right).**

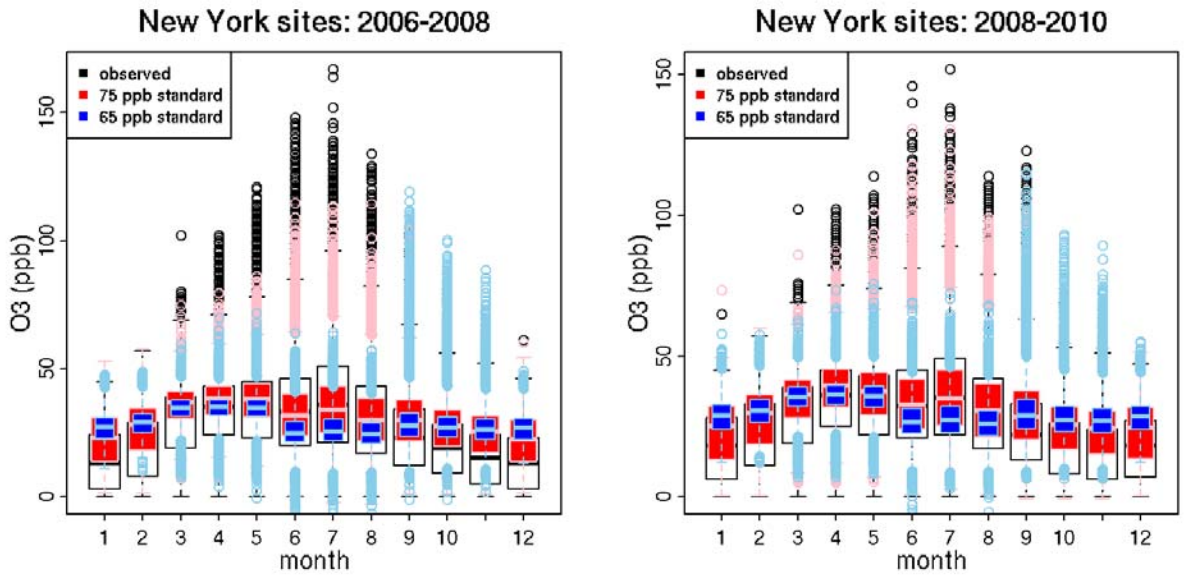


**Figure 38: Monthly $O_3$ distributions at New York area regulatory monitoring sites for observed air quality, and air quality adjusted to meet the existing (75 ppb) and alternative (65 ppb) standards for 2006-2008 (left) and 2008-2010 (right).**

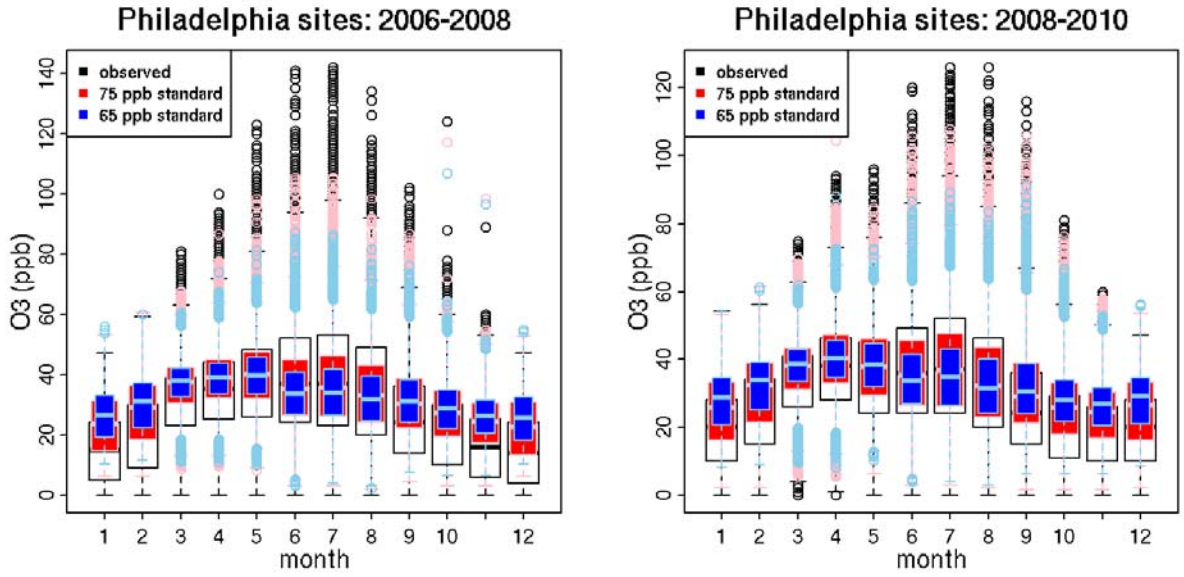


**Figure 39: Monthly $O_3$ distributions at Philadelphia area regulatory monitoring sites for observed air quality, and air quality adjusted to meet the existing (75 ppb) and alternative (65 ppb) standards for 2006-2008 (left) and 2008-2010 (right).**

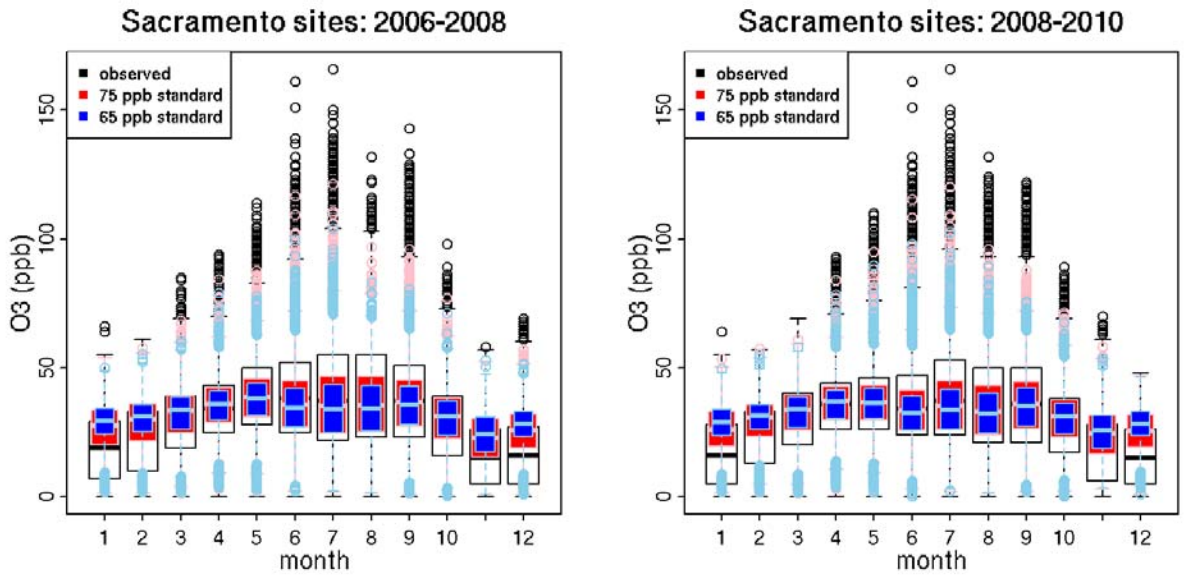


**Figure 40: Monthly $O_3$ distributions at Sacramento area regulatory monitoring sites for observed air quality, and air quality adjusted to meet the existing (75 ppb) and alternative (65 ppb) standards for 2006-2008 (left) and 2008-2010 (right).**

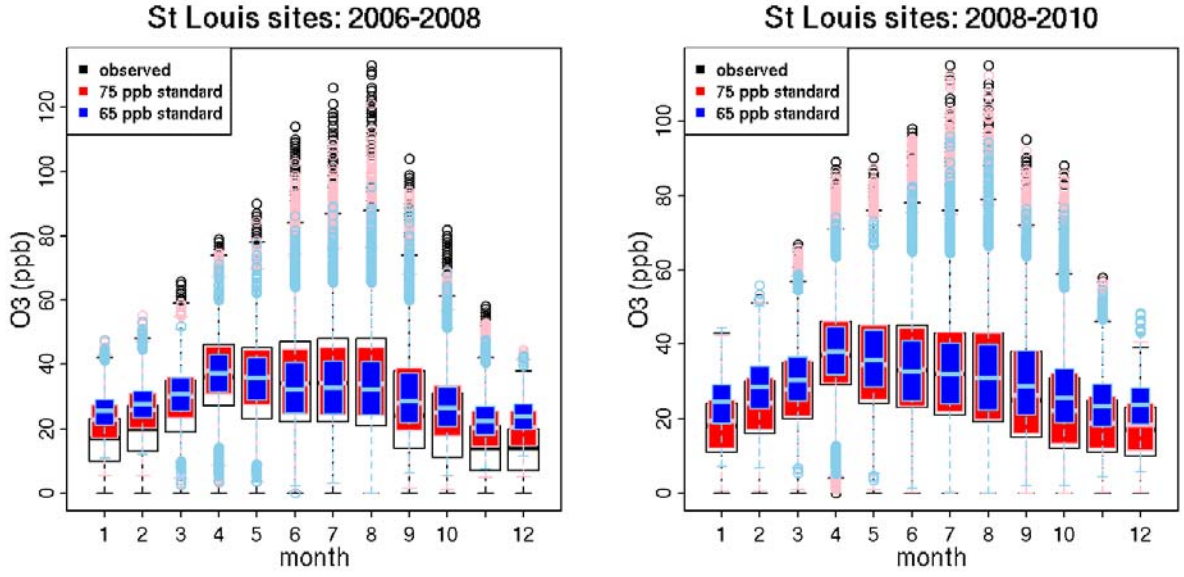


**Figure 41: Monthly $O_3$ distributions at St. Louis area regulatory monitoring sites for observed air quality, and air quality adjusted to meet the existing (75 ppb) and alternative (65 ppb) standards for 2006-2008 (left) and 2008-2010 (right).**

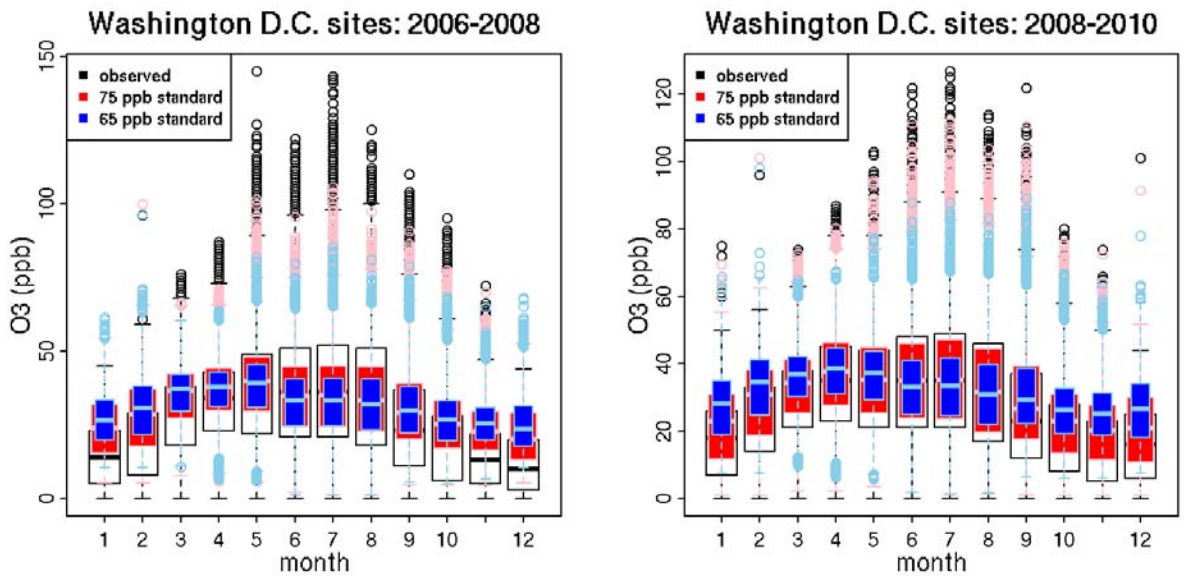


**Figure 42: Monthly $O_3$ distributions at Washington, D.C. area regulatory monitoring sites for observed air quality, and air quality adjusted to meet the existing (75 ppb) and alternative (65 ppb) standards for 2006-2008 (left) and 2008-2010 (right).**

## 4.4 STANDARD ERRORS FOR PREDICTED HOURLY $O_3$ CONCENTRATIONS

Standard error values for predicted hourly $O_3$ were generally small relative to total predicted hourly $O_3$ concentrations. This indicates that even when regression fits had somewhat lower correlation coefficients, the resulting uncertainty from the use of the regression line does not substantially affect predicted $O_3$ concentrations. Table 18 and Table 19 show the mean and 95$^{th}$ percentile standard error for all hourly $O_3$ values (2006-2010) in each urban area for the existing standard of 75 ppb and the potential alternative standards of 70 ppb, 65 ppb, and 60 ppb.

**Table 18: Mean standard error (ppb) in adjusted hourly $O_3$ concentration in each urban area for each standard.**

| Urban Area | Years | Standard Level | | | |
|---|---|---|---|---|---|
| | | 75 ppb† | 70 ppb | 65 ppb | 60 ppb‡ |
| Atlanta | 2006-2008 | 0.65 | 0.69 | 0.74 | 0.81 |
| | 2008-2010 | 0.37 | 0.68 | 0.71 | 0.77 |
| Baltimore | 2006-2008 | 0.62 | 0.65 | 0.70 | 0.78 |
| | 2008-2010 | 0.62 | 0.64 | 0.69 | 0.75 |
| Boston | 2006-2008 | 0.51 | 0.53 | 0.59 | 0.69 |
| | 2008-2010 | 0.16 | 0.51 | 0.54 | 0.63 |
| Chicago* | 2006-2008 | 0.29 | 0.66 | 0.77 | 0.99 |

| | | | | | |
|---|---|---|---|---|---|
| | 2008-2010 | N/A | 0.41 | 0.68 | 0.83 |
| Cleveland | 2006-2008 | 0.60 | 0.65 | 0.76 | 0.96 |
| | 2008-2010 | 0.60 | 0.66 | 0.80 | 0.95 |
| Dallas | 2006-2008 | 0.59 | 0.64 | 0.74 | 0.86 |
| | 2008-2010 | 0.57 | 0.63 | 0.72 | 0.84 |
| Denver* | 2006-2008 | 0.51 | 0.62 | 0.77 | 0.85 |
| | 2008-2010 | 0.17 | 0.48 | 0.58 | 0.82 |
| Detroit | 2006-2008 | 0.60 | 0.70 | 0.80 | 0.92 |
| | 2008-2010 | N/A | 0.56 | 0.65 | 0.81 |
| Houston | 2006-2008 | 0.73 | 0.83 | 0.95 | 1.11 |
| | 2008-2010 | 0.52 | 0.55 | 0.62 | 0.76 |
| Los Angeles* | 2006-2008 | 1.15 | 1.17 | 1.18 | 1.21 |
| | 2008-2010 | 1.14 | 1.15 | 1.17 | 1.19 |
| New York* | 2006-2008 | 0.84 | 1.06 | 1.39 | N/A |
| | 2008-2010 | 0.69 | 0.92 | 1.34 | N/A |
| Philadelphia | 2006-2008 | 0.66 | 0.72 | 0.80 | 0.90 |
| | 2008-2010 | 0.62 | 0.65 | 0.71 | 0.79 |
| Sacramento | 2006-2008 | 0.49 | 0.55 | 0.61 | 0.81 |
| | 2008-2010 | 0.49 | 0.56 | 0.62 | 0.70 |
| Saint Louis | 2006-2008 | 0.57 | 0.61 | 0.70 | 0.81 |
| | 2008-2010 | 0.13 | 0.48 | 0.58 | 0.66 |
| Washington D.C. | 2006-2008 | 0.67 | 0.71 | 0.78 | 0.87 |
| | 2008-2010 | 0.49 | 0.66 | 0.72 | 0.84 |

*Values are from the standard NOx reduction scenario for all cities except Chicago and Denver, for which value are from the standard NOx/VOC reduction scenario and New York and Los Angeles, for which values based on reductions required when using the lower bound of the 95th percentile confidence interval.
†N/A values for the 75 ppb standard level mean that a particular urban area did not have any design values above 75 for that 3-year period so adjustments were made to ambient data.
‡N/A values for the 60 ppb standard level mean that this adjustment methodology was not able to bring design values down to 60 for that particular city and 3-year period.

**Table 19: 95$^{th}$ percentile standard error (ppb) in adjusted hourly $O_3$ concentration in each urban area for each standard.**

| Urban Area | Years | Standard Level | | | |
|---|---|---|---|---|---|
| | | 75 ppb† | 70 ppb | 65 ppb | 60 ppb‡ |
| Atlanta | 2006-2008 | 1.28 | 1.34 | 1.42 | 1.56 |
| | 2008-2010 | 0.72 | 1.33 | 1.38 | 1.47 |
| Baltimore | 2006-2008 | 1.22 | 1.26 | 1.34 | 1.49 |
| | 2008-2010 | 1.21 | 1.26 | 1.33 | 1.46 |

| | | | | | |
|---|---|---|---|---|---|
| Boston | 2006-2008 | 1.02 | 1.05 | 1.19 | 1.41 |
| | 2008-2010 | 0.33 | 1.03 | 1.09 | 1.29 |
| Chicago* | 2006-2008 | 0.54 | 1.22 | 1.43 | 1.89 |
| | 2008-2010 | N/A | 0.78 | 1.27 | 1.56 |
| Cleveland | 2006-2008 | 1.13 | 1.19 | 1.35 | 1.69 |
| | 2008-2010 | 1.13 | 1.22 | 1.42 | 1.69 |
| Dallas | 2006-2008 | 1.16 | 1.26 | 1.48 | 1.79 |
| | 2008-2010 | 1.12 | 1.24 | 1.45 | 1.75 |
| Denver* | 2006-2008 | 1.14 | 1.35 | 1.70 | 1.89 |
| | 2008-2010 | 0.38 | 1.07 | 1.28 | 1.84 |
| Detroit | 2006-2008 | 1.12 | 1.28 | 1.46 | 0.69 |
| | 2008-2010 | N/A | 1.05 | 1.20 | 1.48 |
| Houston | 2006-2008 | 1.45 | 1.66 | 1.96 | 2.41 |
| | 2008-2010 | 0.98 | 1.04 | 1.15 | 1.39 |
| Los Angeles* | 2006-2008 | 2.84 | 2.86 | 2.89 | 2.93 |
| | 2008-2010 | 2.78 | 2.80 | 2.83 | 2.86 |
| New York* | 2006-2008 | 1.64 | 2.15 | 2.87 | N/A |
| | 2008-2010 | 1.34 | 1.87 | 2.98 | N/A |
| Philadelphia | 2006-2008 | 1.29 | 1.39 | 1.56 | 1.78 |
| | 2008-2010 | 1.25 | 1.29 | 1.41 | 1.58 |
| Sacramento | 2006-2008 | 1.10 | 1.22 | 1.35 | 1.54 |
| | 2008-2010 | 1.11 | 1.24 | 1.38 | 1.55 |
| Saint Louis | 2006-2008 | 1.07 | 1.14 | 1.29 | 1.51 |
| | 2008-2010 | 0.26 | 0.90 | 1.07 | 1.21 |
| Washington D.C. | 2006-2008 | 1.29 | 1.35 | 1.46 | 1.63 |
| | 2008-2010 | 0.94 | 1.27 | 1.36 | 1.57 |

*Values are from the standard NOx reduction scenario for all cities except Chicago and Denver, for which value are from the standard NOx/VOC reduction scenario and New York and Los Angeles, for which values based on reductions required when using the lower bound of the 95th percentile confidence interval.

†N/A values for the 75 ppb standard level mean that a particular urban area did not have any design values above 75 for that 3-year period so adjustments were made to ambient data.

‡N/A values for the 60 ppb standard level mean that this adjustment methodology was not able to bring design values down to 60 for that particular city and 3-year period.

## 4.5 AIR QUALITY INPUTS FOR THE EPIDEMIOLOGY-BASED RISK ASSESSMENT

The air quality inputs to the epidemiology-based risk assessment discussed in Chapter 7 were spatially averaged "composite monitor[6]" values for 12 of the 15 urban case study areas. The procedure for calculating these values is described in Appendix 4a. Figure 43 through Figure 54 show boxplots of the composite monitor daily maximum 8-hour values for observed air quality, air quality adjusted to meet the existing standard, and the potential alternative standards of 70 ppb, 65 ppb, and 60 ppb in the 12 urban areas in the epidemiology-based risk assessment. There are eight panels in each figure. The panels are designed to show contrasts based on three factors:

1. Spatial extent of the urban case study area: the top row of panels in each figure are based on the smaller areas from the Zanobetti & Schwartz, 2008 study (Z & S), , while the bottom row of panels are based on the larger Core Based Statistical Areas (CBSAs)..
2. Length of the $O_3$ season: the 1st and 3rd columns of panels in each figure are based on a shorter June – August $O_3$ season, which was used in Z&S, while the 2nd and 4th columns of panels are based on a longer April – October $O_3$ season. The Smith et al, 2009 study was based on the required $O_3$ monitoring season, which varied by area but often encompassed the April-October period.
3. Year: the two left-hand columns of panels in each figure are based on 2007, while the two right-hand columns of panels in each figure are based on 2009. The epidemiology-based risk assessment focused on these two years: 2007, to represent a year with higher $O_3$ concentrations, and 2009, to represent a year with lower $O_3$ concentrations.

There are a few properties common to nearly all of the figures. First, the highest composite monitor values represented by the top whiskers decrease when air quality is adjusted to meet the existing standard, and continue to decrease as air quality is further adjusted to meet lower alternative standard levels. By contrast, the lowest composite monitor values represented by the bottom whiskers increase when air quality is adjusted to meet the existing standard, and continue to increase as air quality is further adjusted to meet lower alternative standard levels. The behavior of the 25th percentile, median, mean, and 75th percentile values making up the boxes varies by urban area and across the three contrasting factors.

The spatial extent contrasts show that the base composite monitor values based on the smaller Z&S study areas tend to be slightly lower than the base composite monitor values based on the CBSAs. This is because the highest ozone concentrations are often located downwind of the urban area's population center, and the smaller Z&S areas often do not capture the highest

[6] Composite monitor values are calculated as the average of all monitors within each CBSA. See Appendix 4-A for more details.

observed concentrations. Two notable exceptions to this tendency are Atlanta and Sacramento, where the highest monitored concentrations are located near the population center. The spatial extent contrasts also show that when air quality is adjusted, the highest composite monitor values tend to decrease more quickly for the CBSAs than for the Z&S areas, and conversely the lowest composite monitor values tend to increase more slowly for the CBSAs than for the Z&S areas. This is consistent with observed air quality patterns, which show that as NOx emissions decrease, $O_3$ concentrations decrease more quickly downwind of the urban population center, and may increase near the population center due to less titration. This phenomenon also affects the center of the distribution, where we see that the 25$^{th}$ percentile, median, mean, and 75$^{th}$ percentile of the composite monitor values decrease more quickly for the CBSAs than for the Z&S areas. In cases where we see increases in these values, the values tend to increase more quickly for the Z&S areas than for the CBSAs.

The seasonal contrasts show that the composite monitor values based on observed air quality tend to be lower in the spring and fall months than in the summer months. The highest composite monitor values tend to occur in the June-August period, so the upper tail of the distribution often does not change, but the center and lower tail values are usually lower for the April-October period. One notable exception is Houston, where the highest $O_3$ concentrations are often observed in the spring and fall months. When $O_3$ concentrations are adjusted to meet the existing standard, there are many cases where net decreases in the 25$^{th}$ percentile, median, and mean composite monitor values for the June-August period turn into net increases in these values for the April-October period. When air quality is further adjusted to meet the potential alternative standards, initial increases in these values for the April–October period often persist, and in a few cases the increases grow larger as the level of the standard decreases. By contrast, initial increases in the 25$^{th}$ percentile, median, and mean composite monitor values are often reversed when air quality is further adjusted to meet the potential alternative standards.

Finally, the year contrasts are meant to show the effects of changes in emissions and meteorology on the composite monitor values. Precursor emissions were generally higher in 2007 than in 2009, and meteorological conditions were generally more favorable to ozone formation in 2007 than in 2009. Thus, the composite monitor values based on observed air quality are generally higher in 2007 than in 2009, with the exception of Houston, where the climate regime was the reverse of most of the rest of the U.S. during those two years. When air quality are adjusted to meet the existing and potential alternative standards, the decreases in the 2007 composite monitor values tend to be larger than in 2009, and there tend to be fewer increases. However, it is worth noting that since the emissions and meteorological inputs used in the CMAQ/HDDM modeling for the air quality adjustments were based on 2007 data, we tend to have more confidence in the adjusted values for 2007 than for 2009.

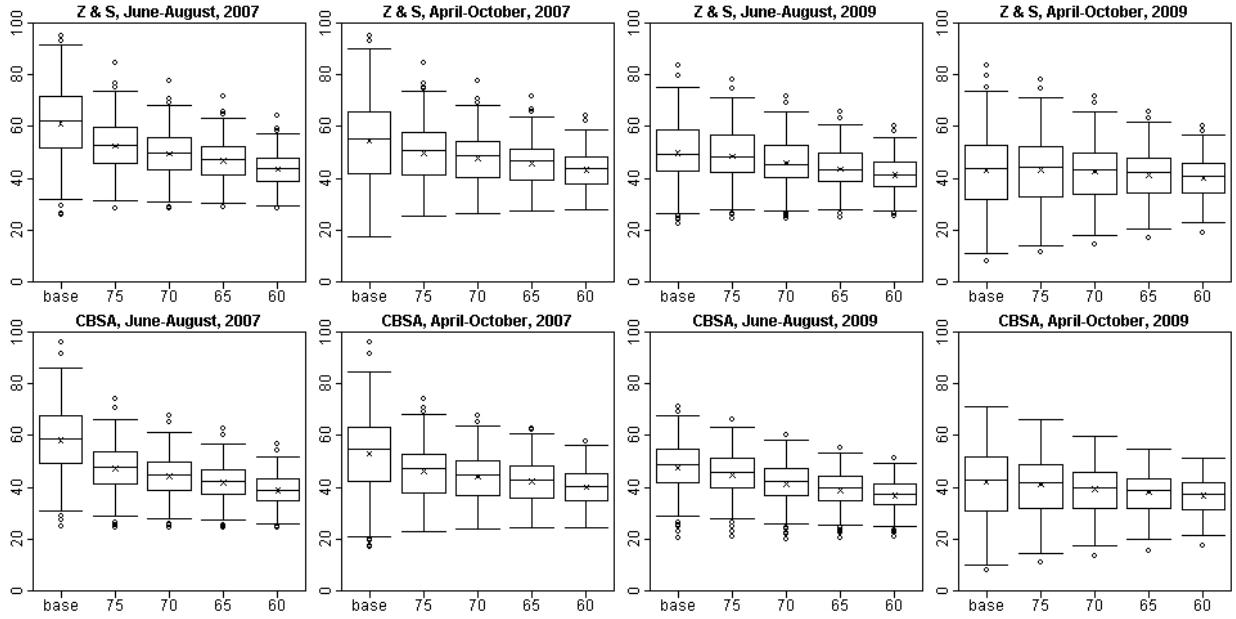


**Figure 43: Composite monitor daily maximum 8-hour $O_3$ values for Atlanta based on observed and adjusted air quality.**

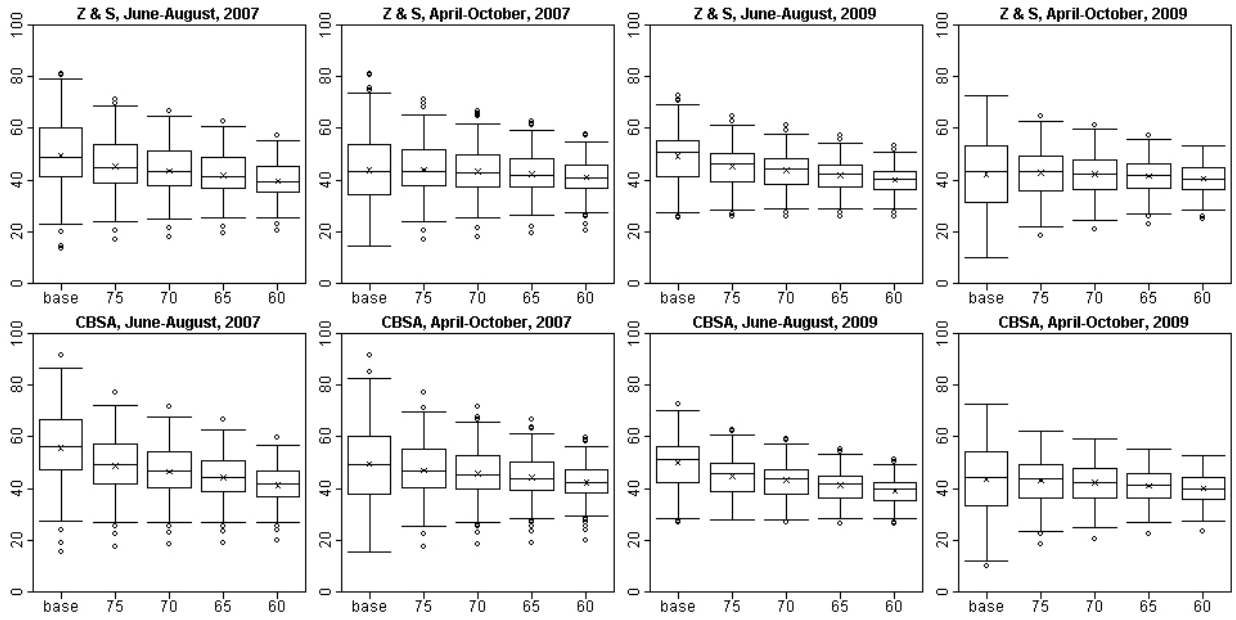


**Figure 44: Composite monitor daily maximum 8-hour $O_3$ values for Baltimore based on observed and adjusted air quality.**

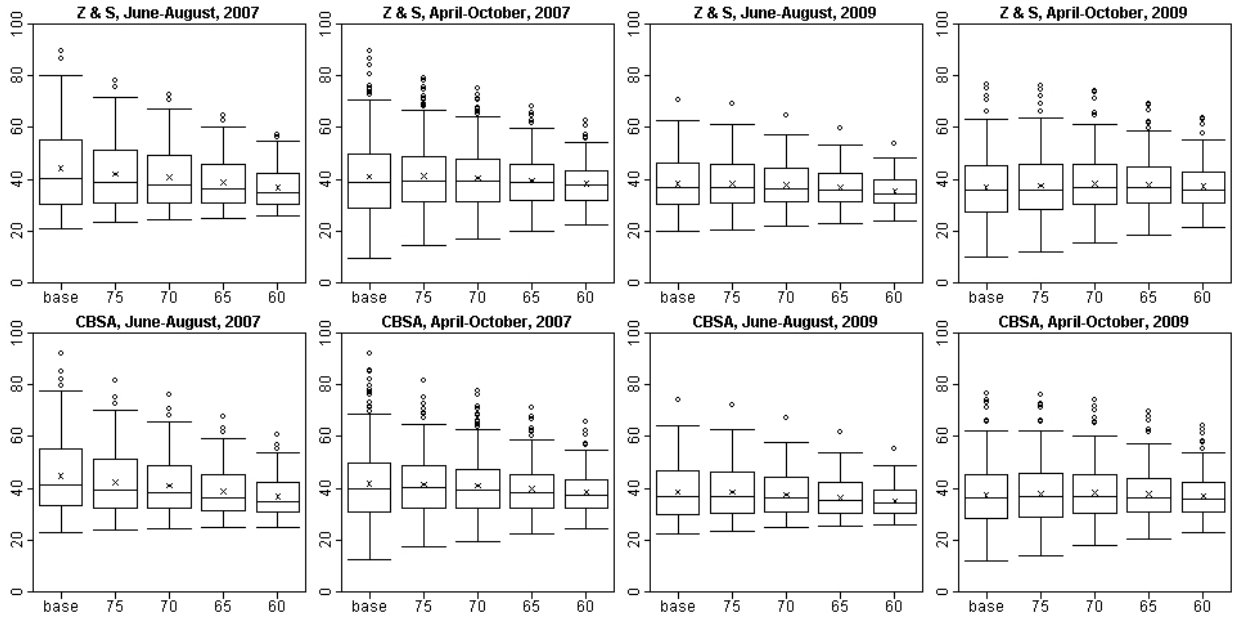


**Figure 45: Composite monitor daily maximum 8-hour $O_3$ values for Boston based on observed and adjusted air quality.**

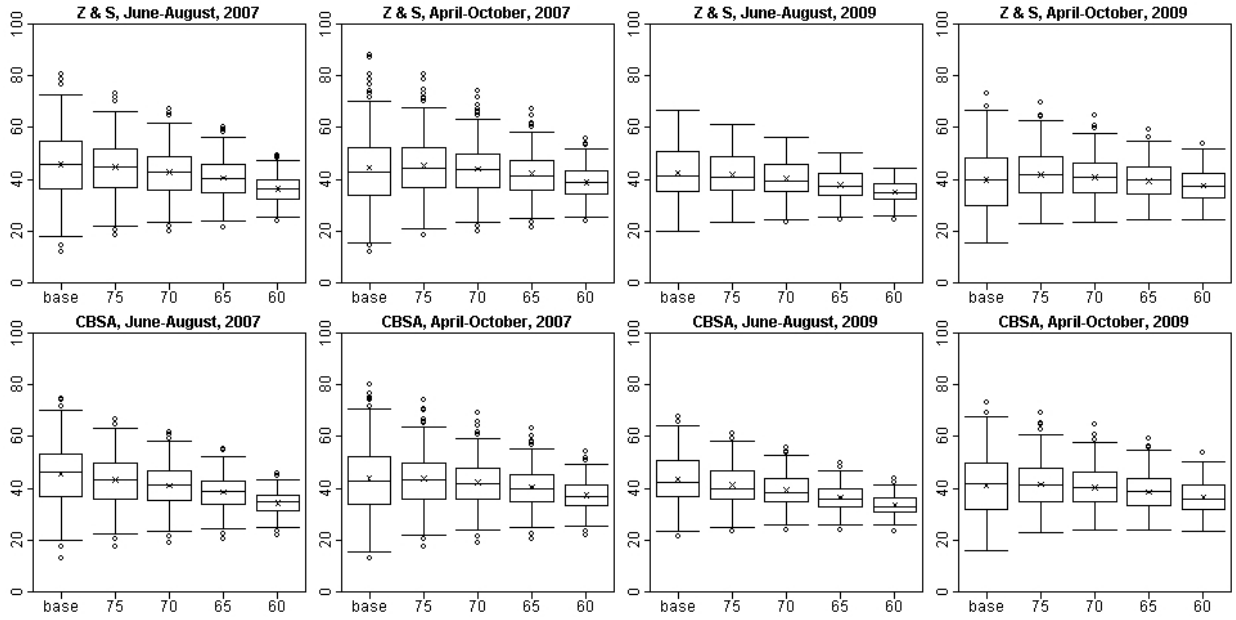


**Figure 46: Composite monitor daily maximum 8-hour $O_3$ values for Cleveland based on observed and adjusted air quality.**

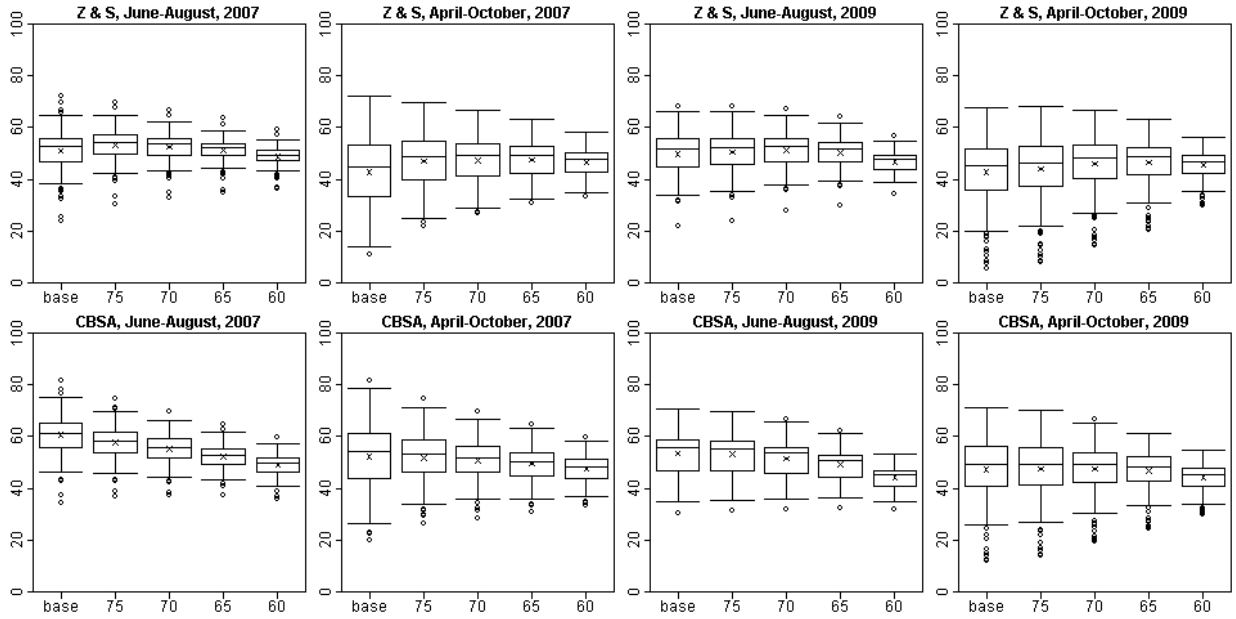


**Figure 47: Composite monitor daily maximum 8-hour $O_3$ values for Denver based on observed and adjusted air quality.**

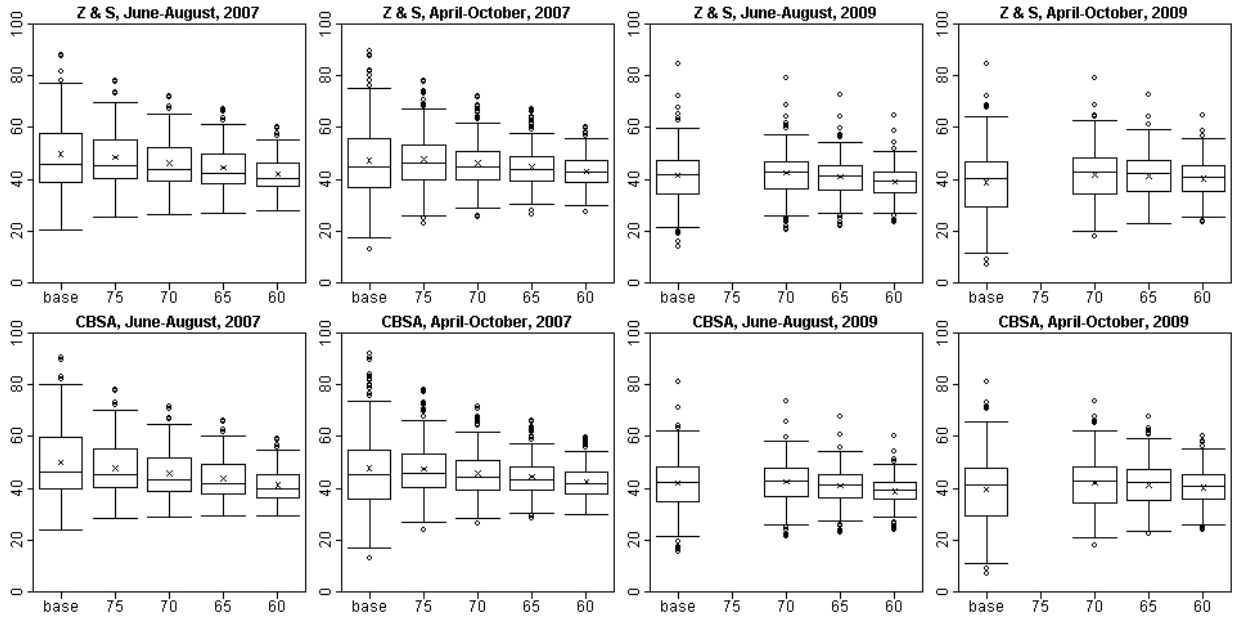


**Figure 48: Composite monitor daily maximum 8-hour $O_3$ values for Detroit based on observed and adjusted air quality.**

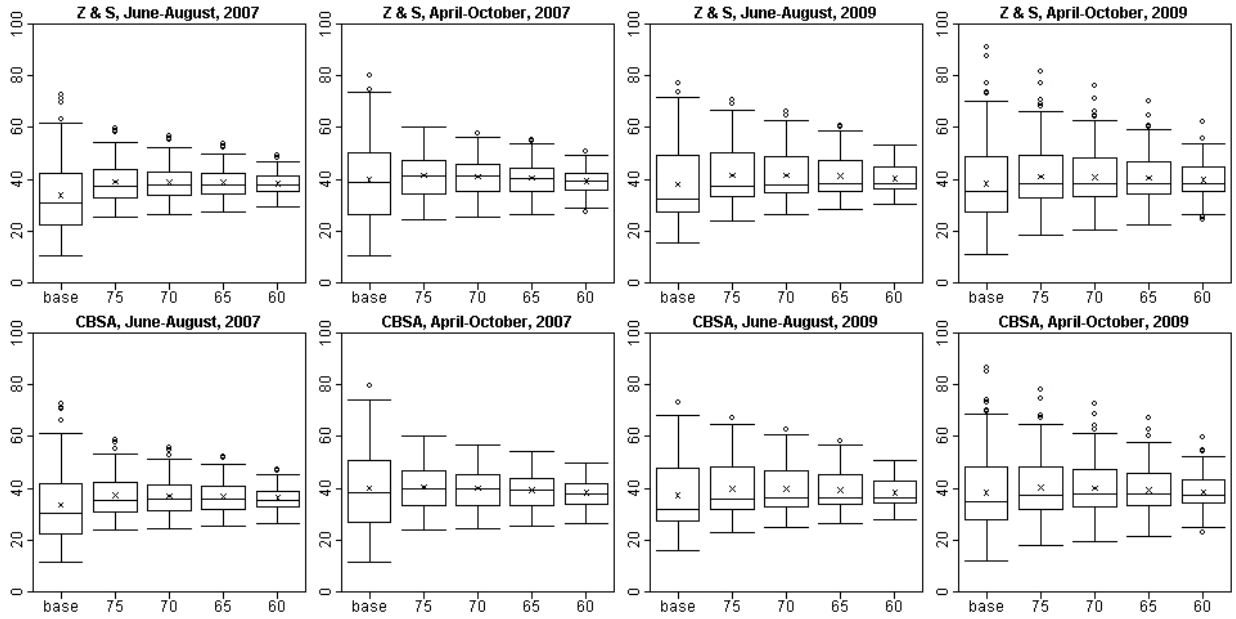


**Figure 49: Composite monitor daily maximum 8-hour $O_3$ values for Houston based on observed and adjusted air quality.**

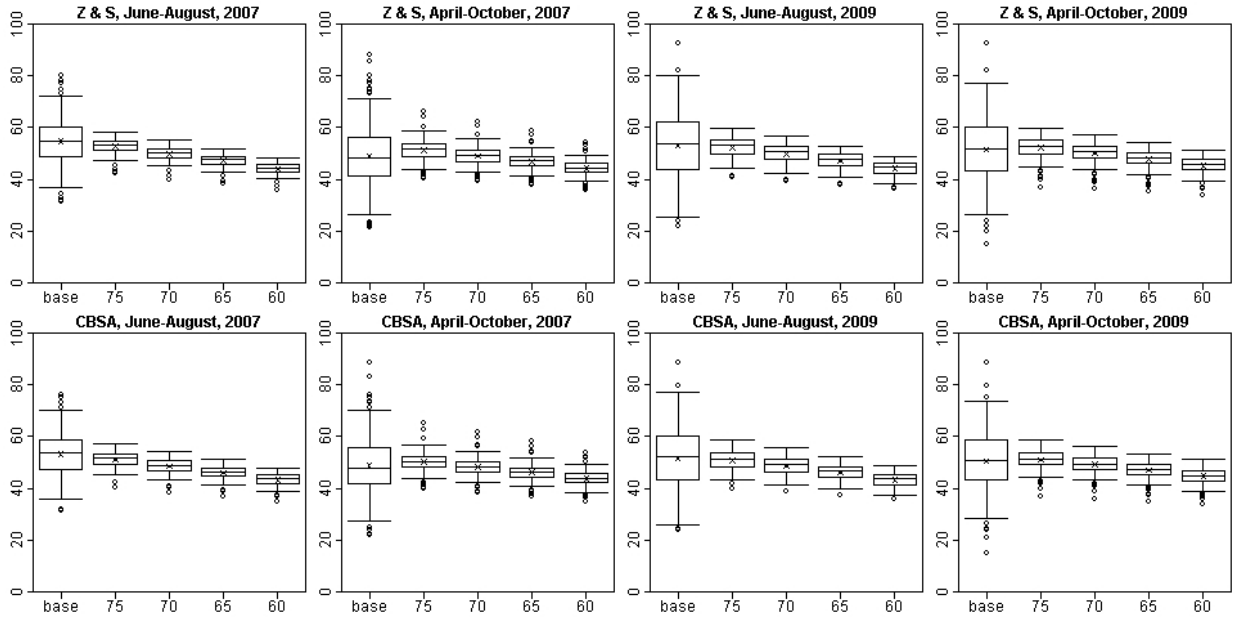


**Figure 50: Composite monitor daily maximum 8-hour $O_3$ values for Los Angeles based on observed and adjusted air quality.**

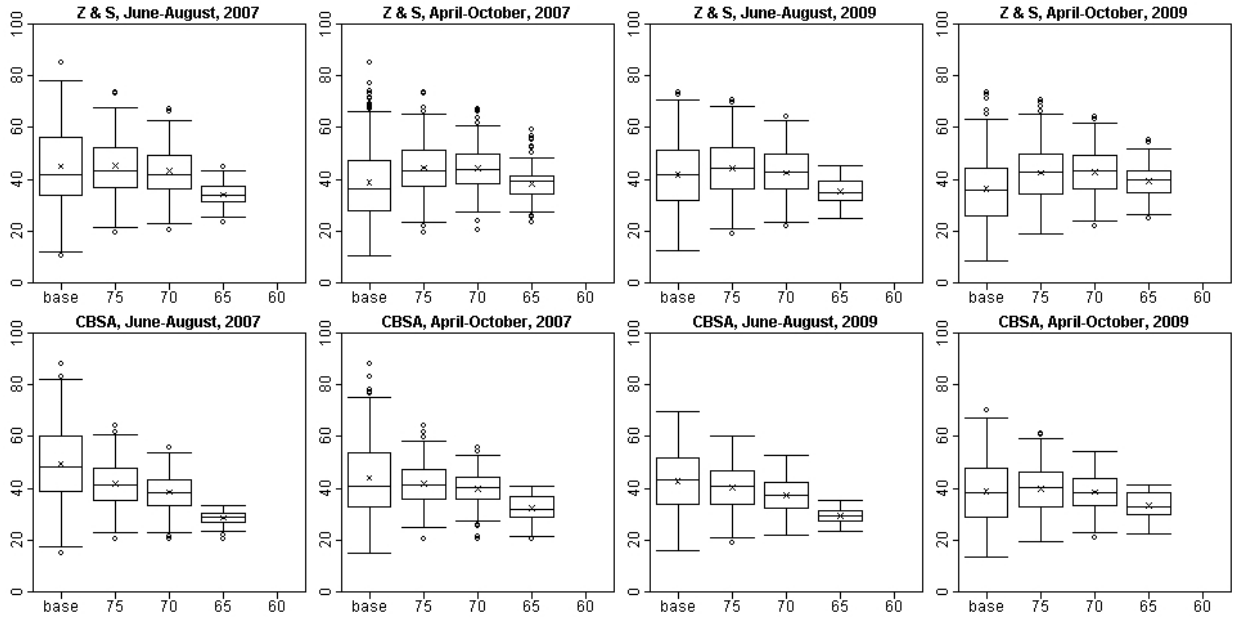


**Figure 51: Composite monitor daily maximum 8-hour $O_3$ values for New York based on observed and adjusted air quality.**

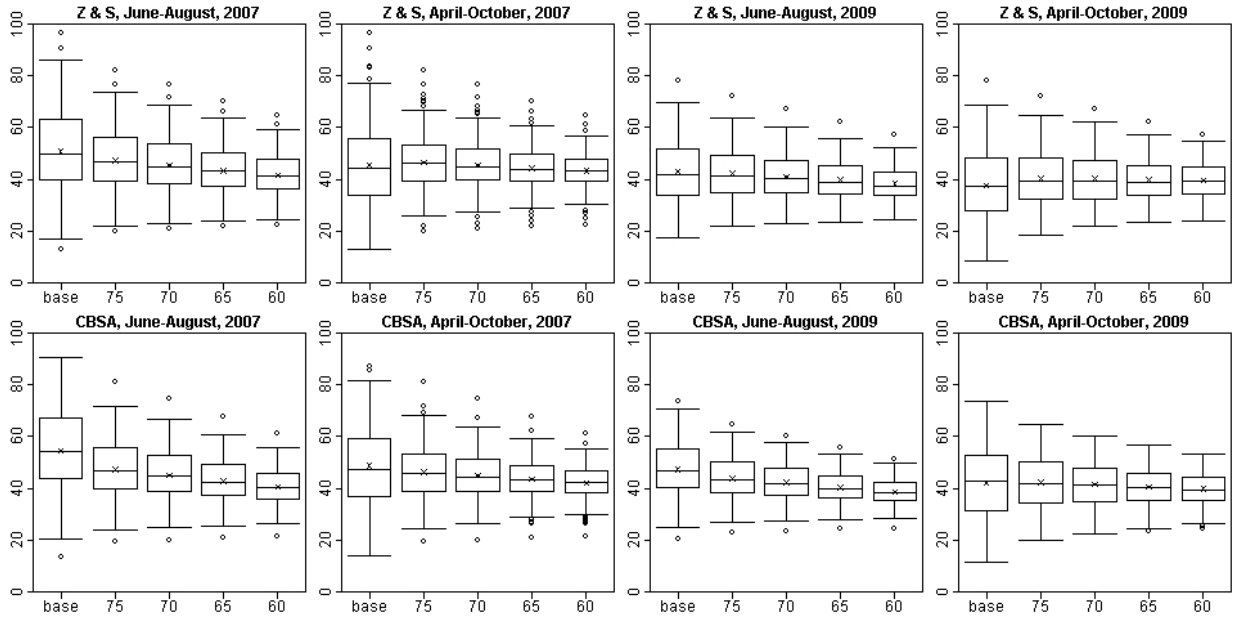


**Figure 52: Composite monitor daily maximum 8-hour $O_3$ values for Philadelphia based on observed and adjusted air quality.**

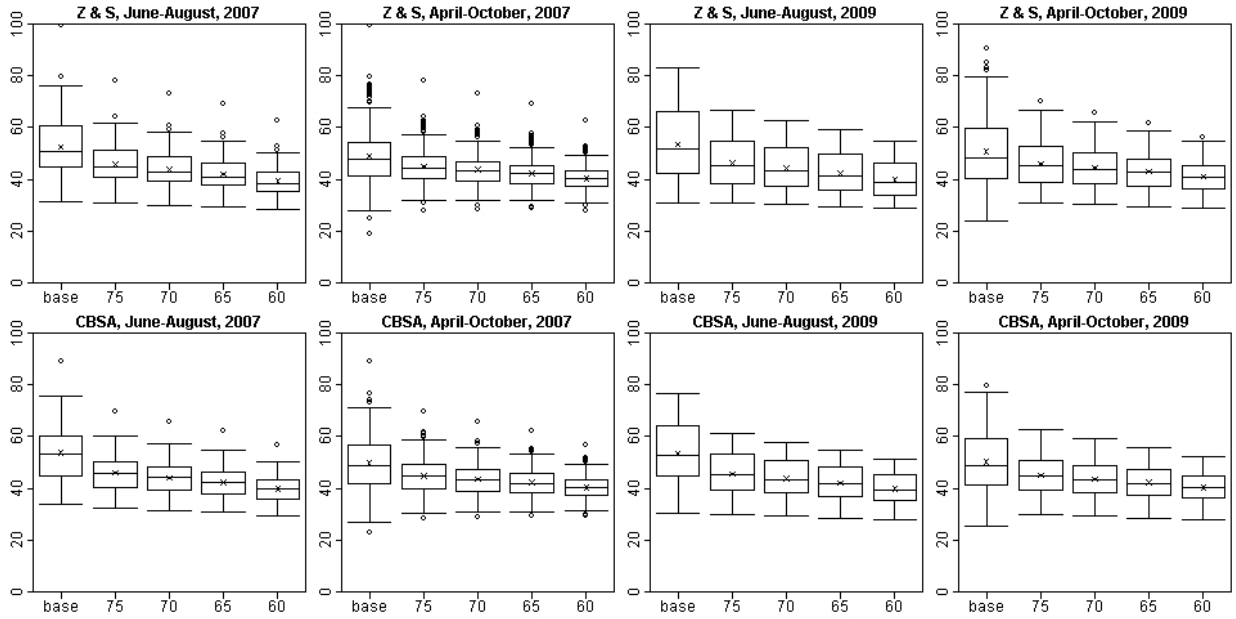


**Figure 53: Composite monitor daily maximum 8-hour $O_3$ values for Sacramento based on observed and adjusted air quality.**

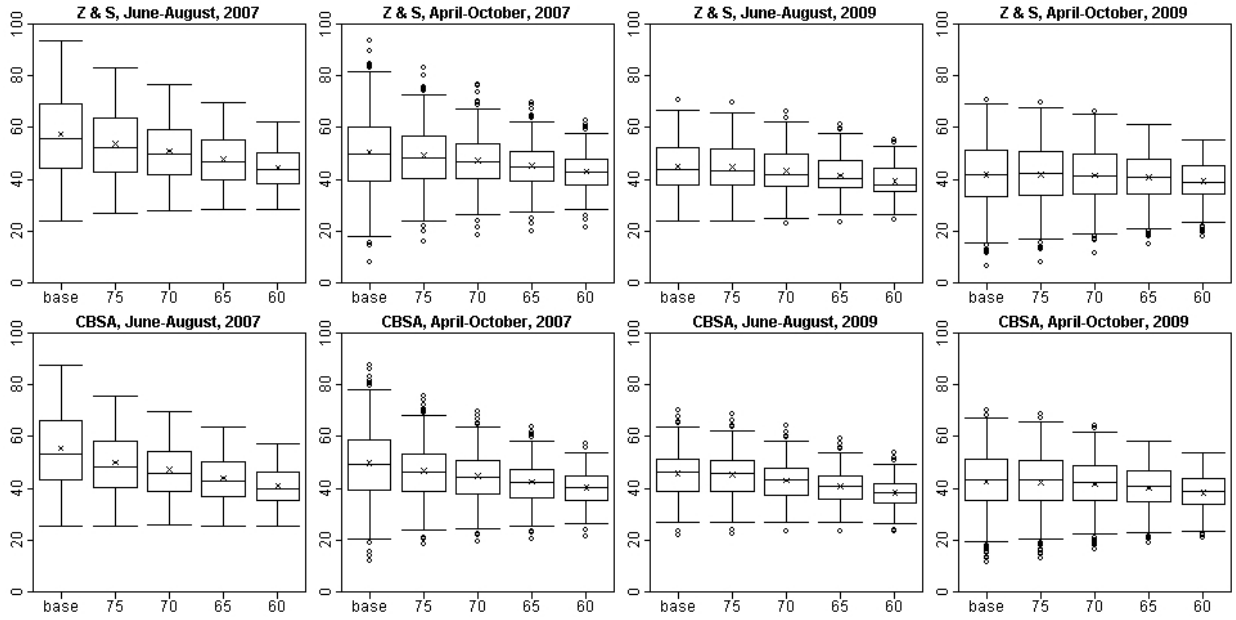


**Figure 54: Composite monitor daily maximum 8-hour $O_3$ values for St. Louis based on observed and adjusted air quality.**

## 4.6 AIR QUALITY INPUTS FOR THE EXPOSURE AND CLINICAL RISK ASSESSMENT

The air quality inputs for the exposure and clinical risk assessments discussed in Chapters 5 and 6 include spatial surfaces of hourly $O_3$ concentrations estimated for each census

tract in the 15 urban case study areas using the Voronoi Neighbor Averaging (VNA) technique. A description of the VNA technique and its application to ambient concentrations are provided in Appendix 4a. In this section, we present three types of figures which summarize the data from the hourly VNA surfaces for observed air quality, air quality adjusted to meet the existing standard[7], and air quality adjusted to meet the potential alternative standard of 65 ppb.

The first set of figures (Figure 55 through Figure 69) show density scatter plots of the change in daily maximum 8-hour average (MDA8) $O_3$ concentrations versus the observed concentration based on the hourly VNA estimates in each area. In each of these figures, the left-hand panels show the observed MDA8 values (x-axis) versus the change in those values that occur when air quality is adjusted to meet the existing standard (y-axis). The right-hand panels show the MDA8 values for air quality adjusted to meet the existing standard[7] (x-axis) versus the additional change in those values that occur when air quality is further adjusted to meet the alternative standard of 65 ppb (y-axis). The top panels show values based on 2006-2008, while the bottom panels show values based on 2008-2010. Within each panel, the x and y values are rounded to the nearest integer and colored to show the relative frequency of each 1 ppb x 1 ppb square within the plot region. Values falling outside of the plot region were set to the nearest value within the plot region, and frequencies above the range in the color bar were set to the highest value within the color bar.

The second set of figures (Figure 70 through Figure 99) show maps of the changes in design values (3-year average of the annual 4$^{th}$ highest MDA8 values) and May – September average MDA8 values based on the ambient data and the hourly VNA surfaces. There are two figures for each of the 15 urban case study areas, one based on 2006-2008 and one based on 2008-2010. In each figure, the panels on the left show the changes in these values that occur when air quality is adjusted to meet the existing standard[7], and the panels on the right show the additional changes in these values that occur when air quality is further adjusted to meet the alternative standard of 65 ppb. The top panels show the changes in the design values, while the bottom panels show the changes in the May – September average MDA8 values. Within each panel, squares show values based on observed data at ambient $O_3$ monitoring sites while circles show values based on VNA estimates at census tract centroids. Regions shaded pink indicate counties in either the Zanobetti & Schwartz, 2008 or the Smith et al, 2009 studies (for the 12 cities in the epidemiology-based risk assessment). The Zanobetti & Schwartz and Smith et al study areas had some counties in common in all 12 cities, and were identical in 6 of the cities. Regions shaded gray indicate additional counties in the CBSA, and regions shaded peach

[7] Chicago and Detroit were already meeting the existing standard in 2008-2010. The 2008-2010 figures for those areas are based on air quality adjusted to meet the 70 ppb alternative standard instead of the existing standard.

indicate any additional counties in the study areas for the exposure and clinical risk assessment. The maps also show some monitors which are located outside of the exposure study areas. These monitors were adjusted along with the other monitors and used in the VNA estimates, but were not used when determining the emissions reductions necessary to meet the various standards.

The third set of figures (Figure 100 through Figure 114) show changes in design values (3-year average of the annual 4$^{th}$ highest MDA8 values) and May – September average MDA8 values in the 15 urban case study areas versus population and population density. The population total and population density information for each census tract were obtained from the U.S. Census Bureau based on the 2010 U.S. Census. Within each figure, the top panels show histograms of the total population stratified by the change in design value or seasonal average, while the bottom panels show scatter plots of population density (x-axis) versus change in design value or seasonal average (y-axis). The left-hand panels are based on 2006-2008, while the right-hand panels are based on 2008-2010. The first and third rows of panels show changes in design values, while the second and fourth rows of panels show changes in May-September average values. Finally, the first and third columns show the changes that occur when air quality is adjusted to meet the existing standard[7], while the second and fourth columns show the additional changes that occur when air quality is further adjusted to meet the alternative standard of 65 ppb. Within each panel, values associated with census tracts falling within the epidemiology study areas as defined previously are colored pink, values associated with additional census tracts falling within the CBSA are colored gray, and values associated with any additional census tracts falling within the exposure study areas are colored peach. Population density values are shown on a logarithmic scale, with values falling outside of the plot region set to the nearest values within the plot region.

In general, the density scatter plots show that the HDDM adjustment procedure predicts increases in MDA8 $O_3$ at low ambient concentrations, and decreases in MDA8 $O_3$ at high concentrations. The vast majority of the increases in MDA8 $O_3$ occur at ambient concentrations below 50 ppb. The relationship between the starting concentrations and the changes in these values based on the HDDM adjustments is fairly linear with strong negative correlation in all 15 urban areas. In some areas, such as Baltimore and Philadelphia, there is a bimodal pattern near the center of the distribution, which may be indicative of differing behavior in the urban population center versus the surrounding suburban areas.

The maps reveal several trends in the spatial pattern of changes in $O_3$ in the urban case study areas. The design values decreased almost universally when air quality was adjusted to

meet the existing standard with a few exceptions[8], and continued to decrease when air quality was further adjusted to meet the 65 ppb alternative standard. The design values also tended to decrease more quickly in suburban and rural areas than in the urban population centers. The May-September "seasonal" average MDA8 values also followed this trend to some extent. However, the decreases in the seasonal average values were nearly universal in the suburban and rural areas, while the behavior in the urban population centers varied amongst the cities. The seasonal average values in the urban population centers followed one of three distinct patterns:

1. The seasonal average values decreased when air quality was adjusted to meet the existing standard, and continued to decrease when air quality was further adjusted to meet the 65 ppb alternative standard. (Atlanta, Sacramento, Washington D.C.)
2. The seasonal average values increased or remained constant when air quality was adjusted to meet the existing standard, then decreased when air quality was adjusted to meet the 65 ppb alternative standard. (Baltimore, Cleveland, Dallas, Detroit, Los Angeles, New York, Philadelphia, St. Louis)
3. The seasonal average values increased when air quality was adjusted to meet the existing standard, and continued to increase or remained constant when air quality was further adjusted to meet the 65 ppb alternative standard. (Boston, Chicago, Houston, Denver)

The population plots show a clear and consistent trend regarding the populations living in areas associated with various changes in design values and seasonal average concentrations. In almost every figure, there is a positive correlation between population density and change in design value or seasonal average concentration. This suggests that in almost every scenario, when NOx emissions were reduced, the suburban areas surrounding the urban population center experience more $O_3$ reductions than in the urban population center. For the 12 urban areas examined in the epidemiology-based risk assessment, the vast majority of the locations associated with increases in the seasonal average concentration occurred within the epidemiology study area, which tended to be focused on the urban population center.

These figures show that using the HDDM adjustment methodology, peak $O_3$ concentrations are reduced in urban areas with large domain-wide reductions in U.S. anthropogenic NOx emissions. In most cases, seasonal average $O_3$ concentrations also decreased with large domain-wide reductions in U.S. anthropogenic NOx emissions. However,

[8] All design values from the VNA surfaces decreased when going from recent conditions to the 75 ppb adjustment scenario with the exceptions of small areas in Boston where design values increased by up to 1 ppb (2008-2010), Chicago where design values increased by up to 2 ppb (2006-2008) and 4 ppb (2008-2010) and New York where design values increased by up to 3 ppb (2008-2010). All areas in which design values increases started with very low design values based on recent conditions.

there were a few cases, such as Chicago and Houston, where current NOx emissions were high enough to cause titration in the urban population centers so that seasonal average $O_3$ concentrations were below regional background levels.

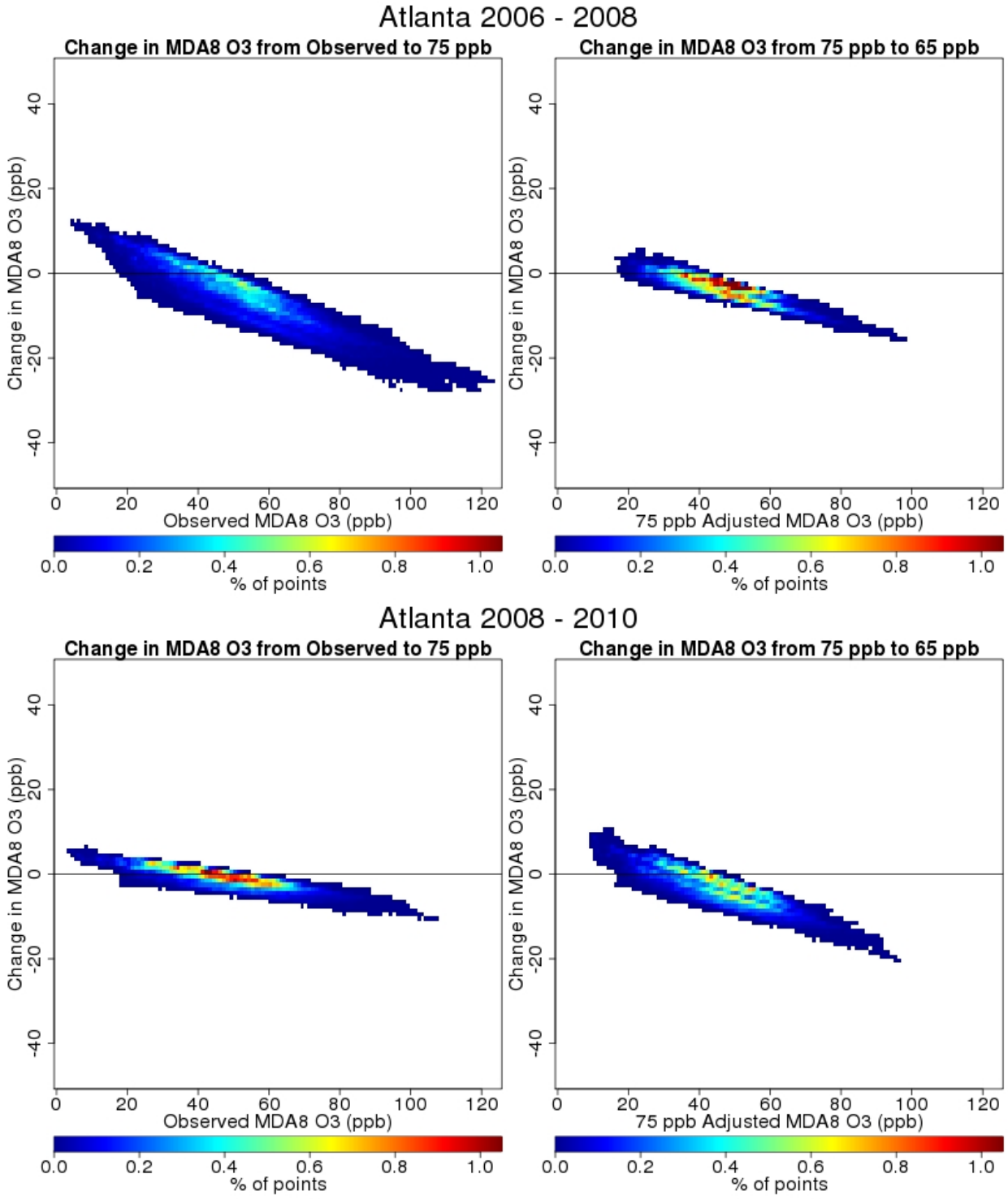


**Figure 55: Change in VNA estimates of the daily maximum 8-hour average (MDA8) $O_3$ concentrations based on HDDM adjustments in Atlanta.**

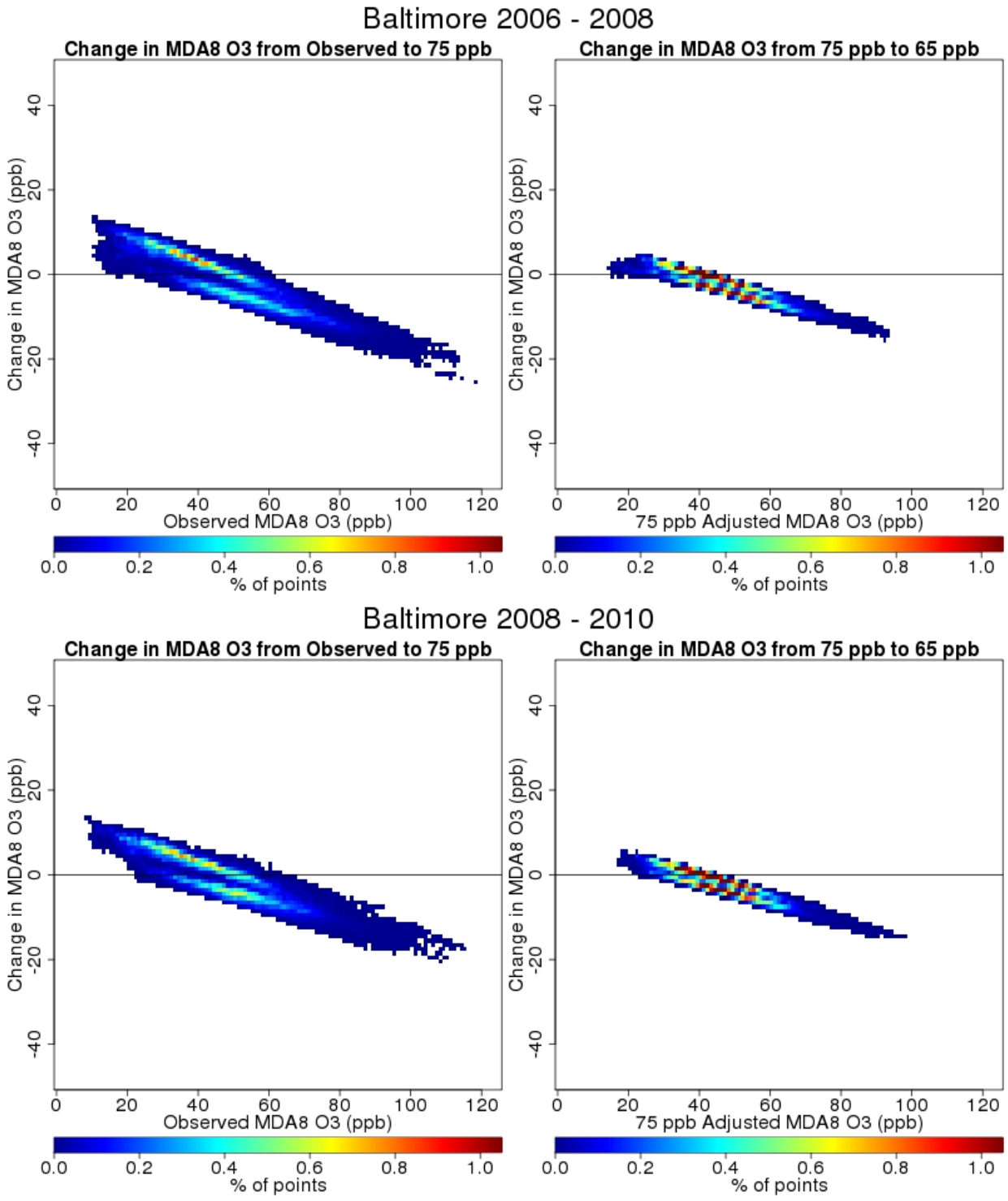


**Figure 56: Change in VNA estimates of the daily maximum 8-hour average (MDA8) $O_3$ concentrations based on HDDM adjustments in Baltimore.**

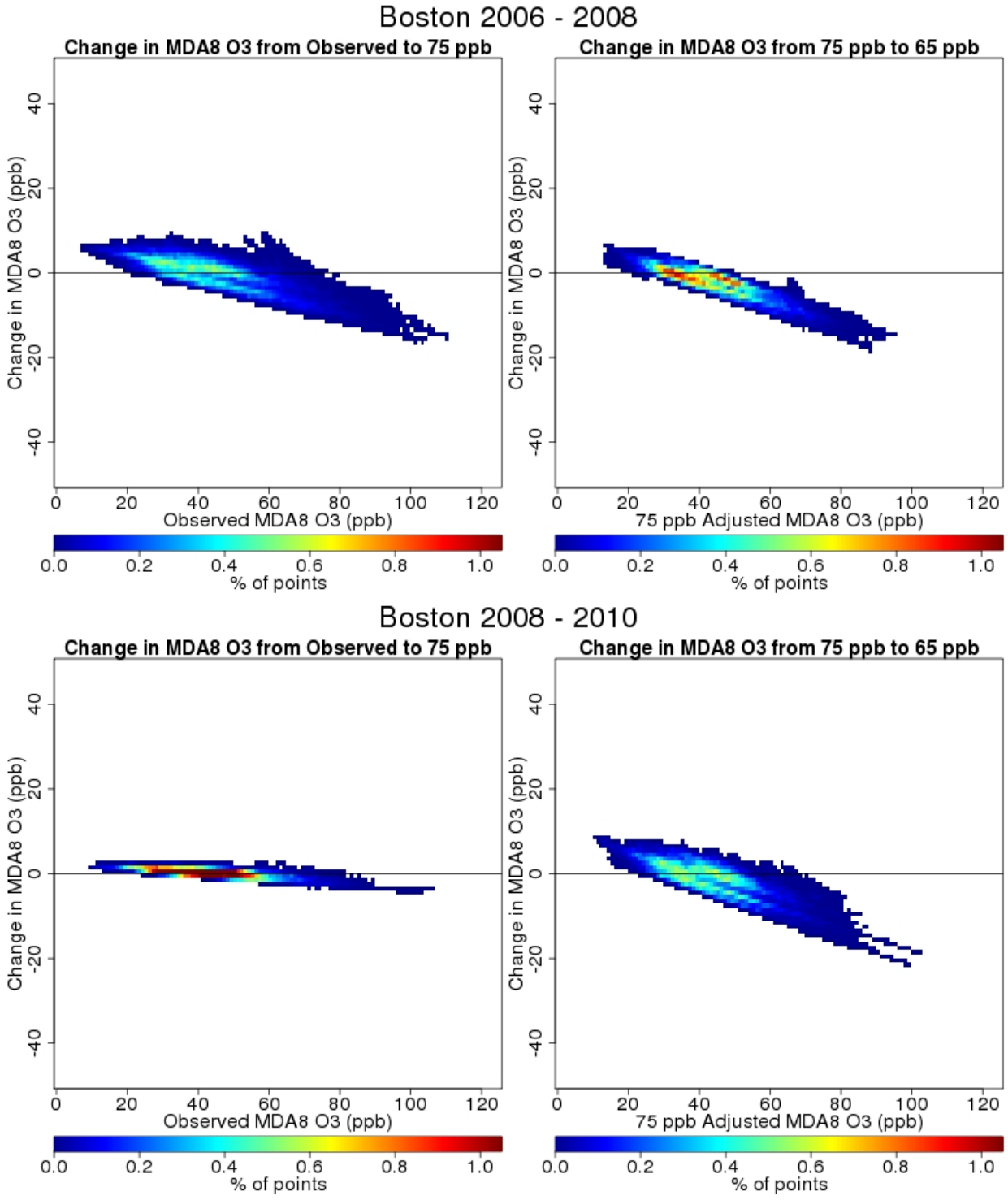


**Figure 57: Change in VNA estimates of the daily maximum 8-hour average (MDA8) $O_3$ concentrations based on HDDM adjustments in Boston.**

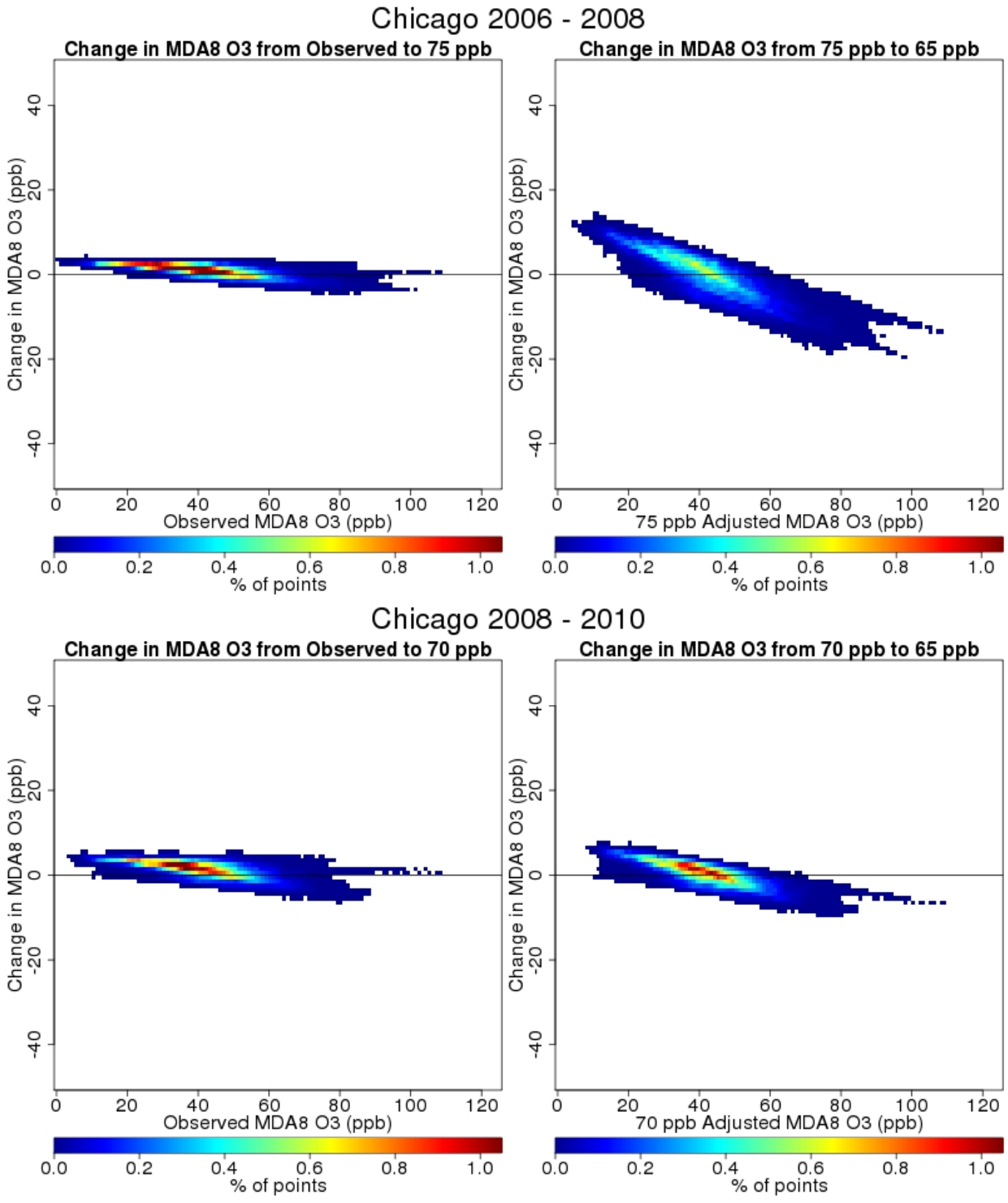


**Figure 58: Change in VNA estimates of the daily maximum 8-hour average (MDA8) $O_3$ concentrations based on HDDM adjustments in Chicago.**

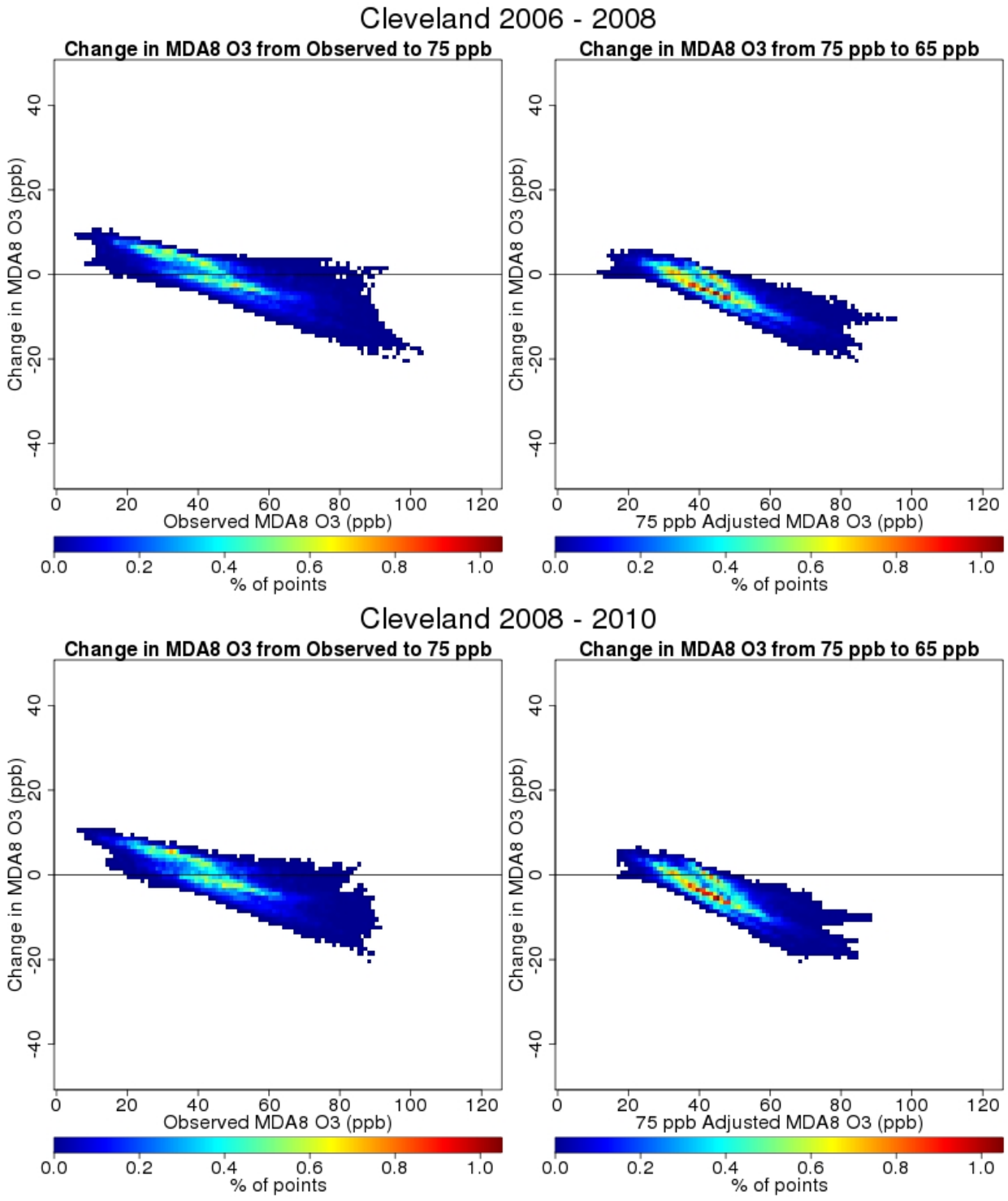


**Figure 59: Change in VNA estimates of the daily maximum 8-hour average (MDA8) $O_3$ concentrations based on HDDM adjustments in Cleveland.**

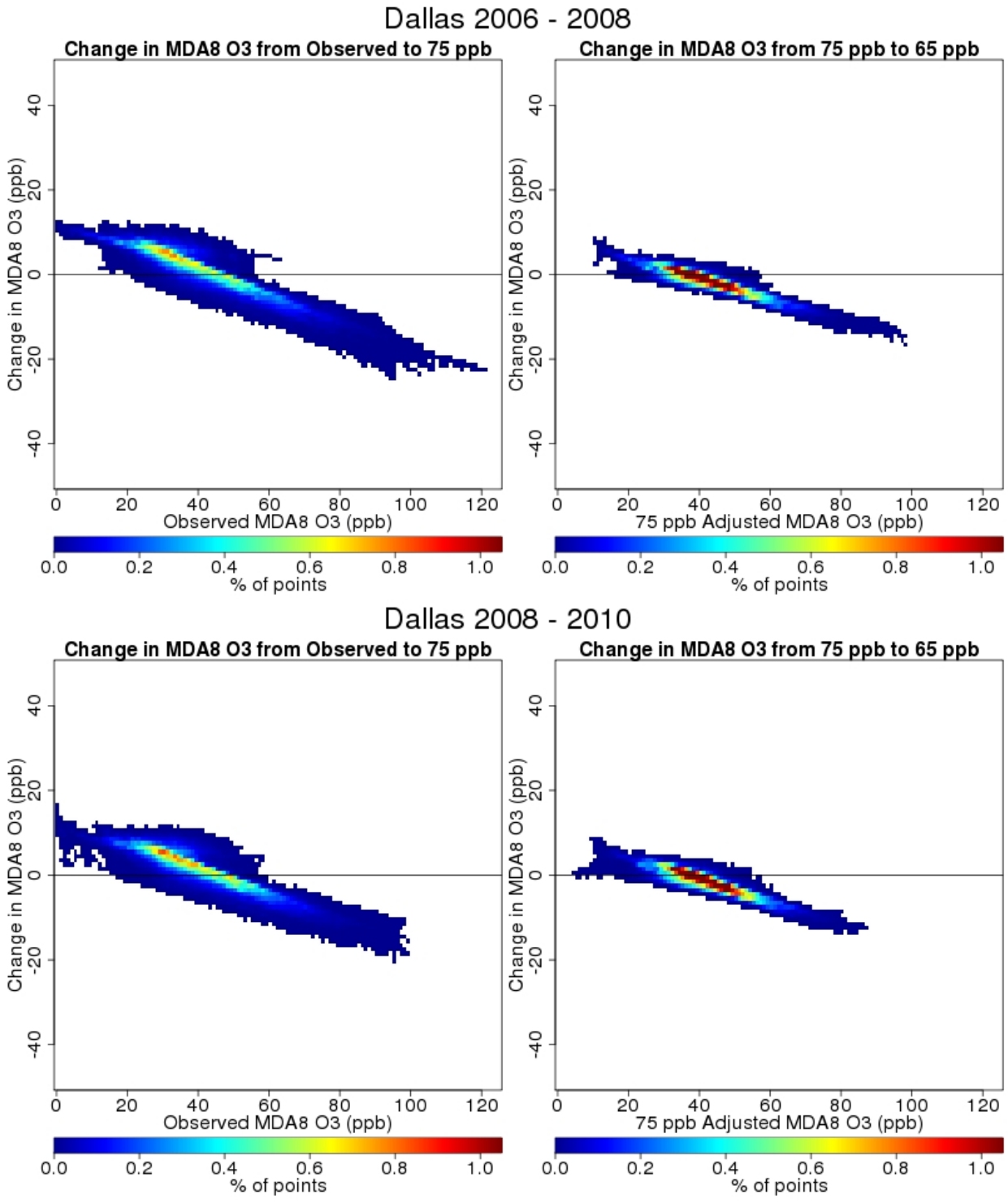


**Figure 60: Change in VNA estimates of the daily maximum 8-hour average (MDA8) $O_3$ concentrations based on HDDM adjustments in Dallas.**

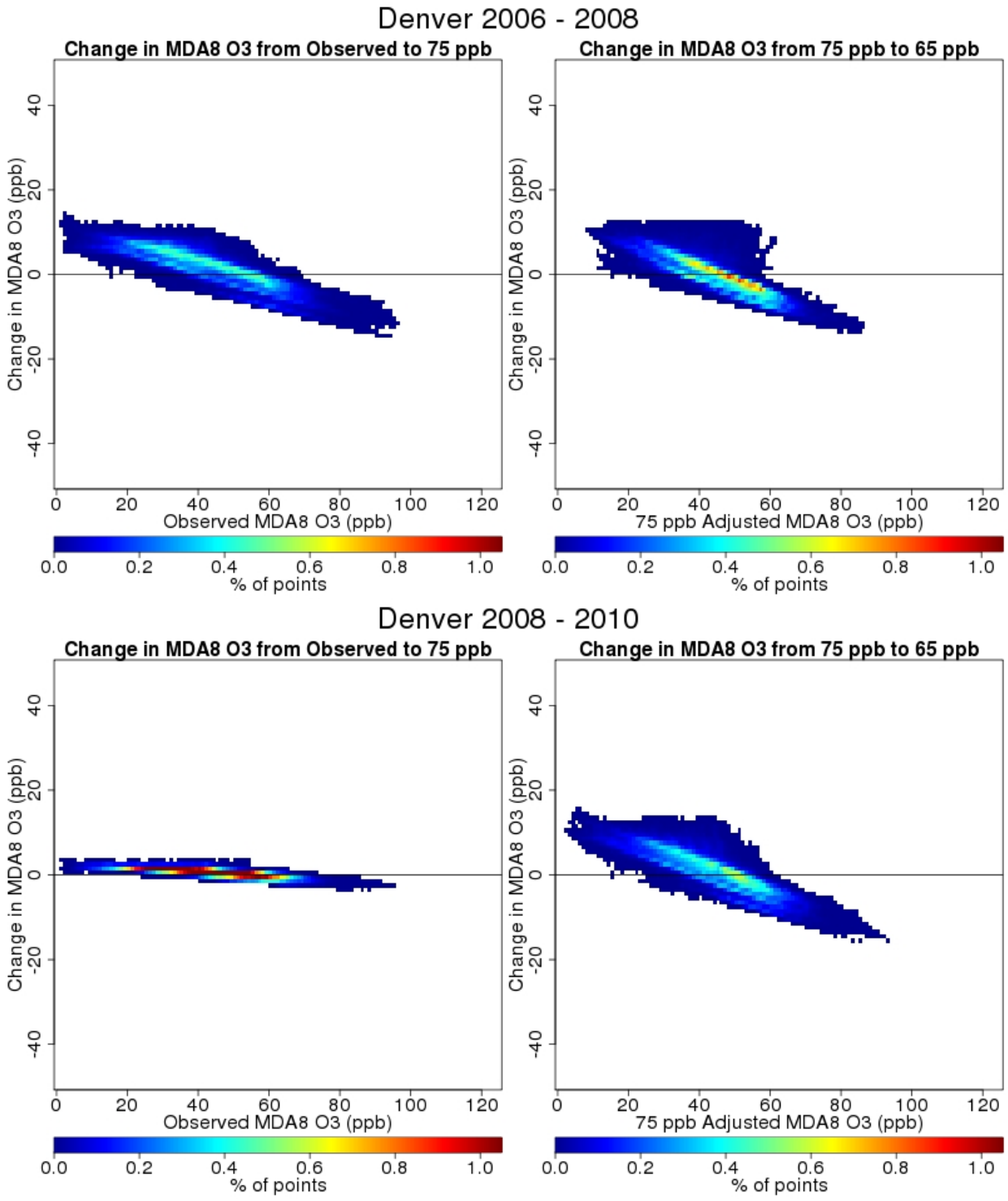


**Figure 61: Change in VNA estimates of the daily maximum 8-hour average (MDA8) $O_3$ concentrations based on HDDM adjustments in Denver.**

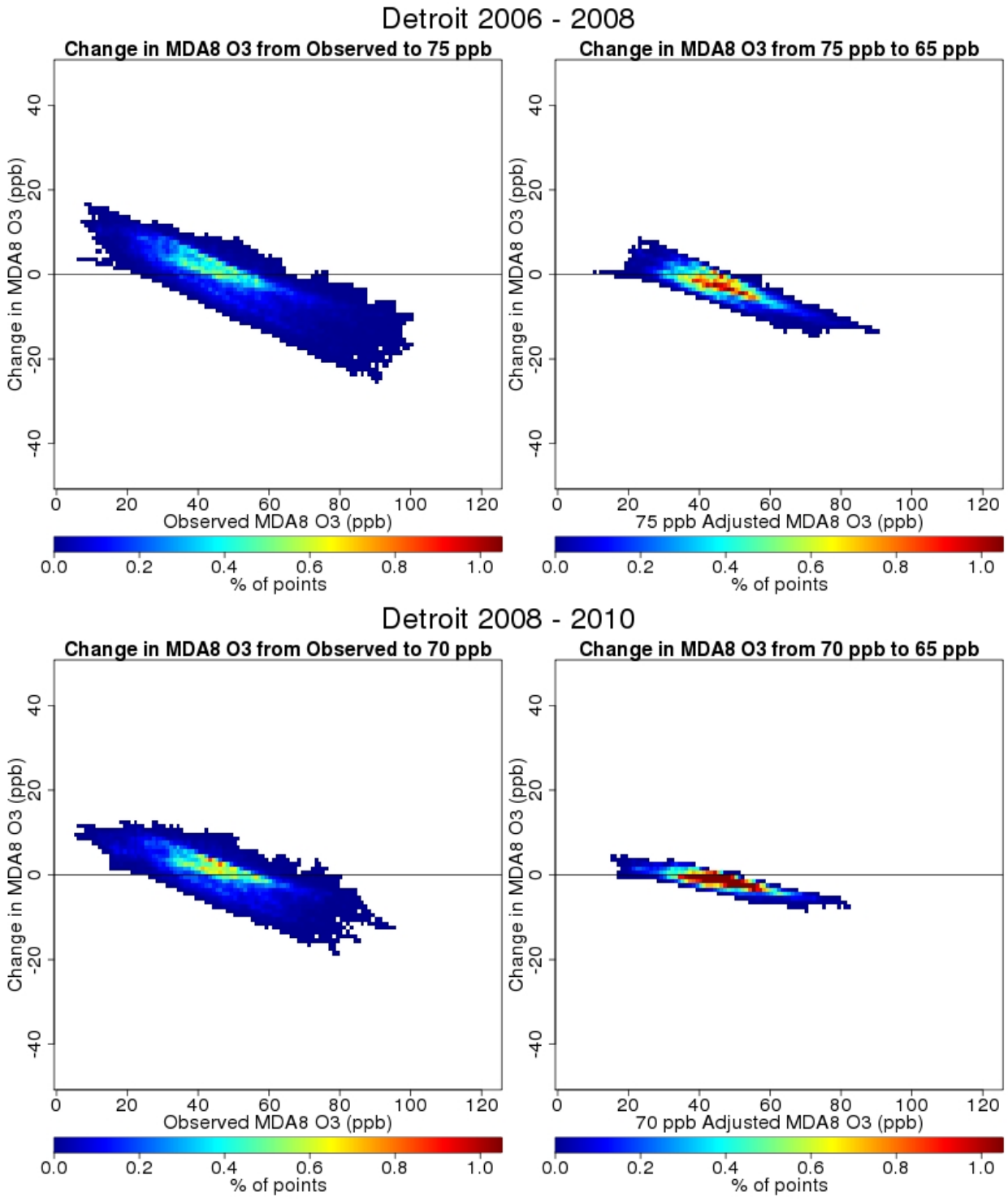


**Figure 62: Change in VNA estimates of the daily maximum 8-hour average (MDA8) $O_3$ concentrations based on HDDM adjustments in Detroit.**

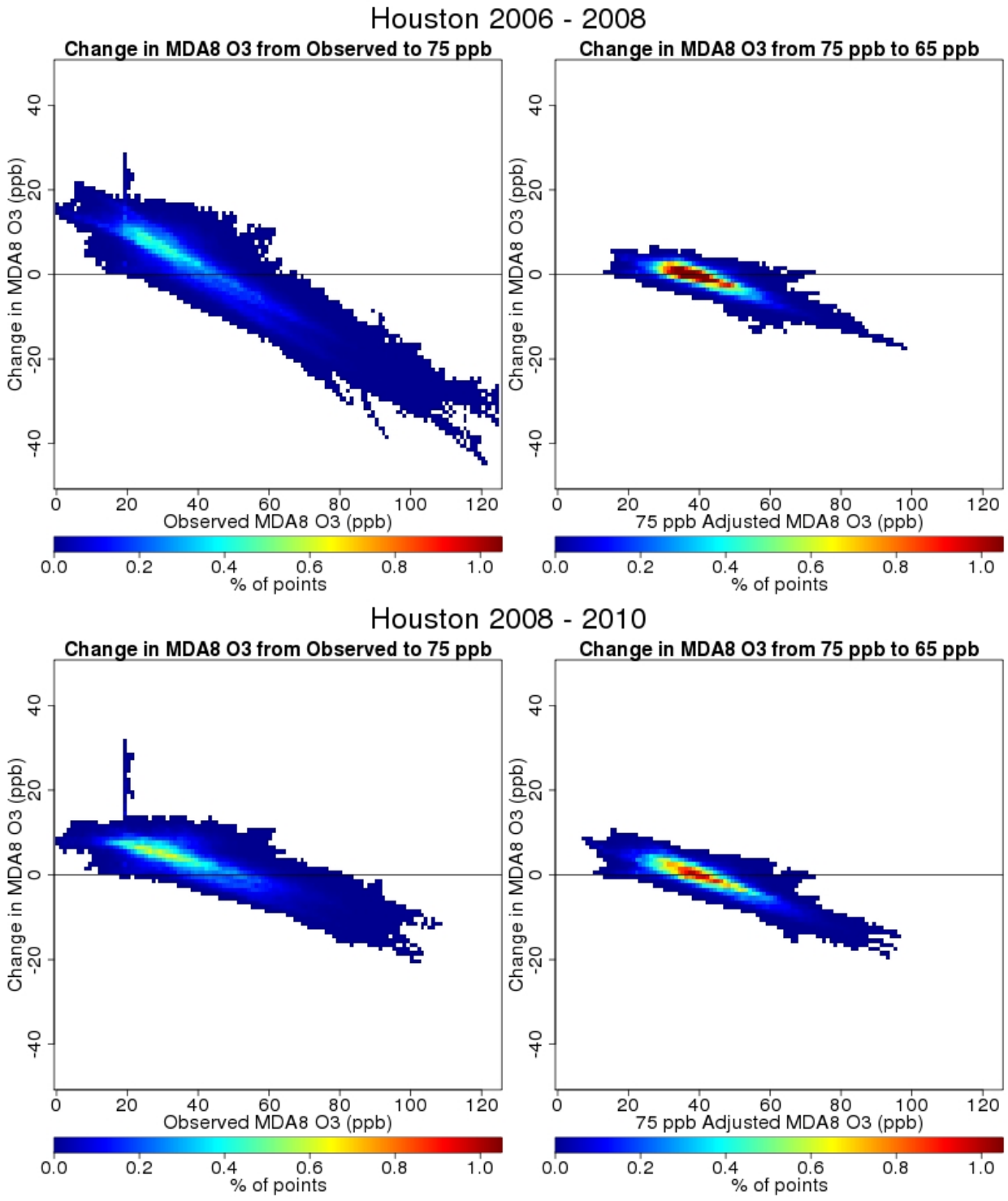


**Figure 63: Change in VNA estimates of the daily maximum 8-hour average (MDA8) $O_3$ concentrations based on HDDM adjustments in Houston.**

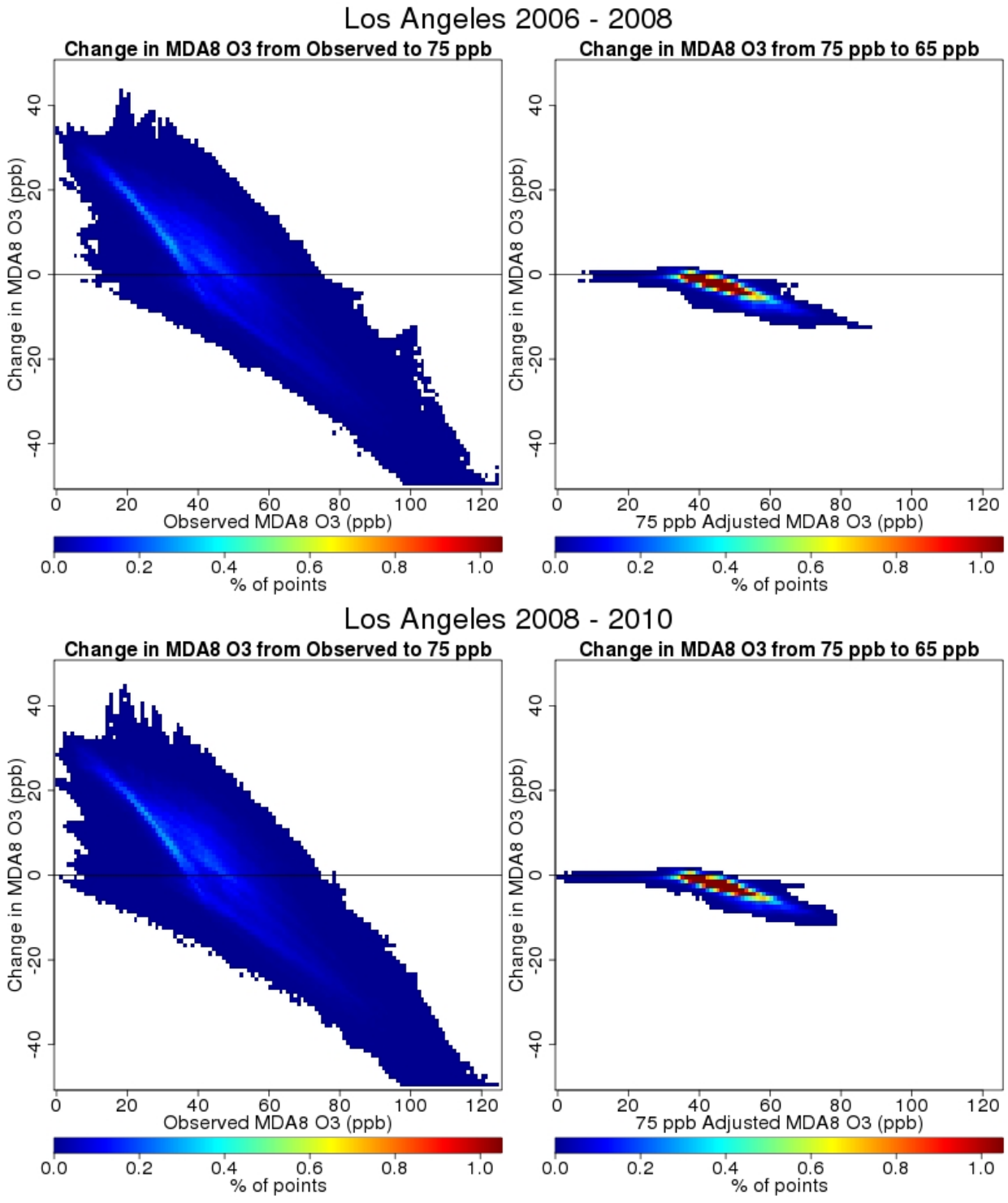


**Figure 64: Change in VNA estimates of the daily maximum 8-hour average (MDA8) $O_3$ concentrations based on HDDM adjustments in Los Angeles.**

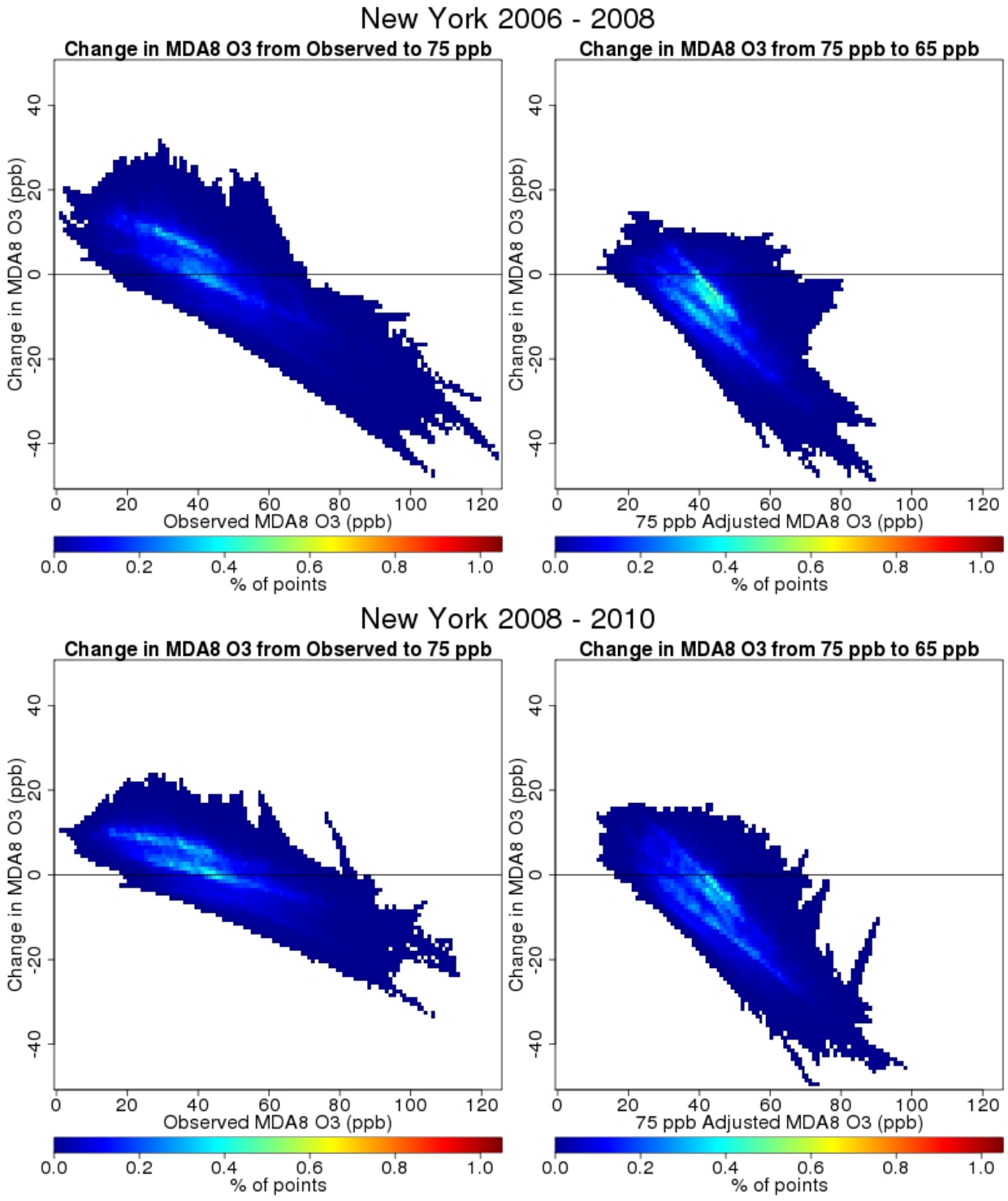


**Figure 65: Change in VNA estimates of the daily maximum 8-hour average (MDA8) $O_3$ concentrations based on HDDM adjustments in New York.**

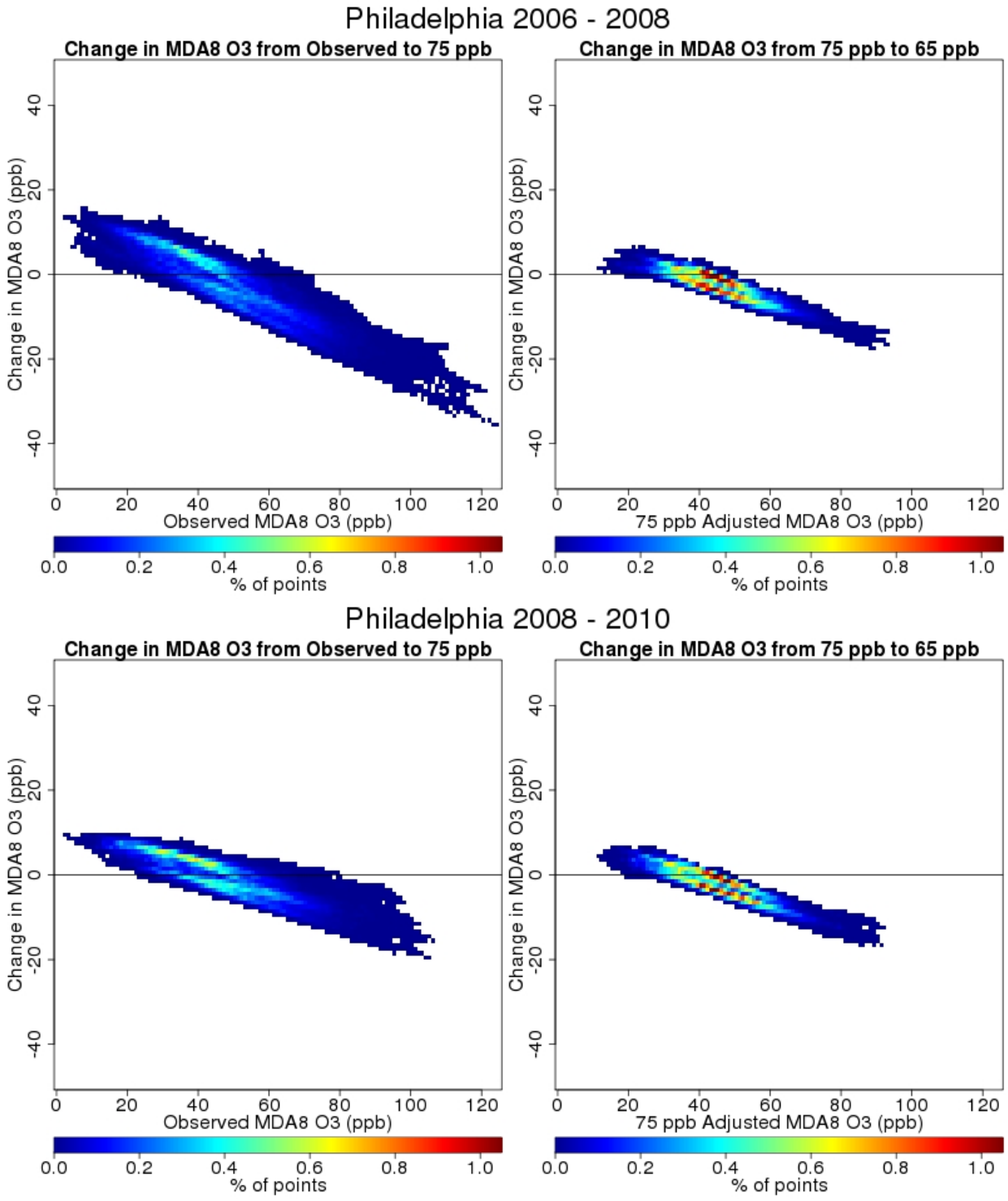


**Figure 66: Change in VNA estimates of the daily maximum 8-hour average (MDA8) $O_3$ concentrations based on HDDM adjustments in Philadelphia.**

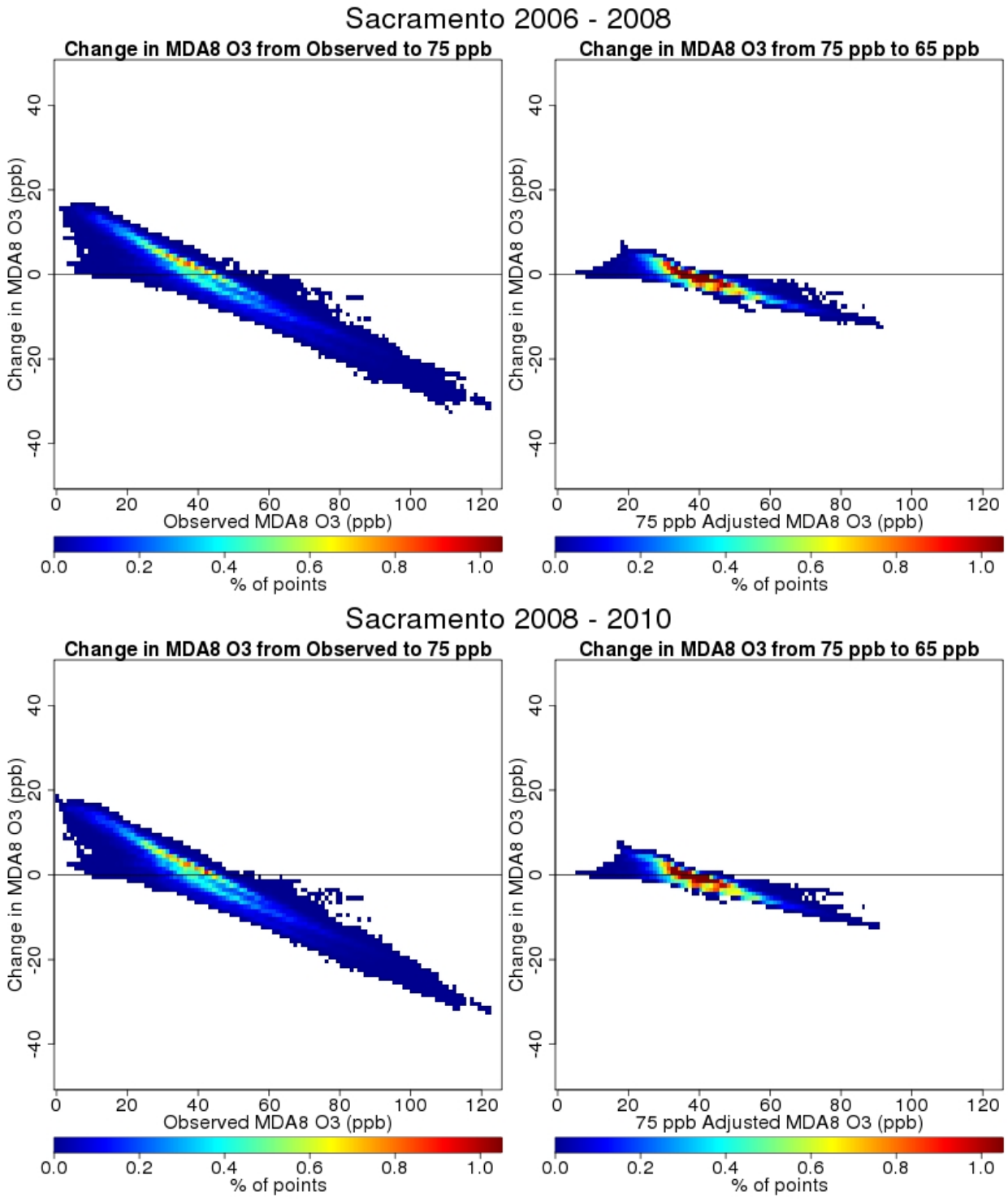


**Figure 67: Change in VNA estimates of the daily maximum 8-hour average (MDA8) $O_3$ concentrations based on HDDM adjustments in Sacramento.**

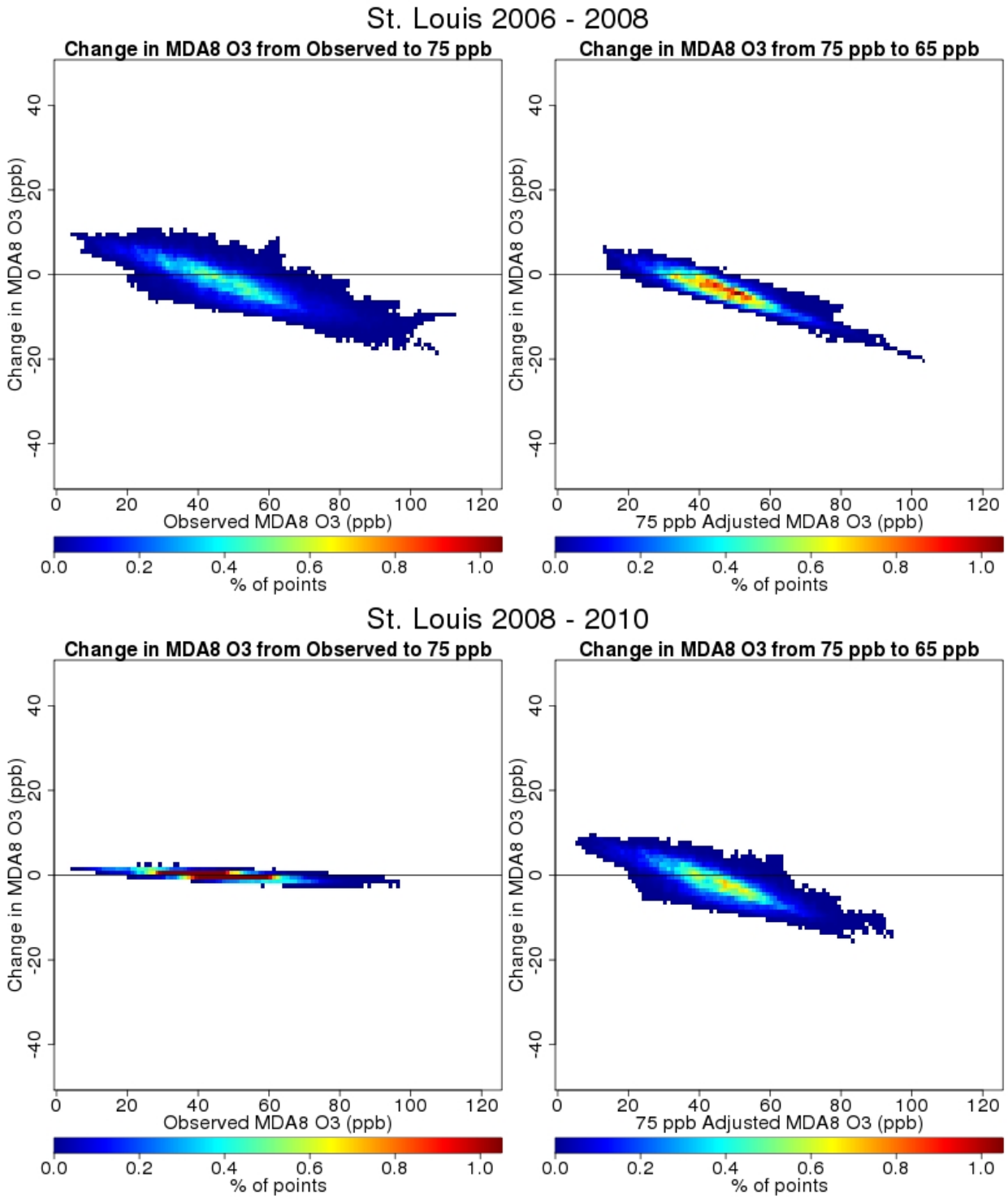


**Figure 68: Change in VNA estimates of the daily maximum 8-hour average (MDA8) $O_3$ concentrations based on HDDM adjustments in St. Louis.**

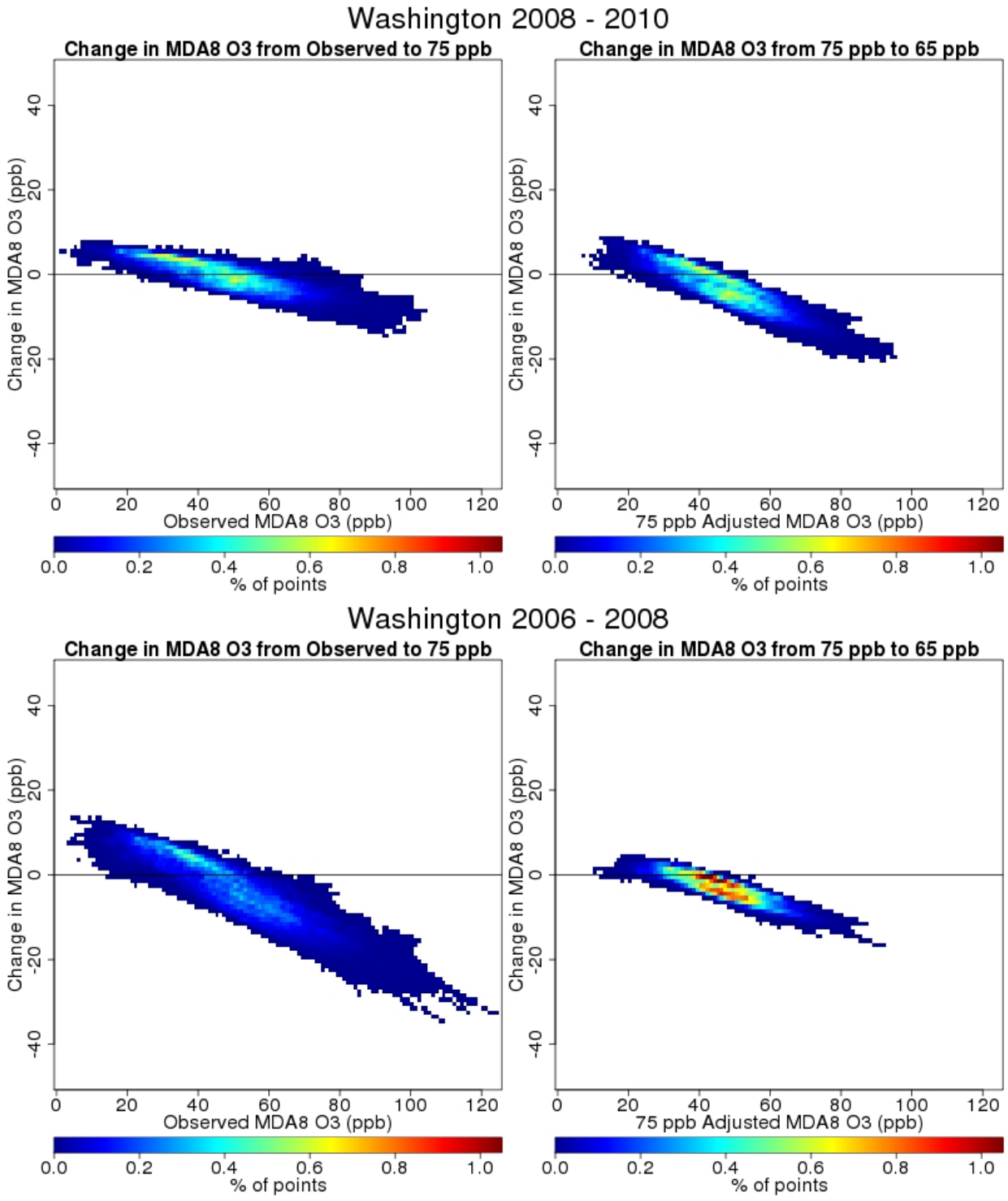


**Figure 69: Change in VNA estimates of the daily maximum 8-hour average (MDA8) O3 concentrations based on HDDM adjustments in Washington, D.C.**

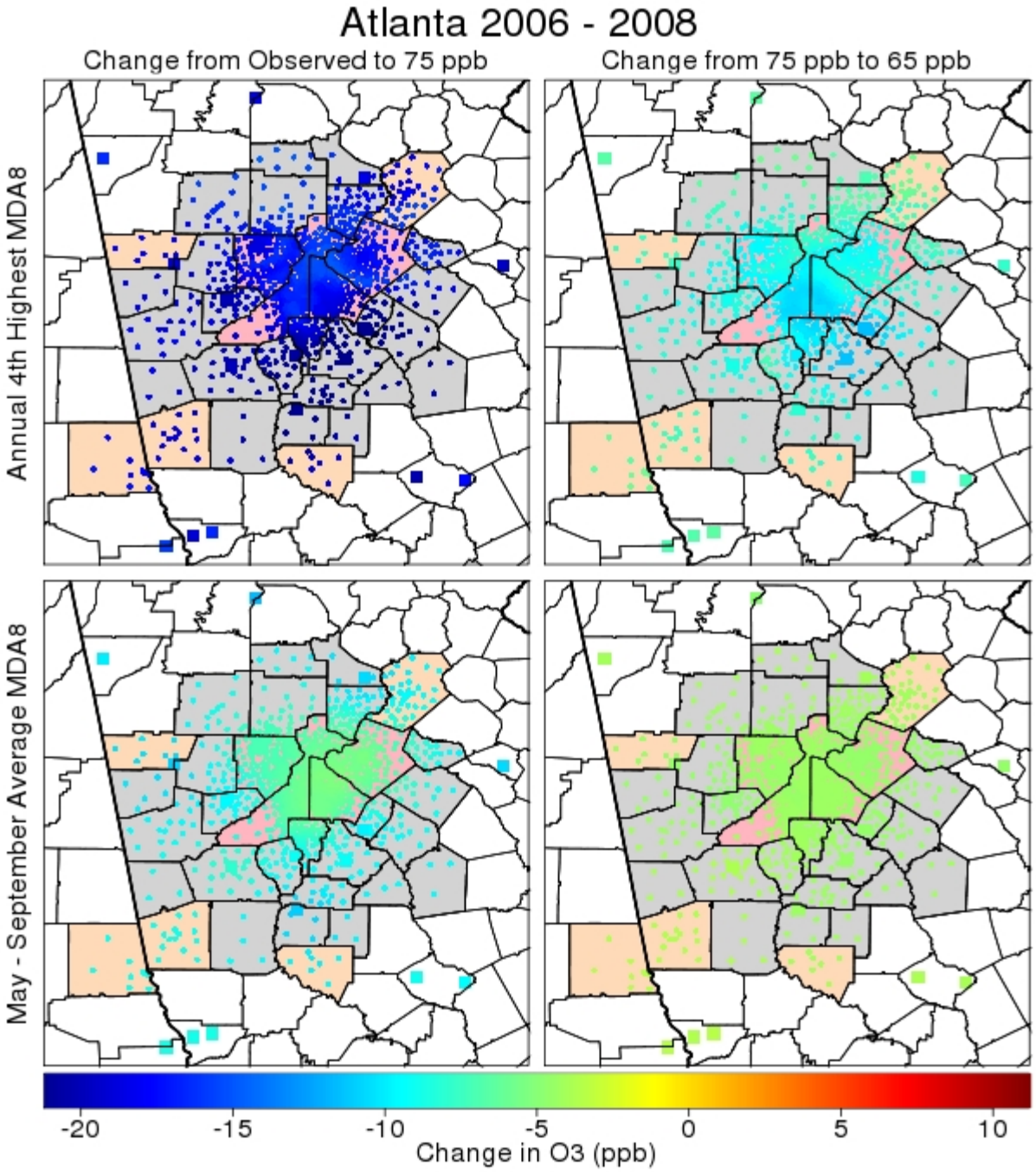


**Figure 70: Changes in annual 4th highest MDA8 and May-September average MDA8 values based on HDDM adjustments for Atlanta, 2006-2008. The points are colored according to the change in ppb, and values falling outside the range in the color bar were set to the nearest value within the color bar.**

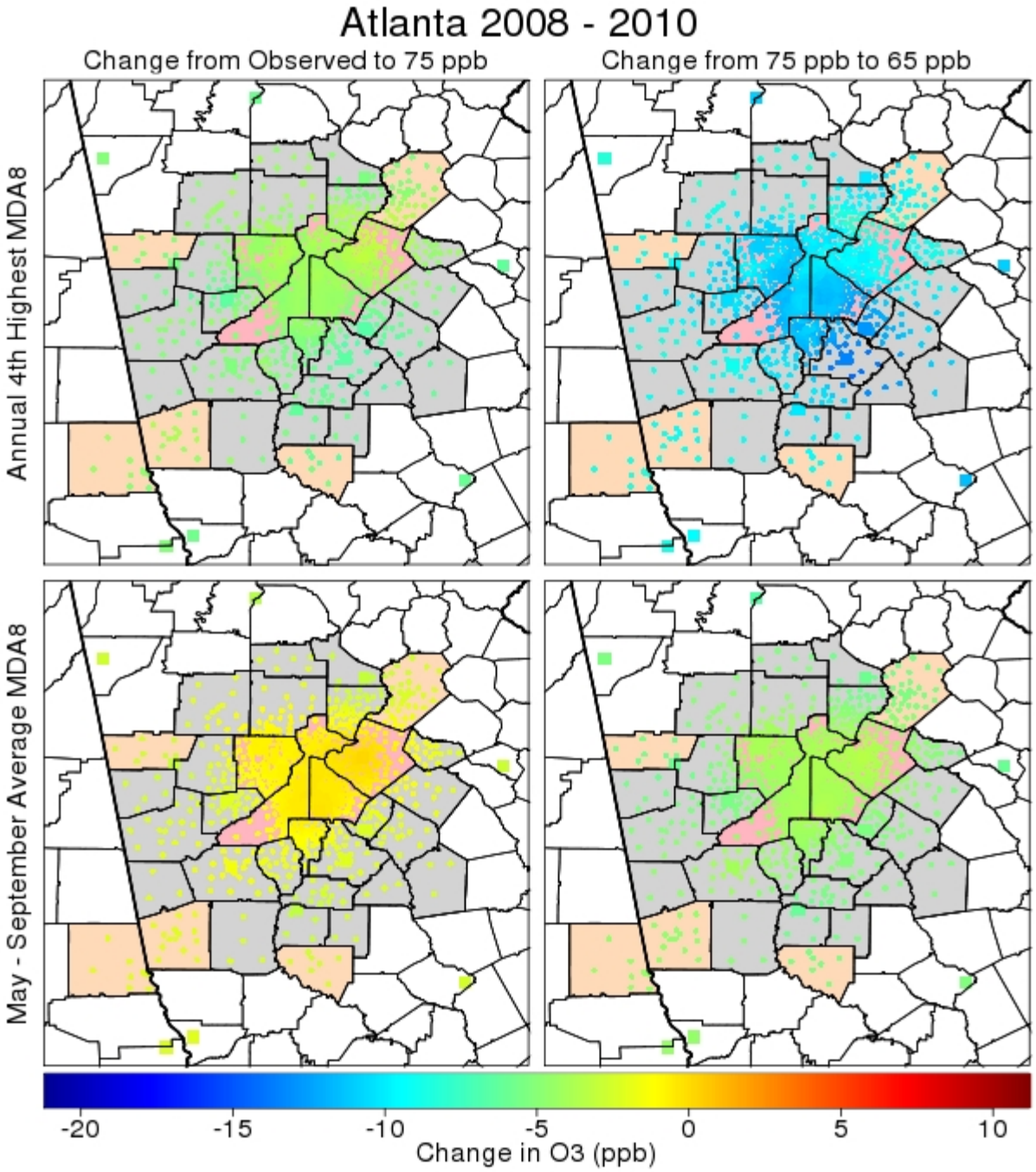


**Figure 71: Changes in annual 4th highest MDA8 and May-September average MDA8 values based on HDDM adjustments for Atlanta, 2008-2010. The points are colored according to the change in ppb, and values falling outside the range in the color bar were set to the nearest value within the color bar.**

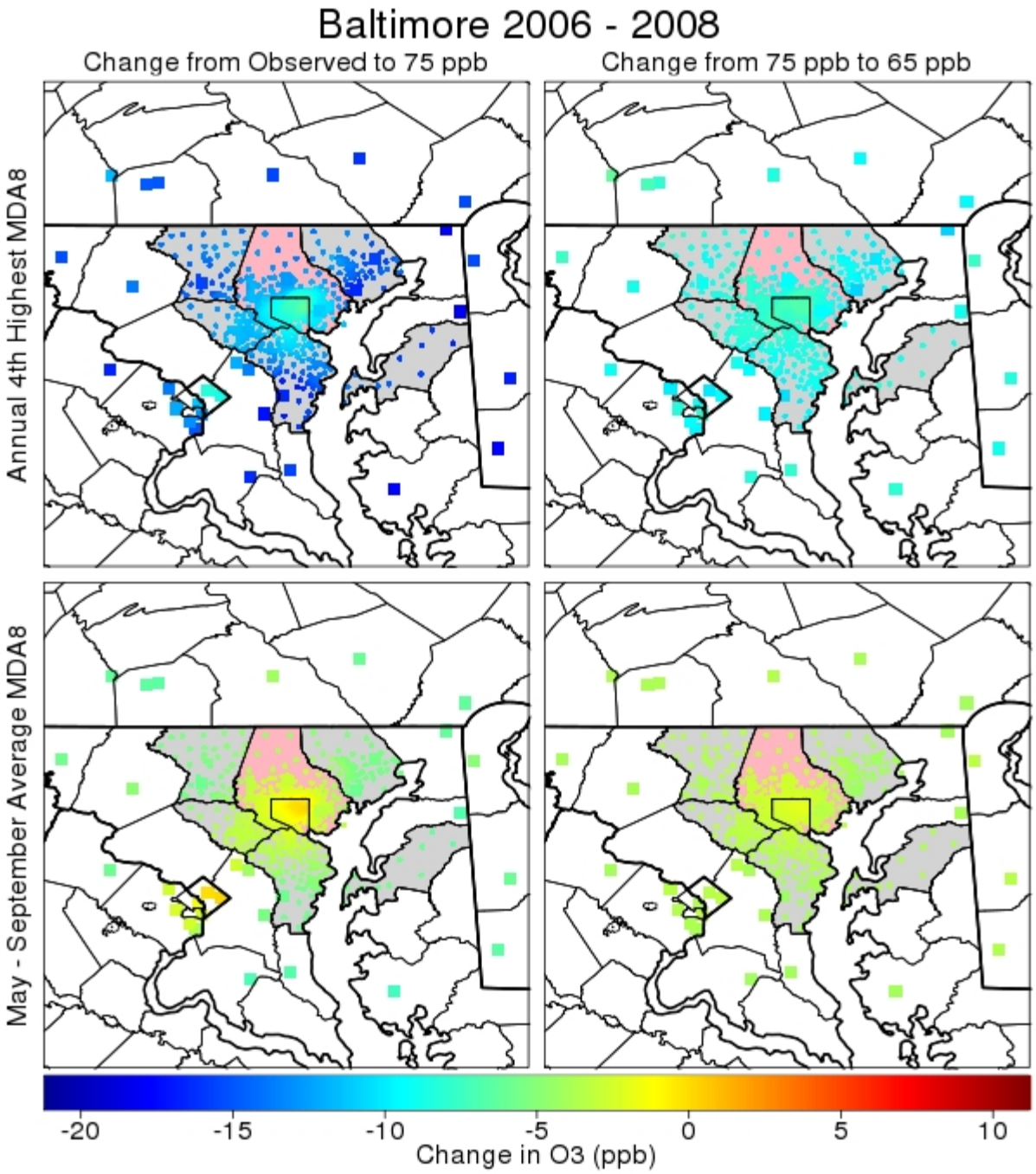


**Figure 72: Changes in annual 4th highest MDA8 and May-September average MDA8 values based on HDDM adjustments for Baltimore, 2006-2008. The points are colored according to the change in ppb, and values falling outside the range in the color bar were set to the nearest value within the color bar.**

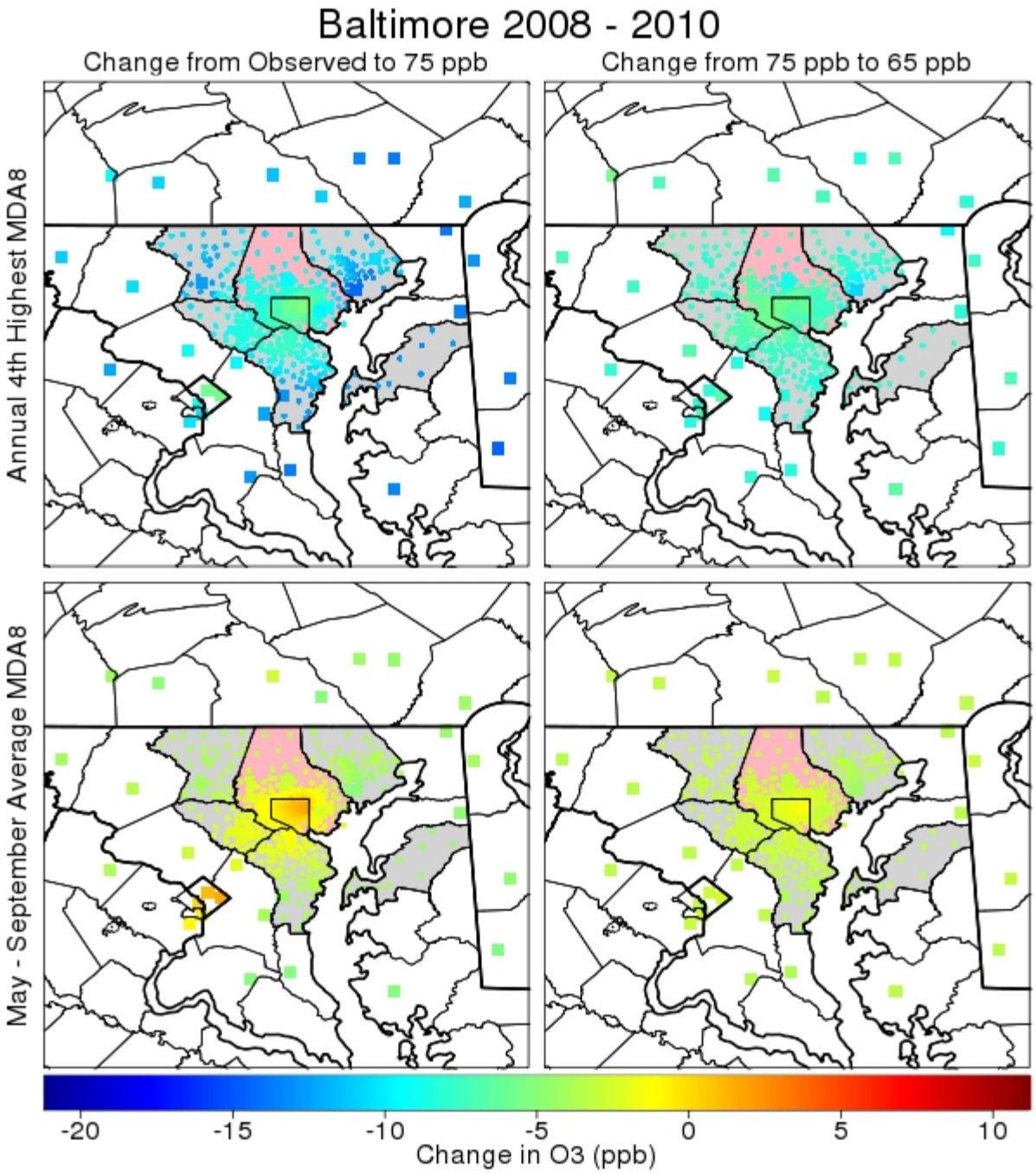


**Figure 73: Changes in annual 4th highest MDA8 and May-September average MDA8 values based on HDDM adjustments for Baltimore, 2008-2010. The points are colored according to the change in ppb, and values falling outside the range in the color bar were set to the nearest value within the color bar.**

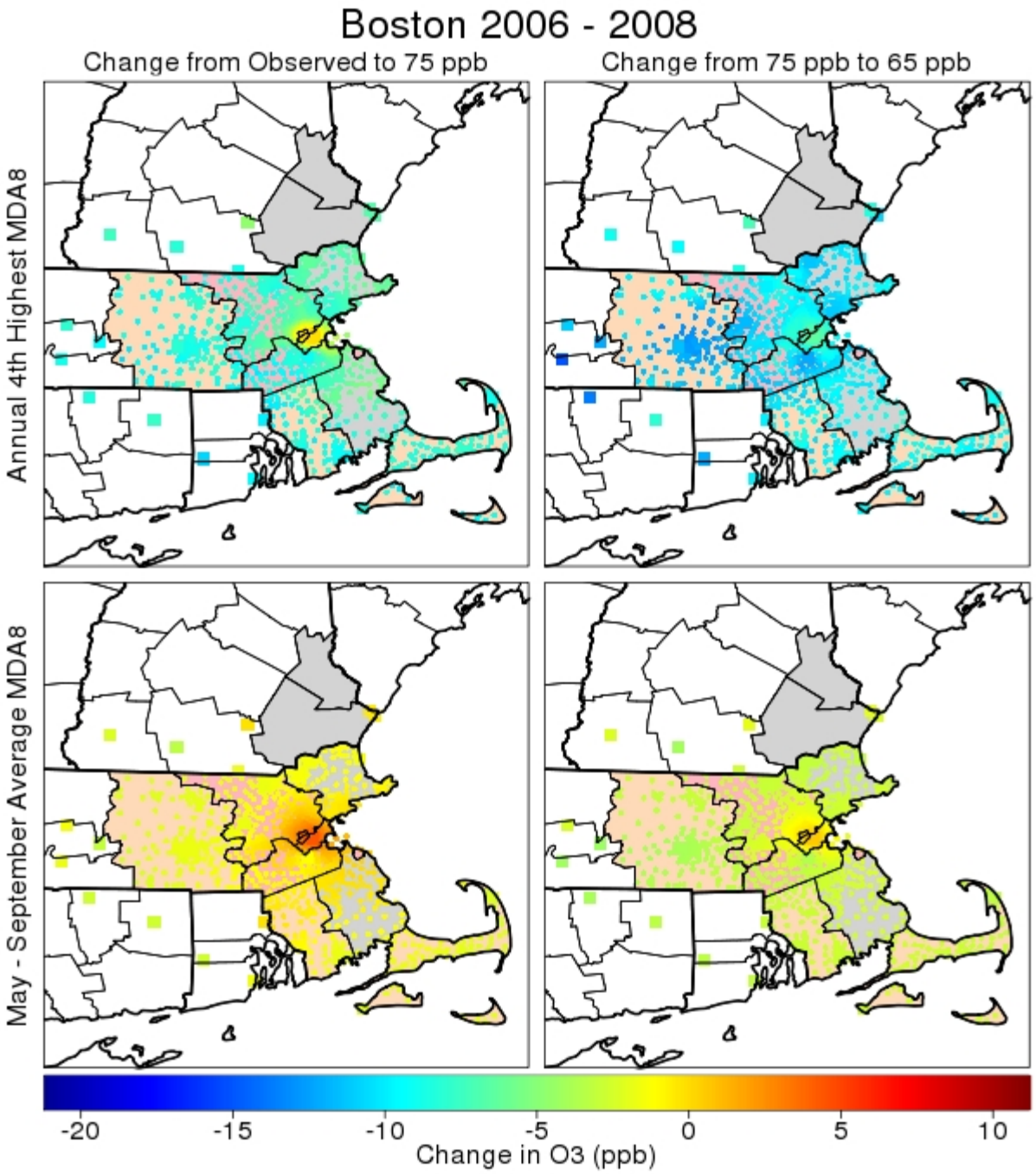


**Figure 74: Changes in annual 4th highest MDA8 and May-September average MDA8 values based on HDDM adjustments for Boston, 2006-2008. The points are colored according to the change in ppb, and values falling outside the range in the color bar were set to the nearest value within the color bar.**

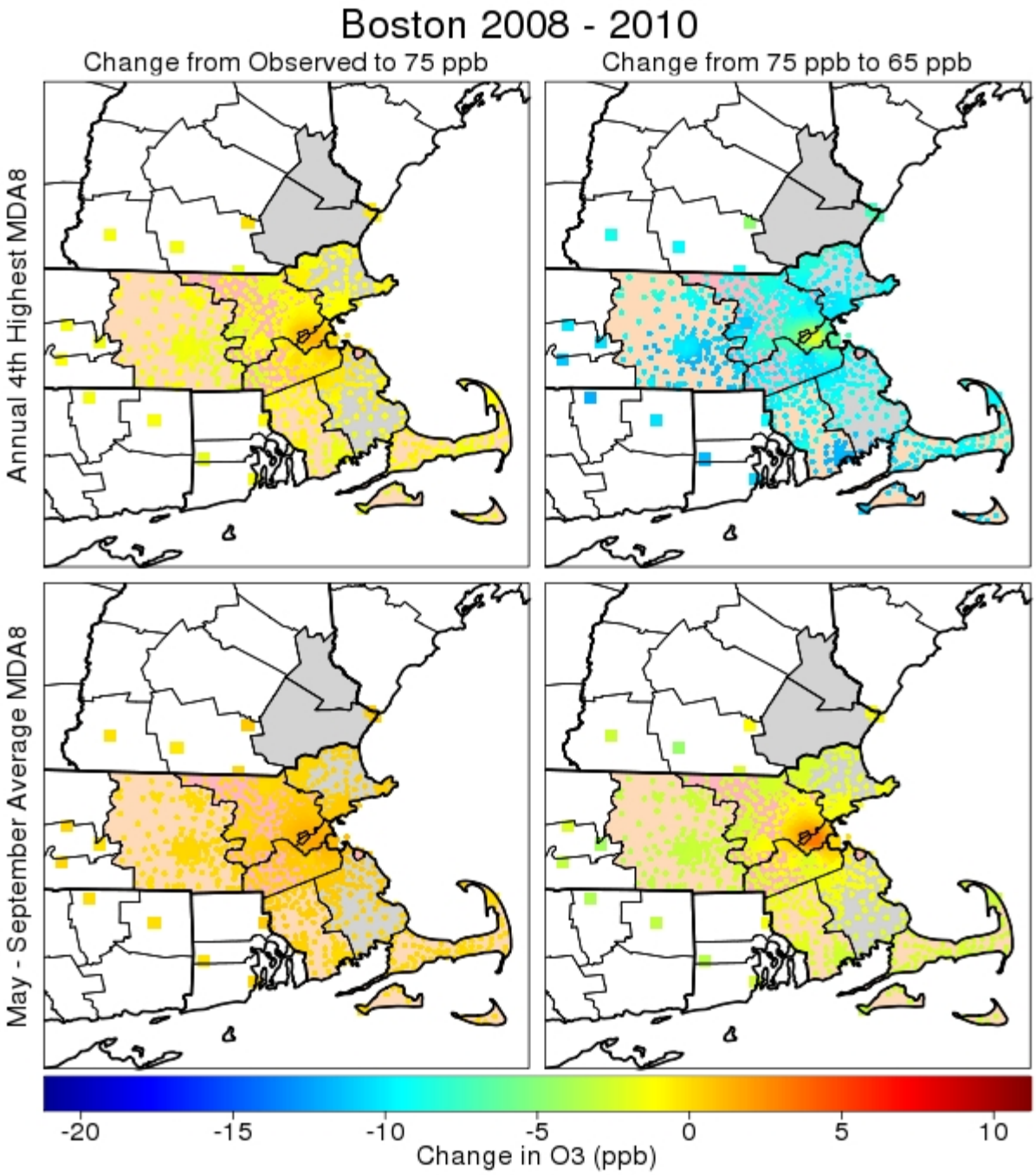


**Figure 75: Changes in annual 4th highest MDA8 and May-September average MDA8 values based on HDDM adjustments for Boston, 2008-2010. The points are colored according to the change in ppb, and values falling outside the range in the color bar were set to the nearest value within the color bar.**

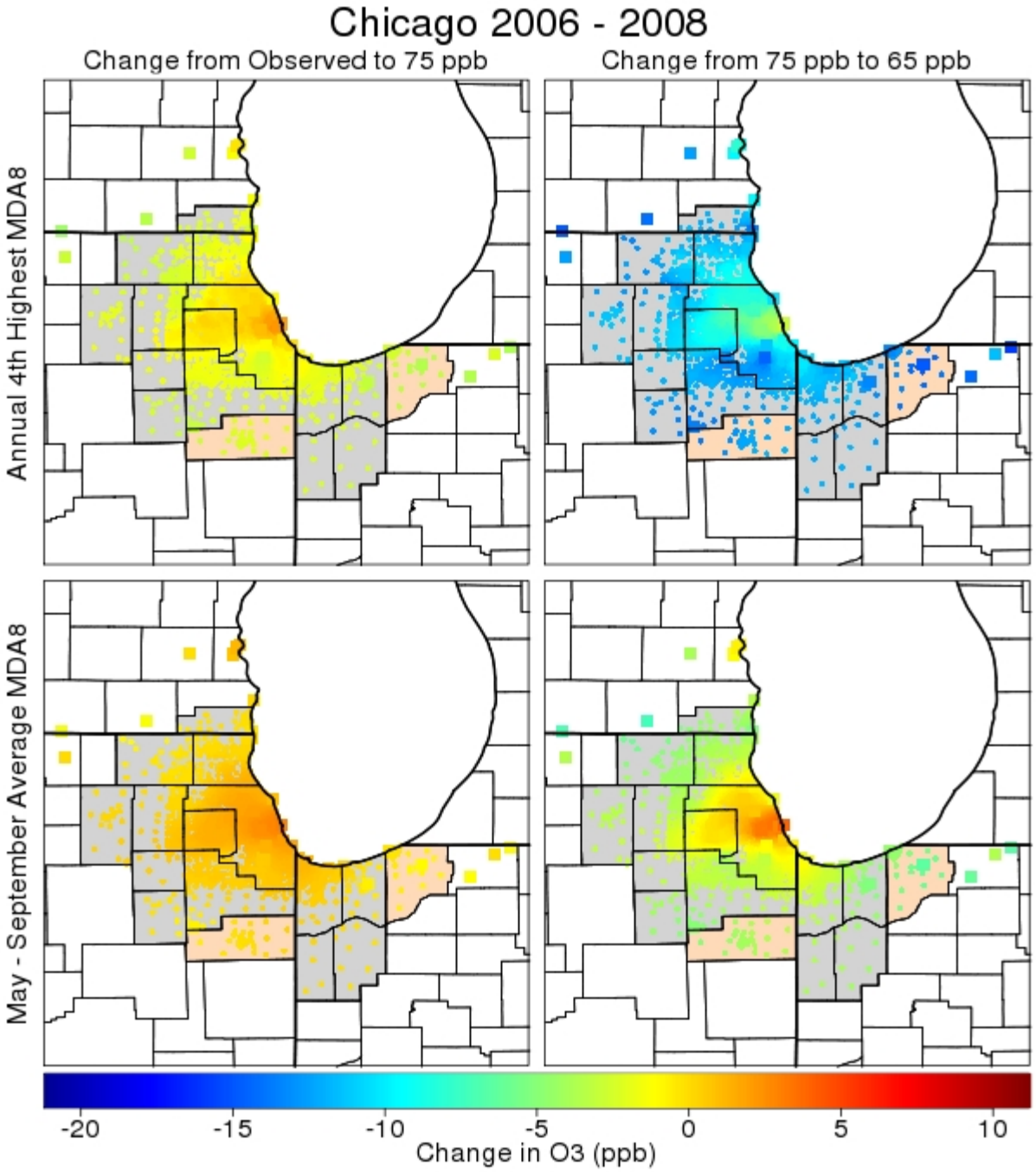


**Figure 76: Changes in annual 4th highest MDA8 and May-September average MDA8 values based on HDDM adjustments for Chicago, 2006-2008. The points are colored according to the change in ppb, and values falling outside the range in the color bar were set to the nearest value within the color bar.**

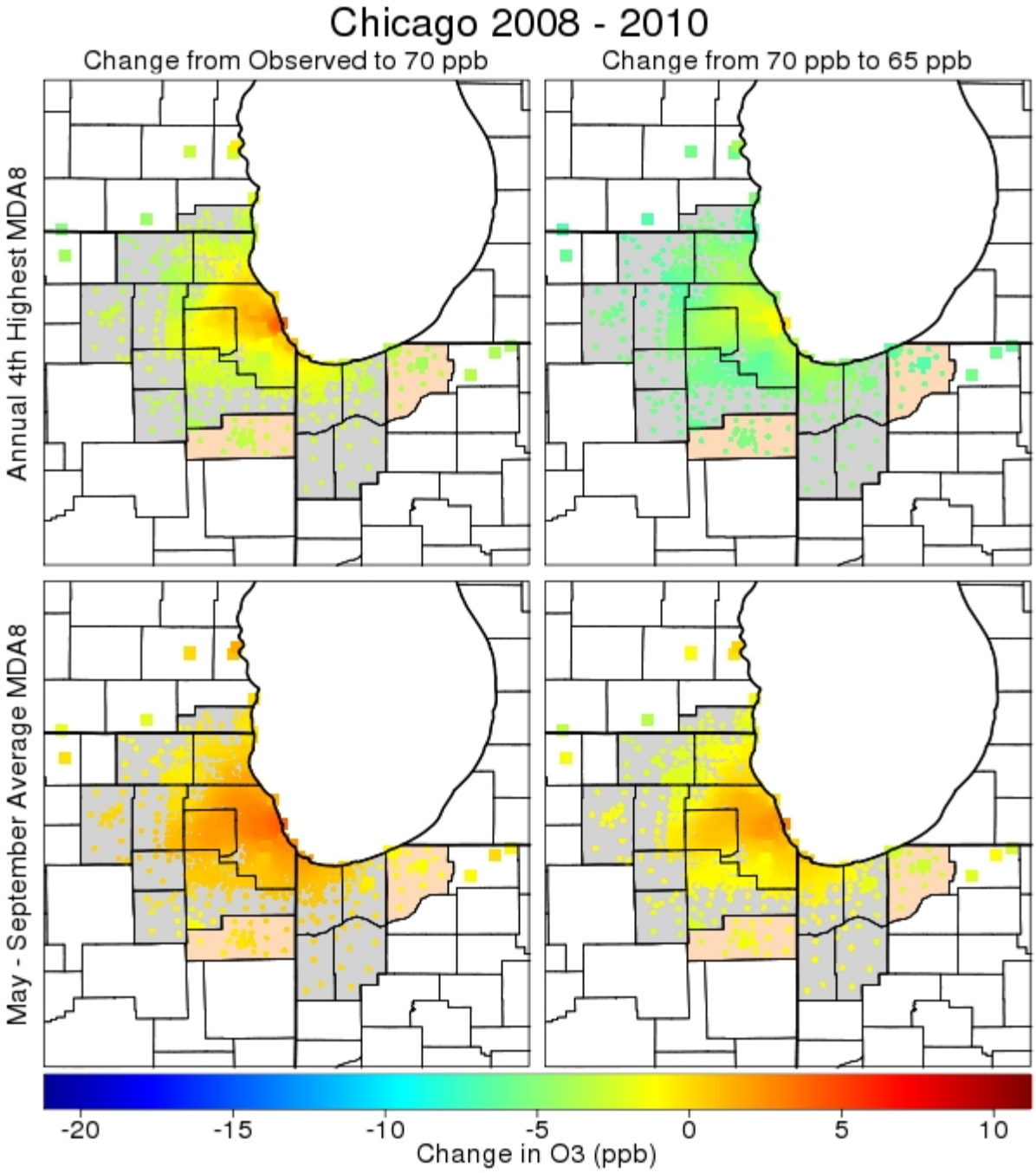


**Figure 77: Changes in annual 4th highest MDA8 and May-September average MDA8 values based on HDDM adjustments for Chicago, 2008-2010. The points are colored according to the change in ppb, and values falling outside the range in the color bar were set to the nearest value within the color bar.**

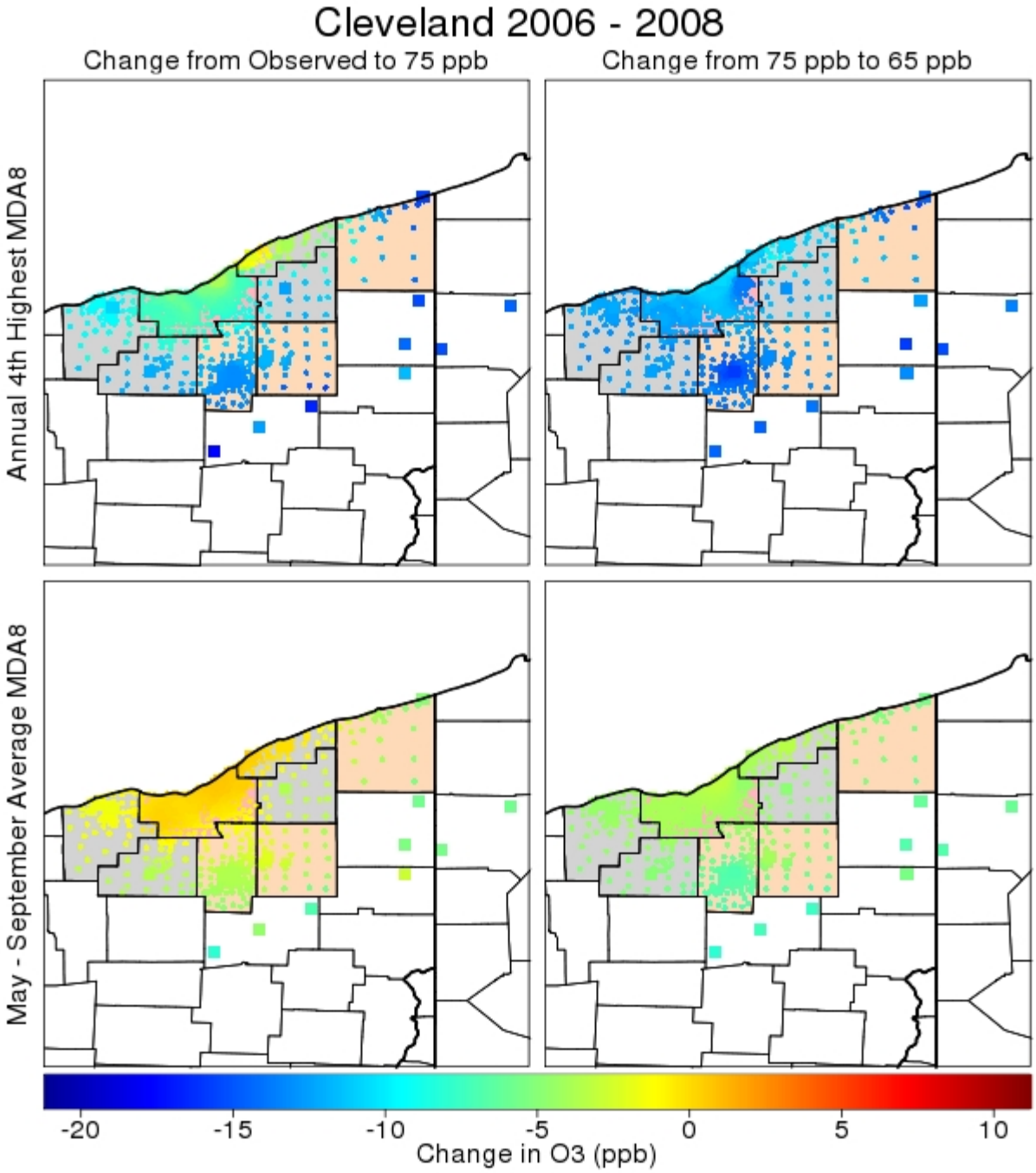


**Figure 78: Changes in annual 4th highest MDA8 and May-September average MDA8 values based on HDDM adjustments for Cleveland, 2006-2008. The points are colored according to the change in ppb, and values falling outside the range in the color bar were set to the nearest value within the color bar.**

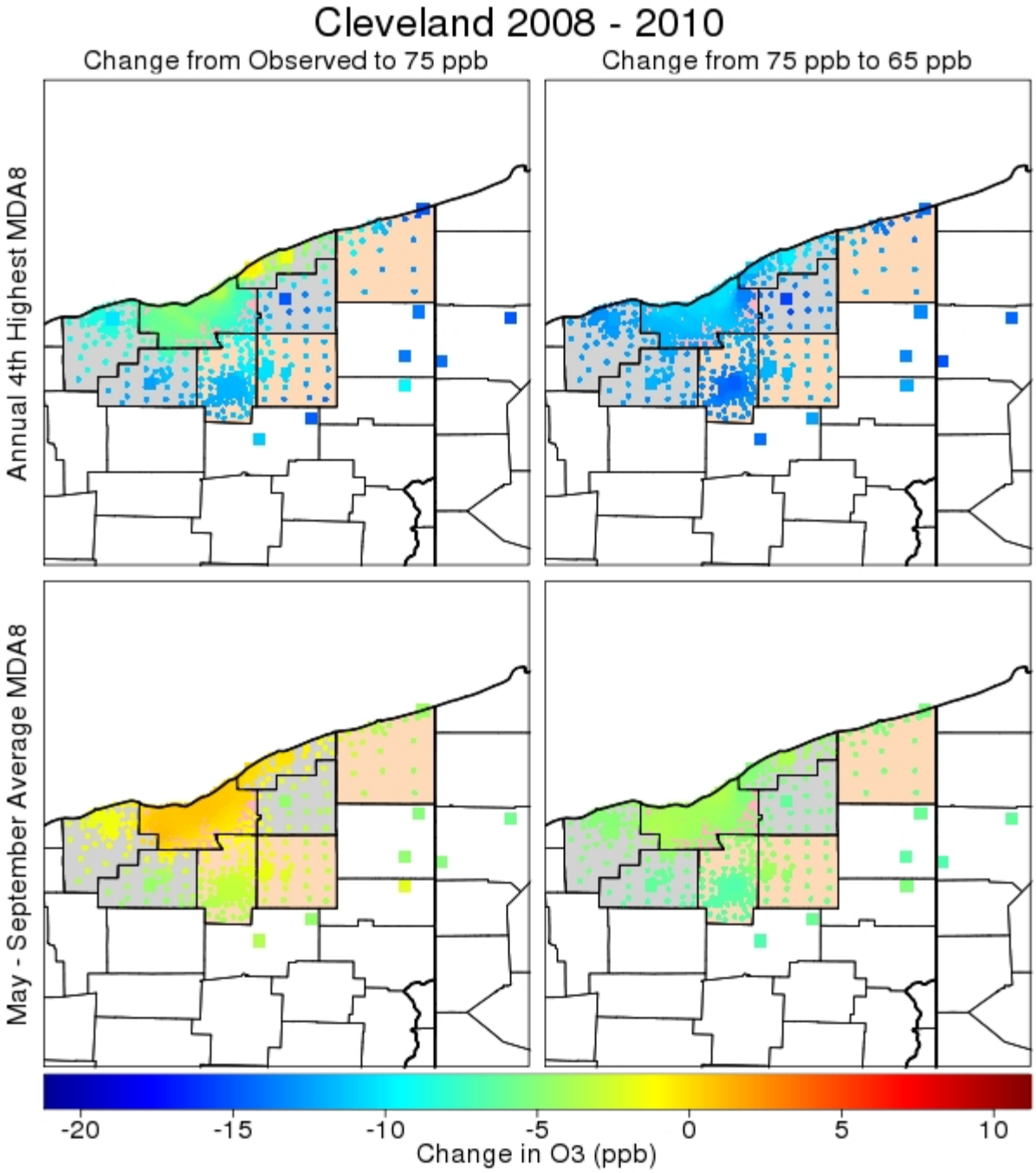


**Figure 79: Changes in annual 4th highest MDA8 and May-September average MDA8 values based on HDDM adjustments for Cleveland, 2008-2010. The points are colored according to the change in ppb, and values falling outside the range in the color bar were set to the nearest value within the color bar.**

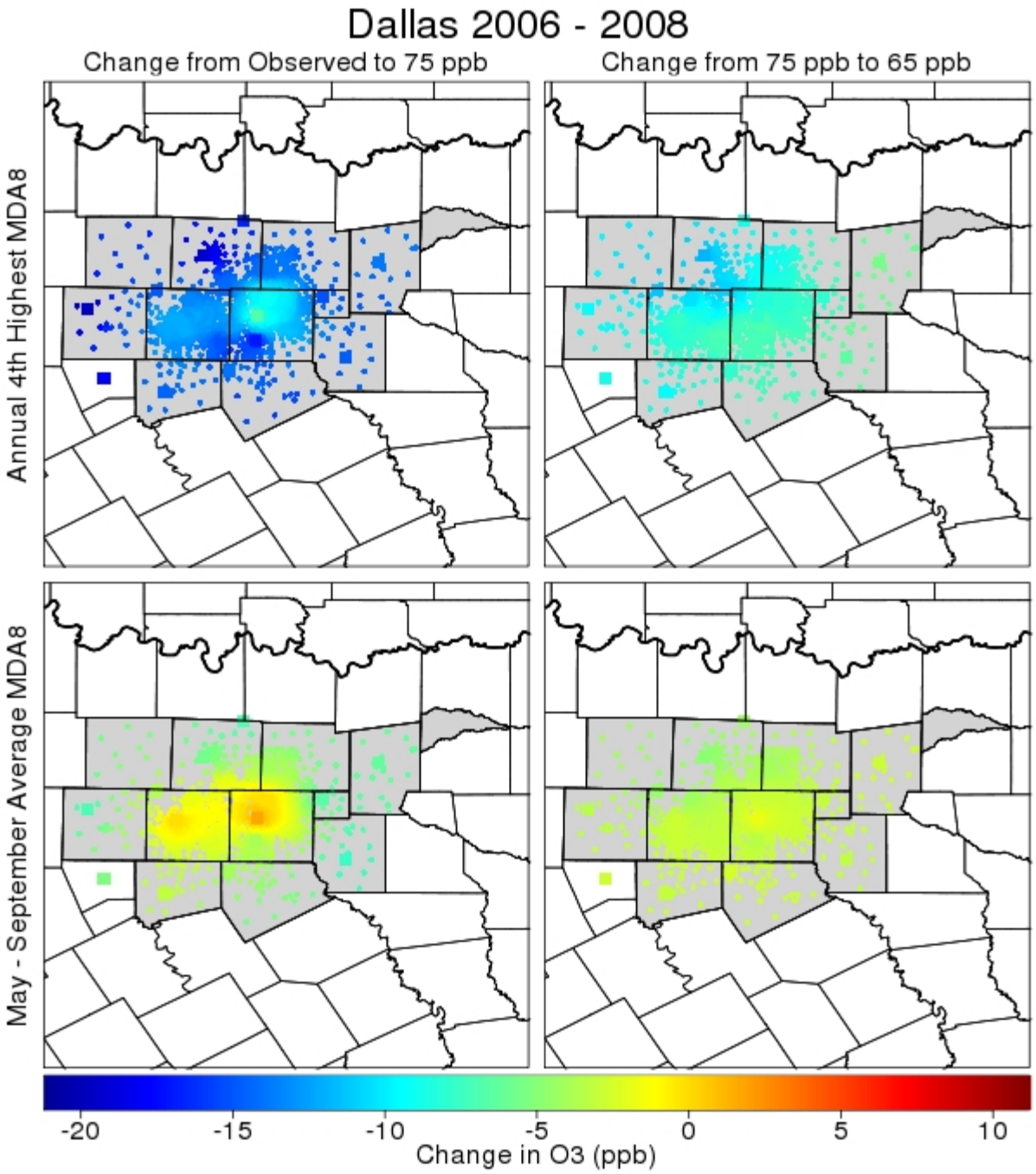


**Figure 80: Changes in annual 4th highest MDA8 and May-September average MDA8 values based on HDDM adjustments for Dallas, 2006-2008. The points are colored according to the change in ppb, and values falling outside the range in the color bar were set to the nearest value within the color bar.**

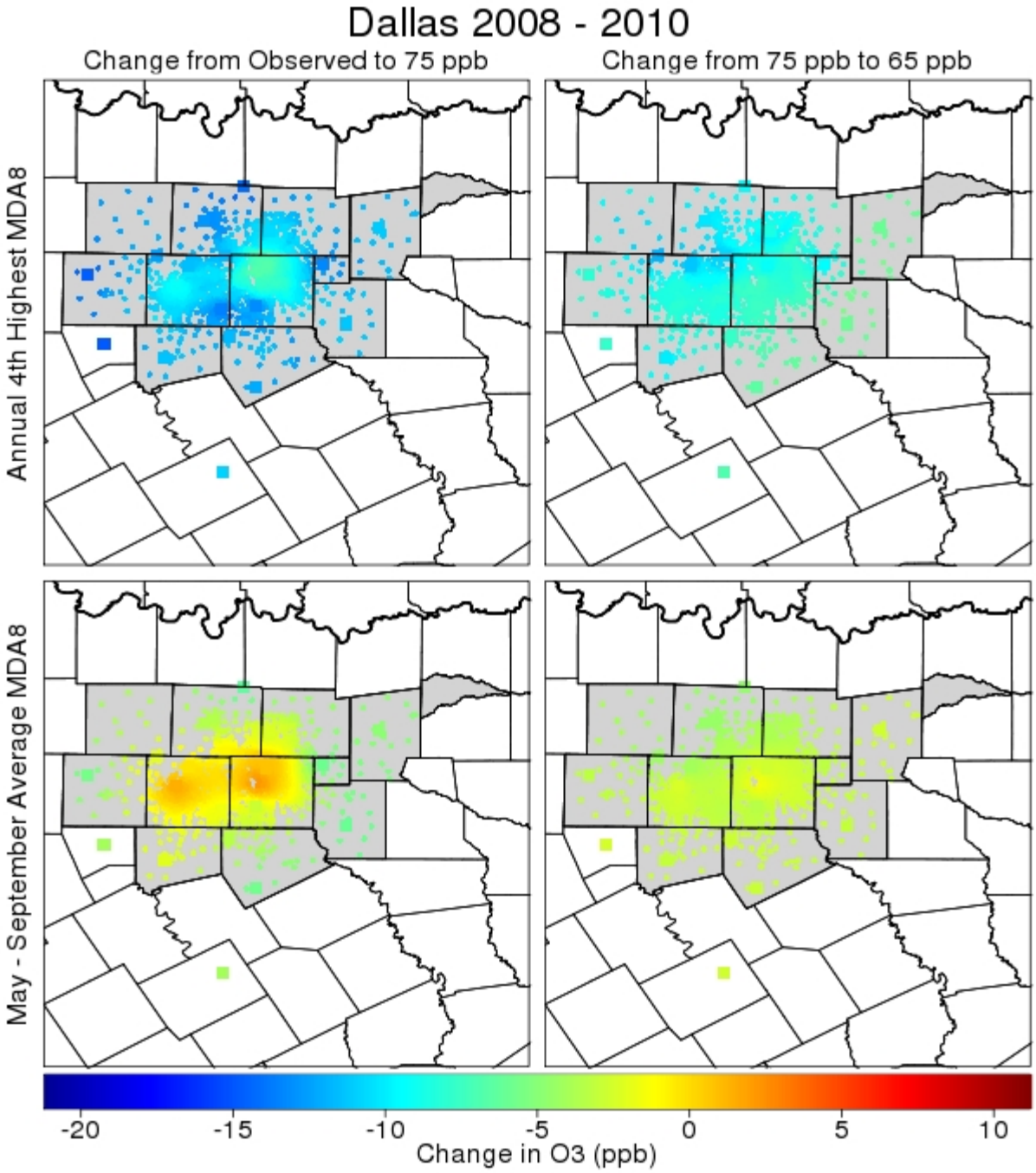


**Figure 81: Changes in annual 4th highest MDA8 and May-September average MDA8 values based on HDDM adjustments for Dallas, 2008-2010. The points are colored according to the change in ppb, and values falling outside the range in the color bar were set to the nearest value within the color bar.**

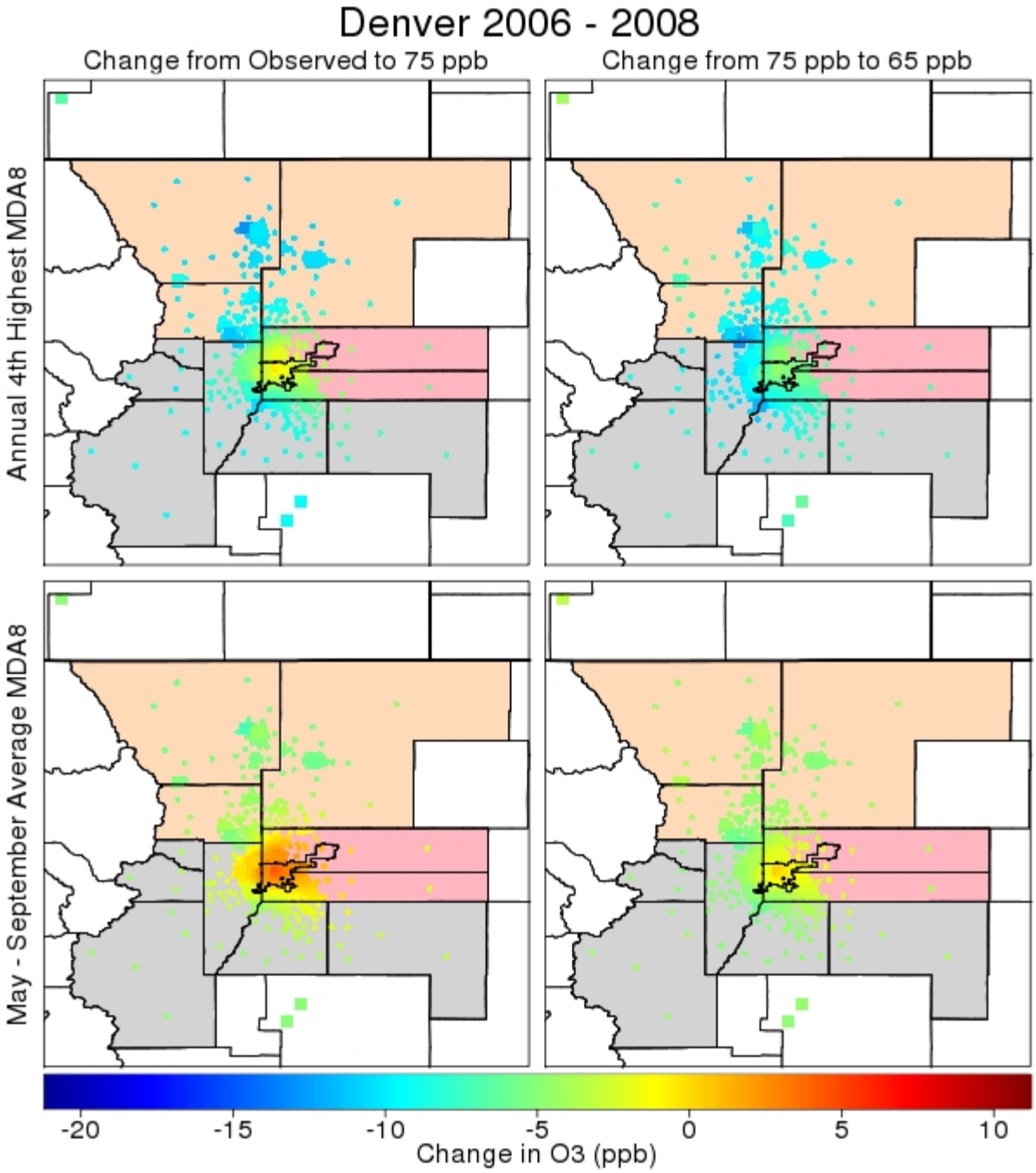


**Figure 82: Changes in annual 4th highest MDA8 and May-September average MDA8 values based on HDDM adjustments for Denver, 2006-2008. The points are colored according to the change in ppb, and values falling outside the range in the color bar were set to the nearest value within the color bar.**

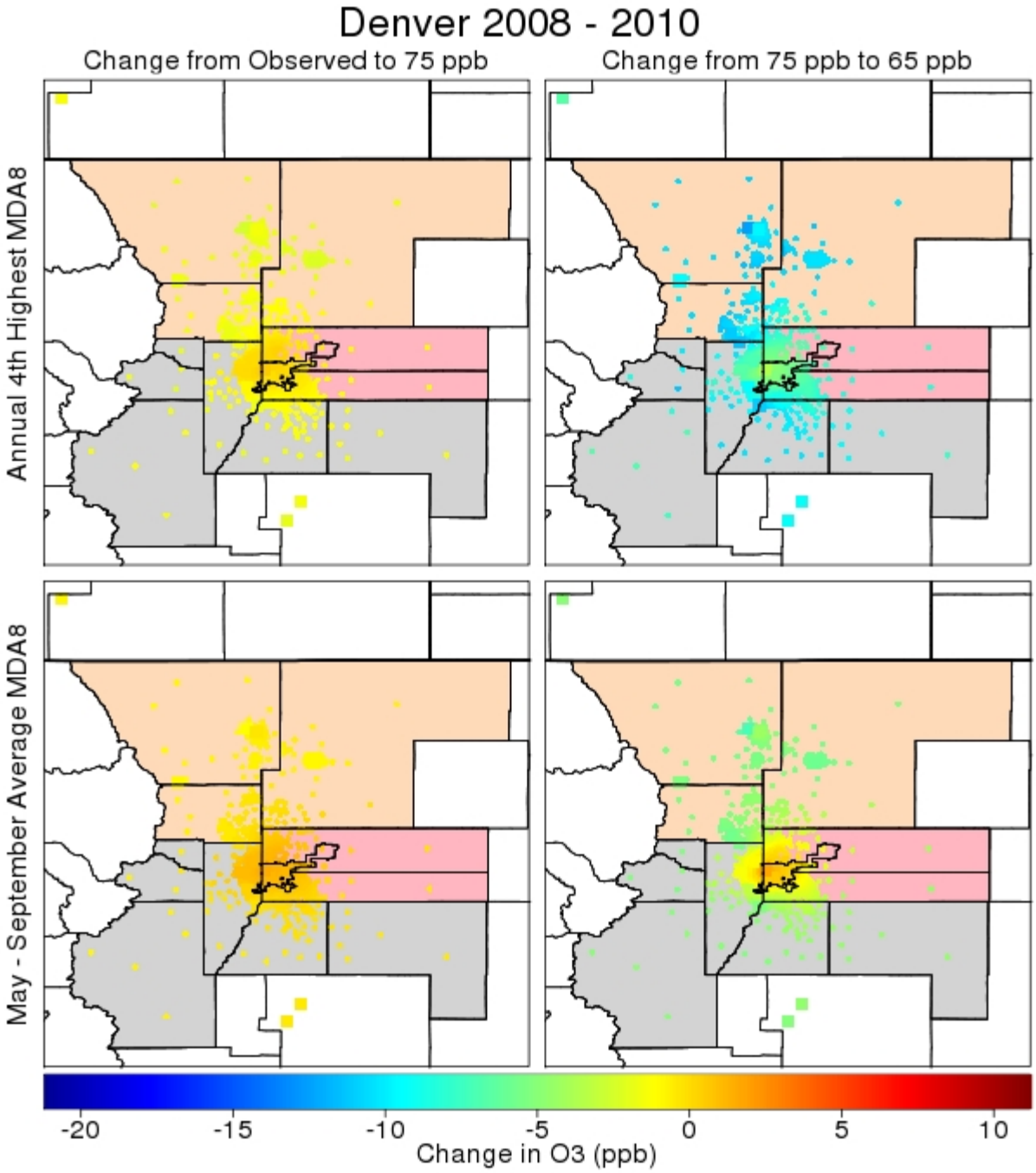


**Figure 83: Changes in annual 4th highest MDA8 and May-September average MDA8 values based on HDDM adjustments for Denver, 2008-2010. The points are colored according to the change in ppb, and values falling outside the range in the color bar were set to the nearest value within the color bar.**

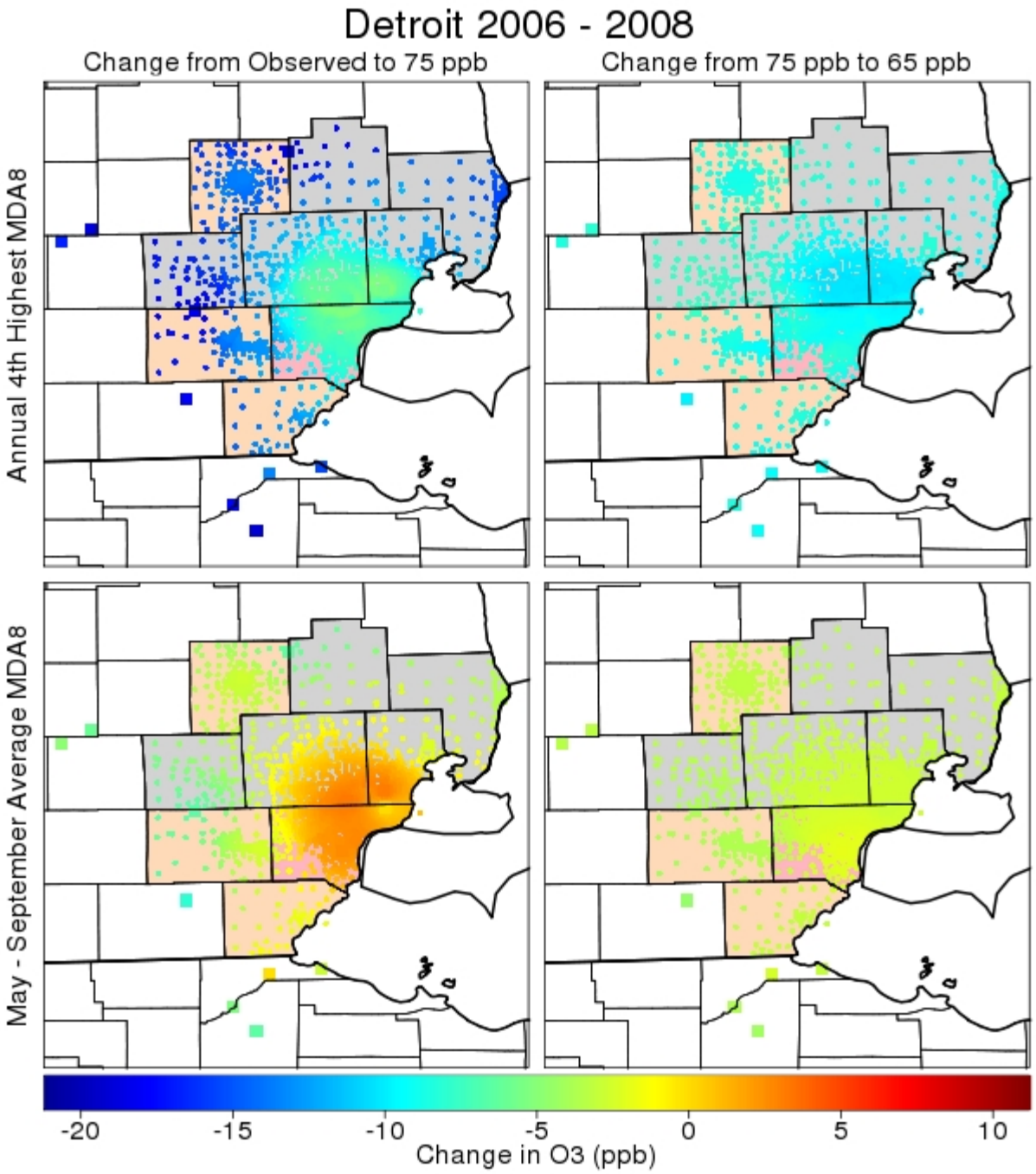


**Figure 84: Changes in annual 4th highest MDA8 and May-September average MDA8 values based on HDDM adjustments for Detroit, 2006-2008. The points are colored according to the change in ppb, and values falling outside the range in the color bar were set to the nearest value within the color bar.**

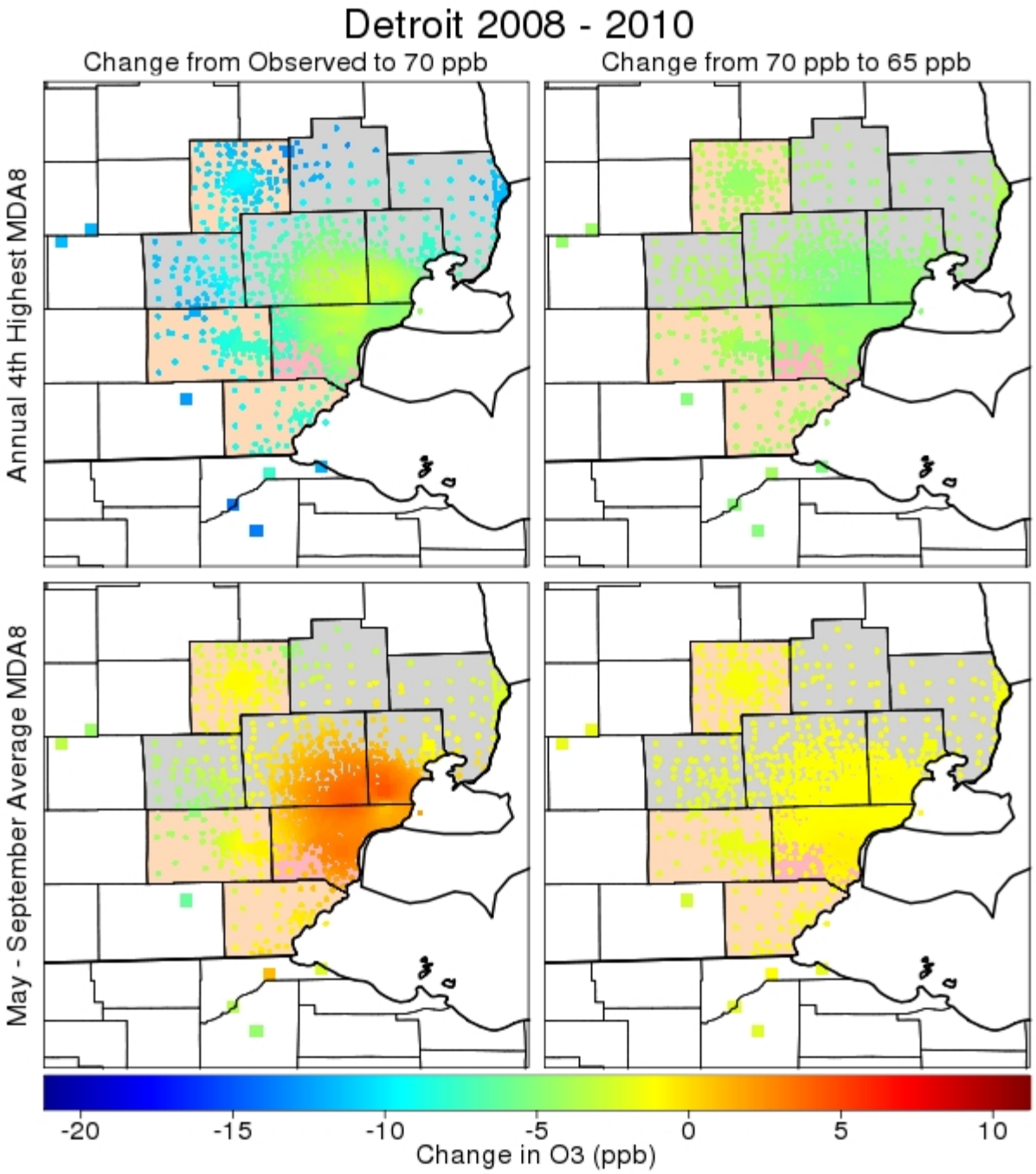


**Figure 85: Changes in annual 4th highest MDA8 and May-September average MDA8 values based on HDDM adjustments for Detroit, 2008-2010. The points are colored according to the change in ppb, and values falling outside the range in the color bar were set to the nearest value within the color bar.**

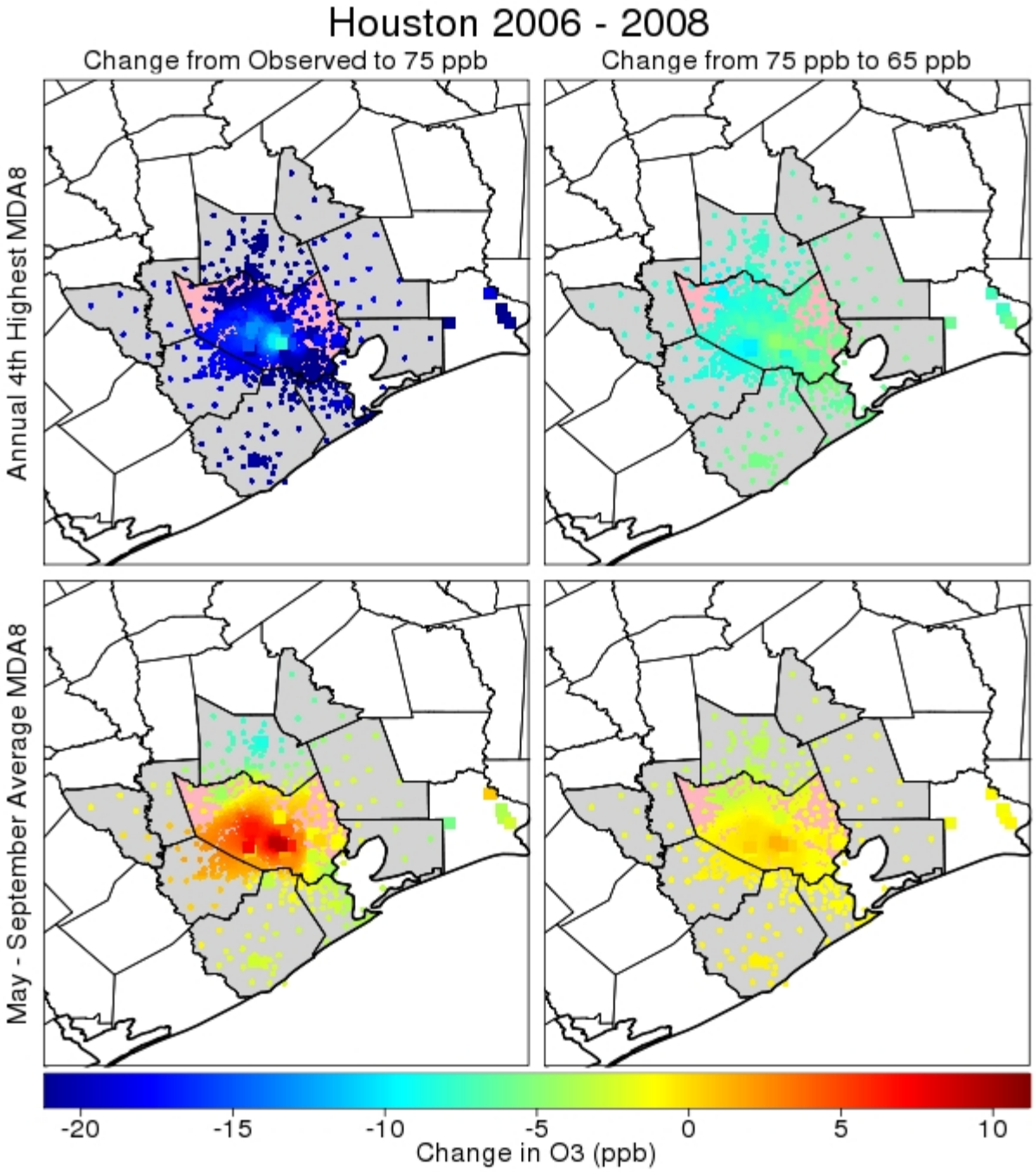


**Figure 86: Changes in annual 4th highest MDA8 and May-September average MDA8 values based on HDDM adjustments for Houston, 2006-2008. The points are colored according to the change in ppb, and values falling outside the range in the color bar were set to the nearest value within the color bar.**

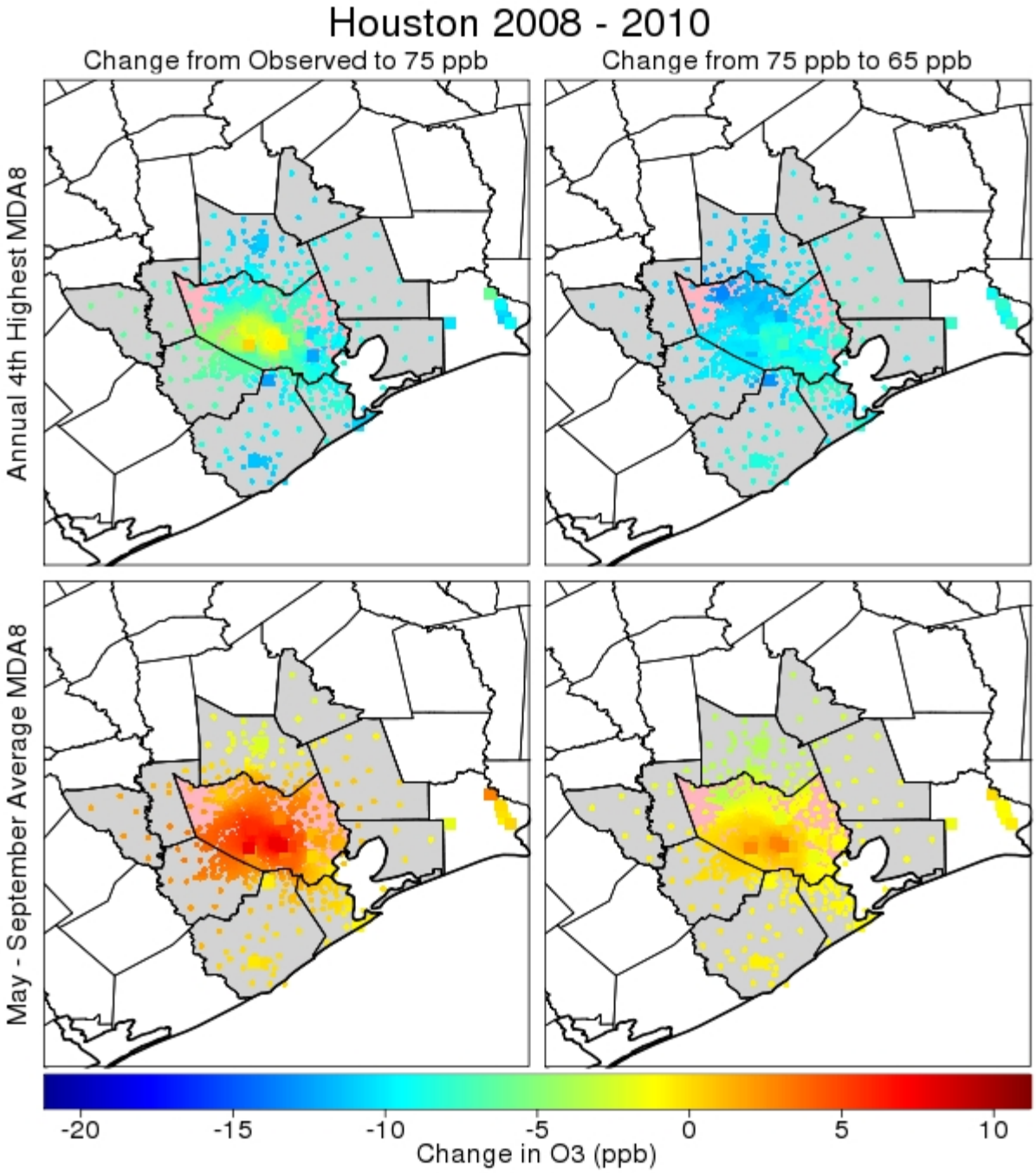


**Figure 87: Changes in annual 4th highest MDA8 and May-September average MDA8 values based on HDDM adjustments for Houston, 2008-2010. The points are colored according to the change in ppb, and values falling outside the range in the color bar were set to the nearest value within the color bar.**

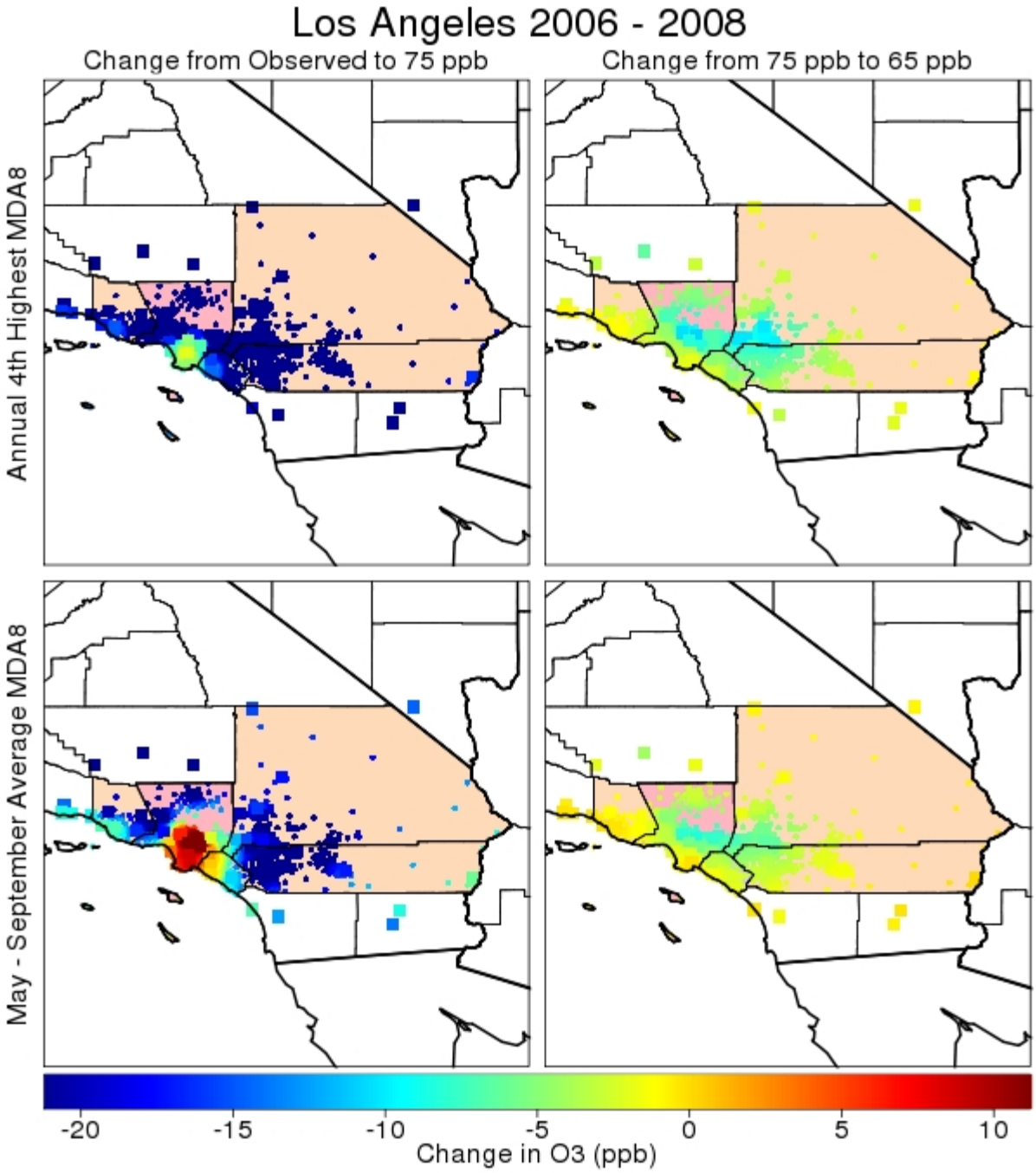


**Figure 88: Changes in annual 4th highest MDA8 and May-September average MDA8 values based on HDDM adjustments for Los Angeles, 2006-2008. The points are colored according to the change in ppb, and values falling outside the range in the color bar were set to the nearest value within the color bar.**

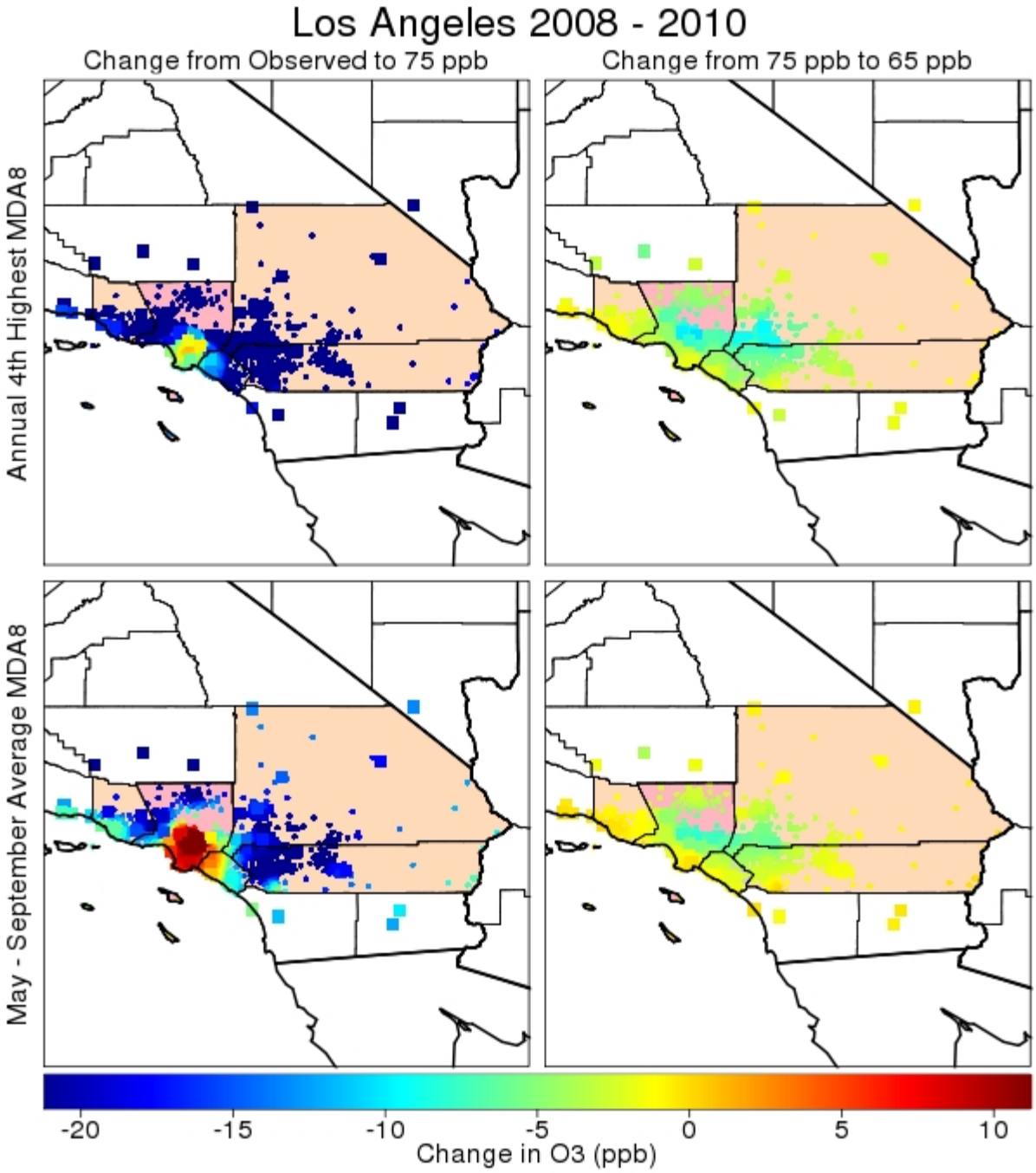


**Figure 89: Changes in annual 4th highest MDA8 and May-September average MDA8 values based on HDDM adjustments for Los Angeles, 2008-2010. The points are colored according to the change in ppb, and values falling outside the range in the color bar were set to the nearest value within the color bar.**

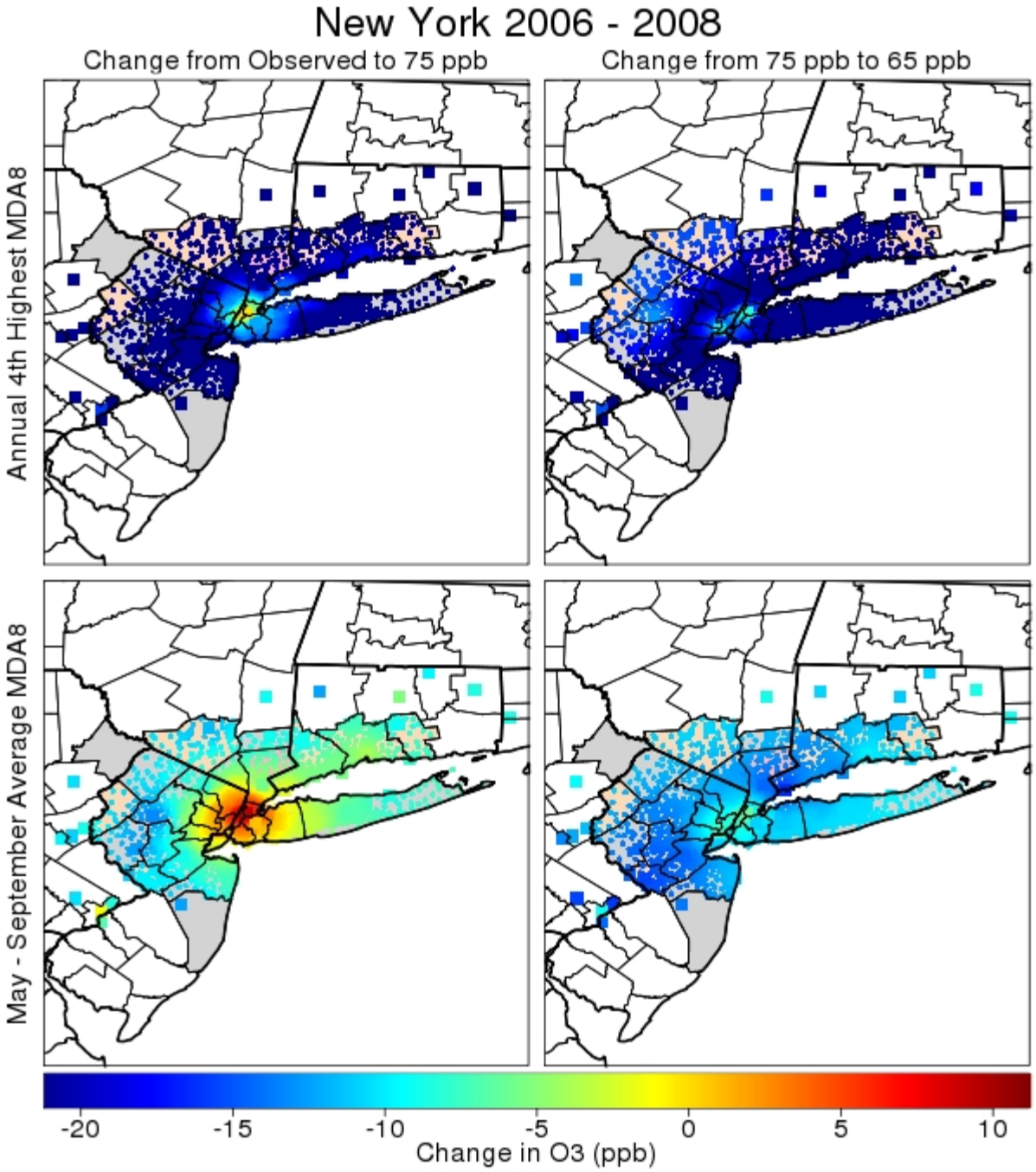


**Figure 90: Changes in annual 4th highest MDA8 and May-September average MDA8 values based on HDDM adjustments for New York, 2006-2008. The points are colored according to the change in ppb, and values falling outside the range in the color bar were set to the nearest value within the color bar.**

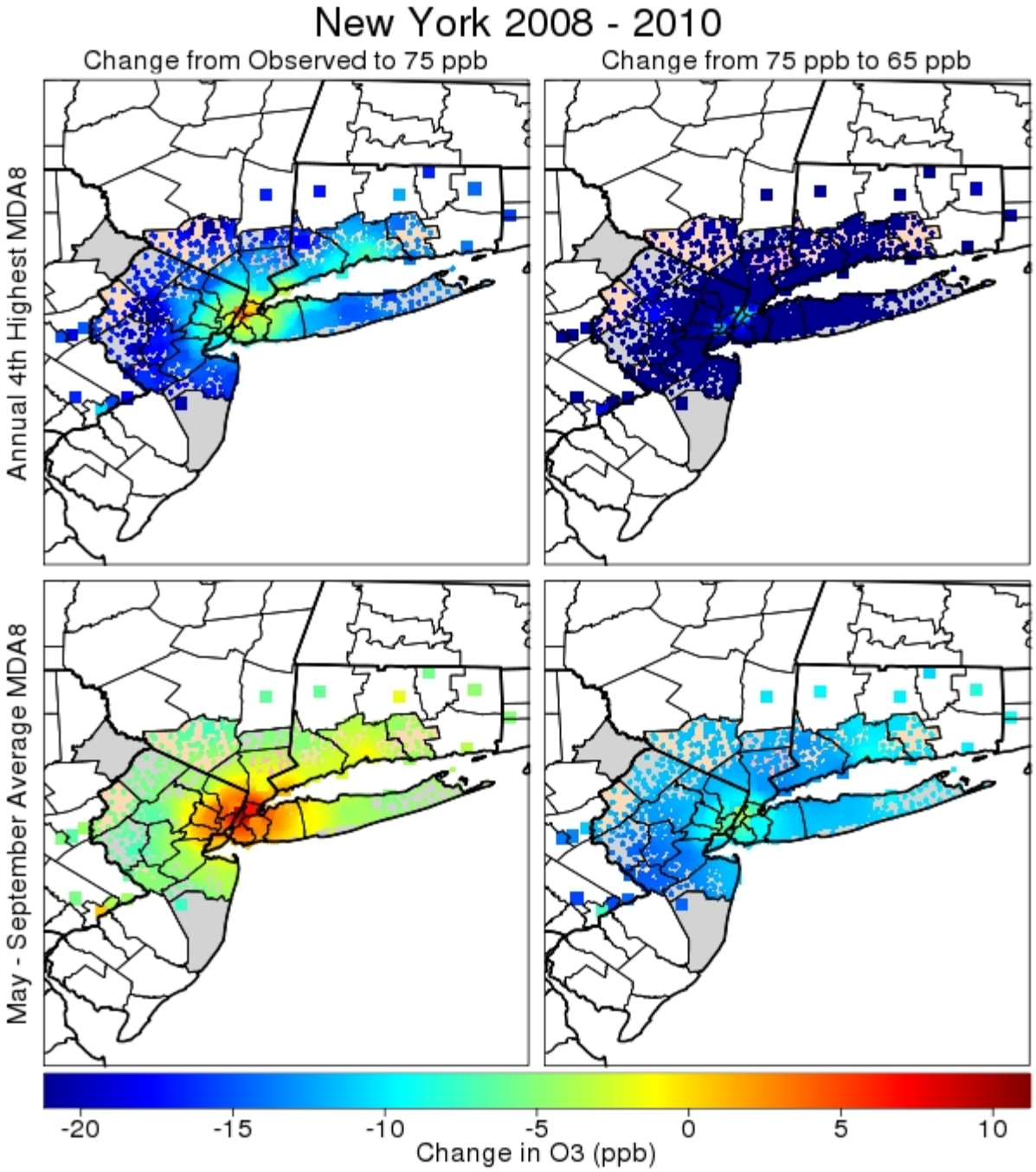


**Figure 91: Changes in annual 4th highest MDA8 and May-September average MDA8 values based on HDDM adjustments for New York, 2008-2010. The points are colored according to the change in ppb, and values falling outside the range in the color bar were set to the nearest value within the color bar.**

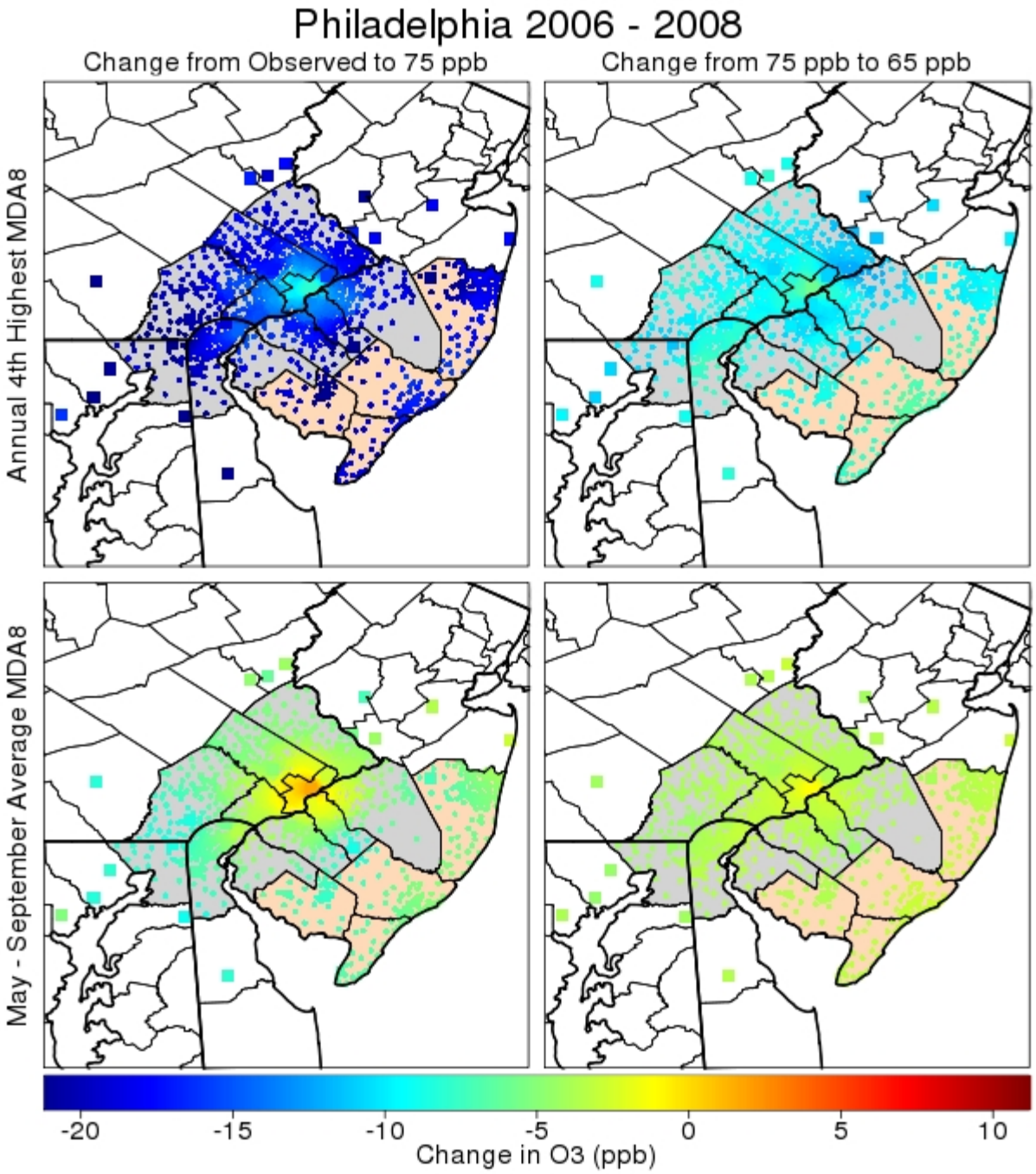


**Figure 92: Changes in annual 4th highest MDA8 and May-September average MDA8 values based on HDDM adjustments for Philadelphia, 2006-2008. The points are colored according to the change in ppb, and values falling outside the range in the color bar were set to the nearest value within the color bar.**

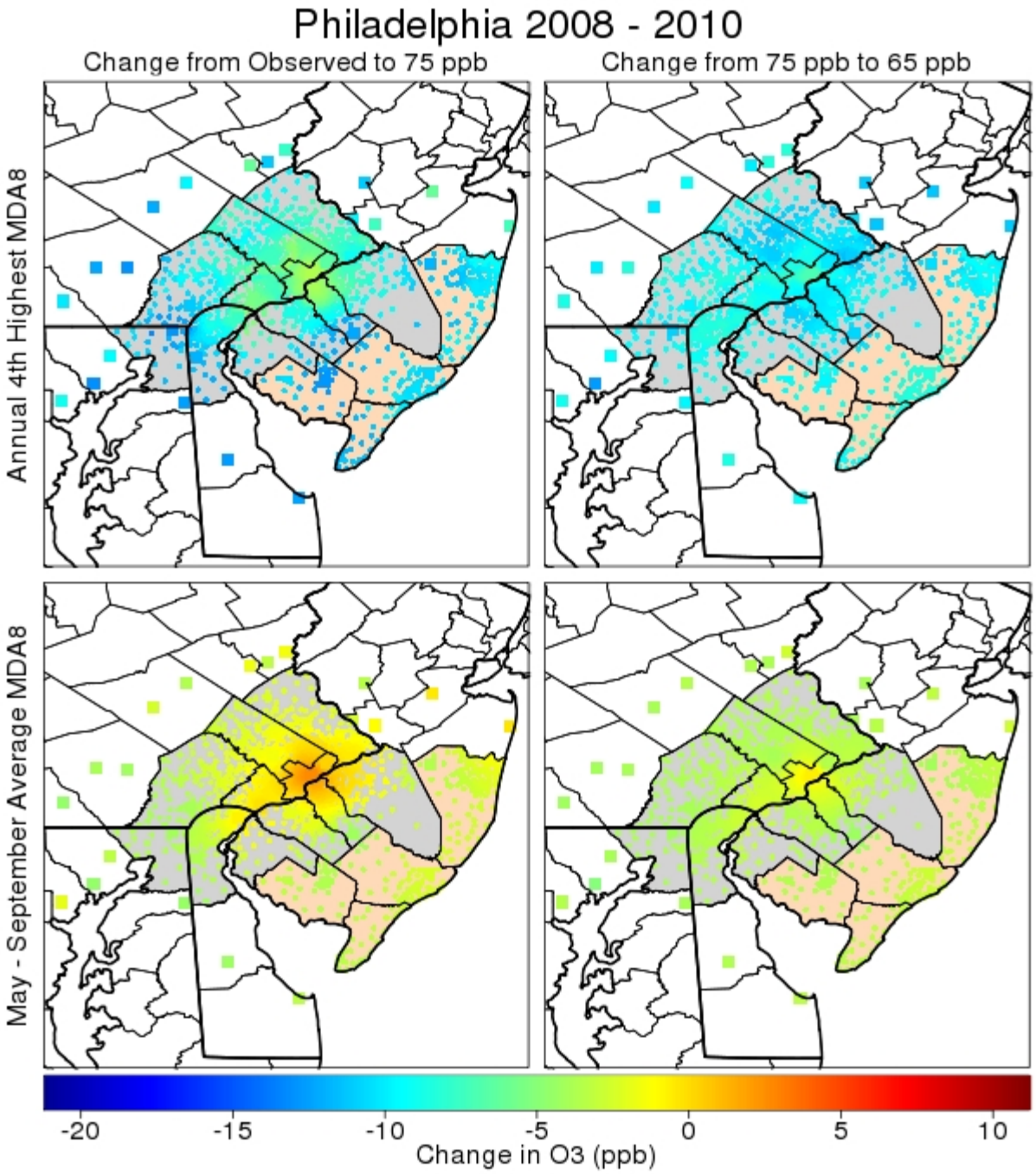


**Figure 93: Changes in annual 4th highest MDA8 and May-September average MDA8 values based on HDDM adjustments for Philadelphia, 2008-2010. The points are colored according to the change in ppb, and values falling outside the range in the color bar were set to the nearest value within the color bar.**

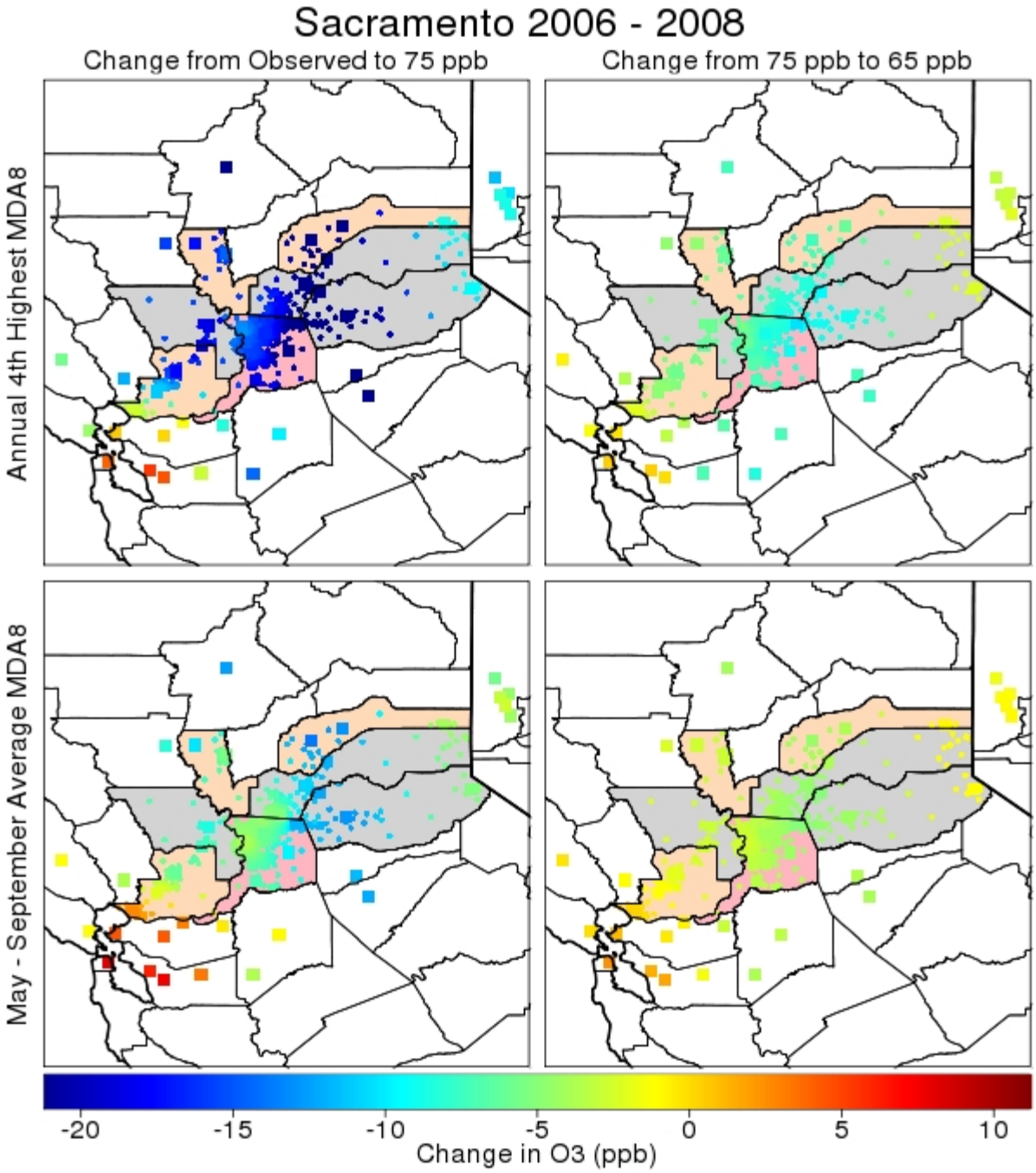


**Figure 94: Changes in annual 4th highest MDA8 and May-September average MDA8 values based on HDDM adjustments for Sacramento, 2006-2008. The points are colored according to the change in ppb, and values falling outside the range in the color bar were set to the nearest value within the color bar.**

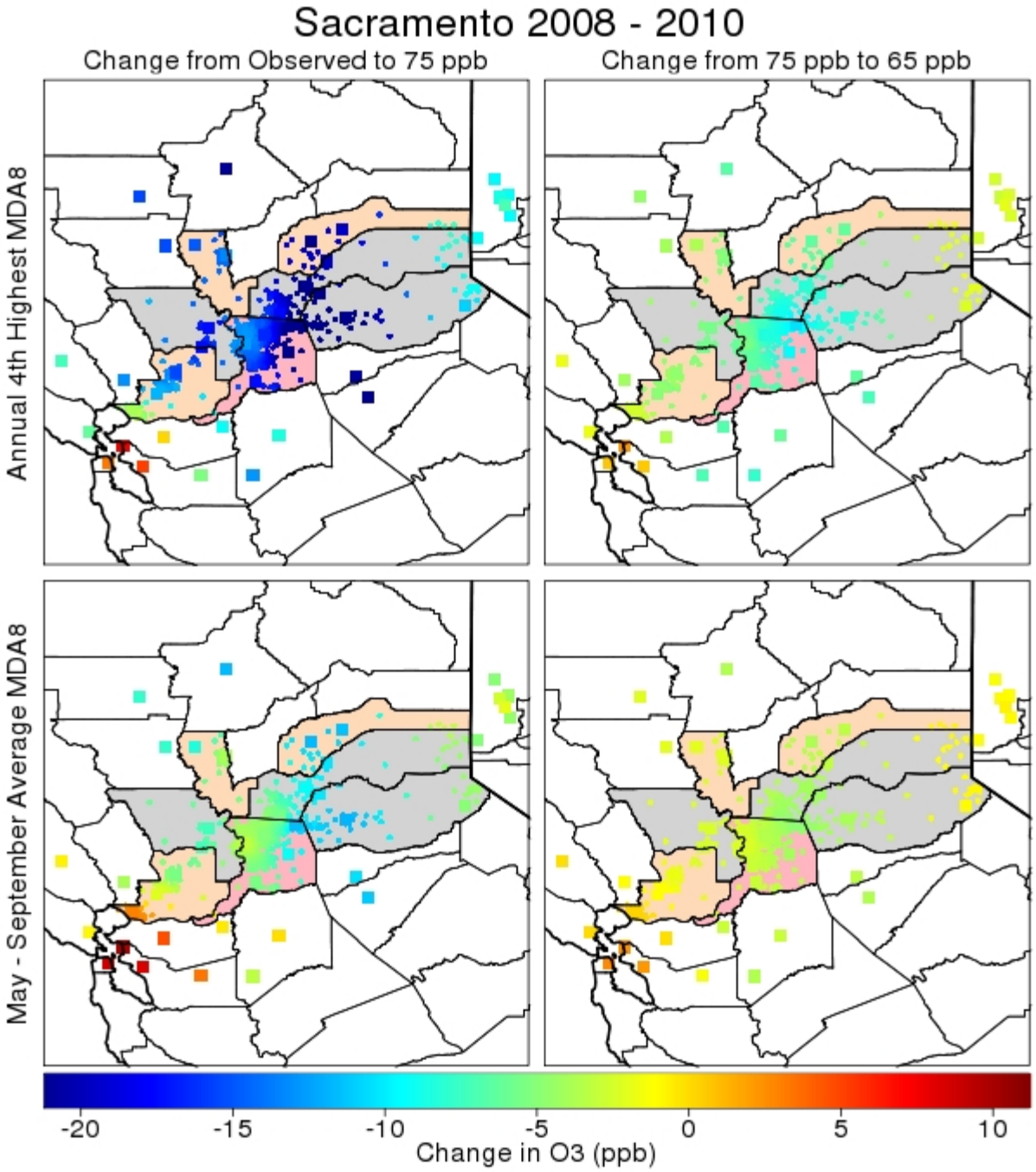


**Figure 95: Changes in annual 4th highest MDA8 and May-September average MDA8 values based on HDDM adjustments for Sacramento, 2008-2010. The points are colored according to the change in ppb, and values falling outside the range in the color bar were set to the nearest value within the color bar.**

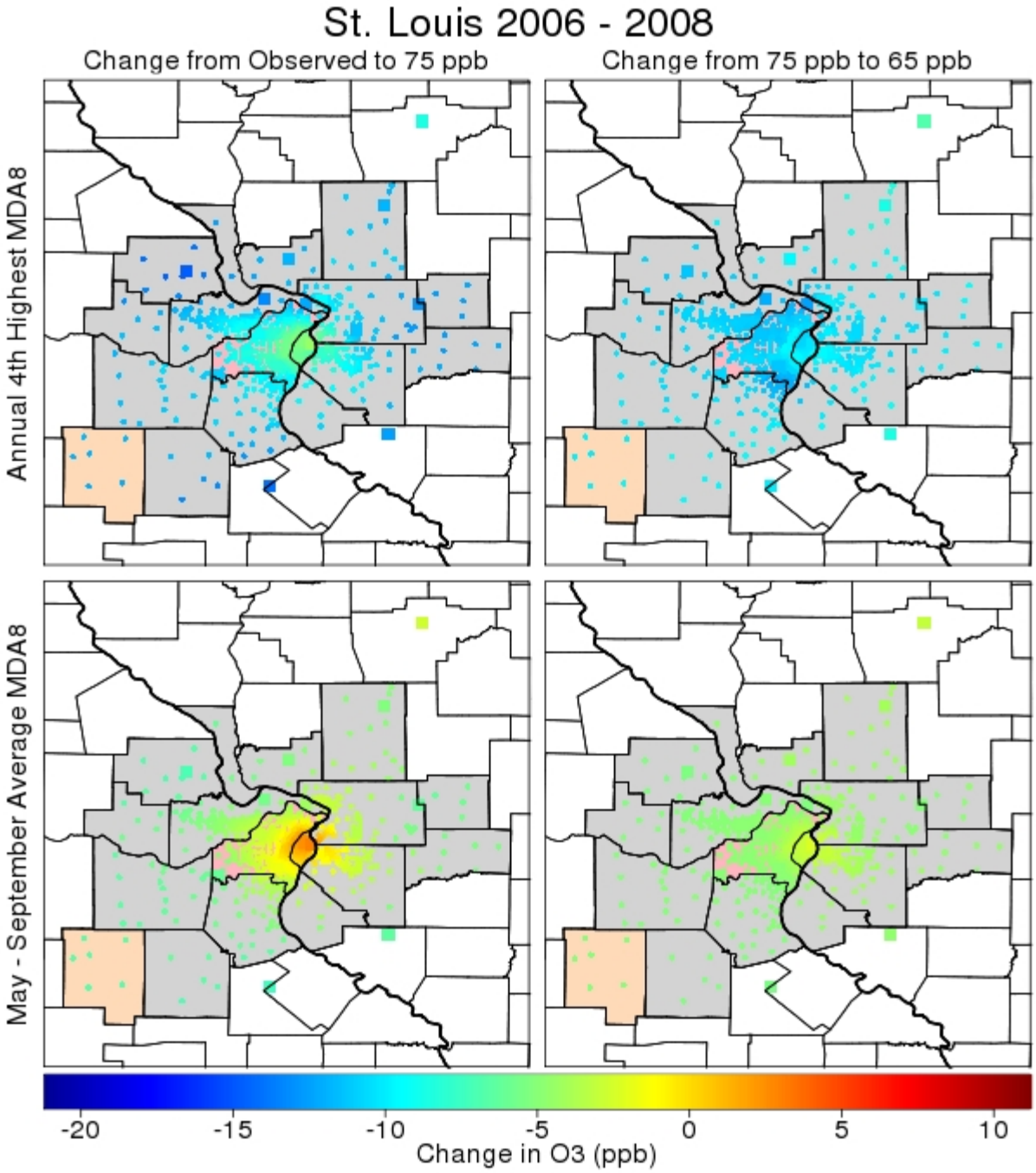


**Figure 96: Changes in annual 4th highest MDA8 and May-September average MDA8 values based on HDDM adjustments for St. Louis, 2006-2008. The points are colored according to the change in ppb, and values falling outside the range in the color bar were set to the nearest value within the color bar.**

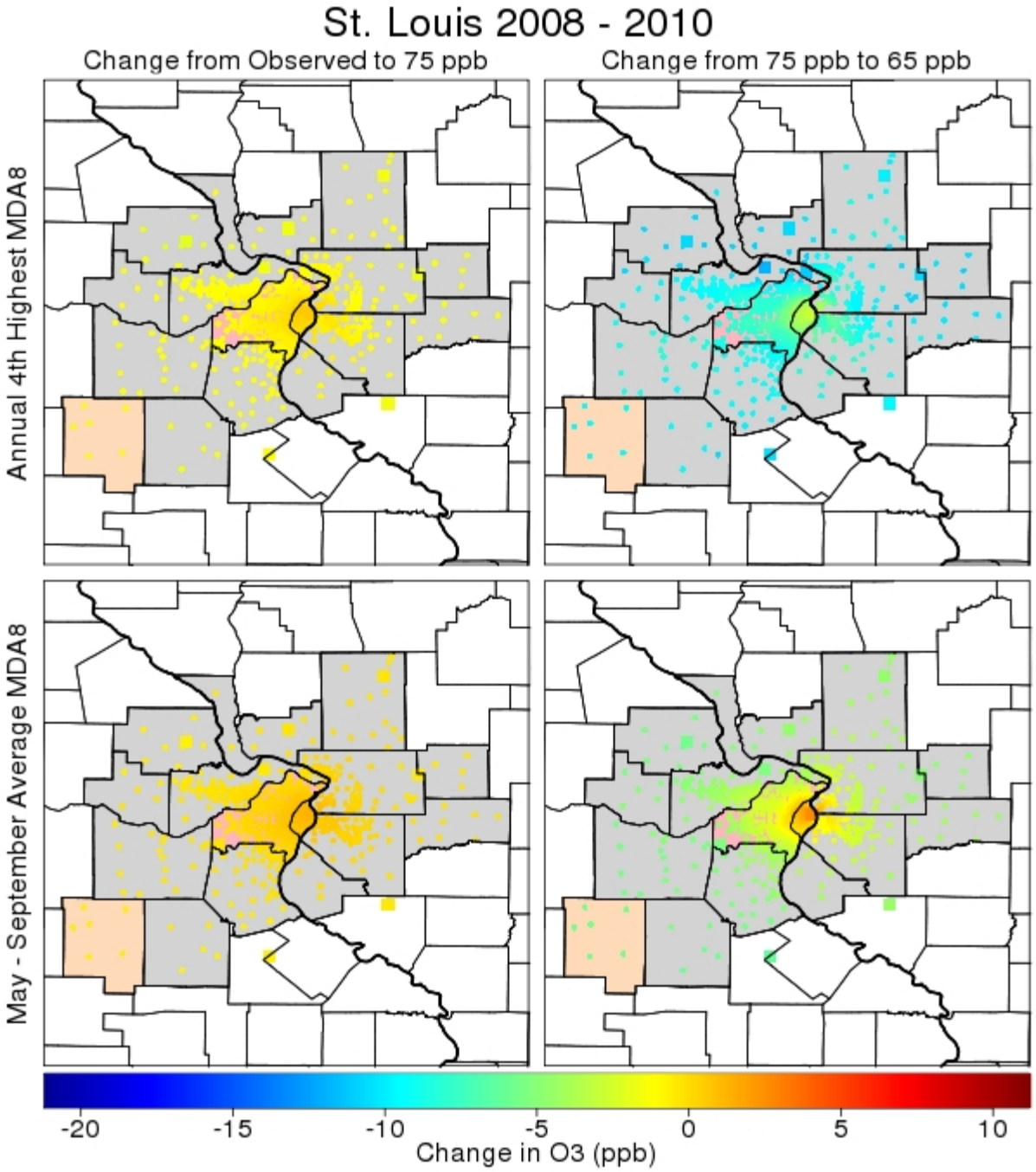


**Figure 97: Changes in annual 4th highest MDA8 and May-September average MDA8 values based on HDDM adjustments for St. Louis, 2008-2010. The points are colored according to the change in ppb, and values falling outside the range in the color bar were set to the nearest value within the color bar.**

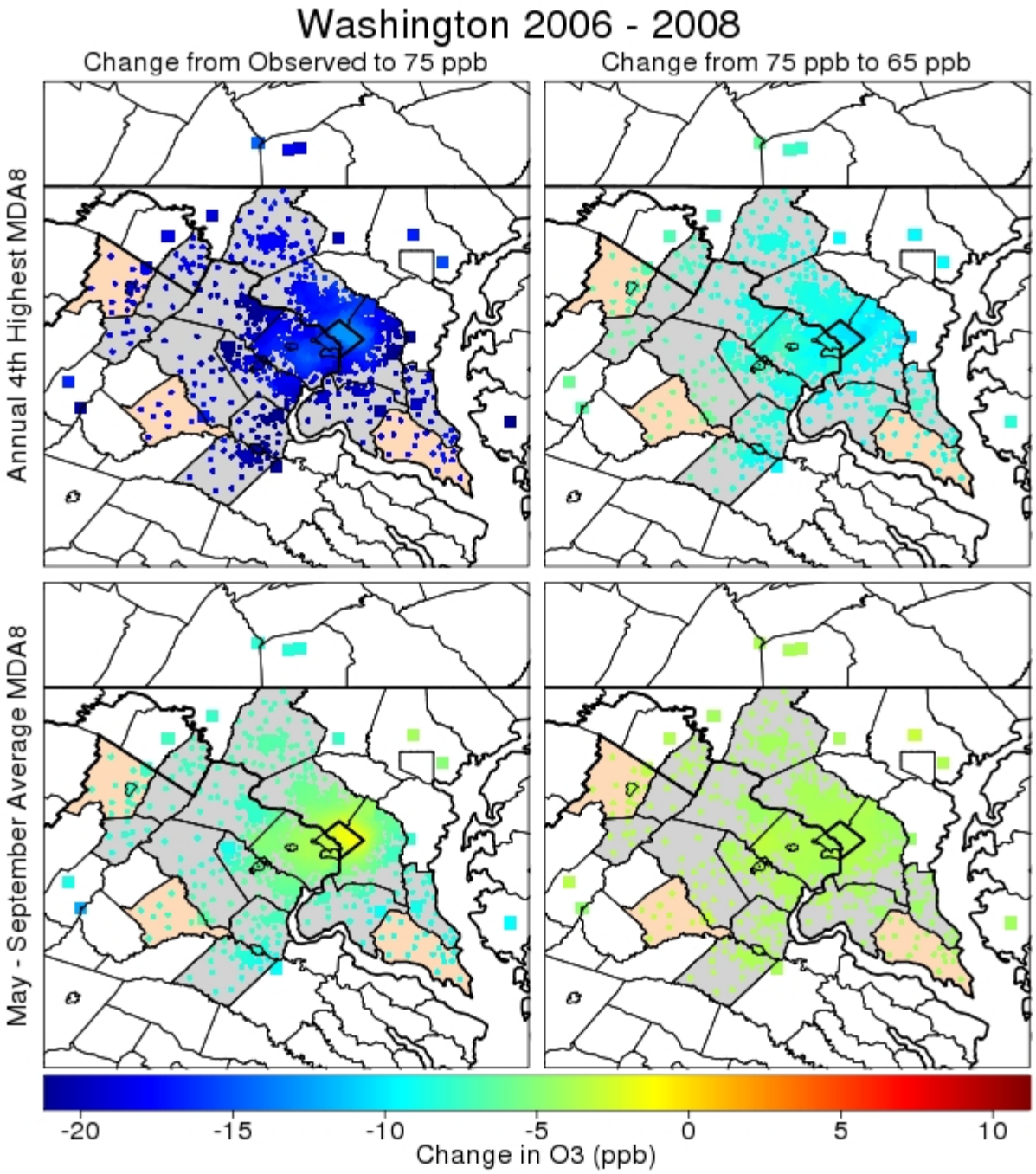


**Figure 98: Changes in annual 4th highest MDA8 and May-September average MDA8 values based on HDDM adjustments for Washington, D.C., 2006-2008. The points are colored according to the change in ppb, and values falling outside the range in the color bar were set to the nearest value within the color bar.**

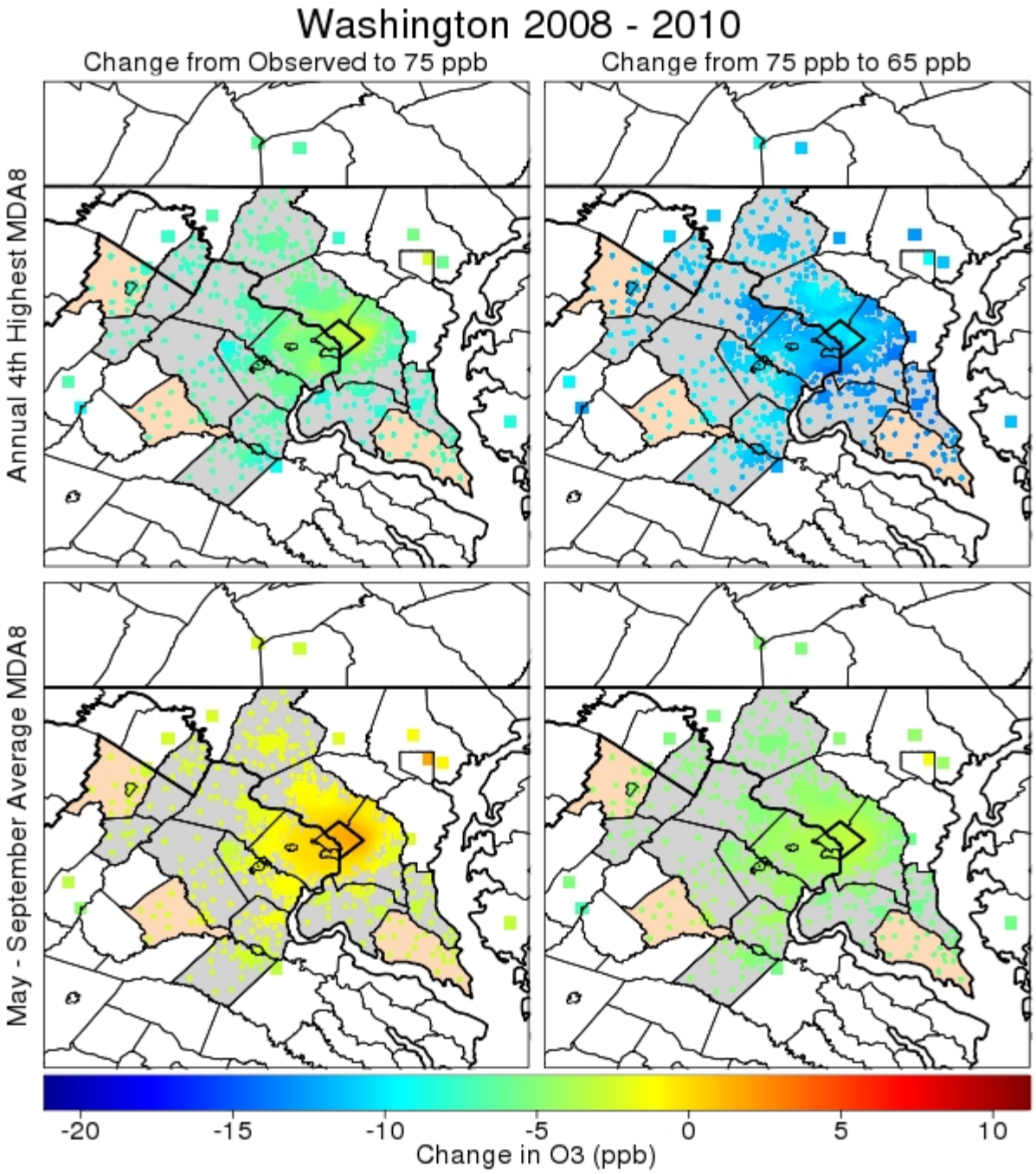


**Figure 99: Changes in annual 4th highest MDA8 and May-September average MDA8 values based on HDDM adjustments for Washington D.C., 2008-2010. The points are colored according to the change in ppb, and values falling outside the range in the color bar were set to the nearest value within the color bar.**

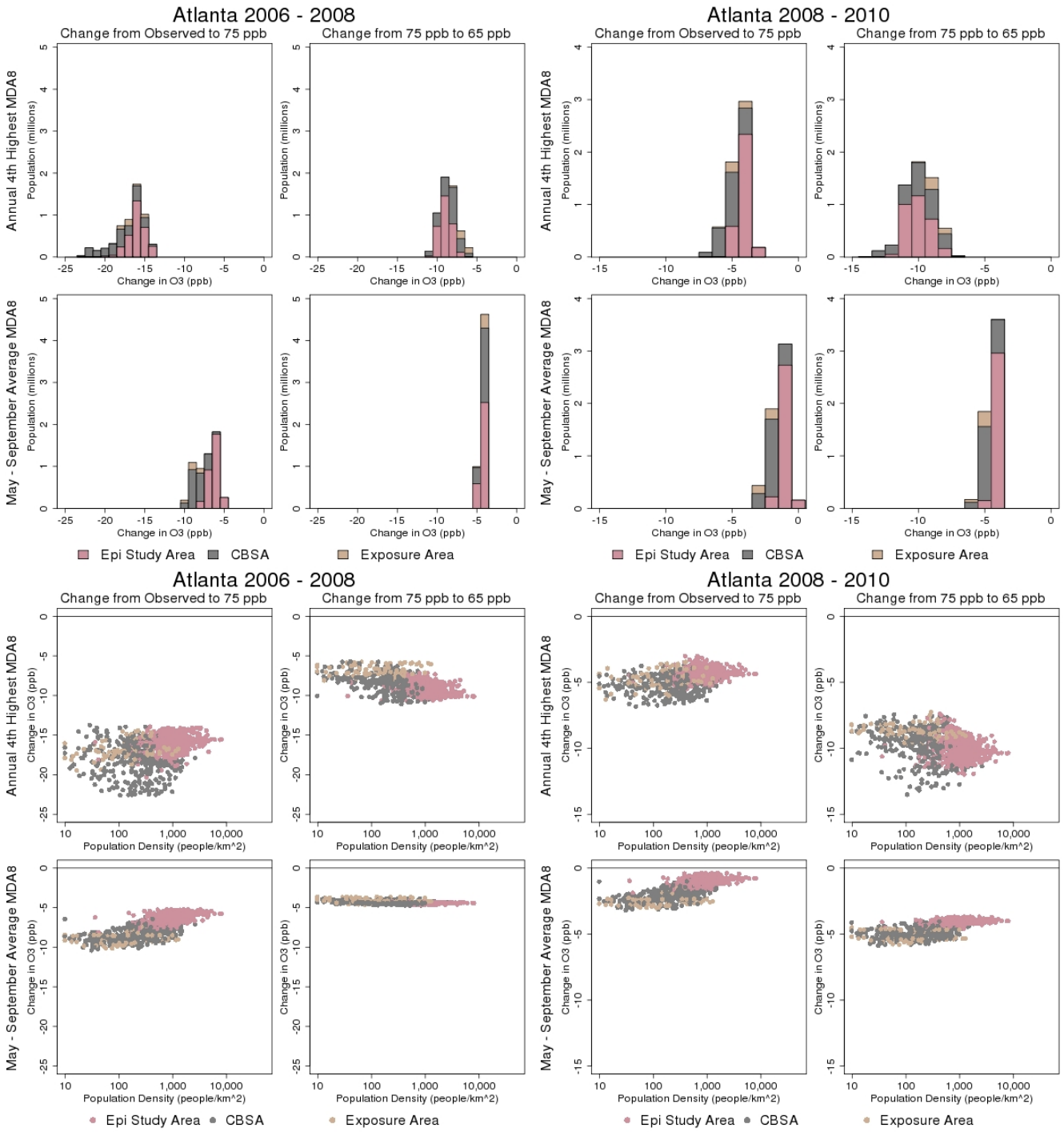


**Figure 100: Changes in VNA estimates of annual 4th highest MDA8 and May – September average MDA8 based on HDDM adjustments for Atlanta versus population and population density.**

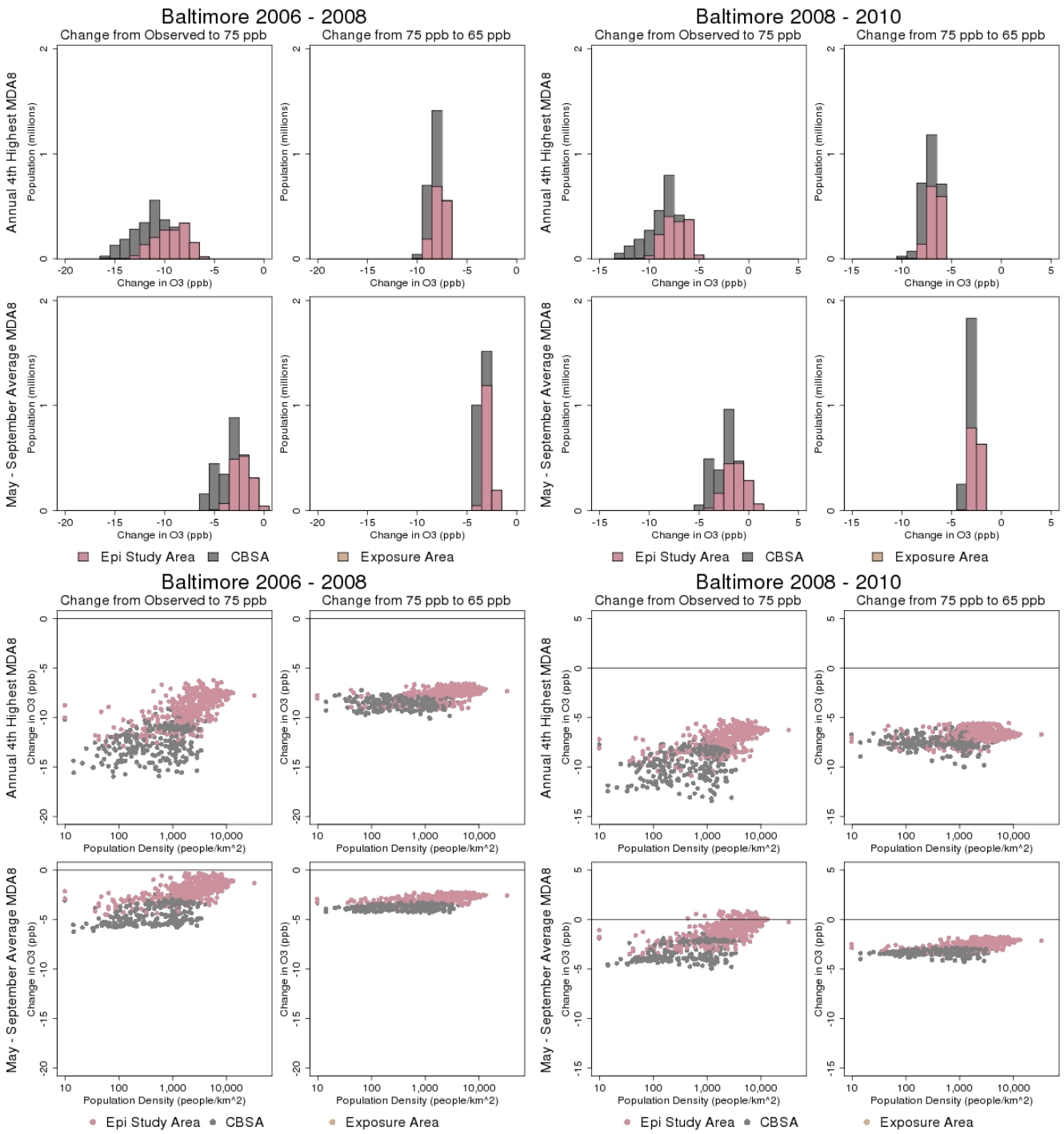


**Figure 101: Changes in VNA estimates of annual 4th highest MDA8 and May – September average MDA8 based on HDDM adjustments for Baltimore versus population and population density.**

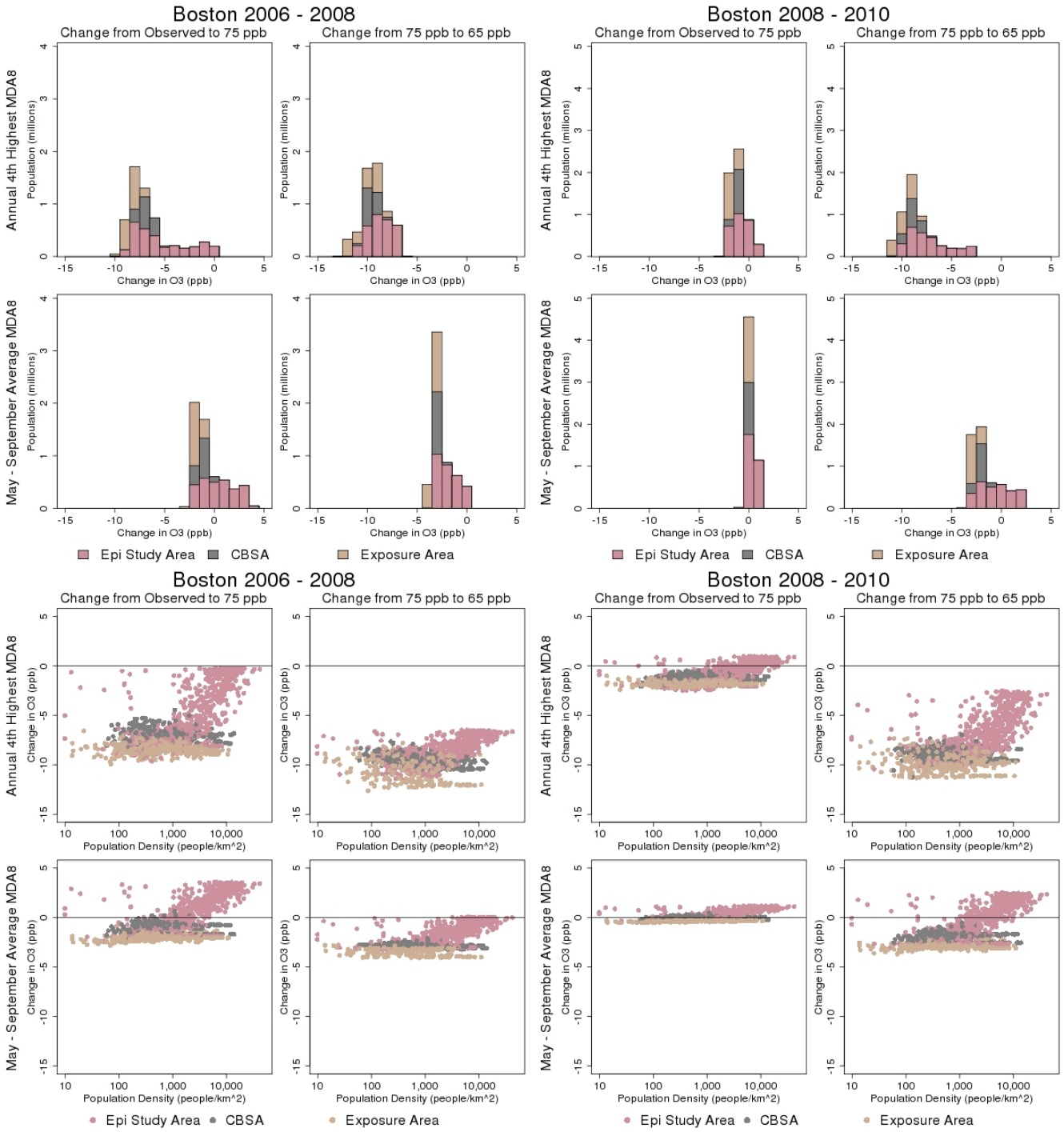


**Figure 102: Changes in VNA estimates of annual 4th highest MDA8 and May – September average MDA8 based on HDDM adjustments for Boston versus population and population density.**

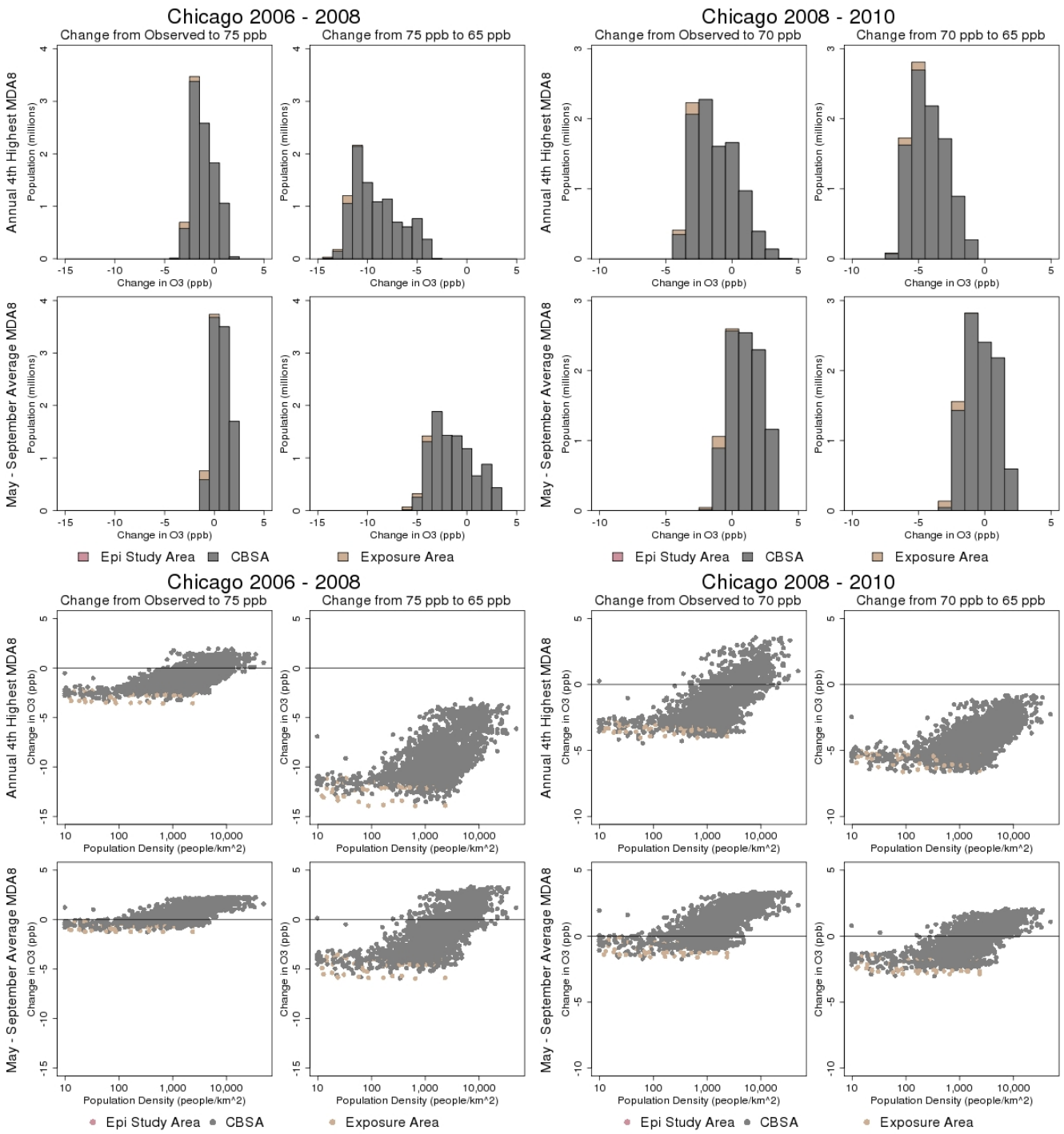


**Figure 103: Changes in VNA estimates of annual 4th highest MDA8 and May – September average MDA8 based on HDDM adjustments for Chicago versus population and population density.**

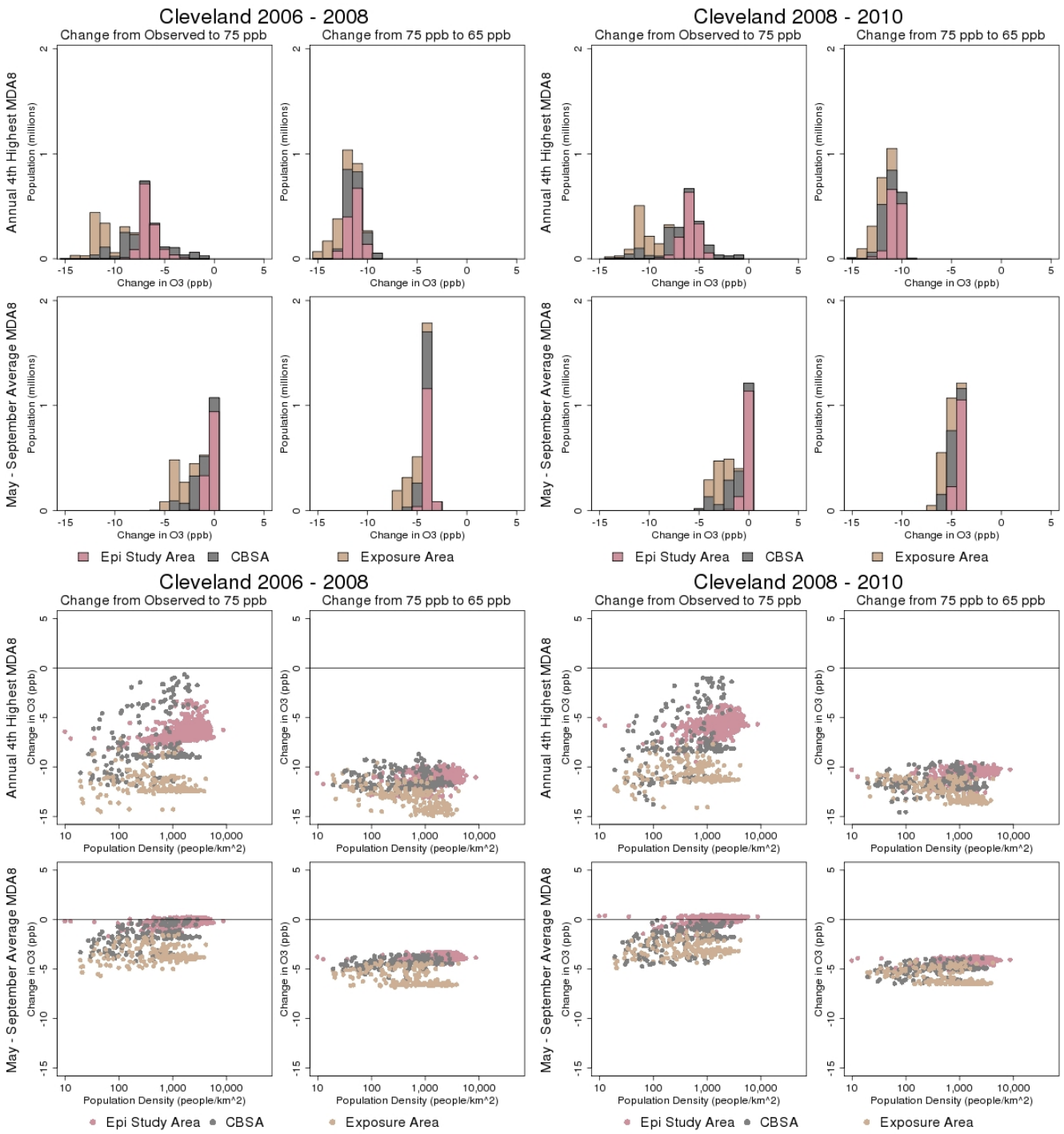


**Figure 104: Changes in VNA estimates of annual 4th highest MDA8 and May – September average MDA8 based on HDDM adjustments for Cleveland versus population and population density.**

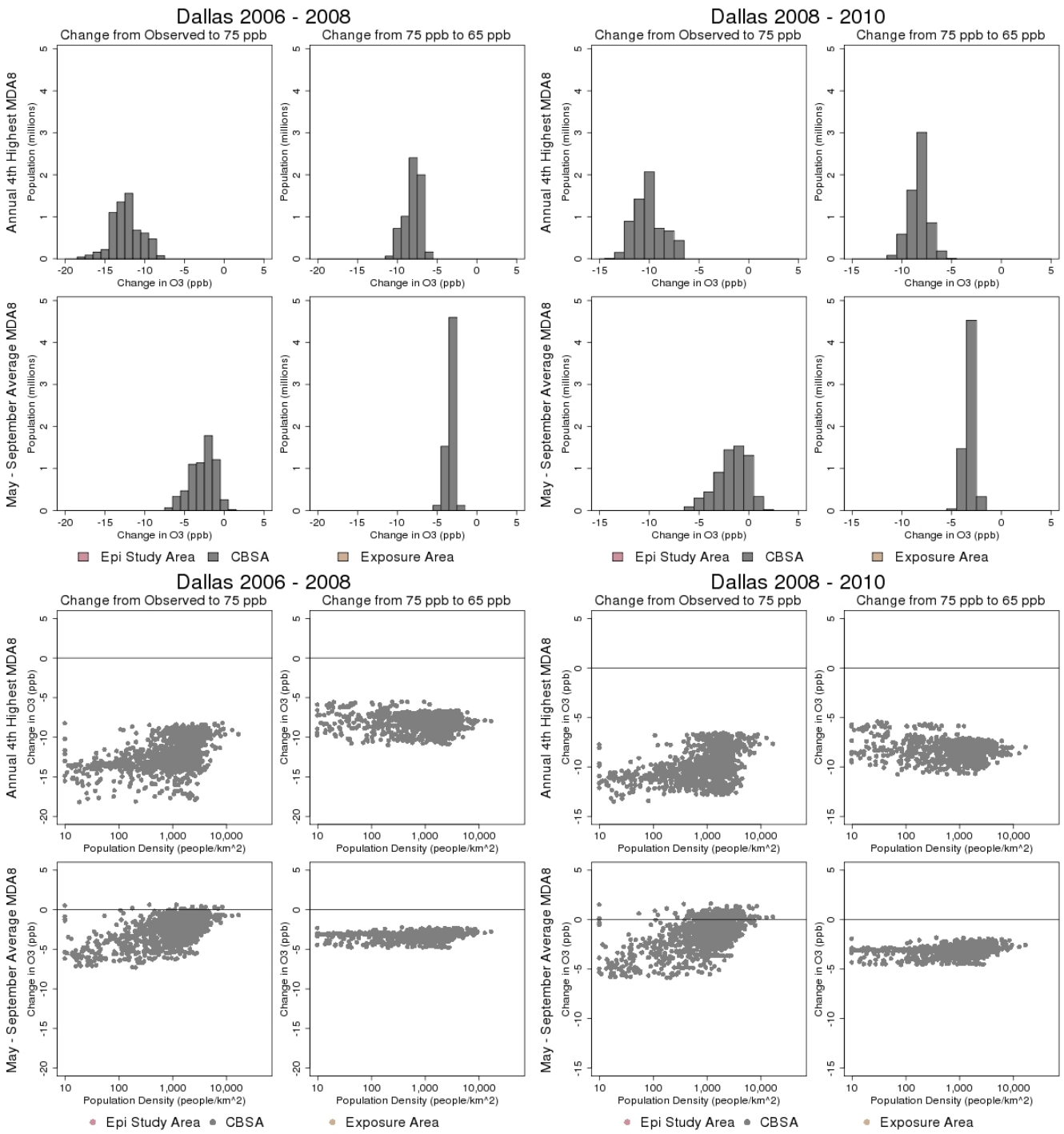


**Figure 105: Changes in VNA estimates of annual 4th highest MDA8 and May – September average MDA8 based on HDDM adjustments for Dallas versus population and population density.**

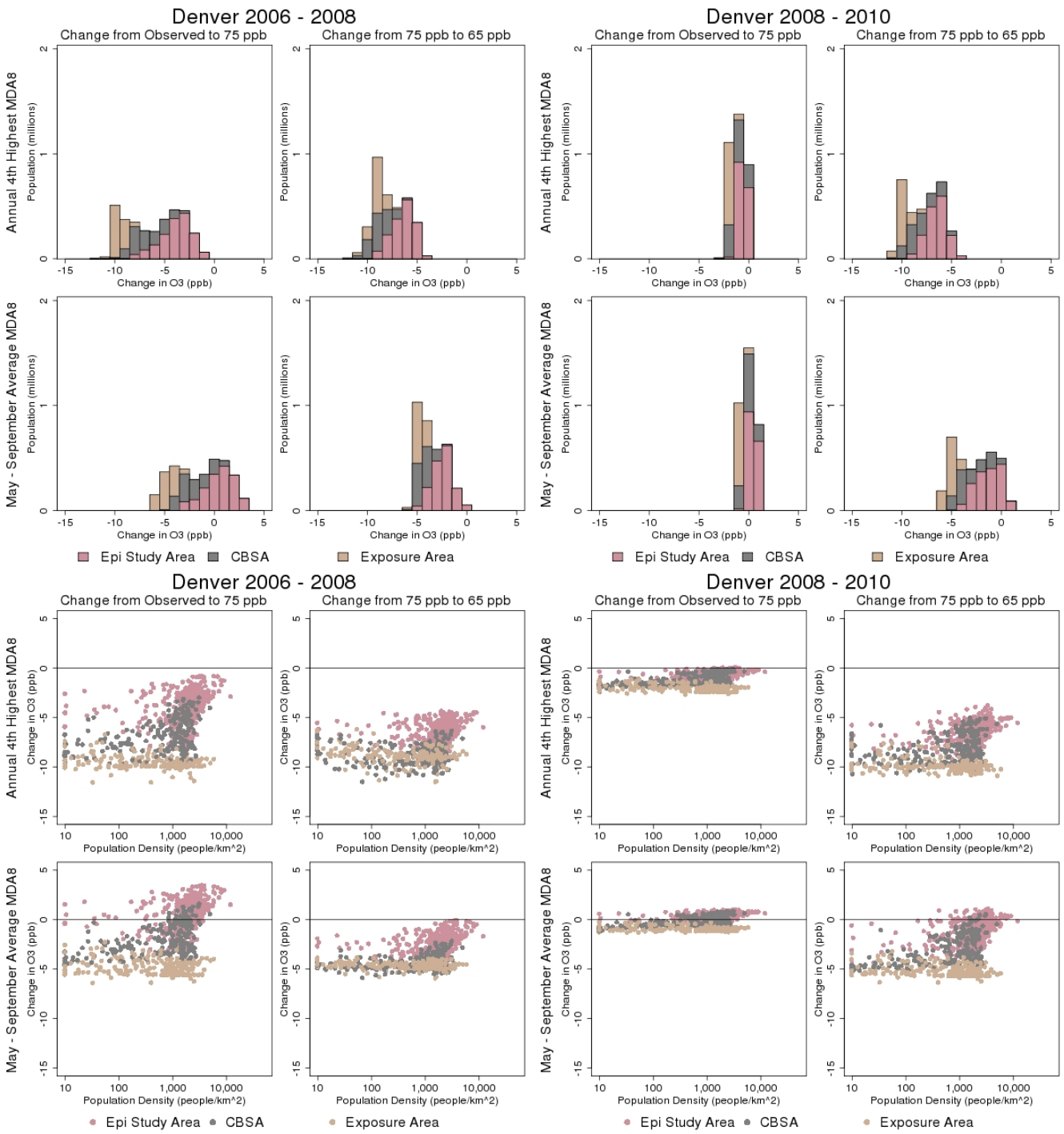


**Figure 106: Changes in VNA estimates of annual 4th highest MDA8 and May – September average MDA8 based on HDDM adjustments for Denver versus population and population density.**

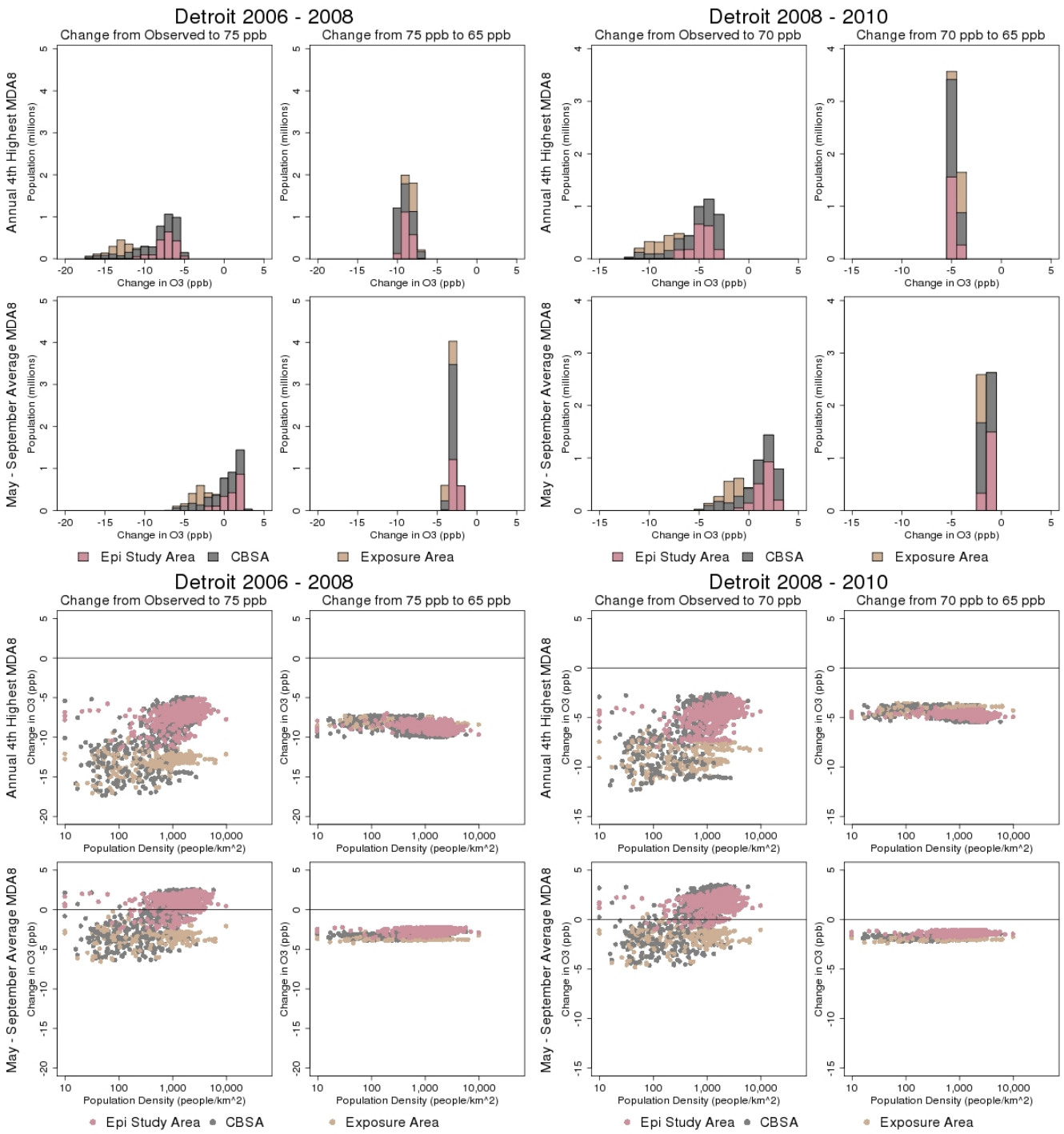


**Figure 107: Changes in VNA estimates of annual 4th highest MDA8 and May – September average MDA8 based on HDDM adjustments for Detroit versus population and population density.**

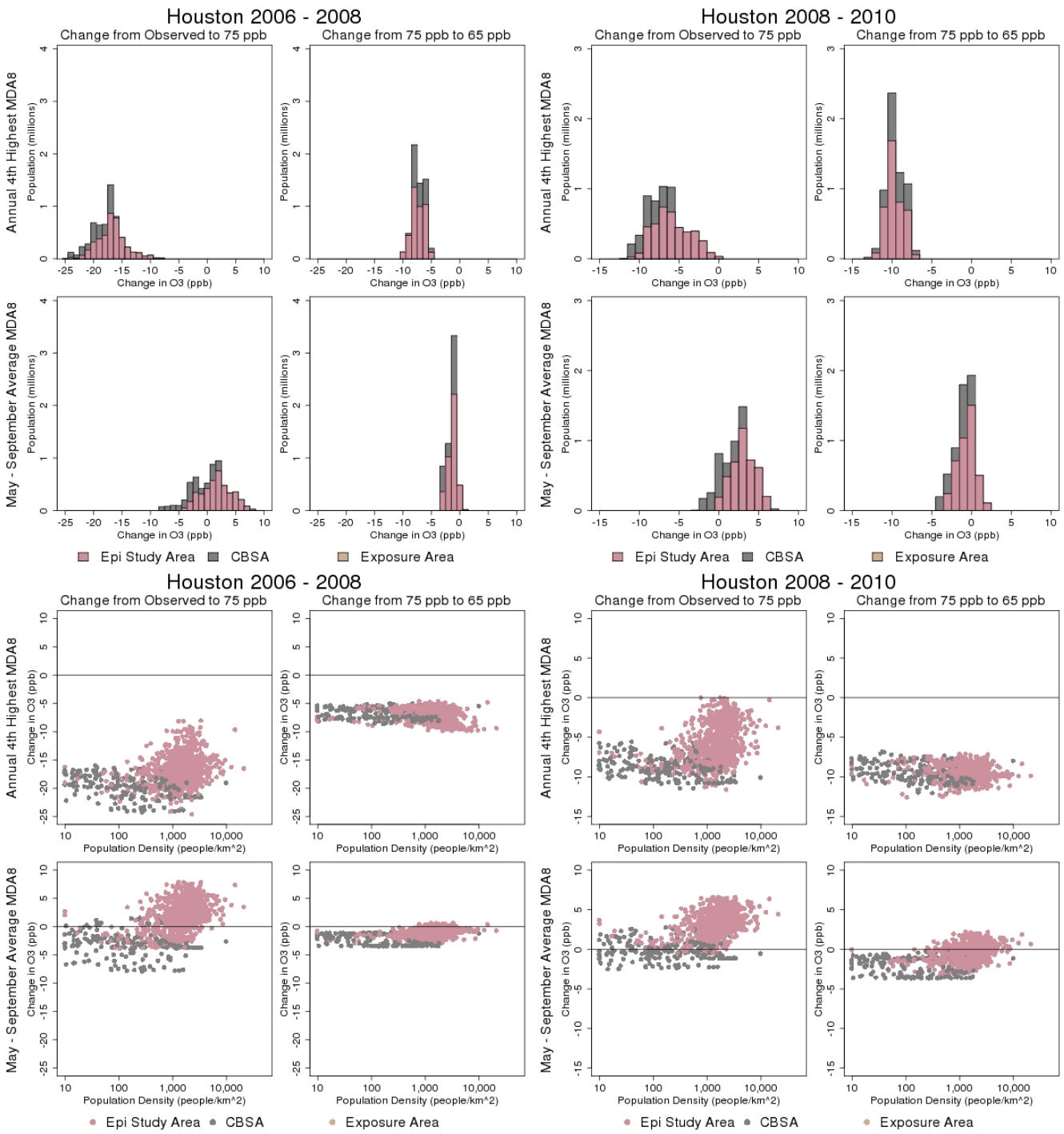


**Figure 108: Changes in VNA estimates of annual 4th highest MDA8 and May – September average MDA8 based on HDDM adjustments for Houston versus population and population density.**

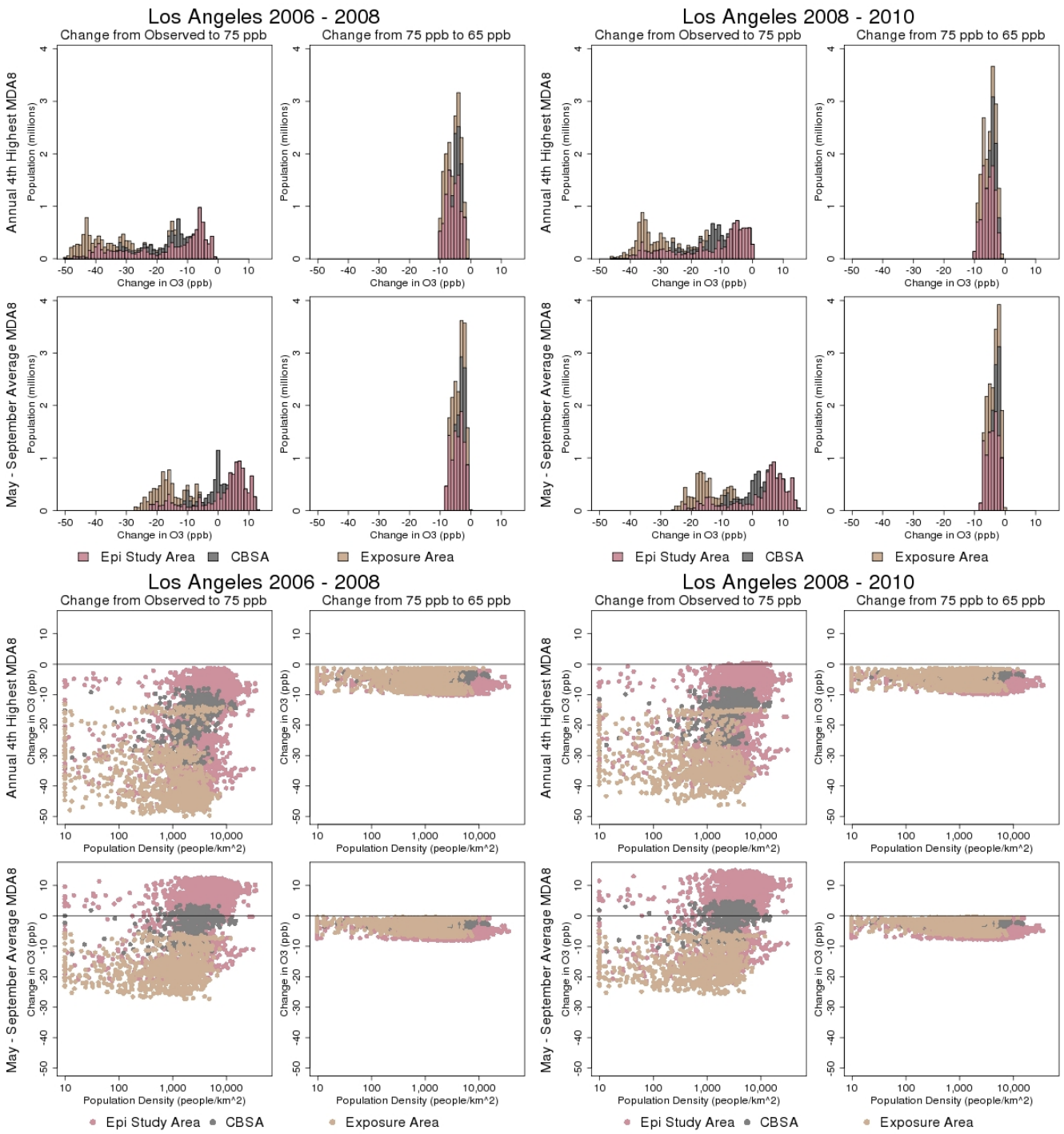


**Figure 109: Changes in VNA estimates of annual 4th highest MDA8 and May – September average MDA8 based on HDDM adjustments for Los Angeles versus population and population density.**

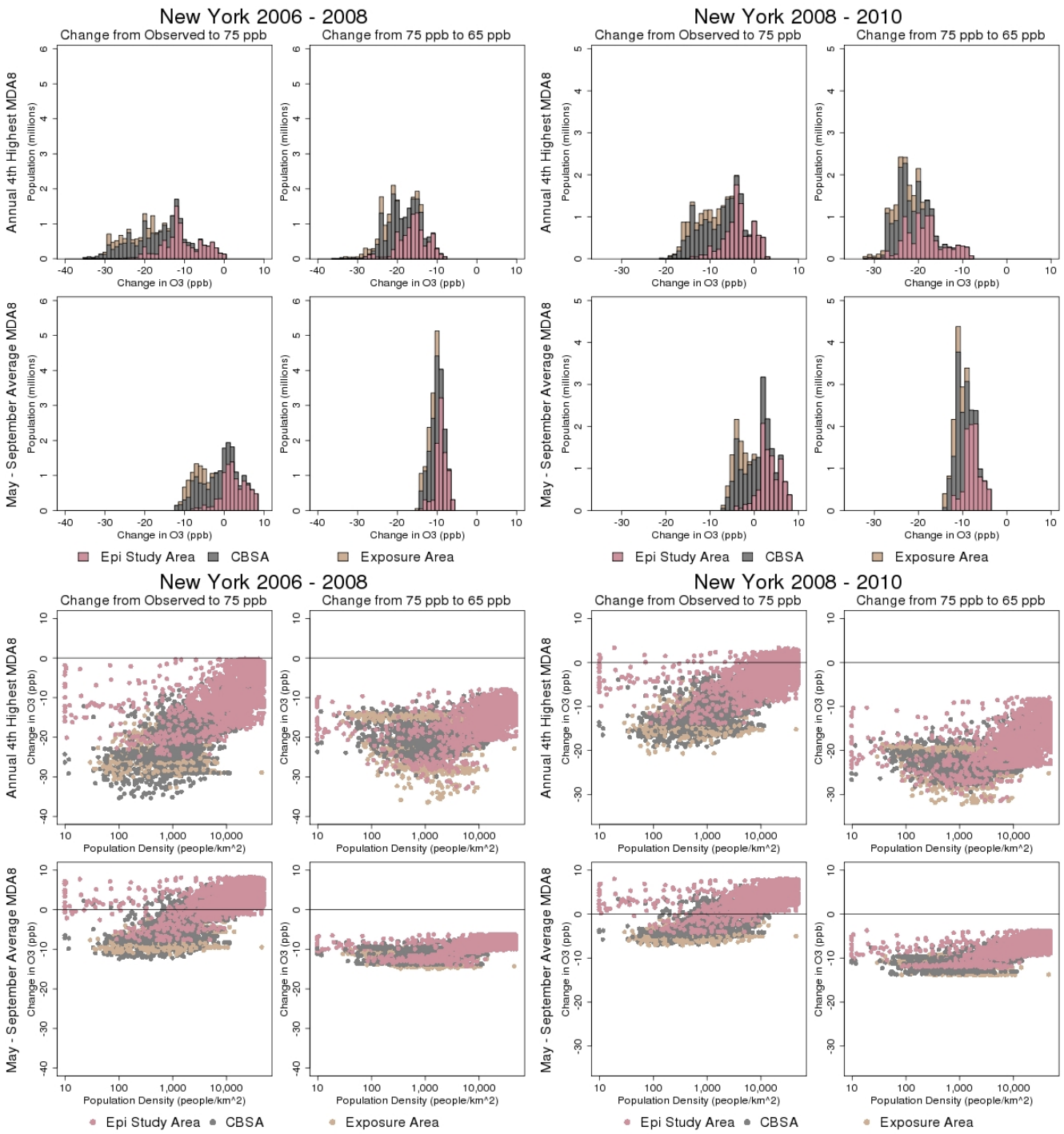


**Figure 110: Changes in VNA estimates of annual 4th highest MDA8 and May – September average MDA8 based on HDDM adjustments for New York versus population and population density.**

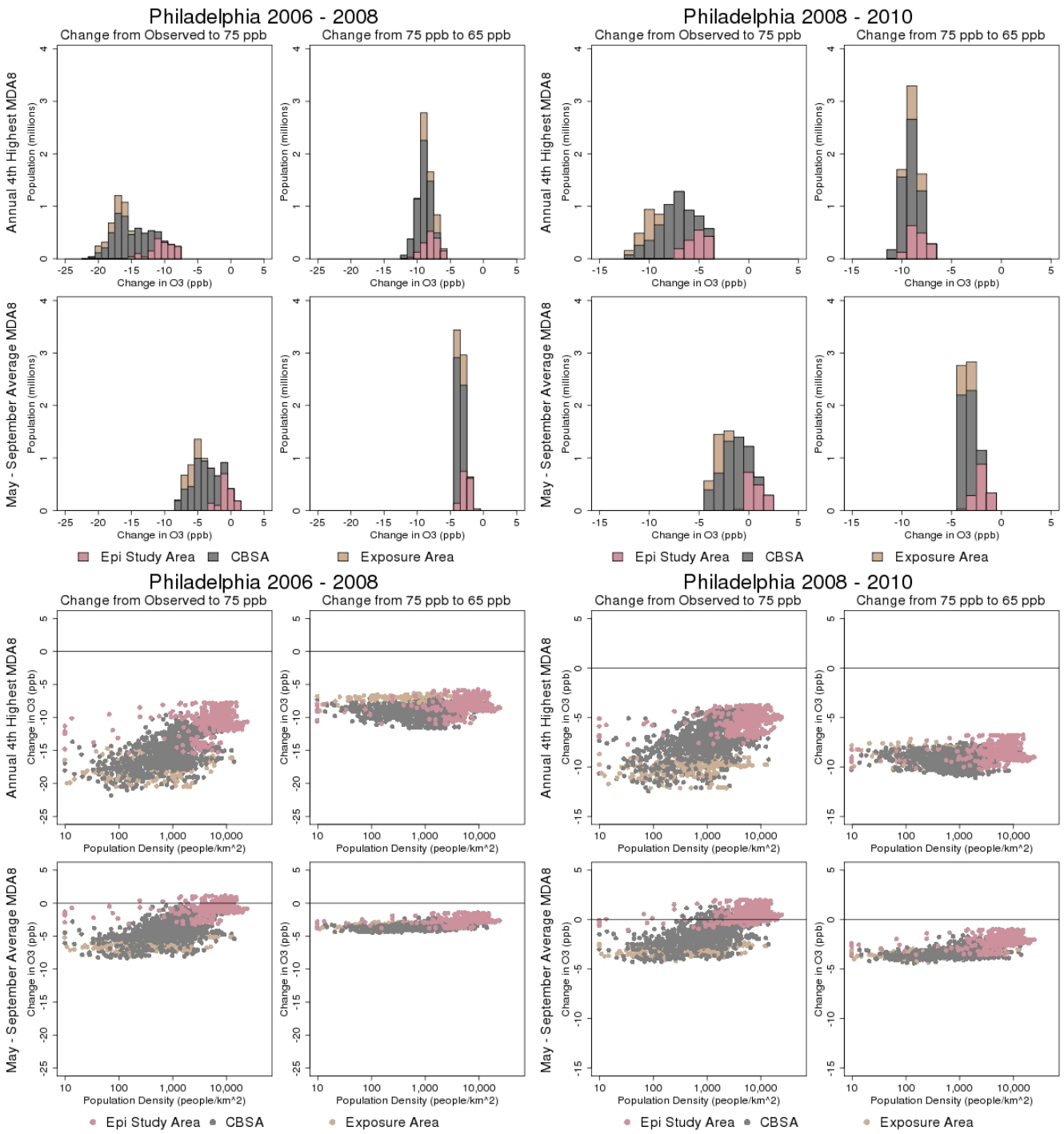


**Figure 111: Changes in VNA estimates of annual 4th highest MDA8 and May – September average MDA8 based on HDDM adjustments for Philadelphia versus population and population density.**

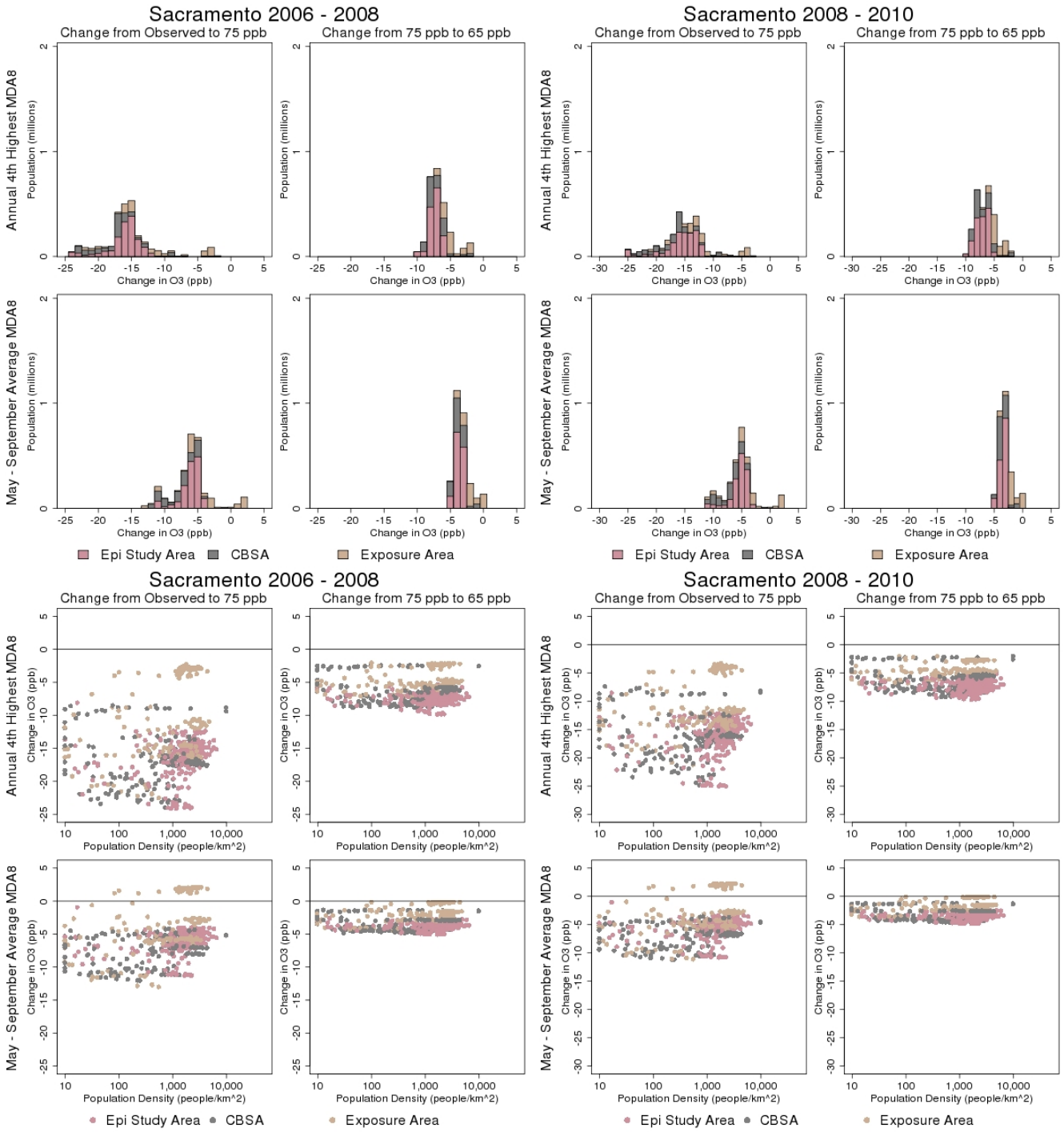


**Figure 112: Changes in VNA estimates of annual 4th highest MDA8 and May – September average MDA8 based on HDDM adjustments for Sacramento versus population and population density.**

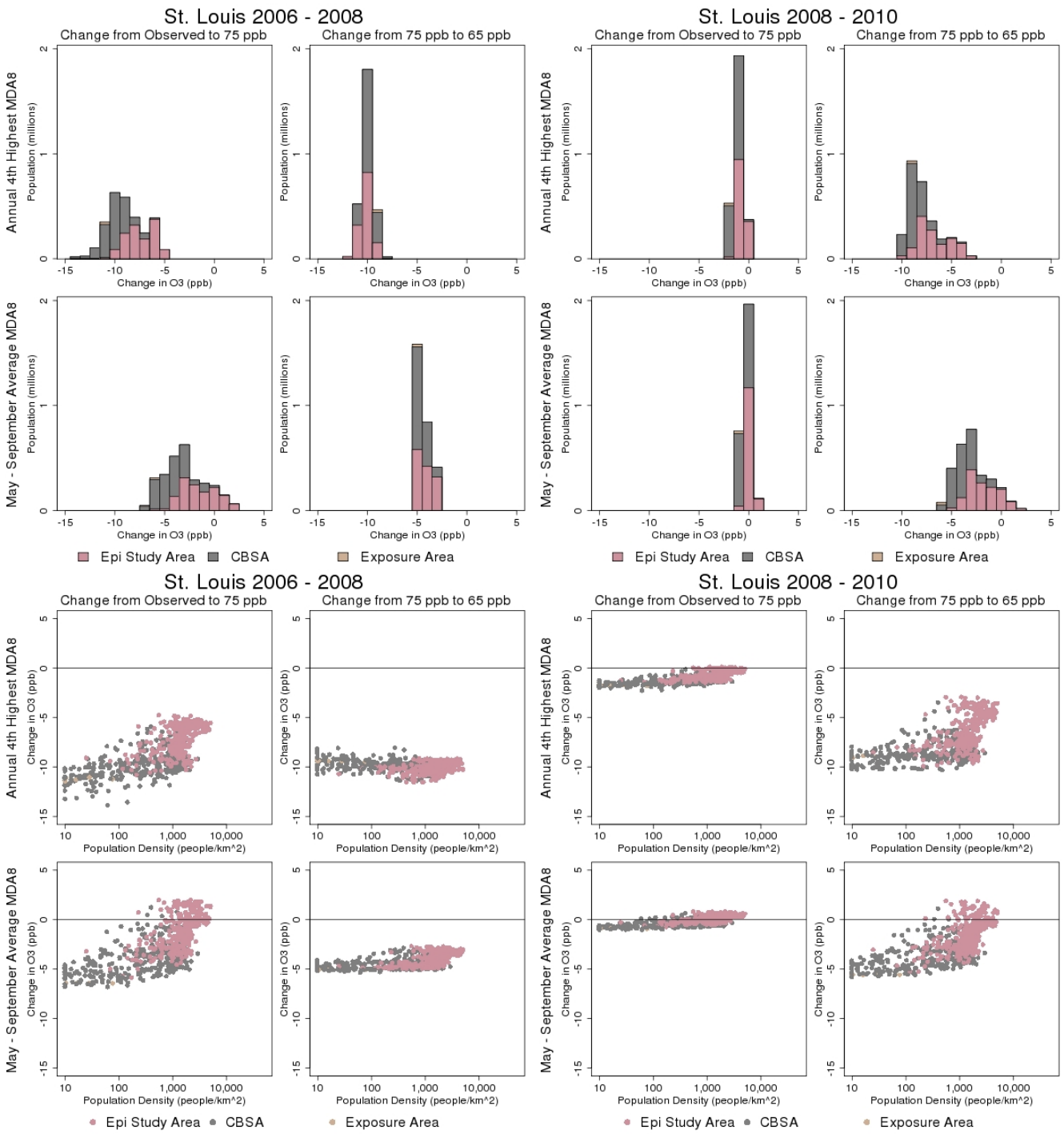


**Figure 113: Changes in VNA estimates of annual 4th highest MDA8 and May – September average MDA8 based on HDDM adjustments for St. Louis versus population and population density.**

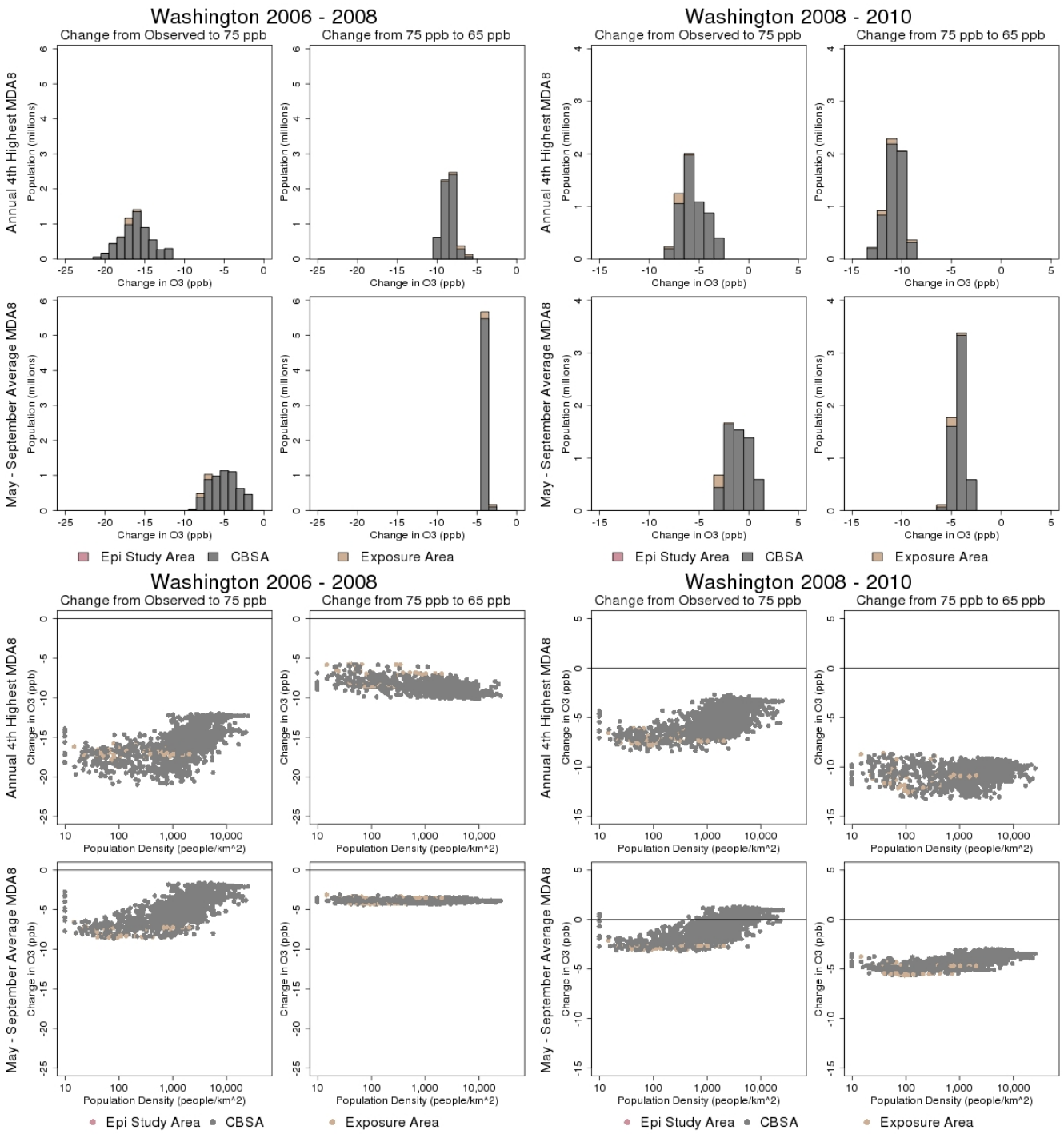


**Figure 114: Changes in VNA estimates of annual 4th highest MDA8 and May – September average MDA8 based on HDDM adjustments for Washington, D.C. versus population and population density.**

## 4.7 COMPARING AIR QUALITY ADJUSTMENTS BASED ON NOX REDUCTIONS ONLY TO AIR QUALITY ADJUSTMENTS BASED ON NOX AND VOC REDUCTIONS

As mentioned in section 3, HDDM-adjustment scenarios could be carried out either by applying across-the-board reductions in U.S. anthropogenic NOx emissions or by applying across-the-board reduction in U.S. anthropogenic NOx and VOC emissions (with equal percentage reductions for the two precursors). The core analysis applied the NOx only reductions to all urban case study areas except Chicago and Denver for which combined NOx and VOC reductions were applied. However, in order to address the question of how the choice of NOx-only emissions reductions affects estimated air quality distributions for adjustments to the current and alternative standard levels we performed sensitivity analyses for seven cities: Denver, Detroit, Houston, Los Angeles, New York, Philadelphia, and Sacramento. For these seven cities, we performed both NOx-only and NOx/VOC emissions reductions scenarios for all standard levels and compared the resulting air quality results. Although in six of these cities the additional VOC reductions did not result in needing lower percentage NOx reductions, we recognize that some VOC reductions are likely to occur in future years due to on-the-books mobile source rules. However, the large VOC cuts applied here are larger than expected reductions from these rules. Several caveats need to be noted for this analysis. First, this is meant as a sensitivity test only and not as a potential realistic alternative control scenario. Second, because the methodology described in section 3 restricts the calculations to equal percentage cuts in NOx and VOC, this sensitivity does not necessarily identify the optimal combination of NOx and VOC reduction levels. Table 20 shows the percentage reductions that were applied in each scenario for each of the seven cities.

**Table 20: Comparison of NOx-only and NOx/VOC emission reductions applied in sensitivity analyses for seven urban areas.**

| City | Years | NOx only | | | | NOx/VOC | | | |
|---|---|---|---|---|---|---|---|---|---|
| | | 75 | 70 | 65 | 60 | 75 | 70 | 65 | 60 |
| Denver | 2006-2008 | 54% | 67% | 76% | 89% | 51% | 65% | 78% | 87% |
| | 2008-2010 | 24% | 53% | 70% | 89% | 15% | 46% | 64% | 87% |
| Detroit | 2006-2008 | 59% | 69% | 76% | 84% | 60% | 73% | 85% | 90% |
| | 2008-2010 | N/A | 54% | 66% | 78% | N/A | 53% | 69% | 85% |
| Houston | 2006-2008 | 62% | 68% | 74% | 82% | 65% | 73% | 81% | 87% |
| | 2008-2010 | 42% | 53% | 63% | 75% | 40% | 52% | 65% | 85% |
| Los Angeles (95% LB) | 2006-2008 | 87% | 89% | 91% | 93% | 95% | 96% | 98% | 99% |
| | 2008-2010 | 87% | 89% | 91% | 93% | 93% | 95% | 97% | 98% |
| New York (95% LB) | 2006-2008 | 64% | 74% | 92% | N/A | 60% | 71% | 89% | N/A |
| | 2008-2010 | 52% | 67% | 89% | N/A | 41% | 55% | 86% | N/A |
| Philadelphia | 2006-2008 | 54% | 61% | 68% | 74% | 57% | 65% | 71% | 79% |
| | 2008-2010 | 42% | 52% | 61% | 68% | 37% | 52% | 62% | 72% |
| Sacramento | 2006-2008 | 63% | 70% | 76% | 84% | 65% | 73% | 80% | 88% |
| | 2008-2010 | 64% | 71% | 77% | 84% | 65% | 74% | 81% | 88% |

Figure 115 through Figure 121 show boxplots of composite monitor daily maximum 8-hr ozone values for recent conditions (base) and each of the eight adjustment scenarios (NOx-only and NOx/VOC for 75, 70, 65, and 60 ppb standard levels) in the seven cities evaluated. A range of results can be seen in different urban areas. Denver, Houston, Los Angeles, and New York showed the largest difference between $O_3$ concentrations in NOx-only versus NOx/VOC scenarios while Detroit, Philadelphia and Sacramento had relatively less difference in the $O_3$ distributions estimated in two types of scenarios. In all cities, the NOx-only and NOx/VOC scenarios had very similar $O_3$ concentrations at the upper end of the distribution (top whiskers and outlier dots in the boxplots). This is not surprising since the adjustment scenarios were implemented to obtain identical $4^{th}$ high $O_3$ concentrations. Mid-range $O_3$

concentrations ($25^{th}$-$75^{th}$ percentiles) were generally lower in the NOx/VOC adjustment scenarios than the NOx-only adjustment scenarios for the same standard level with the exception of New York. The reduction of mid-range $O_3$ concentrations in the NOx/VOC scenarios compared to the NOx-only scenarios tended to be larger in 2007 than in 2009 and tended to be larger at lower alternate standard levels. In most urban case study areas the reduction in mid-level ozone in the NOx/VOC scenario compared to the NOx-only scenario was modest but in Los Angeles it was significant. The change in mid-range ozone concentrations between the two sets of scenarios was so dramatic in Los Angeles that in many cases the $75^{th}$ percentile concentration in the NOx/VOC scenario was lower than the $25^{th}$ percentile concentration in the comparable NOx-only scenario. The most dramatic differences between the NOx-only and the NOx/VOC scenarios occurred at the low end of the ozone distribution. In all urban case study areas, there were smaller increases in ozone at low ozone concentrations in the NOx/VOC scenario when compared to the NOx-only scenario for the same standard level. This is especially evident for extreme low concentrations (bottom whiskers for blue NOx-only scenarios are much higher than bottom whiskers for red NOx/VOC scenarios in the boxplots) but can also be seen in the $25^{th}$ percentile $O_3$ values which are represented by the bottom of the boxes. The reductions were most apparent for Denver, Houston, Los Angeles, New York, and Philadelphia but were more modest in Detroit and Sacramento.

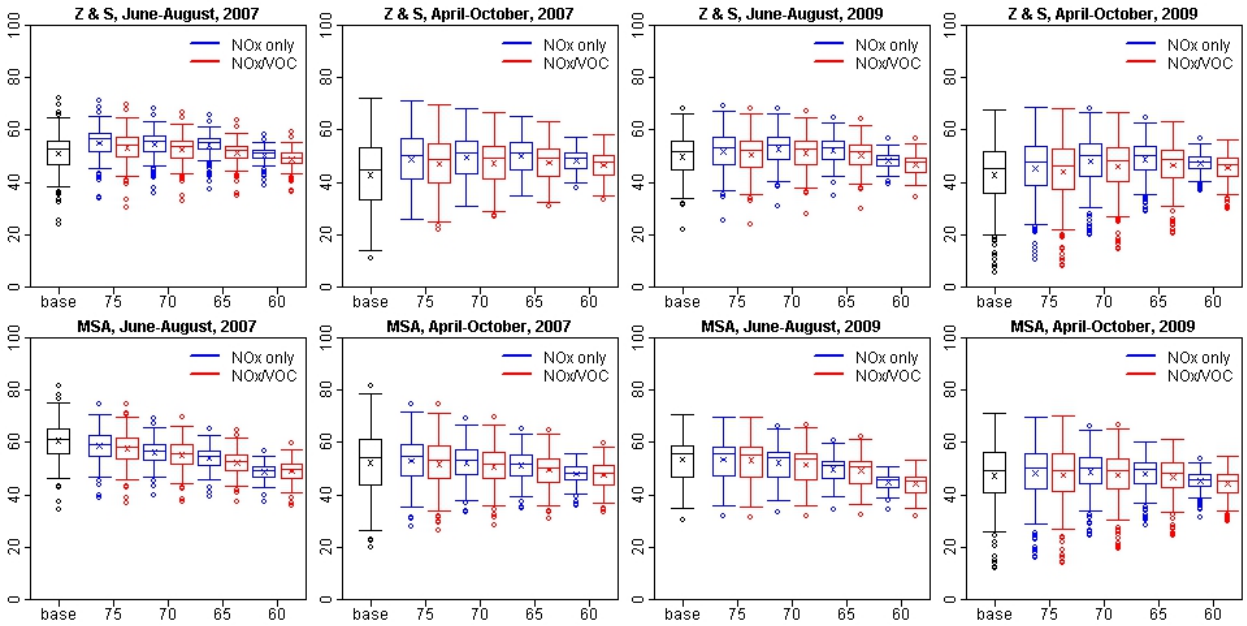


**Figure 115: Composite monitor daily maximum 8-hour $O_3$ values for Denver based on observed and adjusted air quality for the NOx only and NOx/VOC scenarios.**

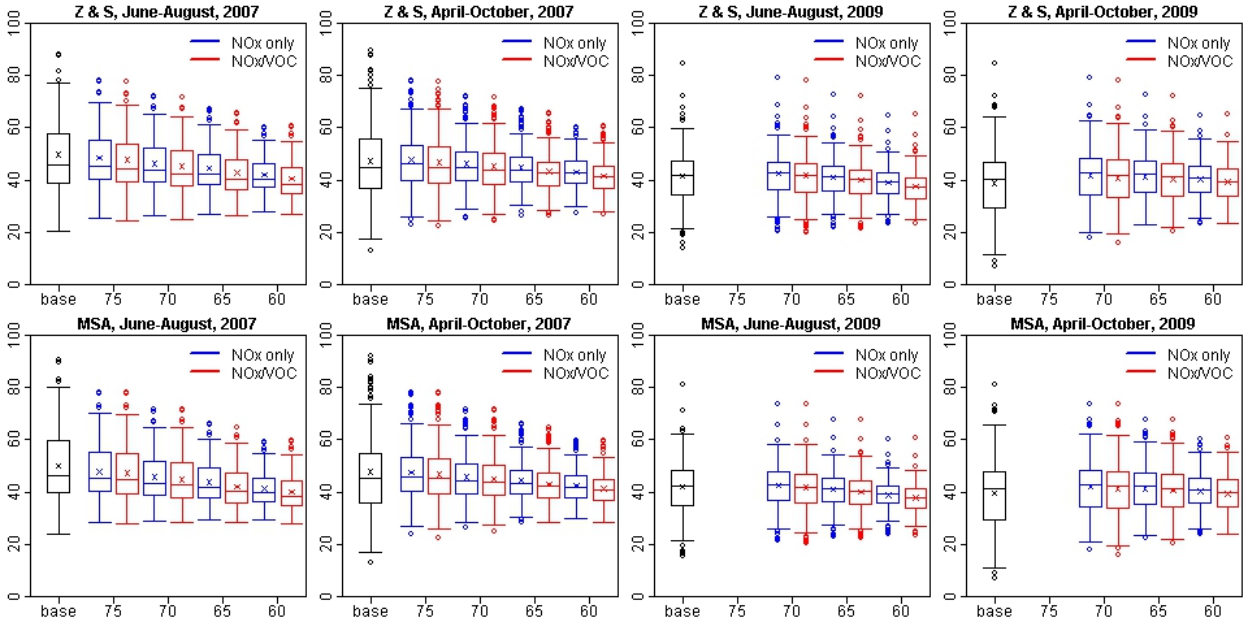


**Figure 116: Composite monitor daily maximum 8-hour $O_3$ values for Detroit based on observed and adjusted air quality for the NOx only and NOx/VOC scenarios.**

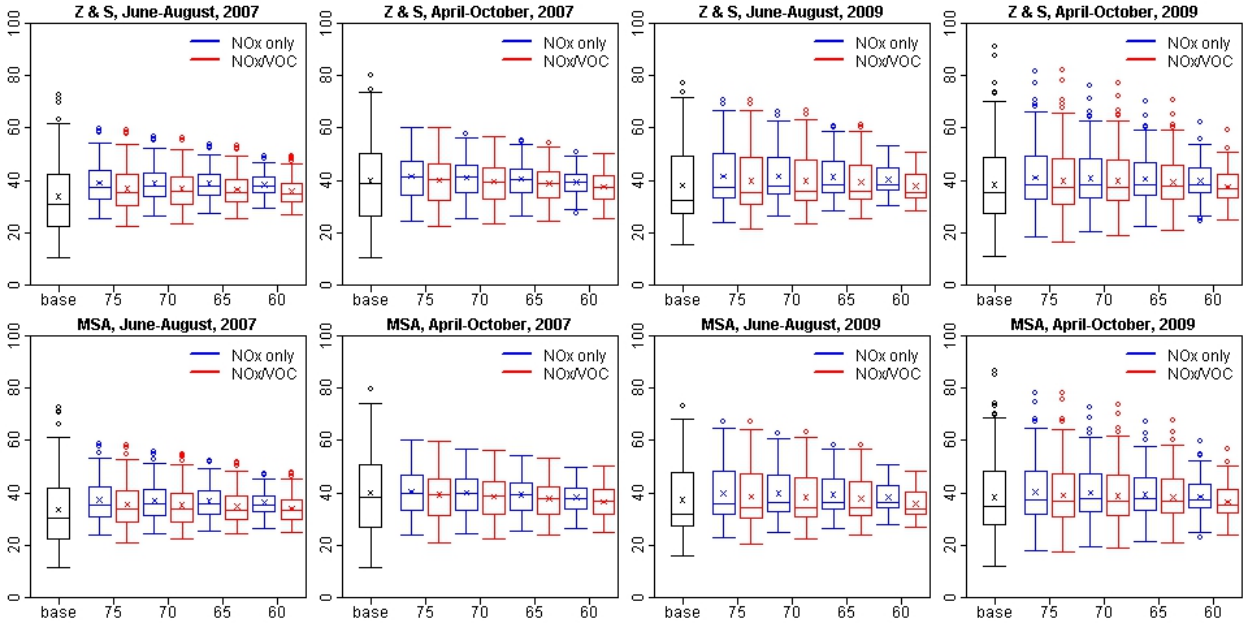


**Figure 117: Composite monitor daily maximum 8-hour $O_3$ values for Houston based on observed and adjusted air quality for the NOx only and NOx/VOC scenarios.**

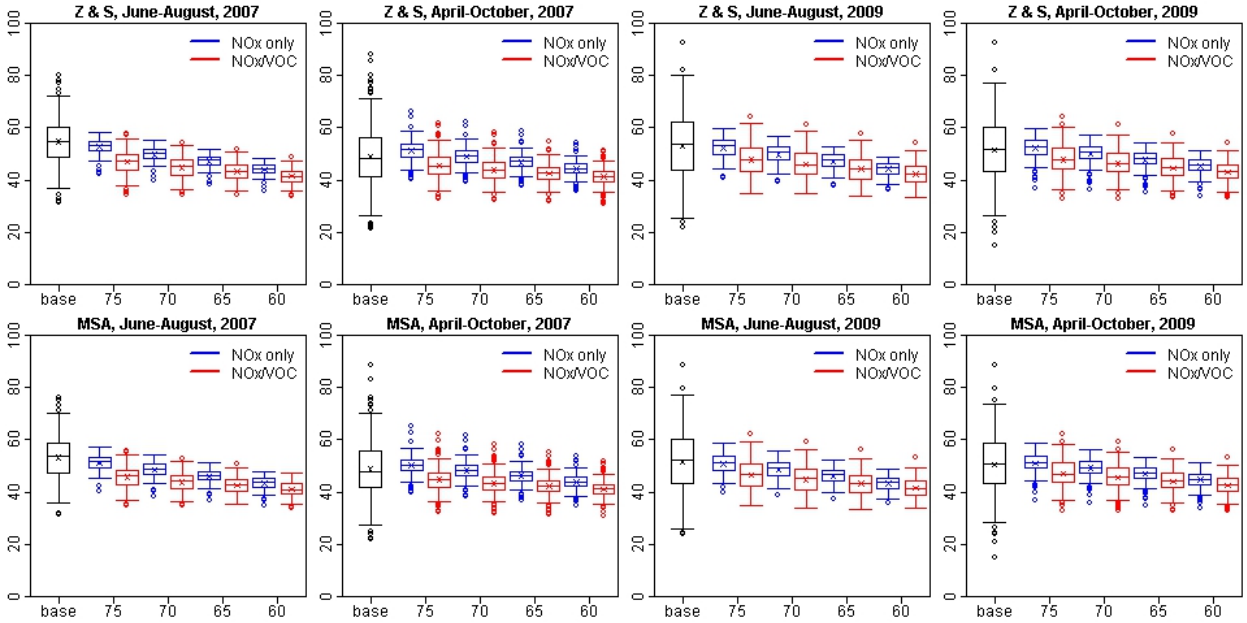


**Figure 118: Composite monitor daily maximum 8-hour $O_3$ values for Los Angeles based on observed and adjusted air quality for the NOx only and NOx/VOC scenarios.**

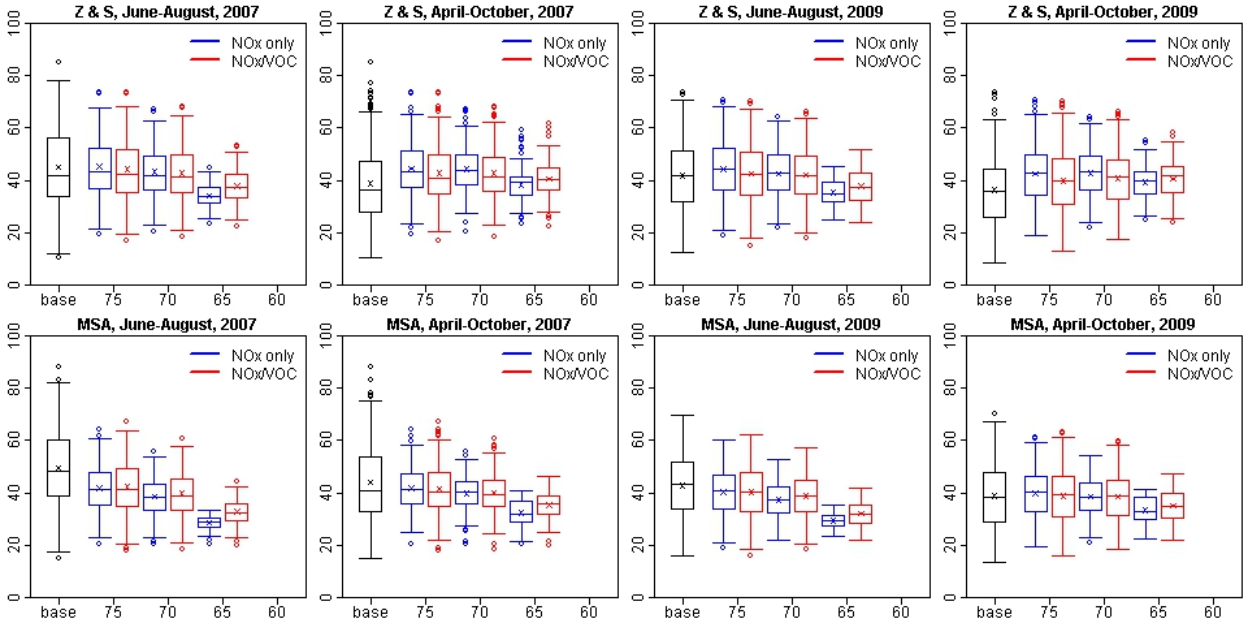


**Figure 119: Composite monitor daily maximum 8-hour $O_3$ values for New York based on observed and adjusted air quality for the NOx only and NOx/VOC scenarios.**

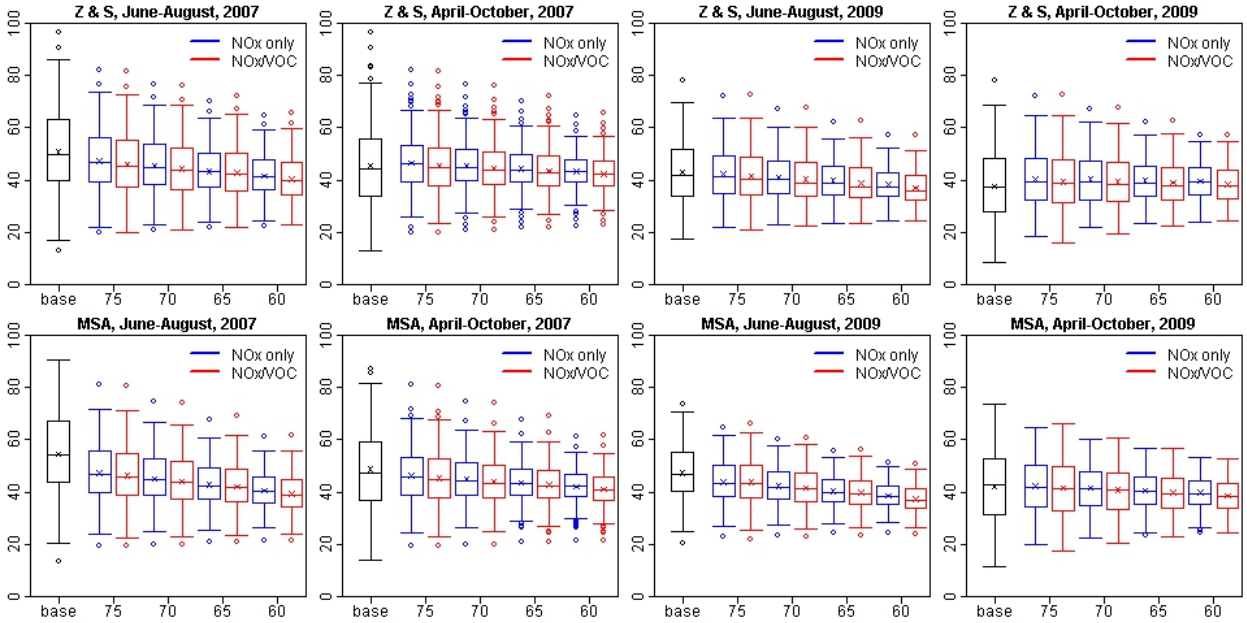


**Figure 120: Composite monitor daily maximum 8-hour $O_3$ values for Philadelphia based on observed and adjusted air quality for the NOx only and NOx/VOC scenarios.**

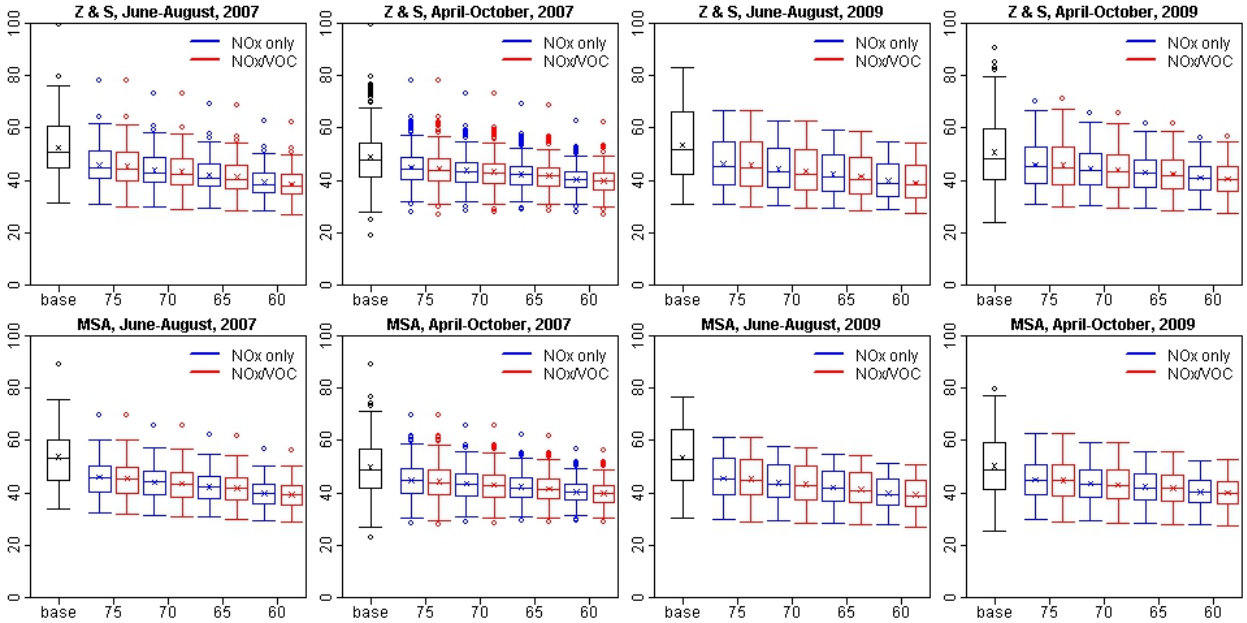


**Figure 121: Composite monitor daily maximum 8-hour $O_3$ values for Sacramento based on observed and adjusted air quality for the NOx only and NOx/VOC scenarios.**

Figure 122 through Figure 128 show maps of the 2006-2008 observed and adjusted April-October seasonal mean of the daily maximum 8-hr ozone value at monitor locations in each of the urban case study areas. Adjusted values are shown for the 75 ppb and 65 ppb NOx-only and NOx/VOC adjustment scenarios. As described earlier in this appendix and in Chapter 4 of the main REA document, these

figures show that for observed 2006-2008 $O_3$ values, the seasonal mean of the daily maximum 8-hr ozone concentration was suppressed in the highly urbanized areas compared to surrounding locations. In these figures, it is clear that ozone concentrations are lower in the center city areas for all cities except Sacramento. The NOx only adjustment scenarios resulted in three types of behavior as demonstrated by the top panels on these maps. First, in Denver, Houston, Los Angeles, and New York the NOx only adjustment cases resulted in increasing seasonal mean concentrations in center city locations where ozone was suppressed in observations and decreasing seasonal mean concentrations in outlying areas where ozone was higher in the observations. This trend is so dramatic in Los Angeles and New York that the spatial gradient becomes inverted in the adjustment cases compared to the observed values (i.e. highest concentrations in urban core areas and lower concentrations in surrounding areas). The second type of response occurred in Detroit where there was little change at the monitor in the center of Wayne County but seasonal mean ozone at the outlying monitors decreased in the NOx-only adjustment cases. Finally, in Sacramento and Philadelphia, the NOx only adjustment cases cause relatively small decreases in seasonal mean ozone throughout the area. When comparing the NOx-only to the NOx/VOC adjustment scenarios three types of patterns emerge. In Denver and Los Angeles, the NOx/VOC adjustment scenarios lead to lower seasonal mean ozone concentrations than the equivalent NOx-only adjustment scenarios in the urban core areas but looked similar to the NOx only adjustment scenario in the outlying areas. In Houston, Detroit, Philadelphia, and Sacramento, seasonal mean ozone concentrations in equivalent NOx-only and NOx/VOC adjustment scenarios were very similar at monitors throughout the areas although the NOx/VOC adjustment scenarios lead to slightly lower concentrations. Finally, in New York the 75 ppb adjustment scenarios were similar for the NOx/VOC and NOx-only cases but for the 65 ppb adjustment scenarios the NOx/VOC case actually lead to higher seasonal mean ozone concentration in the urban core area than the NOx-only case.

An evaluation of the composite monitor and spatial plot maps leads to several general conclusions for this sensitivity analysis. First, the NOx/VOC reduction scenarios tended to mitigate increases that occurred in the NOx-only scenario at the lower end of the ozone distribution. Second the effect on the NOx/VOC scenario versus the NOx-only scenario was less dramatic for mid-range ozone concentrations and varied from city to city. The NOx/VOC scenarios lead to lower mid-range ozone concentrations than the NOx-only scenarios except in the case of New York. Third, the high end ozone concentrations at various standard levels were similar in the NOx-only and the NOx/VOC scenarios. Finally, the VOC reductions tended to have more impact in urban core areas and relatively little impact in outlying areas. The effects of these air quality sensitivity analyses on risk are evaluated and discussed in chapter 7 of the main document.

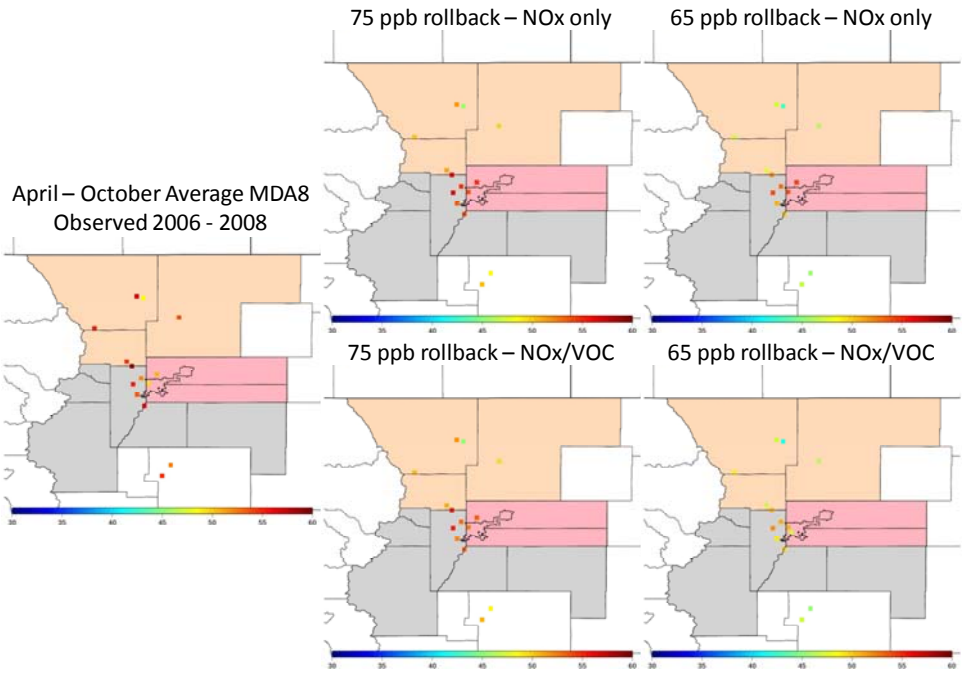


**Figure 122: April-October seasonal average of daily maximum 8-hour $O_3$ values at Denver area monitor locations for observed 2006-2008 conditions (left panel), 75 ppb adjustment scenarios (middle panels), and 65 ppb adjustment scenarios (right panels). NOx only adjustments are shown in top panels, NOx/VOC adjustments are shown in bottom panels.**

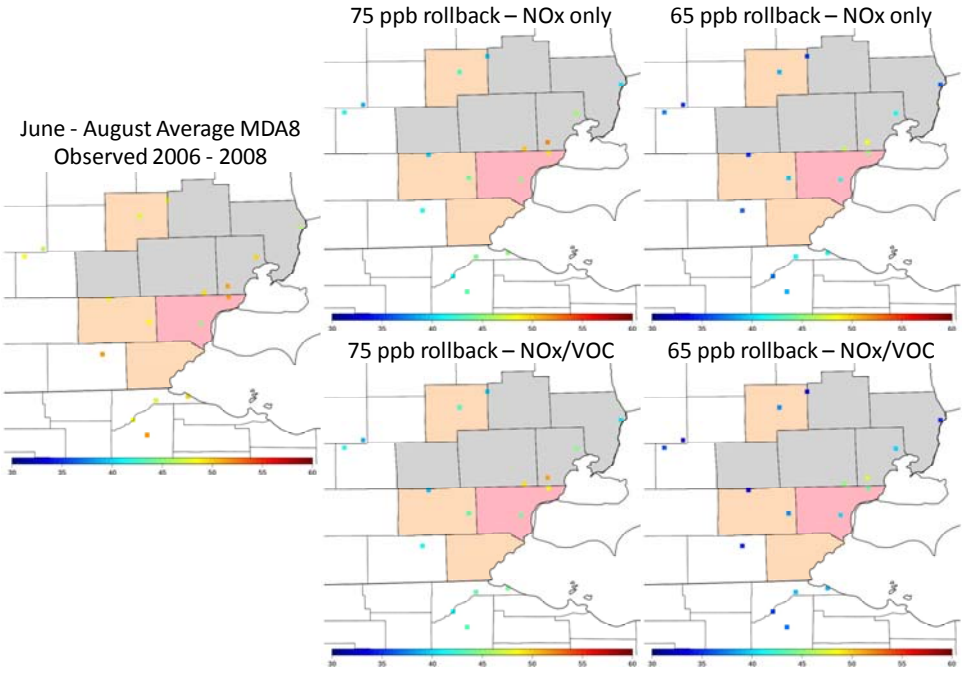


**Figure 123: April-October seasonal average of daily maximum 8-hour $O_3$ values at Detroit area monitor locations for observed 2006-2008 conditions (left panel), 75 ppb adjustment scenarios (middle panels), and 65 ppb adjustment scenarios (right panels). NOx only adjustments are shown in top panels, NOx/VOC adjustments are shown in bottom panels.**

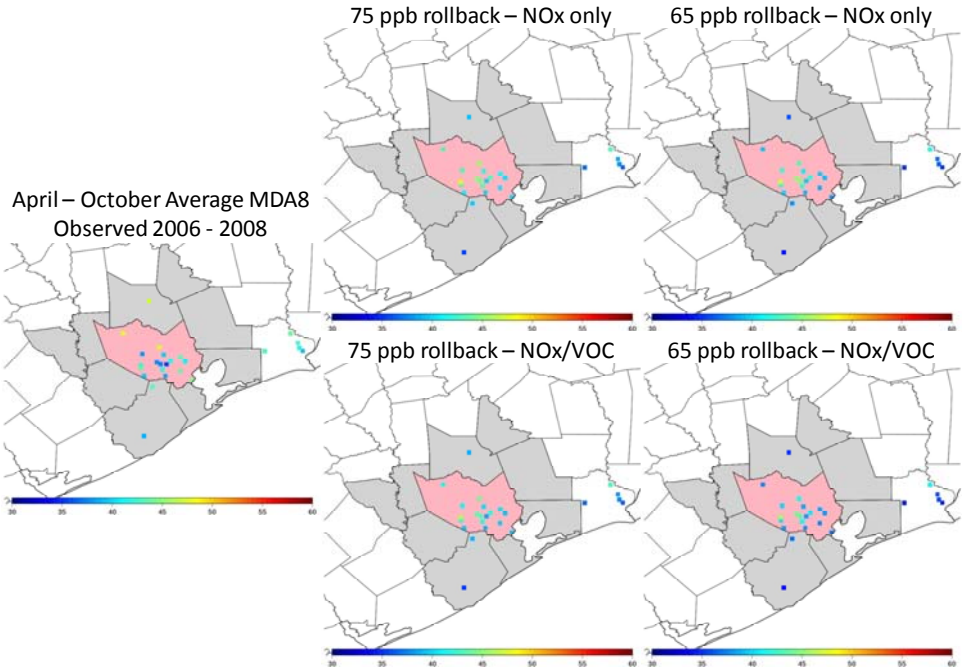


**Figure 124: April-October seasonal average of daily maximum 8-hour $O_3$ values at Houston area monitor locations for observed 2006-2008 conditions (left panel), 75 ppb adjustment scenarios (middle panels), and 65 ppb adjustment scenarios (right panels). NOx only adjustments are shown in top panels, NOx/VOC adjustments are shown in bottom panels.**

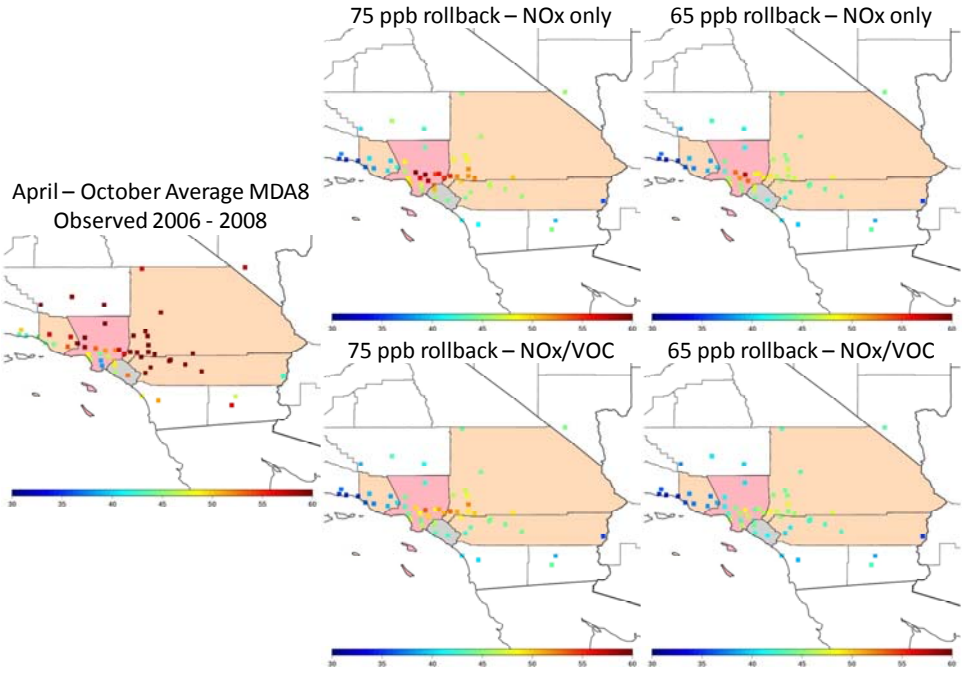


**Figure 125: April-October seasonal average of daily maximum 8-hour $O_3$ values at Los Angeles area monitor locations for observed 2006-2008 conditions (left panel), 75 ppb adjustment scenarios (middle panels), and 65 ppb adjustment scenarios (right panels). NOx only adjustments are shown in top panels, NOx/VOC adjustments are shown in bottom panels.**

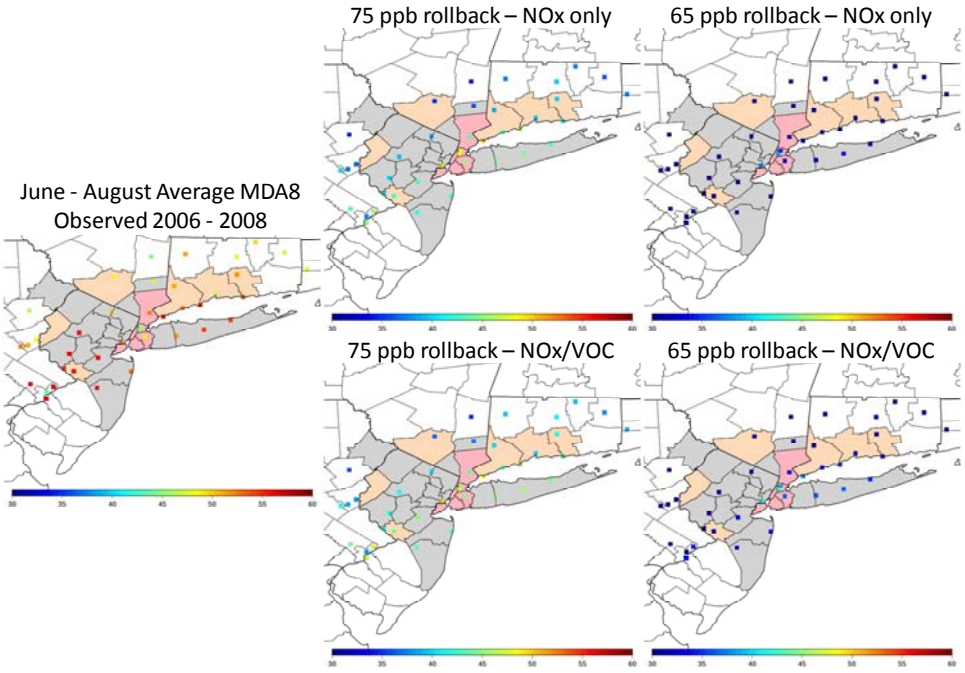


**Figure 126: April-October seasonal average of daily maximum 8-hour $O_3$ values at New York area monitor locations for observed 2006-2008 conditions (left panel), 75 ppb adjustment scenarios (middle panels), and 65 ppb adjustment scenarios (right panels). NOx only adjustments are shown in top panels, NOx/VOC adjustments are shown in bottom panels.**

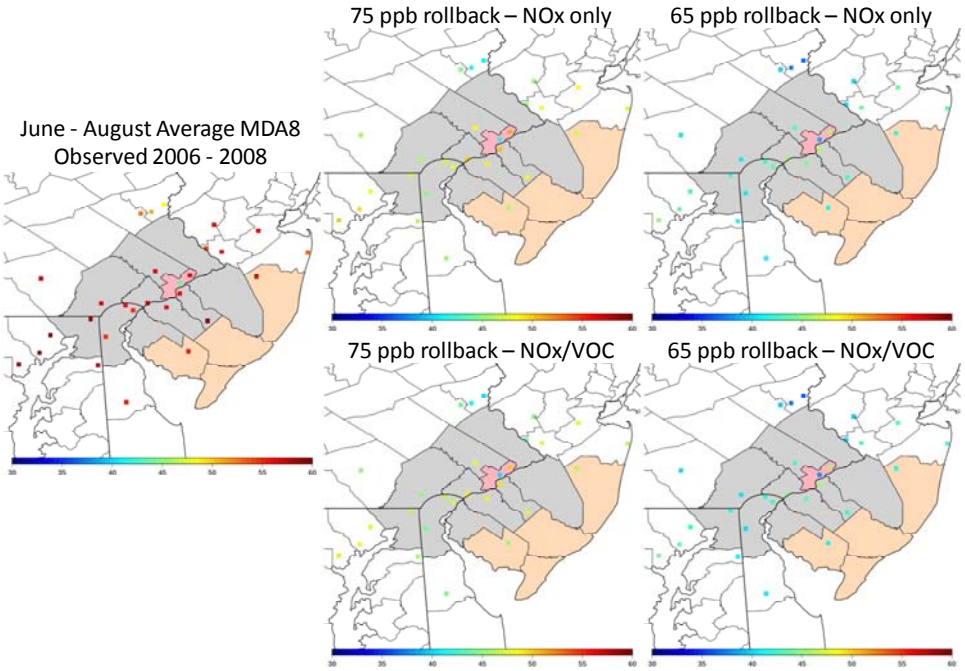


**Figure 127: April-October seasonal average of daily maximum 8-hour $O_3$ values at Philadelphia area monitor locations for observed 2006-2008 conditions (left panel), 75 ppb adjustment scenarios (middle panels), and 65 ppb adjustment scenarios (right panels). NOx only adjustments are shown in top panels, NOx/VOC adjustments are shown in bottom panels.**

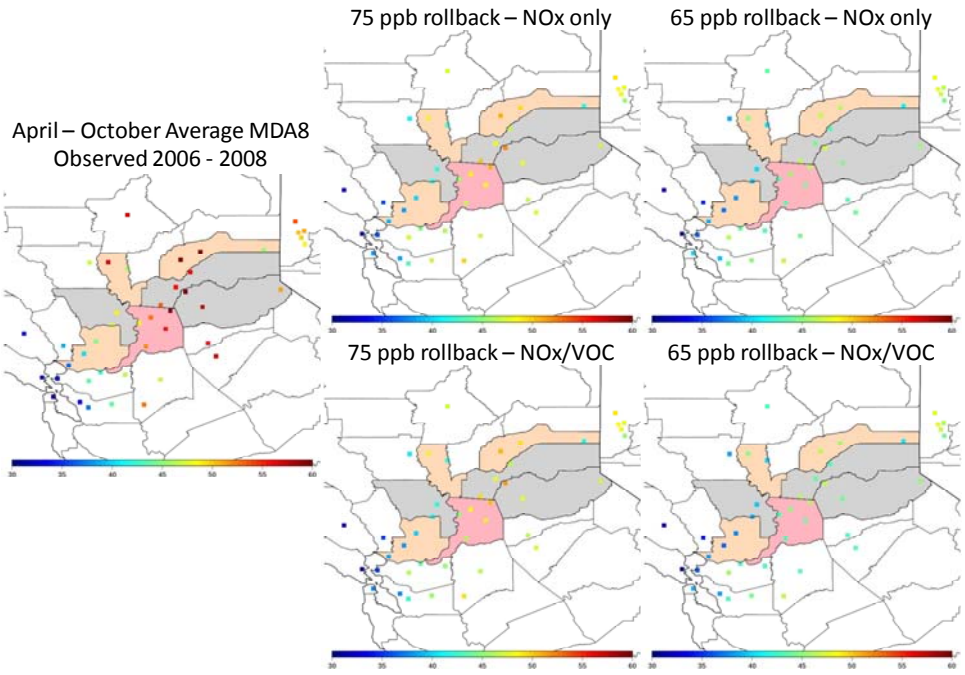


**Figure 128: April-October seasonal average of daily maximum 8-hour $O_3$ values at Sacramento area monitor locations for observed 2006-2008 conditions (left panel), 75 ppb adjustment scenarios (middle panels), and 65 ppb adjustment scenarios (right panels). NOx only adjustments are shown in top panels, NOx/VOC adjustments are shown in bottom panels.**

# 5. REFERENCES


Appel, K.W., Gilliland, A.B., Sarwar, G., Gilliam, R.C. (2007). Evaluation of the Community Multiscale Air Quality(CMAQ) model version 4.5: Sensitivities impacting model performance Part I - Ozone. Atmospheric Environment, 41: 9603-9615.

Appel, K.W., Bhave, P.V., Gilliland, A.B., Sarwar, G., Roselle, S.J. (2008). Evaluation of the community Multiscale air quality (CMAQ) model version 4.5: Sensitivities impacting model performance; Part II - particulate matter. Atmospheric Environment, 42: 6057-6066.

Baker, K. and P. Dolwick. Meteorological Modeling Performance Evaluation for the Annual 2005 Eastern U.S. 12-km Domain Simulation, USEPA/OAQPS, February 2, 2009.

Baker, K. and P. Dolwick. Meteorological Modeling Performance Evaluation for the Annual 2005 Continental U.S. 36-km Domain Simulation, USEPA/OAQPS, February 2, 2009.

Byun, D.W., and Ching, J.K.S., Eds, 1999. Science algorithms of EPA Models-3 Community Multiscale Air Quality (CMAQ modeling system, EPA/600/R-99/030, Office of Research and Development).

Byun, D., Schere, K.L. (2006). Review of the governing equations, computational algorithms, and other components of the models-3 Community Multiscale Air Quality (CMAQ) modeling system. Applied Mechanics Reviews, 59: 51-77.

Cohan, D.S., Hakami, A., Hu, Y., Russell, A.G. (2005). Nonlinear response of ozone to emissions: Source apportionment and sensitivity analysis. Environmental Science & Technology, 39: 6739-6748.

Cohan, D.S., Napelenok, S.L. (2011). Air quality response modeling for decision support. Atmosphere, 2: 407-425; doi:10.3390/atmos2030407.

Dunker, A.M. (1984). The decoupled direct method for calculating sensitivity coefficients in chemical kinetics. Journal of Chemical Physics, 81; 2385-2393.

Foley, K.M., Roselle, S.J., Appel, K.W., Bhave, P.V., Pleim, J.E., Otte, T.L., Mathur, R., Sarwar, G., Young, J.O., Gilliam, R.C., Nolte, C.G., Kelly, J.T., Gilliland, A.B., Bash, J.O. (2010). Incremental testing of the Community Multiscale Air Quality (CMAQ) modeling system version 4.7, Geoscientific Model Development, 3: 205-226.

Grell, G., J. Dudhia, and D. Stauffer (1994). A Description of the Fifth-Generation Penn State/NCAR Mesoscale Model (MM5), NCAR/TN-398+STR., 138 pp, National Center for Atmospheric Research, Boulder CO.

Hakami, A., Odman, M.T., Russell, A.G. (2003). High-order direct sensitivity analysis of multidimensional air quality models. Environmental Science & Technology, 37: 2442-2452.

Hakami, A., Odman, M.T., Russell, A.G. (2004). Nonlinearity in atmospheric response: A direct sensitivity analysis approach. Journal of Geophysical Research, 109: D15303; doi:10.1029/2003JD004502.

Houyoux, M.R., Vukovich, J.M., Coats, C.J., Wheeler, N.J.M., Kasibhatla, P.S. (2000). Emission inventorydevelopment and processing for the Seasonal Model for Regional Air Quality (SMRAQ) project. Journal of Geophysical Research-Atmospheres, 105: 9079-9090.

Koo, B., Dunker, A.M., Yarwood, G. (2007). Implementing the decoupled direct method for sensitivity analysis in a particulate matter air quality model. Environmental Science & Technology, 41: 2847-2854.

Napelenok, S.L., Cohan, D.S., Hu, Y., Russell, A.G. (2006). Decoupled direct 3D sensitivity analysis for particulate matter (DDM-3D/PM). Atmospheric Environment, 40: 6112-6121.

National Research Council of the National Academies (2008). Estimating Mortality Risk Reduction and Economic Benefits from Controlling Ozone Air Pollution. The National Academies Press, Washington, D.C

Pierce, T.; Geron, C.; Bender, L.; Dennis, R.; Tonnesen, G. Guenther, A. (1998). Influence of increased isoprene emissions on regional ozone modeling. J. Geophys. Res., 103: 25611–25629.

Seinfeld, J.H. and S.N. Pandis. (1998). Atmospheric chemistry and physics from air pollution to climate change. John Wiley & Sons, Inc, New York, 1998.

Simon, H., Baker, K.B., Akhtar, F., Napelenok, S.L., Possiel, N., Wells, B., Timin, B. (2013) A direct sensitivity approach to predict hourly ozone resulting from compliance with the national ambient air quality standard, Environmental Science and Technology, 47, 2304-2313.

US EPA, 2007. Guidance on the Use of Models and Other Analyses for Demonstrating Attainment of Air Quality Goals for Ozone, PM2.5, and Regional Haze, Research Triangle Park. EPA-454/B-07-002: http://www.epa.gov/ttn/scram/guidance/guide/final-03-pm-rh-guidance.pdf.

US EPA, Emissions Modeling for the Final Mercury and Air Toxics Standards Technical Support Document, 2011a, EPA-45A/R-11-011: http://epa.gov/ttn/chief/emch/toxics/MATS_Final_Emissions_Modeling_TSD_9Dec2011.pdf.

US EPA, Air Quality Modeling Technical Support Document: Final EGU NESHAP, 2011b, EPA-45A/R-11-009.

US EPA, Health Risk and Exposure Assessment for Ozone: First External Review Draft, 2012, EPA 452/P-12-001.

US EPA Integrated Science Assessment for Ozone and Related Photochemical Oxidants, 2013, EPA 600/R-10/076F

Yang, Y.-J., Wilkinson, J.G., Russell, A.G. (1997). Fast, direct sensitivity analysis of multidimensional photochemical models. Environmental Science & Technology, 31: 2859-2868.

Zhang, W., Capps, S.L., Hu, Y., Nenes, A., Napelenok, S.L., Russell, A.G. (2012). Development of the high-order decoupled direct method in three dimensions for particulate matter: Enabling advanced sensitivity analysis in air quality models. Geoscientific Model Development, 5: 355-368.

# APPENDIX 4E EVALUATION OF SEATTLE AIR QUALITY

Investigation of the monitoring network and ambient data trends in Seattle raised serious concerns about the appropriateness of using 2006 data for the purpose of an exposure analysis. Seattle experienced some high ozone events in 2006 that were substantially higher than any measured ozone that occurred in the modeled time period (Jan, April-October 2007) (Fig 1). The model generally predicted ozone disbenefits to NOx reductions in Seattle on the low ozone days that were predominant in 2007. Because these conditions are not likely to occur on high ozone days, we had serious concerns about extrapolating 2007 sensitivities to 2006 high ozone days.

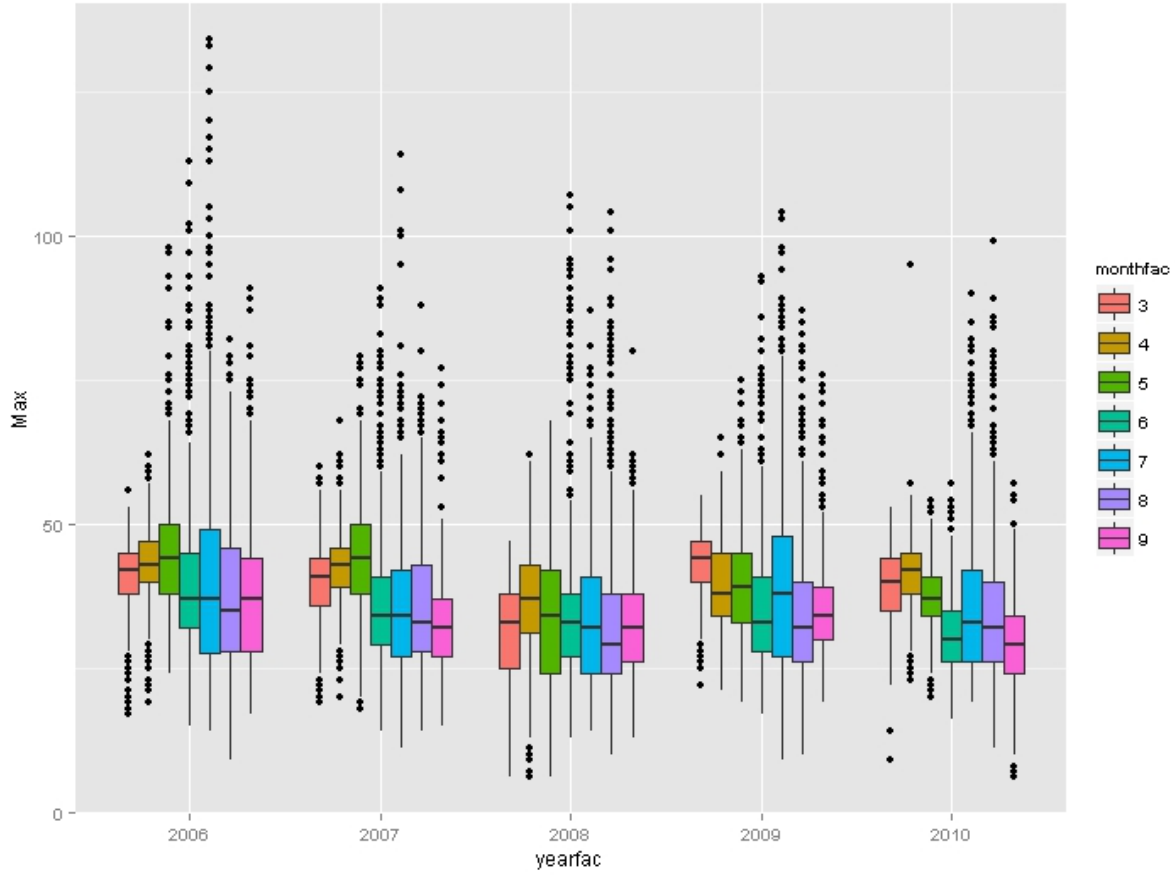


**Figure 1: All-site maximum hourly O3 (ppb) in Seattle by year and month. This figure combines all hourly O3 data from 11 sites in the Seattle area and plots the highest-site value at each hour for Mar-Sep.**

Further concerns come from the lack of measured urban ozone concentrations in all years, but especially in 2006. The Seattle monitoring network is mainly focused on downwind and background areas. There is a single urban monitor in a residential area of downtown Seattle (Fig 2 and Fig 3). The urban monitor was not in operation from January-September of 2006, so no urban measurements were made during most of the 2006 ozone season. Performing a census-tract level exposure analysis for the Seattle and Tacoma urban areas would not be appropriate based solely on ozone values in outlying rural and suburban areas.

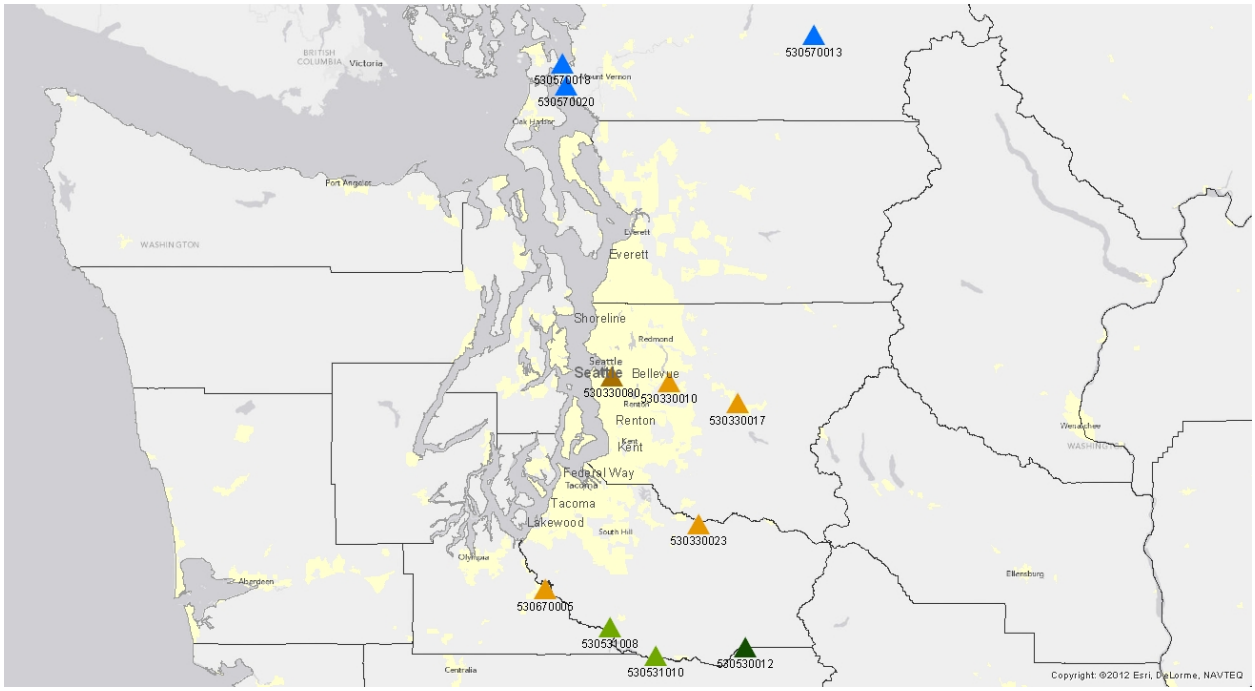


**Figure 2: Map of Seattle area monitoring sites used to create the ozone surfaces for the exposure assessment. Dark brown site is the most urban location (in a residential area of downtown Seattle), orange sites are suburban, sites in the far northern and southern portions of the area are plotted in blue and green respectively, dark green site is a high elevation site.**

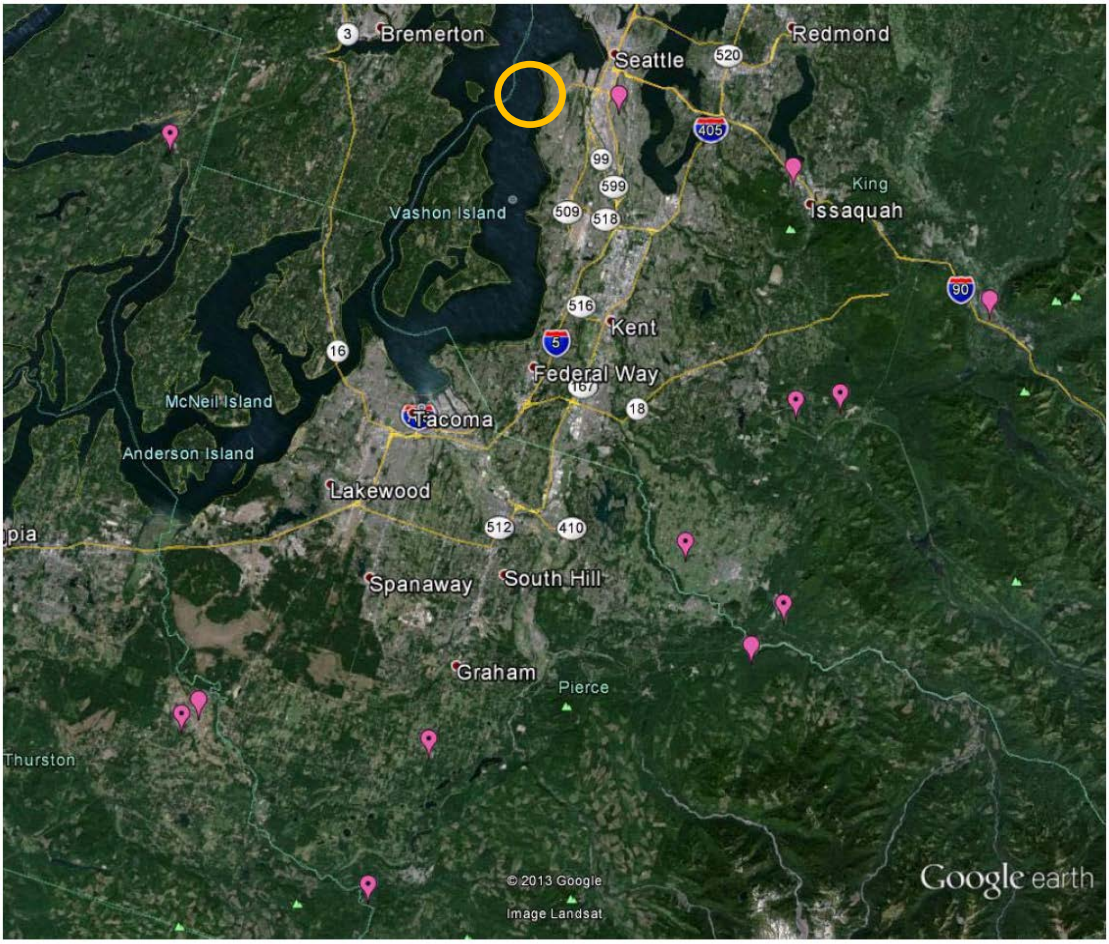


**Figure 3: Map with aerial photography overlay showing where monitors are located with respect to highly urbanized (gray) areas versus suburban and rural areas (green). Downtown Seattle site is circled in orange.**

Additional concerns were raised about the potential insufficient density of the Seattle ozone monitoring network and subsequently its adequacy for use in a census-tract level exposure analysis beyond the concerns above for 2006. The Seattle area ozone monitoring network was designed primarily to address NAAQS compliance. For this purpose it is appropriate to focus on downwind suburban areas where ozone concentrations are expected to be highest. Modeling suggests that there are often large spatial gradients of ozone within the Seattle/Tacoma area. Figures 4, 5, 6, and 7 show 8-hr daily maximum ozone concentration fields for the Seattle area from the 2007 CMAQ modeling described in appendix 4A. Spatial fields for exposure modeling are created using interpolation of monitor data and do not capture any modeled spatial gradients. Therefore it is expected that at many times, interpolation of the single Seattle urban monitor with

downwind suburban monitors will not adequately represent the ozone values in highly populated urban areas such a Tacoma. In addition, unlike most other urban areas, the Seattle monitoring network for the 2006-2010 time period did not include any upwind monitors (on the West side of Puget Sound).

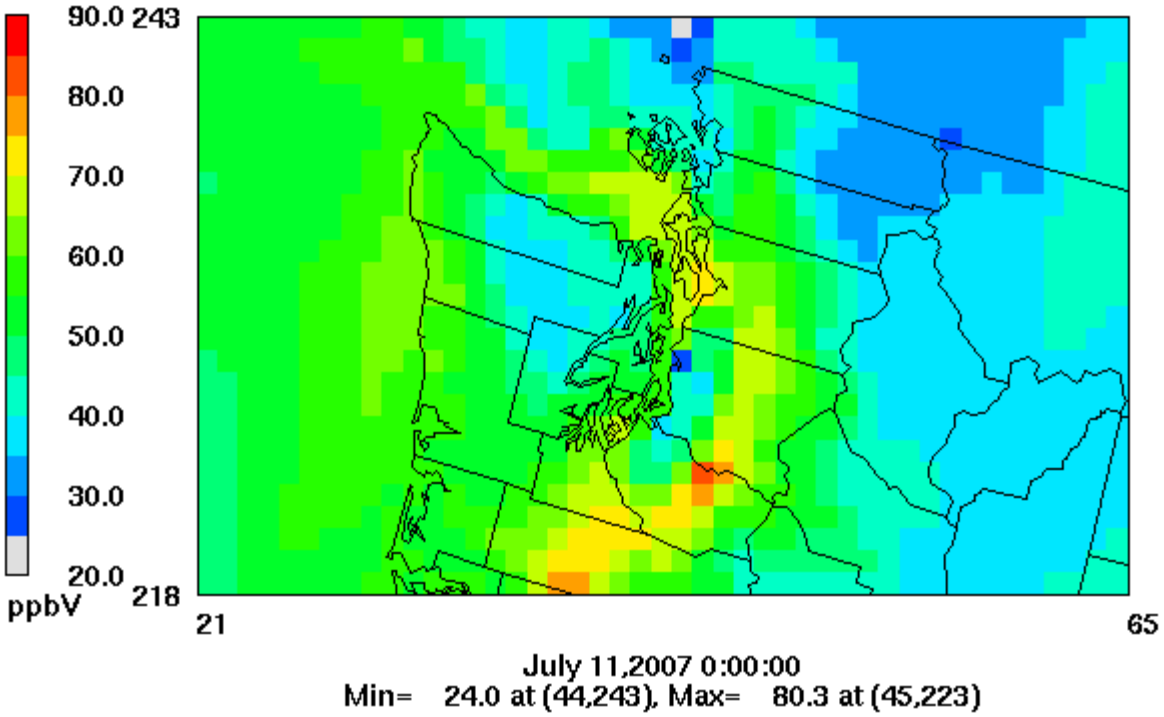


**Figure 4: Example of a day with large spatial ozone gradients in the Seattle area. Maximum 8-hr daily maximum ozone value for July 11, 2007.**

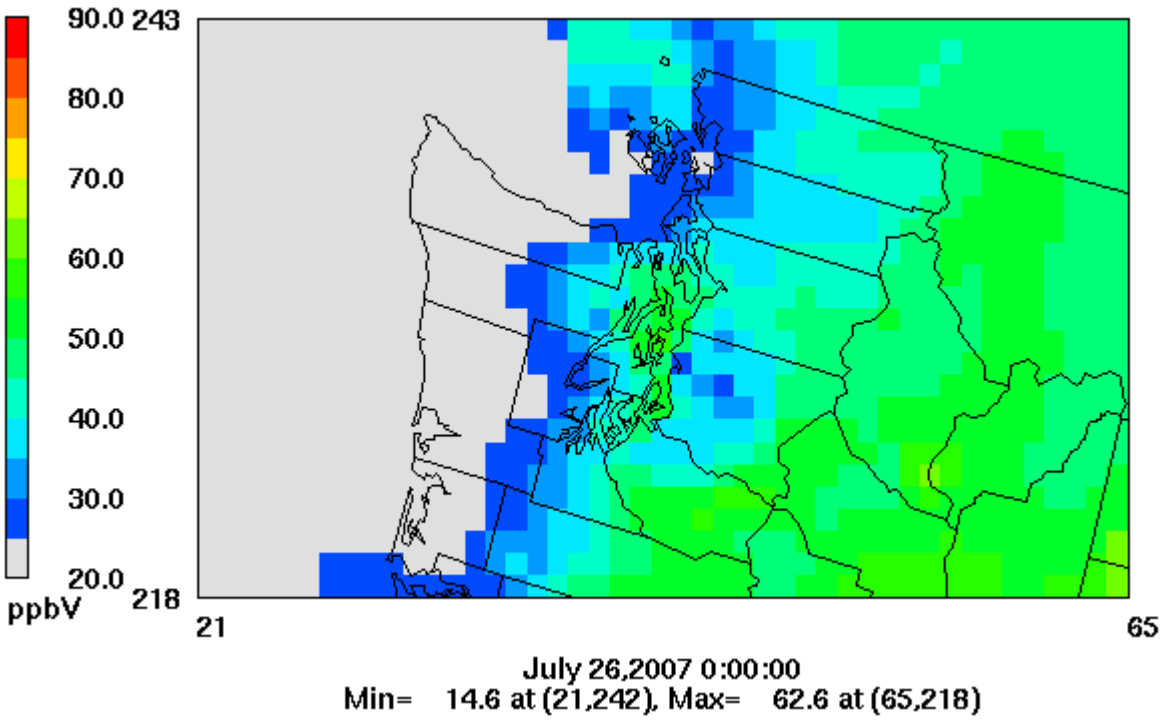


**Figure 5: Example of a day with large spatial ozone gradients in the Seattle area. Maximum 8-hr daily maximum ozone value for July 26, 2007.**

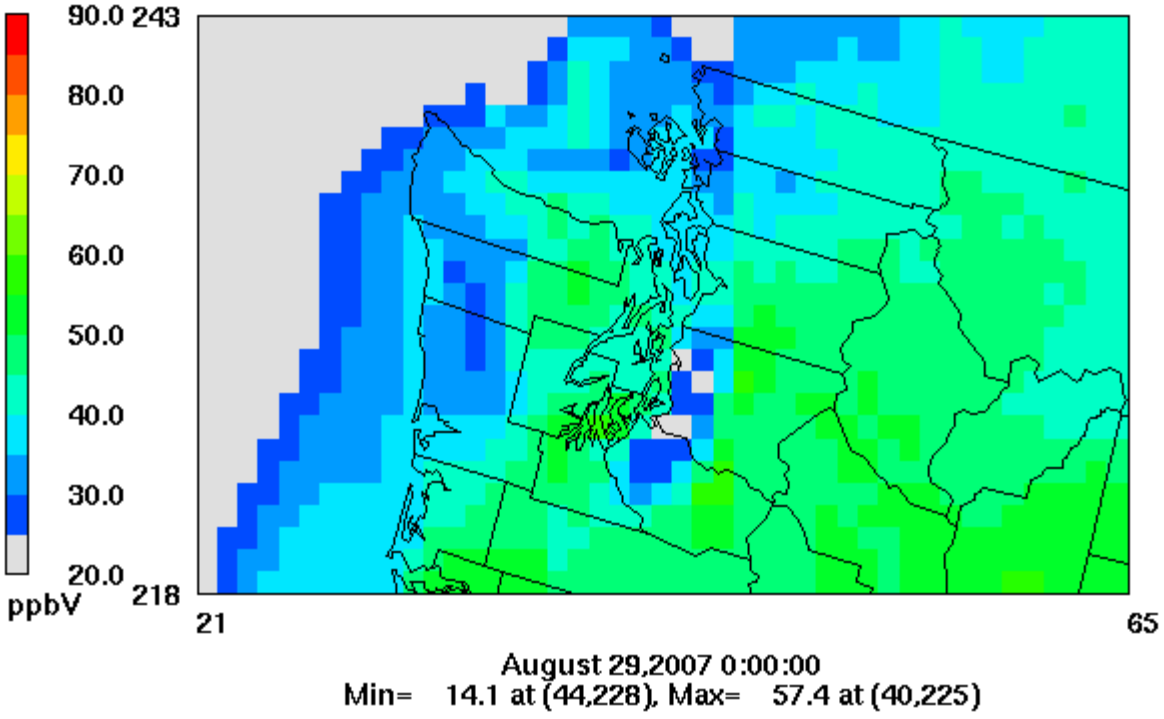


**Figure 6: Example of a day with large spatial ozone gradients in the Seattle area. Maximum 8-hr daily maximum ozone value for August 29, 2007.**

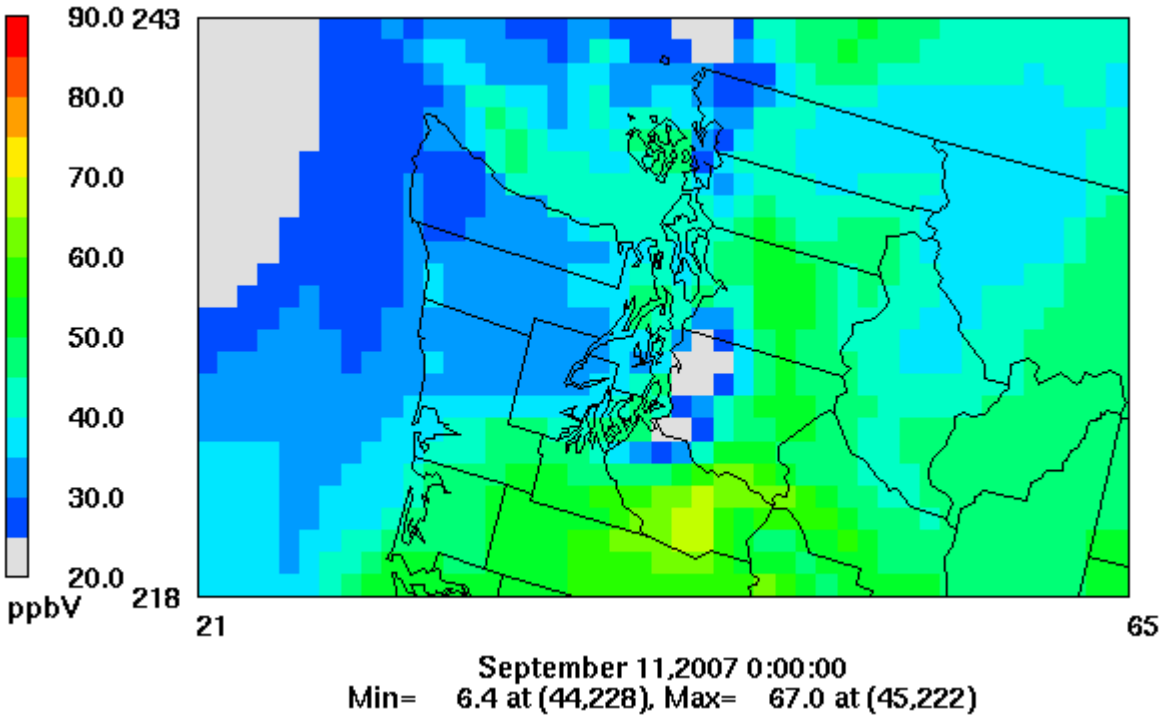


**Figure 7: Example of a day with large spatial ozone gradients in the Seattle area. Maximum 8-hr daily maximum ozone value for September 11, 2007.**

To further analyze the appropriateness of the Seattle monitoring network for the purpose of performing an exposure assessment, the representativeness of the ozone monitoring network to total population in Seattle was compared to all other urban case study areas (Figure 8). This analysis showed that the Seattle monitoring network was much less representative of ozone concentrations where people live than the ozone networks in the other 15 cities. For instance, while more than 75 % of the area-wide population lived within 20km of an ozone monitor in each of the other 15 urban areas, in Seattle only about 55% of the population lives within 20km of an ozone monitor. Furthermore, in 13 cities, more than 50% of the population lives within 10km of an ozone monitor, in 2 cities more than 50% of the population lives within 13 km of an ozone monitor, yet in Seattle, more than 50% of the population lives within 18 km of an ozone monitor. Based on both the sharp spatial gradients predicted by the model and the much sparser monitor coverage in highly populated areas in Seattle compared to other urban case study areas, it was determined that the monitoring network in Seattle likely does not capture ozone values representing levels to which large portions of the population are exposed and therefore it would not be appropriate to rely upon the currently available Seattle ozone monitors for the purpose of the exposure analysis which requires accurate fine scale estimates of ozone concentrations where people are exposed.

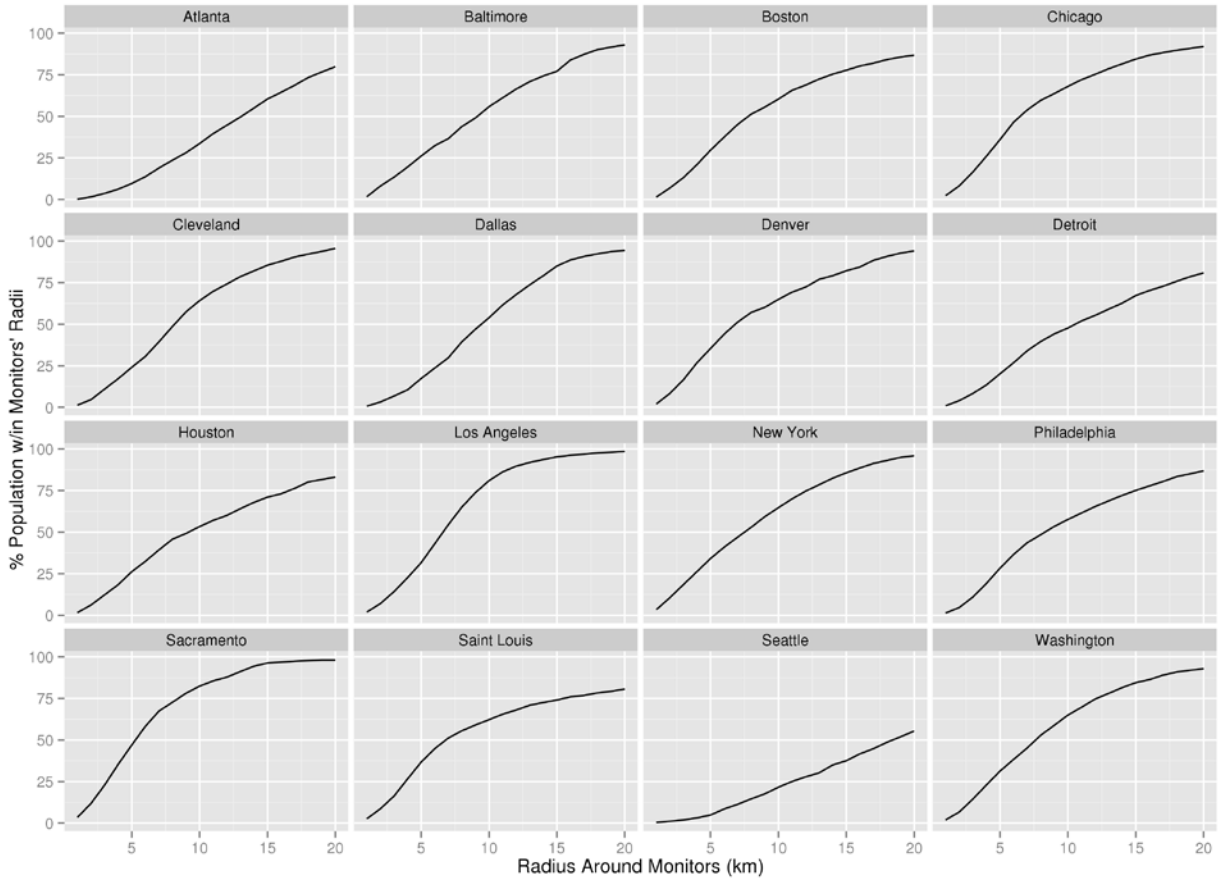


**Figure 8: Cumulative distribution of population living within set distances of an ozone monitor in each urban area.**

United States
Environmental Protection
Agency

Office of Air Quality Planning and Standards
Air Quality Strategies and Standards Division
Research Triangle Park, NC

Publication No. EPA-452/P-14-004b
February 2014